3. DESIGN OF STRUCTURES, COMPONENTS, EQUIPMENT, AND SYSTEMS

The information contained in this section describes design considerations for structures, components, equipment, and systems. Some of the information was prepared in accordance with the original plant licensing requirements and is representative of the site conditions at the time the plant was licensed. Information in this chapter reflects the permanently defueled status unless otherwise noted.

3.1 CONFORMANCE WITH NRC GENERAL DESIGN CRITERIA

This section discusses the extent to which the design criteria for the plant structures, systems, and components important to safety needed to support permanent plant shutdown or defueled operations, meet the applicable NRC General Design Criteria for Nuclear Power Plants specified in Appendix A to 10 CFR Part 50. For each criterion, a summary is provided to show how the principal design features meet the criterion. The design complies with all applicable general design criteria, with no exceptions other than NRC approved exemptions. In the discussion of each criterion, the sections of this UFSAR where more detailed information is presented are referenced to demonstrate compliance with the criterion. Controlled Document 90215, NRC Regulatory Guide Applicability, identifies which NRC Regulatory Guides are applicable and lists exceptions as appropriate.

3.1.1 OVERALL REQUIREMENTS

3.1.1.1 Criterion 1 - Quality Standards and Records

3.1.1.1.1 Criterion

Structures, systems, and components important to safety shall be designed, fabricated, erected, and tested to quality standards commensurate with the importance of the safety functions to be performed. Where generally recognized codes and standards are used, they shall be identified and evaluated to determine their applicability, adequacy, and sufficiency and shall be supplemented or modified as necessary to assure a quality product in keeping with the required safety function. A quality assurance program shall be established and implemented in order to provide adequate assurance that these structures, systems, and components will satisfactorily perform their safety functions. Appropriate records of the design, fabrication, erection, and testing of structures, systems, and components important to safety shall be maintained by or under the control of the nuclear power unit licensee throughout the life of the unit.

3.1.1.1.2 Response

Structures, systems, and components of San Onofre 2 and 3 are classified according to their importance to safety. The seismic and quality classifications are discussed and listed for major structures, systems, and components in Section 3.2. The codes and standards applicable to the design, fabrication, erection, and testing of each component are discussed in the FSAR sections

covering the particular system descriptions. Applicability of NRC Regulatory Guides is discussed in Controlled Document 90215.

A Decommissioning Quality Assurance Program (DQAP) was established in accordance with 10CFR50, Appendix B, to ensure that structures, systems, and components will satisfactorily perform their safety function. The applicants and their special vendors implement the DQAP. The applicants will maintain, either in their possession or under their control, the appropriate records of the design, erection, and testing of structures, systems, and components for the life of the plant.

3.1.1.2 Criterion 2 - Design Bases for Protection Against Natural Phenomena

3.1.1.2.1 Criterion

Structures, systems, and components important to safety shall be designed to withstand the effects of natural phenomena such as earthquakes, tornadoes, hurricanes, floods, tsunami, and seiches without loss of capability to perform their safety functions. The design bases for these structures, systems, and components shall reflect: (1) appropriate consideration of the most severe of the natural phenomena that have been historically reported for the site and surrounding area, with sufficient margin for the limited accuracy, quantity, and period of time in which the historical data have been accumulated, (2) appropriate combinations of the effects of normal and accident conditions with the effects of the natural phenomena, and (3) the importance of the safety functions to be performed.

3.1.1.2.2 Response

Design bases for protection against natural phenomena are in accordance with General Design Criterion 2. Structures, systems, and components important to safety are designed to withstand the effects of natural phenomena such as earthquakes, tornadoes, hurricanes, floods, tsunami, and seiches without loss of the capability to perform those safety functions necessary to cope with appropriate combinations of natural phenomena and plant conditions. The designs are based upon the most severe of the natural phenomena recorded for the site and surrounding area, with an appropriate margin to account for uncertainties in the historical data. The natural phenomena postulated in the design are presented in Chapter 2. The design criteria for the structures, systems, and components affected by each natural phenomenon are presented in Sections 3.2, 3.3, 3.4, 3.5, 3.7, and 3.8. Those combinations of natural phenomena and plant-originated accidents that are considered in the design are identified in Sections 3.8 and 3.9.

3.1.1.3 Criterion 3 - Fire Protection

3.1.1.3.1 Criterion

Structures, systems, and components important to safety are designed and located to minimize, consistent with other safety requirements, the probability and effect of fires and explosions. Noncombustible and heat-resistant materials shall be used wherever practical throughout the unit,

particularly in locations such as the containment and control room. Fire detection and firefighting systems of appropriate capacity and capability shall be provided and designed to minimize the adverse effects of fire on structures, systems, and components important to safety. Firefighting systems shall be designed to ensure that their rupture or inadvertent operation does not significantly impair the safety capability of these structures, systems, and components.

3.1.1.3.2 Response

Structures, systems, and components important to safety meet the requirements of General Design Criterion 3. Fire protection systems meeting the requirements of Criterion 3 are provided.

The plant design minimizes the probability and effect of fires. Noncombustible and fire-resistant materials are used to the degree possible in the containment, Control Room/Command Center, components of safety feature systems, and throughout the plant. The fire protection system (FPS) provides equipment and facilities for fire protection, including detection, alarm, extinguishment, and smoke venting, and protects both plant equipment and personnel from fire and the resultant release of toxic vapors. Both automatic and manual types of firefighting equipment are provided wherever appropriate in accordance with 10CFR50.48(f) requirements. The FPS is described in Chapter 9 and the Updated Fire Hazards Analysis.

Firefighting systems are designed to ensure that their rupture or inadvertent operation will not impair systems important to safety. Section 3.4 discusses the effects of flooding from rupture or inadvertent actuation of FPS components.

3.1.1.4 Criterion 4 - Environmental and Missile Design Bases

3.1.1.4.1 Criterion

Structures, systems, and components important to safety shall be designed to accommodate the effects of and to be compatible with the environmental conditions associated with normal operation, maintenance, testing, and postulated accidents, including loss-of-coolant accidents (LOCAs). These structures, systems, and components shall be appropriately protected against dynamic effects, including the effects of missiles, pipe whipping, and discharging fluids that may result from equipment failures and from events and conditions outside the nuclear power unit.

3.1.1.4.2 Response

Environmental and missile design bases are in accordance with General Design Criterion 4. Structures, systems, and components important to safety are designed to accommodate the effects of and to be compatible with the environmental conditions associated with normal operation, maintenance, testing and postulated accidents, assuming that nonrelated extreme/abnormal events do not occur simultaneously. These structures, systems, and components are appropriately protected against dynamic effects, including the effects of missiles, pipe whipping, and

discharging fluids, that may result from equipment failures and from events and conditions outside the nuclear power unit.

Flood design is discussed in Section 3.4. Missile protection is discussed in Section 3.5.

3.1.1.5 Criterion 5 - Sharing of Structures, Systems, and Components

3.1.1.5.1 Criterion

Structures, systems, and components important to safety shall not be shared among nuclear power units unless it is shown that such sharing will not significantly impair their ability to perform their safety functions including, in the event of an accident in one unit, an orderly shutdown and cooldown of the remaining units.

3.1.1.5.2 Response

Structures, systems, and components that are shared by the two units are identified in Appendix 3B. The effects of sharing these structures, systems, and components are evaluated in Appendix 3B to show that such sharing will not significantly impair their ability to perform their safety functions for each unit in a manner independent of the conditions existing in the second unit.

3.1.2 PROTECTION BY MULTIPLE FISSION PRODUCT BARRIERS

3.1.2.1 Criterion 10 - Reactor Design
(DELETED)

3.1.2.2 Criterion 11 - Reactor Inherent Protection
(DELETED)

3.1.2.3 Criterion 12 - Suppression of Reactor Power Oscillations
(DELETED)

3.1.2.4 Criterion 13 - Instrumentation and Control
(DELETED)

3.1.2.5 Criterion 14 - Reactor Coolant Pressure Boundary (RCPB) (Primary Coolant System Boundary)
(DELETED)

3.1.2.6 Criterion 15 - Reactor Coolant System Design
(DELETED)

3.1.2.7 Criterion 16 - Containment Design
(DELETED)

3.1.2.8 Criterion 17 - Electric Power Systems
(DELETED)

3.1.2.9 Criterion 18 - Inspection and Testing of Electric Power Systems
(DELETED)

3.1.2.10 Criterion 19 - Control Room

3.1.2.10.1 Criterion

A control room shall be provided from which actions can be taken to operate the nuclear power unit safely under normal conditions and to maintain it in a safe condition under accident conditions, including LOCA. Adequate radiation protection shall be provided to permit access and occupancy of the control room under accident conditions without personnel receiving radiation exposures in excess of 5 rem whole body, or its equivalent to any part of the body, for the duration of the accident.

Equipment at appropriate locations outside the control room shall be provided: (1) with a design capability for prompt hot shutdown of the reactor, including necessary instrumentation and controls to maintain the unit in a safe condition during hot shutdown and (2) with a potential capability for subsequent cold shutdown of the reactor through the use of suitable procedures.

3.1.2.10.2 Response

In the permanently defueled condition, Control Room/Command Center actions are no longer an element of accident mitigation. Furthermore, from a personnel protection perspective, the remaining Design Basis Accidents do not produce dose releases that are a substantive threat to Control Room/Command Center personnel.

3.1.3 PROTECTION AND REACTIVITY CONTROL SYSTEMS

3.1.3.1 Criterion 20 - Protection System Functions
(DELETED)

3.1.3.2 Criterion 21 - Protection System Reliability and Testability
(DELETED)

3.1.3.3 Criterion 22 - Protection System Independence
(DELETED)

3.1.3.4 Criterion 23 - Protection System Failure Modes
(DELETED)

3.1.3.5 Criterion 24 - Separation of Protection and Control Systems
(DELETED)

3.1.3.6 Criterion 25 - Protection System Requirements for Reactivity Control Malfunctions
(DELETED)

3.1.3.7 Criterion 26 - Reactivity Control System Redundancy and Capability
(DELETED)

3.1.3.8 Criterion 27 - Combined Reactivity Control Systems Capability
(DELETED)

3.1.3.9 Criterion 28 - Reactivity Limits
(DELETED)

3.1.3.10 Criterion 29 - Protection Against Anticipated Operational Occurrences

3.1.3.10.1 Criterion

The protection and reactivity control systems shall be designed to ensure an extremely high probability of accomplishing their safety functions in the event of anticipated operational occurrences.

3.1.3.10.2 Response

Consideration of redundancy, independence, and testability in the design, coupled with careful component selection, overall system testing, and adherence to detailed quality assurance, ensure an extremely high probability that safety functions are accomplished in the event of these anticipated operational occurrences.

3.1.4 FLUID SYSTEMS

3.1.4.1 Criterion 30 - Quality of Reactor Coolant Pressure Boundary (Primary Coolant System Boundary)
(DELETED)

3.1.4.2 Criterion 31 - Fracture Prevention of Reactor Coolant Pressure Boundary (Primary Coolant System Boundary)
(DELETED)

3.1.4.3 Criterion 32 - Inspection of Reactor Coolant Pressure Boundary (Primary Coolant System Boundary)
(DELETED)

3.1.4.4 Criterion 33 - Reactor Coolant Makeup
(DELETED)

3.1.4.5 Criterion 34 - Residual Heat Removal
(DELETED)

3.1.4.6 Criterion 35 - Emergency Core Cooling
(DELETED)

3.1.4.7 Criterion 36 - Inspection of Emergency Core Cooling System (Core Auxiliary Cooling System)
(DELETED)

3.1.4.8 Criterion 37 - Testing of Emergency Core Cooling System
(DELETED)

3.1.4.9 Criterion 38 - Containment Heat Removal
(DELETED)

3.1.4.10 Criterion 39 - Inspection of Containment Heat Removal System
(DELETED)

3.1.4.11 Criterion 40 - Testing of Containment Heat Removal System
(DELETED)

3.1.4.12 Criterion 41 - Containment Atmosphere Cleanup
(DELETED)

3.1.4.13 Criterion 42 - Inspection of Containment Atmosphere Cleanup systems
(DELETED)

3.1.4.14 Criterion 43 - Testing of Containment Atmosphere Cleanup Systems
(DELETED)

3.1.4.15 Criterion 44 - Cooling Water

3.1.4.15.1 Criterion

A system to transfer heat from structures, systems, and components important to safety to an ultimate heat sink shall be provided. The system safety function shall be to transfer the combined heat load of these structures, systems, and components under normal operating and accident conditions.

Suitable redundancy in components and features, and suitable interconnections, leak detection, and isolation capabilities shall be provided to ensure that for onsite electric power system

operation (assuming offsite power is not available) and for offsite electric power system operation (assuming onsite power is not available) the system safety function can be accomplished, assuming a single failure.

3.1.4.15.2 Response

The Independent Spent Fuel Pool Cooling System (ISFPCS) provides heat transfer from spent fuel pool to the ultimate heat sink (i.e., the atmosphere). This system is designed to transfer the heat loads under all anticipated normal SFP and accident conditions. Suitable redundancy, leak detection, system interconnection, and isolation capabilities ensure the remaining safety function.

A complete description of the ultimate heat sink and the ISFPCS is given in Chapter 9.

3.1.4.16 Criterion 45 - Inspection of Cooling Water System

3.1.4.16.1 Criterion

The cooling water system shall be designed to permit appropriate periodic inspection of important components, such as heat exchangers and piping, to ensure the integrity and capability of the system.

3.1.4.16.2 Response

The integrity and capability of the ISFPCS is monitored during normal SFP operation.

Components of the ISFPCS are in accessible areas to permit appropriate periodic inspection. This system is discussed in Chapter 9.

3.1.4.17 Criterion 46 - Testing of Cooling Water System

3.1.4.17.1 Criterion

The cooling water system shall be designed to permit appropriate periodic pressure and functional testing to ensure: (1) the structural and leaktight integrity of its components, (2) the operability and the performance of the active components of the system, and (3) the operability of the system as a whole, and under conditions as close to design as practicable, the performance of the full operational sequence that brings the system into operation for reactor shutdown and for LOCAs, including operation of applicable portions of the protection system and the transfer between normal and emergency power sources.

3.1.4.17.2 Response

The ISFPCS operates continuously during SFP operation. This operation demonstrates the operability, performance, and structural and leaktight integrity of all cooling water system components.

3.1.5 REACTOR CONTAINMENT

3.1.5.1 Criterion 50 - Containment Design Basis

(DELETED)

3.1.5.2 Criterion 51 - Fracture Prevention of Containment Pressure Boundary

(DELETED)

3.1.5.3 Criterion 52 - Capability for Containment Leakage Rate Testing

(DELETED)

3.1.5.4 Criterion 53 - Provisions for Containment Testing and Inspection

(DELETED)

3.1.5.5 Criterion 54 - Piping Systems Penetrating Containment

(DELETED)

3.1.5.6 Criterion 55 - Reactor Coolant Pressure Boundary Penetrating Containment (Primary Coolant System Boundary)

(DELETED)

3.1.5.7 Criterion 56 - Primary Containment Isolation

(DELETED)

3.1.5.8 Criterion 57 - Closed System Isolation Valves

(DELETED)

3.1.6 FUEL AND RADIOACTIVITY CONTROL

3.1.6.1 Criterion 60 - Control of Releases of Radioactive Materials to the Environment

3.1.6.1.1 Criterion

The nuclear power unit design shall include methods to control the release of radioactive materials in gaseous and liquid effluents and to handle radioactive solid wastes produced during normal reactor operation, including anticipated operational occurrences. Sufficient holdup capacity shall be provided for retention of gaseous and liquid effluents containing radioactive materials, particularly where unfavorable site environmental conditions can be expected to impose unusual operational limitations upon the release of such effluents to the environment.

3.1.6.1.2 Response

The facility controls the release of radioactive materials in gaseous and liquid effluents and handles radioactive solid wastes produced. The radioactive waste management systems minimize the potential for an inadvertent release of radioactivity from the facility and ensure that

the discharge of radioactive wastes is maintained in accordance with the limits of 10CFR20 and 10CFR50, Appendix I. The radioactive waste processing system, the design criteria, and the amounts of estimated releases of radioactive effluents to the environment are described in Chapter 11.

3.1.6.2 Criterion 61 - Fuel Storage and Handling and Radioactivity Control

3.1.6.2.1 Criterion

The fuel storage and handling, radioactive waste, and other systems which may contain radioactivity shall be designed to ensure adequate safety under normal and postulated accident conditions. These systems shall be designed:

A. With a capability to permit appropriate periodic inspection and testing of components important to safety

B. With suitable shielding for radiation protection

C. With appropriate containment, confinement, and filtering systems

D. With a residual heat removal capability having a reliability and testability that reflects the importance to safety of decay heat and other residual heat removal

E. To prevent significant reduction in fuel storage coolant inventory under accident conditions

3.1.6.2.2 Response

The spent fuel pool and associated cooling system, fuel handling system, and radioactive waste processing system ensure adequate safety under normal and postulated accident conditions.

The ISFPCS provides cooling to remove residual heat from the fuel stored in the spent fuel pool. The system is designed with redundancy and testability to ensure continued heat removal. The ISFPCS is described in Chapter 9.

The spent fuel pool meets Seismic Category I requirements so that no postulated accident could cause excessive loss of coolant inventory.

Structures, components, and systems are designed and located so that appropriate periodic inspection and testing may be performed.

Adequate shielding is provided as described in Chapter 12. Radiation monitoring is provided as discussed in Chapters 11 and 12.

Individual components that contain radioactivity are located in confined areas and are ventilated through appropriate filtering systems.

3.1.6.3 Criterion 62 - Prevention of Criticality in Fuel Storage and Handling

3.1.6.3.1 Criterion

Criticality in the fuel storage and handling system shall be prevented by physical systems or processes, preferably by use of geometrically safe configurations.

3.1.6.3.2 Response

The restraints and interlocks provided for safe handling and storage of spent fuel are discussed and illustrated in Chapter 9.

Criticality in the spent fuel storage area is prevented by physical separation and administrative controls based on initial fresh enrichment, discharge burnup (with conservative uncertainty), and cooling time. Inserted CEAs and borated stainless steel guide tube inserts are also credited.

For all postulated accidents involving misplacement or damage to fuel assemblies, dissolved boron ensures a $K_{eff} \leq 0.95$. Layout of the fuel handling area is such that the spent fuel cask is never required to traverse the spent fuel storage pool during removal of the spent fuel assemblies.

3.1.6.4 Criterion 63 - Monitoring Fuel and Waste Storage

3.1.6.4.1 Criterion

Appropriate systems shall be provided in fuel storage and radioactive waste systems and associated handling areas: (1) to detect conditions that may result in loss of residual heat removal capability and excessive radiation levels and (2) to initiate appropriate safety actions.

3.1.6.4.2 Response

Instrumentation in the fuel pool cooling and purification system detects and alarms in the Control Room/Command Center if excessive temperatures or low water levels occur.

The atmosphere above the spent fuel storage pool and the radwaste disposal areas is drawn into ventilation systems and is discharged through the plant vent. Radiation monitors continually measure the gaseous activity in these vents and provide a control room alarm. Further details are provided in Chapter 11.

Area radiation monitors provide general surveillance of the gross gamma activity level in the area of the spent fuel pool, radwaste treatment area, and numerous other locations throughout the plant. Control Room/Command Center and local alarms and Control Room/Command Center recording are provided.

3.1.6.5 Criterion 64 - Monitoring Radioactivity Releases

3.1.6.5.1 Criterion

Methods shall be provided for monitoring the reactor containment atmosphere, spaces containing components for recirculation of LOCA fluids, effluent discharge paths, and the plant environs for radioactivity that may be released from normal operations, anticipated operational occurrences, and postulated accidents.

3.1.6.5.2 Response

Radioactivity levels contained in the facility effluent and discharge paths in the plant environs are continually monitored during normal and accident conditions by the station radiation monitoring system. In addition to the installed detectors, periodic plant environmental surveillance is established. Measurement capability and reporting of effluents are consistent with the recommendations of Regulatory Guides 4.1 and 1.21, with the exception described in Controlled Document 90215.

Chapter 11 discusses the process and effluent radiological monitoring.

3.2 CLASSIFICATION OF STRUCTURES, COMPONENTS, AND SYSTEMS

3.2.1 SEISMIC CLASSIFICATION

General Design Criterion 2 of Appendix A to 10CFR50, General Design Criteria for Nuclear Power Plants, and Appendix A to 10CFR100, Seismic and Geologic Siting Criteria for Nuclear Power Plants, require that nuclear power plant structures, components, and systems important to safety be designed to withstand the effects of earthquakes without loss of capability to perform their safety functions.

Controlled Document 90034, "Q-List" provides a listing of structures, components, and systems and identifies those that are Seismic Category I.

The seismic classifications are consistent with the recommendations of NRC Regulatory Guide 1.29 with exceptions described in Controlled Document 90215.

3.2.2 SYSTEM QUALITY GROUP CLASSIFICATIONS

Controlled Document 90034, "Q-List" identifies systems, and portions of systems, important to safety and lists industry codes and standards applicable to pressure-retaining components and associated safety systems. The design, fabrication, inspection, and testing requirements for each classification provide the required degree of conservatism commensurate with the importance of the safety function to be performed.

Equipment quality group classifications are indicated in Controlled Document 90034, "Q-List". The principal design and construction code or standard is also listed for each major structure, component, and system.

3.2.3 QUALITY ASSURANCE PROGRAM CLASSIFICATIONS

To fulfill the requirements of SONGS Decommissioning Quality Assurance Program Manual (DQAP), those items that fall under the DQAP are identified in Controlled Document 90034, "Q-List".

Controlled Document 90034, "Q-List" provides the quality classification of major plant structures, components, and systems. Four quality classes were established to identify the required quality control and quality assurance procedures for structures, components, and systems relative to their importance to the safety of the nuclear power system. As defined in Controlled Document 90034, "Q-List", those items designated as Quality Classes I, II, III and IV make up the Project Q-List used in development, review, approval, and control of the design of major plant structures, components, and systems. For Quality Class I and II items, the applicable requirements of 10CFR50, Appendix B, Quality Assurance Criteria for Nuclear Power Plants and Fuel Reprocessing Plants, have been met to ensure the highest quality standards.

3.3 WIND AND TORNADO LOADINGS

3.3.1 WIND LOADINGS

Wind loadings for Seismic Category I structures were selected on the basis of ASCE Paper No. 3269, Wind Forces on Structures.[1]

3.3.1.1 Design Wind Velocity

The fastest wind in the vicinity of the San Onofre site based on a recurrent interval of at least 100 years is approximately 90 mi/h as per Figure 1 (b) of Reference 1. All structures are designed, however, to withstand a basic wind speed of 100 mi/h. The vertical wind speed profile is selected from Table 1 (b) of Reference 1. A gust factor of 1.1 is selected for design on the basis of Reference 1.

3.3.1.2 Determination of Applied Forces

The design wind dynamic pressures are calculated by the following formula :[1]

$$q = 0.002558 \ V^2$$

where:

q = dynamic pressure in lb/ft^2

V = velocity in mi/h

To arrive at the local pressure at any point on a surface of a building and the total force on a building, the pressure coefficients (Cp) and the shape or drag coefficients (C_d), respectively, are selected from both the outlined procedures and Table 4 of Reference 1.

3.3.2 TORNADO LOADINGS

All aboveground Seismic Category I structures are designed to withstand tornado pressure loadings and tornado-generated missiles.

3.3.2.1 Applicable Design Parameters

The following three design parameters are applied concurrently, in combinations producing the most critical conditions.

3.3.2.1.1 Dynamic Wind Pressure

The dynamic wind pressure is caused by a tornado funnel having a peripheral tangential speed of 220 mi/h and a translational speed of 40 mi/h. The applicable portions of wind design methods

described in Reference 1 are used, particularly for shape factors. The provisions for gust factors and variation of wind speed with height are not applied.

3.3.2.1.2 Pressure Differential

The atmospheric pressure change is taken as 1.5 lb/in.^{2} in 4.5 seconds, followed by a 3-second calm and then a repressurization at the same rate as the depressurization. The cycle accounts for reduced pressure in the eye of a passing tornado. All Seismic Category I structures are designed to withstand the full 1.5 lb/in^2 pressure differential without considering pressure reduction due to venting.

3.3.2.1.3 Impingement of Generated Missiles

Three types of tornado missiles are postulated and are considered to act independently, with only one type occurring at any one time. The missile types are identified and described in Table 3.5-6.

3.3.2.2 Determination of Forces on Structures

The dynamic wind pressure is applied to the structures in the same manner as the wind loads described in Paragraph 3.3.1.2, with the exception that the gust factor and the variation of wind speed with height do not apply. The procedures used for transforming the impactive dynamic missile loadings into effective loads are discussed in Subsection 3.5.3.

The load combinations involving individual tornado loadings are given in Paragraphs 3.8.1.3, 3.8.4.3, and 3.8.5.3.

The loading combination for the tornado-generated load, W_t, considers the velocity pressure effects, atmospheric pressure change effects, and missile impact effects. The following combinations which produce the most adverse loadings shall be used.

$$W_t = W_{tq}$$

$$W_t = W_{tp}$$

$$W_t = W_{tm}$$

$$W_t = W_{tq} + 0.5\ W_{tp}$$

$$W_t = W_{tq} + W_{tm}$$

$$W_t = W_{tq} + 0.5\ W_{tp} + W_{tm}$$

where:

W_{tq} = velocity pressure effects

W_{tp} = atmospheric pressure change effects

W_{tm} = missile impact effects

The design criteria for tornado loading conditions are presented in Bechtel Topical Report BC-TOP-3, Design Criteria for Nuclear Power Plants Against Tornadoes, (previously submitted to the Commission).[2] The tornado loadings on structures are based on that topical report with the exception that the design parameters in Paragraphs 3.3.2.1.1 and 3.3.2.1.2 and in Table 3.5-6 will be used, and when the tornado loading includes missile impact effects the structure locally may go in the plastic range from the impact. The procedure used is presented in BC-TOP-9A.

3.3.2.3 Effect of Failure of Structures or Components Not Designed for Tornado Loads

The design of all permanent non-Seismic Category I structures, systems, and components not designed for tornado loadings is analytically checked to ensure that: (1) these structures, systems, and components cannot produce missiles, during a tornado, that have more severe effects than the tornado-generated missiles listed in Table 3.5-6 and (2) their failure will not affect the integrity of adjacent Seismic Category I structures. This design ensures that Seismic Category I structures, systems, and components required for safe storage of spent fuel after a tornado will perform their intended functions.

An analysis of the Seismic Category II turbine building shows that it will not collapse on adjacent Seismic Category I structures when subjected to the tornado loads described in Paragraph 3.3.2.1.1.

3.3.3 REFERENCES

(1) "Wind Forces on Structures," Paper No. 3269, American Society of Civil Engineers (ASCE), New York, N.Y., 1961.

(2) "Design Criteria for Nuclear Power Plants Against Tornadoes," BC-TOP-3, Bechtel Power Corporation, San Francisco, California.

3.4 WATER LEVEL (FLOOD) DESIGN

3.4.1 FLOOD PROTECTION

The remaining systems and components for which flood protection is provided are the same as those identified in Paragraph C.1 of Regulatory Guide 1.29 with exceptions described in Controlled Document 90215.

3.4.1.1 Flood Protection for External Flooding

Flood protection of systems and components required to mitigate the consequences of postulated accidents is provided for all postulated flood levels and conditions described in Chapter 2.

The maximum design basis flood level used in the initial design of plant structures was elevation +30.5 feet mean lower low water (mllw). Subsequent hydrological analyses determined that the maximum postulated flood level in the Units 2 and 3 power block is below elevation +31.0 feet mllw as shown on Figure 2.4-13. This flood level is based on the 12.25-inch, 6-hour thunderstorm probable maximum precipitation (PMP). No loss of integrity to the spent fuel pool or impact to equipment required to mitigate the consequences of postulated accidents will result from these flood levels (see Chapter 2).

3.4.1.1.1 Description of Structures

Structures that house the equipment required to mitigate the consequences of postulated accidents and that offer flood protection to this equipment are identified in Table 3.4-1.

The flood level is not the governing criterion for the design of perimeter walls. The structures identified in Section 3.4, the walls of which are to be used for flood protection, are Seismic Category I structures. A description of these structures and their design criteria are provided in Section 3.8.

The groundwater design level is elevation +5 feet mllw. The foundation basemats and exterior walls of the structures that offer flood protection are designed to resist the upward and lateral pressures caused by the hydrostatic groundwater level up to elevation +5 feet mllw.

3.4.1.1.2 Provisions for Flood Protection

The flood protection of all exterior openings and penetrations that are below the probable maximum flood (PMF) level for Seismic Category I Structures that house equipment required to mitigate the consequences of postulated accidents are tabulated in Table 3.4-1. The drawings noted in this table are provided in accordance with Section A.1.8 for Seismic Category I structures. All openings and penetrations below the PMF level are either sealed, protected by watertight doors/hatches, protected by waterstops, or analysis has shown that the PMF cannot impact equipment required to mitigate the consequences of postulated accidents.

Fluid piping penetrations that are below the PMF level and are not protected by waterstops are sealed with a boot seal between the wall sleeve and the pipe. This boot seal system has been tested for watertight seal at a pressure equivalent to a static head of 34.6 feet of water. This test pressure exceeds the static head of water equivalent to the maximum elevation differential between the PMF level and the lowest sealed piping penetration noted in Table 3.4-1.

Electrical duct banks and conduits that are below the PMF level and are not protected by waterstops are sealed using the methods detailed in Controlled Drawing 35153. These sealing methods have a history of successful usage in numerous nuclear power plants.

One complete watertight door assembly of each lot was proof tested for watertight seal at 150% of the design pressures. The proof pressures were: (1) a static head of 31.5 feet of water exerted from either side of the door, and (2) a static head of 64.2 feet of water exerted from the hinge side of the door. All doors were chalk tested after installation. Additional specific provisions for flood protection included administrative procedures and signage to ensure that all remaining required watertight doors, hatch covers and other flooding barriers are controlled. These barriers may be opened subject to limitations defined by the barrier control program.

Tunnels and openings between Seismic Category I buildings that house equipment required to mitigate the consequences of postulated accidents are sealed by waterstops. A typical waterstop installation is shown in Figure 3.4-1. Two specimens of this waterstop system have been subjected to a pressure equivalent to a static head of 139 feet of water for 2 hours after being subjected to a simulated DBE. There was no evidence of water leakage through waterstop specimen 1 and a minor leakage of 0.0024 ft^3/min through waterstop specimen 2. This leakage is insignificant and could not impact equipment required to mitigate the consequences of postulated accidents.

The waterstop hydrostatic test was very conservative since the test pressure was approximately 300% of the static head of water equivalent to the maximum elevation differential between the PMF level and the bottom of the lowest tunnel protected by a waterstop as noted in Table 3.4-1. Additionally, the waterstops are only required to withstand the hydrostatic groundwater level up to elevation +5 feet mllw, not the PMF level. As an additional precaution, metallic bellows seals are installed below elevation +5 feet mllw in addition to the water stops.

Nonwatertight exterior doors and openings between the turbine building and Seismic Category I structures protecting equipment required to mitigate the consequences of postulated accidents are above elevation +9 feet mllw as noted in Table 3.4-1. The volume of storm water that would enter elevation +7 feet mllw of both turbine buildings during the PMF event is calculated to be 230,000 ft^3. There is sufficient volume in the turbine building and the circulating water pump area of the intake structure below elevation +9 feet mllw to prevent the water level from this flood from rising above elevation +9 feet mllw.

Other nonwatertight exterior doors and openings into Seismic Category I structures protecting equipment required to mitigate the consequences of postulated accidents with sills below the PMF level are also listed in Table 3.4-1. These openings either do not permit direct access to

equipment, or negligible water will enter these exterior doors for the reasons previously stated in Chapter 2.

3.4.1.2 Flood Protection for Flooding from Component Failures (Outside Containment)

3.4.1.2.1 Flood Protection Criteria

The design of San Onofre Units 2 and 3 ensure that:

A. Failure of any non-Seismic Category I equipment will not cause flooding or a release of chemicals to a degree that would prevent engineered safety systems from performing their safety functions. In this regard, a loss of redundancy is permitted, but not a loss of function.

B. Failure of Seismic Category I equipment (e.g., piping, vessels) will not cause flooding which would result in failure of redundant equipment required to mitigate the consequences of postulated accidents.

3.4.1.2.2 Implementation of Flood Protection Design Criteria

The following design features have been incorporated to meet the criteria of Paragraph 3.4.1.2.1:

A. Redundant components are either located in separate compartments, are protected from flooding by adequate separation, or are protected from flooding by natural drainage.

B. Failure of the Seismic Category I vessel in the Primary Plant Make-up Storage tank room (Unit 2; 127A, Unit 3; 127B) may result in loss of both trains of Spent Fuel Pool make-up. However, multiple alternate sources for Spent Fuel Pool make-up are available for this scenario. Refer to Appendix 9A.

C. Passages or piping and other penetrations through walls of a room containing equipment important to safety are sealed against water leakage resulting from any postulated failure of non-Seismic Category I water systems. The seals are designed for the design basis earthquake (DBE).

D. Walls, doors, panels, or other compartment closures designed to protect equipment important to safety from damage due to flooding from a non-Seismic Category I system rupture are designed for the DBE.

The effects of flooding as a result of other component failures or actuation of the fire protection system outside containment, analyzed by the procedures discussed in Paragraph 3.4.2.2, are presented in Table 3.4-2. Flooding levels are given for each postulated event. The levels calculated are not sufficient to either impair the operability of essential systems and components or damage essential structures.

Table 3.4-1
OPENINGS AND PENETRATIONS LOCATED BELOW
MAXIMUM POSTULATED FLOOD LEVEL OF +31.0 FT MLLW (Sheet 1 of 5)

Building	Opening or Penetration	Bottom of Opening Elevation		Type of Protection[(a)]	Location	Drawing Number (Reference Section A.1.8)	Comments
		(ft)	(in.)				
Auxiliary Building Radwaste Storage Tank Area Unit 2	Pipe opening	17	3	A	North wall	25173 F2 25174 F1 25174 G1 25408 C3	Pipe opening between auxiliary building and fuel handling building.
	Door	30	9	B	East wall	25173 G7	This door provides access to the tank room. Exterior curb protects opening to +31'-3".
	Piping sleeve	27	0-1/4	A	East wall	25173 F6	
	Piping sleeve	25	0	A	East wall	25173 F7	
	Conduit Ductbank	2	11	C	East wall	25170 G3	Connects manholes AKX202 and IXX201.

(a)
A. Openings and penetrations sealed against flood water by one or more of the following devices: waterstops, boots, conduit pressure rings and sealing grommet, duct terminator (i.e., PVC conduit duct with cemented joints), pipes or sleeve poured in concrete.
B. Openings and penetrations protected from flood water by watertight doors, watertight hatches, curbs or manhole covers.
C. Flood levels will not impact equipment required to mitigate the consequences of postulated accidents (see Chapter 2 and Section 3.4.1.2.)

Table 3.4-1
OPENINGS AND PENETRATIONS LOCATED BELOW MAXIMUM POSTULATED FLOOD LEVEL OF +31.0 FT MLLW (Sheet 2 of 5)

Building	Opening or Penetration	Bottom of Opening Elevation		Type of Protection[a]	Location	Drawing Number (Reference Section A.1.8)	Comments
		(ft)	(in.)				
Auxiliary Building Radwaste Storage Tank Area Unit 3	Pipe opening	17	3	A	South wall	25173 F2 25174 F1 25174 G1 25408 C3	Pipe opening between auxiliary building and fuel handling building.
	Door	30	9	B	East wall	25173 C3	This door provides access to the tank room. Exterior curb protects opening to +31'-3".
	3 Piping sleeves	24	11	A	East wall	25173 C6	
	Piping sleeve	25	0	A	East wall	25173 C3	
	Piping sleeve	24	4-3/4	A	East wall	25173 C5	
	Conduit Ductbank	2	11	C	East wall	25170 G3	Connects manholes AKX202 and IYX301.
	Conduit Ductbank	5	8	C	East wall	25170 D7	Connects manholes AKX214 and IYX213.
Auxiliary Building Penetration Area Unit 2	Pipe tunnel	6	6	A	Basemat and west wall	25200 C7 25206 E4 25206 E6	Shutdown piping tunnel to SEB.
	2 Doors	9	3	B	Corridor (room 112)	10000 25200	Watertight doors C2-102 and C2-103 between penetration area and turbine building.
Auxiliary Building Penetration Area Unit 3	Pipe tunnel	6	6	A	Basemat and west wall	25250 F7 25206 E4 25206 E6	Shutdown piping tunnel to SEB.

Table 3.4-1
OPENINGS AND PENETRATIONS LOCATED BELOW MAXIMUM
POSTULATED FLOOD LEVEL OF +31.0 FT MLLW (Sheet 3 of 5)

Building	Opening or Penetration	Bottom of Opening Elevation		Type of Protection[a]	Location	Drawing Number (Reference Section A.1.8)	Comments
		(ft)	(in.)				
Auxiliary Building Penetration Area Unit 3	1 Door	9	3	B	West wall (corridor, room 112)	10050 25250	Watertight door C3-105 between penetration area and turbine building.

Table 3.4-1
OPENINGS AND PENETRATIONS LOCATED BELOW MAXIMUM
POSTULATED FLOOD LEVEL OF +31.0 FT MLLW (Sheet 4 of 5)

Building	Opening or Penetration	Bottom of Opening Elevation		Type of Protection[a]	Location	Drawing Number (Reference Section A.1.8)	Comments
		(ft)	(in.)				
Fuel Handling Building Unit 2	Electrical trays	17	3	A	North wall	25409 C8 25407 D8	Opening between fuel handling building and underground electrical tunnel.

Table 3.4-1
OPENINGS AND PENETRATIONS LOCATED BELOW MAXIMUM POSTULATED FLOOD LEVEL OF +31.0 FT MLLW (Sheet 5 of 5)

Building	Opening or Penetration	Bottom of Opening Elevation		Type of Protection[a]	Location	Drawing Number (Reference Section A.1.8)	Comments
		(ft)	(in.)				
Fuel Handling Building Unit 2 (cont)	2 Doors	30	0	C	North wall	25418 H3	
	2 Removable block access openings	30	3	A	East wall	25413 D2 25417 D2	Construction opening.
Fuel Handling Building Unit 3	Electrical trays	17	3	A	South wall	25409 C8 25407 D8	Opening between fuel handling building and underground electrical tunnel.
	2 Doors	30	0	C	South wall	25418 H3	
	2 Removable block access openings	30	3	A	East wall	25413 D3 25417 D2	Construction opening.

3.4.2 ANALYSIS PROCEDURES

3.4.2.1 Analysis Procedures for External Flooding

Seismic Category I structures that house the equipment required to mitigate the consequences of postulated accidents are designed to protect the equipment from the PMF and the highest groundwater level. Specific descriptions of each structure, including design loadings, are given in Sections 3.8.

3.4.2.2 Analysis Procedures for Flooding from Component Failures

Postulated failures in liquid-carrying system piping and in actuation of fire protection systems (sprinklers plus hoses) is based on the following criteria.

Table 3.4-2
EFFECTS OF FLOODING FROM COMPONENT FAILURES[a] (Sheet 1 of 5)

Building	Room or Compartment No.	Reference Drawing No.	Postulated Line or Tank Break[b]	Type of Break[c]	Maximum Flood Level (Ft)[d]	Comments
Auxiliary Building Radwaste Area @ El 9ft-0in	127A	10105	T-056 Spent Fuel Pool Makeup Tank	TWF	20.9	See note f.

[a] See last sheet for notes

Table 3.4-2
EFFECTS OF FLOODING FROM COMPONENT FAILURES[a] (Sheet 2 of 5)

Building	Room or Compartment No.	Reference Drawing No.	Postulated Line or Tank Break[b]	Type of Break[c]	Maximum Flood Level (Ft)[d]	Comment
Auxiliary Building Penetration Area	113	10000 10000 10000	1203-266-18-D-LL1 1203-215-10-D-LL1 1203-292-18-D-LL1	CC	0	Flood drains down to penetration rooms 110 and 111.

Table 3.4-2
EFFECTS OF FLOODING FROM COMPONENT FAILURES[a] (Sheet 3 of 5)

Building	Room or Compartment No.	Reference Drawing No.	Postulated Line or Tank Break[b]	Type of Break[c]	Maximum Flood Level (Ft)[d]	Comment
Auxiliary Building-Radwaste Area @ El 9ft-0in.	127B	10105	T-055 Spent Fuel Pool Makeup Tank	TWF	17.5	Flood rises 17.5' to fire protection piping penetrations and then spills into adjacent corridor. (See Note f)

Table 3.4-2
EFFECTS OF FLOODING FROM COMPONENT FAILURES[a] (Sheet 4 of 5)

Building	Room or Compartment No.	Reference Drawing No.	Postulated Line or Tank Break[b]	Type of Break[c]	Maximum Flood Level (Ft)	Comment
Fuel Handling Building	406	10201	1219-025-12-D-LL0	CC	0	Flood drains to spent fuel pool.
	407	10201	See comment	--	0	Piping in room is less than 1-inch diameter. No flooding considered.
	302 309	10201 10201	See comment	--	0	Flooding from actuation of fire protection system will drain down stairway to rooms 101 and 103.
	202	10200	1203-095-3-D-LL1	CC	0	Flood drains down to rooms 101 and 103.
	209	10200	1203-102-16-D-LL1	CC	0	Flooding is less than from fire protection system from rooms 302 and 309.
	Rail car unloading area	10200	See comment	--	0	Flooding from actuation of fire protection system will drain to outside sewer.

Table 3.4-2
EFFECTS OF FLOODING FROM COMPONENT FAILURES[a] (Sheet 5 of 5)

Building	Room or Compartment No.	Reference Drawing No.	Postulated Line or Tank Break[b]	Type of Break[c]	Maximum Flood Level (Ft)	Comment
Fuel Handling Building (cont)	107	10200	1219-010-14-D-LL0	--	0	Flood drains down to rooms 101 and 103. Flooding is less than from fire protection system from rooms 302 and 309.
	101	10200				Non internal piping. Flooding from rooms 302 and 309 will drain into penetration building and then down into shutdown cooling piping tunnel at El (-) 18ft-6in.
	103	10200	See comment	--	0	
	104	10200	See comment	--	0	Flooding from actuation of fire protection system will drain down to east electrical tunnel at El 9ft-6in. Flooding is less than from fire protection system in east electrical tunnel.

NOTES:

(b) Postulated failure selected is most critical to flooding. The process identification numbers included in line numbers (including some systems no longer in service) are as follows:

1203	Component Cooling Water	2301	Fire Protection
1219	Fuel Storage Pool and Refueling		

(c) Type of breaks considered:

CC - Critical crack -- fluid flow from a crack shall be based on an opening of area equal to that of a rectangle one-half pipe-diameter in length and one-half pipe wall thickness in width.

DE - Double ended break - A circumferential break that results in pipe severance and separation amounting to at least a one-diameter lateral displacement of the ruptured piping sections unless physically limited by piping restraints, structural members or piping stiffness as may be demonstrated by elastic limit analysis (e.g., a plastic hinge in the piping is not developed under load).

TWF - Tank wall failure

(d) Maximum steady state flood level is provided unless maximum transient flood level is significant (>2 in.).

(e) (DELETED)

(f) The tank and piping in this room are upgraded to Seismic Category I, so that only random equipment failure during normal plant operation needs to be postulated. Pipe stress analysis performed on the lines in the Spent Fuel Pool Make-up Storage Tank room demonstrates that moderate energy pipe cracks are not credible and do not need to be postulated. Failure of the Spent Fuel Pool Make-Up tank wall may result in damage to the equipment required to mitigate the consequences of postulated accidents located in the room. The equipment located in this room (Spent Fuel Pool makeup pumps and valves) is not required to remain operable in this scenario because multiple alternate sources for Spent Fuel Pool make-up are available for this scenario. Refer to Appendix 9A.

3.4.2.2.1 Determination of Postulated Component Failures

Each postulated failure is considered separately as a single postulated event occurring during normal plant operation. Each area of the plant identified in Table 3.4-2 is reviewed to determine the failure which results in the most adverse flooding conditions. In the evaluation of the most adverse failure of a fluid system piping run, the following criteria was used:

A. High-energy fluid system piping.
(DELETED)

B. Critical cracks are postulated in fluid system piping which is not considered high-energy. Fluid flow from a crack is based on an area equal to that of a rectangle one-half pipe diameter in length and one-half pipe wall thickness in width.

3.4.2.2.2 Analysis of the Effects of Postulated Component Failures

For postulated line failures, the operating temperature and pressure are assumed as initial thermodynamic conditions in calculating outflow. When a postulated pump discharge line breaks, it is assumed that the runout capacity of the pump is the flooding rate unless otherwise noted.

The flow from the postulated failure is assumed to result in a flood in the compartment in which the component is located, except that consideration is given to unprotected communicating compartments. No credit is taken in the analysis for compartment drain lines or operation of sump pumps.

For flooding due to the actuation of fire protection systems, the analysis assumes the maximum design flow rate from both the sprinklers and hose stations in the area.

The volume occupied by equipment in a room is considered negligible except where it is apparent that large equipment occupies a significant proportion of the available room volume. Examples of this are rooms specifically designed to accommodate large storage tanks.

3.5 MISSILE PROTECTION

Missile protection criteria conform to 10CFR50, General Design Criterion 4, Environmental and Missile Design Bases. Protection against the postulated missiles identified in Subsection 3.5.1 is provided to fulfill the following design criteria:

A. Reactor Coolant Pressure Boundary Missiles
(DELETED)

B. Main Steam and Feedwater Missiles
(DELETED)

C. Internal Missiles Other Than Reactor Coolant, Main Steam, or Feedwater

A missile generated from a plant system, other than the reactor coolant system, the main steam system, or the main feedwater pump discharge lines shall not perforate the Control Room/Command Center or cause loss of integrity to the spent fuel pool.

D. Tornado Missiles

Missiles generated by a tornado, which have velocities equal to or less than the design velocities, shall not cause failure of the Control Room/Command Center walls or cause loss of integrity to the spent fuel pool and fuel handling and storage facilities. Exceptions to these missile protection criteria are permitted where it has been demonstrated that the total annual probability (per unit) of damage to exposed critical components due to a tornado missile strike is less than 1.0×10^{-7}, as discussed in Section 3.5.3.

3.5.1 MISSILE SELECTION AND DESCRIPTIONS

3.5.1.1 Internally Generated Missiles (Outside Containment)

There are two general sources of postulated missiles outside containment:

A. Rotating component failures

B. Pressurized component failure

A tabulation of all structures, systems, and components outside the containment required to mitigate the consequences of postulated accidents, their location, seismic category, quality group classification, and the applicable FSAR sections, which include system piping and instrumentation drawings describing safety design features, is given in Controlled Document 90034, “Q-List”. Refer to Controlled Drawings 40000 to 40010 for general arrangement.

3.5.1.1.1 Rotating Component Failure Missiles

A tabulation of missiles generated by postulated failures of rotating components, their source and characteristics, and provided missile protection is given in Table 3.5-1.

Missile selection is based on the following conditions:

A. All rotating components, which are operated during normal operating plant conditions, are capable of becoming missiles.

Table 3.5-1
INTERNALLY GENERATED MISSILES OUTSIDE CONTAINMENT[a] (Sheet 1 of 5)

Missile Identification	Source of Missile	Missile Characteristics			Thickness of Concrete to Prevent Spalling[j] (in.)	Thickness of Steel to Prevent Penetration[j] (in.)	Remarks
		Velocity (ft/s)	Diameter (in.)	Weight (lb)			
Penetration Building: A316, Fan blade A317, Fan blade	 Normal exhaust fan Standby exhaust fan	277	2.26[b]	3.4	-	-	[e]
A359, Fan blade A360, Fan blade	Normal ventilation unit Standby ventilation unit	140.9	0.956[b]	2.052	1.62	0.105	This unit is located above a concrete roof at El. 95' which is at least 12" thick.[d]
A037, Fan blade	Exhaust fan	184	2.03[b]	1.83	-	-	[e]
E361, Fan blade	Normal A/C unit	119	0.90[b]	2.6	-	-	In order to impact essential systems, the fan blade must penetrate the 0.0598" housing, the cooling coils, and the inlet filters.[d]
E360, Fan blade	Normal A/C unit	132	0.69[b]	1.15	1.82	-	This unit is separated from essential systems by concrete walls and floors which are at least 12" thick.[d]

[a] See last sheet of table for notes.

Table 3.5-1
INTERNALLY GENERATED MISSILES OUTSIDE CONTAINMENT[a] (Sheet 2 of 5)

Missile Identification	Source of Missile	Missile Characteristics			Thickness of Concrete to Prevent Spalling[j] (in.)	Thickness of Steel to Prevent Penetration[j] (in.)	Remarks
		Velocity (ft/s)	Diameter (in.)	Weight (lb)			
Auxiliary Building - Radwaste Area:							
P180 Pump impeller	Chemical waste tank	133	8.96[b]	137.4	-	0.186[k]	The steel casing of this pump is 0.5" thick.[h]

Table 3.5-1
INTERNALLY GENERATED MISSILES OUTSIDE CONTAINMENT[a] (Sheet 3 of 5)

Missile Identification	Source of Missile	Missile Characteristics			Thickness of Concrete to Prevent Spalling[j] (in.)	Thickness of Steel to Prevent Penetration[j] (in.)	Remarks
		Velocity (ft/s)	Diameter (in.)	Weight (lb)			
Auxiliary Building - Radwaste Area: (cont)							
P188, Pump impeller	Miscellaneous waste evaporator condenser monitor	-	-	-	-	-	This pump impeller has less energy than P200. Casing thickness is 0.438".[h]
P1018, P1019, Pump impeller	Spent Fuel Pool makeup pumps	-	-	-	-	-	[c]

Table 3.5-1
INTERNALLY GENERATED MISSILES OUTSIDE CONTAINMENT[a] (Sheet 4 of 5)

Missile Identification	Source of Missile	Missile Characteristics			Thickness of Concrete to Prevent Spalling[j] (in.)	Thickness of Steel to Prevent Penetration[j] (in.)	Remarks
		Velocity (ft/s)	Diameter (in.)	Weight (lb)			
Safety Equipment Building:							
E412 Fan blade	Normal A/C unit	-	-	-	-	-	This fan has less energy than E414.

Table 3.5-1
INTERNALLY GENERATED MISSILES OUTSIDE CONTAINMENT[a] (Sheet 5 of 5)

Missile Identification	Source of Missile	Missile Characteristics			Thickness of Concrete to Prevent Spalling[j] (in.)	Thickness of Steel to Prevent Penetration[j] (in.)	Remarks
		Velocity (ft/s)	Diameter (in.)	Weight (lb)			
Auxiliary Building - Control Area:							
E295, Fan blade	Normal A/C unit	129	1.08[b]	4.86	-	-	Failure of this fan cannot impact the control room.[d]
E411, Fan blade	Normal A/C unit	83.5	0.523[b]	0.062	-	0.013[k]	Steel fan housing is 0.0359 inches thick.[e]
A206, E419, E423, E426 Fan blade	Emergency A/C unit	-	-	-	-	-	[c]
Breathing Air Bottle Valve	Self contained breathing apparatus	207	2	1-2	-	0.065	0.31 in. barrier provided by storage rack.

(b) Equivalent missile diameter for noncircular frontal area: $D_{equivalent} = \sqrt{1.274 \times A_{frontal}}$

(c) These potential missiles are installed in equipment which operates infrequently during normal plant operating conditions. Therefore, they are not considered credible potential missiles.

(d) These potential missiles are either remote from or separated by adequate barriers from all essential systems. Therefore, essential systems are protected from these potential missiles.

(e) The blades of these fans do not have enough energy to penetrate the fan housing. Therefore, essential systems are protected from these potential missiles.

(f) (DELETED)

(g) (DELETED)

(h) The potential missiles from these pumps do not have enough energy to penetrate the pump casing. Therefore, essential systems are protected from these potential missiles.

(i) (DELETED)

(j) Minimum thickness of missile barrier to stop missile. For enclosed components (fans, pumps and turbines), this thickness is based on residual missile velocity after penetrating casing unless noted otherwise.

(k) Minimum barrier thickness based on full missile velocity before impacting casing.

B. The energy in a rotating part associated with 120% overspeed is assumed sufficient for component failure.

C. The energy of the missile is sufficient to perforate the protective housing.

3.5.1.2 Internally Generated Missiles (Inside Containment)
(DELETED)

3.5.1.4 Missiles Generated By Natural Phenomena (Tornado)

Tornado-generated missiles are considered in the design of Seismic Category I structures which are required for protection of systems and components required to mitigate the consequences of postulated accidents. The missiles considered in design and their characteristics are listed in Table 3.5-6.

Missiles generated by any other natural phenomena are not considered credible.

3.5.1.5 Missiles Generated By Events Near the Site

As discussed in Section 2.2, there is no credible basis for anticipating site proximity missiles.

Table 3.5-6
TORNADO-GENERATED MISSILES CONSIDERED
IN DESIGN OF STRUCTURES THAT
PROVIDE MISSILE PROTECTION

Description	Weight (lbs)	Impact Area (ft^2)	Maximum Velocity (ft/s)	Kinetic Energy (ft-lbs)
A 12-foot wood plank, 4 x 12 inches in cross-section, weighing 108 pounds, traveling end on at a speed of 220 mi/h, striking the structure at any elevation	108	0.33	322	1.74×10^5
A steel pipe, Schedule 40, 3 inches in diameter by 10 feet long, weighing 75.8 pounds, traveling end on at 100 mi/h, striking the structure at any elevation	75.8	0.067	147	2.54×10^4
An automobile of 4,000 pounds weight, striking the structure at 50 mi/h on a contact area of 20 ft^2, any portion of the impact being not more than 25 feet above grade.	4000	20.0	73.5	3.36×10^5
A utility pole, 13-1/2 inches in diameter, Missile F of SRP 3.5.1.4, any portion of the impact being not more than 25 feet above grade.	1490	0.994	$V_H = 152$ $V_V = 122$	5.35×10^5 3.44×10^5
A steel rod, 1-inch in diameter x 3 feet long, Missile C of SRP 3.5.1.4	8	0.0054	$V_H = 229$ $V_V = 183$	6.51×10^3 4.16×10^3

3.5.1.6 Aircraft Hazards

The information contained in this section was prepared in accordance with the original plant licensing requirements and is representative of the site conditions at the time the plant was licensed.

3.5.1.6.1 Airport Operations

The San Onofre Heliport is located 633 yards northwest of Unit 2 as shown in Figure 3.5-8. It is expected to have an average of eight operations per month, with the takeoffs and landings along the paths indicated in Figure 3.5-8. The National Transportation Safety Board reports seven fatal helicopter crashes on takeoff and landing during 1973.[3] The Federal Aviation Administration tabulated 1.16 million helicopter hours for 1973[4] which implies 4.6 million takeoff or landing operations based on two operations per typical half-hour flight. This implies a fatal crash rate of 1.5×10^{-6} per operation (landing or takeoff). The following conservative analysis leads to an estimate of less than 1.2×10^{-10} per year for the expected frequency of fatal helicopter crashes into Unit 2 or 3.

A. The approach and departure paths are kept away from the plants. Since helicopters operate only under visual flight rule conditions, they would be expected to adhere to the nominal path. The closest they would get to the plant would be in the immediate vicinity of the heliport itself. Possible deviation from the centerline of the landing or takeoff path is conservatively represented by a negative exponential distribution with a decay angle of 30˚ or $P(y) = 1/2e^{-y \tan 30}$ where y is distance from the landing pad. This decay is consistent with the 30˚ vertical approach angle typical of helicopter operations. The negative exponential distribution is more slowly decaying than the more frequently used Gaussian, so it provides a conservative model.

B. The greatest deviation near the plant can occur when the helicopter is 245 feet from the pad, just opposite the northeastern or southwestern boundaries (plus 15 feet for the radius of the rotor circle) of the plant as shown in Figure 3.5-8. At this point the decay angle of 30˚ implies a decay distance of 143 feet (245 tan 30). For a negative exponential distribution with this decay length, the probability of a deviation greater than 633 yards in one direction (the distance required to reach Unit 2 or 3) on either takeoff or landing is 0.85×10^{-6}. This is also a conservative estimate of the conditional probability of impacting the plant, providing the helicopter crashes on landing or takeoff.

C. The expected frequency of fatal crashes per year is then the product of the number of operations per year, multiplied by the national average rate of fatal crashes per operation, multiplied by the conditional probability of crashing into the plant providing the helicopter crashes:

$$(8 \times 12) \times (1.5 \times 10^{-6}) \times (0.85 \times 10^{-6}) = 1.2 \times 10^{-10}/\text{year}$$

Helicopter operations of the San Onofre heliport are no credible hazard to the plant.

3.5.1.6.2 Air Corridor Operations

There are three categories of aircraft operating in air corridors in the vicinity of the San Onofre site.

A. General aviation

B. Commercial aviation and high speed jet business or general aviation and

C. Military aviation (mainly helicopters and high speed jets)

Typical and limiting general aviation aircraft observed in the vicinity of the site are listed in Table 3.5-7 along with local damage parameters for determining the adequacy of plant structures. These parameters are based on engine weight and frontal area[(5)(6)] and maximum plane rated speed.[(5)] Based on these parameters and the barrier design procedures described in Reference 7, it has been determined that general aviation aircraft will not cause unacceptable local damage to plant safety-related structures, and furthermore, the probability of impact which would cause unacceptable consequences to plant safety-related structures is less than 10^{-6} per year.

For the other two categories of aircraft the probability of impacting the plant has been estimated using methodology consistent with Standard Review Plan (SRP) 3.5.1.6 and as described in published literature.[(6)] For a specific type of aircraft flying along a defined corridor near the plant site, the frequency of impact (with safety-related structures) per year is given by:

$$P = CNA\rho$$

where: C is the enroute crash rate for the type of aircraft expressed on a per mile basis, N is the annual number of operations along the corridor past the site, A is the effective plant area (the direct impact area plus skid area), and ρ is the aircraft crash density at the plant site (expressed per mile perpendicular to the nominal corridor centerline).

3.5.1.6.2.1 <u>Effective Area of Plant</u>

A. Direct Impact Area

The effective direct impact area is given by:

$$A = A_\rho + A_s$$

where: A_ρ is the horizontal area of the safety-related plant structures and A_s is the shadow of the plant created by the glide slope angle of an aircraft on a plant

impact course. The smaller the glide slope of the potentially impacting aircraft, the larger this shadow will be. An angle of 10˚ for the glide slope was assumed.[6] For such a shallow glide slope, the shadow areas are found from the formula:

Cylindrical with hemispherical dome:

$$A_s = \left[D\left(h - \frac{D}{2} \right) + \frac{\pi D^2}{8} \right] \cot \alpha - \frac{\pi D^2}{8}$$

where: D is the diameter, h is the altitude to the top of the dome, α is the glide slope angle, and the last term represents the removal of half the cylindrical cross-sectional area which has already been included in $A\rho$.

Rectangular:

$$A_s = bh \cot \alpha$$

where: b is the dimension normal to the assumed flightpath, plus wingspan.

The aircraft nominally flying V23 and V25 will be traveling parallel to the coast, so the impact area is taken normal to this direction with the shadows of the safety-related buildings projected along this direction. The effective areas were calculated for Units 2 and 3 individually. In determining the impact area the size of the aircraft (wingspan) was considered. Building and aircraft dimensions used are given in Tables 3.5-8 and 3.5-9. For military helicopters, no glide slope was assumed. The resulting impact areas are given in Table 3.5-10.

B. Skid Area

The effective plant area should also include the area adjacent to the plant in which an aircraft could fall and still skid into the plant. Soloman, et al.,[8] provides information for determining the maximum potential skid distance.

The San Onofre site is located in an excavation in bluffs along the Pacific Coast. Consideration of local terrain features and nonsafety- related structures results in limiting the skid area to less than that which would be obtained using the formula of Reference 8. The values obtained and used in the probability analysis are given in Table 3.5-10. For helicopters, no skid area was considered.

Table 3.5-7
AIRCRAFT IMPACT CHARACTERISTICS

Aircraft	Engine	Speed (mi/h)	Weight (lb)	Area (ft^2)	Energy Density ($ft\text{-}lb/ft^2$)
Piper Commanche	1	242	440	3.97	2.17×10^5
Beechcraft Bonanza	1	204	480	4.07	1.64×10^5
Piper Navajo	2 Reciprocating	270	1402	9.44	3.62×10^5
Cessna 414	2 Reciprocating	227	974	8.24	2.03×10^5
Mitsubishi MU-2	2 Turbo-prop	350	670	6.26	4.38×10^5
Beechcraft King-Air	2 Turbo-prop	285	622	6.26	2.70×10^5

Table 3.5-8
SIZE OF BUILDINGS FOR EACH UNIT

Building	Length (ft)	Width (ft)	Top Elevation[a]
Fuel handling	122	67	119
Penetration area (abutts containment)	169	106	96
Containment	157	157	191
Safety equipment			
(1)	173	71	82
(2)	51	47	82
Auxiliary	225	140	(only horizontal area appropriate)
Intake	200	110	(only horizontal area appropriate)
Tank and auxiliary feedwater building	100	100	85
Diesel generator building	30	135	49
Recirculation gates	130	55	(only horizontal area appropriate)

[a] Elevation datum is MLLW. Building grade is +30 feet elevation.

Table 3.5-9
CHARACTERISTIC DIMENSIONS FOR AIRCRAFT

Category	Dimension (ft)	Parameter
Air carrier	108	Wing span
Military helicopter	70	Rotor diameter
Military jet	70	Wing span

Table 3.5-10
IMPACT AND SKID AREAS

Category	Impact Area (mi^2)	Skid Area (mi^2)
Air carrier >12,500 lb	0.0153	0.0083
Military helicopter >12,500 lb	0.0062	--
Military jet >12,500 lb	0.0137	0.0072

3.5.1.6.2.2 Crash Rates

The rates of crashes for enroute aircraft which might cause significant damage are taken from historical statistics of crashes which resulted in fatalities. This is a conservative assumption because many fatal crashes involve relatively light impacts, with occupants killed by subsequent fires. It can be argued that there are examples of crash landings without fatality (in open fields or roads) which would certainly have produced fatalities had the plane crashed into a building. On the other hand, there are crash landings (in open fields or roads) which produce fatalities, but in which the pilot had sufficient control while the plane was airborne to avoid any large structures which would prove fatal immediately. Indeed, any landing on a road, and most landings in open fields, are prima-facie evidence that the pilot had sufficient control to select such a relatively safe landing location.

As far as crash rates are concerned, the aircraft are classified in three categories: commercial air carrier, military, and business jet.

A. Commercial Air Carrier

Information from the National Transportation Safety Board shows seven enroute crashes producing fatalities in the years 1970-1975.[9] During these 6 years there were a total of 1.56×10^{10} regularly scheduled plus supplemental air carrier miles flown[10] which implies a fatal crash rate:

$$C = 0.45 \times 10^{-9} \text{ per mile}$$

B. Military

Crash statistics on military aircraft are difficult to obtain and they would not be directly useful since total domestic miles flown do not appear to even be tabulated. Furthermore, the distinction between fatal and nonfatal crashes would not be valid since pilots of high-performance aircraft can safely eject before very serious accidents. It is expected that military experience should fall somewhere between the commercial crash rate and the 200 times higher general aviation total crash rate. Most general aviation crashes are caused by poorly maintained aircraft (particularly running out of fuel), poorly trained pilots (only 50 hours plus a successful check ride required for license), or inadequate navigation instrumentation. Military pilots would have much greater advantages in these areas which suggests a crash rate close to the commercial experience. For purposes of this analysis we have, therefore, estimated the military crash rate to be five times the commercial crash rate:

$$C = 2.25 \times 10^{-9} \text{ per mile}$$

C. Business Jet

In the present analysis this category is distinguished from the rest of general aviation because they fly at much higher speeds and many weigh more than 12,500 pounds. Near the San Onofre site they generally fly the offshore Airway V25, along with the commercial air carrier jets. Since the business jets generally have a high standard of pilot qualification and aircraft maintenance, the crash rate is assumed to correspond to the commercial experience.

3.5.1.6.2.3 Aircraft Crash Density

As indicated in Paragraph 2.2.2.5, aircraft in the vicinity of the San Onofre site were observed by radar from the Coast TRACON Facility at El Toro Naval Air Station. The two categories of air traffic of present concern observed were:

A. Commercial aviation and high-speed jet business or general aviation.

B. Military aviation (mainly helicopters and high-speed jet aircraft).

The resulting distributions of closest approach distances are shown in Figures 2.2-5, 2.2-6, and 2.2-7. The height of the histograms represent the total number of observations at each of the quantized distances from the plant.

It was assumed that the crash density normal to the flight direction is represented by a negative exponential probability density function symmetric about the nominal flight path distance of closest approach:[(7)(11)]

$$f(x) = \frac{\lambda}{2} e^{-\lambda|x|}$$

The aircraft are assumed to be uniformly distributed within each of the 1/2-mile quantization intervals. The probability density function is averaged over the quantization intervals used in obtaining the aircraft flight distributions.

$$\bar{\rho}_n = \frac{\lambda}{2\Delta} \int_{(n-1/2)\Delta}^{(n+1/2)\Delta} e^{-\lambda x} dx = \frac{\text{SINH} \frac{\lambda\Delta}{2}}{\Delta} e^{-n\lambda\Delta}$$

$$\bar{\rho}_o = \frac{2\lambda}{2\Delta} \int_0^{\Delta/2} e^{-\lambda x} dx = \frac{1}{\Delta} (1 - e^{-\lambda\Delta/2})$$

where: n represents the number of quantization intervals deviation from the nominal flight path centerline, and $\Delta = 0.5$ miles, the quantization interval size.

This average density in each interval is then multiplied by the number of aircraft nominally flying in this quantization interval, divided by the total observations and the result is summed to give the aircraft crash density at the plant.

The appropriate values of λ were taken from References 7 and 11. The decay constant for commercial aviation was corrected to consider that the aircraft were flying at a lower altitude near the San Onofre site. The values used for λ were 2.0 mi^{-1} for the general single engine and twin engine categories 1 mi^{-1} for military jet and helicopter and 2.67 mi^{-1} for the air carrier and other high-speed jet categories. The appropriate values for the annual number of flights and crash density are given in Table 3.5-11.

3.5.1.6.2.4 Crash Probabilities

The probability of striking any safety-related portion of the plant is given in Table 3.5-11 for the three aircraft categories. With the exception of military helicopters, which assumed no skid, the probability is the sum of the impact and skid components. All of these probabilities are seen to be less than 10^{-7}. It is concluded that aircraft operations in the vicinity of the San Onofre site result in no credible hazard.

3.5.2 SYSTEMS TO BE PROTECTED

3.5.2.1 General

The sources of missiles which, if generated, could affect the safety of the plant are considered in Subsection 3.5.1. A tabulation of Seismic Category I structures and equipment required to mitigate the consequences of postulated accidents is provided in Controlled Document 90034 "Q-List". Figure 3.5-9 identifies penetrations for the auxiliary building and fuel handling building that require tornado missile protection.

3.5.2.2 Barriers for Internally Generated Missiles (Outside the Containment)

Structures and equipment are protected from internally generated missiles by the separation and independence inherent to redundant systems or by physical barriers as listed in Tables 3.5-1 and 3.5-2.

3.5.2.3 Barriers for Missiles Generated by Natural Phenomena (Tornado)

A tabulation of critical components and the structures, shields, and barriers that are designed to provide protection from tornado-generated missiles is given in Table 3.5-12. The missile barriers indicated are designed utilizing the procedures given in Subsection 3.5.3.

Table 3.5-11
SUMMARY OF AIRCRAFT IMPACT PARAMETERS AND PROBABILITIES

Aircraft	N[(a)] Flights/Year	C Crash Rate/Mile	A_2 mi	ρ Aircraft/Mile	P, Impact + Skid Per Year
Air carrier >12,500 lb	71,656	4.5×10^{-10}	0.0236	0.0186	1.42×10^{-8}
Military helicopter >12,500 lb	7,072	2.25×10^{-9}	0.0062	0.199	1.96×10^{-8}
Military jet >12,500 lb	26,676	2.25×10^{-9}	0.0209	0.037	4.64×10^{-8}

(a) See Subsection 2.2.2.

Table 3.5-12
MISSILE BARRIERS FOR TORNADO MISSILES

Critical Components	Missile Barrier
Control Room/Command Center and critical instrumentation, control, piping, and mechanical equipment in auxiliary building	Auxiliary building
Spent fuel pool and other critical equipment in fuel handling building	Fuel handling building and fuel pool wall

3.5.3 BARRIER DESIGN PROCEDURES

Missile-resistant barriers and structures are designed to withstand and absorb missile impact loads without being perforated in order to prevent damage to critical components. The procedures employed in design of missile-resistant barriers for local effects are described in Section 2 of BC-TOP-9A[12] and EPRI NP-440.[13] The procedures used to predict the overall response of the barrier and portions thereof to missile impact are described in Sections 3 and 4 of BC-TOP-9A.[12]

Due to splintering upon impact, the energy imparted to the targets by the utility pole and the 4" x 12" plank (Table 3.5-6) will be a small fraction (25%) of their initial energy. Table 5-1 of EPRI NP-440[13] provides test data for a 12" diameter steel pipe and a 13.5" diameter utility pole (Test No. 6 & 12 respectively). For almost identical velocities, the load imparted to the test slab by the utility pole is less than 50% of that from the pipe. The utility pole is twice as heavy as the pipe thus indicating a four fold reduction in energy due to splintering. No tests were performed for the 4" x 12" plank, however, it can be concluded that the splintering of the plank will be more severe than that of the utility pole as the velocity of the plank is much higher than utility pole's test velocity (322 fps versus 203 fps). Based on these test results, only 25% of the calculated strain energy should be used for the utility pole and the 4" x 12" plank. However, as an additional design conservatism, 50% of the strain energy for the utility pole is considered in the barrier designs.

The barriers provided for protection against tornado-generated missiles are typically the reinforced concrete walls (1-foot thick minimum) and roof slabs (1-foot thick minimum) of the Seismic Category I structures housing equipment required to mitigate the consequences of postulated accidents. These thicknesses prevent perforation and sustain the impact without concrete spalling on the interior surfaces. In addition, steel grids or framed steel plates (3/4-inch minimum thickness) are provided as covers for required openings. These covers prevent missile perforation and experience structural deflections which are restricted by design so as not to impair the intended safety function of each opening.

Missile-resistant barriers are not required when the total probability (per unit per year) of damage to exposed critical components due to a missile strike is less than 1.0×10^{-7}.

Operator actions are credited to limit the area of exposed critical components. These operator actions, included in an Abnormal Operating Instruction, are able to be completed in an acceptable period of time (approximately 4 hours). One of these actions is to close the set of front entry doors (AC201 & AC201A) to the Control Room/Command Center lobby. These doors are designed as missile barriers and are normally held in an open position. Upon receipt of a severe weather watch or warning, station operators will confirm the weather event, evaluate the hazards implications per pre-approved criteria, and perform the credited actions.

3.5.4 REFERENCES

1. (DELETED)

2. (DELETED)

3. Annual Review of Aircraft Accident Data 1973, National Transportation Safety Board, p 136, NTSB-AGR-75-1, July 1975.

4. Federal Aviation Administration Statistical Handbook of Aviation, Calendar year 1973.

5. Jane's All the Worlds Aircraft, 1975 - 1976.

6. Chelapati, C. V., Kennedy, R. P., and Wall, I. B., "Probabilistic Assessments of Aircraft Hazard for Nuclear Power Plants, "Nuclear Engineering and Design, 19, pp 333-364, 1972.

7. Solomon, K. A., "Hazards Associated With Aircrafts and Missiles," presented at the American and Canadian Nuclear Society Meeting, Toronto, Canada, June 1976.

8. Solomon, K. A., et al., "Airplane Crash Risks to Ground Population," UCLA-ENG-7424, March 1974.

9. Letter from John K. Crawford (Chief Safety Analysis Division, Bureau of Aviation Safety, FAA) to R. Hill (Dames & Moore), June 9, 1976.

10. Federal Aviation Administration Statistical Handbook of Aviation, Calendar year 1974 and earlier; 1975 data from phone conversation with Jack Joe, National Transportation Safety Board, June 10, 1976.

11. Solomon, K. A., "Estimate of the Probability That an Aircraft Will Impact the PVNGS," NUS-1416, June 1975.

12. "Design of Structures for Missile Impact," BC-TOP-9A, Bechtel Power Corporation, San Francisco, California, September 1974.

13. Stephenson, Alan E., "Full-Scale Tornado-Missile Impact Tests," Electrical Power Research Institute, EPRI NP-440, dated July 1977.

3.6 PROTECTION AGAINST DYNAMIC EFFECTS ASSOCIATED WITH THE POSTULATED RUPTURE OF PIPING

The High Energy Piping Systems have been removed from service. They no longer have Design Basis, Licensing Basis, or operational functions. The information contained in this section has been updated to reflect the current status. Although these system have been removed from service, they may still contain fluids, gases, or other hazards such as energized circuits, compressed air, radioactive material, etc. Equipment may not have been physically removed from the plant. See General Arrangement Drawings, P&IDs, and One Line diagrams for the current plant configuration.

This section described the design bases and protective measures that were used to ensure that the containment, essential equipment, and other essential structures were adequately protected from dynamic effects associated with the postulated rupture of high-energy piping, including the reactor, in accordance with General Design Criterion 4, Environmental and Missile Design Bases.

3.7 SEISMIC DESIGN

3.7.1 SEISMIC INPUT

3.7.1.1 Design Response Spectrum

The soil at the site is a thick (900+ feet) deposit of well-graded dense sand, of essentially uniform properties. The design basis earthquake (DBE) is postulated to occur near the site (5 miles), and the accelerations are postulated to be quite high (0.67g). Because of these site-specific characteristics, the site tends to amplify long-period motions, and to attenuate short-period motions. These site-specific characteristics were accounted for in site-specific analyses, as discussed in Appendix 2.5B. In brief, the design spectrum was developed by requiring it to fit over the peaks of the surface response spectra developed from site-specific analyses for input earthquake acceleration time histories scaled to produce a 0.67g ground surface acceleration. Further, the severity of the acceleration time history fitted to the design spectrum (Paragraph 3.7.1.2), was compared to that of many recorded acceleration time histories using several measures of severity and was found to be significantly more severe. The measures of severity included: spectral amplification ratio, spectral intensity, pulse distribution, impulse, kinetic energy, and Housner severity parameters. Details of analyses and results of the severity

comparison study are presented in Appendix 2.5B. The resulting site-specific design spectrum for horizontal motions is shown in Figure 3.7-1.

The spectrum of Figure 3.7-1 is applicable to both horizontal components. The vertical-motion spectrum has the same shape, but is 2/3 times the horizontal, as also shown in Figure 3.7-1. The operating basis earthquake (OBE) response spectra have the same shape but are one-half times those for the DBE, shown in Figure 3.7-1.

The site-specific spectral shapes of Figure 3.7-1 are valid for damping values other than 2%, but the spectral values are altered based on amplification factors suggested by Newmark and Hall[1] normalized to a value of 3.5 at 2% damping as follows:

	Factor by which to multiply 2% spectral value of acceleration control points	
Damping	A (T = 0.2s)	B (T = 1.0s)
0	1.49	1.49
0.5	1.34	1.34
1	1.20	1.20
2	1.00	1.00
5	0.63	0.63
7	0.46	0.46
10	0.40	0.40

3.7.1.2 Design Basis Earthquake Acceleration Time History

The 80-second duration DBE acceleration time history was developed from a simulated strong-motion record, synthesized by Jennings, Housner, and Tsai.[2] This simulated free-field strong-motion record was modified so that its response spectrum approximates the design response spectrum of Figure 3.7-1. Modification of the simulated acceleration time history was accomplished for a response spectrum for 2% damping in 2 steps:

- The acceleration record was scaled linearly to ⅔g maximum- acceleration level, consistent with the zero-period acceleration of the design response spectrum.

- Using the spectrum-suppress and spectrum-raising iterative technique developed by Tsai,[3] the acceleration time history was modified until its spectrum appropriately matched the design spectrum (50 iterations were necessary).

The resulting acceleration time history is given in Figure 3.7-2. The period intervals used for spectrum calculation are:

Period Range (s)	Oscillator Interval (s)
0.01 to 0.20	0.01
0.20 to 1.80	0.02
1.80 to 2.00	0.05

These period intervals were based on the listing of period intervals that was in common usage for spectrum calculation at the time the spectrum matching was completed. Specifically, the listing was published in a sub-routine of a lumped mass program developed at the University of California, Berkeley, for site response analyses.

The resulting spectra for the DBE time history are presented, along with the corresponding design response spectra, in Figures 3.7-3 through 3.7-10.

The DBE acceleration time history of Figure 3.7-2 is applicable to both horizontal components. The DBE acceleration time history for the vertical component has the same shape, but is ⅔ times the horizontal.

3.7.1.3 Critical Damping Values

Damping values for the structures have been taken from reference 3 and the soil dampings, both hysteretic and spatial, have been calculated and measured. All Seismic Category I structures will be founded in the San Mateo Formation sand, so only that material is considered here.

Hysteretic soil damping of the San Mateo Formation sand was measured directly in two ways: laboratory cyclic triaxial tests, and field in-situ wave-propagation tests. The details of the tests are presented in appendix 3.7C. The values used are given in Figure 3.7-11. The appropriate strains to be used for DBE and OBE analyses shown on Figure 3.7-11 were derived from finite-element analyses as described in Appendix 3.7C.

Spatial soil dampings were calculated by elastic theory, using the expressions in Table 3.7-1. The large-scale field tests were performed at the site to check the calculated values of spatial damping. These tests, which did verify the calculated values, are reported in detail in Appendix 3.7C. The calculated values used are given in Table 3.7-2. The values actually used were limited to 10% for the DBE analysis and to 8% for OBE analysis as indicated on Table 3.7-3. Further the viscous damping values used for steel, prestressed concrete, and reinforced concrete are tabulated on Table 3.7-3 and are equal to or less than those recommended in Regulatory Guide 1.61.

3.7.1.4 Supporting Media for Seismic Category I Structures

3.7.1.4.1 Soil Conditions

Soil conditions at the San Onofre site have been described in Paragraphs 2.5.4.1 and 2.5.4.2. Briefly, the native soils at the site consist of approximately 70 feet of terrace deposits (from

elevation 120 to 50), underlain by approximately 900 feet of San Mateo Formation sand which, in turn, is underlain by bedrock of the Capistrano Formation. The soils comprising the terrace deposits are predominantly clayey sands and silty clays. The San Mateo Formation sand is a very dense medium-to-coarse sand which exhibits some apparent cohesion and high shear strength due to efficient grain packing. The San Mateo Formation sand at the site is quite uniform, with no significant continuous layering, although occasional lenses of soils of different grain sizes do occur.

In the plant area, the soil has been excavated to between elevation +29 and -34 feet. Thus all Seismic Category I structures are founded on the San Mateo Formation sand.

3.7.1.4.2 Soil Properties

The static and dynamic properties of the San Mateo Formation sand are presented in Paragraph 2.5.4.2. A general summary of the pertinent static and dynamic properties of the San Mateo Formation sand are summarized in Table 3.7-4, and the variation of shear modulus and hysteretic damping with strain and confinement is presented in Figure 3.7-12 for this material.

A summary of relevant foundation and structure characteristics for the various Seismic Category I structures is presented in Table 3.7-5.

The stiffness parameters used for the design of Seismic Category I structures are presented in Table 3.7-6. Details of the general procedures used in developing these stiffness parameters together with the evaluation of structural sliding of shallowly imbedded structures and design parameters for long critical ductways and piping are presented in Appendix 3.7C.

Table 3.7-1
SPATIAL DAMPING PARAMETERS

Parameters	Mode of Motion			
	Vertical Translation	Horizontal Translation	Rocking	Twisting
Inertia	M, mass of foundation and machine	M, mass of foundation and machine	I_r, mass moment of inertia about rocking axis	I_t, mass moment of inertia about twisting axis
Equivalent[a] Radius	$r = \sqrt{\frac{BL}{\pi}}$	$r = \sqrt{\frac{BL}{\pi}}$	$r = \sqrt[4]{\frac{BL^3}{3\pi}}$	$r = \sqrt[4]{\frac{BL(B^2+L^2)}{6\pi}}$
Inertia[b] ratio	$B_v = \frac{(1-v)m}{4\rho r_e^3}$	$B_h = \frac{(7-8\nu)m}{32(1-\nu)\rho r_e^3}$	$B_r = \frac{3(1-\nu)I_r'}{8\rho r_e^5}$	$B_t = \frac{I_t}{\rho r_e^5}$
Effective inertia for design	m	m	$I_r' = \eta_r I_r$ (reference 4)	I_t
Spatial damping	$D_v = \frac{0.425}{\sqrt{B_v}}$	$D_h = \frac{0.288}{\sqrt{B_h}}$	$D_r = \frac{0.15}{(1+B_r)\sqrt{B_r}}$	$D_t = \frac{0.50}{1+2B_t}$

(a) For square or rectangular footing -
- B = width of foundation in plan (parallel to axis of rotation)
- L = length of foundation in plan (perpendicular to axis of rotation)

(b) where:
- r_e = effective radius = 0.6r for translation modes
- r_e = effective radius = 0.8r for rotational modes
- v = Poisson's ratio = 0.35
- ρ = unit mass density of soil, k-slug/ft^3
- η_r = a factor to account for inertial effects[4]

Table 3.7-2
SUMMARY OF TOTAL DAMPING VALUES
CALCULATED FOR SEISMIC CATEGORY I STRUCTURES (Sheet 1 of 2)

Structure	Spatial Damping (%)	Hysteretic Damping (%)		Total Damping[a] (%)	
		DBE	OBE	DBE	OBE
Containment	D_v=40 D_h=24 D_r=9 D_t=(b)	12.5	10	D_v=52.5 D_h=36.5 D_r=21.5 D_t=(b)	50 34 19 (b)
Auxiliary Building	D_v=56 D_h=34 D_{rxx}=22 D_{ryy}=16 D_t=15	12.5	10	D_v=68.5 D_h=46.5 D_{rxx}=34.5 D_{ryy}=27.5 D_t=27.5	66 44 32 26 25
Intake Structure	D_v=51 D_h=31 D_{rxx}=21 D_{ryy}=22	12.5	10	D_v=63.5 D_h=31.5 D_{rxx}=33.5 D_{ryy}=34.5	61 41 31 32
Fuel Handling Building	D_v=32 D_h=19 D_{rxx}=11 D_{ryy}=11 D_t=(b)	12.5	10	D_v=44.5 D_h=31.5 D_{rxx}=17.5 D_{ryy}=23.5 D_t=(b)	42 29 15 21 (b)

[a] Definitions:

D_v = Damping for translation in vertical direction
D_h = Damping for translation in horizontal direction
D_{rxx} = Damping for rocking about x axis
D_{ryy} = Damping for rocking about y axis
D_t = Damping for twisting about vertical axis

[b] Available structural data insufficient to develop these values

Table 3.7-2
SUMMARY OF TOTAL DAMPING VALUES
CALCULATED FOR SEISMIC CATEGORY I STRUCTURES (Sheet 2 of 2)

Structure	Spatial Damping (%)	Hysteretic Damping (%)		Total Damping[a] (%)	
		DBE	OBE	DBE	OBE
Safety Equipment Building	D_v=47 D_h=41 D_{rxx}=(b) D_{ryy}=(b) D_t=(b)	12.5	10	D_v=59.5 D_h=53.5 D_{rxx}=(b) D_{ryy}=(b) D_t=(b)	57 51 (b) (b) (b)
Electrical and Piping Gallery Structure	D_v=47 D_h=29 D_{rxx}=23 D_{ryy}=25 D_t=14	12.5	10	D_v=59.5 D_h=41.5 D_{rxx}=35.5 D_{ryy}=37.5 D_t=26.5	57 39 33 35 24
Condensate and Refueling Tank Enclosure Structure	D_v=49 D_n=30 D_{rxx}=14 D_{ryy}=19 D_t=13	12.5	10	D_v=61.5 D_n=42.5 D_{rxx}=26.5 D_{ryy}=31.5 D_t=25.5	59 40 25 29 23
Diesel Generator Building	D_v=46 D_n-28 D_{rxx}=8 D_{ryy}=12 D_t=10	12.5	10	D_v=58.5 D_n=40.5 D_{rxx}=20.5 D_{ryy}=24.5 D_t=22.5	56 38 18 22 20

Reviews were made for the use of soil structure interaction parameters developed for various Seismic Category I structures, as outlined in Section 5.0 of Appendix 3.7C. Table 3.7-7 lists the various structures for which these reviews were made. Reviews for other structures are made on an ongoing basis as their designs progress.

Table 3.7-3
DAMPING VALUES (%) USED FOR SEISMIC CATEGORY I STRUCTURES (Sheet 1 of 2)

Building	OBE					DBE				
	Soil	Steel	Rein-forced Concrete	Pre-stressed Concrete	Sub-systems	Soil	Steel	Rein-forced Concrete	Pre-stressed Concrete	Sub-systems
Containment	8	NA	4	2	1[b]	10	NA	7	5	2[b]
Auxiliary building	8	3-4	3	NA	2[c]	10	5	6	NA	5[c]
Fuel handling building	8	3-4	3	NA	2[c] ½ [d]	10	5	6	NA	5[c]
Electrical and piping gallery structure[a]	NA	NA	NA	NA	NA	10	NA	7	NA	NA
Safety equipment building[a]	NA	NA	NA	NA	NA	10	0	7	NA	NA

[a] Separate OBE analysis was not performed. OBE response was taken to be 60% of DBE response based on results of analyses on other structures.

[b] See Table 3.7-22 for values used in NSSS analysis.

[c] Damping values used for subsystem analyses of steel beam-column framing systems.

[d] Damping values used for the liquid content in the fuel pool.

[e] Damping values are for the liquid content in the tanks.

Table 3.7-3
DAMPING VALUES (%) USED FOR SEISMIC CATEGORY I STRUCTURES (Sheet 2 of 2)

Building	OBE					DBE				
	Soil	Steel	Rein-forced Concrete	Pre-stressed Concrete	Sub-systems	Soil	Steel	Rein-forced Concrete	Pre-stressed Concrete	Sub-systems
Condensate and refueling tank enclosure structure	8	NA	3	NA	½ [e]	10	NA	7	NA	1[e]
Diesel generator building	8	NA	4	NA	NA	10	NA	7	NA	NA

Table 3.7-4
SUMMARY OF PROPERTIES OF SAN MATEO FORMATION SAND

Property	Value
In-situ total unit weight	130 lb/ft^3
Unified soil classification	well-graded sand (SW)
Angle of internal friction	41°
Effective cohesion[(a)]	700 lb/ft^2
Shear wave velocity at low strain[(b)]	930 ft/s
Shear modulus at low strain[(b)]	3500 k/ft^2

(a) Back calculated from stability analysis of existing slopes using $\phi = 41°$, assuming slope-stability safety factor of unity.

(b)
- For strain on the order of 10^{-4}%.
- For near-surface material, i.e., upper 15 feet.
- The effect of strain and confinement (or depth) on modulus and hysteretic damping are summarized in Figure 3.7-12.

3.7.2 SEISMIC SYSTEM ANALYSIS

Seismic Category I structures, systems, and components are classified consistent with the recommendations of NRC Regulatory Guide 1.29 as discussed in Section 3.2.1. The above are analyzed for earthquake conditions, the DBE and the OBE as described in Subsections 2.5.2 and 3.7.1.

3.7.2.1 Seismic Category I Structures

3.7.2.1.1 Seismic Analysis Methods for Structures

In the analysis of Seismic Category I structures, two distinct objectives must be satisfied:

A. Development of in structure seismic response characteristics when necessary for use in the analysis and design of Seismic Category I systems, equipment, and components.

B. Determination of stress distributions within the various structures resulting from the design criteria free-field seismic input for use in the design of Seismic Category I structures.

Table 3.7-5
SUMMARY OF STRUCTURAL DIMENSIONS

Structure	Foundation Dimension (ft)	Foundation Embedment [a] (ft)	Total Height (ft)
Containment	92 radius	9[b]	184' - 9"
Auxiliary building	221 x 280	30[d]	~94
Intake structure	226 x ~280[c]	30 - 60	~60
Fuel handling building	Irregular 87 x 134	19.5 avg	106
Safety equipment building	Irregular 74 x 174	10 - 50	70
Electrical and piping junction gallery structure	Irregular 67 x 86	~35	54[e]
Condensate and refueling tank enclosure structure	Irregular 98 x 137	4	44 (average)
Diesel generator building	91 x 60	5 ft 6 in.	40 ft 10 in.
Box conduit	41 x 160	23[f]	23
Auxiliary intake structure	Irregular 27 x 20	~27[g]	38
Circular conduit	20 OD x 24	~20[h]	~20

[a] Embedment is based on the area of foundation walls in contact with soil.
[b] Irregular, varies from 9 feet at the base-slab to 43.5 feet at the base of tendon galleries.
[c] Intake structure foundation is common to two units.
[d] East wall only.
[e] Nominal height, Unit 2 access way has a height of 101 feet.
[f] Structure is completely buried, with depth of cover from 6½ ft to 15 ft.
[g] Conduit portion of structure is completely buried, with a minimum depth of cover of 4 ft.
[h] Structure is completely buried, with a minimum depth of cover of 4 ft.

Table 3.7-6
SUMMARY OF VALUES OF STIFFNESS PARAMETERS FOR SEISMIC CATEGORY 1 STRUCTURES

Structure	Stiffness Parameter	Horizontal	Component Value		Twisting	Depth[a] (ft)
			Vertical	Rocking		
Containment	K	500G	600G	1.9×10^6G	4.25×10^6G	50
Auxiliary Building	C[b]	1.0	0.81	0.66	0.41	37
Intake Structure	K avg. Values	1180G	570G	3.2×10^6G	--	47
Fuel Handling Building	C	2.3	0.98	1.08[c] 0.84[d]	1.19	35
Safety Equipment Building	K	1340G[e] 1240G[f]	450G	5.6×10^5G[d] 12.4×10^6G[c]	3.5×10^6G	30
Electrical and Piping Gallery Structure	K	435G	230G	3.7×10^5G[c] 2.1×10^5G[d]	3×10^5G	20
Condensate and Refueling Tank Enclosure Structure	K	496G	376G	5.6×10^5G[d] 7.5×10^5G[c]	1×10^6G	32
Diesel Generator Building	K	289G	199G	1.3×10^5G[d] 1.9×10^5G[c]	2.5×10^5G	40

(a) Depth = depth below foundation for calculating strain-compatible values of shear modulus G, using Figure 3.7-12
(b) $C = C_1C_2$ where C_1 = stress-distribution factor
C_2 = embedment factor
(c) Rocking about short axis
(d) Rocking about long axis
(e) Along long axis
(f) Along short axis

Table 3.7-7
REVIEW OF INTERACTION PARAMETERS FOR SEISMIC CATEGORY I STRUCTURES

Structure	Parameters Developed	Date of Transmission of Parameters	Review of Use of Parameters
Containment	Stiffness and damping	12 Feb 1973	23 Oct 1973
Auxiliary Building	Stiffness and damping	12 Feb 1973	19 Nov 1973
	Sliding potential	20 Feb 1973	23 Feb 1972
Intake structure	Stiffness and damping	4 Dec 1973	15 Jan 1974
	Critical instantaneous displacement profile	7 Sep 1973	15 Jan 1974
Fuel handling building	Stiffness and damping	11 Sep 1974	(a)
Safety equipment building	Stiffness and damping	21 Mar 1974	(a)
Electrical and piping gallery structure	Stiffness and damping	11 Dec 1974	21 Mar 1975
Condensate and refueling tank enclosure structure	Stiffness and damping	10 Nov 1976	(a)
Diesel generator building	Stiffness and damping	24 June 1977	(a)

(a) Review was made on an on-going basis.

3.7.2.1.1.1 General Methods

Two separate analytical procedures are employed to satisfy the above requirements. A time history analysis is used to develop in structure response data, and a modal response spectra analysis is used to develop stress distributions within the various structures. The mathematical idealization of the structural characteristics of the various Seismic Category I structures was accomplished by either a lumped-parameter beam-stick model or a three-dimensional finite-element model. The general analytical methods and modeling techniques used in these analyses are discussed in Bechtel Topical Report BC-TOP-4A.[5]

Variations in the application of specific details are discussed in the next paragraph and in the applicable sections of this document. The seismic design criteria input is defined in terms of the OBE and DBE design response spectra (Paragraph 3.7.1.1), the free-field time history records (Paragraph 3.7.1.2), and the soil-structure interaction parameters (Paragraph 3.7.1.4).

The seismic ground acceleration was defined as the free-field motion at the ground surface. This motion was applied as input at the foundation level without modification or reduction for embedment depth. Such free-field motion would be exhibited by an embedded basemat of mass-density similar to the soil if the basemat were detached from the superstructure response interaction. The corresponding input for the mathematical models used in the dynamic structural analyses was applied at the base of dimensionless soil-structure-interaction springs attached to

the foundation basemat of each structure. The equations of motion used in the dynamic analyses were formulated to represent the above definition of input motion whereby the basemat without super-structure would track the free field motion. A more detailed description is given in Section 3.6 of reference 6.

Structural damping values are defined in Table 3.7-3 and soil-damping characteristics in Tables 3.7-2 and 3.7-3.

Incorporation of damping into the seismic analyses was accomplished in two ways. For the lumped-parameter time history analyses, the nonproportional damping technique discussed in reference 7 was used. For the three-dimensional finite-element analyses, the composite modal damping technique as described in Sections 3.2 and 3.3 of Reference 5 was used.

Depending upon the degree of embedment, the soil-structure interaction effects are represented either by the lumped-parameter approach using strain-dependent soil springs or by the series combination of a finite-element soil grid multipoint, constrained to a set of discrete springs resulting in the equivalent soil-structure interaction parameters as prescribed by the project geotechnical consultant. A more complete description of this subject is provided in Paragraph 3.7.2.1.4.

General considerations for structural and response coupling, the minimum number of mass points, and the number of degrees-of-freedom per mass point are described in Section 3.2 of Reference 5.

Consideration of maximum relative displacements of Seismic Category I structures is provided by means of a supplementary three-dimensional finite-element analysis of the entire power block area. By means of this analysis, a more realistic assessment of the phase relationship between the response of the various structures can be determined. A more detailed description of the modeling technique can be found in Paragraph 3.7.2.1.3.10. Intra building relative support displacements were established in accordance with Section 5.3 of Reference 5.

Significant effects such as piping interactions, external structural restraints, and hydrodynamic effects are included in the analysis.

3.7.2.1.1.2 Methods Employed in the Analysis of the Intake Structure

Two independent analyses are performed to develop seismic-induced stress distributions within the intake structure. The first, a dynamic equivalent static load analysis, is used to establish member sizes and define reinforcement requirements, while the second, a more rigorous pseudo-dynamic instantaneous displacement profile analysis (refer to Section 3.5 and Appendix H of Appendix 3.7C) is used as a check to verify the magnitude and distribution of the forces and moments from the first analysis. Refer to Paragraph 3.7.2.1.10 for a detailed description of each analysis. These two analyses are justified in lieu of a seismic system dynamic analysis, since the structure is very rigid in both vertical and horizontal directions due to its numerous piers and

partition walls, and being a nearly buried structure filled with water during normal operation, the mass and inertial characteristics of the structure are similar to those of the displaced soil.

3.7.2.1.1.3 Methods Employed in the Analysis of the Offshore Circular Conduits

The intake conduits consist of 20-foot outside diameter pipe segments, 24 feet in length, connected by bell and spigot joints that were designed to accommodate the maximum rotation and translation resulting from the DBE ground motion. Because the joints are designed to articulate and are incapable of transferring tension, and the conduits are completely bedded in the select gravel backfill and formational material, the conduits as a whole are fully compliant with the ground motion. Longitudinal bending stresses cannot be transferred from segment to segment, and lateral shear stresses between the conduits cannot develop since continuity will be maintained in the formation during a DBE (refer to Figure 3.7-13 for an illustration of the conduit behavior during a seismic event). The analysis of individual pipe segments for longitudinal bending and shear is discussed below. The maximum rotations and translations were calculated using the critical instantaneous displacement profile (CIDP) (refer to Appendix 3.7C) and verified using the methodology outlined in the BC-TOP-4 Section 6.0, Analysis of Long Buried Structures.

The seismically-induced transverse stresses on the pipe sections were determined by modeling the pipe as a closed ring and inputting the seismic accelerations statically to the structure as equivalent inertia loads (refer to Paragraph 3.7.2.1.10 for a detailed description of the equivalent static analysis methodology). Calculation of the transverse stresses on the pipe section adjacent to the box conduit at the interface included the additional soil pressure resulting from the differential displacement of the conduit at the interface. Corresponding stresses from the vertical and two horizontal seismic loadings are combined by taking the square root of the sum of the squares (SRSS) of the individual seismic stresses.

Longitudinal bending and shear stresses in the individual pipe sections are calculated using the BC-TOP-4 methodology. This methodology assumes that a long, flexible pipeline will be bent to conform with the seismic wave shape. In this case, the intake pipe segments are rigid with respect to longitudinal bending and will not comply individually with the calculated curvature. The relative soil displacement over the 24-foot pipe segment from the calculated radius of curvature is not sufficient to mobilize additional soil pressure. Thus, there are essentially no longitudinal bending or shear stresses in the individual pipe segments.

The offshore circular conduits interface with the box conduit structure approximately 160 feet seaward of the permanent seawall. The first circular conduit segment is a starter section, 8 feet in length, which is embedded 2½ feet into the box conduit. Because the box conduit is a relatively rigid structure and will not comply with the ground motion, the structure will displace differentially with respect to the soil and the circular conduit segments. The starter section and first 24-foot pipe segment will be subjected to longitudinal bending and shear stresses induced by the soil contact stresses resulting from the differential displacement of the conduit with respect to the soil. Differential displacement was calculated using the BC-TOP-4 methodology, and the corresponding soil pressures were provided by Woodward-Clyde Consultants.

The method of analysis used for the offshore circular conduits is justified in lieu of a seismic system dynamic analysis for the following reasons: (1) the pipes are completely buried

structures filled with water, the mass and inertial characteristics are similar to those of the displaced soil and no significant soil structure interaction will be experienced; (2) the pipe sections are adequately modeled as a beam in the longitudinal direction and a closed ring in the transverse direction.

3.7.2.1.1.4 Methods Employed in the Analysis of the Box Conduit

The box conduit is analyzed and designed for static and equivalent dynamic loads, using the finite element model of the conduit cross-section shown in Figure 3.7-14. The model is constructed using beam elements to model the conduit and soil springs to simulate the stiffness of the soil around the box conduit. The seismically-induced stress distributions for the transverse direction are determined by inputting the maximum unamplified free field accelerations statically to the structure as equivalent inertia loadings (refer to Paragraph 3.7.2.1.10 for a detailed description of the equivalent static analysis).

A separate lumped mass model, representing the conduit structure acting as a longitudinal beam supported by a continuous elastic media, is used to determine the stresses in the longitudinal direction and to check the adequacy of the longitudinal reinforcing steel. Seismically-induced displacements, determined by the critical instantaneous displacement profile, are applied to the three major axes of the structure to determine the longitudinal stresses. (The critical instantaneous displacement profile is discussed in detail in Appendix 3.7C.)

The method of analysis used for the box conduits is justified in lieu of a seismic system dynamic analysis for the following reasons: (1) the box conduit structure is a completely buried structure filled with water under normal operating conditions; the mass and inertial characteristics are similar to those of the displaced soil, and no significant soil structure interaction will be experienced; (2) the overall simplicity of the structural models; the conduit can be adequately modeled in the transverse direction using the finite element model with beam elements, and modeled in the longitudinal direction by the lumped mass model as a beam supported by a continuous elastic media.

3.7.2.1.1.5 Methods Employed in the Analysis of the Auxiliary Intake Structure

The seismically-induced stress distributions within the auxiliary intake structure are calculated using an equivalent static analysis. Seismic accelerations are input statically into the structure as equivalent inertia loadings (refer to Paragraph 3.7.2.1.10 for a detailed description of the equivalent static analysis methodology). The corresponding stresses from the vertical and the two horizontal seismic loadings are combined by taking the square root of the sum of the squares (SRSS) of the individual seismic stresses. In addition to the structural inertia loadings, hydrodynamic and soil loadings induced by the earthquake were considered in the seismic analysis. Three wave loading conditions were also calculated independently. Normal storm

waves are assumed to be concurrent with seismic loadings. They were not included in stress comparisons because the independent calculation showed that they were negligible compared to the seismic stresses. Maximum storm waves produce lower stresses than seismic loadings and are considered independently since they represent an unrelated extreme event. Tsunami loadings are seismically induced but do not occur for at least 5 minutes following the earthquake and are thus nonconcurrent.

The equivalent static analysis is justified in lieu of seismic system dynamic analysis based on the overall simplicity of the structural model. The riser is modeled as a rigid cantilever beam element supported on a rigid buried base. The pipe section can be analyzed as a standard frame element, with the stresses determined by conventional methodology employing analytical techniques based on the principles of virtual work. Soil structure interaction will not be significant because of the use of the select gravel backfill material, the rigidity of the structure, and the similar mass densities of the structure and the backfill.

3.7.2.1.1.6 Mathematical Models

Refer to Figures 3.7-15 through 3.7-30 for either a pictorial representation or an actual sketch of the mathematical model of each Seismic Category I structure. A complete description of the formulation of the mathematical models and their use is provided in Paragraph 3.7.2.1.3.

3.7.2.1.2 Natural Frequencies and Response Loads

A summary of natural frequencies and modal characteristics is given in Tables 3.7-8 through 3.7-14. Selected total response, determined by seismic analyses for each Seismic Category I structure, is given in Figures 3.7-31 through 3.7-36, and Tables 3.7-15 through 3.7-20. The response spectra at selected plant elevations with major equipment and equipment support points for each structure are given in Appendix 3.7A.

The results of the analyses show that the structural response is dominated by the soil-structure interaction modes. Likewise, the effects of the strain-dependent soil springs are clearly shown by the frequency shift between the DBE and OBE results.

The typical in structure response spectra shown in Appendix 3.7A represent an envelope of the response for a given coordinate direction resulting from the square-root-of-the-sum-of-the-squares (SRSS) combination of the response produced from the vertical excitation and a single-axis horizontal excitation.

For the fuel handling building, the first seven modes correspond to fluid oscillation in the spent fuel pool and exhibit little fluid-structure interaction. The summation of participation factors for these modes were less than 8%.

Table 3.7-8
CONTAINMENT STRUCTURE (SHELL AND INTERNAL STRUCTURE) DBE ANALYSIS SUMMARY OF FREQUENCIES AND MODAL CHARACTERISTICS OF LUMPED-PARAMETER COUPLED MODELS

Mode No.	Model Parallel to Hot Leg			Model Perpendicular to Hot Leg		
	Frequency (Hz)	Participation Factor (%)	Critical Damping (%)	Frequency (Hz)	Participation Factor (%)	Critical Damping (%)
1	1.40	76.8 H[a]	9.82	1.40	77.1 H	9.82
2	2.16	90.3 V[b]	9.97	2.16	90.3 V	9.97
3	2.63	15.5 H	9.90	2.63	15.8 H	9.91
4	9.72	1.4 H	5.61	10.89	0.8 H	5.59
5	12.45	0.0 H	3.83	16.48	0.0 H	2.22
6	13.40	0.03 H	4.29	16.51	0.8 H	2.91
7	17.65	0.0 H	2.55	18.45	2.2 V	4.87
8	18.58	2.3 V	4.93	20.04	0.0 H	5.29
9	18.61	1.5 H	5.74	21.06	1.9 H	5.70

[a] H = Horizontal mode

[b] V = Vertical mode

Table 3.7-9
AUXILIARY BUILDING
SUMMARY OF FREQUENCIES AND MODAL CHARACTERISTICS OF THE LUMPED-PARAMETER GEOMETRICALLY COUPLED MODEL

Mode No.	Frequency (Hz)	Critical Damping (%)	Participation Factors, DBE (%)			Type of Main Response[a]
			Horizontal -X	Horizontal -Y	Vertical-Z	
1	1.50	9.95	56.9	0.4	1.1	H_x, T_z, R_y
2	1.57	9.95	0.3	57.1	14.3	H_y, V_z, R_x
3	1.79	9.95	4.4	1.6	0.1	H_y, H_x, T_z, R_y
4	1.83	9.97	1.3	13.9	74.6	V_z, H_y, H_x
5	2.35	9.98	35.6	0.3	0.8	H_x, V_z, R_y, T_z
6	2.55	9.99	0.2	25.6	8.7	H_y, V_z, R_x
7	15.41	6.05	0.6	0.0	0.0	
8	16.32	6.05	0.0	0.6	0.1	
9	17.04	6.03	0.4	0.0	0.0	
10	22.43	6.01	0.01	0.2	0.0	

[a] Direction of main response given in order of importance for first six modes according to the following notation:

H_x = Horizontal translation along X-axis
H_y = Horizontal translation along Y-axis
V_z = Vertical translation along Z-axis
R_x = Rotation about X-axis
R_y = Rotation about Y-axis
T_z = Torsion about Z-axis

Table 3.7-10[a]
FUEL-HANDLING BUILDING SUMMARY OF FREQUENCIES AND MODAL CHARACTERISTICS OF THE LUMPED-PARAMETER GEOMETRICALLY COUPLED MODEL

Mode[b] No.	Frequency (Hz)	Critical Damping (%)	Participation Factor, DBE (%)			Type of Main Response[c]
			Horizontal-X	Horizontal-Y	Vertical-Z	
8	2.38	9.79	0.0	48.6	3.9	H_y, V_z, R_x
9	2.58	9.87	41.9	0.2	10.0	H_x, V_z, R_y
10	2.99	9.98	6.1	2.7	83.9	V_z, H_x, R_y
11	4.57	9.77	4.0	0.6	0.4	H_x, H_y, T_z
12	5.53	9.94	37.4	0.5	1.3	H_x, V_z, R_y
13	5.85	9.87	0.4	38.1	0.6	H_y, V_z, R_x
14	18.80	6.20	0.2	0.2	0.0	
15	21.77	6.11	0.5	0.3	0.0	
16	22.34	6.17	0.2	0.7	0.0	
17	28.57	6.05	0.1	0.9	0.0	
18	31.98	6.06	1.0	0.0	0.0	
19	36.48	6.02	0.0	0.0	0.0	

(a) See Table 3.7-20A for additional modal importance for characteristics information.

(b) The model has seven degrees of freedom associated with fluid mass. The first seven modes correspond to fluid oscillations exhibiting little fluid-structure interaction. The tabulated participation factors do not add up to 100% due to the exclusions of the first seven modes.

(c) Direction of Main Response given in order of 8-13 modes according to the following notation:

H_x = Horizontal translation along X-axis
H_y = Horizontal translation along Y-axis
V_z = Vertical translation along Z-axis
R_x = Rotation about X-axis
R_y = Rotation about Y-axis
T_z = Torsion about Z-axis

Table 3.7-11
SAFETY EQUIPMENT BUILDING
SUMMARY OF FREQUENCIES AND MODAL CHARACTERISTICS OF THREE-DIMENSIONAL FINITE-ELEMENT MODEL

Mode No.	Frequency (Hz)	Modal Damping (%)	Participation Factor, DBE (%)			Type of Main Response[a]
			Horizontal-X	Horizontal-Y	Vertical-Z	
1	2.39	10	46.69	0.78	1.35	H_x, R_y, T_z
2	3.22	10	1.01	0.89	92.43	V_z, H_x, R_x
3	4.12	10	2.22	0.37	0.26	H_x, H_y, R_y
4	5.05	10	0.68	68.55	1.85	H_y, V_z, R_x
5	7.31	10	36.64	3.13	1.16	H_x, H_y, R_y
6	8.85	10	5.84	21.89	1.87	H_y, H_x, R_x
7	12.69	7	3.19	0.95	0.16	
8	13.59	7	3.04	0.62	0.24	
9	15.62	7	0.55	1.96	0.47	
10	17.68	7	0.14	0.87	0.21	

[a] Direction of Main Response given in order of importance for first six modes according to the following notation:

H_x = Horizontal translation along X-axis
H_y = Horizontal translation along Y-axis
V_z = Vertical translation along Z-axis
R_x = Rotation about X-axis
R_y = Rotation about Y-axis
T_z = Torsion about Z-axis

Table 3.7-12
ELECTRICAL AND PIPING GALLERY STRUCTURE
SUMMARY OF FREQUENCIES AND MODAL CHARACTERISTICS OF THREE-DIMENSIONAL FINITE-ELEMENT MODEL

Mode No.	Frequency (Hz)	Modal Damping (%)	Participation Factors, DBE (%)			Type of Main Response[a]
			Horizontal-X	Horizontal-Y	Vertical-Z	
1	2.09	10	2.858	16.967	3.934	H_y, R_x, T_z
2	2.40	10	11.686	4.634	13.512	V_z, H_x, R_y
3	3.28	10	14.502	0.265	16.172	V_z, H_x
4	3.81	10	1.408	5.801	1.115	H_y, R_x, T_z
5	4.82	10	10.959	5.765	4.840	H_x, R_y
6	5.27	10	4.207	10.839	2.752	H_y, T_z
7	8.12	7	0.526	0.745	1.346	
8	9.01	7	0.038	0.691	1.265	
9	10.19	7	0.016	0.393	0.018	
10	11.67	7	0.313	0.231	0.071	

[a] Direction of main response given in order of importance for the first 6 modes according to the following notation:

H_x = Horizontal translation along X-axis
H_y = Horizontal translation along Y-axis
V_z = Vertical translation along Z-axis
R_x = Rotation about X-axis
R_y = Rotation about Y-axis
T_z = Torsion about Z-axis

Table 3.7-13
CONDENSATE AND REFUELING TANK ENCLOSURE STRUCTURE SUMMARY OF FREQUENCIES AND MODAL CHARACTERISTICS OF THREE-DIMENSIONAL FINITE-ELEMENT MODEL (Sheet 1 of 2)

Mode[a] No.	Frequency (Hz)	Modal Damping (%)	Participation Factors, DBE (%)			Type of Main Response[b]
			Horizontal-X	Horizontal-Y	Vertical-Z	
9	4.09	10	5.27	21.89	0.08	H_y, R_x, T_z
10	4.14	10	25.74	5.62	1.00	H_x, R_y, T_z
11	4.44	10	2.11	13.42	0.00	H_y, R_x
12	6.15	10	1.39	0.35	12.40	V_z, H_x
13	6.30	10	0.12	5.51	1.58	H_y, T_z

(a) The model has eight degrees of freedom associated with fluid mass. The first eight modes correspond to fluid oscillations exhibiting little fluid-structure interaction. The tabulated participation factors do not add up to 100% due to exclusions of the first eight modes.

(b) Direction of main response given in order of importance for 9-15 modes according to the following notation:

H_x = Horizontal Translation along X-axis
H_y = Horizontal Translation along Y-axis
V_z = Vertical Translation along Z-axis Rx
R_x = Rotation about X-axis
R_y = Rotation about Y-axis
T_z = Torsion about Z-axis

Table 3.7-13
CONDENSATE AND REFUELING TANK ENCLOSURE STRUCTURE SUMMARY OF FREQUENCIES AND MODAL CHARACTERISTICS OF THREE-DIMENSIONAL FINITE-ELEMENT MODEL (Sheet 2 of 2)

Mode[a] No.	Frequency (Hz)	Modal Damping (%)	Participation Factors, DBE (%)			Type of Main Response[b]
			Horizontal-X	Horizontal-Y	Vertical-Z	
14	6.39	10	4.26	2.23	8.06	Vz, Hx Ry
15	6.55	10	4.27	2.25	3.18	Hx, Ry, Tz
16	8.15	7	0.46	0.07	0.48	
17	9.07	7	0.48	0.46	1.27	
18	9.19	7	0.01	0.21	0.26	
19	9.25	7	0.24	0.18	0.77	
20	9.32	7	0.05	0.33	0.70	
21	9.43	7	0.14	0.38	0.49	
22	9.73	7	0.73	0.31	0.34	

Table 3.7-14
DIESEL GENERATOR BUILDING SUMMARY OF FREQUENCIES AND MODAL CHARACTERISTICS OF THE LUMPED-PARAMETER GEOMETRICALLY COUPLED MODEL

Mode No.	Frequency (Hz)	Critical Damping (%)	Participation Factors, DBE (%)			Type of Main Response[a]
			Horizontal-X	Horizontal-Y	Vertical-Z	
1	3.38	10	0.00	13.88	0.00	H_y, R_x
2	3.39	10	11.85	0.00	0.00	H_x, R_y
3	4.140	10	0.00	0.00	18.68	V_z, R_x, R_y
4	4.26	10	0.00	0.00	0.00	T_z, H_x, H_y
5	5.78	10	14.44	0.00	0.00	R_y, H_x
6	6.38	10	0.00	12.49	0.00	R_x, H_y
7	28.73	7	0.00	0.43	0.00	
8	33.59	7	0.34	0.00	0.00	
9	34.63	7	0.00	0.00	0.00	
10	42.23	7	0.00	0.07	0.00	

[a] Direction of main response given in order of importance for the first 6 modes according to the following notation:

H_x = Horizontal translation along x-axis
H_y = Horizontal translation along y-axis
V_z = Vertical translation along z-axis
R_x = Rotation about x-axis
R_y = Rotation about y-axis
T_z = Torsion about z-axis

Table 3.7-15
AUXILIARY BUILDING NODAL FORCES, ACCELERATIONS, AND DISPLACEMENTS FROM DBE ANALYSIS
(N-S AND VERTICAL EXCITATION)

Node[a] No.	Nodal Weight (x 10^4 k)	Forces[b] (x 10^4 k)			Accelerations[b] (ft/s^2)			Displacements[b]					
								(x 10^{-2} ft)			(x 10^{-4} rad)		
		F_x	F_y	F_z	$\ddot{u}_x$	$\ddot{u}_y$	$\ddot{u}_z$	u_x	u_y	u_z	θ_x	θ_y	θ_z
1	10.66	7.00	1.78	6.38	21.1	5.4	19.3	19.6	4.3	14.7	2.3	19.8	4.8
2	1.65	1.17	0.28	1.01	22.8	5.4	19.6	23.6	4.5	14.9	2.3	19.9	4.8
3	0.09	0.07	0.02	0.10	23.4	8.0	34.6	24.8	7.4	28.4	2.4	20.0	4.8
4	0.09	0.07	0.02	0.10	23.4	8.2	34.5	24.8	7.7	28.7	2.4	20.0	4.8
5	1.34	0.85	0.22	0.78	20.4	5.4	18.9	19.7	4.6	14.3	2.3	19.9	4.8
6	2.56	1.93	0.43	1.57	24.3	5.4	19.7	26.4	4.7	15.0	2.4	19.9	4.8
7	0.20	0.14	0.05	0.21	23.5	8.1	34.7	25.4	7.6	28.5	2.4	20.0	4.8
8	0.20	0.14	0.05	0.21	23.5	8.3	34.7	25.4	7.9	28.9	2.4	20.0	4.8
9	2.67	1.98	0.45	1.60	23.9	5.5	19.3	26.1	4.8	14.6	2.4	19.9	4.8
10	3.03	2.58	0.53	1.85	27.4	5.6	19.7	30.8	5.0	15.0	2.4	20.0	4.8
11	0.93	0.69	0.16	0.55	24.0	5.7	19.0	26.6	5.1	14.4	2.4	20.0	4.8
12	2.75	2.48	0.50	1.66	29.0	5.9	19.4	32.8	5.4	14.7	2.4	20.0	4.8
13	0.18	0.18	0.05	0.20	30.8	8.5	35.2	34.9	8.1	28.9	2.4	20.1	5.0
14	0.18	0.18	0.05	0.20	30.8	8.9	35.2	34.9	8.5	29.3	2.4	20.1	5.0

(a) Refer to Figure 3.7-21 for node location.

(b) Nomenclature:

x, y, z = axes of coordinate system according to Figure 3.7-19

F_i = translational force along I-axis

u_i = translational displacement along I-axis

θ_i = rotational displacement about I-axis

$\ddot{u}_i$ = translational acceleration along I-axis

Table 3.7-16
AUXILIARY BUILDING NODAL FORCES, ACCELERATIONS, AND DISPLACEMENTS FROM DBE ANALYSIS
(E-W AND VERTICAL EXCITATION)

Node[a] No.	Nodal Weight (x 10^4 k)	Forces[b] (x 10^4 k)			Accelerations[b] (ft/s^2)			Displacements[b]					
								(x 10^{-2} ft)			(x 10^{-4} rad)		
		F_x	F_y	F_z	$\ddot{u}_x$	$\ddot{u}_y$	$\ddot{u}_z$	u_x	u_y	u_z	θ_x	θ_y	θ_z
1	10.66	0.21	8.06	8.38	0.6	24.3	25.3	0.5	22.8	19.5	17.2	0.4	0.9
2	1.65	0.03	1.33	1.38	0.7	25.9	26.8	0.6	25.3	21.1	17.3	0.4	0.9
3	0.09	0.002	0.07	0.08	0.7	25.8	26.8	0.6	25.5	21.1	17.3	0.5	1.0
4	0.09	0.002	0.08	0.08	0.7	27.6	27.1	0.6	27.4	21.4	17.3	0.5	1.0
5	1.34	0.05	1.11	1.13	1.1	26.6	27.2	1.0	26.4	19.9	17.3	0.4	0.9
6	2.56	0.06	2.18	2.18	0.7	27.5	27.5	0.6	27.5	21.7	17.3	0.4	0.9
7	0.20	0.004	0.27	0.15	0.7	27.7	25.2	0.6	27.9	19.1	17.3	0.5	1.0
8	0.20	0.004	0.18	0.15	0.7	29.5	25.3	0.6	29.9	19.3	17.3	0.5	1.0
9	2.67	0.06	2.42	2.09	0.7	29.2	25.2	0.7	29.6	19.1	17.3	0.4	0.9
10	3.03	0.06	2.94	2.53	0.7	31.3	26.9	0.7	31.9	21.2	17.4	0.4	0.9
11	0.93	0.04	0.94	0.80	1.3	32.4	27.7	1.13	33.1	20.2	17.4	0.4	0.9
12	2.75	0.07	2.98	2.16	0.8	34.9	25.3	0.8	35.6	19.3	17.4	0.4	0.9
13	0.18	0.005	0.21	0.14	0.9	35.7	25.2	0.8	36.3	19.2	17.4	0.5	1.0
14	0.18	0.005	0.22	0.15	0.8	37.7	25.4	0.8	38.3	19.3	17.4	0.5	1.0

(a) Refer to Figure 3.7-21 for node location.

(b) Nomenclature:

x, y, z = axes of coordinate system according to Figure 3.7-19

F_i = translational force along I-axis

u_i = translational displacement along I-axis

θ_i = rotational displacement about I-axis

$\ddot{u}_i$ = translational acceleration along I-axis

Table 3.7-17
AUXILIARY BUILDING MAXIMUM CONNECTIVITY FORCES FROM DBE ANALYSIS (Sheet 1 of 3)

Connectivity (Nodes)[a]	N-S and Vertical Excitation						E-W and Vertical Excitation					
	Forces[b] (x 10^4 k)			Moments[b] (x 10^6 k-ft)			Forces[b] (x 10^4 k)			Moments[b] (x 10^6 k-ft)		
	F_x	F_y	F_z	M_x	M_y	M_z	F_x	F_y	F_z	M_x	M_y	M_z
1 - 2	8.31	1.96	5.89	1.79	6.10	3.21	0.14	10.79	8.21	4.46	0.19	0.15
1 - 3	0.00	0.00	0.12	0.06	0.16	0.00	0.00	0.00	0.06	0.03	0.09	0.00
1 - 4	0.00	0.00	0.12	0.06	0.16	0.00	0.00	0.00	0.06	0.03	0.09	0.00
1 - 5	3.35	0.60	3.36	3.21	4.24	3.26	0.24	3.18	5.22	5.46	0.16	0.45
1 - 6	1.18	0.24	0.61	0.47	0.59	1.47	0.07	1.34	1.77	2.36	0.05	0.14
1 – 10	0.15	0.05	0.14	0.16	0.50	0.19	0.007	0.29	0.53	0.71	0.01	0.02
2 - 3	0.16	0.18	0.53	0.03	0.58	0.19	0.005	0.87	0.34	0.10	0.37	0.95
2 - 4	0.16	0.20	0.57	0.03	0.63	0.22	0.01	1.01	0.39	0.11	0.43	1.12
2 - 5	0.50	0.03	0.19	0.12	0.07	0.33	0.02	0.13	0.25	0.16	0.08	0.05
2 - 6	6.50	1.33	4.21	0.30	3.50	0.52	0.15	7.48	5.90	1.10	0.13	0.23

(a) Refer to Figure 3.7-21 for relative location of nodes

(b) Nomenclature:

x, y, z = axes of coordinate system according to Figure 3.7-19

F_i = translational force along the I-axis

M_i = rotational force about the I-axis

Table 3.7-17
AUXILIARY BUILDING MAXIMUM CONNECTIVITY FORCES FROM DBE ANALYSIS (Sheet 2 of 3)

Connectivity (Nodes)[a]	N-S and Vertical Excitation						E-W and Vertical Excitation					
	Forces[b] (x 10^4 k) (x 10^4 k)			Moments[b] (x 10^6 k-ft) (x 10^6 k-ft)			Forces[b] (x 10^4 k) (x 10^4 k)			Moments[b] (x 10^6 k-ft) (x 10^6 k-ft)		
	F_x	F_y	F_z	M_x	M_y	M_z	F_x	F_y	F_z	M_x	M_y	M_z
3 - 5	0	0.002	0	0	0	0.002	0	0.002	0	0	0	0
3 - 6	0.11	0.16	0.50	0.03	0.55	0.18	0.004	0.80	0.30	0.05	0.33	0.87
3 - 7	0	0	0.06	0.04	0.007	0	0	0	0.03	0.02	0.003	0
4 - 5	0	0.002	0	0	0	0.002	0	0.002	0	0	0	0.002
4 - 6	0.11	0.18	0.54	0.03	0.58	0.20	0.008	0.94	0.35	0.05	0.38	1.01
4 - 8	0	0	0.06	0.04	0.007	0	0	0	0.03	0.02	0.003	0
5 - 6	1.41	0.13	0.81	0.59	0.83	1.13	0.09	0.62	1.18	0.85	0.05	0.13
5 - 7	0.18	0.05	0.44	0.23	0.56	0.11	0.007	0.25	0.36	0.18	0.44	0.27
5 - 8	0.18	0.06	0.46	0.24	0.58	0.11	0.02	0.28	0.37	0.18	0.45	0.30
5 - 9	1.30	0.19	1.45	1.65	1.31	1.77	0.11	1.09	2.46	2.81	0.03	0.19
6 - 7	0.12	0.18	0.59	0.23	0.65	0.21	0.004	0.88	0.34	0.14	0.38	0.97
6 - 8	0.12	0.18	0.60	0.23	0.64	0.21	0.01	0.91	0.35	0.14	0.38	0.98
6 - 9	6.90	1.17	3.79	1.69	2.88	3.23	0.16	6.66	5.24	2.36	0.07	0.11
6 – 10	0.47	0.10	0.20	0.17	0.20	0.44	0.02	0.58	0.62	0.53	0.01	0.04
7 - 9	0.21	0.19	0.75	0.13	0.83	0.21	0.009	0.97	0.40	0.12	0.44	1.04
7 – 10	0.15	0.001	0.15	0.13	0.20	0.17	0.01	0.008	0.13	0.13	0.17	0.03

Table 3.7-17
AUXILIARY BUILDING MAXIMUM CONNECTIVITY FORCES FROM DBE ANALYSIS (Sheet 3 of 3)

Connectivity (Nodes)[a]	N-S and Vertical Excitation						E-W and Vertical Excitation					
	Forces[b] (x 10^4 k)			Moments[b] (x 10^6 k-ft)			Forces[b] (x 10^4 k)			Moments[b] (x 10^6 k-ft)		
	F_x	F_y	F_z	M_x	M_y	M_z	F_x	F_y	F_z	M_x	M_y	M_z
8 - 9	0.21	0.20	0.76	0.13	0.83	0.21	0.009	1.01	0.41	0.13	0.45	1.09
8 – 10	0.15	0.001	0.16	0.14	0.20	0.17	0.006	0.008	0.13	0.14	0.18	0.01
9 – 10	5.16	1.14	3.43	1.07	3.25	2.20	0.13	6.65	4.53	1.89	0.10	0.23
9 – 11	0.78	0.11	0.82	0.95	0.71	1.06	0.04	0.68	1.31	1.57	0.03	0.07
10 – 11	1.10	0.20	0.55	0.39	0.60	0.70	0.03	1.19	0.74	0.54	0.01	0.04
10 – 12	2.25	0.57	1.42	0.72	1.22	1.42	0.07	3.40	2.01	0.97	0.05	0.13
10 – 13	0.10	0.00	0.15	0.13	0.22	0.10	0.004	0.002	0.08	0.07	0.11	0.006
10 – 14	0.09	0.00	0.16	0.14	0.23	0.10	0.01	0.002	0.09	0.08	0.12	0.01
11 – 12	1.19	0.15	0.81	0.66	0.80	0.81	0.04	0.94	1.19	1.00	0.05	0.07
12 – 13	0.07	0.06	0.10	0.04	0.12	0.13	0.03	0.28	0.09	0.07	0.10	0.33
12 – 14	0.07	0.07	0.12	0.03	0.13	0.14	0.02	0.32	0.11	0.08	0.12	0.36

Table 3.7-18
FUEL HANDLING BUILDING NODAL FORCES, DISPLACEMENTS, AND ACCELERATIONS FROM DBE ANALYSIS
(N-S AND VERTICAL EXCITATION)

Node[a] No.	Nodal Weight (x 10^4 k)		Forces[b] (x 10^4 k)			Accelerations[b] (ft/s^2)			Displacements[b]					
									(x 10^{-2} ft)			(x 10^{-4} rad)		
	Horiz. Trans.	Vert. Trans.	F_x	F_y	F_z	$\ddot{u}_x$	$\ddot{u}_y$	$\ddot{u}_z$	u_x	u_y	u_z	θ_x	θ_y	θ_z
1	1.63	2.02	1.51	0.04	1.44	29.8	0.8	22.9	3.87	0.20	6.49	0.7	12.8	0.7
2	0.96	0.83	0.79	0.03	0.59	26.5	0.9	22.9	5.40	0.31	6.54	0.7	12.8	0.8
3	0.73	0.55	0.56	0.02	0.40	26.0	1.2	23.1	7.21	0.42	6.58	0.7	12.9	0.8
4	0.86	0.84	0.72	0.04	0.60	26.9	1.6	23.1	9.49	0.56	6.59	0.7	13.0	0.8
5	0.44	0.44	0.50	0.03	0.32	36.5	2.2	23.1	13.74	0.81	6.60	0.7	13.1	0.9
6	0.30	0.30	0.41	0.02	0.21	44.2	2.6	23.2	16.17	0.95	6.63	0.7	13.1	0.9

(a) Refer to Figure 3.7-22 for node location

(b) Nomenclature:

x, y, z = axes of coordinate system according to Figure 3.7-20

F_i = translational force along I-axis

u_i = translational displacement along I-axis

θ_i = rotational displacement about I-axis

$\ddot{u}_i$ = translational acceleration along I-axis

Table 3.7-19
FUEL HANDLING BUILDING NODAL FORCES, ACCELERATIONS, AND DISPLACEMENTS FROM DBE ANALYSIS
(E-W AND VERTICAL EXCITATION)

Node[a] No.	Nodal Weight ($x 10^4$ k)		Forces[b] ($x 10^4$ k)			Accelerations[b] (ft/s^2)			Displacements[b]					
									($x 10^{-2}$ ft)			($x 10^{-4}$ rad)		
	Horiz. Trans.	Vert. Trans.	F_x	F_y	F_z	$\ddot{u}_x$	$\ddot{u}_y$	$\ddot{u}_z$	u_x	u_y	u_z	θ_x	θ_y	θ_z
1	1.63	2.02	0.08	1.51	1.33	1.6	29.7	21.1	0.46	4.02	6.03	16.3	1.5	0.7
2	0.96	0.83	0.07	0.77	0.54	2.2	25.9	21.1	0.70	6.29	6.02	16.6	1.5	0.7
3	0.73	0.55	0.06	0.56	0.38	2.9	24.6	22.2	0.95	8.71	6.19	16.9	1.5	0.7
4	0.86	0.84	0.10	0.72	0.55	3.8	27.4	21.0	1.24	11.92	5.98	17.1	1.5	0.7
5	0.44	0.44	0.07	0.56	0.29	5.3	41.1	21.2	1.77	17.59	6.02	17.3	1.6	0.7
6	0.30	0.30	0.06	0.47	0.19	6.2	51.3	21.2	2.07	20.86	6.01	17.3	1.6	0.7

(a) Refer to Figure 3.7-22 for node location

(b) Nomenclature:

x, y, z = axes of coordinate system according to Figure 3.7-20

F_i = translational force along I-axis

u_i = translational displacement along I-axis

θ_i = rotational displacement about I-axis

$\ddot{u}_i$ = translational acceleration along I-axis

Table 3.7-20
FUEL HANDLING BUILDING MAXIMUM CONNECTIVITY FORCES FROM DBE-ANALYSIS

Connectivity (Nodes)[a]	N-S and Vertical Excitation						E-W and Vertical Excitation					
	Forces[b] (x 10^4 k)			Moments[b] (x 10^6 k-ft)			Forces[b] (x 10^4 k)			Moments[b] (x 10^6 k-ft)		
	F_x	F_y	F_z	M_x	M_y	Mz	F_x	F_y	F_z	M_x	M_y	M_z
1 – 2	2.63	0.15	2.11	0.19	1.79	0.25	0.36	2.64	1.93	1.66	0.22	0.20
2 – 3	1.75	0.12	1.37	0.23	1.20	0.30	0.25	2.10	1.62	0.93	0.20	0.06
2 – 4	0.27	0.001	0.16	0.06	0.11	0.10	0.04	0.01	1.02	0.39	0.05	0.02
3 – 4	1.28	0.09	0.98	0.09	0.88	0.15	0.19	1.67	1.29	0.42	0.14	0.07
4 – 5	0.90	0.05	0.53	0.03	0.52	0.05	0.13	1.02	0.48	0.52	0.07	0.02
5 – 6	0.41	0.02	0.21	0.007	0.13	0.02	0.06	0.47	0.19	0.13	0.01	0.02

(a) Refer to Figure 3.7-22 for relative location of nodes.
(b) Nomenclature:
x, y, z = axes of coordinate system according to Figure 3.7-20
F_i = translational force along the I-axis
M_I = rotational force about the I-axis

3.7.2.1.3 Procedure Used for Modeling

3.7.2.1.3.1 Designation of Systems Versus Subsystems

Major Seismic Category I structures that are considered in conjunction with foundation media in forming a soil-structure interaction model are defined as "seismic systems." Other Seismic Category I structures, systems, and components that are not designated as "seismic systems" are considered as "seismic subsystems."

3.7.2.1.3.2 Decoupling Criteria

Decoupling of systems and subsystems was performed in accordance with the provisions of Section 3.2 of Reference 5. Although a simplified model of the NSSS has been incorporated into the lumped parameter analysis of the containment structure to account for potential coupling, the detailed analysis of the NSSS was performed using a decoupled model as discussed in Paragraph 3.7.2.2.

3.7.2.1.3.3 Lumped Mass Considerations

A description of the procedure used to locate lumped masses for the seismic analyses of Seismic Category I structures and equipment is provided in Section 3.2 of Reference 5.

3.7.2.1.3.4 Lumped Parameter Models for the Containment Structure

The two-dimensional lumped-parameter coupled models of the containment structure and the NSSS used for time-history analyses were developed to obtain response characteristics along the two principal axes of the containment exterior structure and the NSSS. Each model consists of five separate subsystems: Soil, basemat, containment shell, internal structure, and the NSSS.

In considering the interactions between subsystems as mentioned above, it was recognized that the proper geometrical relationships must be maintained. This is extremely important when significant rocking of the structure occurs due to soil-structure interaction. This rocking causes a geometric coupling between the horizontal and vertical motions of points on the structure away from the centerline. If the structure is modeled as a beam, with stiffness and inertia properties lumped at the centerline (elastic axis), the response will be decoupled. Vertical motions computed at the centerline will not account for geometric coupling due to rocking. However, geometric coupling can be accounted for by considering the simple transformation of centerline response to points away from the centerline.

This application has been termed a "multipoint constraint" and is equivalent to the introduction of a rigid massless link. In this manner, the proper geometric relationship may be maintained between subsystems whose interfaces are not on the elastic axis. In addition, coupling between horizontal and vertical motions due to rocking can be accounted for in the model itself. Using the multipoint constraint concept, two-dimensional elements with flexural, shear, and axial

stiffness were developed for the basemat, containment shell, interior structure, and the NSSS. The interface between the containment shell and basemat was made using a set of multipoint constraints that approximated the actual connection. An axisymmetric model of the containment and basemat was used to verify the constraint system. This procedure was repeated for the internal structure and basemat interface.

Soil compliance was incorporated into the model by use of a set of discrete springs attached to the basemat. The spring rates were determined by the soil consultant and were based on data obtained from analysis and the field test discussed in Section 2.2 and Appendix E of Appendix 3.7C. Since the soil structure interaction parameters are strain dependent, different spring rates were used for OBE and DBE inputs. The vertical and horizontal springs were distributed to the nodes in the basemat. The actual stiffness of the spring assigned to each node was determined by multiplying the appropriate total spring rate by a weighting ratio. The weighting ratio for a given node is the ratio of the effective area of the basemat represented by that node divided by the total effective area of all of the nodes. An additional rotational spring rate was applied at the center node. This was necessary since the couple produced by the vertical springs accounts for only a portion of the rotational stiffness. The effective spring rates were checked by applying several static loads to the model.

A beam model of the NSSS, which was considered an adequate representation of the mass and stiffness of the subsystem, was provided by the NSSS supplier. The local deflection characteristics of each interface between the NSSS and the interior structure were studied and then incorporated into the model with an appropriate multipoint constraint. An example of this is the steam generator snubber support. This support is located on a wall panel that has significant local deflection characteristics. A horizontal spring was used to include this effect. The spring rate was determined from static loads applied to a three-dimensional fixed-base finite-element model of the interior structure.

Inertial properties were developed by assigning material density properties to the various beam elements within the structural model and then generating a consistent mass matrix. Additional nodal masses were applied at the appropriate locations to account for the mass associated with floor slabs and equipment.

3.7.2.1.3.5 Axisymmetric Finite-Element Model for the Containment Structure

An axisymmetric finite-element model of the containment structure was developed to obtain the resulting stress distributions within the exterior shell and basemat when subjected to postulated axisymmetric and nonaxisymmetric loading conditions. For the seismic induced loads, the response spectra technique was employed.

For this analysis the interior structure was idealized as an axisymmetric structure in order to account for its stiffness and inertial influence on the total structural response. Figures 3.7-16 and 3.7-17 present a pictorial representation of the computer models used. Damping was incorporated by the use of the composite modal damping technique, wherein the individual modal damping coefficients are based on the predominate response characteristic of a given

mode. For example, if the predominate modal response characteristic is soil structure interaction, then the modal damping coefficient is related to soil damping value, and if the predominant modal response characteristic is in the form of differential building motion, then the modal damping coefficient is related to the corresponding structural damping values.

The seismic stress distributions were obtained from a two-component absolute summation technique, considering the worst case response from a single axis horizontal excitation in combination with the vertical excitation, using the design criteria response spectra as input.

3.7.2.1.3.6 Three-Dimensional Finite-Element Model for the Containment Structure

A three-dimensional finite-element model of the containment structure was developed to obtain the resulting stress distributions within the internal structure when subjected to postulated loading conditions. For seismic induced loads, the response spectra technique was employed. Figure 3.7-18 presents a pictorial representation of the computer model used. For this analysis the containment exterior shell was idealized as a single lumped-parameter beam stick in order to account for its stiffness and inertial influence on the total structural response. A pictorial representation of interior containment is shown in Figures 3.7-19 and 3.7-20. The basemat flexibility was ignored and the soil-structure interaction was represented by a set of discrete springs that are multipoint constrained to the interior structure basemat interface. Damping was again incorporated by the use of the composite modal damping technique.

The three-component SRSS modal response spectra technique was used to determine the seismic stress distribution.

3.7.2.1.3.7 Three-Dimensional Geometrically Coupled Lumped-Parameter Models

The lumped-parameter geometrically coupled models for the auxiliary building, the fuel handling building, and the diesel generator building used for both time history and response spectra analyses were developed to account for coupling between the various modes of response independent of the orientation of input, and to facilitate the definition of the system physical properties that are required to formulate the equations of motion. The system response is defined by nodal coordinates originating at the center of mass of the various floor levels. This was done since the center of mass for a given floor level can be uniquely defined at a single point independent of the orientation of motion.

The aforementioned results in a geometrically uncoupled mass matrix with diagonal terms that are conveniently evaluated to represent the translational and rotational inertia of the masses tributary to each nodal point. The stiffness matrix, on the other hand, becomes geometrically coupled. It is developed by considering all the resisting assemblies affecting the connectivity between nodal points and transforming these local element stiffnesses to the common nodal coordinate system. This approach permits analysis of the structure as a three-dimensional geometrically coupled system, allows for full consideration of the coupling of translation, torsion, and rocking response, and provides for the evaluation of the coupled natural frequencies.

It also permits the representation of partial floors by allowing multiple connectivity between nodal points and affords the use of a single model to study input motion in any direction.

A pictorial representation of the lumped-parameter model for the auxiliary building is shown in Figure 3.7-21 and a similar model for the fuel handling building and the diesel generator building is shown in Figures 3.7-22 and 3.7-36, respectively.

For these models a diagonal mass matrix was used. The resisting elements to be considered in the formulation of the stiffness matrix are the various shear walls, and to a lesser extent, the columns connecting the nodal points under consideration. These assemblies are treated as three-dimensional elements with flexural, shear, and axial stiffness characteristics. Finite element studies were performed to establish guidelines to be used in determining the effectiveness of specific assemblies and the type of boundary conditions to be assumed. Once resisting assemblies had been identified, and their stiffness effects calculated relative to their local coordinate system with due regard to their directional effectiveness and assumed boundary conditions, the results were transformed and summed with respect to the nodal coordinate system. This was equivalent to introducing a unit displacement in each of the nodal degrees of freedom, performing a rigid-body transformation to the local coordinate system of the resisting assembly, calculating the forces developed in the resisting assemblies, and finally algebraically adding all of the forces about the nodal points.

This whole development was based upon the fundamental definition of the stiffness matrix: Each column of a stiffness matrix was associated with a degree of freedom and represented the vector of forces in every degree of freedom that resulted from a unit displacement imparted to the given degree of freedom.

A similar concept was applied to the soil stiffness characteristics when the modeling was extended to the soil-structure interaction. The discrete springs representing the soil-structure interaction were assumed to act at the geometric center of the basemat, which was not coincident with the basemat nodal point location (center of mass). Therefore, a coordinate transformation was required to incorporate the soil stiffness characteristics into the unconstrained system stiffness matrix of the structural system already defined.

In order to account for all potentially significant interaction phenomena, the model of the fuel handling building also incorporates the hydrodynamic effects of the fluid content in the spent fuel pool. This is accomplished by use of both stationary and oscillatory masses in accordance with the transmissibility characteristics of the fluid.

Utilizing the lumped-parameter model, a modal response spectra analysis was performed to aid in the initial seismic evaluation of the structure and to develop representative stress distributions within the structure. Once the final structural configuration and anticipated member sizes were established, a time-history analysis was performed to develop in structure acceleration time-history records and associated response spectra.

The final step in the seismic analysis of the auxiliary, fuel handling, and diesel generator buildings was to translate the seismic response characteristics defined by the lumped-parameter model into stress distributions within the structure. Specific subsystem finite-element models were developed where necessary to aid in this analysis.

A supplemental lumped-parameter model was developed for the control area of the auxiliary building to account for the potential amplification to the vertical response resulting from the more flexible steel column support system. Typical column lines together with their associated tributary areas were excited with the basemat acceleration time history developed above with due consideration for the geometric rigid-body transformation associated with the location of column bases.

Subsequent to completion of the seismic analysis of the auxiliary building, the concrete walls and roof which were designed to enclose the upper level (elevation 85 feet), over the radwaste area and part of the control area, were deleted. The deletion represents a slight reduction in overall mass and in geometric eccentricity, neither of which significantly affects the seismic response. The validity of the original analysis was confirmed by a partial re-analysis of the building utilizing a mathematical model that incorporated the revised configuration. The re-analysis demonstrated that the dominant soil-structure interaction frequencies were virtually unchanged and that the base shear seismic response was slightly decreased. The results of the re-analysis were used to evaluate the effects of torsional seismic excitation in response to NRC inquiries.

In 1985 evaluations were performed for the addition of a non-safety related building on top of the roof of a part of the existing auxiliary building. The new addition is to be built on top of the "Radwaste Storage Tank Area." The new building is a light-weight structural steel framework covered with light-gage metal sidings and conventional roofing. A new floor system is also added to provide an independent support; separating the building from the existing auxiliary building roof. In order to demonstrate the structural integrity of the existing building a refined 3-dimensional thin shell finite element model that accurately represents the main load carrying shear walls of the auxiliary building was prepared. This model was coupled to the elevated floor subsystem representing the new building addition. Static and dynamic response spectrum analyses were done to evaluate the status of the representative main shear walls. Time-history analyses were also performed to develop floor response spectra at key points for comparison with the original analysis. The new model and the analyses followed the criteria and the basic assumption used in the original analyses of the building. It was demonstrated that the effect of the proposed addition on the dynamic characteristics of the existing structure will be negligible. The evaluation of the main shear walls showed that they have sufficient reserve capacity to resist the effects of adding a new light-weight structure. Comparison of the selected floor response spectra indicated that the original spectra are conservative. Therefore, it was concluded that there will be no discernible adverse effect of the new building addition on the existing structure.

A finite element model (FEM) of the fuel handling building (FHB) was used to evaluate the effects of installing the high density racks in the spent fuel pool. This current FEM is consistent with the original lumped mass model shown in Figure 3.7-22. The Table 3.7-20A comparison shows that the current FEM behaves very similar to the lumped parameter model. The dynamic

characteristic of the current FEM are compared with those stated in Table 3.7-10. The two dominant modes for each direction are compared. The model (lumped vs. FEM) comparisons show that the FEM accurately depicts the FHB and the differences in the model frequencies are as expected (more mass - lower frequency). The verified FEM was used to compute the resulting stresses (see Table 3.8-7B) from the new spent fuel racks and additional stored fuel for the structural evaluation of the FHB.

3.7.2.1.3.8 Three-Dimensional Finite-Element Subsystem Models

The purpose of the subsystem analysis was to develop the stress distributions within the various subsystem assemblies resulting from the seismic-induced loads. Typical three-dimensional finite-element subsystem models were then developed for the areas of major concern. Appropriate boundary conditions were applied to the structural interfaces of the subsystem models compatible with the physical constraints present in the actual structure. The input data used in this analysis were in the form of modal force and displacement responses developed from the lumped-parameter model using the modal response spectra technique. The specific modal response characteristics such as the relative sign of the various force components within the modal force vectors were preserved by evaluating each mode independently in a mode-by-mode step procedure. The resulting stress distributions from each mode are then combined by the methods described in Paragraphs 3.7.2.1.6 and 3.7.2.1.7 and added to the seismic induced inertial effects generated within the subsystem assembly itself.

3.7.2.1.3.9 Three-Dimensional Finite-Element Models

Three-dimensional finite-element models of the safety equipment building, electrical and piping gallery structure, and condensate and refueling tank enclosure structure were developed for use in establishing both time-history acceleration response data and modal response spectra stress distributions. The use of a single model for use in the evaluation of the dynamic response characteristics of a structure was made possible by the incorporation of numerous advanced capabilities of an existing three-dimensional finite element computer code.

For these analyses the structural finite-element meshes are sized to adequately describe the structural response characteristics of the structure and to produce enough data to determine maximum stress levels. Four node quadrilateral plate elements and three node triangular elements were used for this purpose. These elements exhibit both membrane and flexural stiffness characteristics with prescribed material characteristics (i.e., density, modulus of elasticity and Poisson's ratio) and element thickness. Figure 3.7-23 gives a pictorial representation of the mathematical model for the safety equipment building while Figures 3.7-25 and 3.7-35 depict a similar pictorial representation for the electrical and piping gallery structure and condensate and refueling tank enclosure structure, respectively. Figure 3.7-24 represents a typical mesh size used in these analyses. The refueling water storage tanks and condensate tanks were modeled as beam elements with masses lumped at the nodes according to the criteria given in Reference 8. The "stick model" bases (master nodes) are multipoint constrained to the foundation slab to simulate the effect of tank stiffness upon it.

Due to the varied embedment conditions, the soil-structure interaction characteristics were modeled by a combination of three-dimensional brick elements that were multipoint constrained to a master node and a set of discrete springs attached between the master node and ground. The brick elements were assigned physical parameters consistent with the soil properties defined by the project geotechnical consultant. The set of discrete springs was so proportioned that the series combination of the spring and brick elements will produce the desired soil-structure interaction parameters defined by the project geotechnical consultant. This was verified by applying static loads to the system independently in each of the principal coordinate directions and monitoring the displacement response. For this model, a composite modal damping technique was utilized in both the time-history analysis and the response spectra analysis. The seismic stress distributions were obtained by the methods described in Paragraphs 3.7.2.1.6 and 3.7.2.1.7 using the design criteria response spectra as input.

3.7.2.1.3.10 Power Block Analysis

The model used in the analysis of the relative response between adjacent structures is shown in Figure 3.7-26. The model takes into account the fact that the site is symmetrical about the east-west centerline and therefore it is necessary to model only one-half of the total site. However, in order to obtain the complete response characteristics, two separate analyses must be performed and the results superimposed. The first analysis incorporates symmetrical boundary conditions along the plane of symmetry, while the second analysis uses the antisymmetrical boundary conditions.

Each structure was modeled as a six degree-of-freedom, rigid body attached to the appropriate soil contact surface. The nodes to which a structure is attached are therefore forced to displace (both in translations as well as rotations and in three-dimensional space) as the master node representing the building. The translational and rotational masses were applied to the building master nodes, at the elevation of the center of gravity for each structure. The soil was modeled in two ways. First a soil grid of 489 by 694 plan dimension and 80 feet deep was modeled using eight-node solid brick elements. The contact surface between the soil and each of the structures was included, in as much detail as possible. Second, the exterior boundary of the soil grid, excluding the plane of symmetry, was multipoint constrained to a master node with a set of discrete springs attached between the master node and ground. The brick elements are assigned physical parameters consistent with the soil properties defined by the project geotechnical consultant. The set of discrete springs is so proportioned that the series combination of the spring and brick elements will produce the desired soil-structure interaction parameters defined by the project geotechnical consultant.

The analyses were performed using composite modal damping and the design criteria free-field response spectra as input. The resulting relative building motions are then obtained through use of the response characteristics for the master nodes of the various buildings. A rigid body transformation is used to translate the individual building responses from the master node location (i.e., center of gravity of the structure) to the desired attachment interface location on the perimeter of the structure. Furthermore, the relative building motions are established on a mode-by-mode step procedure in order to retain the appropriate sign relationship between the

various response components. The resulting "modal" relative displacements can then be combined by use of the three-component SRSS combination technique for use in the analysis of piping systems.

Table 3.7-20A
FUEL HANDLING BUILDING
COMPARISON OF MODEL CHARACTERISTICS FOR THE ORIGINAL CONFIGURATION VERSUS THE CURRENT CONFIGURATION[a]

Direction	Frequency (Hz)		Participation Factor		Critical Damping	
	Original	Current	Original	Current	Original	Current
East-West	2.38	2.53	48.6	54.9	9.79	9.72
North-South	2.58	2.67	41.9	34.5	9.87	9.87
Vertical	2.58	2.67	10.0[b]	25.4[b]	9.87	9.87
Vertical	2.99	2.89	83.9[b]	71.5[b]	9.98	9.93
North-South	5.53	4.84	37.4	36.2	9.94	9.21
East-West	5.85	5.16	38.1	38.8	9.87	9.77

Original values in the above table are obtained from Table 3.7-10.

[a] Original Configuration: Original Spent Fuel Storage Racks
Current Configuration: New High Density Spent Fuel Storage Racks

[b] The summation of participation of vertical masses for the original and the current configurations are approximately the same. The frequencies for the two modes are closer spaced for the current evaluation which accounts for the participation shift.

A review of the mode shapes and frequencies from both the symmetrical and antisymmetric models indicated reasonable correlation with those from the individual building analyses. However, it should be emphasized that the results of these analyses were used only to establish inter-building response characteristics. For response characteristics totally within a given structure the separate building analyses are used.

3.7.2.1.4 Soil/Structure Interaction

In general, the methods used to analyze the soil-structure interaction effects are in accordance with Section 3.3 and Appendices D and H of Reference 5, with other modifiers for geometric configuration and embedment provided by the project geotechnical consultant (see Section 3.2 and Appendix E of Appendix 3.7C). Strain-dependent soil properties are introduced into the analysis by using different rates for OBE and DBE analysis.

The lumped parameter models for the containment time-history analysis utilize beam elements to model the flexibility of the basemat. Vertical and horizontal springs are distributed to the nodes in the basemat. Actual stiffness of the spring assigned to each node is determined by multiplying the appropriate total spring rate by a weighting ratio. The weighting ratio for a given node is the ratio of the effective area of the basemat represented by that node divided by the total effective area of all of the nodes. An additional rotation spring is applied at the center node. This additional spring is necessary since the couple produced by the vertical springs accounts for only a portion of the rotational stiffness. The effective spring rates are checked by applying several static loads to the model.

For three-dimensional geometrically coupled lumped parameter models in which the flexibility of the basemat is not modeled (i.e., auxiliary building and fuel handling building), the discrete springs representing the soil-structure interaction are assumed to act at the geometric center of the basemat, which is not necessarily coincident with the basemat nodal point location (center of mass). Therefore, a coordinate transformation is performed to incorporate the soil stiffness characteristics into the unconstrained system stiffness matrix of the structural system.

For three-dimensional finite-element models (i.e., safety equipment building and piping electrical junction structure), due to the varied embedment conditions, the soil-structure interaction characteristics are modeled by a combination of three-dimensional brick elements that are multipoint constrained to a master node from their exterior boundary and a set of discrete springs attached between the master node and ground. The brick elements are assigned physical parameters consistent with the soil properties. The set of discrete springs is so proportioned that the series combination of the spring and brick elements produce the desired soil-structure interaction parameters. Spring equivalence is verified by applying static loads to the system independently in each of the principal coordinate directions and monitoring the displacement response.

3.7.2.1.5 Development of Floor Response Spectra

The time-history analysis method is used to develop floor response spectra. It is described in Sections 4.2, 4.3, and 5.2 of Reference 5.

Independent analyses are performed for each of the principal coordinate directions.

Due to the geometric coupling within the structures, input in any one coordinate direction can produce response in each coordinate direction. Therefore, the response spectra represent an envelope of the response produced from the vertical excitation and a single-axis horizontal input.

The typical in structure response is an envelope of the response obtained from the SRSS combination of the vertical response and either of the single-axis horizontal responses.

3.7.2.1.6 Components of Earthquake Motion

Although independent analyses were performed for each of the three principal coordinate directions, response characteristics used in the design of Seismic Category I structures were established considering several different combination techniques for combining the responses resulting from excitation in the three independent coordinate directions. More specifically, three distinct methods were employed for the combination of seismic response characteristics. The choice of a specific technique evolved as industry and regulatory practice changed. Those structures designed early in the project utilized either a modified two-component SRSS or a two component absolute summation technique, while the structures designed most recently incorporated the three-component SRSS technique.

For the auxiliary building and fuel handling building, the resultant seismic load distributions used in design were established from the direct combination of the individual modal responses resulting from the maximum single axis horizontal excitation and the vertical excitation. This combination of individual modal responses was performed to account for modal superposition of geometrically coupled modes. In this combination technique, the sign relationship between the various response terms was maintained while considering the worst case of either a positive and negative combination of the individual modal response terms. The resulting combined individual responses were then combined by an SRSS technique.

For the following structures, the resultant seismic load distributions used in design were established by a two-component absolute summation technique considering the worst case response from a single axis horizontal excitation in combination with the vertical excitation:

- Intake Structure and Transition Section
- Containment Exterior Shell
- Safety Equipment Building
- Electric and Piping Gallery Structure

For the following structures, the resultant seismic load distributions used in design were established by a three-component SRSS combination technique considering seismic excitation in all three coordinate directions acting concurrently:

- Containment Interior Structure
- Condensate and Refueling Water Tank Enclosure Structure
- Diesel Generator Building
- Offshore Intake Conduit and Auxiliary Intake Structure

For development of in structure response spectra refer to Paragraph 3.7.2.1.5.

3.7.2.1.7 Combination of Modal Responses

In general, modal responses are combined as described in Section 4.2.1 of Reference 5. The major exception is for the auxiliary building and fuel handling building where an alternate technique was employed. This alternate procedure is discussed in depth in the third paragraph below.

In the application of the modal response spectra technique, the individual modal responses are combined by the SRSS modal summation. This method is based upon probability considerations and provides an excellent approximation of the maximum anticipated response. It takes into account the random nature of the seismic disturbance and the relatively short duration of the response, while at the same time not completely ignoring potential modal superposition. Where modal frequencies are closely spaced, the contribution from these modes are first summed using the sum of their absolute values. These results are then considered as a pseudo-mode when the overall SRSS modal summation is made. The total system response is then established by the methods described in Paragraph 3.7.2.1.6.

In the analyses of the auxiliary building and fuel handling building, the individual modal responses from the maximum single axis horizontal excitation and the vertical excitation were directly combined prior to any SRSS combination. This combination of individual modal responses was performed by the algebraic combination of the response terms, considering the worst case of either an in-phase or out-of-phase combination of the various response characteristics. This modal combination technique was employed to account for the superposition of geometrically coupled modes while at the same time preserving the relative sign relationship between the various response terms within a given mode. The resulting combined individual modal responses were then combined by an SRSS technique, as discussed in Paragraph 3.7.2.1.6.

3.7.2.1.8 Interaction of Non-Category I structures with Seismic Category I Structures

To ensure that Seismic Category I structures will perform their intended functions after a DBE, non-Category I structures are designed to meet one of the following two conditions:

A. The non-Category I structure, which is not checked for DBE equivalent loads, is sufficiently isolated from Seismic Category I structures so as to preclude interaction.

B. The non-Category I structure is analytically checked to assure that it will not collapse on or otherwise impair the integrity of adjacent Seismic Category I structures when subjected to DBE equivalent loads.

3.7.2.1.9 Effects of Parameter Variations on Floor Response Spectra

Sections 5.2 and 5.3.2 of Reference 5 describe the various considerations in the seismic analyses. These include the effects on floor response spectra of expected variations of structural properties, damping, soil properties, soil-structure interaction, etc.

3.7.2.1.10 Use of Static Load Factors

3.7.2.1.10.1 Equivalent Static Analysis for the Intake Structure

In the equivalent static load analysis, the maximum unamplified free-field acceleration levels are input statically into the structure, as equivalent inertia loadings. The structure is idealized by various two-dimensional finite-element models representing typical cross-sections through the structure, taking into account the tributary mass associated with each section. Figure 3.7-27 represents typical models used in the analysis. Soil-structure interaction characteristics are modeled as a set of discrete springs. Seismic-induced lateral soil pressure conditions are also applied. The stress distributions resulting from this analysis are then combined with the various operating loading conditions to establish the reinforcements. Justification for using the maximum unamplified free-field acceleration as the design input is provided in Paragraph 3.7.2.1.10.5.

3.7.2.1.10.2 Equivalent Static Analysis for the Offshore Conduits

For the equivalent static analysis of the offshore conduits, the calculated acceleration levels were input statically as equivalent inertia loadings. To obtain the design acceleration levels, a factor of 1.5 was applied to the peak response from the applicable project ground motion response spectra. The operating basis earthquake (OBE) and DBE loadings were determined using structural damping of 4% and 7% of critical, respectively, for the conventionally reinforced concrete sections; and 2% and 5%, respectively, for the prestressed concrete sections.

The pipe sections were analyzed as a closed ring. The stress distributions resulting from the seismic analysis were combined with the various operating loading conditions to establish the reinforcement requirements. Soil structure interaction is not expected to be significant because of the rigidity of the pipe sections, and because the completely buried pipe sections filled with water have similar mass and inertial characteristics as the displaced soil.

3.7.2.1.10.3 Equivalent Static Analysis for the Auxiliary Intake Structure

For the equivalent static analysis of the auxiliary intake structure, the calculated acceleration levels are input statically into the structure as equivalent inertia loads. To obtain the seismic loadings for structural elements subject to oscillatory motion, a factor of 1.5 was applied to the peak response from the applicable project ground motion response spectra. The OBE and DBE loadings were determined using structural damping of 4% and 7% of critical, respectively.

Stress distributions resulting from the equivalent static analysis are combined with the various operating loading conditions to establish the reinforcement requirements. Soil structure interaction will not be significant because of the select gravel backfill, the rigidity of the

structure, and the similar mass densities and inertial characteristics of the structure and the backfill.

3.7.2.1.10.4 Equivalent Static Analysis for the Box Conduits

For the equivalent static analysis, the maximum unamplified free-field acceleration levels were input statically to the box conduit cross-section as equivalent inertial loads. Seismically-induced lateral soil pressures were also applied. Seismic loads were combined with the various operating loading conditions and, in using the finite element model, the stresses were calculated and the reinforcing requirements established.

The use of unamplified free-field accelerations is justified for the following reasons: (1) the box conduit is a completely buried structure, filled with water during normal operation, and has similar mass and inertial characteristics as the displaced soil; and (2) the box conduits, being completely buried, are highly damped and thus amplification of the free-field accelerations will be insignificant.

3.7.2.1.10.5 Instantaneous Displacement Profile Analysis

The intent of this analysis is to verify the magnitude and stress distribution obtained in the previous analysis. The critical instantaneous displacement profile (CIDP) is defined as the deflected shape that the structure will assume at an instant during the earthquake, which would cause maximum stresses within the structural elements. The determination of the CIDP is made using a traveling shear-wave finite-element model and evaluating the displacement profile along the base of the structural elements in the finite-element mesh at every instant in time. The critical profile is found using maximum slope change across the profile (maximum bending) as a criterion. In the development of the CIDP, only the gross structural stiffness characteristics are included.

For a more detailed discussion please refer to Section 3.5 and Appendix H of Appendix 3.7C. Once the CIDP has been developed, it is used as a boundary displacement input to a more refined three-dimensional finite-element model. The resulting stress distributions are then combined with the lateral soil pressure conditions and compared to the stress distributions obtained in the equivalent static load analysis. The pictorial representation of the instantaneous displacement profile analysis is shown in Figure 3.7-28.

3.7.2.1.11 Method Used to Account for Torsional Effects

Torsional effects are accounted for directly in the modeling of either three-dimensional geometrically-coupled lumped-parameter models or three-dimensional finite-element models.

3.7.2.1.12 Comparison of Responses

A comparison of the results of a modal response spectrum analysis and the modal time-history analysis for the containment structure is given in Table 3.7-21.

3.7.2.1.13 Methods for Seismic Analysis of Dams

This section does not apply to this plant since there are no dams which could affect safe shutdown of the plant.

3.7.2.1.14 Determination of Seismic Category I Structure Overturning Moments

The effects of overturning moments are evaluated by the methods shown in Section 4.4 of Reference 5.

Vertical and single-axis horizontal responses are combined using the SRSS method.

3.7.2.1.15 Analysis Procedure for Damping

Incorporation of damping into the seismic analysis was accomplished by one of the following procedures. For the lumped parameter time-history analyses, the nonproportional damping technique was used. While for the three-dimensional finite-element analyses, the composite modal damping technique was employed.

The nonproportional damping technique is described in Reference 7. For this procedure, the damping characteristics of each major subsystem within a given model is defined independently and is dependent solely upon the physical characteristics of the particular subsystem and the anticipated stress levels. Application of this procedure results in equations of motion that will not uncouple in the generalized modal degrees of freedom, unless the same value of damping has been used in each subsystem. Consequently, the equations of motion must be solved using a direct integration procedure. The Newmark β method was selected for this purpose.

Table 3.7-21
CONTAINMENT STRUCTURE
DBE SEISMIC RESPONSES[a]

Eleva-tion (ft)	Horizontal Earthquake						Vertical Earthquake					
	Horizontal Response			Vertical Response			Horizontal Response			Vertical Response		
	SMIS[b]	ASHSD[c]	% Diff.[d]	SMIS[b]	ASHSD[c]	% Diff.[d]	SMIS[b]	ASHSD[c]	% Diff.[d]	SMIS[b]	ASHSD[c]	% Diff.[d]
10.5	23.27	20.67	11.2	20.76	19.03	8.3	0	0	0	21.60	18.74	13.2
35.875	24.15	22.13	8.4	20.76	19.22	7.4	0	0	0	21.69	18.81	13.3
61.25	28.83	25.73	10.8	20.76	19.44	6.4	0	0	0	21.78	18.91	13.2
86.625	33.52	30.22	9.8	20.76	19.61	5.5	0	0	0	21.83	19.03	13.4
112.0	38.06	35.50	6.7	20.76	19.73	5.0	0	0	0	21.91	19.07	13.0
140.39	44.04	41.78	5.1	--	--	--	0	0	0	21.91	19.13	12.7
177.5	52.45	50.41	3.9	--	--	--	0	0	0	21.93	19.39	11.9
Center of Basemat	22.05	20.29	8.0	0.00	0.13	--	0	0	0	21.65	21.29	1.7

(a) Units are feet/second^2
(b) Time-history response data are obtained from computer runs sequence No. F370A1A, FS07AEE and F323HLP.
(c) Response spectrum response data are obtained from computer runs sequence No. F742B65 and F694B20.
(d) With reference to SMIS.

Application of the nonproportional damping technique was restricted conservatively by the selection of soil-damping values to values that result in structural response no less than that resulting from an overall proportional modal damping of 10% for the DBE or 8% for the OBE, even though significantly larger values can be justified (see Section 3.0 and Appendix D of Appendix 3.7C). To ensure this requirement, soil damping values are first selected based upon a comparison of steady-state analyses, using various damping values, and then confirmed by comparison of in structure response spectra from proportional and nonproportional time-history analyses.

As discussed previously, the structural response of all the major structures is dominated by soil-structure interaction modes, and consequently, the overall energy dissipation characteristics of the model are controlled by the damping assigned to the soil subsystem. Therefore, the final damping values used for the soil subsystem are consistent with the preestablished upper-bound proportional damping limit of 10% of the DBE and 8% for the OBE.

The composite modal damping technique is discussed in Sections 3.2 and 3.3 of Reference 5. Again damping values are defined independently for each subsystem, based upon the physical characteristics of the particular subsystem and the predicted stress levels, but are then weighted by the response characteristics of the particular modes, which results in an equivalent diagonalized modal damping matrix. By this method, the equations of motion are uncoupled and can be solved using the normal mode solution technique. Damping values used in the soil subsystem again were restricted conservatively to 10% for the DBE or 8% for the OBE.

3.7.2.2 Reactor Coolant System

The Reactor Coolant System has been removed from service. It no longer has Design Basis, Licensing Basis, or operational functions. The information contained in this section has been updated to reflect the current status. Although this system has been removed from service, it may still contain fluids, gases, or other hazards such as energized circuits, compressed air, radioactive material, etc. Equipment may not have been physically removed from the plant. See General Arrangement Drawings, P&IDs, and One Line diagrams for the current plant configuration.

3.7.3 REFERENCES

1. Newmark, N. M. and Hall, W. J., "Seismic Design Criteria for Nuclear Reactor Facilities," Proceedings, 3rd World Conference on Earthquake Engineering Vol 2, Santiago, Chile, 1969.

2. Jennings, P. C., Housner, G. W., and Tsai, N. C., "Simulated Earthquake Motions," Earthquake .Engineering Research Laboratory, California Institute of Technology, April 1968.

3. Tsai, N. C., "Spectrum-Compatible Motions for Design Purposes," Journal of Engineering Mechanics Division, ASCE, Vol 98, EM2, April 1972.

4. McNeill, R. L., "Machine Foundations: The State-of-the-Art," Proceedings of Specialty Session 2, Seventh International Conference on Soil Mechanics and Foundation Engineering, Mexico city, Mexico, August 1969.

5. "Seismic Analyses of Structures and Equipment for Nuclear Power Plants," BC-TOP-4A, Revision 3, Bechtel Power Corporation, San Francisco, California, November 1974.

6. "Final In-Structure Response Spectra Analysis for the Containment and Interior Structure, San Onofre Nuclear Generating Station Units 2 and 3; Bechtel Power Corporation, LAPD, August 1973.

7. "Methods of Direct Application of Element Damping, San Onofre Units 2 and 3," Bechtel Power Corporation, Los Angeles office, January 1972.

8. "Nuclear Reactors and Earthquake," TID 7024, U.S. Atomic Energy Commission, Division of Technical Information, August 1963. Distributed by National Technical Information Service, U.S. Department of Commerce.

3.8 DESIGN OF CATEGORY I STRUCTURES

3.8.1 CONCRETE CONTAINMENT

Not all subsystems of the Containment System are required to support permanent plant shutdown or defueled operations. The status of these subsystems is listed in the table below. Design Basis, Licensing Basis, and operational information contained in this section has been updated to reflect the current status. Although the subsystems removed or partially removed from service no longer support operation, they may still contain fluids, gases, or other hazards such as energized circuits, compressed air, radioactive material, etc. Equipment may not have been physically removed from the plant. See General Arrangement Drawings, P&IDs, and One Line diagrams for the current plant configuration.

STRUCTURES/SYSTEMS/COMPONENTS	STATUS
High Energy Piping	Removed from Service
Containment	Partially Removed from Service
Containment Tendons	Removed from Service
Containment Liner	Removed from Service
Equipment and Personnel Penetrations	Removed from Service
Process Pipe Penetrations	Removed from Service
Electrical Penetrations	Removed from Service
Fuel Transfer Tube	Partially Removed from Service
Attachment and Brackets	Partially Removed from Service
Wall-to-Base Slab Connection	Partially Removed from Service
Buttresses	Removed from Service
Large Penetrations	Removed from Service
Temporary Construction Opening for the Steam Generator Replacement Project	Partially Removed from Service

This section describes the structural design considerations for the containment. Further information relative to the containment is covered in Topical Report BC-TOP-5[(1)] which provides the bases for design, construction, testing, and surveillance of the prestressed concrete containment.

During the Steam Generator Replacement Project (SGRP) performed in 2009 for Unit 2 and in 2010 for Unit 3, a temporary construction opening was created in the cylindrical wall of the containment building to facilitate the transfer of major equipment components out of and into the containment. This opening was closed and the containment building restored to its original design basis prior to operation of each unit. The closure of this opening and restoration of the containment is further described in the following subsections.

3.8.1.1 Description of the Containment

3.8.1.1.1 General

The basic configuration of each containment structure consists of a prestressed, reinforced concrete cylindrical structure with a hemispherical dome and a conventionally reinforced concrete basemat with a reactor cavity approximately at its center. Controlled Drawings 23000, 23101, 23102, 23104, and 23105 illustrates this configuration and also shows the relationship between the external shell and the internal floors and walls. The internal structure is separated from the shell by a nominal 6 inch peripheral gap at each floor elevation to avoid interaction between the internal structure concrete slab and the exterior shell during a seismic event. Components such as, steel grating and electrical conduits, are located within the peripheral gap. These components are provided with sufficient clearance to avoid adverse interaction. The walls are connected to the basemat by means of reinforcing steel and cadwelds welded to the liner plate. The arrangement of the containment in relation to the surrounding buildings is illustrated in Controlled Drawings 40002, 40006 and 40007. As indicated in these figures, the containment is separated from the surrounding buildings by means of a 12-inch gap to avoid any interaction with the surrounding building during a seismic event.

The dome and cylinder are reinforced with bonded reinforcing steel as required by the design loading conditions. The quantity of reinforcing steel provided satisfies the minimum requirement specified for crack control (refer to Controlled Drawings 23017, 23025, 23024, 23031 and 23032 for typical details). Additional bonded reinforcing is provided at discontinuities and around openings in the shell. A continuous tendon access gallery below the basemat is provided for installation and inspection of the vertical post-tensioning system (refer to Controlled Drawings 23011 and 23014). A welded carbon steel liner plate is provided on the inside surface of the basemat, shell wall, and dome (refer to Controlled Drawings 23040, 23044, 23053, 23059, and 23061). The basemat liner plate system is covered with concrete for protection. Typical basemat, shell wall, and dome reinforcing steel details are shown in Controlled Drawings 23017, 23025, 23024, 23031, 23032, 23011, and 23014.

Principal nominal dimensions of the containment are as follows:

Interior diameter	150 ft
Interior height (above filler slab)	170 ft
Cylindrical wall thickness	4 ft - 4 in. (nominal)
Dome thickness	Varies from 4 ft - 4 in. (nominal) at the springline to 3 ft - 9 in. (minimum) at the top of the dome
Basemat thickness	9 ft
Liner plate thickness	1/4 in.

Internal free volume	2,355,000 ft^3 (nominal)

3.8.1.1.2 Fuel Transfer Tube

A fuel transfer tube penetration is provided for refueling. An inner pipe acts as the refueling tube with an outer pipe as the housing. The tube is fitted with a gasketed blind flange in the refueling canal and a standard gate valve in the spent fuel pool. The gasketed blind flange and gate valve arrangement prevents leakage through the fuel transfer tube. The blind flange gasket is cast polyurethane with two concentric seating surfaces. Outer sleeves permit the transfer tube to penetrate the secondary shield wall, the containment shell, and the exterior wall of the fuel handling building, while maintaining a pressure-tight boundary at each wall. The sleeves are anchored into each wall, respectively, and are welded to each wall's liner plate. Sleeve bellows at the interior face of both the containment shell and the exterior wall of the fuel handling building permit thermal expansion of the transfer tube. The same expansion bellows permit differential movement between structures. Details are shown in Controlled Drawing 23065.

3.8.1.1.2.1 Attachments and Brackets

Attachments to the shell wall are brackets for support of the service polar crane, electrical conduit and cable tray, spray piping, dome lighting, dome ventilation, and safety injection valves. The polar crane support brackets consist of built-up steel plate, the top flange penetrating the thickened liner plate, and are anchored in the concrete of the shell wall.

3.8.1.1.2.2 Wall-to-Base-Slab Connection

The shell wall interface at the base slab incorporate a haunched design in order to accommodate large moments due to horizontal seismic excitation. Refer to Controlled Drawings 23017, 23024 and 23025 and Controlled Drawings 23011 and 23014, for details of the lower wall configuration.

3.8.1.2 Applicable Codes, Standards, and Specifications

The following codes, standards, regulations, specifications, design criteria, and NRC Regulatory Guides constitute the basis for the design, fabrication, construction, testing, and inservice inspection of both containment structures. Modifications to these codes, standards, etc., are made when necessary to meet the specific requirements of the structure. These modifications are indicated in the sections where references to the codes, standards, etc., are made.

3.8.1.2.1 Codes

A. Uniform Building Code (UBC), 1970 Edition

B. American Institute of Steel Construction (AISC), Manual of Steel Construction, 1970 Edition

C. American Concrete Institute (ACI) 318-71, Building Code Requirements for Reinforced Concrete

D. American Society of Mechanical Engineers (ASME), Boiler and Pressure Vessel Code, 1971 Edition and Addenda through Winter 1972

1. Section II, Material Specifications - Part A - Ferrous

2. Section III, Nuclear Power Plant Components, Division 1

3. Section V, Nondestructive Examination

4. Section VIII, Pressure Vessels, Division 1

5. Section IX, Welding and Brazing Qualifications

E. American Welding Society (AWS), AWS D1.1-72, Structural Welding Code

3.8.1.2.2 Standards and Regulations

A. Occupational Safety and Health Act (OSHA)

B. State of California, Division of Industrial Safety, General Industry Safety Orders

C. Property Loss Prevention Standard for Nuclear Generating Stations, Nuclear Mutual Limited (NML), June 1974 Edition.

D. National Fire Protection Association (NFPA), NFPA No. 24, 1973 Edition, Outside Protection.

3.8.1.2.3 Specifications

A. Industry Specifications

1. American Society for Testing and Materials (ASTM)

ASTM standard specifications are used whenever possible to describe material properties, testing procedures, and fabrication and construction methods. The standards used and the exceptions to these standards, if any, are identified in the applicable sections.

2. American Concrete Institute (ACI), ACI 301, Specification for Structural Concrete for Buildings, May 1972

3. American Iron and Steel Institute (AISI), Specification for the Design of Light Gage, Cold-Formed Steel Structural Members, 1968 Edition

4. Crane Manufacturers Association of America (CMAA), CMAA Specification No. 70, 1971

B. Project Design and Construction Specifications

Project design and construction specifications are prepared to cover the areas related to design and construction of the containment. These specifications, prepared specifically for the San Onofre Nuclear Generating Station, Units 2 and 3, emphasize important points of the industry standards for the design and construction of the containment and reduce options that otherwise would be permitted by the industry standards. Unless specifically noted otherwise, these specifications do not deviate from the applicable industry standards. They cover the following subject headings:

1. Excavation and Backfill

2. Concrete Placement

3. Inspection of Concrete Production

4. Reinforcement Steel Placement

5. Structural Steel Erection

6. Miscellaneous Metalwork Installation

7. Stainless Steel Liner Plate System Installation

8. Post-tensioning System Embedded Items Installation

9. Concrete and Concrete Products

10. Reinforcing Steel and Associated Products

11. Prestressing Steel and Related Accessories

12. Structural Steel

13. Miscellaneous Steel and Embedded Materials

14. Stainless Steel Liner Plate

15. Containment Polar Cranes

16. Containment Liner plate System including Locks and Hatches

17. Fuel transfer tube.

Design Criteria

A. Project Design Criteria

Project design criteria included comprehensive design requirements of the containment. The criteria contained specific references to prescribed Bechtel internal design guides, applicable industry standards, and pertinent technical texts, journals, and published reports.

B. Bechtel Topical Reports

1. BC-TOP-1, Containment Building Liner Plate Design Report, Revision 1, December 1972 with additional information dated September 1973

2. BC-TOP-4, Seismic Analysis of Structures and Equipment for Nuclear Power Plants, Revision 1, September 1972

3. BC-TOP-5-A, Prestressed Concrete Nuclear Reactor Containment Structures, Revision 1, February 1972

4. BC-TOP-7, Full-Scale Buttress Test for Prestressed Nuclear Containment Structures, August 1971 (reprinted September 1972)

5. BC-TOP-8, Tendon End Anchor Reinforcement Test, November 1971

6. BC-TOP-9A, Design of Structures for Missile Impact, Revision 2, September 1974

7. BN-TOP-1, Testing Criteria for Integrated Leakage Rate Testing of Primary Containment Structures for Nuclear Power Plants, Revision 1, November 1972

8. BN-TOP-2, Design for Pipe Break Effects, Revision 1, September 1973

9. BP-TOP-1, Seismic Analysis of Piping Systems, Revision 0, April 1973

10. BC-TOP-5-A, Prestressed Concrete Nuclear Reactor Containment Structures, Revision 3, February 1975

C. Project Reports

1. Seismic and Foundation Studies, April 15, 1970, Dames and Moore

2. Methods of Direct Application of Element Damping - San Onofre Units 2 and 3, January 1972, Bechtel Power Corporation, Los Angeles office

3. Development of Soil-Structure Interaction Parameters, Proposed Units 2 and 3 San Onofre Generating Station, January 31, 1974, Woodward-McNeill & Associates

4. Elastic and Damping Properties, Laydown Area, San Onofre Nuclear Generating Station, Woodward-McNeill & Associates, Orange, CA, October 14, 1971

5. Preliminary Safety Analysis Report - San Onofre Units 2 and 3

3.8.1.3 Loads and Load Combinations

3.8.1.3.1 Load Definitions

The containment is designed for all credible loading conditions. The design load categories are identified as preoperational pressure test loads, normal loads, severe environmental loads, extreme environmental loads, and abnormal loads.

3.8.1.3.1.1 Preoperational Pressure Test Load

Upon completion of construction, the containment and its penetrations were tested at 115% of the design LOCA pressure as discussed in Paragraph 3.8.1.7.1.

3.8.1.3.1.2 Normal Loads

Normal loads are those loads to be encountered during normal plant operation and shutdown. They include:

A. Dead Loads

Dead load consists of the weight of the concrete wall, dome, base slab, steel, and permanently attached equipment. In addition, dead load includes hydrostatic loads that consist of lateral hydrostatic pressure resulting from ground or flood water, as well as buoyant forces resulting from the displacement of ground water or flood water by the structure.

B. Live Loads

Live loads consist of any movable equipment loads and other loads with variable intensity and occurrence, such as soil pressures.

C. Prestressing Loads

Prestressing loads consist of the compressive forces due to prestressing tendons.

3.8.1.3.1.3 Severe Environmental Loads

Severe environmental loads are those loads that could infrequently be encountered during the plant life. Included in this category are:

A. Operating Basis Earthquake (OBE)

The OBE consists of a static equivalent seismic load for which the dynamic effects have been included in its determination. A more detailed discussion is presented in Subsection 3.7.1.

B. Wind Loads

Refer to Subsection 3.3.1 for a detailed description of wind loads.

3.8.1.3.1.4 Extreme Environmental Loads

Extreme environmental loads are those loads that are credible but are highly improbable. They include the following:

A. Design Bases Earthquake (DBE)

The DBE consists of a static equivalent seismic load for which the dynamic effects have been included in its determination. A more detailed discussion is presented in Subsection 3.7.1.

B. Tornado Loads

Tornado loads consist of the combined effects of tornado wind pressure, pressure differential, and missile impingement. Refer to Subsection 3.3.2 for a detailed description.

3.8.1.3.1.5 Abnormal Loads

Abnormal loads are those loads generated by a postulated high-energy pipe break accident within a building and/or compartment thereof. NOTE: Abnormal loads listed below are no longer applicable following cessation of power operation and permanent plant shutdown of the units.

Abnormal Loads
Pipe Rupture and Miscellaneous Missile Loads
Design Pressure Load
Abnormal Thermal Loads
Abnormal Pipe Expansion Loads

3.8.1.3.2 Load Combinations

Two types of loading cases are considered in the design of the containment:

A. The service load conditions for which the working stress method is used.

B. The factored load conditions for which the strength design method is used.

The following nomenclature is used in the loading combination equations:

C = required capacity of the containment to resist factored loads

ϕ = capacity reduction factor (defined in Paragraph 3.8.1.3.2.3)

D = dead loads

L = appropriate live load

F_T = prestress at transfer load

F = sustained prestress load

T_o = normal thermal loads*

H_o = normal pipe expansion load*

E = operating basis earthquake load

W = wind load

E' = design basis earthquake load

W_T = tornado load

R = pipe rupture and miscellaneous missile loads

P = LOCA or MSLB pressure load*

P_T = preoperational pressure test load*

T_A = abnormal thermal loads*

H_A = abnormal pipe expansion load*

*These loads are no longer applicable following cessation of power operation and permanent plant shutdown of the units.

3.8.1.3.2.1 Service Load Conditions

A. Preoperational Pressure Test Case

$D + F + P_T$

B. Normal Case

$D + F + L + T_o$

C. Abnormal Case

$D + F + L + P + T_A$

3.8.1.3.2.2 Factored Load Conditions

A. Abnormal Case

$1.0\ D + 1.5\ P + 1.0\ T_A + 1.0\ F$

B. Abnormal/Severe Environmental Case

$1.0\ D + 1.25\ P + 1.0\ T_A + 1.0\ H_A + 1.25\ E + 1.0\ F$

C. Abnormal/Severe Environmental Case

$1.0\ D + 1.25\ P + 1.0\ T_o + 1.25\ H_o + 1.25\ E + 1.0\ F$

D. Abnormal/Severe Environmental Case

$1.0\ D + 1.0\ H_A + 1.0\ R + 1.0\ F + 1.25\ E + 1.0\ T_A$

E. Abnormal/Severe Environmental Case

$1.0\ D + 1.25\ H_o + 1.0\ R + 1.0\ F + 1.25\ E + 1.0\ T_o$

F. Abnormal/Extreme Environmental Case

$1.0\ D + 1.0\ P + 1.0\ T_A + 1.0\ H_A + 1.0\ E' + 1.0\ F$

G. Abnormal/Extreme Environmental Case

$1.0\ D + 1.0\ P + 1.0\ T_o + 1.25\ H_o + 1.0\ E' + 1.0\ F$

H. Abnormal/Extreme Environmental Case

$1.0\ D + 1.0\ H_A + 1.0\ R + 1.0\ E' + 1.0\ F + 1.0\ T_A$

I. Abnormal/Extreme Environmental Case

$1.0\ D + 1.25\ H_o + 1.0\ R + 1.0\ E' + 1.0\ F + 1.0\ T_o$

J. Extreme Environmental Case

$1.0\ D + 1.25\ H_o + 1.0\ F + 1.0\ T_o + 1.0\ W_T$

3.8.1.3.2.3 Capacity Reduction Factors

The capacity reduction factor provides for the possibility that small adverse variations in material strengths, workmanship, dimensions, control, and degree of supervision, while individually within required tolerances and the limits of good practice, occasionally may combine to result in undercapacity. It is applied to the ultimate strength capacity of the section being designed and to the allowable stresses. Capacity reduction factors are:

ϕ = 0.90 for concrete in flexure with or without axial tension

ϕ = 0.85 for shear and torsion

ϕ = 0.75 for spirally reinforced concrete compression members

ϕ = 0.70 for tied compression members

ϕ = 0.90 for reinforcing steel in direct tension

ϕ = 0.90 for mechanical splices of reinforcing steel

ϕ = 0.95 for prestressed tendons in direct tension

For members subject to flexure and axial compression, the provisions of ACI 318-71 apply.

3.8.1.4 Design and Analysis Procedures

The containment was analyzed for various loading combinations, considering the values of individual loads that generate the most significant stress condition for each component and member of the structure.

The critical areas for analysis are the basemat, the intersection between cylinder wall and basemat, the liner plate system, the tendon anchorage zones, and the penetration openings.

Computer programs were relied upon to perform many of the computations required for the containment analysis. However, classical theory, empirical equations, and numerical methods were applied as necessary for analysis of localized areas and for preliminary proportioning. They are described in Subsection 7.1 of BC-TOP-5.[1]

The design methods incorporate several phases as described in Sections 6.2 and 6.3, of BC-TOP-5. Improved assumptions as to material properties, including the effects of creep, shrinkage, and cracking on concrete, are used in design. Analysis and design of tendon anchorage zones and reinforcement in buttresses are discussed in Section 6.6 of BC-TOP-5, BC-TOP-7,[2] and BC-TOP-8.[3] The method of analyzing the effects of penetrations, the thickening of walls, reinforcements, and embedments, etc., is discussed in Section 7.3 of BC-TOP-5. The design of the liner and its anchorage system is covered in BC-TOP-1[4] and Section 7.5 of BC-TOP-5. Information on analyses for computation of seismic loads is provided in Section 3.7.

3.8.1.4.1 Analytical Techniques

The analysis of the containment consists of two parts, the overall analysis of the containment and the local analysis. The overall analysis, given axisymmetric loads, is performed by utilizing the FINEL finite-element computer program for combinations of the individual loading cases of dead, live, thermal, pressure, and pre-stress loads (see Subsection 7.2.1 of BC-TOP-5). In the case of nonaxisymmetric loads; i.e., seismic loads, the analysis is performed using the ASHSD finite-element computer program (see Subsection 7.2.2, BC-TOP-5).

The axisymmetric finite-element representation of the containment assumes that the structure is axisymmetric. This does not account for the buttresses, penetrations, brackets, and liner plate anchors. These items are considered in the local analysis using either computer programs; e.g., equipment hatch analysis, or principles of structural analysis; e.g., polar crane bracket analysis.

In addition, some of the design; e.g., buttresses, BC-TOP-5, Subsection 6.6.2, and BC-TOP-7, is based on test results.

3.8.1.4.1.1 Overall Analysis

The containment is considered an axisymmetric structure for the overall analysis (Subsection 7.2.1, BC-TOP-5). Although there are deviations from this ideal shape, the deviations are usually localized and can be handled by special analyses; hence, axisymmetric analyses are considered acceptable.

The overall analysis of the containment, given the application of axisymmetric loads, is performed by Bechtel's nonlinear FINEL finite-element computer program (BC-TOP-5, Section 7.1.2). A detailed description of this program is provided in Appendix 3C, Section 3C.1. The entire containment is modeled with one finite-element mesh consisting of the shell wall, basemat, internal structure, and soil.

The entire concrete structure is modeled by continuously interconnected elements. The geometry of the mesh allows the representation of reinforcing steel superimposed on the corresponding concrete elements.

The liner plate is simulated by a layer of elements attached to the interior surfaces of the concrete structure.

The finite-element mesh of the structure is extended into the soil to account for the elastic nature of the soil material and its effect on the behavior of the basemat. The tendon access gallery is analyzed as a separate structure.

The use of the nonlinear finite-element analysis permits accurate determination of the stress pattern at any location of the structure.

The FINEL finite-element mathematical model for axisymmetric loads is shown on Controlled Drawings 23520, 23521, 23522, and 23523.

The overall analysis of the containment, given the application of non-axisymmetric loads, is performed by Bechtel's linear elastic ASHSD finite-element computer program. A detailed description of this program is provided in Appendix 3C, Section 3C.2. Details of the seismic analysis are described in Section 3.7. Wind and tornado loadings are discussed in Subsections 3.3.1 and 3.3.2.

3.8.1.4.1.2 Local Analysis

The local analyses of the containment include the following:

A. Buttress and Tendon Anchorage Zones

The containment has three buttresses. At each buttress, two out of any group of three hoop tendons are anchored on the opposite faces of the buttress, with the third tendon continuous through the buttress.

Between the opposite anchorages in the buttress, the compressive forces exerted by the anchored tendons are larger than elsewhere in the shell wall. This value, combined with the effect of the tendon, which is continuous throughout the buttress, is 1.5 times the prestressing forces acting outside the buttress. The thickness of the buttress is approximately 1.5 times the thickness of the wall. Hence, the hoop stresses and strains, as well as the radial displacements, may be considered as being nearly constant all around the structure.

The design of the tendon anchorage zones is based on two test programs conducted by Bechtel to demonstrate the adequacy of several reinforcing patterns for use in anchorage-zone concrete in the basemat and buttresses. These tests have been undertaken to develop a more efficient design to reduce reinforcement congestion, and thereby facilitate the placement of high quality concrete around the tendon anchorages. The test programs are as follows:

1. A full-scale model of a simulated containment buttress containing several patterns of reinforcement and types of tendon anchorages was constructed and tested. A detailed description of the test is presented in BC-TOP-7.[(2)]

2. Two large concrete test blocks containing two patterns of reinforcement with different proportions of reinforcing bars were constructed and tested. A detailed description of the test is presented in BC-TOP-8.[(3)]

The test results demonstrate satisfactory performance of the test anchorages. The design of the tendon anchorage zones is based on the results and recommendations of these tests.

B. Large Penetration Openings

Large penetrations are defined as those having an inside diameter equal to or greater than 2.5 times the containment nominal shell wall thickness. The equipment hatch falls into this category.

The stresses at the opening are predicted by an analysis performed using Bechtel's computer program SAP, described in Appendix 3C, Section 3C.5, which is capable of performing a static analysis of linear elastic three-dimensional structures utilizing the finite-element method. The points delineating the outermost boundaries of the analytical model are located at approximately two penetration diameters beyond the center of the opening, so that the behavior of the model along the boundaries is compatible with that of the undisturbed cylindrical wall.

Typical details of the equipment hatch are shown in Controlled Drawings 23017 and 23025. Figure 3.8-15 shows the equipment hatch boundary conditions. Figure 3.8-16 shows the finite-element model geometry. Figure 3.8-17 shows the finite-element mesh for truss elements and brick elements, used for the analyses of the equipment hatch. The brick elements are used to model the concrete, and the truss elements are used to represent the post-tensioning system. Figure 3.8-18 shows a section through the equipment hatch wall showing the layered elements.

C. Small Penetration Openings

Small penetration openings are defined as those having an inside diameter less than 2.5 times the containment nominal shell wall thickness. The stresses at the openings due to applied moments and forces are determined using the methods outlined in Reference 5.

Results of these analyses show the stresses to be well within the allowable limits. Typical details of small penetrations are shown in Controlled Drawings 23054 and 23055.

D. Temporary Construction Opening for SGRP

The containment structure was reanalyzed for the effects of the creation and closure of the temporary construction opening. This re-analysis of the containment was performed using the methods for evaluating large penetration openings contained in reference 5. The analysis was performed with the ANSYS finite-element computer program. The entire shell above the basemat was modeled with a 3D finite-element mesh consisting of plate elements and the explicit modeling of tendons using truss elements. Load redistributions due to the creation of the temporary opening and the creep and shrinkage effects of the restored concrete were evaluated.

A plan and elevation drawing of the containment structure hatches and locks is provided in Controlled Drawing 23063. The personnel lock and escape lock are illustrated in greater detail in Figures 3.8-20 and 3.8-21, respectively.

3.8.1.4.1.3 Variations in Analytical Assumptions and Material Properties

The treatment of the effects of expected variations in assumptions and material properties on the analysis results is discussed in Paragraphs 3.7.2.1.9 and 3.8.1.3.2.3.

Table 3.8-1
ALLOWABLE STRESSES AND STRAINS

Loading Condition	Allowables		
	Concrete	Reinforcement	Liner
	$(f'_c)90 = 6$ k/in.^{2}	$f_y = 60$ k/in.^{2}	$f_y = 24$ k/in.^{2} and 38 k/in.^{2}
At transfer of prestress	Mem. = $0.3\ f'_c$		
	Mem. + Bend. = $-0.6\ f'_c$	$f_s = \pm 0.5\ f_y$	$f_s = 0.5\ f_y$ (ten.)
	Memb. Ten. = $\sqrt{f'_c}$		$\gamma_s = 0.004$ (Comp.)
Design loads	Mem. + Bend. = $-0.6\ f'_c$	$f_s = \pm 0.5\ f_y$	$f_s = 0.5\ f_y$ (Ten.)
	Mem. Ten. = 0		$\gamma_s = 0.004$ (Comp.)
Factored loads[a]	Mem. + Bend. = $-0.9\ f'_c$		
	Comp. Strain = -0.003	$f_s = \pm 0.9\ f_y$	$\gamma_s = \pm 0.005$

[a] In the San Onofre Units 2 and 3 PSAR, the capacity reduction factors were applied to the loading combinations. In this table, the capacity reduction factors are applied to the allowable stresses.

3.8.1.4.2 Description of Computer Programs

Computer programs used in the design and analysis of the containment are described in Appendix 3C.

3.8.1.5 Structural Acceptance Criteria

The fundamental acceptance criterion for the containment as a prototype is the successful completion of the structural integrity test, with measured responses within the allowable limits, including strain measurements in the concrete sufficient to permit a complete evaluation of strain distribution at prescribed locations. Strain measurements are taken with the exception that no measurement is taken under a vertical tendon anchor, since full-scale tests on the size of tendon used have shown the adequacy of the anchorage system as discussed in BC-TOP-7[2] and BC-TOP-8.[3] The limits for allowable values for stress and strain are given in Table 3.8-1. In this way, the margins of safety associated with the design and construction of the containment are, as a minimum, the accepted margins associated with nationally recognized codes of practice. The accepted margins will be compatible with the provisions of ASME Section III, Division I, and the ACI 318-71 codes. In addition, the measured responses are compared to those predicted by the analyses.

The structural integrity test is planned to yield information on both the overall response of the containment and the response of localized areas, such as major penetrations and buttresses, which are important to the design functions, of the containment.

The design and analytical methods, as well as the type of construction and construction materials, are chosen to allow assessment of the capability of the structure throughout its service life. Additionally, surveillance testing provides further assurances of the continuing ability of the structure to meet its design functions.

Table 3.8-2 shows the calculated stresses and strains, respectively, as well as the allowables, taken from critical sections of the containment structure. The ratios of the allowable stresses and strains to the calculated stresses and strains yield the margins of safety at selected critical sections.

Similar to the original containment structure evaluation, the provisions of the ASME Section III, Division I and ACI 318-71 codes are used to evaluate the containments' structural integrity following restoration of the SGRP temporary construction opening. Tables 3.8-2A and 3.8-2B show the Unit 2 and 3 calculated stresses and strains, as well as the allowables, for the containment restored condition, post-SGRP, at locations within or immediately adjacent to the restored opening area. In addition, interaction diagram at these locations are provided in Figure 3.8-22.

Interaction diagrams for each critical section identified in Table 3.8-2, together with a graphical plot of the actual axial load with its accompanying moment for each principal load combination are furnished in Figure 3.8-22.

The effect of three-dimensional stress/strain fields on the behavior of the structure has been considered in the FINEL computer program described in Appendix 3C, Subsection 3C.1.

LOADING CONDITIONS[A]	LOADING COMBINATIONS[A]	ANALYSIS PERFORMED (YES OR NO)
AT TRANSFER OF PRESTRESS	$D + F_T$	YES
LOAD UNDER SUSTAINED PRESTRESS	D + F	NO[B]
PREOPERATIONAL PRESSURE TEST	$D+F+P_T$	YES
SERVICE LOADS	$D+F+T_O$	YES
	$D+F+T_A+P$	YES
FACTORED LOADS	$D+F+T_A+1.5P$	YES
	$D+F+T_A+1.25P+1.25E$	YES
	$D+F+T_O+1.25P+1.25E$	NO[C]
	$D+F+T_A+1.25E$	YES
	$D+F+T_O+1.25E$	NO[C]
	$D+F+T_A+P+E'$	YES
	$D+F+T_O+P+E'$	NO[C]
	$D+F+T_A+E'$	YES
	$D+F+T_O+E'$	NO[C]
	$D+F+T_O+W_T$	NO[D]

NOTATION

D = DEAD LOAD
E = OPERATING BASIS EARTHQUAKE
E' = DESIGN BASIS EARTHQUAKE
F = PRESTRESS LOAD
F_T = PRESTRESS AT TRANSFER
P = LOCA/MSLB PRESSURE LOAD
P_T = PREOPERATIONAL PRESSURE TEST LOAD
T_A = ABNORMAL THERMAL LOAD
T_O = NORMAL THERMAL LOADS
W_T = TORNADO LOAD

[A] Loading conditions and corresponding loading combinations are taken from Paragraphs 3.8.1.3.2.1 and 3.8.1.3.2.2 and since they are intended to reflect an overall stress and strain distribution, they exclude the local effects of live load (L), normal and abnormal pipe reaction loads (H_O and H_A), and pipe rupture and miscellaneous missile loads (R).

[B] The case of loading under sustained prestress was not analyzed since concrete stresses will be lower than the preceding case. Reinforcement stresses will be higher however, but they are mainly compressive and are well within the allowable limits. Liner plate stresses also will be higher (in compression); however, liner stresses and strains under sustained prestress (including creep and shrinkage effects) have already been evaluated and taken into account per Bechtel Topical Report (BC-TOP-1)

[C] Each of these loading cases is less critical than the preceding one since accident thermal effects are more significant.

[D] The effects of tornado loads were previously evaluated and were found to be less critical than the seismic forces. Thus, this loading case is, for example, less critical than that of the last case analyzed.

Table 3.8-2

STRESS ANALYSIS RESULTS (Sheet 1 of 10)

FINAL ANALYSIS LOADING COMBINATIONS
OF CONTAINMENT SHELL
(Refer to Figure 3.8-51 for the Key Elevation
that shows the location of the twelve reference sections)

The following notes are common to all tabular material on sheets 2 through 10:

1. Results given in tables are from the nonlinear finite element analysis except for the seismic loads.

2. Seismic analysis results are taken from San Onofre 2 and 3 preliminary containment analysis and superimposed on finite element analysis results.

3. Only the compressive concrete stresses are included.

4. Fully cracked sections are shown thus (*). Partially cracked sections are not indicated.

5. Deflections for the basemat are vertical; for the wall radial. Deflections for the dome are normal to the surface.

6. Radial shears and deflections do not include the effects of seismic loads.

7. Allowable stresses are based on songs 2 and 3 psar except for the liner allowable compressive strains shown in the tables, which are based on ASME Code, Section III, Division 2.

8. Material properties are:
   - $f'c$ = 6 ksi = compressive strength of concrete (90 days)
     <u>Exception</u>: $f'c$ = 4 ksi (28 DAYS), Three 24" diameter construction vent plugs, See Dwg # 23060
   - f_y = 60 ksi = reinforcement yield strength
   - f_y = 24 ksi = 1/4 inch liner plate yield point
   - f_y = 38 ksi = yield point of liner plate greater than 1/4 inch

9. SIGN CONVENTIONS ARE:

STRESSES AND STRAINS	(+) TENSILE	(-) COMPRESSIVE
DEFLECTIONS	(+) OUTWARD	(-) INWARD
SECTION AXIAL FORCES	(+) TENSILE	(-) COMPRESSIVE
MOMENTS	(+) TENSION	(-) COMPRESSION
	ON THE OUTSIDE FACE	ON THE OUTSIDE FACE

Table 3.8-2
STRESS ANALYSIS RESULTS (Sheet 2 of 10)
DEAD LOAD + PRESTRESS AT TRANSFER LOAD
($D + F_t$)

PORTION	SECTION	CONCRETE STRESS		LINER STRAINS		REINFORCING STRESS				SECTION RESULTANTS					DEFLECTION
						INSIDE		OUTSIDE							
		MER PSI	HOOP PSI	MER X 10^{-6} IN./IN.	HOOP X 10^{-6} IN./IN.	MER KSI	HOOP KSI	MER KSI	HOOP KSI	MER FORCE K/FT	HOOP FORCE K/FT	MER MOMENT K/FT/FT	HOOP MOMENT K/FT/FT	RADIAL SHEAR K/FT	INCHES
ALLOWABLE		-3600	-3600	+400 -2000	+400 -2000	±30	±30	±30	±30	--	--	--	--	--	--
DOME	1	-893	-890	-210	-200	-4.6	-4.5	-4.7	-4.7	-504	-500	15	22	-2	-0.60
	2	-1190	-1050	-270	-250	-6.1	-5.3	-6.5	-5.0	-662	-585	13	49	13	-0.46
	3	-1270	-1070	-310	-260	-6.5	-5.3	-5.1	-5.0	-641	-590	95	57	6	-0.21
WALL	4	-1070	-1211	-250	-290	-5.3	-6.5	-5.0	-6.2	-652	-769	116	95	24	-0.20
	5	-1090	-1542	-240	-360	-4.5	-8.7	-5.2	-8.3	-687	-1004	-19	80	6	-0.27
	6	-1100	-775	-220	-190	-5.2	-3.8	-6.2	-3.6	-709	-521	-47	33	-38	-0.13
	7	-1550	-495	-450	-180	-5.9	-0.7	-0.7	-0.1	-698	-288	1110	302	13	-0.03
BASE SLAB	8	-253	-140	-30	-50	-1.4	-0.5	5.1	0.5	-20	-55	643	264	47	0.20
	9	-192	-101	-30	-60	-1.0	-0.3	0.7	0.2	-28	-33	410	188	-34	0.26
	10	-44	-39	-10	-10	-0.2	-0.2	0.2	0	-20	-28	95	52	2	0.27
REACTOR CAVITY	11	-83	-24	-10	-10	-0.4	0	-0.5	0	-70	-21	-12	2	18	0.27
	12	-4	5	0	0	0	0.1	0.2	0.1	9	7	20	-2	21	0.27

Table 3.8-2
STRESS ANALYSIS RESULTS (Sheet 3 of 10)
DEAD LOAD + PRESTRESS LOAD + PREOPERATIONAL PRESSURE TEST LOAD
($D + F + P_T$)

PORTION	SECTION	CONCRETE STRESS		LINER STRAINS		REINFORCING STRESS				SECTION RESULTANTS					DEFLECTION
						INSIDE		OUTSIDE							
		MER PSI	HOOP PSI	MER X 10^{-6} IN./IN.	HOOP X 10^{-6} IN./IN.	MER KSI	HOOP KSI	MER KSI	HOOP KSI	MER FORCE K/FT	HOOP FORCE K/FT	MER MOMENT K/FT/FT	HOOP MOMENT K/FT/FT	RADIAL SHEAR K/FT	INCHES
ALLOWABLE		-3600	-3600	+400 -2000	+400 -2000	±30	±30	±30	±30	--	--	--	--	--	--
DOME	1	-154	-151	-19	0	-0.5	-0.5	-0.8	-0.8	-74	-71	-9	-8	-1	-0.20
	2	-405	-269	-73	-62	-1.9	-2.0	-2.4	-1.1	-212	-147	-9	15	11	-0.13
	3	-378	-139	-85	-34	-2.1	-0.3	-1.8	-0.3	-196	-72	25	12	2	-0.01
WALL	4	-358	-128	-80	-32	-2.1	-0.3	-1.8	-0.3	-208	-73	49	20	4	-0.01
	5	-404	-177	-91	-43	-2.3	-0.5	-1.9	-0.5	-242	-105	32	19	0	-0.02
	6	-785	-309	18	-30	-0.5	-1.0	-4.7	-1.0	-264	-160	-260	-33	25	-0.03
	7	-527	-156	343	151	-0.9	-0.1	-3.4	-0.5	-284	-21	-509	-48	104	-0.01
BASE SLAB	8	-353	-62	563	128	13.9	-0.3	-2.3	2.8	9	48	-1082	55	-197	0.10
	9	-702	-374	-242	-124	-3.6	-1.0	8.7	3.0	-75	-11	1277	616	-123	0.47
	10	-331	-161	-94	-47	-1.9	-0.5	4.1	0.7	-25	-28	687	279	39	0.57
REACTOR CAVITY	11	-199	-7	-32	0	-1.0	0.3	-1.3	0.2	-165	0	-38	-7	42	0.58
	12	101	95	25	25	0.5	0.5	0.7	0.6	98	98	3	-6	6	0.58

Table 3.8-2
STRESS ANALYSIS RESULTS (Sheet 4 of 10)
DEAD LOAD + PRESTRESS LOAD + NORMAL THERMAL LOAD
($D + F + T_o$)

PORTION	SECTION	CONCRETE STRESS		LINER STRAINS		REINFORCING STRESS				SECTION RESULTANTS					DEFLECTION
						INSIDE		OUTSIDE							
		MER PSI	HOOP PSI	MER X 10^{-6} IN./IN.	HOOP X 10^{-6} IN./IN.	MER KSI	HOOP KSI	MER KSI	HOOP KSI	MER FORCE K/FT	HOOP FORCE K/FT	MER MOMENT K/FT/FT	HOOP MOMENT K/FT/FT	RADIAL SHEAR K/FT	INCHES
ALLOWABLE		-3600	-3600	+400 -2000	+400 -2000	±30	±30	±30	±30	--	--	--	--	--	--
DOME	1	-1490	-1488	-450	-450	-6.7	-6.7	0.2	0.3	-438	-440	371	378	-2	-0.40
	2	-1720	-1656	-510	-500	-8.0	-7.3	-1.3	0	-576	-514	369	401	11	-0.29
	3	-1880	-1639	-550	-500	-8.5	-7.0	0	0.3	-559	-491	456	418	3	-0.10
WALL	4	-1650	-1817	-490	-530	-7.7	-8.9	-1.5	-2.6	-570	-671	526	554	15	-0.10
	5	-1610	-2119	-480	-600	-7.3	-11.0	-0.2	-2.4	-604	-873	467	562	8	-0.17
	6	-1600	-1345	-480	-420	-8.4	-7.0	-0.9	-3.0	-626	-594	513	343	-41	0.02
	7	-1830	-829	-590	-320	-7.1	-2.7	0.4	0.5	-614	-277	1512	807	26	0.10
BASE SLAB	8	-651	-388	-210	-160	-4.6	-2.5	5.2	3.4	-217	-120	1256	518	25	0.22
	9	-923	-548	-340	-230	-6.3	-3.3	3.5	2.6	-307	-162	1462	926	-60	0.23
	10	-680	-418	-240	-180	-5.2	-3.1	0.8	2.3	-333	-144	1202	754	-11	0.22
REACTOR CAVITY	11	34	(*)	20	80	-0.1	2.3	0.4	4.2	22	38	-16	-28	39	0.23
	12	89	85	-100	-90	-0.3	-0.3	8.8	7.6	40	34	101	85	22	0.25

Table 3.8-2
STRESS ANALYSIS RESULTS (Sheet 5 of 10)
DEAD LOAD + PRESTRESS LOAD + LOCA/MSLB PRESSURE LOAD + ABNORMAL THERMAL LOAD
($D + F + P + T_A$)

PORTION	SECTION	CONCRETE STRESS		LINER STRAINS		REINFORCING STRESS				SECTION RESULTANTS					DEFLECTION
						INSIDE		OUTSIDE							
		MER PSI	HOOP PSI	MER X 10^{-6} IN./IN.	HOOP X 10^{-6} IN./IN.	MER KSI	HOOP KSI	MER KSI	HOOP KSI	MER FORCE K/FT	HOOP FORCE K/FT	MER MOMENT K/FT/FT	HOOP MOMENT K/FT/FT	RADIAL SHEAR K/FT	INCHES
ALLOWABLE		-3600	-3600	+400 -2000	+400 -2000	±30	±30	±30	±30	--	--	--	--	--	--
DOME	1	-845	-830	-380	-380	-1.8	-1.7	8.5	8.6	-115	-114	211	212	-1	0.13
	2	-1370	-1364	-500	-510	-5.4	-4.1	1.3	7.4	-257	-216	377	355	8	0.14
	3	-1510	-905	-550	-420	-5.3	-1.0	7.3	10.0	-242	-113	384	248	-1	0.22
WALL	4	-1400	-1012	-510	-430	-5.8	-2.3	0.7	7.7	-255	-157	469	313	2	0.21
	5	-1620	-1256	-570	-490	-6.3	-3.6	6.7	8.4	-289	-189	535	397	-3	0.17
	6	-1150	-1620	-430	-540	-5.2	-7.9	-0.4	-0.5	-311	-451	410	546	25	0.11
	7	-404	-504	-90	170	-1.8	-2.0	-2.4	1.4	-322	-71	47	425	138	0.13
BASE SLAB	8	-251	-206	-180	-60	4.8	-2.2	-1.7	5.7	-124	-32	-556	262	-191	0.12
	9	-1240	-690	-470	-300	-7.8	-3.5	9.7	5.7	-267	-118	2054	1157	-140	0.40
	10	-870	-446	-310	-210	-6.3	-3.0	6.0	3.7	-241	-97	1560	796	15	0.42
REACTOR CAVITY	11	38	(*)	20	130	-0.5	-0.5	-0.7	4.9	-59	57	-64	-57	66	0.50
	12	-3	(*)	30	50	3.0	3.0	10.0	9.9	57	60	54	42	10	0.52

Table 3.8-2
STRESS ANALYSIS RESULTS (Sheet 6 of 10)
DEAD LOAD + PRESTRESS LOAD + ABNORMAL THERMAL LOAD + 150% LOCA/MSLB PRESSURE LOAD
($D + F + T_A + 1.5P$)

PORTION	SECTION	CONCRETE STRESS		LINER STRAINS		REINFORCING STRESS				SECTION RESULTANTS					DEFLECTION
						INSIDE		OUTSIDE							
		MER PSI	HOOP PSI	MER X 10^{-6} IN./IN.	HOOP X 10^{-6} IN./IN.	MER KSI	HOOP KSI	MER KSI	HOOP KSI	MER FORCE K/FT	HOOP FORCE K/FT	MER MOMENT K/FT/FT	HOOP MOMENT K/FT/FT	RADIAL SHEAR K/FT	INCHES
ALLOWABLE		-5400	-5400	±5000	±5000	±54	±54	±54	±54	--	--	--	--	--	--
DOME	1	(*)	(*)	290	330	11.4	11.8	18.2	17.5	55	59	-16	-26	0	0.48
	2	-656	-511	-310	-300	-2.9	0.6	0.9	12.5	-100	-60	192	150	9	0.43
	3	-660	(*)	-250	90	-1.8	11.5	7.6	22.0	-85	75	161	46	-2	0.62
WALL	4	-758	(*)	-200	290	-3.5	16.7	0.8	26.1	-98	93	244	-45	-6	0.81
	5	-1100	(*)	-320	300	-3.7	25.0	14.6	36.0	-132	146	356	-55	-3	1.08
	6	-453	-880	-200	-380	-1.7	-4.3	-3.5	2.8	-154	-166	-46	306	47	0.22
	7	-800	-296	370	30	4.8	-1.1	-5.6	2.8	-182	32	-826	82	156	0.17
BASE SLAB	8	-465	-124	590	50	16.3	-1.7	-2.4	7.4	-113	22	-1404	120	-302	-0.01
	9	-1410	-841	-540	-340	-8.6	-4.1	11.9	7.2	-272	-127	2346	1399	-169	0.48
	10	-1050	-531	-370	-240	-7.4	-3.3	9.2	4.5	-248	-104	1911	931	36	0.63
REACTOR CAVITY	11	-203	(*)	20	140	-0.8	4.2	-1.2	5.3	-117	63	-93	-66	76	0.65
	12	(*)	(*)	80	90	3.6	3.9	10.8	10.8	73	75	23	16	6	0.68

Table 3.8-2
STRESS ANALYSIS RESULTS (Sheet 7 of 10)
DEAD LOAD + PRESTRESS LOAD + ABNORMAL THERMAL LOAD
+ 125% LOCA/MSLB PRESSURE LOAD + 125% OPERATING BASIS EARTHQUAKE
($D + F + T_A + 1.25P + 1.25E$)

PORTION	SECTION	CONCRETE STRESS		LINER STRAINS		REINFORCING STRESS				SECTION RESULTANTS					DEFLECTION
						INSIDE		OUTSIDE							
		MER PSI	HOOP PSI	MER X 10^{-6} IN./IN.	HOOP X 10^{-6} IN./IN.	MER KSI	HOOP KSI	MER KSI	HOOP KSI	MER FORCE K/FT	HOOP FORCE K/FT	MER MOMENT K/FT/FT	HOOP MOMENT K/FT/FT	RADIAL SHEAR K/FT	INCHES
ALLOWABLE		-5400	-5400	±5000	±5000	±54	±54	±54	±54	--	--	--	--	--	--
DOME	1	-260	-230	-230	-230	1.3	1.5	11.1	10.9	-40 -14	-12 -38	86 94	84 90	-2	0.02
	2	-1120	-1090	-430	-440	-4.5	-2.6	1.6	1.3	-206 -148	-106 -194	302 300	261 259	7	0.26
	3	-1270	-500	-480	-310	-4.1	3.0	9.9	14.0	-231 -95	56 -104	298 262	143 133	-1	0.33
WALL	4	-1160	-440	-430		-5.3	2.6	1.4	12.6	-231 -121	45 -111	372 354	127 117	-1	0.34
	5	-1720	-410	-580	-300	-7.2	3.0	10.6	14.9	-405 -17	-1 -67	480 422	161 145	-4	0.37
	6	-1940	-1910	-390	-400	-4.0	-8.9	5.0	3.9	-513 +47	-578 -70	-67 553	442 572	37	0.14
	7	-1520	-790	30	-90	2.1	-2.3	2.8	4.1	-525 -23	-240 180	-1269 559	79 457	151	0.14
BASE SLAB	8	-600	-340	420	-130	11.1	-3.0	-3.3	6.8	-137 -79	-227 -151	-501 -1317	472 -10	-244	0.07
	9	-1620	-1070	-560	-390	-9.7	-4.5	11.8	7.6	-297 -207	-166 -64	2714 1548	1783 767	-149	0.44
	10	-1250	-600	-540	-240	-8.1	-3.7	9.5	4.5	-204 -270	-115 -67	2249 1237	1037 685	28	0.56
REACTOR CAVITY	11	-260	(*)	40	120	-1.1	4.3	-1.1	5.3	-67 -119	86 36	-137 -29	-75 -49	71	0.58
	12	(*)	(*)	50	65	3.2	3.5	10.6	10.6	97 29	115 15	77 5	65 -1	9	0.61

Table 3.8-2
STRESS ANALYSIS RESULTS (Sheet 8 of 10)
DEAD LOAD + PRESTRESS LOAD + ABNORMAL THERMAL LOAD
+ 125% OPERATING BASIS EARTHQUAKE
($D + F + T_A + 1.25E$)

PORTION	SECTION	CONCRETE STRESS		LINER STRAINS		REINFORCING STRESS				SECTION RESULTANTS					DEFLECTION
						INSIDE		OUTSIDE							
		MER PSI	HOOP PSI	MER X 10^{-6} IN./IN.	HOOP X 10^{-6} IN./IN.	MER KSI	HOOP KSI	MER KSI	HOOP KSI	MER FORCE K/FT	HOOP FORCE K/FT	MER MOMENT K/FT/FT	HOOP MOMENT K/FT/FT	RADIAL SHEAR K/FT	INCHES
ALLOWABLE		-5400	-5400	±5000	±5000	±54	±54	±54	±54	--	--	--	--	--	--
DOME	1	-2075	-2061	-680	-680	-8.0	-8.0	3.1	3.0	-449 -423	-427 -453	533 541	543 549	-2	-0.28
	2	-2378	-2345	-750	-750	-10.1	-9.3	1.0	3.1	-603 -545	-483 -571	599 597	598 596	10	-0.18
	3	-2736	-2354	-840	-750	-11.0	-9.0	4.3	4.2	-627 -491	-400 -560	685 649	603 593	1	0.02
WALL	4	-2350	-2575	-750	-800	-10.0	11.3	0.5	0.6	-625 -515	-577 -733	776 758	821 811	14	-0.04
	5	-2700	-2899	-820	-820	-11.6	-13.3	4.5	3.2	-798 -410	-838 -904	812 754	885 869	4	-0.12
	6	-3270	-2670	-730	-730	-10.0	-12.1	6.0	0.9	-906 -346	-972 -466	460 1080	566 696	-26	0.03
	7	-3050	-1390	-810	-440	-8.8	-3.2	6.0	2.9	-887 -339	-484 -64	638 2466	423 1101	51	0.11
BASE SLAB	8	-840	-540	-250	-190	-5.6	-3.2	5.5	3.9	-229 -171	-143 -67	1556 840	735 253	23	0.22
	9	-1244	-840	-410	-300	-8.0	-4.9	4.6	3.7	-332 -242	-193 -91	2021 855	1423 409	-61	0.23
	10	-940	-430	-340	-230	-6.5	-3.7	3.5	2.8	-283 -349	-144 -96	1708 696	941 696	-12	0.21
REACTOR CAVITY	11	-50	(*)	50	100	0.5	2.9	0.3	4.1	59 7	67 17	-82 26	-48 -22	39	0.23
	12	190	-200	-120	-100	-0.4	0.4	9.1	8.8	77 9	108 8	120 48	71 5	23	0.25

Table 3.8-2
STRESS ANALYSIS RESULTS (Sheet 9 of 10)
DEAD LOAD + PRESTRESS LOAD + ABNORMAL THERMAL LOAD
+ LOCA/MSLB PRESSURE LOAD + DESIGN BASIS EARTHQUAKE LOAD
($D + F + T_A + P + E'$)

PORTION	SECTION	CONCRETE STRESS		LINER STRAINS		REINFORCING STRESS				SECTION RESULTANTS					DEFLECTION
						INSIDE		OUTSIDE							
		MER PSI	HOOP PSI	MER X 10^{-6} IN./IN.	HOOP X 10^{-6} IN./IN.	MER KSI	HOOP KSI	MER KSI	HOOP KSI	MER FORCE K/FT	HOOP FORCE K/FT	MER MOMENT K/FT/FT	HOOP MOMENT K/FT/FT	RADIAL SHEAR K/FT	INCHES
ALLOWABLE		-5400	-5400	±5000	±5000	±54	±54	±54	±54	--	--	--	--	--	--
DOME	1	-896	-869	-390	-390	-1.9	-1.9	8.8	8.8	-131 -99	-99 -129	204 218	207 217	-1	0.13
	2	-1446	-1476	-510	-530	-5.8	-4.8	1.7	8.1	-295 -219	-159 -273	379 375	357 353	8	0.14
	3	-1739	-1116	-600	-450	-6.6	0.2	8.0	11.3	-329 -155	-8 -218	407 361	255 241	-1	0.22
WALL	4	-1539	-1194	-540	-460	-6.6	-.3	1.3	8.8	-327 -183	-55 -259	480 458	320 306	2	0.21
	5	-2110	-1347	-680	-500	-9.3	-4.0	8.9	9.0	-542 -36	-145 -233	573 497	406 388	-3	0.17
	6	-2646	-2345	-500	-620	-5.7	-10.8	8.2	4.0	-678 56	-784 -118	1 819	460 632	25	0.11
	7	-1782	-988	-230	-180	0.8	-2.8	5.8	4.4	-682 48	-346 -204	-1154 1248	177 673	138	0.13
BASE SLAB	8	-525	-407	-240	-100	6.1	-3.3	-2.5	6.2	-160 88	-81 17	-78 -1034	580 -56	-191	0.12
	9	-1666	-1072	-560	-380	-10.1	-5.6	11.2	6.9	-324 -210	-184 -52	2797 1311	1801 513	-140	0.40
	10	-1230	-586	-380	-230	-7.8	-3.8	7.7	4.1	-200 -282	-130 -64	1198 -78	1020 572	15	0.42
REACTOR CAVITY	11	-164	(*)	50	150	0.1	-0.9	-0.9	5.1	-24 -94	92 22	-138 10	-73 -41	66	0.50
	12	-7	(*)	30	-30	2.4	3.3	10.6	10.6	106 8	139 -19	116 -8	91 -7	10	0.52

Table 3.8-2
STRESS ANALYSIS RESULTS (Sheet 10 of 10)
DEAD LOAD + PRESTRESS LOAD + ABNORMAL THERMAL LOAD
+ DESIGN BASIS EARTHQUAKE LOAD
($D + F + T_A + E'$)

PORTION	SECTION	CONCRETE STRESS		LINER STRAINS		REINFORCING STRESS				SECTION RESULTANTS					DEFLECTION
						INSIDE		OUTSIDE							
		MER PSI	HOOP PSI	MER X 10^{-6} IN./IN.	HOOP X 10^{-6} IN./IN.	MER KSI	HOOP KSI	MER KSI	HOOP KSI	MER FORCE K/FT	HOOP FORCE K/FT	MER MOMENT K/FT/FT	HOOP MOMENT K/FT/FT	RADIAL SHEAR K/FT	INCHES
ALLOWABLE		-5400	-5400	±5000	±5000	±54	±54	±54	±54	--	--	--	--	--	--
DOME	1	-2091	-2067	-680	-680	-8.0	-8.1	3.2	3.0	-452 -420	-424 -455	530 544	541 551	-2	-0.28
	2	-2396	-2372	-750	-750	-10.2	-9.5	1.1	3.3	-612 -536	-470 -584	600 596	599 595	10	-0.18
	3	-2789	-2405	-850	-760	-11.4	-9.3	4.5	4.5	-646 -472	-375 -585	690 644	605 591	1	0.02
WALL	4	-2379	-2630	-750	-800	-10.2	-11.6	0.6	0.8	-642 -498	-553 -757	778 756	823 809	14	-0.04
	5	-2820	-2921	-850	-820	-12.3	-13.4	5.0	3.4	-857 -915	-827 -915	821 745	886 868	4	0.12
	6	-3626	-2835	-750	-750	-10.1	-12.8	9.1	2.0	-993 -259	-1052 -386	361 1179	545 717	-26	0.03
	7	-3378	-1604	-840	-440	-9.4	-3.4	8.4	3.6	-973 -253	-549 1	351 2753	663 1159	51	0.11
BASE SLAB	8	-906	-580	-270	-210	-6.0	-3.6	5.7	4.0	-236 -164	-154 -56	1676 720	812 176	23	0.22
	9	-1335	-924	-440	-310	-8.5	-5.4	5.0	4.0	-344 -230	-208 -76	2181 695	1561 273	-61	0.23
	10	-1062	-564	-350	-230	-6.8	-3.8	3.8	2.9	-275 -357	-153 -87	1840 564	989 541	-12	0.21
REACTOR CAVITY	11	170	(*)	50	100	0.7	3.0	0.4	4.2	68 -2	77 7	-102 46	-41 -19	39	0.23
	12	(*)	(*)	-120	-110	-0.1	0.5	9.3	9.0	92 -6	137 -21	146 22	87 -11	23	0.25

Table 3.8-2A
CONTAINMENT RESTORED CONDITION
STRESS ANALYSIS RESULTS WITHIN THE RESTORED OPENING AREA

(a) Service Loads: Membrane + Bending Forces

Load Comb.	Section Resultants				Internal Stresses/Strains									
	Mer. Force (kip/ft)	Hoop Force (kip/ft)	Mer. Moment (ft·kip/ft)	Hoop Moment (ft·kip/ft)	Conc., Inside (ksi)		Conc., Outside (ksi)		Reinf, Inside (ksi)		Reinf, Outside (ksi)		Liner Plate ($x10^{-6}$, in./in.)	
					Mer.	Hoop	Mer.	Hoop	Mer.	Hoop	Mer.	Hoop	Mer.	Hoop
I	-221	-634	267	455	-1.0	-2.0	-	-	-4.5	-10	1.4	-1.2	-232	-462
II	82	12	335	290	-1.2	-1.1	-	-	3.6	1.0	34.9	22.6	-275	-251
			Allowable		*-3.6*	*-3.6*	*-3.6*	*-3.6*	*±40****	*±40****	*±40****	*±40****	*-4000*	*4000*

(b) Factored Loads: Membrane + Bending Forces

Load Comb.	Section Resultants				Internal Stresses/Strains									
	Mer. Force (kip/ft)	Hoop Force (kip/ft)	Mer. Moment (ft±kip/ft)	Hoop Moment (ft±kip/ft)	Conc., Inside (ksi)		Conc., Outside (ksi)		Reinf, Inside (ksi)		Reinf, Outside (ksi)		Liner Plate ($x10^{-6}$, in./in.)	
					Mer.	Hoop	Mer.	Hoop	Mer.	Hoop	Mer.	Hoop	Mer.	Hoop
III	84	38	267	-71	-0.9	-	-	-0.8	3.9	48.0	30.3	2.1	-205	2207
IV	-27	-11	280	133	-1.2	-0.5	-	-	-1.0	-0.2	17.2	8.3	-266	-120
	194	-77	311	117	-0.3	-0.4	-	-	11.8	-1.7	48.5	1.5	-61	-100
V	-406	-563	612	778	-2.3	-2.9	-	-	-9.4	-11.8	6.9	7.5	-533	-664
	-18	-629	554	762	-2.3	-2.9	-	-	-0.7	-12.4	38.2	4.8	-521	-665
VI	-159	102	373	299	-1.5	-0.8	-	-	-4.5	5.7	10.0	35.0	-342	-194
	181	14	367	281	-0.9	-1.1	-	-	9.4	1.1	50.6	22.2	-201	-242
VII	-462	-542	621	779	-2.4	-2.9	-	-	-10.0	-11.6	4.9	8.4	-538	-665
	-520	-630	545	761	-2.1	-2.9	-	-	-9.9	-12.4	1.2	4.8	-483	-654
			Allowable		*-5.4*	*-5.4*	*-5.4*	*-5.4*	*±54*	*±54*	*±54*	*±54*	*±5000*	*±5000*

*** Allowable steel stress is increased by 33-1/3 percent as the temperature effects are included which is based on Bechtel Topical Report BC-TOP-5-A, Rev. 3

\+ Liner plate strains induced by dead and prestressing loads are small. As such, the increase of liner plate strains due to concrete creep is ignored.

Table 3.8-2B
CONTAINMENT RESTORED CONDITION
STRESS ANALYSIS RESULTS WITHIN THE RESTORED OPENING AREA

(a) Service Loads: Membrane + Bending Forces

Load Comb.	Section Resultants				Internal Stresses/Strains									
	Mer. Force (kip/ft)	Hoop Force (kip/ft)	Mer. Moment (ft·kip/ft)	Hoop Moment (ft·kip/ft)	Conc., Inside (ksi)		Conc., Outside (ksi)		Reinf, Inside (ksi)		Reinf, Outside (ksi)		Liner Plate ($x10^{-6}$, in./in.)	
					Mer.	Hoop	Mer.	Hoop	Mer.	Hoop	Mer.	Hoop	Mer.	Hoop
I	-988	-1245	298	485	-2.2*	-3.1*	-0.9*	-0.9*	-12.7*	-16.6*	-7.3*	-7.4*	-509	-697
II	-684	-599	366	320	-1.9*	-1.7*	-0.3*	-0.3*	-10.1*	-8.6*	-3.4*	-2.5*	-433	-379
			Allowable		*-3.6*	*-3.6*	*-3.6*	*-3.6*	*±40****	*±40****	*±40****	*±40****	*4000*	4000

(b) Factored Loads: Membrane + Bending Forces

Load Comb.	Section Resultants				Internal Stresses/Strains									
	Mer. Force (kip/ft)	Hoop Force (kip/ft)	Mer. Moment (ft·kip/ft)	Hoop Moment (ft·kip/ft)	Conc., Inside (ksi)		Conc., Outside (ksi)		Reinf, Inside (ksi)		Reinf, Outside (ksi)		Liner Plate ($x10^{-6}$, in./in.)	
					Mer.	Hoop	Mer.	Hoop	Mer.	Hoop	Mer.	Hoop	Mer.	Hoop
III	-454	12	383	-141	-1.6*	0.3*	0.1*	-0.3*	-7.8*	1.2*	-0.8*	-1.5*	-358	76
IV	-794	-164	311	81	-2.0*	-0.4*	-0.6*	-0.1*	-10.8*	-2.3*	-5.1*	-0.8*	-445	-100
	-304	-230	405	65	-1.4*	-0.5*	0.4*	-0.2*	-6.4*	-2.9*	1.1*	-1.7*	-315	-116
V	-1173	-1174	643	808	-3.3*	-3.7*	-0.5*	-0.1*	-17.4*	-18.2*	-5.6*	-2.8*	-750	-834
	-785	-1240	585	792	-2.6	-3.7*	-	-0.2*	-12.9	-18.8*	-1.9	-3.7*	-584	-850
VI	-925	-509	404	329	-2.4*	-1.6*	-0.6*	-0.1*	-12.9*	-7.8	-5.5*	-1.5*	-540	-351
	-307	-597	442	311	-1.7	-1.7*	-	-0.3*	-6.9	-8.6	4.4	-2.6*	-384	-374
VII	-1229	-1153	652	809	-3.4*	-3.6*	-0.5*	-0.1*	-18.1*	-18.0*	-6.1*	-2.6*	-775	-827
	-1287	-1241	576	791	-3.3*	-3.7*	-0.8*	-0.2*	-18.1*	-18.8*	-7.5*	-3.8*	-758	-850
			Allowable		*-5.4*	*-5.4*	*-5.4*	*-5.4*	*±54*	*±54*	*±54*	*±54*	*±5000*	*±5000*

* Uncracked sections; All other sections are partially-cracked sections

*** Allowable steel stress is increased by 33-1/3 percent as the temperature effects are included. Approach is based on Bechtel Topical Report BC-TOP-5-A, Rev. 3

\+ Liner plate strains induced by dead and prestressing loads are small. As such, the increase of liner plate strains due to concrete creep is ignored.

3.8.1.6 Materials, Quality Control, and Special Construction Techniques

The following basic materials are used in the construction of the containment structure.

A. Concrete

Tendon access gallery		f_c (lb/in.^{2}) = 6,000 at 90 days
Base slab		f_c (lb/in.^{2}) = 6,000 at 90 days
Cylindrical wall and dome		f_c (lb/in.^{2}) = 6,000 at 90 days
	Exception:	f_c (lb/in.^{2}) = 4,000 at 28 days Three 24" diameter construction vent plugs, See Dwg # 23060
Containment opening closure of SGRP Temporary construction opening		f_c (lb/in.^{2}) = 6,000 at 7 days (see 3.8.1.6.3.5)

B. Reinforcing Steel

Deformed bars	ASTM A615 Grade 60	f_y (lb/in.^{2}) = 60,000

C. Structural and Miscellaneous Steel

Structural steel shapes, plates, and bars	ASTM A36	f_y (lb/in.^{2}) = 36,000
High-strength structural steel shapes, plates, and bars	ASTM A572	f_y (lb/in.^{2}) = 42,000 to 65,000 (varies depending on grade of the material)
Pipe used as structural members	ASTM A53	f_y (lb/in.^{2}) = 25,000 to 35,000 (varies depending on grade used)
Forgings	ASTM A237 Class C	f_y (lb/in.^{2}) = 58,000 to 60,000 (varies depending on material thickness)
Pins	ASTM A307	f_t (lb/in.^{2}) = 60,000 minimum

	ASTM A325	f_y (lb/in.^{2}) =	81,000 to 92,000 (varies depending on diameter of pins)
	ASTM A449	f_y (lb/in.^{2}) =	58,000 to 92,000 (varies depending on diameter of material)
	ASTM A490	f_y (lb/in.^{2}) =	130,000 (varies depending on diameter of pins)
	ASTM A540	f_y (lb/in.^{2}) =	105,000 to 150,000 (varies depending on diameter, class, and grade of material)
Polar crane rail	AISI 175 lb/yd		
Refueling machine rail	ASTM A36	f_y (lb/in.^{2}) =	36,000 minimum
CEA change mechanism rail	Stainless steel		
Anchor bolts	ASTM A36	f_y (lb/in.^{2}) =	36,000 minimum
	ASTM A307	f_t (lb/in.^{2}) =	60,000 minimum
	ASTM A325	f_y (lb/in.^{2}) =	81,000 to 92,000 (varies depending on diameter of bolts)
	ASTM A449	f_y (lb/in.^{2}) =	58,000 to 42,000 (varies depending on diameter of bolts)
	ASTM A490	f_y (lb/in.^{2}) =	130,000 minimum (varies depending on diameter of bolts)
	ASTM A540	f_y (lb/in.^{2}) =	105,000 to 150,000 (varies depending on diameter, class, and grade of material)
Bolts	ASTM A307	f_t (lb/in.^{2}) =	60,000 minimum

High strength bolts	ASTM A325	f_y (lb/in.^{2}) =	81,000 to 92,000 (varies depending on diameter of bolts)
	ASTM A490	f_y (lb/in.^{2}) =	130,000 minimum (varies depending on diameter of bolts)
	ASTM A540	f_y (lb/in.^{2}) =	105,000 to 150,000 (varies depending on diameter, class, and grade of material)
Nelson shear studs	ASTM A108	f_y (lb/in.^{2}) =	f_y = 50,000

D. Containment Steel Liner Plate and Penetration Sleeves

1/4-in. liner plate	ASME SA-285 Grade A	f_y (lb/in.^{2}) =	24,000
	ASME SA-285, Grade C (f_y = 30,000 lb/in.^{2}) used for liner repairs		
Greater than 1/4-in. liner plate	ASME SA-516 Grade 70	f_y (lb/in.^{2}) =	38,000
Embedded items	ASME SA-36	f_y (lb/in.^{2}) =	36,000
	ASME SA-285 Grade A	f_y (lb/in.^{2}) =	24,000
	ASME SA-516 Grade 70	f_y (lb/in.^{2}) =	38,000
	ASME SA-106 Grade B	f_y (lb/in.^{2}) =	35,000
Cadweld connectors	AISI C1026	f_y (lb/in.^{2}) =	72,000
	AISI C1018	f_y (lb/in.^{2}) =	72,000
Nelson shear studs	ASTM A108	f_y (lb/in.^{2}) =	50,000

Penetration sleeves		
Seamless pipes	ASME SA-333 Grade 1 Grade 6	 f_y (lb/in.^{2}) = 30,000 f_y (lb/in.^{2}) = 35,000
Welded pipes	ASME SA-516 Grade 70	(f_y) (lb/in.^{2}) = 38,000
	ASME SA-155 Grade-KCF-70 Class 1	(f_y) (lb/in.^{2}) = 38,000

E. Post-Tensioning System

Prestressing strands	ASTM A416-74 Grade 270	(f_s) (lb/in.^{2}) = 270,000
Prestressing strands installed to restore SGRP temporary construction opening	ASTM A416-06 Grade 270	(f_s) (lb/in.^{2}) = 270,000
Bearing plates	ASTM A537-67a Grade A	(f_y) (lb/in.^{2}) = 45,000
Sheathing	ASTM A527	
Sheathing, adapters couplers installed to restore SGRP temporary construction opening	ASTM A513	
Anchor heads	AISI 1026	(fy) (lb/in.^{2}) = 50,000
Anchorheads replaced during SGRP	EN10025-1993 Grade S355J2G3 N	(fy) (lb/in.^{2}) = 50,000

Materials and their quality control requirements are described in the following paragraphs.

3.8.1.6.1 Reinforced Concrete

3.8.1.6.1.1 Concrete

All concrete work was done in accordance with ACI 318-71, Building Code Requirements for Reinforced Concrete, and ACI 301-72, Specifications for Structural Concrete for Buildings, except as otherwise stated herein.

The concrete is a dense, durable mixture of sound coarse aggregates, fine aggregates, cement, and water. Admixtures are added to improve the quality and workability of the plastic concrete during placement and, in some areas to retard the set of concrete. When pozzolan admixtures are used, the pozzolan is substituted for portions of cement in the concrete mix. The sizes of aggregates, water-reducing additives, and slumps were selected to maintain low limits on shrinkage and creep.

3.8.1.6.1.2 Cement

Cement is Type II, low alkali, moderate heat of hydration or Type V, high sulfate resistant conforming to the Specification for Portland Cement (ASTM C150-70) including Table 1A for moderate heat of hydration or a Portland-pozzolan cement, conforming to the Specification for Blended Hydraulic Cements (ASTM C595-75), Type 1P. Certified copies of mill test reports showing the chemical composition and physical properties were obtained for each load of cement delivered. The limitation of the alkali content of the cement may be waived provided that the aggregates pass required laboratory tests and have no history of alkali-aggregate incompatibility.

In addition to the tests required by the cement manufacturers, the following tests were performed:

ASTM C109 - Compressive Strength

ASTM C114 - Chemical Analysis

ASTM C115 or C204 - Fineness of Portland Cement

ASTM C151 - Autoclave Expansion

ASTM C191 or C266 - Time of Set

The purpose of the above tests was to ascertain conformance with ASTM Specifications C150 or C595. In addition, tests ASTM C191 or ASTM C266, ASTM C109, and ASTM C451 were repeated periodically during construction to check storage environmental effects on cement characteristics. The tests supplement visual inspection of material storage procedures.

3.8.1.6.1.3 Aggregates

All aggregates conformed to either the Standard Specifications for Concrete Aggregate (ASTM C33-69) or the Standard Specifications for Public Works Construction (SSPWC-1979)[11]. In addition to the specified gradation, the fine aggregate (sand) had a fineness modulus of not less than 2.3 or more than 3.1 during normal operations; at least 9 of 10 test samples should not vary in fineness modulus more than 0.20 from the average. Coarse aggregate may be rejected, if the loss when subjected to the Los Angeles abrasion test, ASTM C131-69 using grading A, exceeds 40% by weight at 500 revolutions.

Acceptance of aggregates was based on the following tests:

ASTM Test No.	Name of Test
C131	Los Angeles Abrasion
C142	Clay Lumps and Friable Particles
C117	Material Finer than No. 200 Sieve
C87	Mortar Making Properties
C40	Organic Impurities
C289	Potential Reactivity (Chemical)
C136	Sieve Analysis
C88	Soundness
C127	Specific Gravity and Absorption
C128	Specific Gravity and Absorption
C295	Petrographic

In addition to the foregoing initial tests, a daily inspection control program was carried on during construction to ascertain consistency in potentially variable characteristics such as gradation and organic content.

3.8.1.6.1.4 Water

Water and ice used in mixing concrete was free of injurious amounts of oil, acid, alkali, organic matter, or other deleterious substances as determined by American Association of State Highway Officials (AASHO) Methods of Sampling and Testing, Designation T26. Water shall not contain

impurities in amounts that will cause either a change in the time of setting of Portland cement or more than 25% or a reduction in the compressive strength of mortar of more than 5% compared with results obtained with distilled water. The water shall not contain more than 250 ppm of chlorides as C1 when used in concrete for the containment structure, nor more than 350 ppm of chloride as C1 when used in concrete for the balance of the Seismic Category I structures. In addition, the water shall not contain more than 800 ppm of sulfates as SO_4, nor more than 2000 ppm total dissolved solids. The pH range shall be within 6.0 to 9.0.

3.8.1.6.1.5 Admixtures

The concrete also contains an air entraining admixture, a water reducing admixture, and a pozzolan. The air entraining admixture is in accordance with the Specification for Air Entraining Admixtures for Concrete (ASTM C260). It is capable of entraining 3 to 5% air, is completely water soluble, and is completely dissolved when it enters the batch. The water reducing admixture may be a type that retards the set of the concrete and that conforms to the Standard Specification for Chemical Admixtures for Concrete (ASTM C494-68), Types A and D.

Pozzolans conform to Specifications for Fly Ash and Raw or Calcined Natural Pozzolans for Use in Portland Cement Concrete (ASTM C618) except that ignition loss shall not exceed 6%. In limited instances (less than 1.0% of total concrete), where enhancement of workability and sulfate resistance by pozzolans is not essential, the pozzolan admixture is omitted.

3.8.1.6.1.6 Concrete Mix Design

Concrete mixes were designed in accordance with the American Concrete Institute Standard (ACI) 211.1.70. Only concrete mixes meeting the design requirements specified for the structures were used.

Trial mixes were tested in accordance with the applicable ASTM specifications as indicated below:

ASTM	Test
C39-66	Compressive strength of molded concrete cylinders
C143-69	Slump of Portland cement concrete
C192-69	Making and curing concrete test specimens, in the laboratory
C231-68	Air content of freshly-mixed concrete by the pressure method
C232-58	Bleeding of concrete

Concrete test cylinders were cast from the mix proportions selected for use in the prestressed concrete for the containment to determine the following properties:

- Compressive strength
- Thermal diffusivity
- Autogenous shrinkage
- Thermal coefficient of expansion
- Modulus of elasticity and Poisson's ratio
- Uniaxial creep

The restoration of the containment building temporary construction opening for SGRP used a concrete mix design similar to the original mix design. The mix used ingredients similar to those used in the original design, with appropriate adjustments to the slump, air content and strength as necessary to ensure workability during concrete placement operations. Ingredients conforming to the specific testing requirements were used. The mix is qualified for strength per Section 4.2.3 of ACI 301.

3.8.1.6.1.7 Concrete Testing

During construction, concrete was sampled and tested for slump, air content, temperature, and unit weight prior to casting comprehensive strength cylinders.

Compressive strength cylinders were cast from representative samples taken in accordance with Sampling Fresh Concrete (ASTM C172-71).

Cylinders were made, cured, and tested in accordance with the Standard Method for Making and Curing Compression and Flexure Tests in the Field (ASTM C31-69) and the Standard Test for Compressive Strength of Molded Concrete Cylinders (ASTM C39-66).

The requirements for taking cylinders were as follows:

A. One set of test specimens is made not less than once a day or less than once for each 100 cubic yards of concrete placed, or fraction thereof, for each mix design. For large concrete placements exceeding 500 cubic yards, one set of test specimens is made not less than once for each 250 cubic yards of concrete placed, or fraction thereof, for each design mix.

B. The procedures for securing strength test samples and molding test specimens comply with the above mentioned standards. A set of test specimens consists of six 6-inch diameter by 12-inch cylinders.

C. Two cylinders from each set of test specimens are tested at the designated test intervals. Tests are performed at 3, 7, 28, and 90 days. The 3-day test is only made on occasion to correlate 3-day strength. When these tests are made, the 90-day tests are not made.

D. When a correlation of test data is established for each mix, the 90-day test cylinders are discontinued except for prestressed concrete.

Concrete cylinders were maintained at a temperature of 60°F to 80°F prior to stripping, stripped within 24 hours after casting, marked and stored in the curing room until the designated date for testing.

Standards of concrete control were in accordance with the criteria established in ACI 214 for "excellent" concrete. An acceptable correlation was based upon test results from at least the first 10,000 cubic yards of concrete placed for each mix design.

The average of all of the compressive strength tests representing each class of concrete, as well as the average of any five consecutive strength tests representing each class of concrete, was required to be equal to or greater than the specified strength, and no more than one strength test in ten had an average value less than the specified strength. The strength of an individual test was the average of the strengths of the two specimens.

The concrete mix used to restore the temporary construction opening for SGRP was tested to requirements that are similar to those used for the original concrete mix with the following notable exceptions: the test specimens were made at the beginning of each 50 cubic yards placed and at the end of the pour; and the compressive strength test specimens consisted of either 6” diameter by 12” long or 4” diameter by 8” long cylinders prepared in accordance with ASTM C31. In addition, this concrete mix was tested for creep and modulus of elasticity. Creep testing is in accordance with ASTM C512, “Standard Test Method for Creep of Concrete in Compression.” The modulus of elasticity complies with the requirements of ASTM C469, “Standard Test Method for Static Modulus of Elasticity and Poisson’s Ration of Concrete in Compression.”

3.8.1.6.1.8 Concrete Placement.

A. General

Conveying and placing of concrete was performed in accordance with ACI 301, ACI 318, ACI 304, ACI SP2, ASTM C94, and as specified herein. No aluminum pipe or other conveying equipment containing aluminum that would be in contact with the fresh concrete was used for conveying concrete to the point of placement. Steel pipe were used for concrete pumps or pneumatic placers. Pipe sizes were limited to 5 inches minimum diameter for 3/4- to 1-1/2-inch maximum size aggregate mixes and may be reduced to smaller pipe sizes for aggregate mix size less than 3/4-inch maximum. For second stage concrete placements within completed areas, pipe sizes or rubber hoses of 4 inches minimum diameter may be used for 3/4-inch maximum size aggregate mixes.

B. Clean-Up Preparation

Before depositing concrete, all equipment was cleaned. Debris was removed from spaces to receive concrete. Reinforcement and other metal to be embedded was thoroughly cleaned of all loose rust, scale, and/or coatings that might impair the bond. All compacted soil, rock, or concrete surfaces to receive concrete were thoroughly wetted before placement.

C. Construction Joint Placement

To the maximum extent possible, concrete was deposited continuously to provide monolithic units in the construction as shown on the approved engineering design drawings. Construction joints were provided in accordance with details as shown on the approved engineering design drawings where the size of large slabs or lengths of continuous strips so dictate. Adjacent vertical placements had a minimum curing time of 3 days. In all cases, concrete was deposited in such a way as to prevent water from collecting at the ends and corners of forms and along form faces during placement.

All contiguous vertical concrete construction joints to receive additional lifts of concrete were moist cured. Newly placed concrete was moist cured by continuous application of water for the first 7 days after the concrete had been placed. As soon as unformed surfaces of concrete had hardened sufficiently to prevent surface damage through application of curing procedures, an intermittent fine spray of water was applied as necessary to keep such surfaces continually moist for not less than 7 days.

Construction joints and curing of concrete for the restoration of the temporary construction opening for SGRP were in accordance with project design and construction specifications listed in Section 3.8.1.2.3.B, except that a commercial coating compound was used for joint preparation in accordance with the manufacturer's instructions.

D. Placement Limitations

Concrete was deposited in horizontal layers between 12 to 24 inches in depth and was not allowed to flow a distance of more than 5 feet from the point of deposition.

E. Segregation

Concrete was not dropped through dense reinforcing steel which might cause segregation of the coarse aggregate. Concrete was not dropped free from a height of more than 6 feet.

F. Concrete Temperature Control

The target temperature of concrete shall be less than 50°F for placements that exceed 6 feet in thickness; i.e., the least dimension in any direction.

The target temperature for placements greater than 3 feet in the least dimension and less than or equal to 6 feet in the least dimension shall be 70°F. The target temperature for placements less than or equal to 3 feet in the least dimension shall be 85°F and the maximum temperature for placement shall not exceed 90°F.

The total thickness for consecutive placements shall be determined by adding all placements made within a lapsed time of 14 days. This total thickness in the least dimension shall be used in determining the target temperature as indicated in the above paragraph.

G. Weather Precautions

During cold weather, if the air temperature drops below freezing at night, or if the mean daily temperature falls below 40°F for more than 1 day during the period when concrete is being placed, concrete is placed in accordance with the Recommended Practice for Cold Weather Concreting, ACI 306. The concrete shall be maintained at a temperature no lower than 50°F for at least 72 hours after it is placed. No additional protection from freezing will be required if that temperature is maintained for that length of time by means of insulation in contact with the form or concrete surfaces. Foundation forms can be stripped 24 hours after concrete is placed.

Concrete, when deposited in the forms during cold weather, is required to have a temperature of not less than the following:

Air Temperature (°F)	Less than 2-1/2 feet in Least Dimension (°F)	Mass Concrete In excess of 2-1/2 feet Least Dimension (°F)
30 to 45	60	50
0 to 30	65	55

Type V cement is not to be used in cold weather concrete placements.

During hot weather, when the ambient temperature is greater than 80°F, concrete is placed in accordance with ACI 305, Recommended Practice for Hot Weather Concreting.

Before depositing concrete in any form or on any surface, cool water is sprinkled on all surfaces and reinforcement steel. Wind breakers are used to prevent wind from blowing over the concrete surface prior to the initiation of curing.

Curing is started as soon as the concrete has hardened to withstand surface damage.

H. Consolidation of Concrete

Concrete was placed with the aid of mechanical vibrating equipment supplemented by hand spading and tamping. The vibrating equipment is of the internal type. The frequency of vibration is not less than 7000 cycles per minute. Vibration is not allowed to cause segregation. In consolidating each layer of concrete, the vibrator is operated in a near vertical position. The vibrating head is allowed to penetrate under the action of its own weight and to re-vibrate the concrete in the upper portion of the underlying layer. Neither form nor surface vibrators are used without specific approval from engineering.

Vibrators are not used to move or spread concrete. A ratio of not less than one spare vibrator in good working condition to each three vibrators required for vibration of the concrete being placed is kept available for immediate use at the placement location. Vibration commences within 15 minutes following the time of placement.

I. Bonding of Concrete Between Lifts

Horizontal construction joints are prepared for receiving the next lift by either sandblasting or water blasting. Sandblasting or water blasting will be performed before placing forms. The operation shall be continued until all laitance, coatings, stains, and other foreign materials are removed. The surface of the concrete is washed thoroughly to remove all loose materials. The horizontal surface is wet immediately before the concrete is placed.

Surface set retardant compounds are not used.

3.8.1.6.2 Reinforcing Steel

Reinforcing steel was deformed billet steel, conforming to ASTM Designation A615-72. This steel has a minimum yield strength of 60,000 lb/in.^{2}, a minimum tensile strength of 90,000 lb/in.^{2}, and a minimum elongation of 7% in an 8-inch specimen. Grade 60 was used throughout the project.

Mill test results are obtained from the reinforcing steel supplier for each heat of steel to show proof that the reinforcing steel has the specified composition, strength, and ductility. Splicing of reinforcing bars is done in accordance with ACI 318-71. Mechanical splices (Cadweld) are used for all bars larger than No. 11 and for bar size No. 11 and smaller where lap splices are impractical. Reinforcing steel ends may be prepared by hand wire brushing, in accordance with the manufacturer's instructions, where access prohibits the use of power wire brushing or sandblasting. Cadweld splices are made in accordance with the manufacturer's instructions as presented in Erico Products Bulletin, RB20M-173-1973, Cadweld Rebar Splicing.

In the intake concrete structure, only, mechanical splices (coupler S-series) are used for bar size No. 11 and smaller where lap splices are impractical. Coupler splices are made in accordance

with the manufacturer's instructions as presented in Bar-locks Installation Guidelines, Attachment I, CS-C04.

To restore the temporary construction opening in the containment structure for SGRP, the original reinforcing steel bars located in temporary construction opening are replaced with new reinforcing steel bars or, for Unit 3, restored when possible using the removed material. Connections to the original reinforcing steel are made by Cadweld or weld splices. When Cadwelding is not feasible, reinforcing steel located in the temporary containment opening is spliced by welding. To minimize the size of the temporary construction opening for the SGRP,not all Cadweld and welded splice locations are staggered.

All new reinforcing steel bars placed in the temporary construction opening are the same material used in the original construction of containment.

3.8.1.6.3 Structural and Miscellaneous Steel

Mill test reports of all structural and miscellaneous steel are obtained for all materials used with the exceptions of hand rails, toe plates, kick plates, stairs, and ladders.

Detailing, fabrication, and erection of the structural and miscellaneous steel are in accordance with the AISC Manual of Steel Construction, 1969 edition. An exception is that plate washers to cover long slotted holes need not be provided for bearing type connections in which the primary bolt load is shear, not tension, and in which the bolt loading is oriented normal to the long slot direction.

Welding is done in accordance with AWS D1.1-72, Structural Welding Code, except, Paragraph 4.9.2 is replaced as follows: All electrodes having low-hydrogen coverings conforming to AWS A5.1 shall be received, stored, and disbursed in accordance with Bechtel Power Corporation Welding Standard WFMC-1, Revision 6, dated February 24, 1978. References 7 and 8 provide justification for this modification, and procedure WFMC-1, Revision 6, is part of Appendix C of Reference 7. The acceptance criteria for visual inspection of welding done in accordance with AWS D1.1-72 are provided in Appendix 3.8A.

3.8.1.6.4 Quality Control

Quality control procedures were established and implemented during construction and inspection. The quality control procedures are specified in the technical specifications covering the fabrication, furnishing, and installation of each structural component and provide inspection and documentation to assure that the codes and construction practices are met. Table 3.8-3 provides a listing of all pertinent concrete related tests.

3.8.1.6.4.1 <u>Control Tests for Concrete</u>

Concrete for the containment structure is tested in accordance with ACI 214, Recommended Practice for Evaluation of Compressive Test Results of Field Concrete.

3.8.1.6.4.2 Control Tests for Reinforcing Steel

Full diameter specimens of each size of reinforcing steel are taken for tests. Frequency of tests conform to Regulatory Guide 1.15 (Withdrawn by NRC, 8/71).

Placement tolerances used for reinforcing steel conform to the following allowable variances:

A. Concrete cover, No. 3 through No. 11: ±1/2 inch

B. Concrete cover, No. 14 and No. 18: +1 inch, -1/2 inch

C. Spacing between bars, No. 3 through No. 11: ±1 inch

D. Spacing between bars, No. 14 and No. 18: ±3 inches

E. Lengthwise of bars: ±2 inches

F. Allowable movement of bars for other embedments were maintained to the following:

   1. Bottoms of beams and elevated slabs: ±2 inches (horizontally)

   2. All other walls, slabs on grade, columns, etc.: ±4 inches

G. Stirrups, hairpins, and ties were uniformly sloped up to 1 in 4, with the requirement that the spacing on one place be maintained within ±1-1/2 inches of the specified location.

Table 3.8-3
CONTROL TESTS FOR CONCRETE (Sheet 1 of 4)

Onsite Testing			
Material	Test	Procedure	Frequency
Cement	Time of setting False set Compressive strength	ASTM C191 ASTM C451 ASTM C109	Monthly Monthly Monthly
Coarse aggregate	Gradation Flat and elongated particles Clay lumps	ASTM C136 CRD C119 ASTM C142	1 test per shift 1 test per week If required
Fine aggregate	Gradation Organic impurities Fineness modulus Material finer than No. 200 sieve	ASTM C136 ASTM C40 ASTM C136 ASTM C117	2 tests per shift[(a)] 1 test per shift 2 tests per shift[(a)] 1 test per shift
Concrete	Slump (also temperature)	ASTM C143	1 each 100 yd^3 per placement per mix
	Air content Unit weight Compressive strength	ASTM C138/C231 ASTM C138 ASTM C39	1 each 100 yd^3 or fraction thereof per mix or 1 each 250 yd^3 or fraction thereof per mix for pours over 500 yd^3.
	Capping cylindrical concrete specimens	ASTM C617	Not applicable
	Accelerated curing of concrete specimens	ASTM C684	Testing program to be determined upon request of the engineer.
	Standard method of sample fresh concrete	ASTM C172-71	Not applicable.

(a) Two tests per shift when using ASTM C150, Type II Cement; 1 test per shift when using ASTM C595, Type 1P, Cement, but twice daily during production if more than 200 yds^3 are batched for San Onofre 2&3.

Table 3.8-3
CONTROL TESTS FOR CONCRETE (Sheet 2 of 4)

Onsite Testing			
Material	Test	Procedure	Frequency
Cement	Chemical analysis Strength False set Fineness Heat of hydration Soundness by autoclave expansion Time of setting Sulfate expansion Tensile strength Sieve No. 325 Pozzolanic activity of blended pozzolan	ASTM C114 ASTM C109 ASTM C451[b] ASTM C204[b] or C115 ASTM C186 ASTM C151 ASTM C191 or C266 ASTM C452[b] ASTM C190[b] ASTM C430[c] ASTM C595[c]	1 set of tests per source
Pozzolan	Fly ash and pozzolan	ASTM C618	1 test for every 1,000 tons used (required only when pozzolan is included as a separate ingredient in the concrete mix)

[b] Required only when Portland Cement, Type II, ASTM C150, is used.
[c] Required only when blended hydraulic cement, ASTM C595, Type 1P, is used.

Table 3.8-3
CONTROL TESTS FOR CONCRETE (Sheet 3 of 4)

Onsite Testing			
Material	Test	Procedure	Frequency
Admixtures	Water reducing	ASTM C494	1 physical test per source and a chemical test with each 1,000 ton pozzolan test when pozzolan is included as a separate ingredient in the concrete mix otherwise
	Air entraining	ASTM C260	1 physical test and a chemical test initially and each time the source is changed
Aggregates	L.A. abrasion	ASTM C131	Once every 10,000 yd^3 of concrete when concrete is produced onsite but every 6 months when concrete is produced and delivered from an offsite plant.
	Soundness	ASTM C88	
	Mortar making prop.	ASTM C87	
	Pot. reactivity (chem.)	ASTM C289	
	Pot. reactivity (mortar bar)	ASTM C227	Once every 40,000 yd^3 of concrete when concrete is produced onsite but initially and each time the source is changed when concrete is produced and delivered from an offsite plant.

Table 3.8-3
CONTROL TESTS FOR CONCRETE (Sheet 4 of 4)

Onsite Testing			
Material	Test	Procedure	Frequency
Aggregates (cont)	Sp. Cr. and absorp. (coarse) Sp. Cr. and absorp. (fine)	ASTM C127 ASTM C128	Once every 10,000 yd[3] of concrete when concrete is produced onsite but monthly when concrete is produced and delivered from an offsite plant.
	Petrographic	ASTM C295	When aggregate tests indicate a significant change has occurred in the characteristics of the aggregate.
Concrete	Radiation shielding properties	ASTM C637	1 test per design mix when high density aggregates are used.
Water and Ice	Chloride ion Sulfates Time of set False set Compressive strength pH Total dissolved solids	ASTM D512 ASTM D516 ASTM C191 ASTM C451[b] ASTM C109 ASTM D1293 AASHO T26	Initially and monthly thereafter until reliability is established then semi-annually thereafter, or as directed by the engineer contractor
Concrete Mixes	Design Making and curing test specimens Air content Slump Bleeding Compressive strength Bond developed with reinforcing	ACI 211.1 ASTM C192 ASTM C231 ASTM C143 ASTM C232[b] ASTM C39 ASTM C234[b]	Upon mix adjustment

3.8.1.6.4.3 Control of Mechanical Splices of Reinforcing

Control of mechanical splices utilizing filler metal and an enclosing sleeve (Cadweld and Bar-lock type splices) are in accordance with Regulatory Guide 1.10 (Withdrawn by NRC 8/71).

3.8.2 STEEL CONTAINMENT

The containment is a prestressed, reinforced concrete structure; therefore this subsection does not apply.

3.8.3 CONCRETE AND STEEL INTERNAL STRUCTURES OF STEEL OR CONCRETE CONTAINMENTS

The internal structures of the containment buildings are not required to support permanent plant shutdown or defueled operations. The operational information has been removed from the UFSAR (DSAR) to indicate that the systems perform no licensing bases or design bases function. Although the systems do not support operation, they may still contain fluids, gases or other hazards such as energized circuits, compressed air, radioactive material, etc. Equipment may not have been physically removed from the plant. See P&IDs, One-Line diagrams, and General Arrangement Drawings for current plant configuration.

3.8.3.1 Description of the Internal Structures

The internal structures located in the containment consist of the reactor vessel supports, steam generator supports and stops, reactor coolant pump supports, reactor coolant pipe restraints, primary shield wall and reactor cavity, secondary shield walls, pressurizer supports, refueling canal walls, fuel transfer tube and the operating and intermediate floors.

3.8.4 OTHER SEISMIC CATEGORY I STRUCTURES

3.8.4.1 Description of the Structures

Seismic Category I structures other than the containment and its internal structure are listed below:

A. Auxiliary building

B. Fuel handling building

C. Safety equipment building

D. Intake structure

E. Electrical/piping junction structure

F. Diesel generator building

G. Condensate and refueling tank enclosure structure

3.8.4.1.1 Auxiliary Building

The auxiliary building is a conventional reinforced concrete structure containing the control area, radwaste area, primary plant makeup, and radwaste storage tank area, and two pipe-penetration areas. The plan dimension of the structure is approximately 220 x 280 feet with a maximum height of approximately 94 feet. Several typical plans and sections are shown in Controlled Drawings 10105 and 25068 and Figure 3.8-32.

The diverse functional requirements of the various entities housed within the auxiliary building have resulted in structural systems with correspondingly diverse physical characteristics. The control area is a relatively open, steel-framed, beam-column system supporting the floor slabs with a perimeter shear wall and light interior partition walls. The radwaste area consists of heavy shear walls to satisfy the compartmentalization and biological shielding requirements associated with its functional characteristics. The tankage area also incorporates a shear wall design concept. However, the story heights within this area are greatly increased over those in the adjoining sectors of the building, and the east perimeter wall is partially embedded. Finally, the penetration areas consist of a steel-framed, beam-column system supporting the cantilevered floor slabs and a partial perimeter shear wall.

3.8.4.1.2 Fuel Handling Building

1. The fuel-handling building is a conventional reinforced concrete structure containing the new- and spent-fuel handling, storage, and shipment facilities[1], fuel pool water cooling equipment, and decontamination area. The overall plan dimension of the structure is approximately 134 x 86 feet, with a maximum height of 110 feet. Several typical plans and sections are shown in Controlled Drawings 25402, 25410, 23105, and 25416. The structure is of heavy shear wall construction with a concrete-slab, steel-frame, composite-action roof system. Partial soil embedment of about 20 feet is present on three sides of the structure with no embedment on the fourth side.

3.8.4.1.3 Safety-Equipment Building

The safety-equipment building is an unsymmetrical, conventionally reinforced concrete structure that houses the safety-injection system, containment spray system, component cooling water system, and engineered safety features (ESF) electrical gallery. The safety-injection area and

[1] No new fuel is stored at SONGS in the permanently defueled condition. However, portions of this system will remain available during the decommissioning process for various activities not related to new fuel storage.

component cooling water area are located in the below-grade portion of the structure with the ESF electrical gallery occupying the roof elevation. The maximum plan dimension of the structure is 174 x 74 feet with an overall height of 70 feet. The minimum dimension of the structure is 48 feet in width. Several typical plans and sections are shown in Controlled Drawings 23600, 23608, and 23605. The safety-injection area consists of a uniform distribution of heavy shear walls to satisfy the separation and shielding requirements. The component cooling water area consists of large, open rooms with a minimum amount of shear walls. The one exception is in the lower elevation, where a more uniform distribution of shear walls is required to satisfy compartmentalization and to provide structural support for the component cooling water heat exchangers. The ESF electrical gallery consists of an open tunnel way with longitudinal shear walls and a heavy roof diaphragm. The basement elevations of the safety-injection portion are not co-planar with the component cooling water portion, and the embedment characteristics vary on all four sides of the structure. The safety injection system piping is located in a tunnel attached to, and below, the basemat of the component cooling water area. The interfaces of the safety equipment building with the emergency sump tunnel of the containment, penetration area, and tunnel under the auxiliary building, are connected by a flexible stainless steel and Inconel bellows to allow movement in any direction due to seismic excitation.

3.8.4.1.4 Intake Structure

The intake structure is a conventional reinforced concrete buried structure that houses the major components of the circulating water system and the pumps associated with the saltwater cooling system (component cooling water system). The structure is quite irregular in shape with numerous piers, partition walls, and localized slab elevations (see Controlled Drawings 22007 and 22008). The maximum plan dimension is approximately 110 by 280 feet with a maximum height of approximately 60 feet. It is situated adjacent to the auxiliary building and the turbine building and is embedded in the soil to a varying degree, with the major portion of the structure completely below grade. Controlled Drawing 22030 also represents an isometric of the Unit 2 intake structure. The Unit 3 structure is symmetrical about an east-west axis along the south edge of the Unit 2 facility. Plant grade is at elevation +30 feet. The saltwater cooling tunnel leading from the intake structure to the plant is located between column lines J and K extending from column line 14 to column line 25 in the intake structure area (see Controlled Drawings 23017, 23025, and 23024). It continues through a portion of the turbine building mat where column lines 12 through 14 and 25 through 27 intersect column lines J and K and connects to the component cooling water heat exchanger area of the safety equipment building. The saltwater cooling tunnel is a conventional reinforced concrete structure and houses the component cooling water heat exchanger saltwater supply and return lines.

3.8.4.1.5 Electrical and Piping Gallery Structure

The electrical and piping gallery structure is a partially buried conventional reinforced concrete shear-wall structure. The structure provides a transition area for Seismic Category I piping and electrical cable from the underground tunnels and duct runs into the safety-equipment building. The overall plan dimension of the structure is 85 x 67 feet with a maximum height of 54 feet.

Several typical plans and sections are shown in Controlled Drawings 23700 and 23701. The interior of the structure consists of numerous partial floor slabs, partition walls, and vertical risers. Due to the physical proximity to other structures, the embedment characteristics vary on each side of the structure.

3.8.4.1.6 Diesel Generator Building

The diesel generator building is a conventional two-story reinforced concrete structure. The overall plan dimensions of the structure are 91 x 60 feet with a maximum height of 41 feet. The structure system consists of shear walls and concrete slabs, supported by a 5.5-foot thick basemat which is integrated with the equipment foundation blocks. Typical plans and sections are shown on Controlled Drawings 23850, 23853, and 23854. The structure contains two 4700-kW diesel generators with complete auxiliary equipment required for independent operation. The diesel generators are located on the lower floor at finished grade elevation and most of the auxiliary equipment is located on the upper floor. The two independent systems are separated by a concrete bearing wall. All of the equipment is protected against tornado missiles by concrete walls and slabs. The resulting structure is regular in shape and exhibits little or no geometric eccentricities.

3.8.4.1.7 Condensate and Refueling Tank Enclosure Structure

This structure is a conventional reinforced concrete structure that contains two steel-plate condensate storage tanks, two steel-plate refueling water storage tanks, one steel-plate nuclear service water storage tank, and all of the associated piping, valves, and pumps. Each tank is installed in a separate compartment, and the foundations are located at grade. The resulting structure is fairly regular in shape but does exhibit some geometric eccentricities between the center of mass and the center of rigidity, due to the difference in size between the condensate storage tanks and the refueling water tanks.

The overall plan dimensions of the concrete structure are approximately 137 x 98 feet with a maximum height of approximately 44 feet. The structure is of heavy shear wall construction with partial concrete roof for missile protection of the condensate storage tank and pump room. A light structural steel frame supports a vinyl-coated fabric screen roof over the refueling water storage tanks to protect them against falling transmission lines. The embedment of the building is 4 feet below the plant grade (elevation +30 ft). Typical plans and sections are shown in Controlled Drawings 23800 and 23803. The two refueling water storage tanks are each 36 feet in diameter with a height of 40 feet. One condensate storage tank is 50 feet in diameter by 39 feet high, while the second tank is 30 feet in diameter by 36 feet high.

Additional information pertaining to the watertightness of the concrete enclosure walls around the large condensate storage tank is covered in Reference (10).

3.8.4.1.8 Miscellaneous "Category I" Structures

The miscellaneous Category I structures consist of electrical tunnels, electrical duct banks, and electrical manholes.

The tunnels are conventional reinforced concrete structures which connect the electrical and piping gallery structure to the containment building and main and auxiliary transformers. The tunnels are completely buried and are rectangular in cross-section. The top slab, which is 2 feet thick, is covered with a 4-foot layer of soil. The bottom slab is 2 feet thick and the sidewalls are 1.5 feet thick. During the decommissioning of well No. 8, cavities adjacent to the well were discovered. This well is located under a section of the Unit 3 electrical tunnel. A thorough discussion of the cavities is provided in Paragraph 2.5.4.14.1. The method of analysis of the effects of the cavity on this structure and the results are given in Paragraph 3.8.4.4 and Table 3.8-7 respectively.

The duct banks are composed of Quality Class II electrical cables and are embedded in the compacted sand backfill. These duct banks are interrupted by several concrete manholes to provide accessibility to pull the cables during installation and maintenance.

Design criteria for these structures are in accordance with Paragraphs 3.8.4.2 through 3.8.4.6.

3.8.4.1.9 Box Conduit Structure

The offshore intake and discharge box conduits are conventionally reinforced concrete buried structures that extend 160 feet seaward of the permanent seawall. They interface with the intake structure at the seawall and with the offshore circulating water conduits on the seaward end. There are a total of four box conduits with square cross-sectional areas for the two units. The interior dimensions of each box section are 16 feet by 16 feet. Each unit has one discharge and one intake box conduit integrated into one structure and separated by a wall 2 feet 6 inches thick. The exterior walls are 3 feet thick, the top slab 3 feet 6 inches thick, and the foundation slab 3 feet 8 inches thick. The invert elevation is at elevation (-) 26.0 feet, and the top slab which is horizontal is at elevation (-) 6.5 feet. A shear key, a cold joint, and continuous water stop are provided at the interface with the intake structure. This joint will act as a hinge and will allow some rotation to take place under applied seismic motions. Controlled Drawings 22044 and 22045, show the plan, sections, and reinforcing details of the structure.

Table 3.8-7
ELECTRICAL TUNNEL SUMMARY OF GOVERNING LOAD INTERACTIONS FOR PRINCIPAL REINFORCED CONCRETE MEMBERS

Description of Principal Members	Governing Load Combination Number(1)	Calculated Axial Load (Pμ) and Flexural Load (Mμ)		Maximum Flexural Capacity (Mμ) For No Axial Load	Maximum Flexural Interaction Capacity (Mμ) Given Axial Load	Remarks
		Pμ (Kips)	Mμ (ft-Kips)			
Roof Slab - el. (+) 25'-6", 2' thick	10(a)	19.0	44.3	91.0	110.0	
Base slab – el. (+)9'-6" 2' thick	10(a)	23.0	34.8	55.4	80.0	
Side Wall – 1'-6" thick	10(a)	10.7	39.8	39.8	40.0	
Tunnel Box Beam Section	10(a)	-	3250	9750	-	

(1) Refer to Paragraph 3.8.4.3.2.A for description of load combination number.

3.8.4.1.10 Auxiliary Intake Structure

The auxiliary intake structure is a conventionally-reinforced concrete conduit modified to support a riser and velocity cap configuration. The riser is designed to pass the 34,000 gal/min flow required for the saltwater cooling system of both Units 2 and 3 during emergency conditions. A separate structure is provided for each unit and is located approximately 3100 feet offshore, directly on the alignment of the intake conduit, and 92 feet shoreward of the primary intake structure. The auxiliary intake structure is designed to be placed in an excavated trench approximately 30 feet below MLLW and backfilled with select granular material. The riser projects approximately 9 feet above this backfill material.

The auxiliary intake riser is a 4-foot inside diameter, reinforced concrete cylinder, with 9-inch walls. It is 11-1/2 feet tall and is topped by a 9-1/2 foot diameter concrete velocity cap. The riser is attached monolithically to a rigid base block that improves resistance to overturning loads and spreads these loads to more favorable application points on the conduit section (see Controlled Drawing 5131363).

The riser and base block are attached mechanically to a specially modified 18-foot inside diameter conduit, 20 feet in length, with a 15-inch wall thickness. The pipe section is monolithically attached to, and supported by, two buttresses, each 5 feet long and 27 feet wide. These buttresses are provided with projections that widen the structure's base to resist lateral overturning and to develop a passive pullout soil wedge for increased stability.

3.8.4.1.11 Offshore Intake Conduits

The offshore intake circular conduits are 18-foot inside diameter concrete pipes that extend approximately 3200 feet seaward from the box conduit interface to the primary offshore intake structure. An auxiliary intake structure, discussed in Paragraph 3.8.4.1.10, is located directly on the intake conduit alignment approximately 92 feet shoreward of the primary offshore intake structure. The intake conduits are classified as Seismic Category I from the onshore intake structure to one pipe section seaward of the auxiliary intake structure. The remainder of the pipe sections and the primary offshore intake structure are Seismic Category II.

With the exception of three sections containing access manholes, the pipe sections are prestressed concrete with 10-inch walls. The pipe sections are 24 feet in length. The manhole sections have an 8-foot section of conventionally reinforced concrete around the manhole opening, while each end of the pipe is prestressed. The pipe sections are connected by bell and spigot joints (Figure 3.8-50) that are designed to accommodate the maximum rotation and translation resulting from the DBE ground motion as determined by the critical instantaneous displacement profile (refer to Appendix 3.7C). The joints are wrapped circumferentially with a 3-foot wide sheet of 1/2-inch thick neoprene rubber to provide a seal and prevent gravel entry in the event of joint movement.

The intake conduit is placed in a trench separated from the discharge conduit trench by a septum of undisturbed San Mateo sand. The intake conduit trench is backfilled with a select gravel material from the box conduit interface to and including the primary offshore intake structure. The gravel backfill material was selected such that it will not behave as a heavy fluid during a DBE.

3.8.4.2 Applicable Codes, Standards and Specifications

The following codes, standards and regulations, specifications, design criteria, and NRC Regulatory Guides constitute the basis for the design, fabrication, and construction of other Seismic Category I structures. Modifications to these codes, standards, etc., are made when necessary to meet the specific requirements of the structure. These modifications are indicated in the sections where references to the codes, standards, etc., are made.

3.8.4.2.1 Codes

A. Uniform Building Code (UBC), 1970 Edition

B. American Institute of Steel Construction (AISC), Manual of Steel Construction, 1969 Edition

C. American Concrete Institute (ACI) 318-71, Building Code Requirements for Reinforced Concrete

D. American Welding Society (AWS), AWS D1.1-72, Structural Welding Code

3.8.4.2.2 Standards and Regulations

A. Occupational Safety and Health Act (OSHA)

B. State of California, Division of Industrial Safety General Industry Safety Orders

C. Nuclear Property Insurance Association - Mutual Atomic Energy Reinsurance Pool (NEPIA-MAERP), Basic Fire Protection for Nuclear Plants

D. National Fire Protection Association (NFPA), NFPA No. 24, Outside Protection

E. Hydraulic Institute (HI) Standards

3.8.4.2.3 Specifications

A. Industry Specifications

1. American Society for Testing and Materials (ASTM)

ASTM standard specifications are used whenever possible to describe material properties, testing procedures, and fabrication and construction methods. The standards used, and the exceptions to these standards, if any, are identified in the applicable sections.

2. American Concrete Institute (ACI), ACI 301, Specification for Structural Concrete for Buildings, May 1972

3. American Iron and Steel Institute (AISI), Specification for the Design of Light Gage, Cold-Formed Steel Structural Members, 1968 Edition

4. Crane Manufacturers Association of America (CMAA), CMAA Specification No. 70, 1971

B. Project Design and Construction Specifications

Project design and construction specifications were prepared to cover the areas related to design and construction of other Seismic Category I structures. These specifications, prepared specifically for the San Onofre Nuclear Generating Station, Units 2 and 3, emphasized important points of the industry standards for the design and construction of the Seismic Category I structures and reduced options that otherwise would be permitted by the industry standards. Unless specifically noted otherwise, these specifications do not deviate from the applicable industry standards. They covered the following subject headings:

1. Excavation and Backfill

2. Concrete Placement

3. Inspection of Concrete Production

4. Reinforcement Steel Placement

5. Structural Steel Erection

6. Miscellaneous Metalwork Installation

7. Stainless Steel Liner Plate System Installation

8. Concrete and Concrete Products

9. Reinforcing Steel and Associated Products

10. Structural Steel

11. Miscellaneous Steel and Embedded Materials

12. Stainless Steel Liner Plate

3.8.4.2.4 Design Criteria

A. Project Design Criteria

Project design criteria were prepared to include comprehensive design requirements of the other Seismic Category I structures and contained specific references to prescribed Bechtel internal design guides, applicable industry standards, and pertinent technical texts, journals, and reports used in preparing the criteria.

B. Bechtel Topical Reports

1. BC-TOP-4, Seismic Analyses of Structures and Equipment for Nuclear Power Plants, Rev. 1, September 1972

2. BC-TOP-9A, Design of Structures for Missile Impact, Revision 2, September 1974

3. BN-TOP-2, Design for Pipe Break Effects, Revision 1, September 1973

C. Project Reports

1. Seismic and Foundation Studies, Dames and Moore, April 15, 1970

2. Methods of Direct Application of Element Damping - San Onofre Units 2 and 3, Bechtel Power Corporation, Los Angeles Office, January 1972

3. Development of Soil-Structure Interaction Parameters, Proposed Units 2 and 3 San Onofre Generating Station. Woodward-McNeill & Associates, Orange, California, January 31, 1974

4. Elastic and Damping Properties, Laydown Area, San Onofre Nuclear Generating Station, Woodward-McNeill and Associates, Orange, California, October 14, 1971

5. Preliminary Safety Analysis Report - San Onofre Units 2 and 3

3.8.4.2.5 NRC Regulatory Guides

A. Regulatory Guide 1.10, Mechanical (Cadweld) Splices in Reinforcing Bars of Category I Concrete Structures (Withdrawn by NRC, 7/81)

B. Regulatory Guide 1.15, Testing of Reinforcing Bars for Category I Concrete Structures (Withdrawn by NRC, 8/71)

C. Regulatory Guide 1.55, Concrete Placement in Category I Structures (Withdrawn by NRC, 8/71)

3.8.4.3 Loads and Load Combinations

3.8.4.3.1 Load Definitions

The other Seismic Category I structures were designed for all credible conditions of loading. The design load categories were identified as normal loads, severe environmental loads, extreme environmental loads, and abnormal loads.

3.8.4.3.1.1 Normal Loads

Normal loads are those loads to be encountered during normal plant operation and shutdown. They include the following:

A. Dead Loads

Dead load consists of the weight of the concrete wall, roof, base slab, steel, and permanently attached equipment, and, in addition, includes hydrostatic loads which consist of lateral hydrostatic pressure resulting from ground water or flood water, as well as buoyant forces resulting from the displacement of ground water or flood water by the structure.

B. Live Loads

Live loads consist of any movable equipment loads and other loads which vary with intensity and occurrence, such as floor occupancies and soil pressures.

C. Normal Thermal Loads

Normal thermal loads are produced due to the temperature distribution through the wall during normal operating or shutdown conditions, based on the most critical transient or steady-state conditions.

D. Normal Pipe Expansion Loads

Normal pipe expansion loads consist of forces on the structure caused by thermal expansion of piping during normal operating or shutdown conditions based on the most critical transient or steady-state condition.

E. Transient Water Pressure Loads (Water Hammer)

The water hammer load consists of the rapid temporary increase in internal pressure in the circulating water system conduits resulting from a simultaneous trip of all the main circulating water pumps.

3.8.4.3.1.2 Severe Environmental Loads

Severe environmental loads are those loads that could infrequently be encountered during the plant life. Included in this category are:

A. Operating Basis Earthquake (OBE)

The OBE consists of a static equivalent seismic load for which the dynamic effects have been included in its determination. A more detailed discussion is presented in Subsection 3.7.1.

B. Wind Loads

Refer to Subsection 3.3.1 for a detailed description of wind loads.

3.8.4.3.1.3 Extreme Environmental Loads

Extreme environmental loads are those loads that are credible, but are highly improbable. They include:

A. Design Basis Earthquake (DBE)

The DBE consists of a static equivalent seismic load for which the dynamic effects have been included in its determination. A more detailed discussion is presented in Subsection 3.7.1.

B. Tornado Loads

Tornado loads consist of the combined effects of tornado wind pressure, pressure differential, and missile impingement. Refer to Subsection 3.3.2 for a detailed description.

Load Combinations

The following nomenclature is used in the load combinations.

D = Dead Load
L = Appropriate live load
T_o = Normal thermal loads*
H_o = Normal pipe expansion load*
E = Operating basis earthquake load
W = Wind loads
E' = Design basis earthquake load
W_t = Tornado loads
R = Pipe rupture and miscellaneous missile loads*
T_A = Abnormal thermal load*
H_A = Abnormal pipe expansion load*
F_H = Water hammer load

* While these loads were part of the design basis they are no longer applicable following cessation of operation and permanent plant shutdown or the units.

The load combinations and factors for which the strength method is used are as follows:

A. Concrete

1. Normal Case

$1.4D + 1.7L$

2. Severe Environmental Case

$1.25D + 1.25L \pm 1.25E/W + 1.0H_o$

3. Severe Environmental Case

$1.25D + 1.25L \pm 1.25E/W + 1.0T_o$

4. Abnormal/Severe Environmental Case

$1.0D + 1.0L \pm 1.25E + 1.0T_A + 1.0R + 1.0H_A$

5. Abnormal/Severe Environmental Case

$1.0D \pm 1.25E + 1.0T_A + 1.0R + 1.0H_A$

6. Abnormal/Extreme Environmental Case

   $1.0D + 1.0L \pm 1.0E' + 1.0T_o + 1.0R + 1.25\ H_o$

7. Abnormal/Extreme Environmental Case

   $1.0D + 1.0L \pm 1.0E' \pm 1.0T_A + 1.0R + 1.0H_A$

8. Abnormal Case

   $1.0D + 1.0L + 1.0W_t + 1.0T_o + 1.25H_o$

The box conduits and offshore circular conduits were originally classified as Seismic Category II structures. However, they were designed to withstand DBE loadings. Since they have been reclassified as Seismic Category I structures, a reanalysis of the box conduits and offshore circular conduits was performed using the load combinations and factors outlined below. The load combinations and factors used in the design of the auxiliary intake structure are also given below:

9. Normal Case

   $1.4D + 1.7L$

10. Severe Environmental Case

    (a) $1.4D + 1.7L + 1.9E/1.7W$

    (b) $1.2D + 1.9E/1.7W$

    (c) $0.75\ (1.4D + 1.7L + 1.9E + 1.7F_H)$

11. Abnormal/Extreme Environmental Case

$1.0D + 1.0L + 1.0E'/1.0W + 1.0F_H$

Where soil and hydrostatic pressures are present, in addition to all the above combination where they may have been included in L and D respectively, the requirements of Sections 9.3.4 and 9.3.5 of ACI 318-71 are also satisfied.

In the case of the electrical tunnel, a reanalysis of the portion of the structure located over the cavity adjacent to well 8, described in Paragraph 2.5.4.14.1, was performed using load combinations 9, 10, and 11.

B. Structural Steel

Steel structures shall satisfy the following loading combinations without exceeding the allowable working stress for equations 1, 2, and 3 and 90% of the elastic yield capacity (with full regard to elastic stability) for equations 4 through 7.

1. Normal Case

$D + L$

2. Severe Environmental Case

$D + L + T_o + H_o + E$ or W

3. Severe Environmental Case

[(a)]$D + L + H_o + E$

4. Abnormal/Extreme Environmental Case

$D + L + R + T_o + H_o + E'$

5. Abnormal/Extreme Environmental Case

$D + L + R + T_A + H_A + E'$

6. Abnormal Case

$D + L + R + T_o + H_o$

[(a)] For structural elements carrying mainly earthquake forces only; e.g., struts and bracing.

7. Extreme Environmental Case

$D + L + T_o + H_o + W_t$

The stress levels reflected in the above load combinations are based upon the specific nature of the loading condition and the actual function of the structure. In general, for the operating basis seismic design, the structure is designed for elastic behavior using load factors based upon stresses significantly below the strength capacity in the case of concrete and using working stress levels in the case of structural steel. For the accident basis design, stress analysis is based upon load levels at or just below the strength capacity for concrete and just below the elastic capacity for structural steel.

3.8.4.4 Design and Analysis Procedures

The analysis procedures, including assumptions of load distribution and boundary conditions for other Seismic Category I structures, listed in Paragraph 3.8.4.1, are based on conventional methods. The basic analytical techniques may be classified in two groups: methods involving simplifying assumptions, such as those found in beam theory, and those based on plate theories of different degree of approximation. The structures are designed to behave under loading as structural units and are provided with connections capable of transmitting vertical and lateral loads by axial and diaphragm action to their foundations.

The structures are designed to maintain elastic behavior when subjected to various combinations of dead, live, thermal, seismic, tornado, and accident loads. The upper limit of elastic behavior is considered to be the yield strength of the effective load-carrying structural material. The yield strength F_y for steel (including reinforcing steel) is considered to be the guaranteed minimum in appropriate ASTM specifications. The yield strength for reinforced concrete structures is considered to be the ultimate resisting capacity as calculated from the ACI 318-71 code. Reinforced concrete structures are designed for ductile behavior.

Under seismic loading, no plastic analysis is considered. Local yielding or erosion of barriers is considered permissible due to pipe rupture loading or missile impact, provided there is no general failure.

Structural steel is designed in accordance with basic working stress design methods as outlined in the 1970 AISC manual of steel construction.

The range of design variables that influence the results of the analyses is considered as follows:

A. Accuracy of design loads

B. Variation from assumed load distributions

C. Future changes in type or magnitude of loads

D. Frequency of loading and impact

E. Accuracy of analysis

F. Design accuracy of member sizing and proportioning

G. Reliability of specified material strengths

H. Construction dimensional variations

I. Function of structure

For the working stress design methods, the effects of the design variables are included in the values of the allowable stresses. For the strength design method, the effects of the design variables are accounted through load factors and capacity reduction factors.

Computer programs used in the analysis and design of reinforcing steel of the other Seismic Category I structures are as follows:

	Computer Program
A. Auxiliary and Fuel Handling Building	
1. Compute equivalent stiffness matrix	COPK (refer to Section 3C.7)
2. Dynamic analysis	SUPER SMIS (refer to Section 3C.3), BSAP
3. Static stress analysis	SAP (refer to Section 3C.5), BSAP
4. Design reinforcing steel	RESCOS (refer to Section 3C.8) OPTCON (refer to Section 3C.9)
B. Safety Equipment Building	
1. Dynamic and static stress analyses	SAP
2. Design reinforcing steel	RESCOS
C. Intake Structure	
1. Static stress analysis	ICES STRUDL-II (refer to Section 3C.6)

D. Electrical and Piping Gallery Structure

1. Dynamic and static stress analyses	SAP
2. Design reinforcing steel	OPTCON

E. Diesel Generator Building and Condensate and Refueling Tank Enclosure Structure

1. Dynamic and static stress analyses	SAP
2. Design reinforcing steel	OPTCON

3.8.4.4.1 Electrical Tunnel Reanalysis

The formation of cavities associated with construction dewatering wells resulted in subsurface conditions that varied from the original soil parameters used in design of the tunnel structure. A reanalysis was performed to evaluate the structural integrity of this tunnel in the cavity region, considering seismic, as well as static loading. In the reanalysis, stiffness of foundation material was assumed to be negligible within the area beneath the structure, where the ratio of pore pressure over the confining pressure was greater than 0.3. This loss of stiffness results from a buildup of excess pore pressure within the cavity region and affects an approximately 25-foot length of the tunnel. A detailed discussion of this effect is contained in Reference 103 to Section 2.5.

The tunnel was reanalyzed both as a continuous box-beam element spanning the cavity region and as a closed box section subjected to pressures that will exist in the cavity region. Local effects on the floor slab were also evaluated. The following conditions and loadings were considered in this reanalysis.

- Dead and live loads
- Seismic loads equal to 1.5 times peak free-field design response spectra acceleration for 8% combined soil-structure damping for OBE and 10% for DBE conditions (Equivalent Static Analysis Methodology). These values are consistent with values determined by dynamic analysis of other plant Seismic Category I structures and would be conservative for a totally buried structure.
- Static and dynamic soil pressure.

- Surcharge loads resulting from soil situated above the tunnel. Foundations of adjacent structures do not impose surcharge loadings since they are located at elevations similar to that of the tunnel.

- Effects of actual construction joint locations. A review of construction details disclosed that no transverse construction joints or seismic separation joints exist in the region considered for the reanalysis (a length equal to three times the cavity affected zone).

- Interface area with other structures. No structural continuity exists between adjacent structures. Seismic gaps are provided to prevent the transfer of any seismically induced actions or loads to the tunnel structure.

3.8.4.5 Structural Acceptance Criteria

The limiting values of stress, strain, and gross deformations are established by the following criteria:

A. To maintain the structural integrity when subjected to the worst load combinations

B. To prevent structural deformations from disturbing the Seismic Category I equipment to the extent that it suffers a loss of function

The allowable stresses are those specified in the applicable codes. The stress contributions due to earthquake loading are included in the load combinations described in Paragraph 3.8.4.3.

Structural deformations were not found to be a controlling criterion in the design of other Seismic Category I structures listed in Paragraph 3.8.4.1.

The tables listed below summarize (1) the governing load interactions and maximum capacity of principal reinforced concrete members (see category A) and, where applicable, (2) the governing combined stress ratios from the beam/column interaction equation for principal structural steel members (see category B).

Structure	Reference Table Number Category A[a,b]	Category B
Auxiliary building	3.8-8	3.8-9
Fuel handling building	3.8-10	-
Safety equipment building	3.8-11	3.8-12 3.8-13
Intake structure	3.8-14	-
Electrical and piping gallery structure	3.8-15	-
Circular conduits	3.8-16	-

Structure	Reference Table Number Category A[a,b]	Category B
Box conduit	3.8-17	-
Auxiliary intake structure	3.8-18	-
Electrical cable tunnel structure	3.8-7	

(a) The ratio of the maximum capacity to the required capacity yields the safety margin.

(b) The installation of high density spent fuel storage racks in the fuel handling building coupled with the application of rigorous structural evaluations have resulted in changes in governing loading conditions. Tables 3.8-7A and 3.8-7B provide additional loading data and comparisons (original conditions vs. current conditions) for the affected portions of the structure (pool walls and basemat).

Table 3.8-7A
CURRENT EVALUATION RESULTS FOR THE
SPENT FUEL POOL WALLS AND BASEMAT

	Governing Load Combination[a]	Utilization Factor (5)[b]
North and South Walls:		
Horizontal Reinforcement	7	88.4
Vertical Reinforcement	7	37.4
East Wall:		
Horizontal Reinforcement	7	23.1
Vertical Reinforcement	7	47.0
West Wall:		
Horizontal Reinforcement	7	28.1
Vertical Reinforcement	6	79.5
Basemat:		
North-South Reinforcement	7	51.7
East-West Reinforcement	6	81.4

(a) Refer to Paragraph 3.8.4.3.2.A
(b) The Utilization Factor is defined as the percentage of resistance to the reinforced concrete section that has been utilized relative to the zero curvature line.

Table 3.8-7B
COMPARISON OF GOVERNING RESULTS FOR
THE ORIGINAL DESIGN VERSUS THE CURRENT
EVALUATION FOR THE SPENT FUEL POOL

Location in Spent Fuel Pool	(a)	Governing Load Combination (b)	Axial Load Pu (kips) (c)	Flexural Load Mu (K-ft/ft)	Max Flexural Load Mu (Max) (K-ft/ft) (d)	Mu/Mu(Max)
7-Foot Thick Basemat in Pool Area (E-W Reinf)	ORIGINAL	7	-527	2604	2660	0.98
	CURRENT EVALUATION	6	92	1465	1793	0.82
4-Foot Thick (N or S) Spent Fuel Pool Wall (Vert Reinf)	ORIGINAL	7	-404	445	947	0.47
	CURRENT EVALUATION	7	-67	208	554	0.38
5-Foot Thick (West) Spent Fuel Pool Wall (Vert Reinf)	ORIGINAL	7	0	666	674	0.99
	CURRENT EVALUATION	6	208	215	257	0.84

(a) The current evaluations are the maximum values obtained and not necessarily at the previous locations.
(b) Refer to Paragraph 3.8.4.3.2.A.
(c) Sign convention for Pu: Compression (-), Tension (+)
(d) Maximum flexural interaction capacity (Mu(Max)) given the axial load shown (Pu).

Table 3.8-8
AUXILIARY BUILDING SUMMARY OF GOVERNING LOAD INTERACTIONS FOR PRINCIPAL REINFORCED CONCRETE MEMBERS (Sheet 1 of 5)

Description of Member	Location of Principal Member	Governing Load Combination Number[a]	Calculated Axial Load (P_u) and Flexural Load (M_u)		Maximum Flexural Interaction Capacity (M_u), Given Axial Load (P_u)[b][c]	Calculated Shear Load (V_u)[b]	Maximum Shear Capacity (V_u)[b]
			P_u[b]	M_u[c]			
	Radwaste Area						
2'-6" thick wall – vertical reinforcement	Exterior south wall @ El 9'-0"	6	-36	161	278	--	--
2'6" x 73'6" wall – vertical reinforcement	Exterior south wall @ El 9'-0"	6	+2,929	8.31×10^4	33.2×10^4	--	--
2'-6" x 73'6" wall - vertical and horizontal reinforcement	Exterior south wall @ El 9'-0"	6	-10,388	9.41×10^4	60.2×10^4	10,975	11,719
3'-0" thick wall – vertical reinforcement	Interior wall @ El 9'-0"	6	-43	260	291	--	--
3'-0" x 28'-6" wall - vertical and horizontal reinforcement	Interior wall @ El 9'-0"	6	-4,477	1.21×10^4	9.7×10^4	5,709	6,387
3'-0" x 28'-6" wall - vertical reinforcement	Interior wall @ El 9'-0"	6	+685	1.07×10^4	5.5×10^4	--	--
1'-0" thick wall - vertical reinforcement	Interior wall @ El 9'-0"	6	-15	12	48	--	--
1'-0" x 11'-2" wall - vertical and horizontal reinforcement	Interior wall @ El 9'-0"	6	-655	161	4,645	408	615
1'-0" x 11'-2" wall - vertical reinforcement	Interior wall @ El 9'-0"	6	+229	142	1,606	--	--

[a] Refer to Paragraph 3.8.4.3.2.A for description of load combination number.
[b] P_u and V_u are in kips; Sign convention for P_u: compression (-), Tension (+).
[c] M_u is in ft-k/ft

Table 3.8-8
AUXILIARY BUILDING SUMMARY OF GOVERNING LOAD INTERACTIONS FOR PRINCIPAL REINFORCED CONCRETE MEMBERS (Sheet 2 of 5)

Description of Member	Location of Principal Member	Governing Load Combination Number[a]	Calculated Axial Load (P_u) and Flexural Load (M_u)		Maximum Flexural Interaction Capacity (M_u), Given Axial Load (P_u)[b][c]	Calculated Shear Load (V_u)[b]	Maximum Shear Capacity (V_u)[b]
			P_u[b]	M_u[c]			
2'-0" thick wall - vertical reinforcement	Interior wall @ El 9'-0"	6	-29	67	81	--	--
2'-0" thick wall - vertical reinforcement	Exterior south wall @ El 50'-0"	6	-16	93	98	--	--
2'-0" x 153'-6" wall - vertical and horizontal reinforcement	Exterior south wall @ El 50'-0"	6	-7,797	139,937	1,393,770	7,758	20,030
2'-0" x 153'-6" wall - vertical reinforcement	Exterior south wall @ El 50'-0"	6	+962	139,937	969,222	--	--
2'-6" thick wall - vertical reinforcement	Interior wall @ El 50'-0"	6	-19	121	183	--	--
2'-6" x 218'-6" wall - vertical and horizontal reinforcement	Interior wall @ El 50'-0"	6	-10,569	454,826	3,282,980	9,674	29,229
2'-6" x 218'-6" wall - vertical reinforcement	Interior wall @ El 50'-0"	6	-822	454,826	2,605,940	--	--
8'-0" thick basemat - E-W reinforcement	@ El 9'-0"	3	--	1,936	2.343	--	--
2'-0" thick slab - E-W reinforcement	@ El 24'-0"	3	--	60	73	--	--
	Radwaste Storage Tank Area						
2'-6" thick wall - vertical reinforcement	Exterior south wall @ El 9'-0"	6	-14	185	217	--	--
2'-6" x 32'-6" wall - vertical and horizontal reinforcement	Exterior south wall @ El 9'-0"	6	3,802	4,568	11.18×10^4	1,499	4,699

Table 3.8-8
AUXILIARY BUILDING SUMMARY OF GOVERNING LOAD INTERACTIONS FOR PRINCIPAL REINFORCED CONCRETE MEMBERS (Sheet 3 of 5)

Description of Member	Location of Principal Member	Governing Load Combination Number	Calculated Axial Load (P_u) and Flexural Load (M_u)		Maximum Flexural Interaction Capacity (M_u), Given Axial Load (P_u)[b][c]	Calculated Shear Load (V_u)[b]	Maximum Shear Capacity (V_u)[b]
			P_u[b]	M_u[c]			
2'-6" x 32'-6" wall - vertical reinforcement	Exterior south wall @ El 9'-0"	6	+2,477	4,568	5.18×10^4	--	--
4'-0" thick wall - vertical reinforcement	Exterior east wall @ El 9'-0"	6	--	907	1,044	--	--
2'-0" thick wall - vertical reinforcement	Exterior east wall @ El 37'-0"	6	-10	60	89	--	--
2'-0" x 60'-0" wall - vertical and horizontal reinforcement	Exterior east wall @ El 37'-0"	6	-2,133	14,629	168,267	4,470	6,639
2'-0" x 60'-0" wall - vertical reinforcement	Exterior east wall @ El 37'-0"	6	+863	732	107,052	--	--
2'-6" thick wall - vertical reinforcement	Interior wall @ El 37'-0"	6	-12	103	142	--	--
2'-6" x 42'-0" wall - vertical and horizontal reinforcement	Interior wall @ El 37'-0"	6	-3,427	7,526	110,556	3,072	4,353
2'-6" x 42'-0" wall - vertical reinforcement	Interior wall @ El 37'-0"		+2,002	7,526	30,637	--	--
8'-0" thick basemat - E-W reinforcement	El 9'-0"	3	--	991	1,167	--	--
2'-0" thick slab - N-S reinforcement	El 37'-0"	3	--	75	96	--	--
	Control Area						
2'-6" thick wall - vertical reinforcement	Exterior west wall @ El 9'-0"	6	-239	450	458	--	--
2'-6" x 218'-6" wall - vertical and horizontal reinforcement	Exterior west wall @ El 9'-0"	6	-23,700	901,000	4.13×10^6	27,979	27,973

Table 3.8-8
AUXILIARY BUILDING SUMMARY OF GOVERNING LOAD INTERACTIONS FOR PRINCIPAL REINFORCED CONCRETE MEMBERS (Sheet 4 of 5)

Description of Member	Location of Principal Member	Governing Load Combination Number[a]	Calculated Axial Load (P_u) and Flexural Load (M_u)		Maximum Flexural Interaction Capacity (M_u), Given Axial Load (P_u)[b][c]	Calculated Shear Load (V_u)[b]	Maximum Shear Capacity (V_u)[b]
			P_u[b]	M_u[c]			
2'-6" x 218'-6" wall - vertical reinforcement	Exterior west wall @ E1 9'-0"	6	-1,198	879,750	2.78×10^6	--	--
2'-0" x 60'-6" wall - vertical and horizontal reinforcement	Interior wall @ E1 9'-0"	6	-7,890	14,730	268,223	3,324	5,072
2'-0" x 60'-6" wall - vertical reinforcement	Interior wall @ E1 9'-0"	6	+3,310	14,730	52,982	--	--
2'-0" thick wall - vertical reinforcement	Exterior west wall @ E1 50'-0"	6	-24	61	107	--	--
2'-0" x 2'3'-0" wall - vertical and horizontal reinforcement	Exterior west wall @ 50'-0"	6	-13,058	306,431	2.6×10^6	13,241	19,852
2'-0" x 219'-0" wall - vertical reinforcement	Exterior west wall @ E1 50'-0"	6	-742	306,431	$1.73 \text{ X } 10^6$	--	--
2'-0" thick wall - vertical reinforcement	Exterior south wall @ E1 50'-0"	6	-24	52	127	--	--
2'-0" x 74'-6" wall - vertical and horizontal reinforcement	Exterior south wall @ E1 50'-0"	6	-7,430	26,315	363,666	3,503	6,982
2'-0" x 74'-6" wall - vertical reinforcement	Exterior south wall @ E1 50'-0"	6	+2,653	26,315	121,403	--	--
8'-0" thick basemat - E-W reinforcement	E1 9'-0"	3	--	5,736	5,765	--	--
1'-0" thick slab - E-W reinforcement	E1 30'-0"	3	--	33	38	--	--
1'-0" thick slab - E-W reinforcement	E1 50'-0"	3	--	41	41	--	--

Table 3.8-8
AUXILIARY BUILDING SUMMARY OF GOVERNING LOAD INTERACTIONS FOR PRINCIPAL REINFORCED CONCRETE MEMBERS (Sheet 5 of 5)

Description of Member	Location of Principal Member	Governing Load Combination Number[a]	Calculated Axial Load (P_u) and Flexural Load (M_u)		Maximum Flexural Interaction Capacity (M_u), Given Axial Load (P_u)[b][c]	Calculated Shear Load (V_u)[b]	Maximum Shear Capacity (V_u)[b]
			P_u[b]	M_u[c]			
	Penetration Area						
2'-0" x 45'-6" wall – vertical and horizontal reinforcement	Exterior west wall @ El 9'-0"	6	-6,730	9,140	173,522	3,426	6,127
2'-0" x 45'-6" wall – vertical reinforcement	Exterior west wall @ El 9'-0"	6	+2,360	8,924	51,464	--	--
8'-0" thick basemat - N-S reinforcement	El 9'-0"	3	--	3,927	4,181	--	--
1'-0" thick slab - E-W reinforcement	El 30'-0"	3	--	44	48	--	--

Table 3.8-9
AUXILIARY BUILDING SUMMARY OF GOVERNING COMBINED STRESS RATIOS FROM THE BEAM/COLUMN INTERACTION
EQUATION FOR PRINCIPAL STRUCTURAL STEEL MEMBERS (Sheet 1 of 2)

Description of Principal Members	Location of Principal Members	Governing Load Combination Number[a]	Combined Stress Ratio (≤1.0)
	Penetration Area - Fuel Handling Building Side		
W 24 x 68	Main girder @ El 30'-0"	2	0.89
W 12 x 65 with 3/4 x 10 plate	Knee brace @ El 30'-0"	2	0.89
W 24 x 110	Main girder @ El 45'-0"	2	0.96
W 24 x 84	Main girder @ El 63'-6"	2	0.83
W 12 x 58	Knee brace @ El 45'-0"	2	0.76
	Column @ El 63'-6"	2	0.74
	Column @ El 9'-0"	2	0.99
	Penetration Area - Radwaste Side		
W 30 x 116 with 1-1/2 x 9 plate	Girder @ El 30'-0"	2	0.83
W 12 x 65	Knee brace @ El 30'-0"	2	0.92
W 30 x 116 with 1-1/2 x 9 plate	Girder @ El 45'-0"	2	0.95
W 12 x 65	Knee brace @ El 45'-0"	2	0.80
W 14 x 127	Column @ El 63'-6"	2	0.82
W 14 x 228	Column @ El 45'-0"	2	0.65
	Radwaste Storage Tank Area		
W 27 x 145 with 12 x 1/2 plate	Girder @ El 37'-0"	1	0.77
W 36 x 194 with 10 x 1-1/2 plate	Girder @ El 63'-6"	2	0.85

[a] Refer to Paragraph 3.8.3.3.2.B for description of load combination number.

Table 3.8-9
AUXILIARY BUILDING SUMMARY OF GOVERNING COMBINED STRESS RATIOS FROM THE BEAM/COLUMN INTERACTION
EQUATION FOR PRINCIPAL STRUCTURAL STEEL MEMBERS (Sheet 2 of 2)

Description of Principal Members	Location of Principal Members	Governing Load Combination Number[a]	Combined Stress Ratio (≤1.0)
	Radwaste Area		
W 16 x 64	Girder @ El 24'-0"	2	0.5
C 10 x 15.3	Staircase stringer	2	0.91
	Control Area		
W 30 x 190 with 13 x 3/4 plate	Main girder @ El 30'-0"	2	0.75
W 21 x 55 with 7 x 3/4 plate	Floor beam @ El 30'-0"	2	0.67
W 33 x 220	Main girder @ El 70'-0"	2	0.99
W 36 x 245	Top chord of truss @ El 70'-0"	2	0.90
W 36 x 300	Bottom chord of truss @ El 50'-0"	2	1.00
W 14 x 287	Diagonal of truss @ El 50'-0"	2	0.95
W 14 x 605	Column supporting truss @ El 9'-0"	2	0.86
W 14 x 426	Column supporting truss @ El 70'-0"	2	0.91
W 14 x 426	Column @ El 9'-0"	2	0.93
W 14 x 119	Column @ El 85'-0"	2	0.96

Table 3.8-10[a]
FUEL HANDLING BUILDING SUMMARY OF GOVERNING LOAD INTERACTIONS
FOR PRINCIPAL REINFORCED CONCRETE MEMBERS (Sheet 1 of 2)

Description of Member	Location of Principal Member	Governing Load Combination Number[a]	Calculated Axial Load P(u) and Flexural Load (M_u)		Maximum Flexural Interaction Capacity (M_u), Given Axial Load (P_u)	Calculated Shear Load (V_u)[b]	Maximum Shear Capacity (V_u)[b]
			P_u[b]	M_u[c]	M_u[c]		
2'-6" x 103'-0" wall - vertical and horizontal reinforcement	Exterior east wall @ El 17'-6"	6	-7,413	12.44×10^4	83.43×10^4	5,437	12,840
2'-6" x 103'-0" wall - vertical reinforcement	Exterior east wall @ El 17'-6"	6	-1,362	10.08×10^4	66.21×10^4	--	--
5'-0" x 79'-6" wall - vertical and horizontal reinforcement	West wall @ 17'-6"	6	-11,181	19.4×10^4	110.37×10^4	8,743	29,958
5'-0" x 79'-6" wall - vertical reinforcement	West wall @ El 17'-6"	6	-1,463	15.72×10^4	87.9×10^4	--	--
5'-0" x 36'-10" wall - vertical and horizontal reinforcement	Interior wall @ El 17'-6"	6	-6,962	1.61×10^5	2.54×10^5	5,410	16,856
5'-0" x 36'-10" wall - vertical reinforcement	Interior wall @ El 17'-6"	6	-1,247	1.49×10^5	1.95×10^5	--	--
2'-6" x 49'-6" wall - vertical and horizontal reinforcement	Exterior south wall @ El 30'-0"	6	-5,586	45,294	204,673	2,102	5,154
2'-6" x 49'-6" wall - vertical reinforcement	Exterior south wall @ El 30'-0"	6	+3,013	45,294	70,271	--	--
2'-6" x 103'-6" wall - vertical and horizontal reinforcement	West wall @ El 63'-6"	6	-3,457	56,885	602,355	3,043	10,216

(a) See Tables 3.8.7A and 3.8.7B for the governing load interactions for the spent fuel pool basemat and walls.
(b) Refer to Paragraph 3.8.4.3.2.A for description of load combination number
(c) P_u and V are in kips; sign convention for P_u:Compression (-), Tension (+)
(d) M_u is in ft-k/ft

Table 3.8-10[a]
FUEL HANDLING BUILDING SUMMARY OF GOVERNING LOAD INTERACTIONS
FOR PRINCIPAL REINFORCED CONCRETE MEMBERS (Sheet 2 of 2)

Description of Member	Location of Principal Member	Governing Load Combination Number[a]	Calculated Axial Load P(u) and Flexural Load (M_u)		Maximum Flexural Interaction Capacity (M_u), Given Axial Load (P_u) M_u[c]	Calculated Shear Load (V_u)[b]	Maximum Shear Capacity (V_u)[b]
			P_u[b]	M_u[c]			
2'-6" x 103'-6" wall - vertical reinforcement	West Wall @ El 63'-6"	6	+75	56,885	473,948	--	--
2'-6" thick wall - vertical reinforcement	Exterior south wall (crane location)	6	-122	224	332		
8'-0" thick basemat - E-W reinforcement	Basemat in penetration area	6	--	3,533	5,500	224	304
2'-6" thick wall - vertical reinforcement	Exterior east wall @ El 17'-6"	6	-24	158	223		

Table 3.8-11
SAFETY EQUIPMENT BUILDING SUMMARY OF GOVERNING LOAD INTERACTIONS
FOR PRINCIPAL REINFORCED CONCRETE MEMBERS (Sheet 1 of 2)

Description of Principal Members	Location of Principal Members	Governing Load Combination Number[a]	Calculated Axial Load (P_u) and Flexural Load (M_u)		Maximum Flexural Interaction Capacity (M_u), Given Axial Load P_u M_u[c]
			P_u[b]	M_u[c]	
Basemat slab - E-W reinforcement	Pump rooms El (-) 15'-6": Safety injection area	7	9	307	442
Basemat slab - E-W reinforcement	Pump rooms El (-) 5'-3" Component cooling water area	7	9	196	442
West wall - vertical reinforcement	Pump room Between El (-) 15'-6" & (+) 8'-0"	4	21	131	160
West Wall - vertical reinforcement	Piping room Between El (-) 5'-3" & (+) 8'-0"	7	49	70	86
Center wall - vertical reinforcement	Shutdown heat exchanger room walls Between El (-) 5'-6" & (+) 8'-0"	4	10	100	118
East wall- vertical reinforcement	Pump rooms Between El (-) 15'-6" & (+) 8'-0"	7	117	68	95
North wall - vertical reinforcement	Shutdown heat exchanger room Between El (-) 15'-6" & (+) 8'-0"	4	25	83	108

[a] Refer to Paragraph 3.8.4.3.2.A for description of load combination number.
[b] P_u is in kips.
[c] M_u is ft-k/ft.

Table 3.8-11
SAFETY EQUIPMENT BUILDING SUMMARY OF GOVERNING LOAD INTERACTIONS
FOR PRINCIPAL REINFORCED CONCRETE MEMBERS (Sheet 2 of 2)

Description of Principal Members	Location of Principal Members	Governing Load Combination Number[a]	Calculated Axial Load (P_u) and Flexural Load (M_u)		Maximum Flexural Interaction Capacity (M_u), Given Axial Load P_u M_u[c]
			P_u[b]	M_u[c]	
South wall - vertical reinforcement	Piping room Between El (-) 15'-6" & (+) 8'-0"	7	30	88	101
Slab - E-W reinforcement	Piping room El (+) 8'-0"	4	21	104	115
East wall - vertical reinforcement	Chemical storage tank room Between (+) 8'-0" & (+) 30' 6"	4	117	176	284
Slab - E-W reinforcement	Electrical cable tray tunnel (+) 30'-6"	7	12	88	117
West wall - vertical reinforcement	Cable tray tunnel room Between (+) 30'-6" & (+) 50'-6"	2	19	36	86
Slab - E-W reinforcement	Main steam line & feedwater line support slab (+) 50'-6"	4	25	225	268
Slab - N-S reinforcement	Main steam line and feedwater line support slab (+) 50'-6"	4	12	158	284

Table 3.8-12
SAFETY EQUIPMENT BUILDING SUMMARY OF GOVERNING COMBINED STRESS RATIOS
FROM THE BEAM/COLUMN INTERACTION EQUATION
FOR PRINCIPAL STRUCTURAL STEEL MEMBERS

Description of Principal Members	Location of Principal Members	Governing Load Combination Number[a]	Combined Stress Ratio (≤1.0)
Low pressure safety injection pump support columns	El (-) 15'-6" Pump rooms	4	0.245
Containment spray pump support columns	El (-) 15'-6" Pump rooms	4	0.245
Shutdown heat exchanger support beams	El 8'-0" Heat exchanger rooms	4	0.432

[a] Refer to Paragraph 3.8.4.3.2.B for description of load combination number.

Table 3.8-13
SAFETY EQUIPMENT BUILDING SUMMARY OF DUCTILITY RATIOS
FOR PIPE WHIP RESTRAINTS

Description of Principal Members	Location of Principal Members	Governing Load Combination Number[a]	Ductility Ratios		Remark
			Actual	Allowable	
Pipe whip restraint	Main steam line restraint	4	71	100	Tension
Pipe whip restraint	Feedwater line restraint	4	41	100	Tension

[a] Refer to Paragraph 3.8.4.3.2.B for description of load combination number.

Table 3.8-14
INTAKE STRUCTURE SUMMARY OF GOVERNING LOAD INTERACTIONS FOR PRINCIPAL REINFORCED CONCRETE MEMBERS (Sheet 1 of 4)

Description of Principal Members	Location of Principal Members	Governing Load Combination Number[a]	Calculated Axial Load (P_u) and Flexural Load (M_u)		Maximum Flexural Interaction Capacity (M_u) Given Axial Load[c]	Remarks
			P_u[b]	M_u[c]		
Base slab	Recirculation system: crossover box	7	16	169	230	
North wall	Recirculation system: crossover box	7	46	131	157	
South wall	Recirculation system: crossover box	7	29	471	548	
Roof slab	Recirculation system: crossover box	7	29	115	151	
Base slab	Recirculation system: seal well	7	97	491	516	
Walls: north above (+)10'-0"	Recirculation system: seal well	7	18	220	257	
Walls: north below (+) 10'-0"	Recirculation system: seal well	7	29	471	548	
Walls: south above (-)6'-0"	Recirculation system: seal well	1	26	330	361	
Walls: south below (-)6'-0"	Recirculation system: seal well	1	139	467	651	
Roof slab	Recirculation system: seal well	7	49	248	264	
Base slab	Intake conduit	7	97	491	516	
Walls: north	Intake conduit	1	139	467	651	

[a] Refer to Paragraph 3.8.4.3.2.A for description of load combination number.
[b] P_u is in kips.
[c] M_u is in ft-k/ft except as noted.

Table 3.8-14
INTAKE STRUCTURE SUMMARY OF GOVERNING LOAD INTERACTIONS FOR PRINCIPAL REINFORCED CONCRETE MEMBERS (Sheet 2 of 4)

Description of Principal Members	Location of Principal Members	Governing Load Combination Number[a]	Calculated Axial load (P_u) and Flexural Load (M_u)		Maximum Flexural Interaction Capacity (M_u) Given Axial Load[c]	Remarks
			P_u[b]	M_u[c]		
Walls south	Intake conduit	1	84	262	423	
Roof slab	Intake conduit	7	35	224	257	
Base slab	Discharge conduit	7	97	491	516	
Walls	Discharge conduit	1	84	262	639	
Roof slab	Discharge conduit	7	35	224	257	
Base slab	Transition	7	1	350	389	
Walls: north	Transition	7	47	358	544	
Walls: center	Transition	7	123	78	582	
Walls: south	Transition	7	79	378	592	
Roof slab	Transition	7	69	335	396	
Crane column supports	Salt water tunnel area El (-)9'-0" to El (+)7'-0"	7	1,640K	5,667 Ft-K	5,857 Ft-K	
Crane column supports	Salt water tunnel area El (+)7'-0" to (+)30'-0"	7	513K	2,802 Ft-K	3,240 Ft-K	Axial tension
Crane column supports	Tsunami wall area	7	426K	302 Ft-K	843 Ft-K	Axial tension
Walls	Stop-gate structure	7	0	650	1,049	

Table 3.8-14
INTAKE STRUCTURE SUMMARY OF GOVERNING LOAD INTERACTIONS FOR PRINCIPAL REINFORCED CONCRETE MEMBERS (Sheet 3 of 4)

Description Principal Members	Location of Principal Members	Governing Load Combination Number[a]	Calculated Axial Load (P_u) and Flexural Load (M_u)		Maximum Flexural Interaction Capacity (M_u) Given Axial Load[c]	Remarks
			P_u[b]	M_u[c]		
Walls	Recirculating gate structures	7	14	117	117	
Slab	Slab El (-) 26'-0", thickness = 4' screen well area	1	5	310	313	
Slab	Slab El (-)26'-0", thickness = 5' screen well area	7	29	68	333	Axial tension
Slab	Slab El (-)26'-0", thickness = 7'-3" screen well area	7	30	177	1,127	
Slab	Slab El (+)9'-0" screen well area	7	38	30	90	Axial tension
Slab	Slab El (+)35'-0" screen well area	7	11	74	83	
Slab	(+) 16'-0" deck screen well area	1	0	43	147	
Beams	(+)16'-0" deck - traveling water screen area	7	49	1,252	2,088	Axial tension
Beams	(+)16'-0" deck - fish elevator area	1	351	661	4,797	Axial tension
Walls	Center wall	1	40	360	421	Axial tension
Walls	Baffle walls	7	38	31	95	

Table 3.8-14
INTAKE STRUCTURE SUMMARY OF GOVERNING LOAD INTERACTIONS FOR PRINCIPAL REINFORCED CONCRETE MEMBERS (Sheet 4 of 4)

Description of Principal Members	Location of Principal Members	Governing Load Combination Number[a]	Calculated Axial Load (P_u) and Flexural Load (M_u)		Maximum Flexural Interaction Capacity (M_u) Given Axial Load[c]	Remarks
			P_u[b]	M_u[c]		
Slab	Pump slab El (-)7'-5"	7	90	253	347	
Slab	Pump well slab El (-)22'-9"	7	14	243	335	Axial tension
Walls - interior	Pump well area	7	52	250	269	
Walls - west exterior	Pump well area	7	24	348	544	
Walls - east exterior	Pump well area	7	36	53	313	
Walls	Tsunami walls	7	0	190	235	
Base slab	Salt-water tunnel area Slab at El (-)9'-0"	7	100	263	446	
Walls	Salt-water tunnel area West walls El (-)9' to El (+)4'	7	23	434	514	
Walls	Salt-water tunnel area East walls El (-)9' to El (+)4'	7	64	228	270	Axial tension
Walls	Salt-water tunnel area West walls El (+)7'-0" to (+)27'-6"	7	2	38	337	Axial tension
Walls	Salt-water tunnel area East walls El (+)7'-0" to (+)27'-6"	7	90	20	238	Axial tension
Slab	Salt-water tunnel area Slab El (+)7'-0"	7	25	283	375	
Slab	Salt-water tunnel area Slab El (+)30'-0"	7	17	172	207	

Table 3.8-15
ELECTRICAL AND PIPING GALLERY STRUCTURE SUMMARY OF GOVERNING LOAD INTERACTIONS FOR PRINCIPAL REINFORCED CONCRETE MEMBERS

Description of Principal Members	Location of Principal Members	Governing Load Combination Number[a]	Calculated Axial Load (P_u) and Flexural Load (M_u)		Maximum Flexural Interaction Capacity (M_u), Given Axial Load P_u[c]
			P_u[b]	M_u[c]	
3'-0" thick basemat N-S reinforcement	Basemat at El (-) 2'-6"	4	87.56	138.78	177.56
3'-0" thick basemat E-W reinforcement	Basemat at El (-) 2'-6"	4	70.06	177.18	200.50
2'-0" thick slab E-W reinforcement	Slab at El 9'-6"	2	23.92	61.53	118.62
1'-6" thick slab N-S reinforcement	Floor at El 30'-6"	5	142.01	35.39	46.22
1'-6" thick slab E-W reinforcement	Floor at El 30'-6"	4	51.71	41.00	64.84
1'-8" thick slab N-S reinforcement	Floor at El 48'-6"	5	81.87	43.98	91.11
1'-6" thick wall horizontal reinforcement	North end exterior wall	7	81.41	39.49	74.99
1'-6" thick wall vertical reinforcement	North end exterior wall	6	79.75	38.66	68.57
1'-6" thick wall vertical reinforcement	Mid-north exterior wall	5	115.32	38.20	69.47
1'-6" thick wall vertical reinforcement	Mid-south exterior wall	4	79.77	50.95	60.99
2'-6" thick wall horizontal reinforcement	South end exterior wall	3	77.81	139.11	162.61
2'-6" thick wall vertical reinforcement	South end exterior wall	7	114.18	76.27	153.03
2'-0" thick wall horizontal reinforcement	West end exterior wall	5	115.20	56.17	152.10
2'-0" thick wall vertical reinforcement	West end exterior wall	5	42.43	53.26	152.96
1'-6" thick wall horizontal reinforcement	Mid-east exterior wall	4	58.43	42.59	81.39
1'-6" thick wall vertical reinforcement	Mid-east exterior wall	5	62.79	43.85	77.23
1'-6" thick wall vertical reinforcement	Interior wall running N-S direction	2	19.65	20.58	58.63

[a] Refer to Paragraph 3.8.4.3.2.A for description of load combination number.
[b] P_u is in kips.
[c] M_u is in ft-k/ft.

Table 3.8-16
OFFSHORE CIRCULAR CONDUITS SUMMARY OF GOVERNING LOAD INTERACTIONS

Description Member	Governing Load Combination	Calculated Axial Load (P_u)[(a)] and Flexural Load (M_u)		Maximum Flexural Capacity (M_u) Given Axial Load (P_u)	DBE Loadings[(b)] M_u (ft-kips)	Remarks
		P_u (kips)	M_u (ft-kips)			
Prestressed Conduit sections	10a	33.0	50.2	58.0	38.0	
Conventionally reinforced Manhole conduit Section	10a	29.2	48.2	52	38.5	
Prestressed Conduit Section Adjacent, to Box Conduit	10a	35.9	57.1	58.0	45.6	
First Conduit Section Longitudinal Bending	11	-	975.4	1,364	-	
Joint Shear - First Conduit Section	11	-	-	-	-	Actual Shear V_u = 216.6^k Shear Capacity = 283^k

(a) Loads are calculated using E = 1.5 x peak response from the OBE response spectrum and an SRSS combination of responses from two horizontal directions and the vertical direction.

(b) Loads are calculated using E' = 1.5 x peak response from the DBE response spectrum and SRSS continuation of responses from two horizontal directions and the vertical direction using load combination 11. They are provided as supplementary information only where this load combination did not govern the design.

Table 3.8-17
OFFSHORE INTAKE AND DISCHARGE BOX CONDUIT SUMMARY OF GOVERNING LOAD INTERACTIONS FOR PRINCIPAL CONDUIT COMPONENTS

Description of Member	Governing Load Combination	Calculated Axial Load (P_u) and Flexural Load (M_u)		Maximum Flexural Capacity (M_u) for no Axial Load	Maximum Flexural Interaction Capacity (M_u) Given Axial Load	Remarks
		P_u (kips)	M_u (ft-kips)			
Roof slab	10(a)	91.2	180.8	320	418	
Base slab	10(a)	102.2	170.5	338	451	Water hammer in one conduit
Side wall	10(a)	94.7	133.9	214	293	Water hammer in one conduit
Interior wall	10(a)	170.9	67.9	119	239	

Table 3.8-18
AUXILIARY INTAKE STRUCTURE SUMMARY OF GOVERNING LOAD INTERACTIONS
FOR PRINCIPAL REINFORCED CONCRETE MEMBERS

Description of Member	Governing Load Combination Number[a]	Calculated Axial Load (P_u) and Flexural Load (M_u)		Maximum Flexural Capacity (M_u), Given Axial Load (P_u) (kips)	Calculated Shear Load (V_u) kips	Maximum Shear Capacity (V_u)kips
		P_u (kips)	M_u (ft-kips)			
Velocity cap	10(a)	-	$4^{ft\text{-}kip}/ft$	$4^{ft\text{-}kip}/ft$	16	29
Columns	10(a)	16	4.5	17	3	43
Riser	10(a)	102.6	908	1042[b]	138	645
Base Block	10(a)	-	0.73[c]	(478)	110	115
(+Bending)			0.58	(478)		
(-Bending)						
Conduit	10(a)	-	$71^{ft\text{-}kip}/ft$	$82^{ft\text{-}kip}/ft$	94 k/ft	97 k/ft
Buttresses	10(a)	-	444	770	95	118
Footing	10(a)	-	$120^{ft\text{-}kip}/ft$	$120^{ft\text{-}kip}/ft$	65 k/ft	68 k/ft
Base Block End	10(a)	-	0.98[c]	(308)	77	84
Beam			0.93	(232)		
(+Bending)						
(-Bending)						

[a] Refer to Paragraph 3.8.4.3.2A for description of load combination number.
[b] For $P_u = 0$.
[c] Because of the complex interaction of the loads on the base block, the actual loadings are given as a percentage of the capacity. The calculated percentage is based on peak localized stresses occurring in the base block and does not represent the total level of stress within the block.

3.8.4.6 Materials, Quality Control, and Special Construction Techniques

The following basic materials are used in the construction of the Seismic Category I structures listed in Paragraph 3.8.4.1, excluding the offshore intake conduits and auxiliary intake structure which are described in Paragraph 3.8.4.6.3.

3.8.4.6.1 Other Seismic Category I Structures

A.	Concrete		f'_c (1b/in.^{2}) = 4,000
B.	Reinforcing steel deformed bars	ASTM A615 Grade 60	f_y (lb/in.^{2}) = 60,000
C.	Structural and miscellaneous steel rolled shapes, bars, and plates	ASTM A36	f_y (lb/in.^{2}) = 36,000
	High-strength	ASTM A325	f_y (lb/in.^{2}) = 81,000 to 92,000 (Varies depending on diameter of bolts)
		ASTM A449	f_y (lb/in.^{2}) = 58,000 to 92,000 (Varies depending on diameter of bolts)
		ASTM A490	f_y (lb/in.^{2}) = 130,000 minimum
	Anchor bolts	ASTM A307	f_t (lb/in.^{2}) = 60,000 minimum
	Stainless steel	ASTM A167 Type 304	f_y (lb/in.^{2}) = 30,000
		ASTM A240 Type 304L	f_y (lb/in.^{2}) = 25,000
	Stainless steel Bars and shapes	ASTM A276 Type 304	f_y (lb/in.^{2}) = 30,000
	Stainless steel Tubing	ASTM A554 Type 304	f_y (lb/in.^{2}) = 30,000

Stainless steel	ASTM A193	f_y (lb/in.^{2}) = 30,000
Bolts, nuts and threaded studs	Grade B8	
Insert plates	ASTM A36	f_y (lb/in.^{2}) = 36,000

The materials and quality control procedures are described in Paragraph 3.8.1.6.

The other Seismic Category I structures listed in Paragraph 3.8.4.1 are built of reinforced concrete and structural steel, using proven methods common to heavy industrial construction. No special construction techniques have been employed in the construction of these structures.

3.8.4.6.2 Offshore Intake Conduits

The following basic materials are used in construction of the conduits.

A. Concrete		f'_c (lb/in.^{2}) = 5500 @ 28 days
B. Reinforcing Steel		
(Deformed bars)	ASTM A615 Gr. 40	f_y (lb/in.^{2}) = 40,000
C. Prestressing Wire	ASTM A648 Class III	f'_s (lb/in.^{2}) = 252,000

3.8.4.6.2.1 <u>Reinforced Concrete - Offshore Intake Conduits</u>

A. Concrete

All concrete work is done in accordance with ACI 318, Building Code Requirements for Reinforced Concrete; ACI 301, Specifications for Structural Concrete for Buildings; and ASTM C361, Specifications for Reinforced Concrete Pipe, except as otherwise stated herein.

The concrete is a dense, durable mixture of sound coarse aggregates, cement, and water. Admixtures are added to improve the quality and workability during placement.

B. Cement

The cement is Type II, low alkali, conforming to the Specification for Portland Cement, ASTM C150. Certified copies of mill test reports showing the chemical

composition and physical properties are obtained for each load of cement delivered representing each batch from which the load was taken.

C. Aggregates

All aggregates conform to the Standard Specification for Concrete Aggregate, ASTM C33. The same supplier provides aggregate for all QCI and QCII concrete work at the site.

D. Water

Water for mixing concrete is a potable quality having less than 350 ppm of chloride as C1. Mixing water is obtained from a direct tie with the Metropolitan Water District, a public water supplier, which supplies water for all QC I and II concrete work. This water meets the above requirements.

E. Admixtures

The concrete contains water reducing and set-controlling admixtures conforming to the Standard Specifications for Chemical Admixtures in Concrete, ASTM C494, Type D.

F. Concrete Testing

During pipe fabrication, the concrete is sampled and tested for slump and temperature prior to casting compressive strength cylinders. The compressive strength cylinders are cast from representative samples taken in accordance with the Standard Method of Sampling Fresh Concrete, ASTM C172.

The cylinders are made, cured, and tested in accordance with the Standard Method for Making and Curing Compression and Flexure Tests in the Field, ASTM C31, and the Standard Test for Compressive Strength of Molded Concrete Cylinders, ASTM C39. For each day's work, or approximately 100 cubic yards, two sets of cylinders are made for each mix design. The cylinders are subjected to the same curing cycle as the pipe sections.

The average of all the compressive strength tests representing each class of concrete, as well as the average of any five consecutive strength tests representing each class, is required to be equal to or greater than the specified strength, and no more than one strength test in 10 can have an average value less than the specified strength. The strength of an individual test is the average of the strengths of the two specimens.

G. Concrete Placement

Conveying and placing concrete is performed in accordance with ACI 301, ACI 304, and ACI 318. Before the concrete is placed, all equipment is cleaned. Debris is

removed from the spaces to receive concrete. Reinforcement and other metal to be embedded is thoroughly cleaned of all loose rust, scale, and/or coatings that might impair the bond. The pipe sections are cast vertically in one monolithic pour. The concrete is consolidated by using external vibrators.

H. Reinforcing Steel

Reinforcing steel is deformed billet steel conforming to ASTM A-615. Grade 40 steel is used for all pipe sections. Mill test results are obtained from the reinforcing steel supplier for each heat of steel to show that the reinforcing steel meets the specified ASTM requirements. The circumferential bars in the pipe are spliced by flash-resistance butt welding. Per ACI 318 and AWS D12.1, the splices are tested for a minimum strength of 50 ksi or 125% of the design yield strength of the bar. At least two reinforcing steel splice samples are made each day for each bar size used in the manufacture of the reinforcing steel cages.

I. Prestressing Wire

The prestressing wire used in the pipe section is No. 6 gage wire conforming to ASTM A648 Class III. This steel wire has a minimum ultimate strength of 252,000 lb/in.^{2}. Mill test results are obtained from the steel wire supplier for each heat of steel to show that the wire meets the ASTM requirements. In addition, per Ameron Quality Control Procedures, user tests are performed on each heat of steel wire received to ensure compliance with the specifications for tensile strength and out-of-roundness.

J. Prestressing Operation

The conduit sections are prestressed after the minimum concrete strength for prestressing $f'c$ = 3000 lb/in.^{2}, has been attained. Concrete cylinders were tested at 3 days, and all were found to be in excess of the required strength. The prestressing operation consists of a helical winding of the prestressing wire around the pipe core under measured and recorded tension at the design spacing. The prestressing wire and the wire anchor blocks are user tested. The records for the pre-stress wrapping tension and the user test results are maintained on file. The load recording mechanism of the prestressing machine is calibrated weekly, and the dynamometer used in the calibration is calibrated every 6 months.

K. Quality Control

Quality control procedures are established and implemented during construction and inspection. The conduit sections are fabricated by Ameron, using essentially an assembly line technique. Ameron developed a Process Standards and Quality Control Manual specifically for the San Onofre Project. SCE's Construction and Material Inspection Organization (CMI) provides additional independent inspection for the

conduit fabrication and is responsible to ensure the appropriate documentation is maintained.

The conduit installation is performed by the Guy F. Atkinson Company. Quality control for the installation process is the responsibility of SCE Construction, Construction and Material Inspection (CMI), and Parker Diving Service. Parker Diving is an independent contractor to SCE, specifically hired for underwater inspection of the conduit installation. Parker Diving, under the guidance of SCE Construction, inspects the excavation of the subgrade, the conduit joint makeup and the backfilling for conformance to the design requirements. The joint gap measurements are logged several times and form a basis for demonstrating the adequacy of the bedding. To date, the measurements have shown little change in the joint gaps after makeup. CMI has the responsibility to ensure proper documentation is maintained.

3.8.4.6.3 Auxiliary Intake Structure

The following basic materials are used in the construction of the auxiliary intake structure:

A.	Concrete		f'_c(lb/in.^{2}) = 4,000
B.	Reinforcing steel deformed bars	ASTM A615	
		Grade 40	f_y (lb/in.^{2}) = 40,000
		Grade 60	f_y (lb/in.^{2}) = 60,000
C.	Structural and miscellaneous steel, rolled shapes, bars and plates	ASTM A36	f_y (lb/in.^{2}) = 36,000

3.8.4.6.3.1 <u>Reinforced Concrete - Auxiliary Intake Structure</u>

A. Concrete

All concrete work is done in accordance with ACI 318, Building Code Requirements for Reinforced Concrete, and ACI 301, Specifications for Structural Concrete for Buildings, except as otherwise stated herein.

The concrete is a dense, durable mixture of sound coarse aggregates, fine aggregates, cement, and water. Admixtures are added to improve the quality and workability of the plastic concrete during placement and to improve the durability of the concrete during its service life. The sizes of aggregates, water reducing additives, and slumps are selected to maintain low limits on shrinkage and creep.

B. Cement

Cement is Type II, low alkali, moderate heat of hydration conforming to Standard Specification for Portland Cement, ASTM C150. Certified copies of mill test reports showing the chemical and physical properties are obtained for each load of cement delivered.

C. Aggregates

All granitic aggregates conform to ASTM C33, Standard Specification for Concrete Aggregates. Aggregates for structural lightweight concrete conform to ASTM C330, Standard Specifications for Light-weight Aggregates for Structural Concrete.

D. Water

Water used in mixing concrete is of potable quality having less than 350 ppm of chloride as C1. Mixing water is obtained from a direct tie with the Metropolitan Water District, a public water supplier, which supplies water for all QCI and QCII concrete work at the job site. This water meets the above requirements.

E. Admixtures

Admixtures used in concrete conform to ASTM C260, Standard Specification for Air-Entraining Admixtures for Concrete; ASTM C494, Standard Specification for Chemical Admixtures for Concrete; and ASTM C618, Standard Specifications for Fly Ash and Raw or Calcined Natural Pozzolans for use in Portland Cement Concrete.

F. Concrete Testing

During construction, concrete is sampled and tested for slump, air content, temperature, and unit weight prior to casting compressive strength cylinders. Compressive strength cylinders are cast from representative samples taken in accordance with ASTM C172, Standard Method of Sampling Fresh Concrete.

Cylinders are made, cured, and tested in accordance with ASTM C31, Standard Method for Making and Curing Compression and Flexure Tests in the Field, and ASTM C39, Standard Method of Test for Compressive Strength of Molded Concrete Cylinders. A total of six cylinders per load are tested per ACI 318, Section 4.3. The average of all the compressive strength tests representing each class of concrete, as well as the average of any five consecutive strength tests representing each class of concrete, is required to be equal to or greater than the specified strength, and no more than one strength test in 10 can have an average value less than the specified strength. The strength of an individual test is the average of the strengths of the two specimens.

G. Concrete Placement

Conveying and placing concrete for the auxiliary intake structure is performed in accordance with ACI 304, ACI 318, and ASTM C94. Before depositing concrete, all equipment is cleaned and debris is removed from spaces to receive concrete. Reinforcing and metal embedments are thoroughly cleaned of all loose rust, scale, and/or coatings that might impair the bond.

The conduit and riser portions of the auxiliary intake structure are cast vertically in monolithic pours. Steel pipe forms are used for these structures, and the concrete is consolidated using external form vibrators. The buttresses and foundations are deposited in two pours with a construction joint between pours. Construction joints are provided in accordance with details on the approved engineering design drawings. Internal vibrators are used to consolidate concrete used in the buttresses, riser base block, and velocity cap. The conduit is steam cured, while the buttresses and foundations are air cured following application of a liquid membrane curing compound to all exposed concrete surfaces.

H. Reinforcing Steel

Reinforcing steel is deformed billet steel conforming to ASTM A615. Grade 40 is used for the entire structure with the exception of the structural ties between the riser base block and the conduit. These bars are Grade 60 bars, which are supplied by a separate steel supplier and are delivered to the job site in a unique configuration such that substitution of Grade 40 bars is not possible. Source inspections and mill test reports are used to verify conformance to ASTM specifications for physical and mechanical properties. Splices of reinforcing bars are limited to either lap splices or mechanical splices meeting the requirements of ACI 318. Welding of reinforcing steel for construction of cage assemblies meets the requirements of AWS D12.1, Reinforcing Steel Welding Code. Four samples of each bar size in each weld configuration are tested prior to production to assure that the mechanical properties of the reinforcing are not degraded by the welding process. In addition, a 2% sample of every type of welded reinforcing bar connection used is tested during production.

For the No. 14 bars in the riser base block and for all the reinforcing steel in the Unit 3 Buttresses, Grade 60 steel was substituted for the Grade 40 steel because Grade 40 steel was not readily available in the larger bar sizes. No welding of the Grade 60 bars was allowed.

I. Quality Control

Quality control procedures are established by SCE Construction and Material Inspection (CMI) prior to the start of construction. CMI makes use of an independent testing laboratory, Smith-Emery Company, for quality control of concrete materials; and Parker Diving Service, a professional construction diving company, is used to verify proper

placement and alignment of the auxiliary intake structure in the intake line. CMI's procedures are reviewed by SCE QA and Engineering to assure consistency with QA objectives and design intent. CMI inspectors assure that the work conforms to the design drawings. CMI also has the responsibility to ensure that all quality-related documentation is filed with the Corporate Documentation Management Center (CDMC).

3.8.4.7 Testing and Inservice Inspection Requirements

Testing and inservice surveillance are not required for Seismic Category I structures other than containment and no formal program of testing and inservice surveillance is planned.

3.8.5 FOUNDATIONS

3.8.5.1 Description of the Foundations

3.8.5.1.1 Containment

The containment foundation is a conventionally reinforced, circular concrete mat, 9 feet thick with a diameter of 184 feet, bearing directly on the San Mateo formation. The reactor cavity is located near the center of the mat and forms an integral part of the foundation. Controlled Drawings 23000, 23101, 23102, 23104 and 23105 show the relative position of the two containment foundations.

Controlled Drawings 23011 and 23014 show cross-sections of the containment base slab.

The internal structures that support the large equipment, such as steam generators and reactor coolant pumps, are anchored to the base slab in order to transfer the loads. Controlled Drawings 23203, 23145, 23180 and 23207 show a typical detail of anchorage to the base slab for the steam generator and reactor coolant pumps.

Controlled Drawings 23011 and 23014 shows the reinforcing pattern at the junction of the base slab and containment wall.

3.8.5.1.2 Auxiliary Building

The auxiliary building foundation is a reinforced concrete slab 8 feet thick, 280 feet long, and approximately 221 feet wide, bearing directly on the San Mateo Formation. A piping gallery extending 11 feet below the bottom of the basemat in the control area is an integral part of the foundation.

Refer to Controlled Drawing 10105 for location of auxiliary building foundation in relation to other Seismic Category I structures.

Figures 3.8-32 and Controlled Drawing 25068 show typical base slab sections and foundation details.

3.8.5.1.3 Fuel Handling Building

The fuel handling foundation is a reinforced concrete slab which varies in thickness from 4 feet 6 inches to 8 feet, and is 134 feet 6 inches long by 87 feet 6 inches wide, bearing directly on the San Mateo Formation.

Refer to Controlled Drawings 25402, 25410 and 23105 for location of the fuel handling foundation in relation to other Seismic Category I structures.

Controlled Drawing 25416 shows typical base slab and foundation details.

3.8.5.1.4 Safety Equipment Building

The safety equipment building foundation is a stepped reinforced concrete slab which is 4 feet thick, 174 feet long, and 74 feet wide, bearing directly on the San Mateo formation.

Refer to Controlled Drawing 23600 for location of the safety equipment building in relation to other Seismic Category I structures.

Controlled Drawings 23608 and 23605 shows typical base slab and foundation details.

3.8.5.1.5 Intake Structure

The intake structure foundation is a reinforced concrete slab, which is 4 feet thick, 119 feet 6 inches long and 109 feet 10 inches wide, bearing directly on the San Mateo formation.

Refer to Controlled Drawing 22030 for location of the intake structure foundation in relation to other Seismic Category I structures.

Controlled Drawings 22077 and 22008 show typical base slab and foundation details.

3.8.5.1.6 Electrical and Piping Gallery Structure

The electrical/piping junction structure is a partially buried conventional reinforced concrete shear-wall structure. The structure provides a transition area for Seismic Category I piping and electrical cable from the underground tunnels and duct runs into the safety equipment building. The overall plan dimension of the structure is 85 x 67 feet with a maximum height of 54 feet. The interior of the structure is a maze of partial floor slabs, partition walls, and vertical risers. Due to the physical proximity to other structures, the embedment characteristics vary on each side of the structure. The resulting structure exhibits geometric eccentricity between the center of mass and the center of rigidity at the various elevations within the structure and at the soil-structure interface.

Refer to Controlled Drawing 23700 for location of the electrical and piping gallery structure foundation in relation to other Seismic Category I structures.

Controlled Drawing 23701 shows typical base slab and foundation details.

3.8.5.1.7 Condensate and Refueling Tank Enclosure Structure

The condensate and refueling tank enclosure foundation is a reinforced concrete slab which varies in thickness from 2 feet to 3 feet. The foundation is 137 feet long by 98 feet wide and bears directly on the San Mateo Formation. Controlled Drawing 23803 shows typical slab sections.

3.8.5.1.8 Diesel Generator Building

The diesel generator building foundation is a conventionally reinforced, rectangular concrete mat which is 5 feet 6 inches thick, 91 feet long by 60 feet wide, bearing directly on the San Mateo Formation.

Controlled Drawings 23850, 23853 and 23854 show typical basemat and foundation details.

3.8.5.1.9 Intake Circular Conduits

The intake circular conduit is a completely buried structure and is described in detail in Subsection 3.8.4.

3.8.5.1.10 Auxiliary Intake Structure

The auxiliary intake structure is placed directly in line with the intake conduits and is located approximately 92 feet shoreward of the primary offshore intake structure. The pipe section of the structure is 20 feet in length and is monolithically attached to, and supported by two buttresses, each 5 feet long and 27 feet wide. The buttresses are provided with projections that widen the structure's base to resist lateral overturning and to develop a passive pullout soil wedge for increased stability. The pipe section and buttresses are bedded in the select gravel material, which is also used to backfill around the structure (see Paragraph 3.8.4.1.10).

3.8.5.1.11 Box Conduit Structure

The box conduit structure extends seaward 160 feet from the permanent seawall to the offshore circular conduits. The box conduit structure is a completely buried structure supported directly on San Mateo sand. The foundation slab of the conduit is 3 feet 8 inches thick (see Paragraph 3.8.4.1.9).

3.8.5.2 Applicable Codes, Standards, and Specifications

The applicable codes, standards, specifications, regulatory guides, and other documents used in the structural design, fabrication, and construction of foundations are covered in the following paragraphs.

Containment, Paragraph 3.8.1.2

Internal Structures, Paragraph 3.8.3.2

Other Seismic Category I Structures, Paragraph 3.8.4.2

3.8.5.3 Loads and Load Combinations

Containment foundation loads and loading combinations are discussed in Paragraph 3.8.1.3.

Foundation loads and loading combinations for other Seismic Category I structures are discussed in Paragraph 3.8.4.3.

3.8.5.4 Design and Analysis Procedures

Design and analysis procedures used, including the computer programs employed, in the design of foundations are discussed in Paragraph 3.8.1.4 for the containment, in paragraph 3.8.3.4 for the internal structures, which include the major concrete support structures, and in Paragraph 3.8.4.4 for the other Seismic Category I structures.

3.8.5.5 Structural Acceptance Criteria

The foundations of all Seismic Category I structures are designed to meet the same structural acceptance criteria as the structures themselves. These criteria are discussed in Paragraphs 3.8.1.5 and 3.8.4.5.

A minimum factor of safety of 1.5 against overturning is maintained for all structures and supports as shown in Table 3.8-19. The procedure used to determine the stability ratio against structural overturning is discussed in detail in Section 4.4 of BC-TOP-4-A.[6]

The foundation bearing pressures shown in Table 3.8-19 when compared with the allowable bearing pressures, show that the foundation medium can safely support the pressures caused by overturning moments. The ratio of the allowable bearing pressure to the actual bearing pressure yields the safety margin.

A study of the potential sliding of structures under a seismic event was performed specifically for the auxiliary building, and a detailed description is given in Appendix 3.7C.

The basic concept of the study is: (1) the ratio of dynamic shear stress to net normal stress developed at the soil-mat interface (τ / σ_m) a measure of the friction mobilized by the imposed base motion, and (2) no sliding is anticipated if the stress ratio is less than the available friction between soil and concrete.

The instantaneous stress ratio obtained from a time-history analysis was evaluated at several locations within the foundation interface. Care was exercised in the transient analysis to account

Table 3.8-19 SUMMARY
OF ACTUAL AND ALLOWABLE FOUNDATION BEARING PRESSURES, SETTLEMENTS, AND FACTORS OF SAFETY AGAINST OVERTURNING FOR SEISMIC CATEGORY I STRUCTURES

Structure	Foundation Medium	Foundation Bearing Pressure (D+L+Seismic) (k/ft^2)	Foundation Allowable Bearing Pressure (k/ft^2)	Estimated Short-Term Settlements of Structure (in.)	Estimated Long-Term Settlements of Structure (in.)	Minimum Factor of Safety (1.5) Against Overturning	Remarks
Containment	Undisturbed natural San Mateo sand	18	54(72)	0.25	0.3	40	
Auxiliary Building	Undisturbed natural San Mateo sand	15	68(88)	0.30	See Chapter 2, FSAR	150	Foundation allowable value is lower bound dictated by shear capacity of soil, neglecting actual horizontal extent of basemats.
Fuel Handling Building	Undisturbed natural San Mateo sand	21	33(44)	0.75	See Chapter 2, FSAR	10	Foundation allowable value is lower bound dictated by shear capacity of soil, neglecting actual horizontal extent of basemats.
Safety Equipment Building	Undisturbed natural San Mateo sand	(DBE) 9.022 (OBE) 7.326	36(48)	<0.25	0.40	Not applicable (See Remarks)	More than 2/3 of structure is embedded in soil
Intake Structure	Undisturbed natural San Mateo sand	(DBE) 18.0 (OBE) 13.0	36(48)	<0.25	0.40	Not applicable	Structure is below grade.
Electrical and Piping Gallery Structure	Undisturbed natural San Mateo sand	(DBE) 11.154 (OBE) 10.497	36(48)	<0.25	0.40	Not applicable (See Remarks)	Approximately 2/3 of structure is embedded

NOTE--Bearing capacity values in parenthesis are for seismic loading and include 1/3 increase over bearing capacity for static loading.

for phase shifts in recognition of the nonlinearly-independent horizontal and vertical acceleration input records that were used. The maximum stress ratio obtained was 0.57, which is below the available friction evaluated at 0.59. This finding is indicative of adequate stability since (1) the reported maximum stress ratio represents only a peak value for an instant of time at a single location, and (2) it is not representative of the more favorable overall state of stress that would result from an integration over a period of time and over the whole foundation interface.

The factor of safety against sliding, as it is normally conceived in pseudostatic analyses, can be developed by considering the average absolute value of the stress ratio. From the transient analysis, the average stress ratio was evaluated as 2/3 of the peak value. Accordingly, the following factor of safety of 1.55 is derived, and it is considered adequate:

$$F.S._{(DBE)} \approx \left(\frac{0.59}{0.57}\right)\left(\frac{1}{2/3}\right) \approx 1.55 > 1.1$$

In regard to the sliding tendency of other Seismic Category I structures, a comparison of their inertial and embedment characteristics with respect to those of the auxiliary building indicated that the auxiliary building is the governing case for sliding analysis. Consequently, specific transient analyses of the sliding stability of these other structures were not performed. It was concluded from the auxiliary building data that their factors of safety are higher than 1.6.

Buoyancy is not a major concern for most of the Seismic Category I structures because the ground water level established at elevation 5 feet 0 inch is relatively low with respect to their foundation levels. The high ground water level is completely below the basemats of the containment structure, fuel handling building, diesel generator building, and condensate and refueling tank enclosure building. For the auxiliary building the ground water level is 4 feet below the top of the 8-foot-thick basemat which is essentially solid concrete, thus buoyancy is precluded.

For the Seismic Category I structures in which buoyancy is pertinent, the factors of safety against buoyant forces are as follows:

- Safety equipment building - 5.0
- Electrical and piping gallery structure - 3.7
- Intake structure - 1.3 (empty condition)

3.8.5.6 Materials, Quality-Control, and Special Construction Techniques

The foundations and equipment supports are built of reinforced concrete using conventional methods for heavy industrial construction. The description of the materials, and the quality control procedures, as well as special construction techniques for foundations, are the same as those discussed in Paragraphs 3.8.1.6, 3.8.3.6, and 3.8.4.6.

3.8.5.7 Testing and Inservice Inspection Requirements

Testing and inservice surveillance are not required and are not planned for foundations of structures or for concrete supports. A discussion of the test program that serves as the basis for the Soils Investigations and Foundation Report may be found in Section 2.5, Geology, Seismology and Geotechnical Engineering.

3.8.6 REFERENCES

1. "Prestressed Concrete Nuclear Reactor Containment Structures," BC-TOP-5, Revision 1, Bechtel Power Corporation, San Francisco, California, December 1972.

2. "Full Scale Buttress Test for Prestressed Nuclear Containment Structures," BC-TOP-7, Bechtel Corporation, San Francisco, California, August 1971 (Reprinted September 1972).

3. "Tendon End Anchor Reinforcement Test," BC-TOP-8, Bechtel Corporation, San Francisco, California, November 1971.

4. "Containment Building Liner Plate Design Report," BC-TOP-1, Revision 1, Bechtel Power Corporation, San Francisco, California, December 1972, including supplemental information entitled "Additional Information Requested by the Atomic Energy Commission on BC-TOP-1, Revision 1, Containment Building Liner Plate Design Report," dated September 1973.

5. Eringer, A. C., Naghdi, A. K., and Thiel, C. C., State of Stress in Circular Cylindrical Shell with a Circular Hole, Welding Research Council Bulletin No. 102, January 1965.

6. "Seismic Analyses of Structures and Equipment for Nuclear Power Plants," BC-TOP-4A, Revision 3, Bechtel Power Corporation, San Francisco, California, November 1974.

7. "Qualification of an Alternative Electrode Control Program for AWS D1.1" ANPP submittal to NRC, dated March 15, 1978, Docket Numbers STN-50-528, STN-50-529, STN-50-530.

8. "Moisture Control of Low Hydrogen Covered Arc-Welding Electrodes at Palo Verde Nuclear Generating Station, Units 1, 2 and 3" is the subject of the letter addressed to Mr. E. E. Van Brunt, Jr, of Arizona Public Service Company from NRC, dated April 24, 1978, referring to Docket No. STN-50-528, STN-50-259, STN-50-350.

9. (DELETED)

10. "Watertight Reliability of Condensate Storage Tank and its Concrete Enclosure Walls under DBE and Tornado Events," dated December 15, 1980.

11. Standard Specifications for Public Works Construction SSPWC-1979, written and promulgated by Southern California Chapter American Public Works Association and Southern California District Associated General Contractors of California Joint Cooperative Committee.

3.9 MECHANICAL SYSTEMS AND COMPONENTS

All subsystems and programs of the Mechanical System are not required to support permanent plant shutdown or defueled operations. The operational information has been removed from the UFSAR to indicate that the systems perform no licensing bases or design basis function. Although the subsystems and programs no longer support operation, they may still contain fluids, gases, or other hazards such as energized circuits, compressed air, radioactive material, etc. Equipment may not have been physically removed from the plant. See P&IDs, One Line Diagrams, and General Arrangement Drawings for current plant configuration.

STRUCTURES/SYSTEMS/COMPONENTS	STATUS
Design Transients	Removed from Service
Pump and Valve Operability Assurance	Removed from Service
Control Element Drive Mechanism	Removed from Service
Reactor Pressure Vessel Internals	Removed from Service
Inservice Inspection Program	Removed from Service

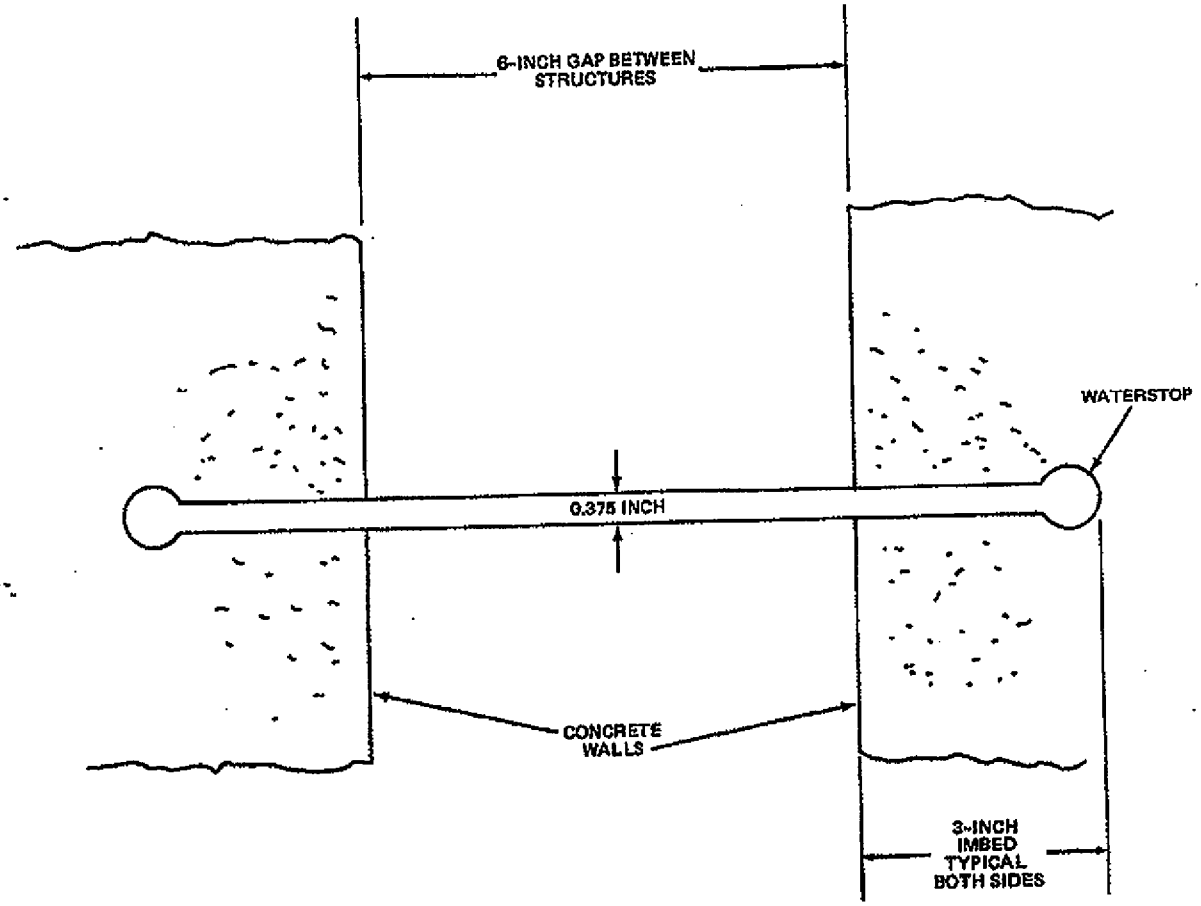

SAN ONOFRE NUCLEAR GENERATING STATION Units 2 & 3
TYPICAL WATERSTOP INSTALLATION
Figure 3.4-1

Site File Copy

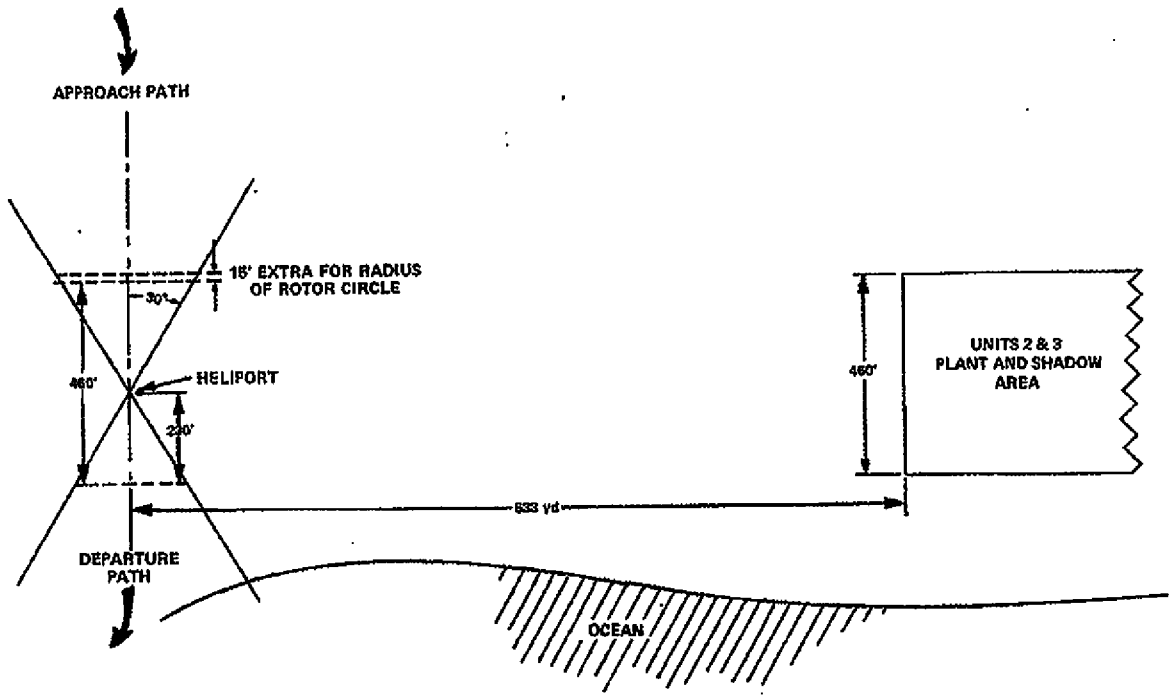

SAN ONOFRE NUCLEAR GENERATING STATION Units 2 & 3
SCHEMATIC OF HELIPORT AND FLIGHT PATHS
Figure 3.5-8

Amended: April 2009 TL: E047997

Site File Copy

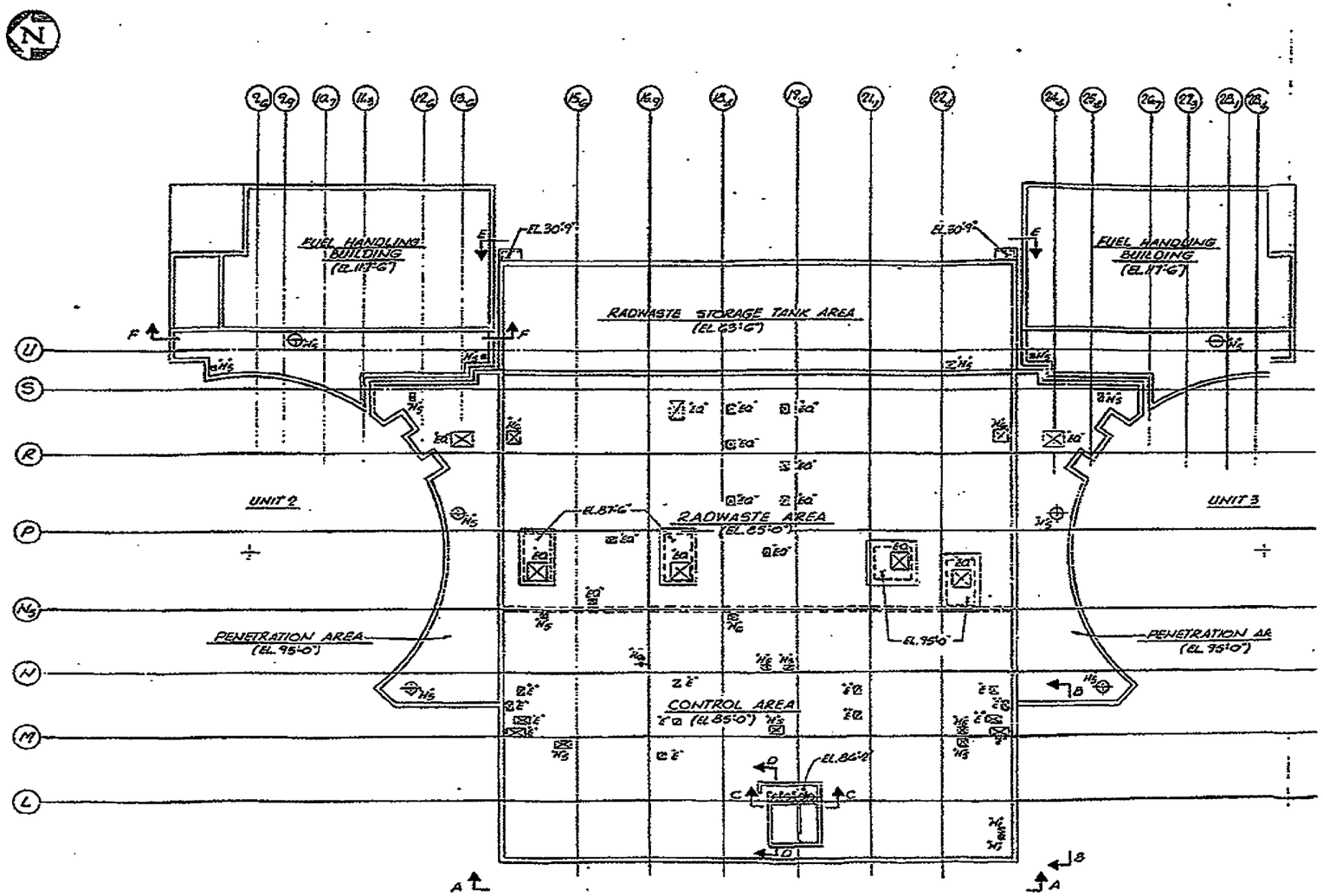

ROOF PLAN

"H" - OPENINGS FOR HVAC SYSTEMS, NUMERICAL SUBSRIPTS ARE AS FOLLOWS:
- "1"/"2" - EMERGENCY CHILLER ROOM SUPPY/EXHAUST, RESPECTIVELY
- "3" CONTROL ROOM EMERGENCY SUPPLY
- "4" BATTERY ROOM EXHAUST
- "5"/"6" - EXHAUST OR SUPPLY FOR OTHER NORMAL SYSTEMS, PROTECTIONED/ UNPROTECTED, RESPECTIVELY
- "7" - EXHAUST OR SUPPLY FOR OTHER NORMAL SYSTTEMS, SHIELDED

"M" - OPENINGS FOR MECHANICAL EQUIPMENT, UNPROTECTED
"E" - OPENINGS FOR NON-SAFETY RELATED ELECTRICAL CABLE TRAYS
"EQ" - ACCESS OPENINGS FOR EQUIPMENT
"D_1" - DOORWAYS, PROTECTED
"D_2" - DOORWAYS, SHIELDED
"D_3" - DOORWAYS, UNPROTECTED

PROTECTION AGAINST TORNADO-GENERATED MISSLES IS PROVIDED AS FOLLOWS:

"H_1", "H_2", "H_3" - FRAMED STEEL PLATE ENCLOSURES DESIGNED TO PREVENT PERFORATION AND UNDERGO LIMITED STRUCTURE REPSONSE TO AVOID DISTORTION AND ASSURE FUNCTIONALITY OF THE SYSTEMS

"H_4" - REINFORCED CONCRETE ENCLOSURE DESIGNED TO PREVENT PERFORATION AND ASSURE FUNCTIONALITY OF THE SYSTEM

"H_5" - FRAMED STEEL PLATE ENCLOSURRE DESIGNED TO PREVENT PERFORARTION

"H_7" - SHIELDING OF OPENING IS PROVIDED BY EXTERIOR PIPING AND/OR STEEL FRAMING OF TURBINE BUILDING

"E" - STEEL CLOSURE PLATES FITTING AROUND TRAYS TO PREVENT

"EQ" - STRUCTURAL STEEL COVERS TO PREVENT PERFORATION

"D_1" - CONCRETE ENCLOSURES AND CLOSED RECESSED BULLET RESISTAND DOORS PROVIDE PROTECTION AGAINST TORNADO MISSLE PERFORATION AND SPALLED CONCRETE

"D_2" - DOORWAY IS PROVIDED WITH BULLET-PROOF DOORS AND IS SHIELDED BY TURBINE BUILDING

"D3" - DOORWAY FOR SHIPPING OR ACCESS, NO EXPOSURE OF SAFETY-RELATED EQUIPMENT

REFER TO TABLE 3.5-13, ITEM 5, FOR EXCEPTIONS

SAN ONOFRE NUCLEAR GENERATING STATION Units 2 & 3 Updated Final Safety Analysis Report
IDENTIFICATION OF SAFETY-RELATED PENETRATIONS ON ROOF AND EXPOSED WALL OF AUXILIARY BUILDING AND FUEL HANDLING BUILDING (Sheet 1 of 2)
Figure 3.5-9

Site File Copy

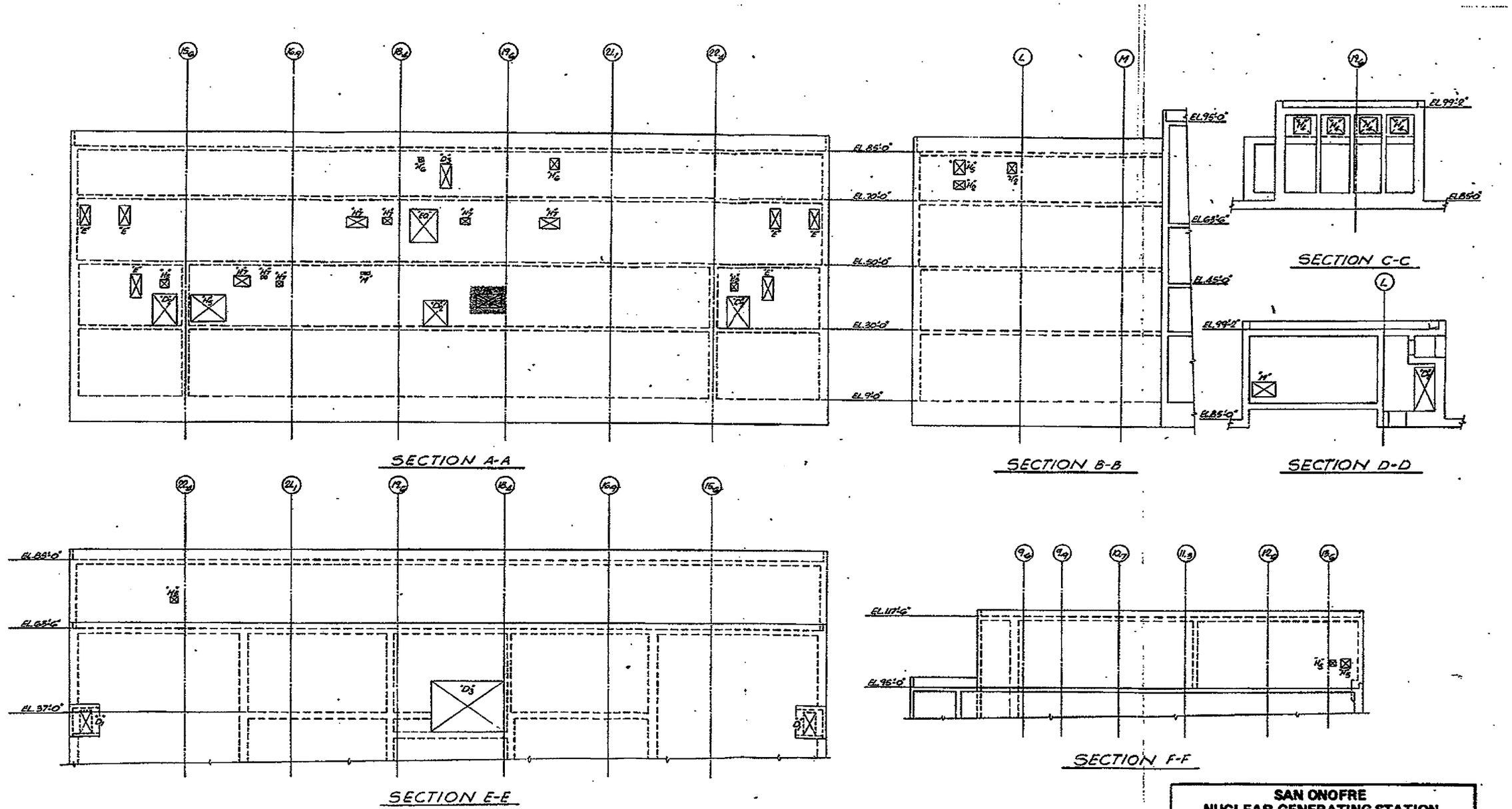

CHANGE

SAN ONOFRE
NUCLEAR GENERATING STATION
Units 2 & 3

IDENTIFICATION OF SAFETY-RELATED PENETRATIONS ON ROOF AND EXPOSED WALLS OF AUXILIARY BUILDING AND FUEL HANDLING BUILDING (Sheet 2 of 2)

Figure 3.5-9

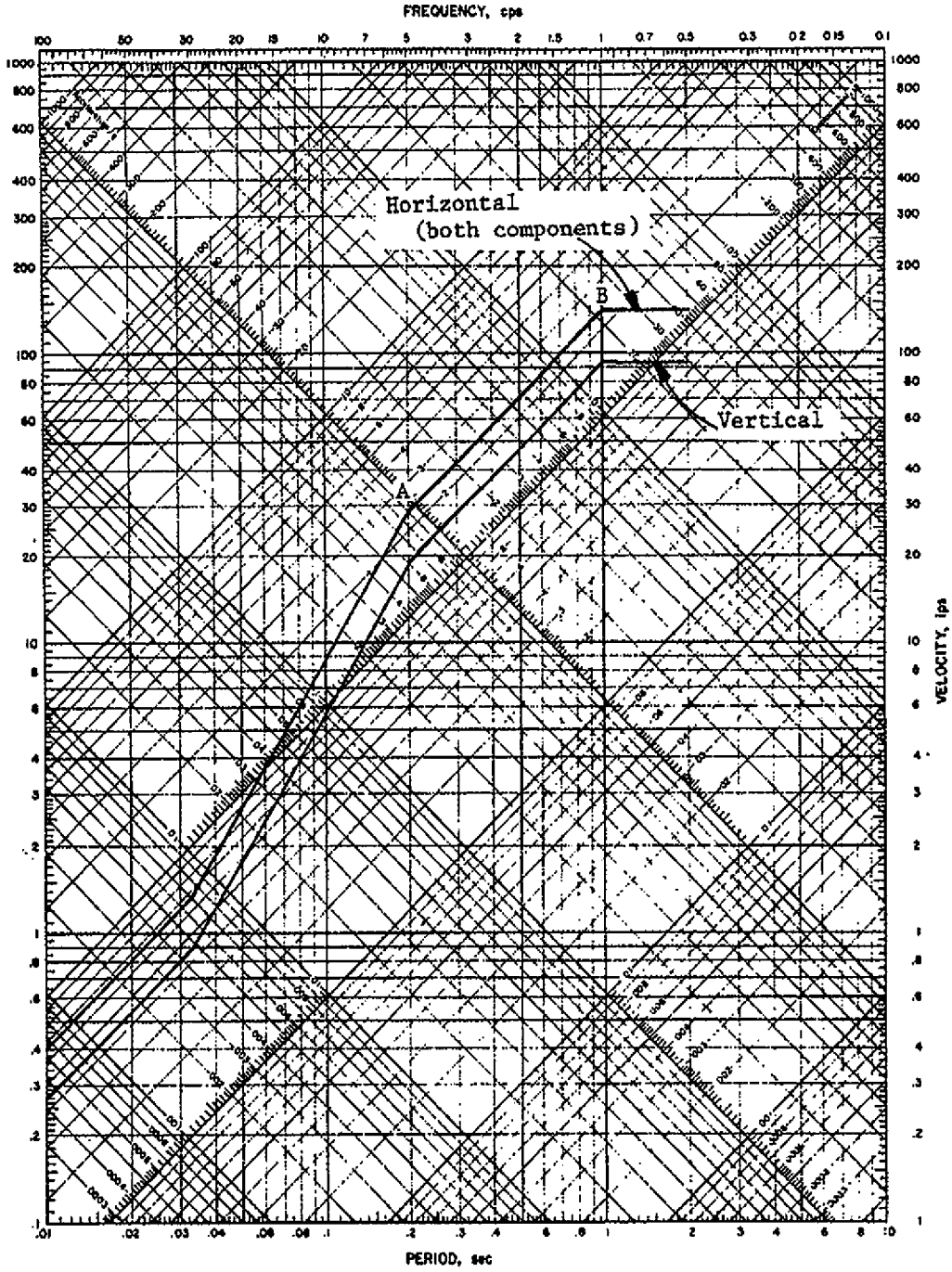

SAN ONOFRE NUCLEAR GENERATING STATION Units 2 & 3
SITE SPECIFIC DESIGN RESPONSE SPECTRA FOR 2% DAMPING
Figure 3.7-1

10079-11D-570
12AU6

Amended: April 2009 TL: E047997

Site File Copy

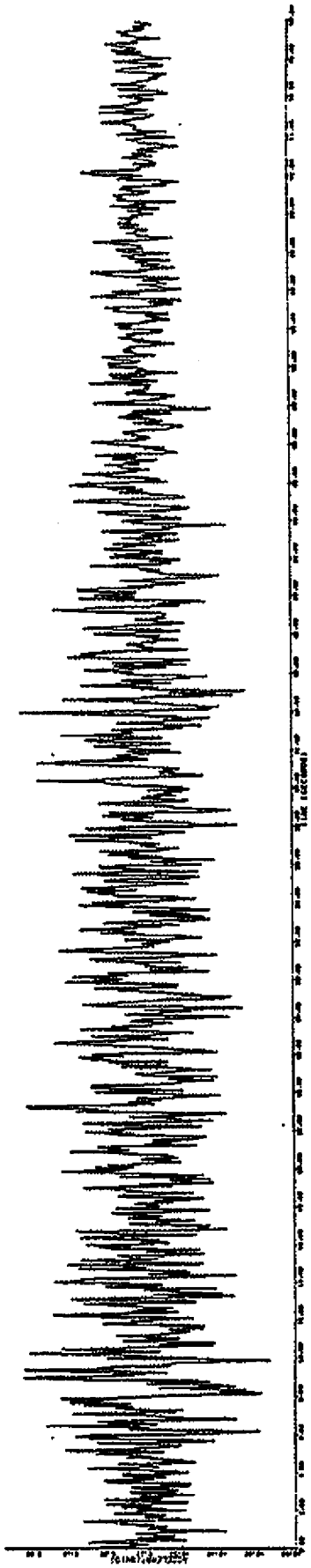

10079-11D-571
12AU6

SAN ONOFRE NUCLEAR GENERATING STATION Units 2 & 3
DBE ACCELERATION TIME HISTORY
Figure 3.7-2

Site File Copy

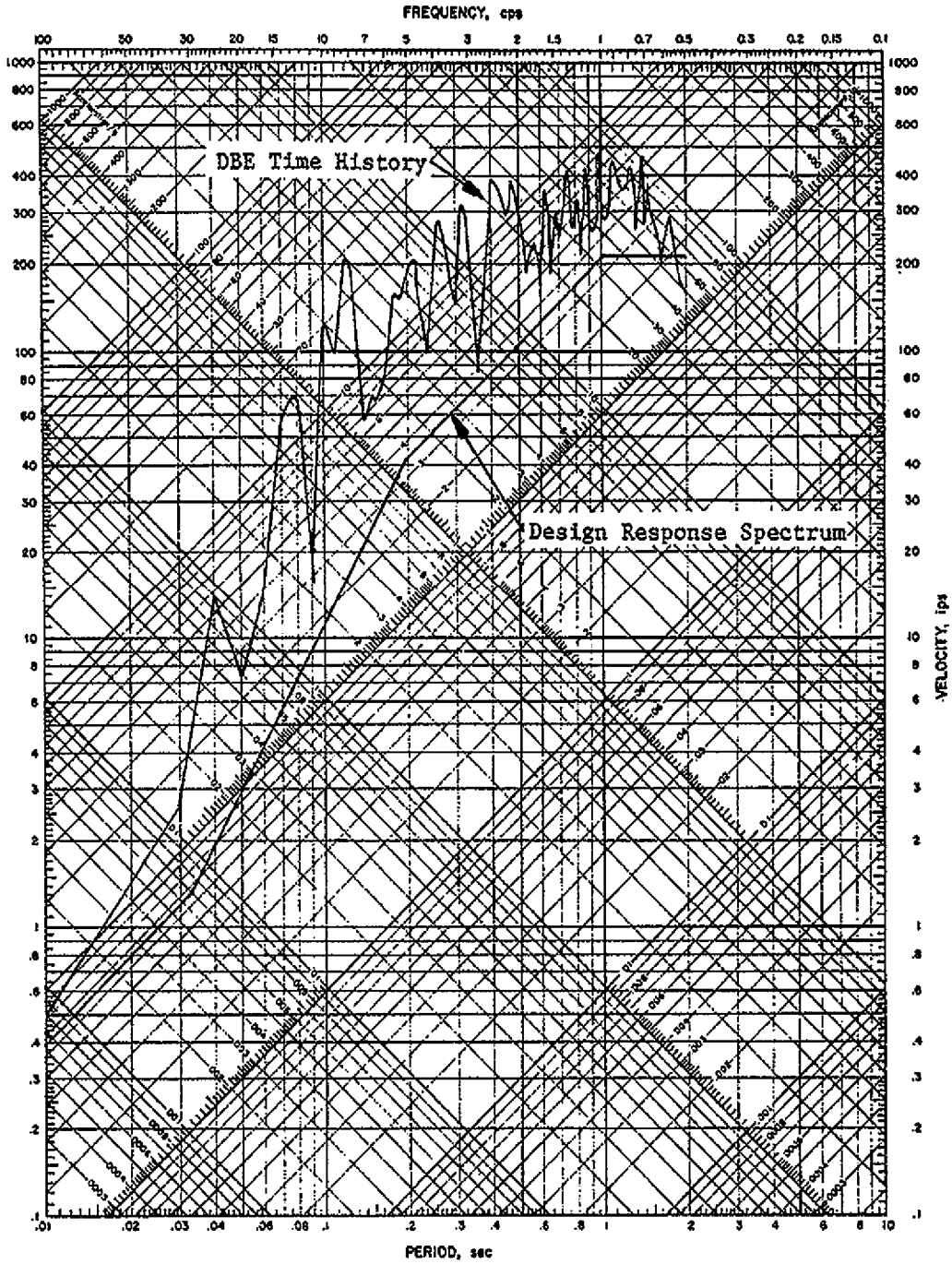

SAN ONOFRE NUCLEAR GENERATING STATION Units 2 & 3
DESIGN AND TIME-HISTORY SPECTRA 0% DAMPING
Figure 3.7-3

10079-11D-572
12AU6

Amended: April 2009 TL: E047997

Site File Copy

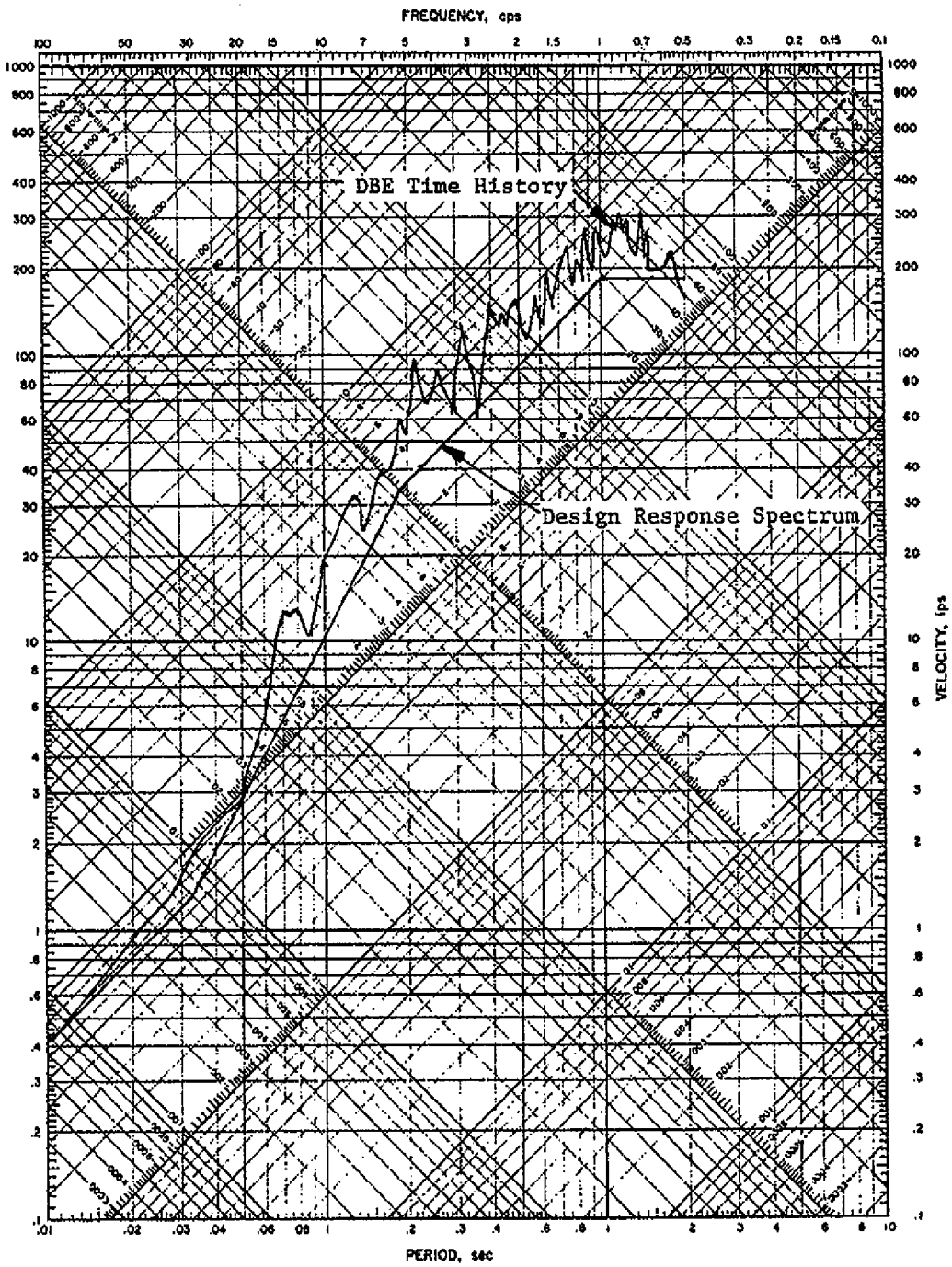

SAN ONOFRE NUCLEAR GENERATING STATION Units 2 & 3
DESIGN AND TIME-HISTORY SPECTRA 0.5% DAMPING
Figure 3.7-4

10079-11D-573
12AU6

Amended: April 2009 TL: E047997

Site File Copy

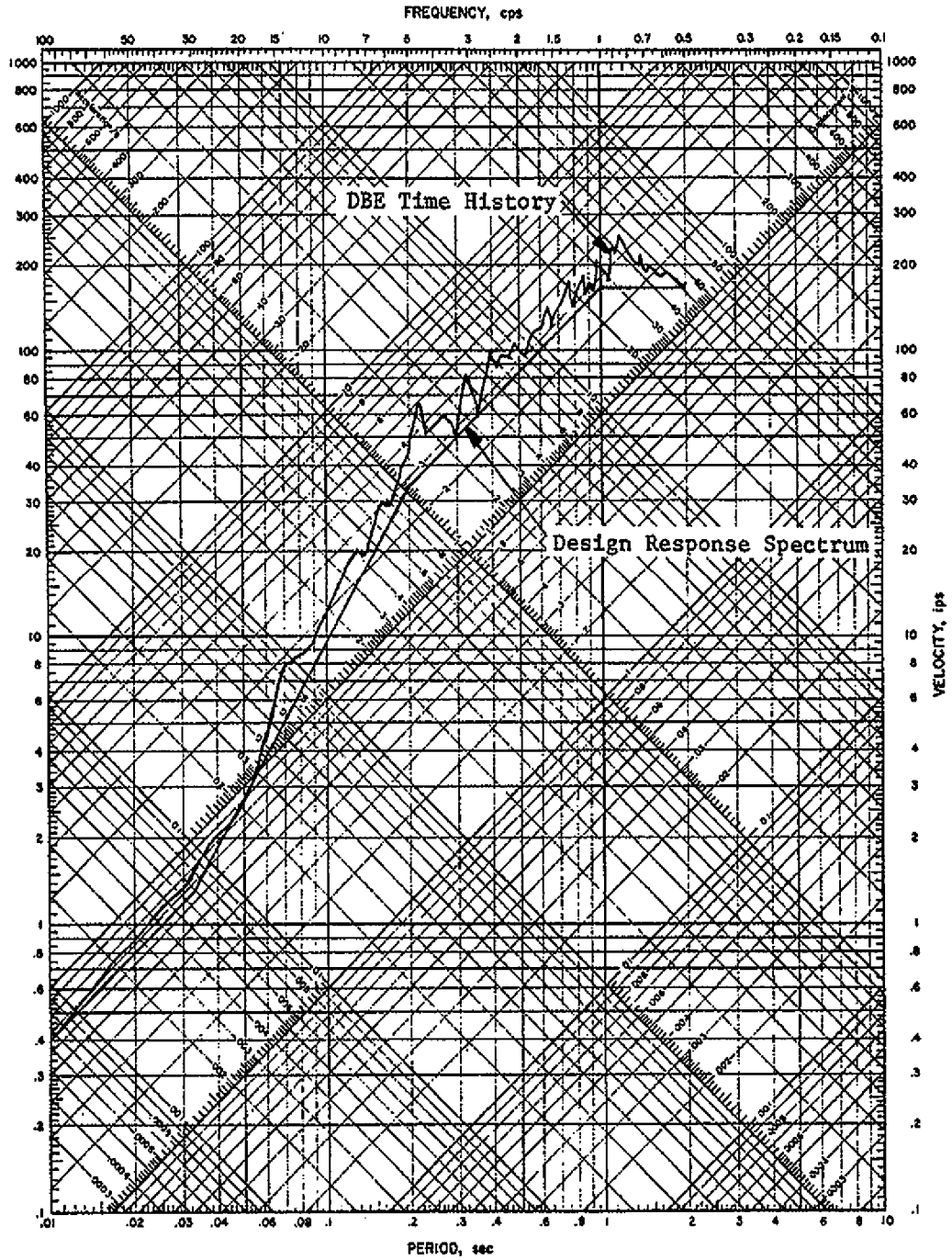

SAN ONOFRE NUCLEAR GENERATING STATION Units 2 & 3
DESIGN AND TIME-HISTORY SPECTRA 1% DAMPING
Figure 3.7-5

50079-t1D-574
12AU6

Site File Copy

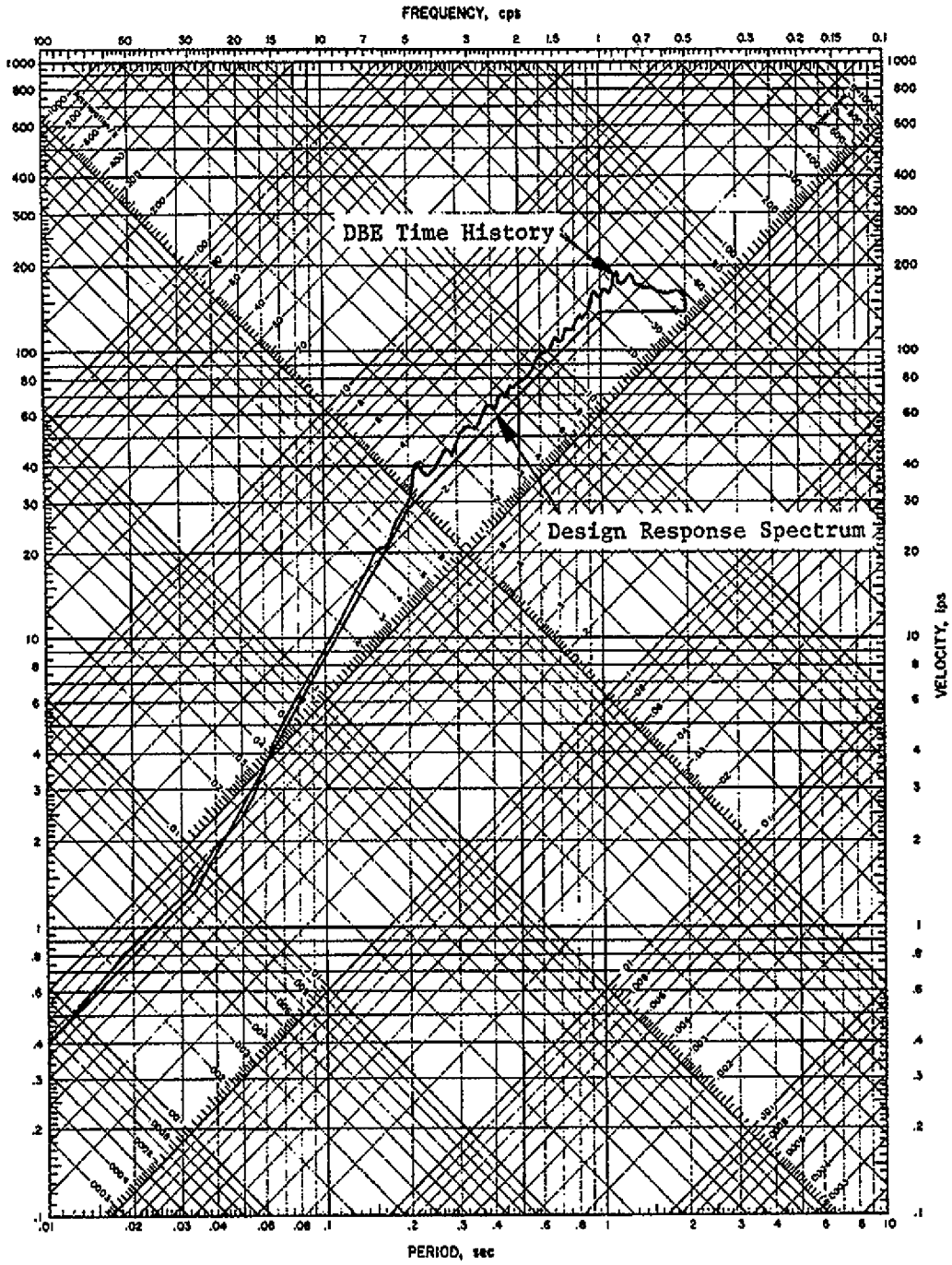

SAN ONOFRE NUCLEAR GENERATING STATION Units 2 & 3
DESIGN AND TIME-HISTORY SPECTRA 2% DAMPING
Figure 3.7-6

10079-11D-575
12AU6

Amended: April 2009 TL: E047997

Site File Copy

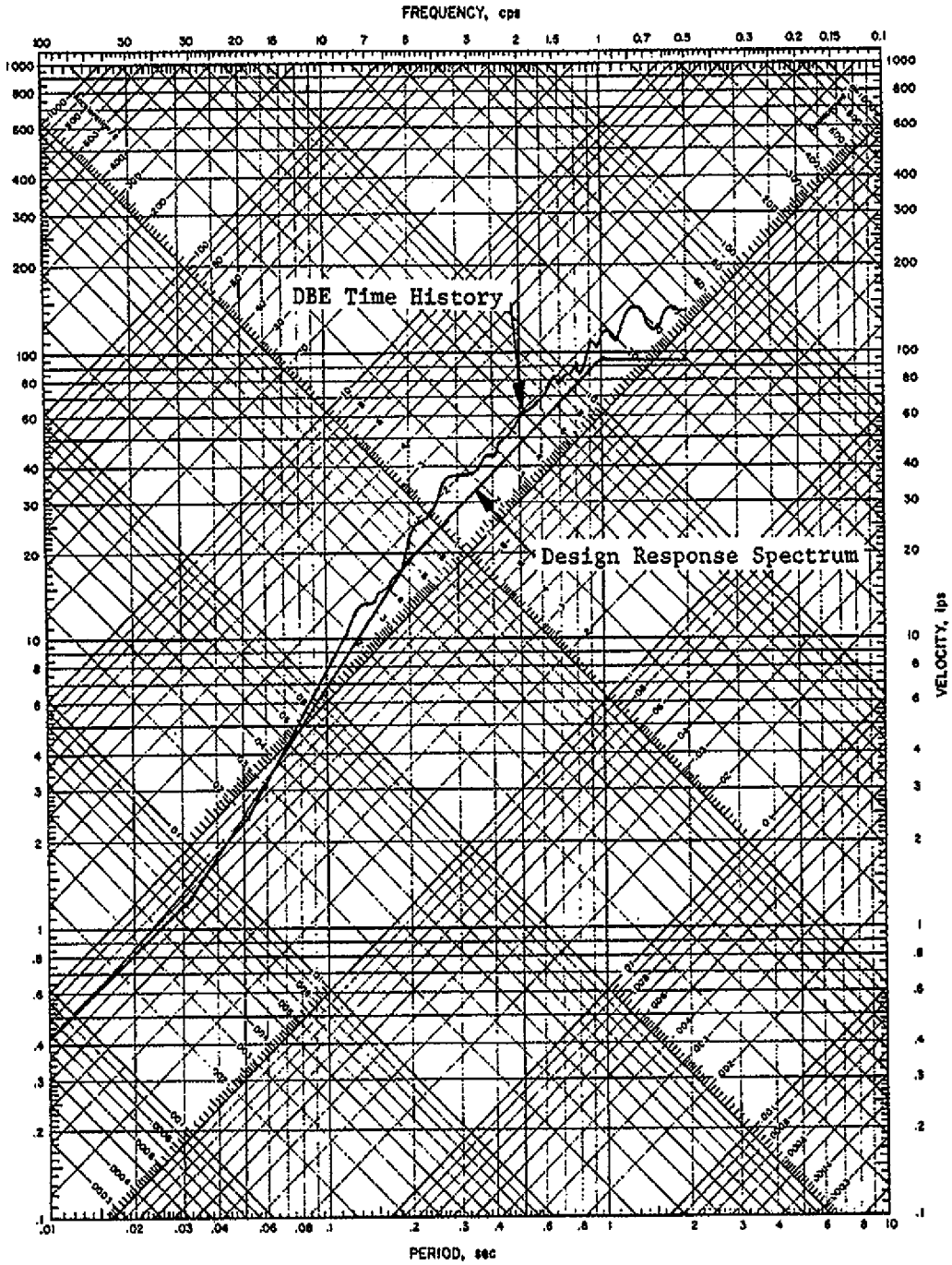

SAN ONOFRE NUCLEAR GENERATING STATION Units 2 & 3
DESIGN AND TIME-HISTORY SPECTRA 5% DAMPING
Figure 3.7-7

10079-11D-576
12AU6

Amended: April 2009 TL: E047997

Site File Copy

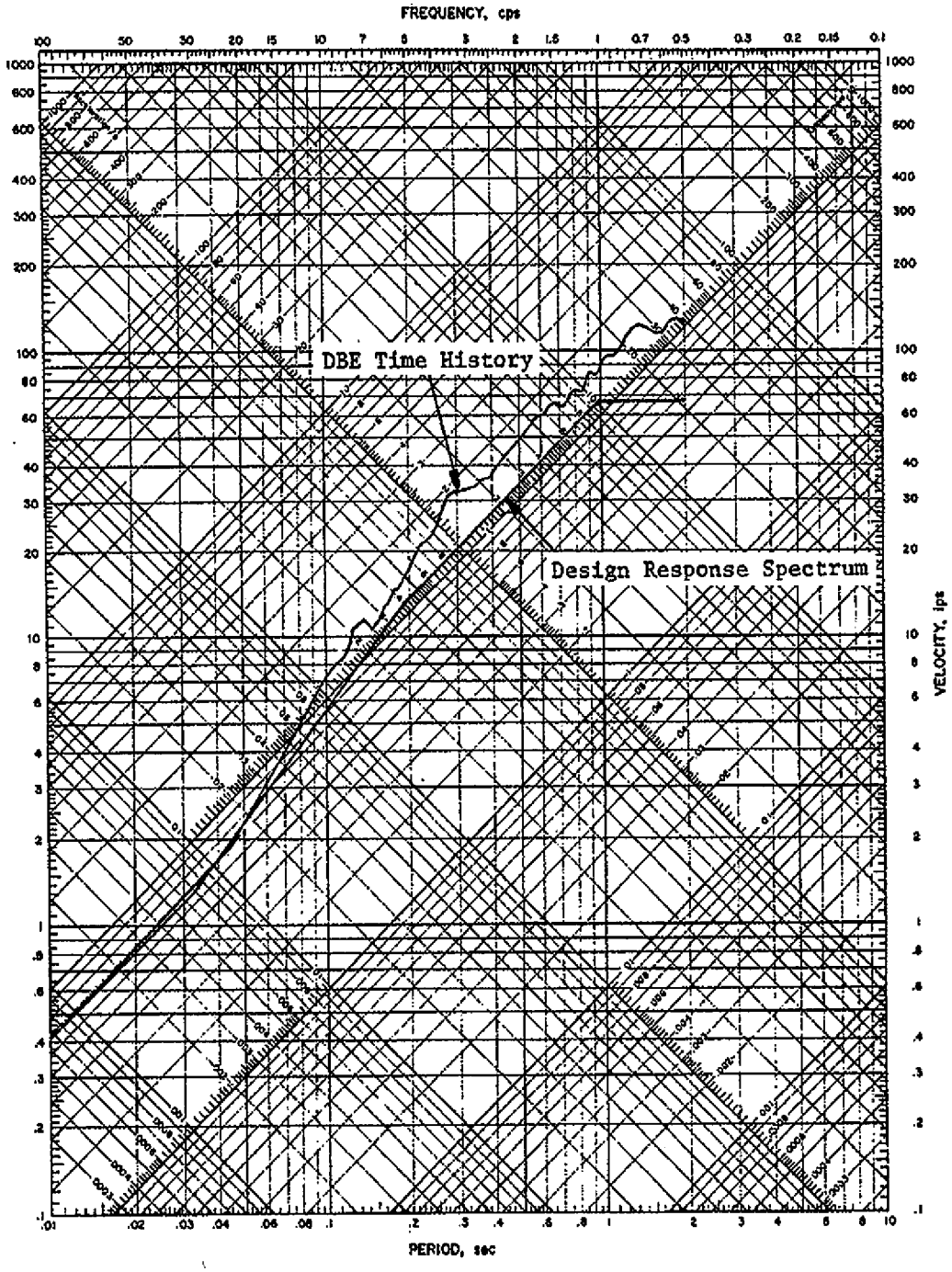

SAN ONOFRE NUCLEAR GENERATING STATION Units 2 & 3
DESIGN AND TIME-HISTORY SPECTRA 7% DAMPING
Figure 3.7-8

10079-11D-577
12AU6

Amended: April 2009 TL: E047997

Site File Copy

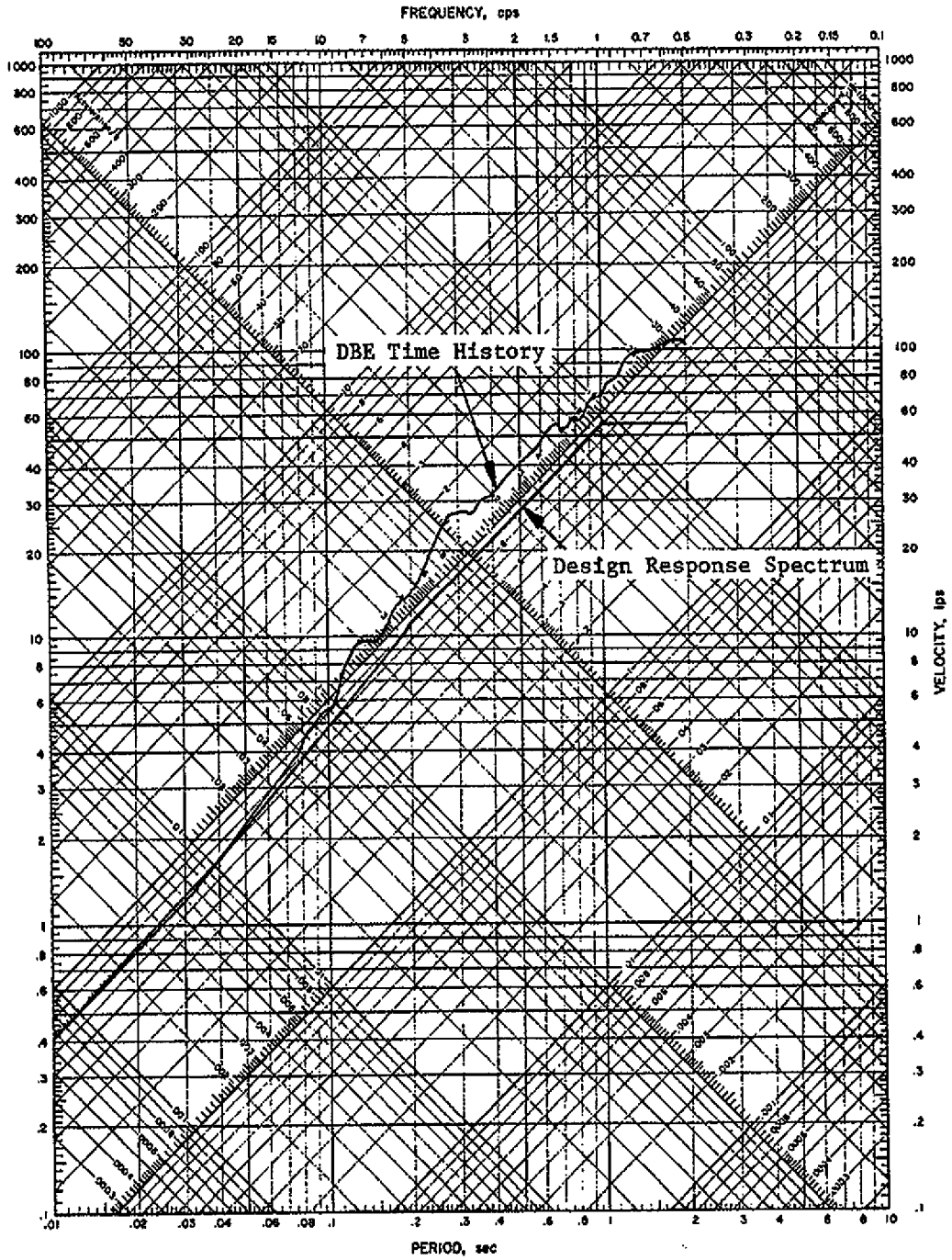

SAN ONOFRE NUCLEAR GENERATING STATION Units 2 & 3
DESIGN AND TIME-HISTORY SPECTRA 10% DAMPING
Figure 3.7-9

10079-11D-578
12AU6

Site File Copy

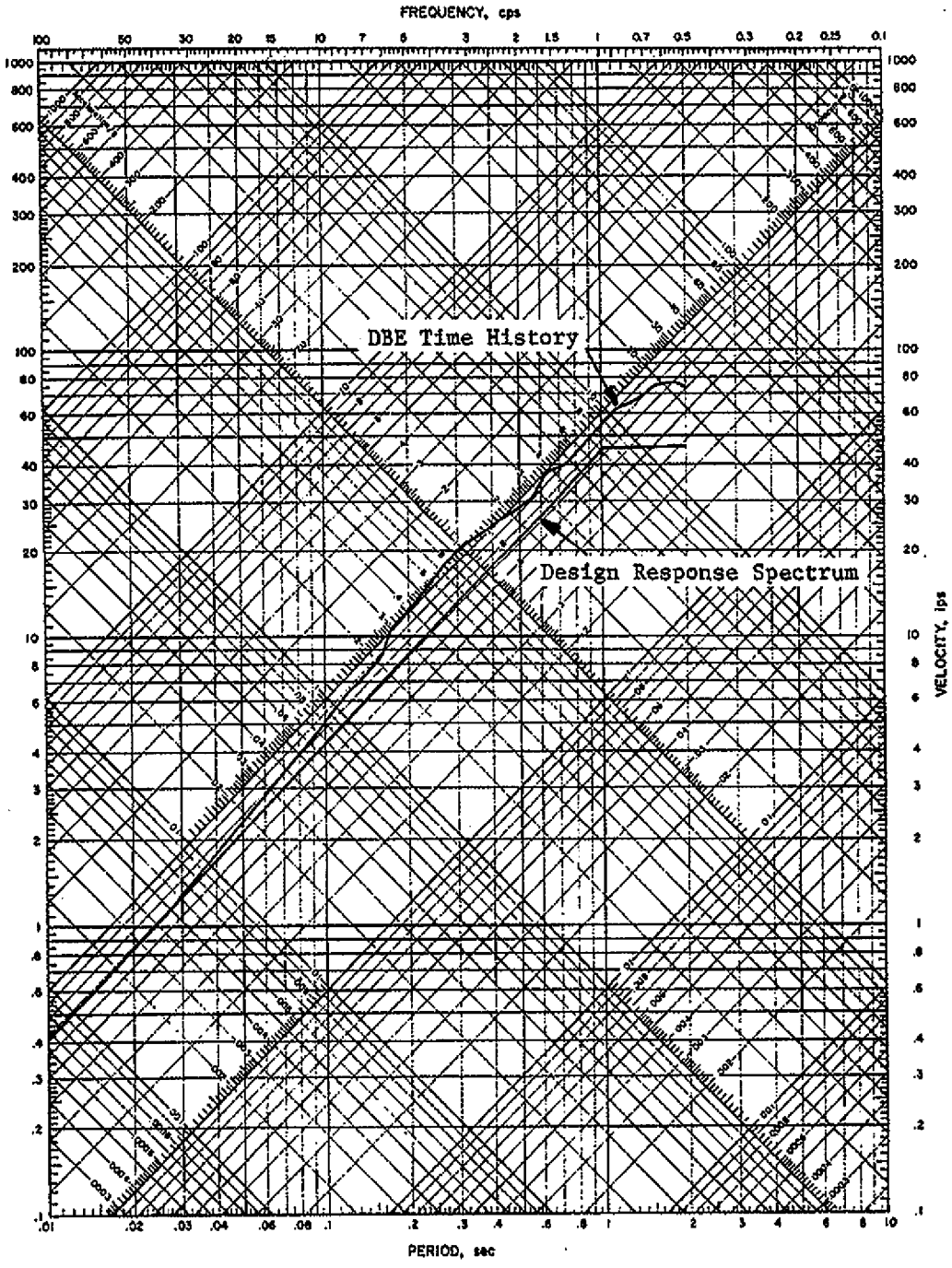

SAN ONOFRE NUCLEAR GENERATING STATION Units 2 & 3
DESIGN AND TIME-HISTORY SPECTRA 20% DAMPING
Figure 3.7-10

16079-11D-579
12AU6

Site File Copy

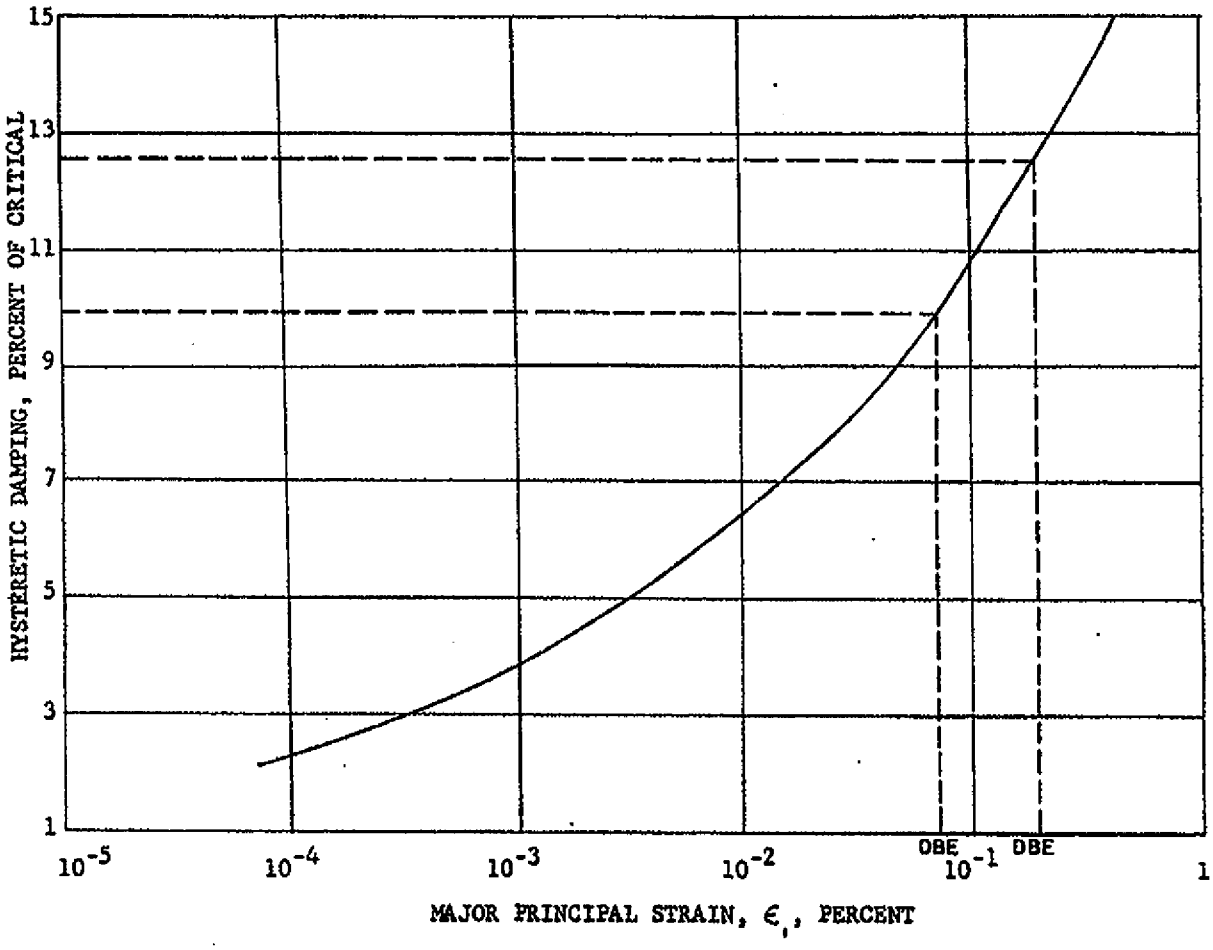

SAN ONOFRE NUCLEAR GENERATING STATION Units 2 & 3
HYSTERETIC DAMPING SAN MATEO FORMATION SAND
Figure 3.7-11

10079-11D-580
12AU6

Site File Copy

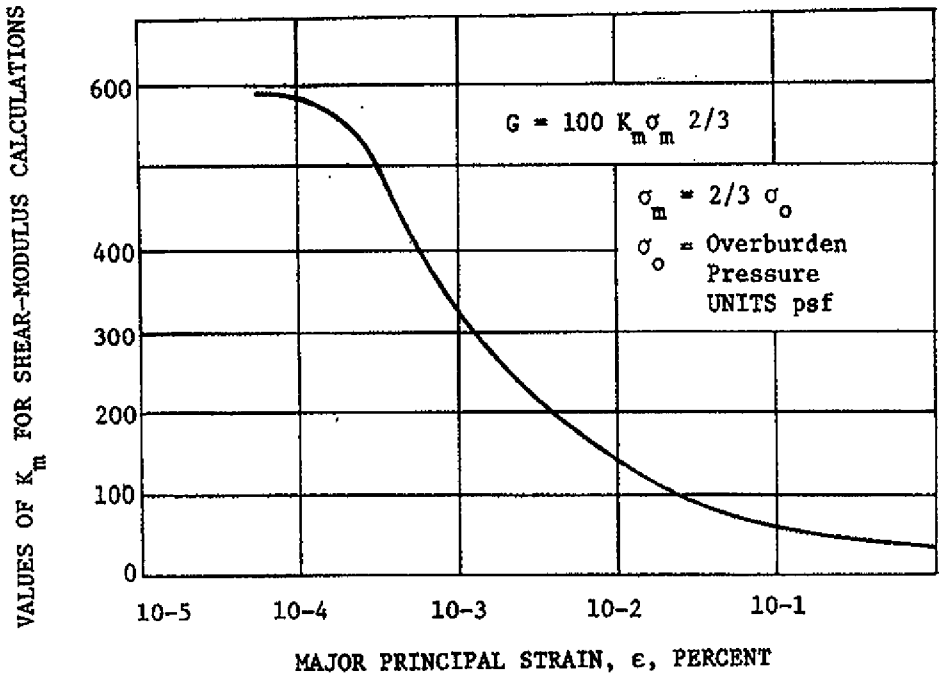

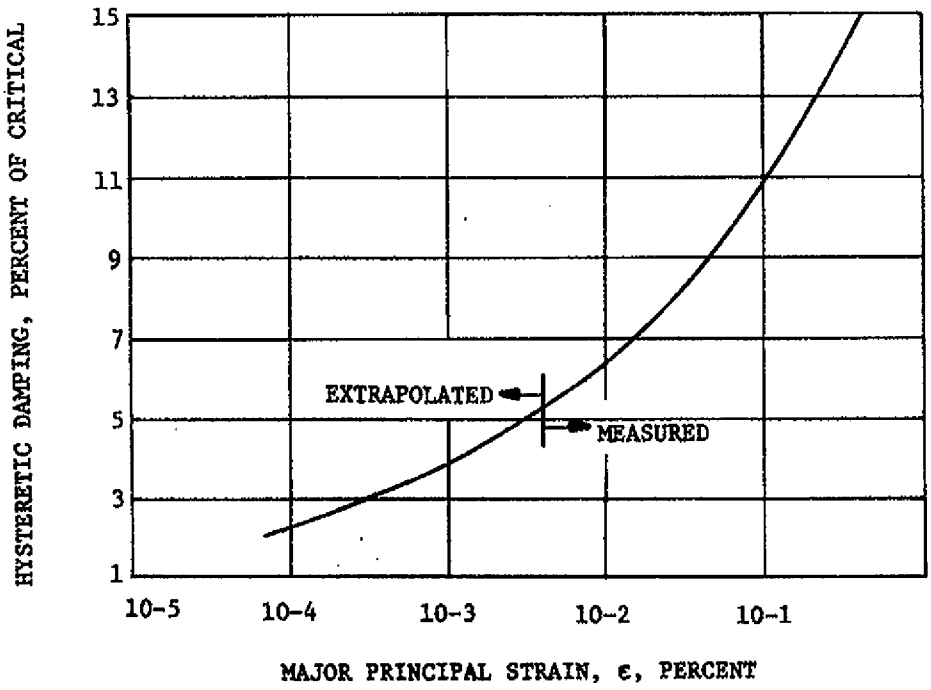

SAN ONOFRE NUCLEAR GENERATING STATION Units 2 & 3
MODULUS AND DAMPING vs. STRAIN SAN MATEO FORMATION SAND
Figure 3.7-12

10079-11D-581
12AU6

Site File Copy

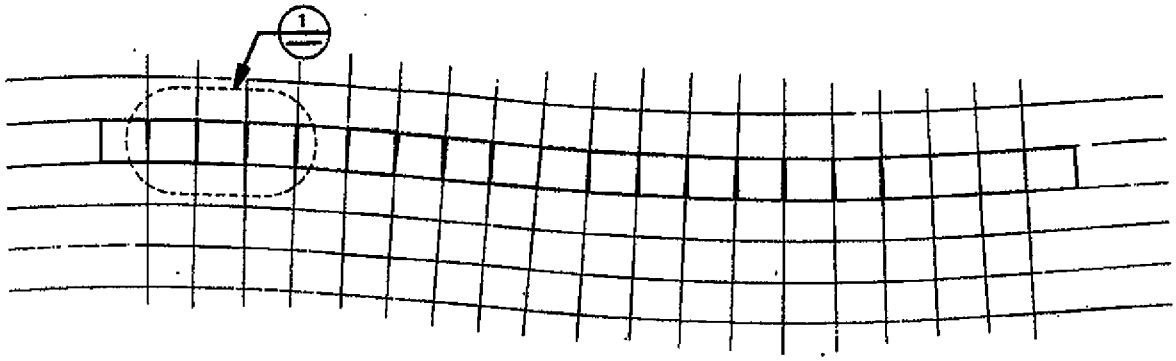

ILLUSTRATION OF CONDUIT COMPLIANCE WITH GROUND MOTION

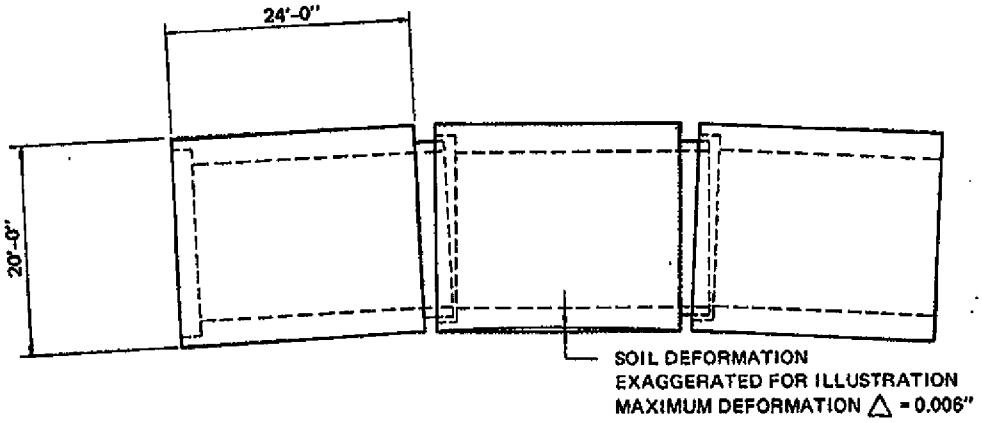

DETAIL 1

SAN ONOFRE NUCLEAR GENERATING STATION Units 2 & 3
CONDUIT BEHAVIOR DURING A SEISMIC EVENT
Figure 3.7-13

10079
29SEP78

Site File Copy

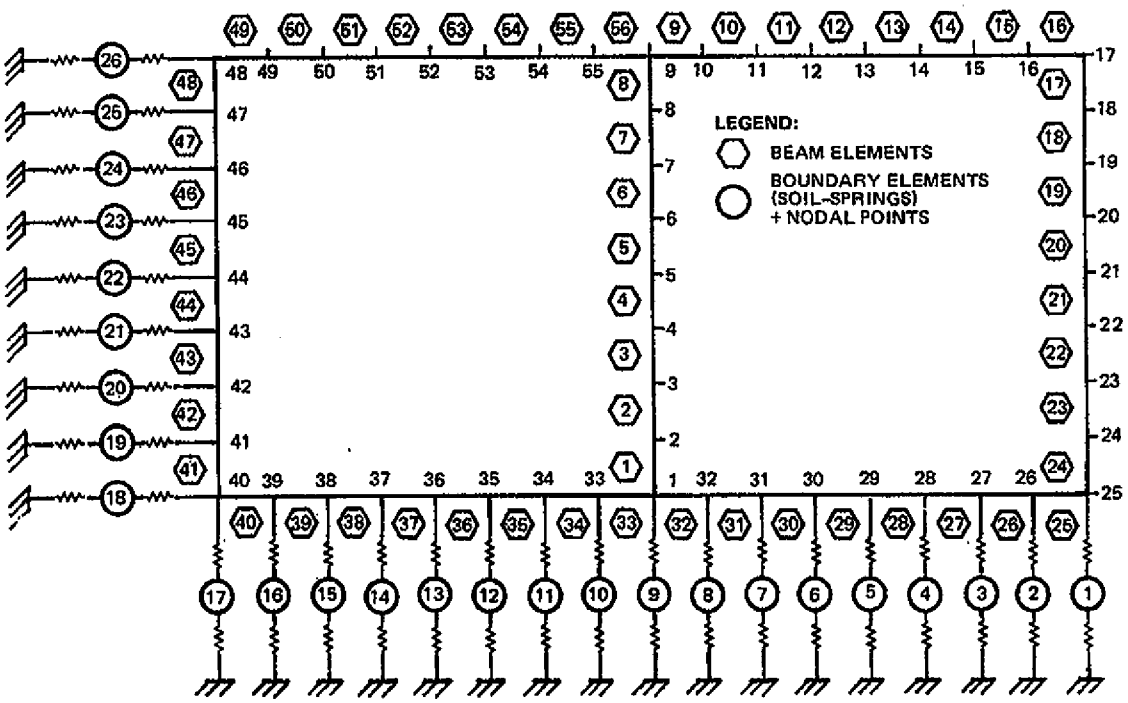

SAN ONOFRE NUCLEAR GENERATING STATION Units 2 & 3
BSAP MODEL USED FOR BOX CONDUIT ANALYSIS AND DESIGN
Figure 3.7-14

10079
29SEP78

Site File Copy

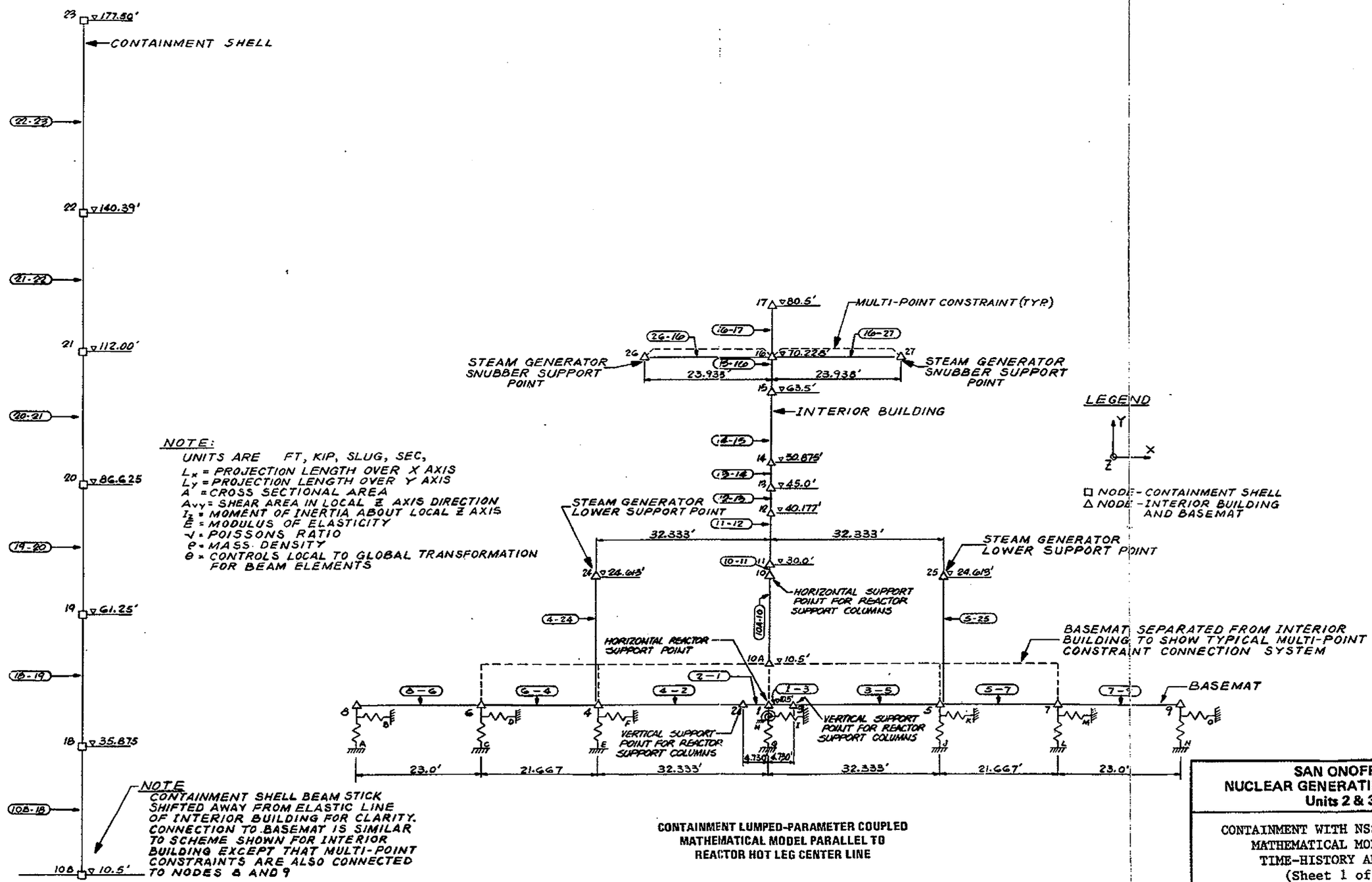

CONTAINMENT LUMPED-PARAMETER COUPLED MATHEMATICAL MODEL PARALLEL TO REACTOR HOT LEG CENTER LINE

SAN ONOFRE NUCLEAR GENERATING STATION Units 2 & 3

CONTAINMENT WITH NSSS EQUIPMENT MATHEMATICAL MODEL FOR TIME-HISTORY ANALYSIS (Sheet 1 of 2)

Figure 3.7-15

Amended: April 2009 TL: E047997

Site File Copy

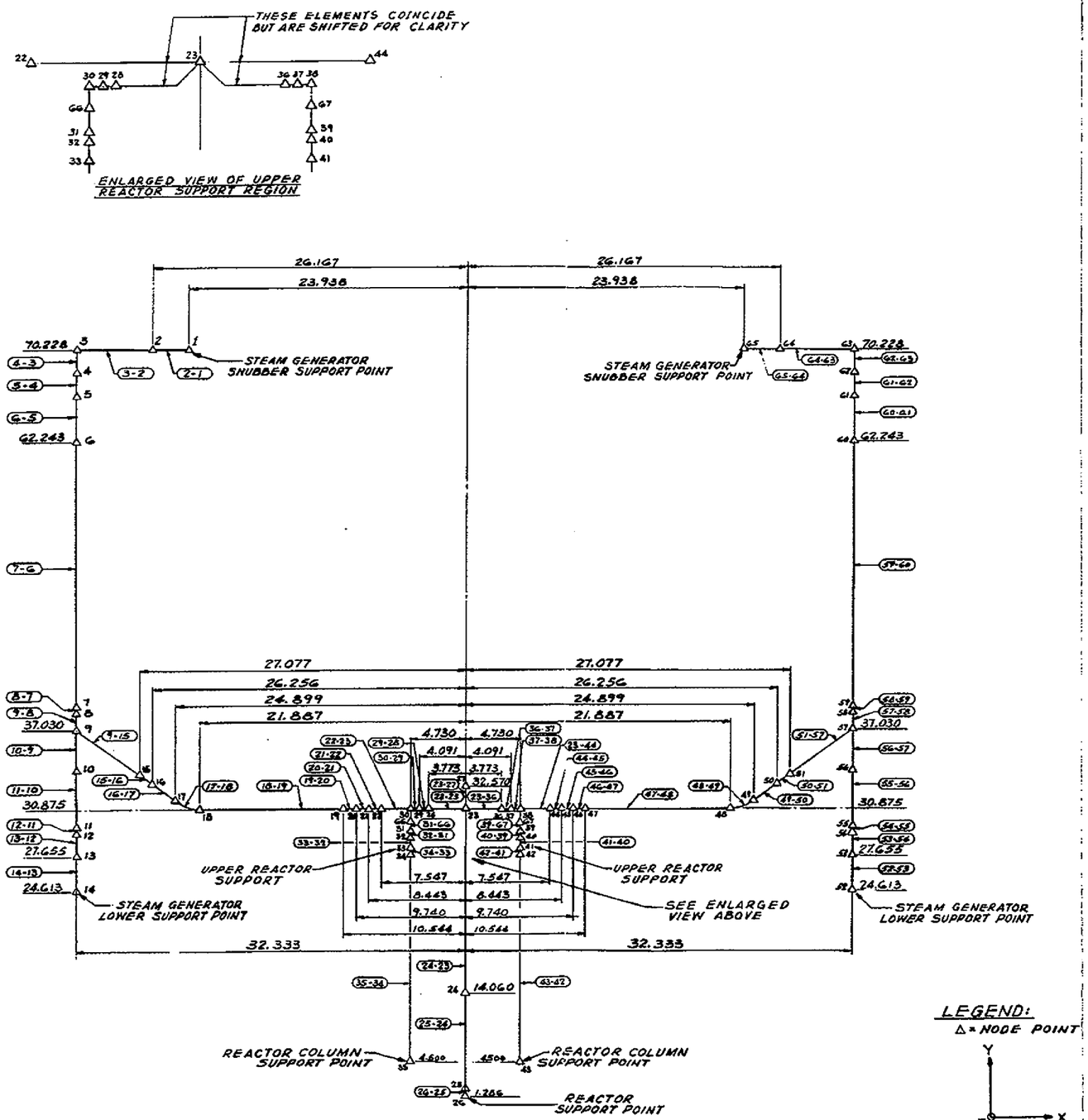

LUMPED-PARAMETER NSSS MATHEMATICAL MODEL
(PLANE PARALLEL TO REACTOR HOT LEG ℄)

NOTE

DIMENSIONS ARE IN FT.

NODES GG-30 & G7-38 ARE CONNECTED BY MULTI-POINT CONSTRAINTS

SAN ONOFRE NUCLEAR GENERATING STATION Units 2 & 3
CONTAINMENT WITH NSSS EQUIPMENT MATHEMATICAL MODEL FOR TIME-HISTORY ANALYSIS (Sheet 2 of 2)
Figure 3.7-15

10079-11D-266
12OC6

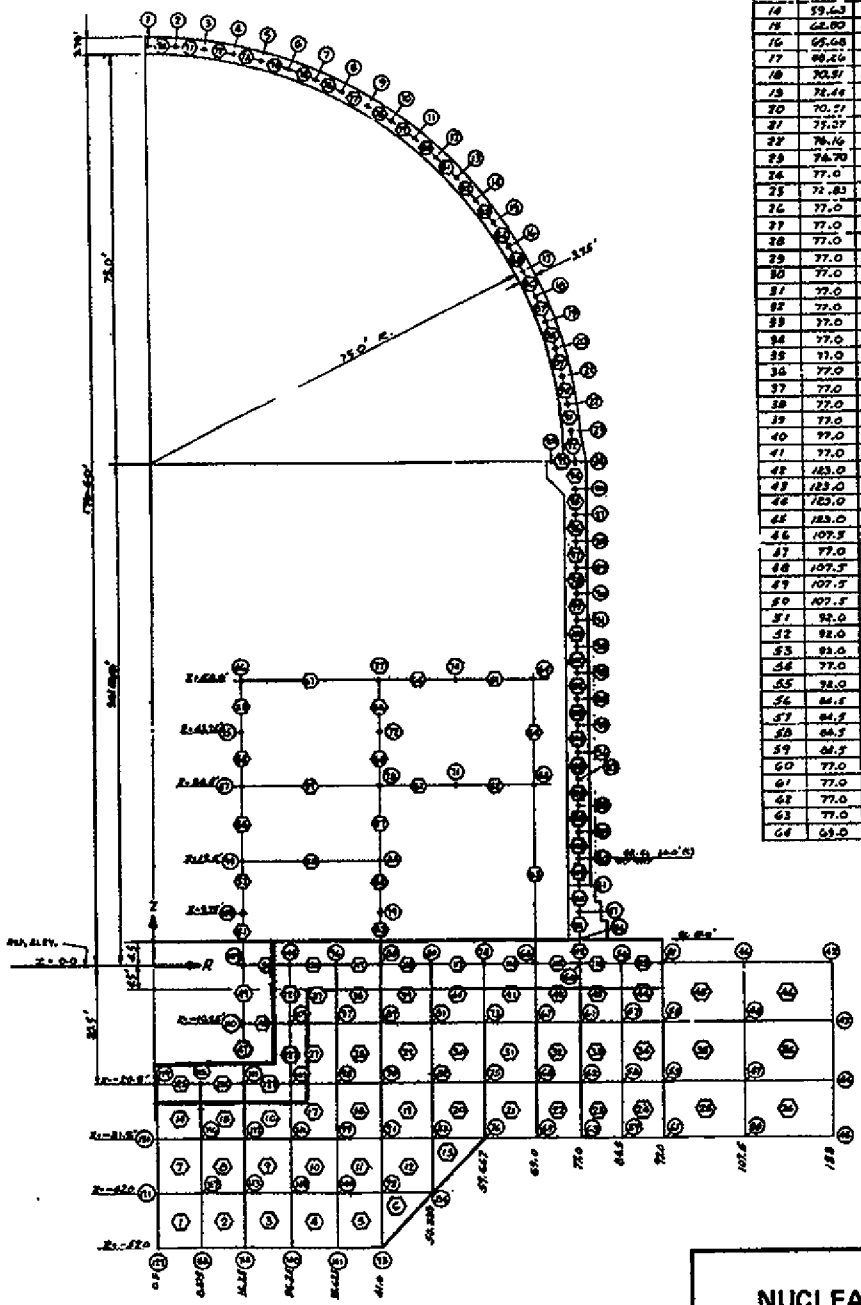

TABLE OF COORDINATES			
NODE	R (FT)	Z (FT)	THK. (FT)
1	0.50	178.38	
2	5.25	178.20	
3	10.87	177.66	
4	15.64	176.77	
5	20.74	175.52	
6	25.74	173.94	
7	30.63	172.01	
8	35.37	169.76	
9	39.94	167.18	
10	44.33	164.30	
11	48.51	161.13	
12	52.47	157.68	
13	56.18	153.97	
14	59.63	150.01	
15	62.80	145.83	
16	65.68	141.46	
17	68.26	136.87	
18	70.51	132.13	
19	72.44	127.24	
20	70.71	122.24	
21	75.27	117.16	
22	76.16	111.97	
23	76.70	106.75	
24	77.0	101.50	
25	72.85	101.50	
26	77.0	97.50	
27	77.0	93.50	
28	77.0	89.50	
29	77.0	84.75	
30	77.0	80.00	
31	77.0	74.00	
32	77.0	68.00	
33	77.0	62.00	
34	77.0	56.00	
35	77.0	50.00	
36	77.0	40.00	
37	77.0	38.00	
38	77.0	38.00	
39	77.0	26.00	
40	77.0	20.00	
41	77.0	14.50	
42	123.0	—	
43	123.0	- 10.25	
44	123.0	- 20.5	
45	123.0	- 31.5	
46	107.5	—	
47	77.0	9.5	
48	107.5	- 10.25	
49	107.5	- 20.5	
50	107.5	- 31.5	
51	92.0	—	
52	92.0	- 10.25	
53	92.0	- 20.5	
54	77.0	4.5	
55	92.0	- 31.5	
56	84.5	—	
57	84.5	- 10.25	
58	84.5	- 20.5	
59	84.5	- 31.5	
60	77.0	—	
61	77.0	- 10.25	
62	77.0	- 20.5	
63	77.0	- 31.5	
64	69.0	53.0	

NODE	R (FT)	Z (FT)	THK. (FT)
65	69.0	34.5	
66	69.0	—	
67	69.0	- 10.25	
68	69.0	- 20.5	
69	69.0	- 31.5	
70	55.0	53.0	
71	55.0	34.5	
72	41.0	43.75	
73	59.667	- 10.25	
74	59.667	—	
75	59.667	- 20.5	
76	59.667	- 31.5	
77	41.0	53.0	
78	41.0	34.5	
79	41.0	9.75	
80	50.333	—	
81	50.333	- 10.25	
82	50.333	- 20.5	
83	50.333	- 31.5	
84	50.333	- 42.0	
85	41.0	19.5	
86	16.25	53.0	
87	16.25	34.5	
88	41.0	—	
89	41.0	- 10.25	
90	41.0	- 20.5	
91	41.0	- 31.5	
92	41.0	- 42.0	
93	41.0	- 52.0	
94	16.25	19.50	
95	16.25	43.75	
96	33.625	—	
97	33.625	- 10.25	
98	33.625	- 20.5	
99	33.625	- 31.5	
100	33.625	- 42.0	
101	33.625	- 52.0	
102	16.25	9.75	
103	16.25	- 10.25	
104	16.25	—	
105	16.25	- 20.5	
106	16.25	- 31.5	
107	16.25	- 42.0	
108	16.25	- 52.0	
109	16.25	—	
110	16.25	- 10.25	
111	16.25	- 20.5	
112	16.25	- 31.5	
113	16.25	- 42.0	
114	16.25	- 52.0	
115	0.375	- 20.5	
116	0.375	- 31.5	
117	0.375	- 42.0	
118	0.375	- 52.0	
119	0.5	- 20.5	
120	0.5	- 31.5	
121	0.5	- 42.0	
122	0.5	- 52.0	

ASHSD AXISYMMETRIC MATHEMATICAL MODEL WITH SMALL SOIL GRID

10079-11D-267
13JL6

SAN ONOFRE NUCLEAR GENERATING STATION Units 2 & 3

CONTAINMENT STRUCTURE
ASHSD AXISYMMETRIC MATHEMATICAL MODEL
FOR STATIC AND DYNAMIC ANALYSES

Figure 3.7-16

Site File Copy

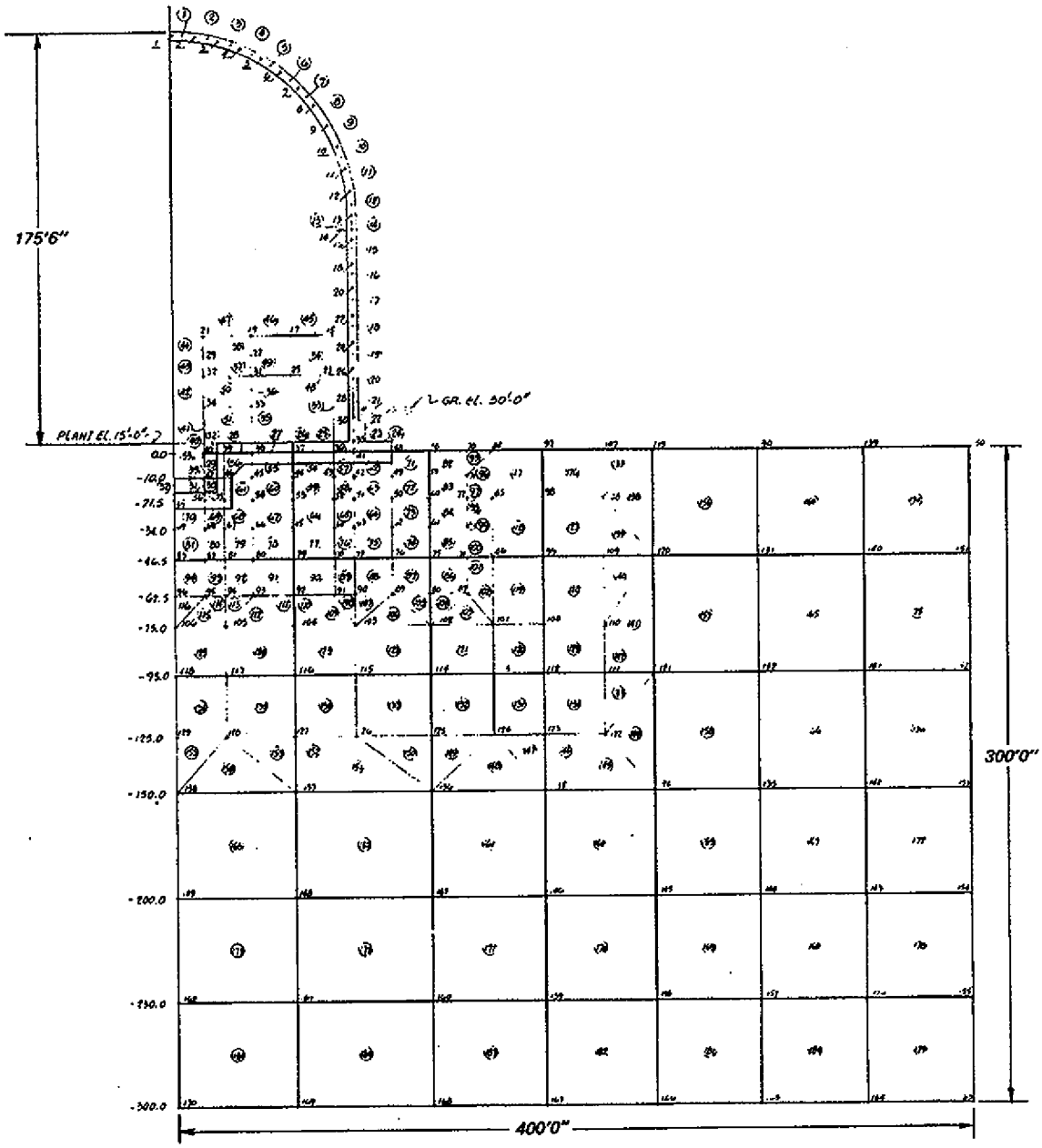

ASHSD AXISYMMETRIC MATHEMATICAL MODEL WITH LARGE SOIL GRID

SAN ONOFRE NUCLEAR GENERATING STATION Units 2 & 3
CONTAINMENT STRUCTURE ASHSD AXISYMMETRIC MATHEMATICAL MODEL FOR STATIC AND DYNAMIC ANALYSES
Figure 3.7-17

10079-11D-268
13JL6

Site File Copy

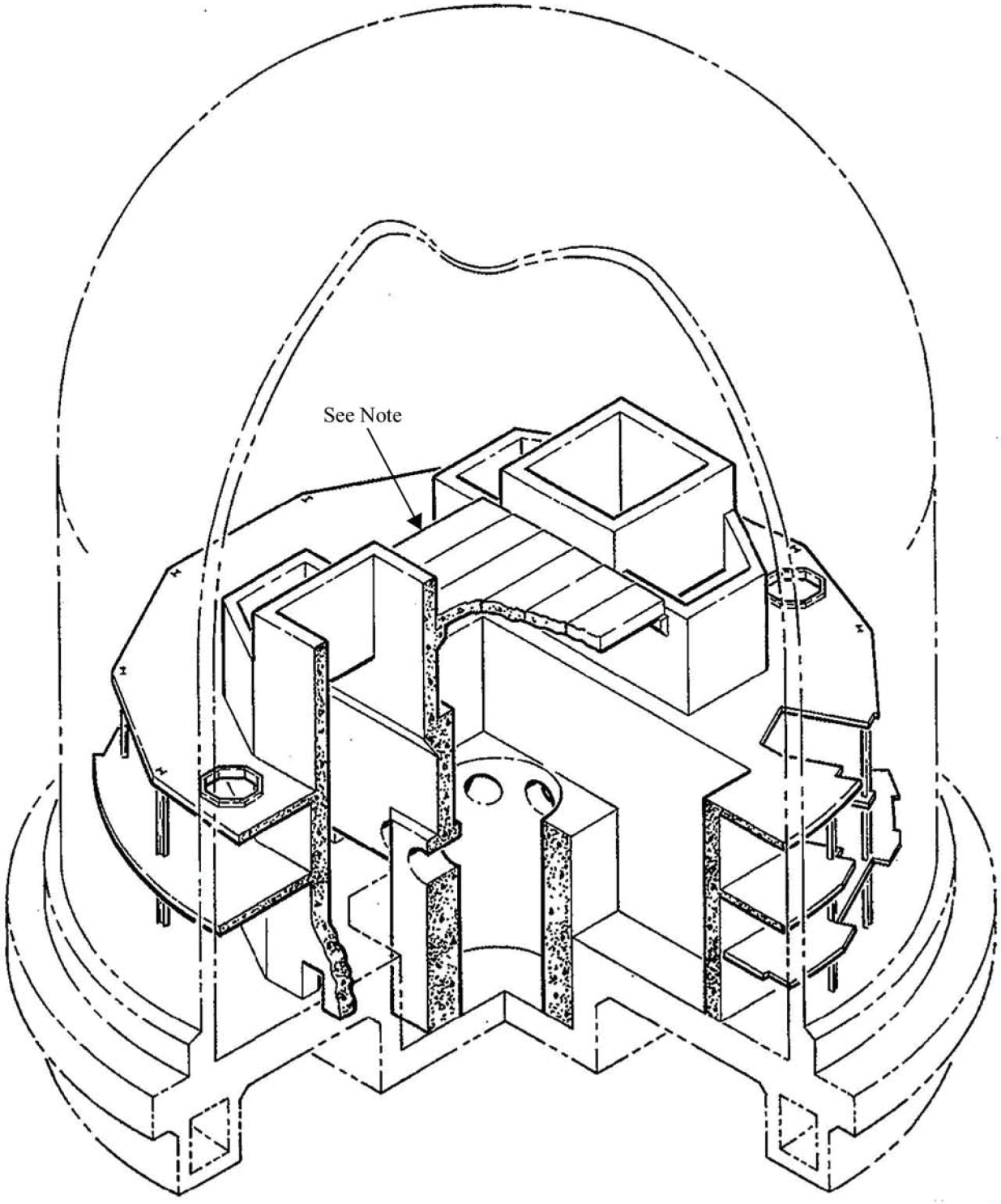

PICTORIAL REPRESENTATION OF THE THREE DIMENSIONAL FINITE ELEMENT MATHEMATICAL MODELS

Note: The concrete missile shield panels have been replaced by the missile shield / cable support structure (UNIT 2 ONLY)

SAN ONOFRE NUCLEAR GENERATING STATION Units 2 & 3
INTERNAL STRUCTURE OF THE CONTAINMENT MATHEMATICAL MODELS FOR STATIC AND DYNAMIC ANALYSES
Figure 3.7-18

23508-A

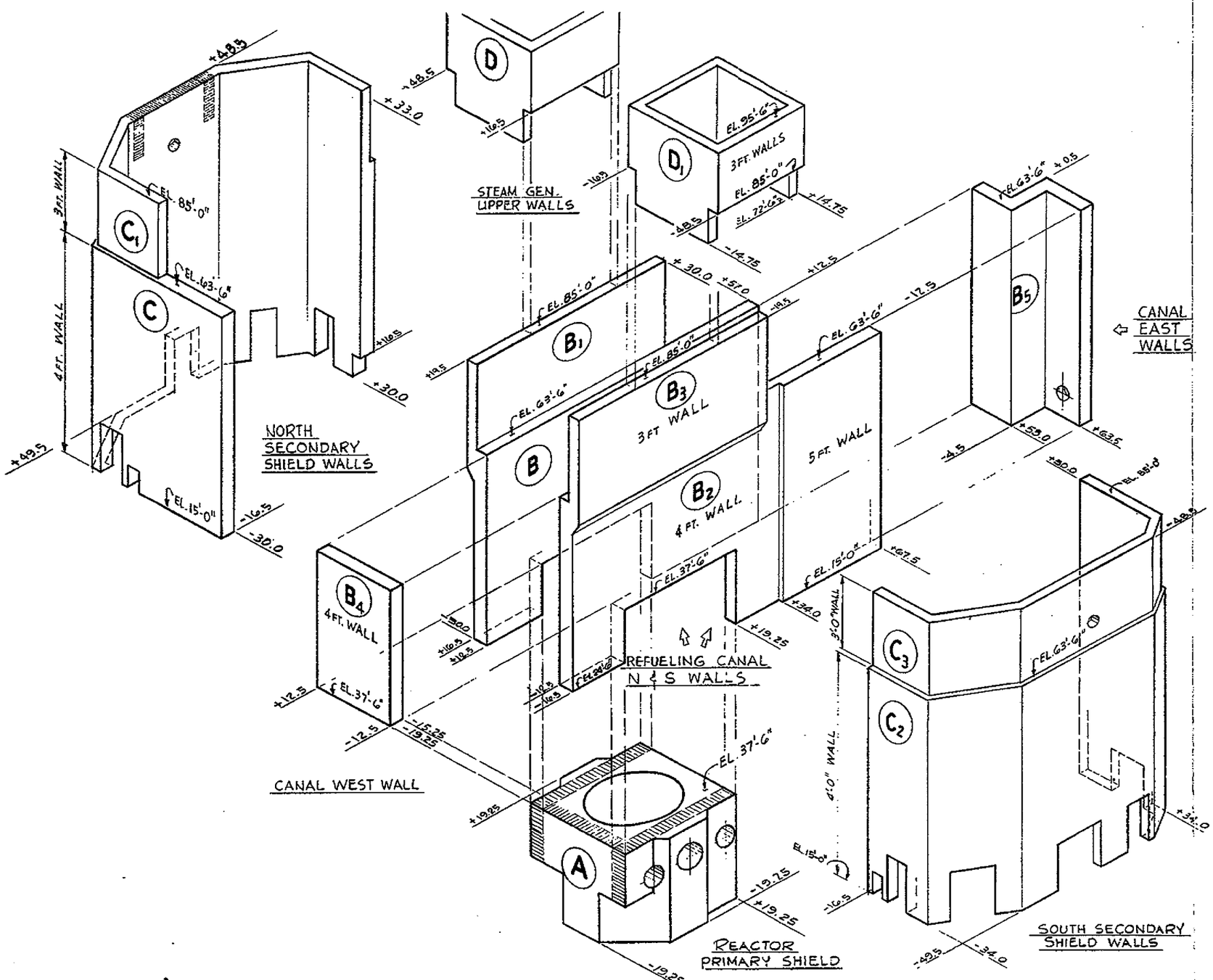

SAN ONOFRE NUCLEAR GENERATING STATION Units 2 & 3
CONTAINMENT INTERIOR (SAP MODEL) EXPLODED ISOMETRIC
Figure 3.7-19

Amended: April 2009 TL: E047997

Site File Copy

23512-A

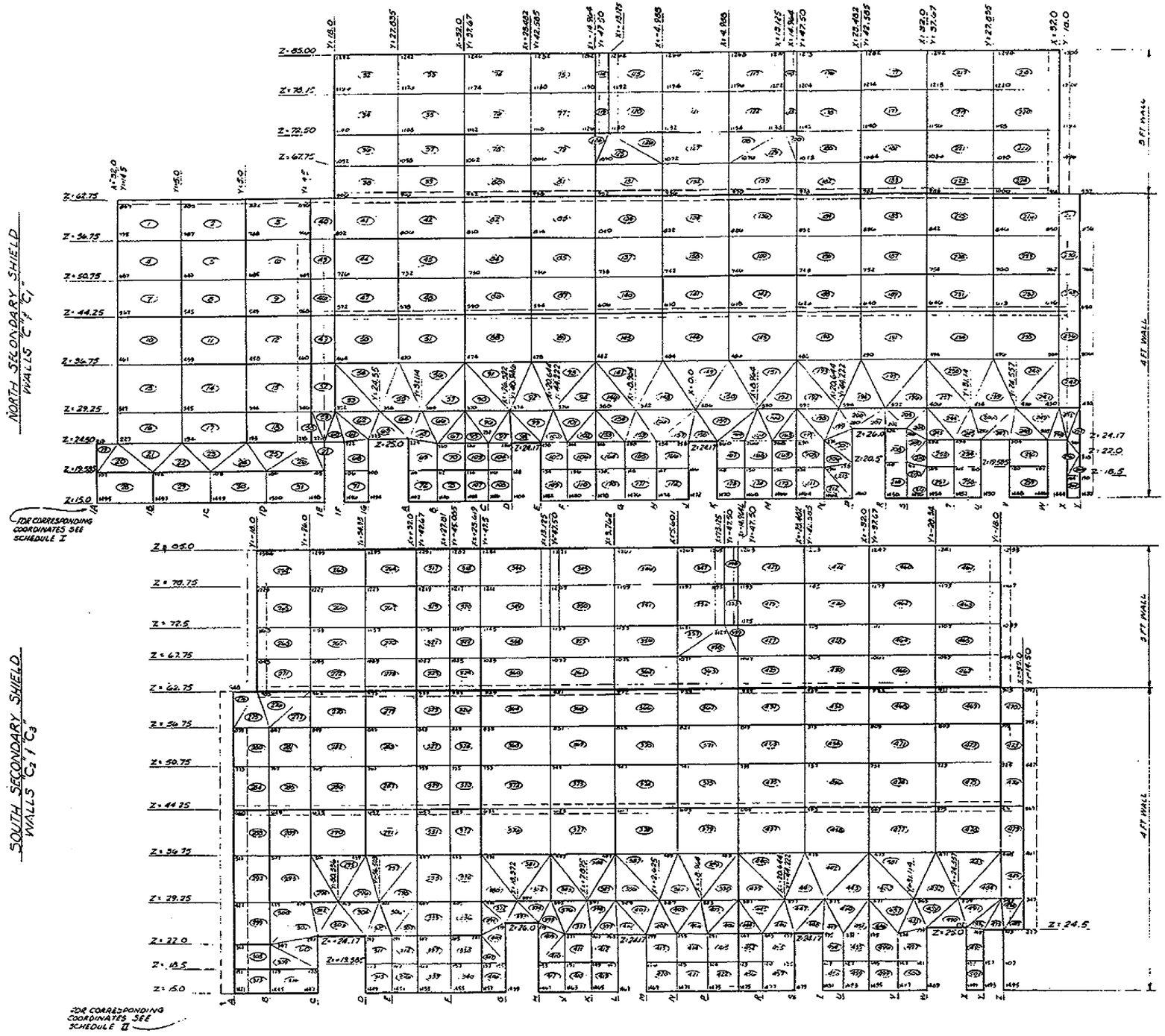

SCHEDULE I

1A	Y= -17.5
1B	Y= -19.0
1C	Y= -20.5
1D	Y= -25.0
1E	Y= 16.5
1F	Y= 19.5
1G	Y= 23.17
A	Y= 29.17
B	Y= 35.42
C	X= -28.95 Y= 39.428
D	X= -28.401 Y= 41.186
E	X= -22.149 Y= 43.552
F	X= -16.556 Y= 45.620
G	X= -10.966
H	X= -5.768
J	X= -1.17
K	X= 3.17
L	X= 6.966
M	X= 10.966
N	X= 16.593 Y= 45.405
P	X= 22.222 Y= 43.310
R	X= 27.552 Y= 41.610
S	X= 31.776 Y= 39.282
T	Y= 35.585
U	Y= 29.50
V	Y= 25.17
W	Y= 17.50
X	Y= 10.50
Y	X= 32.0 Y= 10.50

SCHEDULE II

A	X= -32.0 Y= -14.50
B	Y= -20.25
C	X= +32.0 Y= -22.5
D	X= +32.0 Y= -34.67
E	Y= -38.67
F	X= -22.810 Y= -45.065
G	X= +20.083 Y= -47.50
H	X= +15.083 Y= -47.50
J	X= +11.111
K	X= +7.139
L	X= +3.167
M	X= -1.17
N	X= -5.768
P	X= -10.966
R	X= -16.556 Y= -45.620
S	X= -22.149 Y= -43.552
T	X= -25.901 Y= -41.186
U	X= -28.950 Y= -39.428
V	Y= -33.34
W	Y= -29.0
X	X= +32.0 Y= -23.0
Y	Y= +20.50
Z	Y= -13.50

SAN ONOFRE NUCLEAR GENERATING STATION Units 2 & 3

CONTAINMENT INTERIOR (SAP MODEL) DEVELOPED SECONDARY SHIELD WALLS

Figure 3.7-20

1E079-11D-424
13JL6

Site File Copy

25318-B

NODE DESCRIPTION SCHEDULE

NODE NO.	BUILDING AREAS INCLUDED: RADWASTE	CONTROL	NORTH PENET.	SOUTH PENET.	REF. ELEVATION AT TOP OF SLAB	CONNECTING NODES: BELOW	ABOVE	HORIZONTAL COORDINATES: X (FT)	Y (FT)
1	●	●	●	●	9'-0"		2,3,4,5,6,10	0.0	-28.8
2	●				24'-0"	1	3,4,5,6	0.6	-65.1
3			●		30'-0"	1,2 PLUS 5 A	5 A, SAME EL.	104.8	-66.7
4				●	30'-0"	1,2 PLUS 5 A	5 A, SAME EL.	-108.8	-66.7
5		●	●	●	30'-0"	1,2,3,4 PLUS 5 A	6 A, SAME EL. 30'-0" EL.	0.0	57.5
6	●				37'-0"	1,2,3,4,5	7,8,9,10	-1.0	-74.6
7			●		45'-0"	3,5,6	9,10	126.0	-17.4
8				●	45'-0"	4,5,6	9,10	-126.0	-17.4
9	●	●			50'-0"	5,6,7,8	10,11	-0.5	-12.5
10	●		●	●	60'-6"	1,6,7,8,9	11,12,13,14	-2.1	-64.6
11		●			70'-0"	9,10	12	-2.5	61.9
12	●	●			85'-0"	10,11	13,14,	-4.5	-13.9
13			●		95'-0"	10,12		127.8	-17.0
14				●	95'-0"	10,12		-127.8	-17.0
9A*		●			50'-0"	5	11	0.0	59.2
10A*		●			85'-0"	11		0.0	59.2

* DENOTES NODAL POINTS USED ONLY FOR VERTICAL RESPONSE IN CONTROL AREA.

● DENOTES AREA OF BUILDING ASSOCIATED WITH RESPONSE OF EACH NODE.

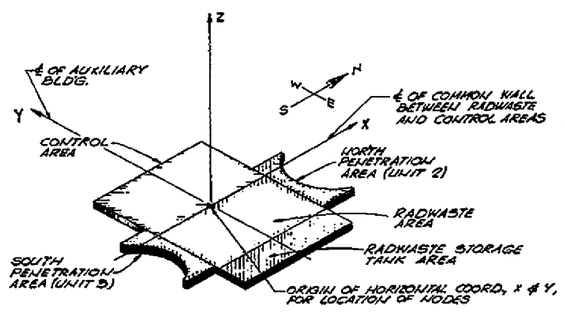

AUXILIARY BUILDING FLOOR SLAB OUTLINE

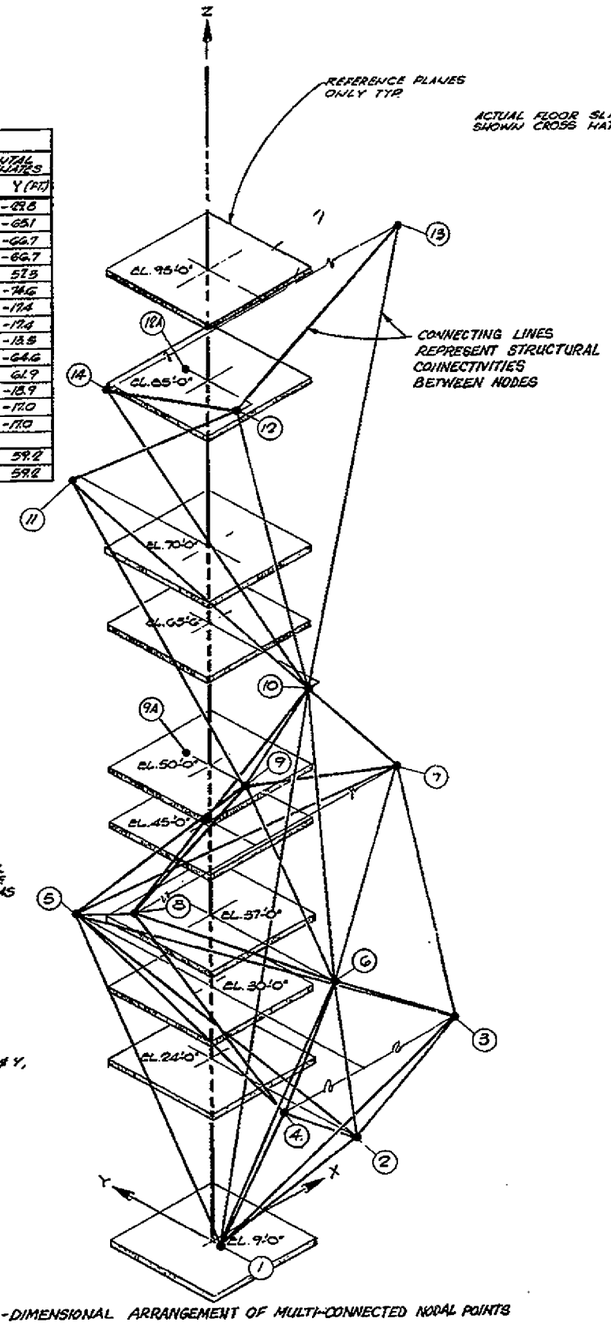

THREE-DIMENSIONAL ARRANGEMENT OF MULTI-CONNECTED NODAL POINTS

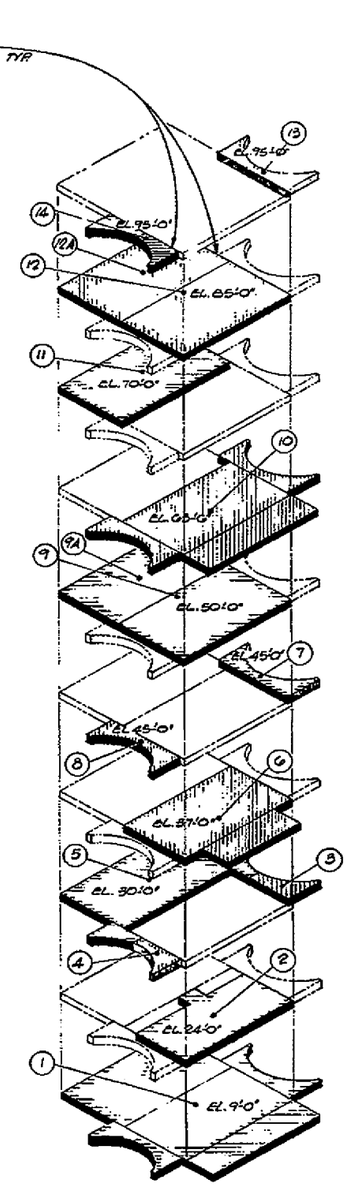

LUMPED MASSES (NODAL POINTS @ C.G. OF MASSES)

LUMPED PARAMETER GEOMETRICALLY COUPLED MATHEMATICAL MODEL

10079-11D-269

SAN ONOFRE NUCLEAR GENERATING STATION Units 2 & 3

AUXILIARY BUILDING MATHEMATICAL MODEL FOR DYNAMIC ANALYSES

Figure 3.7-21

Site File Copy

25305-B

NODE DESCRIPTION SCHEDULE					
NODE NO.	REF. ELEV. AT TOP OF SLAB	CONNECTING NODES		HORIZONTAL COORDINATES	
		BELOW	ABOVE	X FT	Y FT
1	17'-6"	—	2	-3.03	-0.47
2	30'-0"	1	3,4	-0.93	-9.23
3	45'-0"	2	4	-17.58	-4.63
4	63'-6"	2,3	5	-6.16	-8.66
5	95'-0"	4	6	-7.45	-6.01
6	114'-0"	5	—	-8.20	-8.42
7,8,9		3	4		

NOTE:
NODES 7,8 AND 9 REPRESENT THE OSCILLATING WATER MASSES IN THE POOLS.

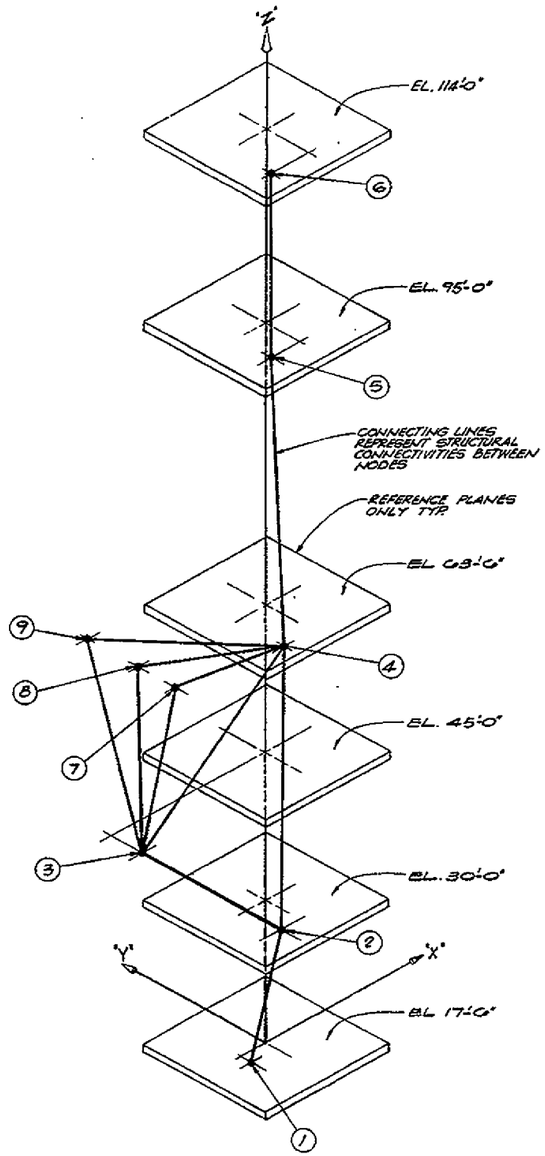

THREE-DIMENSIONAL ARRANGEMENT OF MULTI-CONNECTED NODAL POINTS

LUMPED PARAMETER GEOMETRICALLY COUPLED MATHEMATICAL MODEL

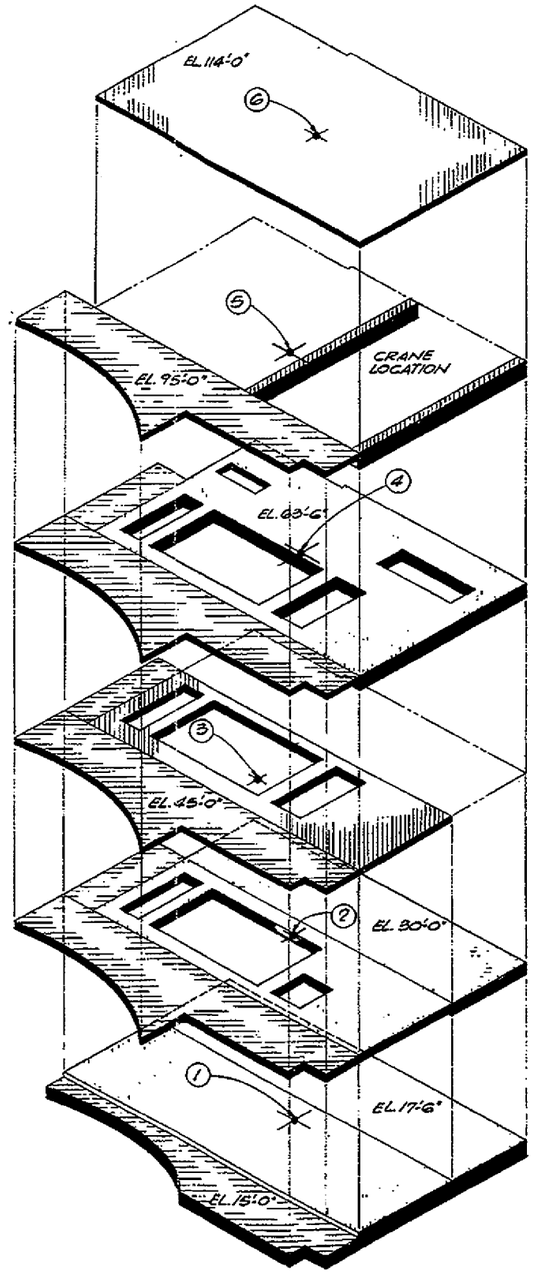

LUMPED MASSES
(NODAL POINTS & C.G. OF MASSES)

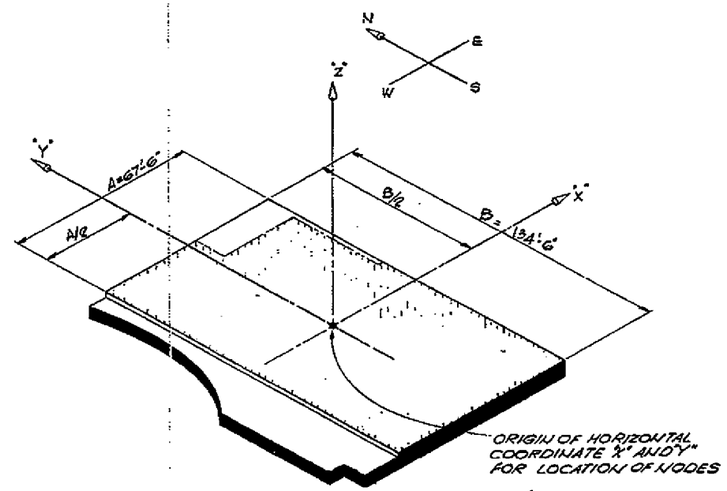

FUEL HANDLING BUILDING FLOOR SLAB OUTLINE

SAN ONOFRE NUCLEAR GENERATING STATION Units 2 & 3

FUEL HANDLING BUILDING MATHEMATICAL MODEL FOR DYNAMIC ANALYSIS

Figure 3.7-22

Site File Copy

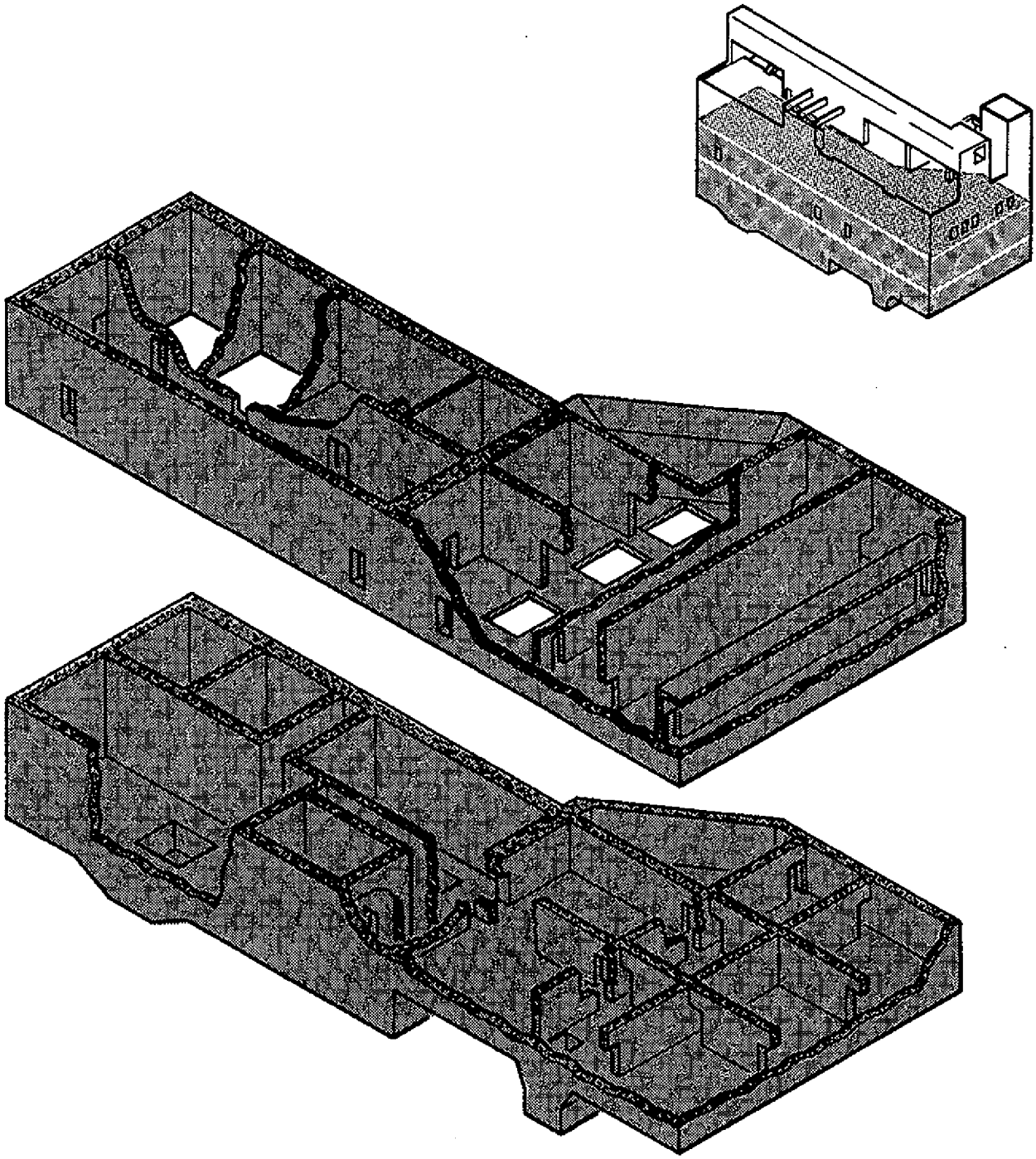

PICTORIAL REPRESENTATION OF THE THREE DIMENSIONAL FINITE ELEMENT MATHEMATICAL MODEL

SAN ONOFRE NUCLEAR GENERATING STATION Units 2 & 3
SAFETY EQUIPMENT BUILDING MATHEMATICAL MODEL FOR STATIC AND DYNAMIC ANALYSES (Sheet 1 of 2)
Figure 3.7-23

10079-11D-251
13JL6

Site File Copy

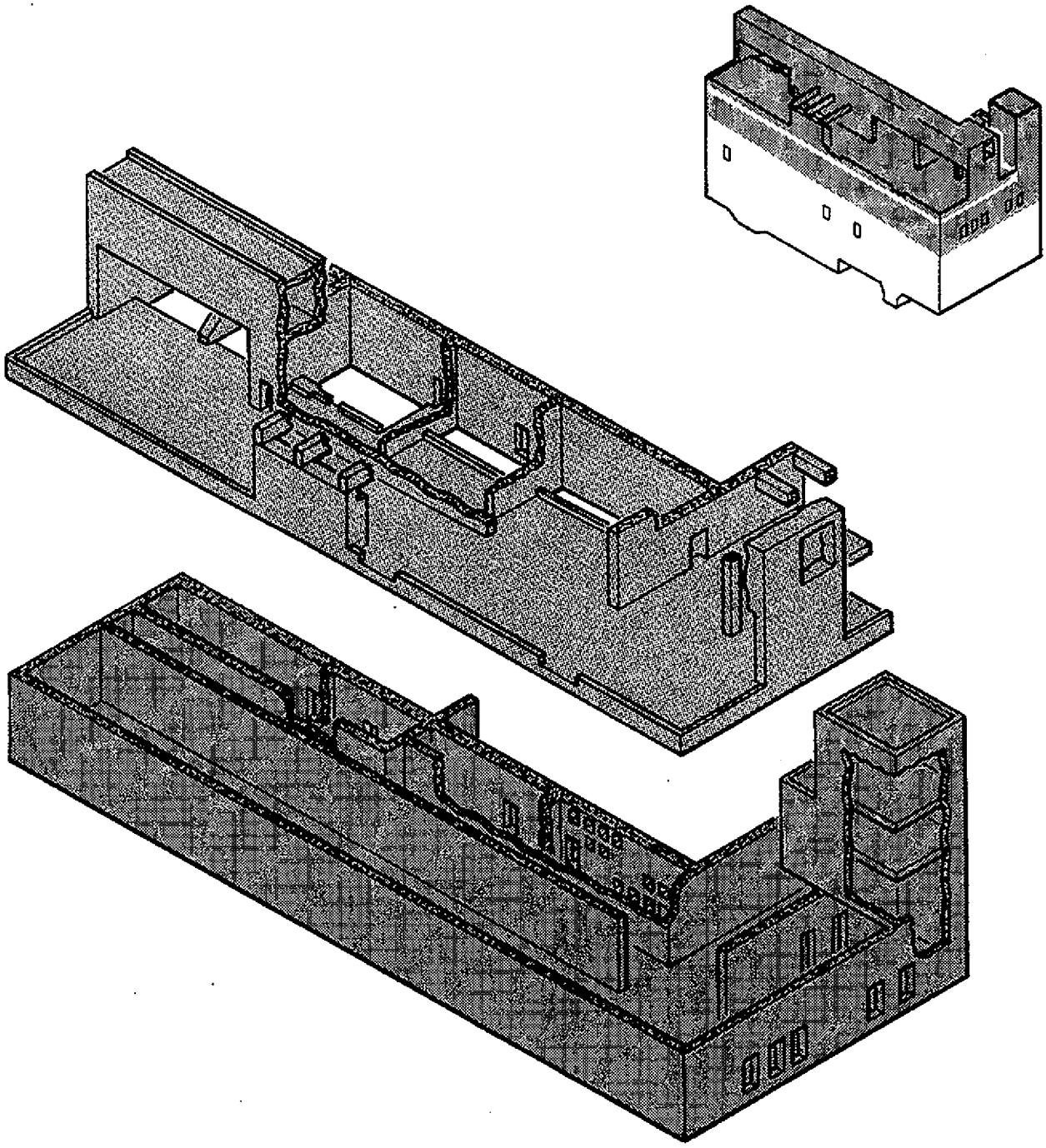

PICTORIAL REPRESENTATION OF THE THREE DIMENSIONAL FINITE ELEMENT MATHEMATICAL MODEL

SAN ONOFRE NUCLEAR GENERATING STATION Units 2 & 3
SAFETY EQUIPMENT BUILDING MATHEMATICAL MODEL FOR STATIC AND DYNAMIC ANALYSES (Sheet 2 of 2)
Figure 3.7-23

10079-11D-252
13JL6

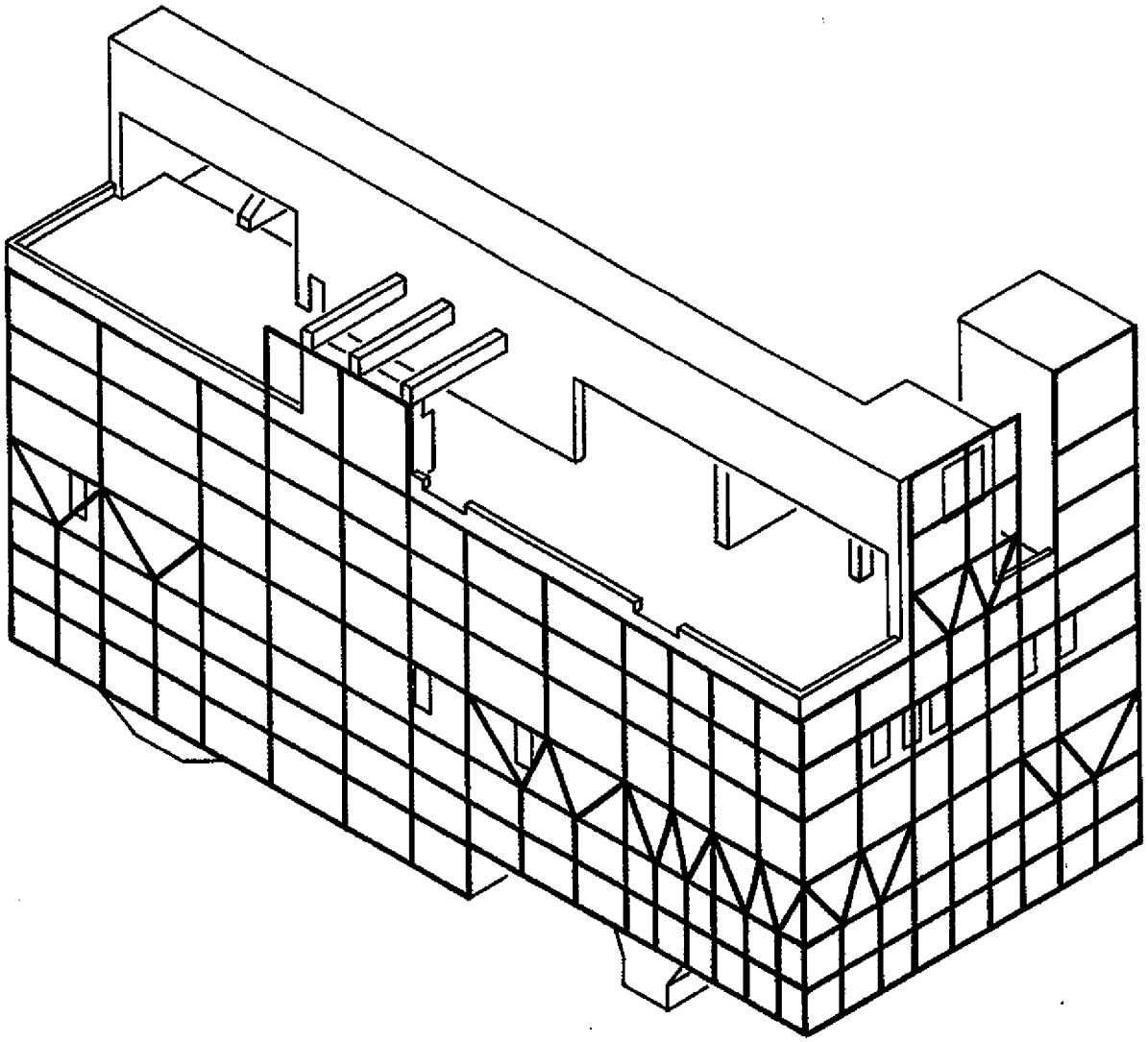

SAN ONOFRE NUCLEAR GENERATING STATION Units 2 & 3
SAFETY EQUIPMENT BUILDING TYPICAL MESH SIZE REPRESENTATION
Figure 3.7-24

10079-11D-425
13JL6

Site File Copy

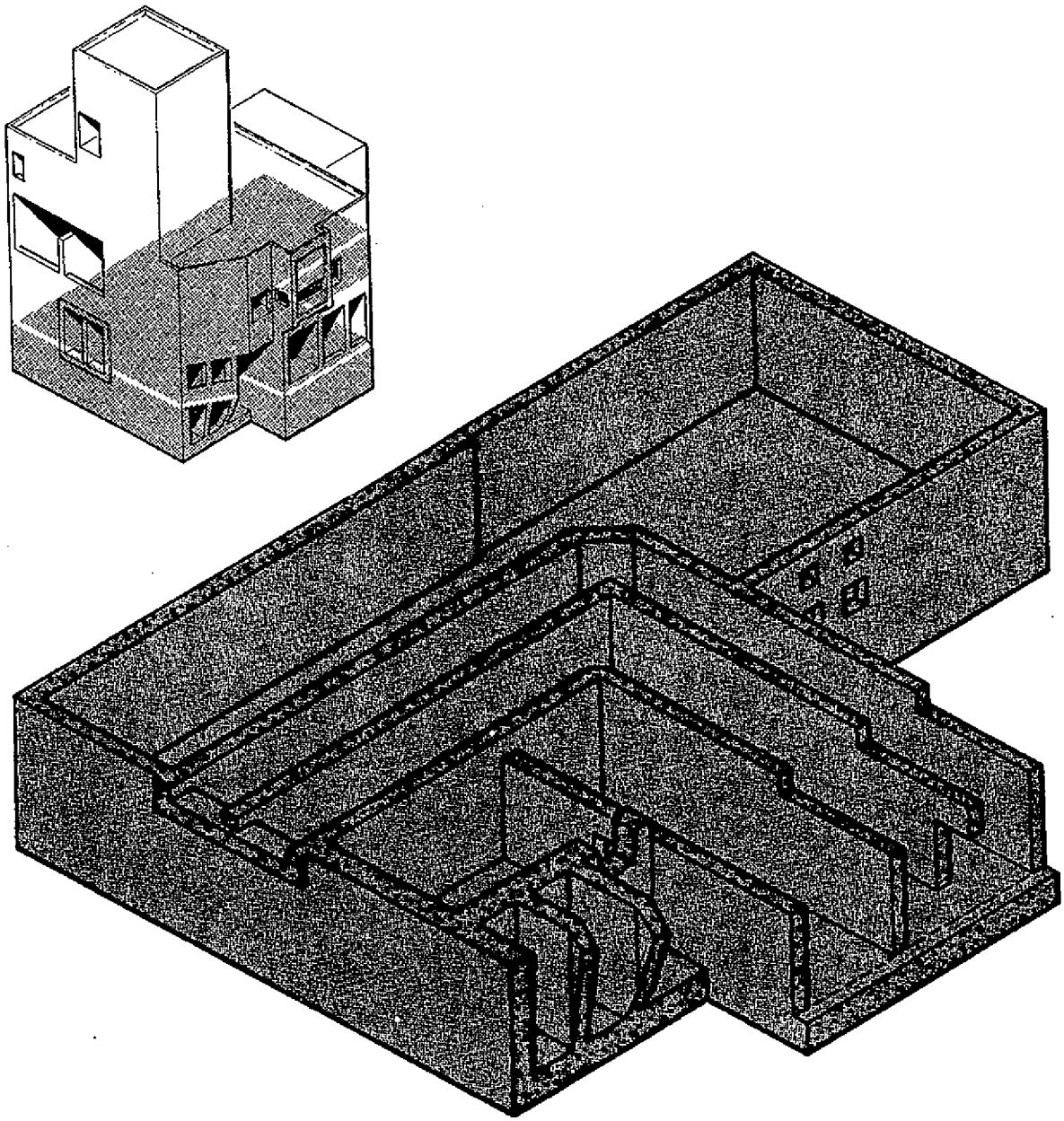

PICTORIAL REPRESENTATION OF THE THREE DIMENSIONAL FINITE ELEMENT MATHEMATICAL MODEL

SAN ONOFRE NUCLEAR GENERATING STATION Units 2 & 3
ELECTRICAL AND PIPING GALLERY STRUCTURE MATHEMATICAL MODEL FOR STATIC AND DYNAMIC ANALYSES (Sheet 1 of 4)
Figure 3.7-25

10079-11D-255
13JL6

Site File Copy

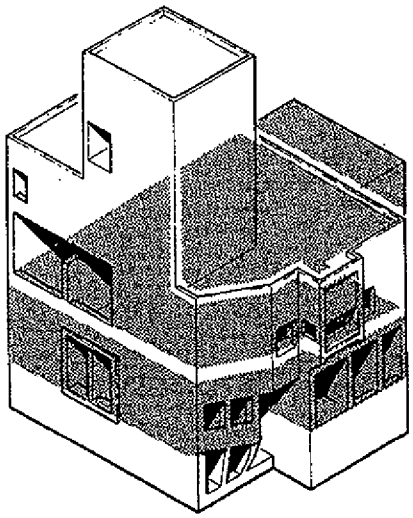

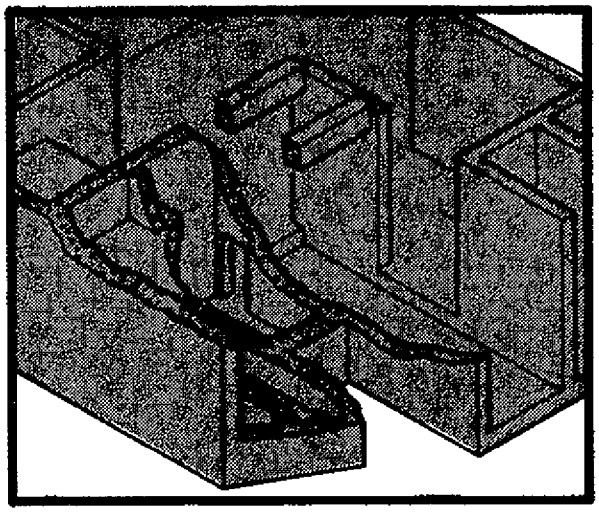

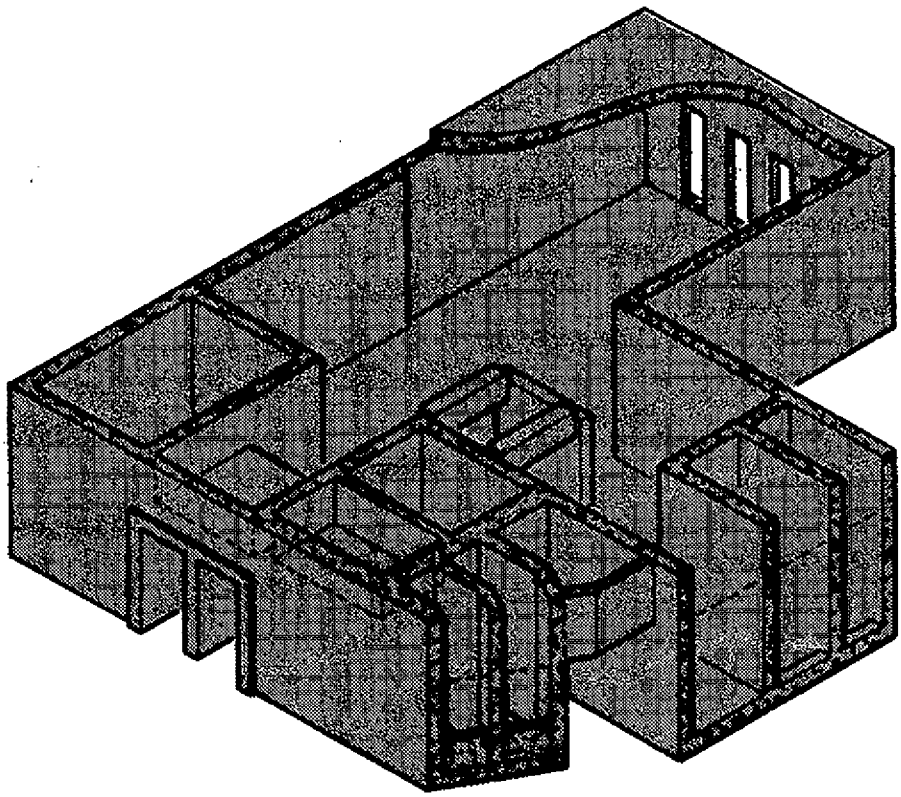

PICTORIAL REPRESENTATION OF THE THREE DIMENSIONAL FINITE ELEMENT MATHEMATICAL MODEL

SAN ONOFRE NUCLEAR GENERATING STATION Units 2 & 3
ELECTRICAL AND PIPING GALLERY STRUCTURE MATHEMATICAL MODEL FOR STATIC AND DYNAMIC ANALYSES (Sheet 2 of 4)
Figure 3.7-25

10079-11D-256
13JL6

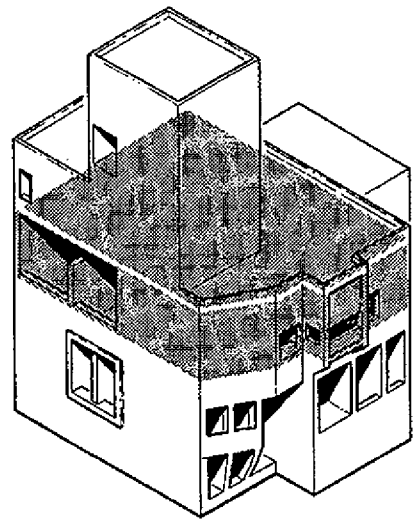

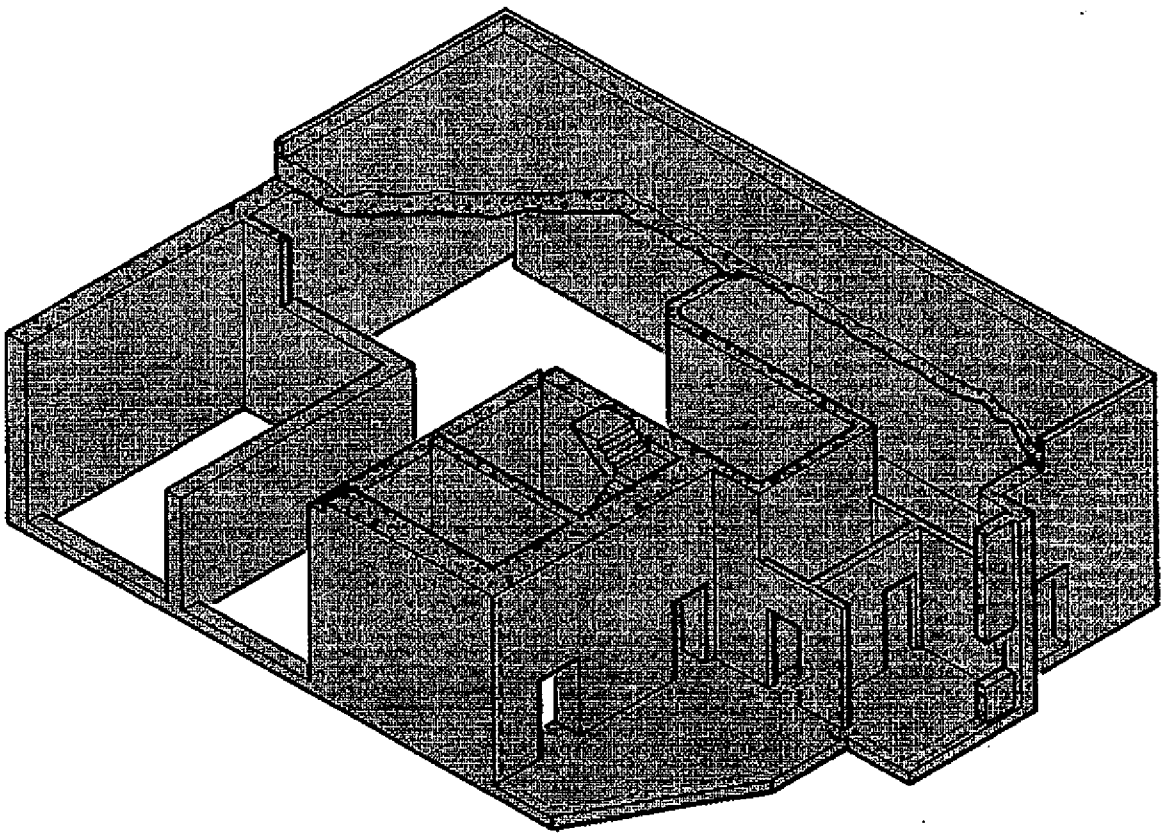

PICTORIAL REPRESENTATION OF THE THREE DIMENSIONAL FINITE ELEMENT MATHEMATICAL MODEL

SAN ONOFRE NUCLEAR GENERATING STATION Units 2 & 3
ELECTRICAL AND PIPING GALLERY STRUCTURE MATHEMATICAL MODEL FOR STATIC AND DYNAMIC ANALYSES (Sheet 3 of 4)
Figure 3.7-25

10079-11D-257
13JL6

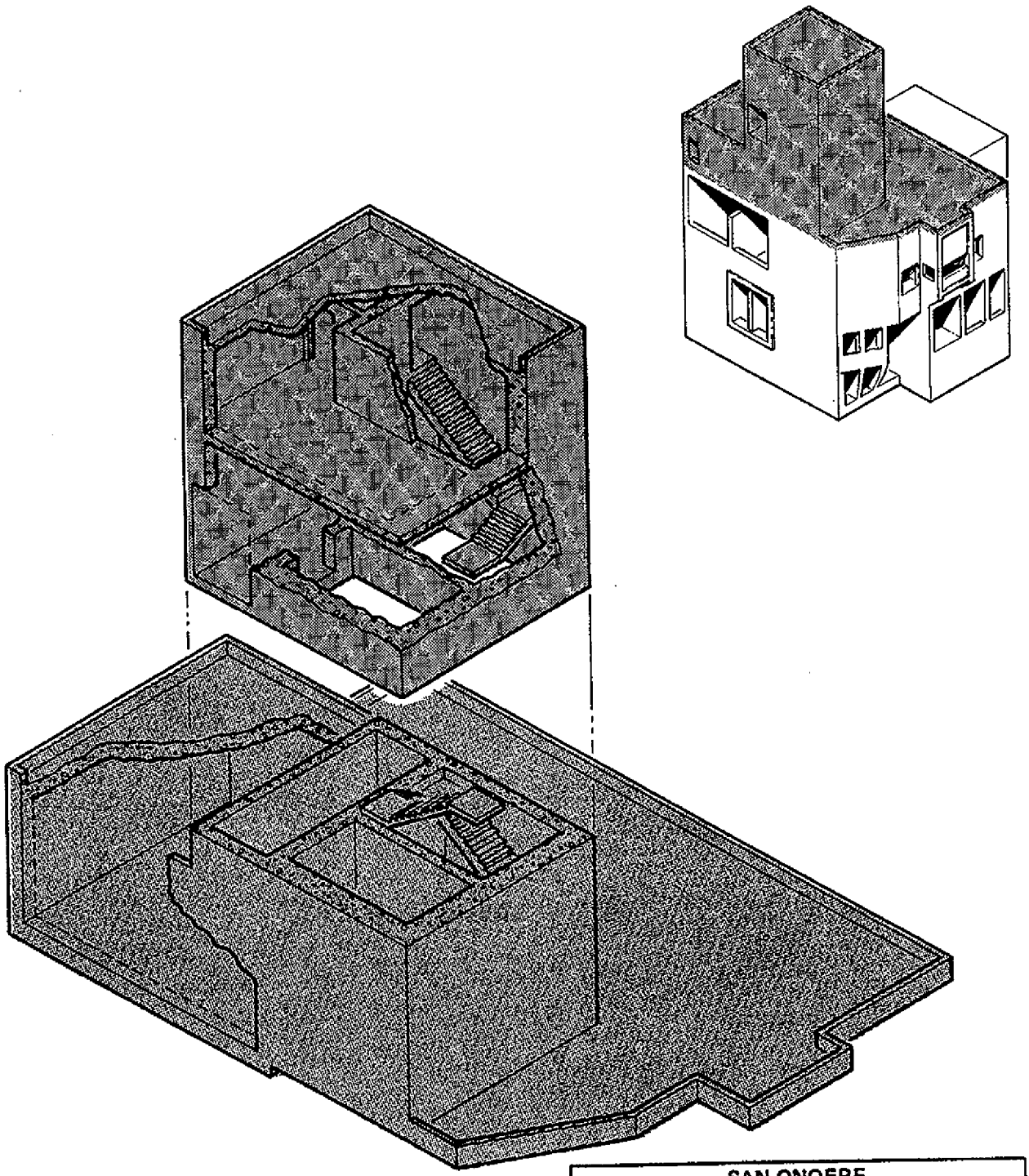

PICTORIAL REPRESENTATION OF THE THREE DIMENSIONAL FINITE ELEMENT MATHEMATICAL MODEL

SAN ONOFRE NUCLEAR GENERATING STATION Units 2 & 3
ELECTRICAL AND PIPING GALLERY STRUCTURE MATHEMATICAL MODEL FOR STATIC AND DYNAMIC ANALYSES (Sheet 4 of 4)
Figure 3.7-25

10079-11D-258
13JL6

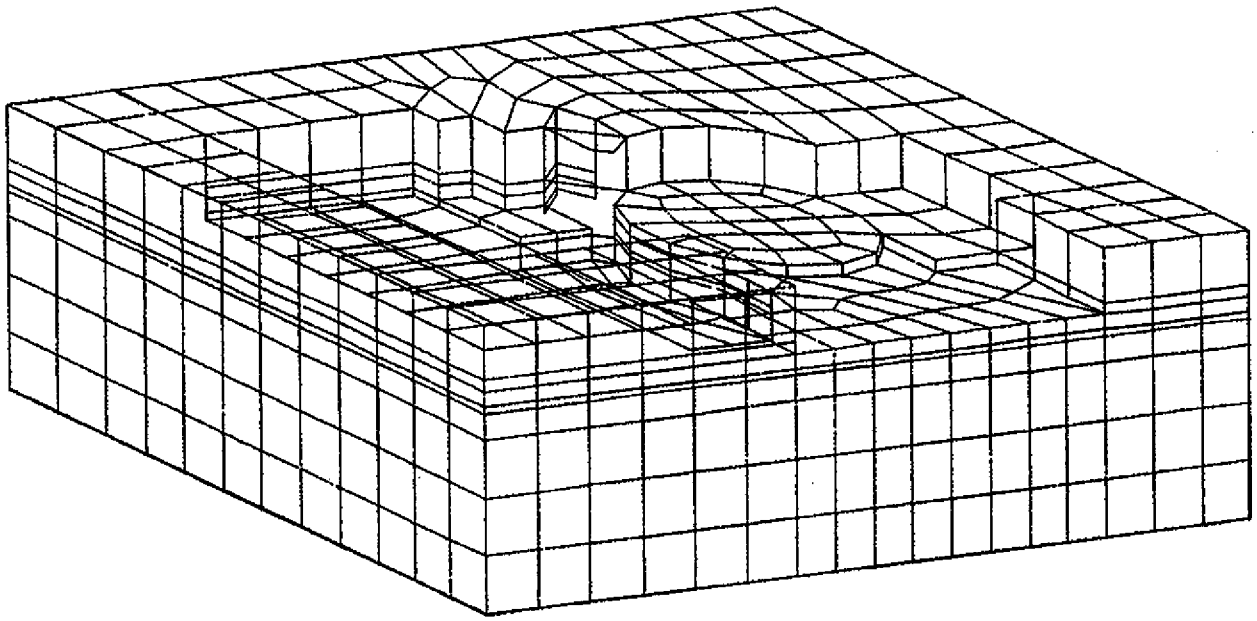

SAN ONOFRE NUCLEAR GENERATING STATION Units 2 & 3
SAP ANTISYMMETRIC MODEL OF SAN ONOFRE 2 AND 3 POWER BLOCK
Figure 3.7-26

10079-11D-426
13JL6

Site File Copy

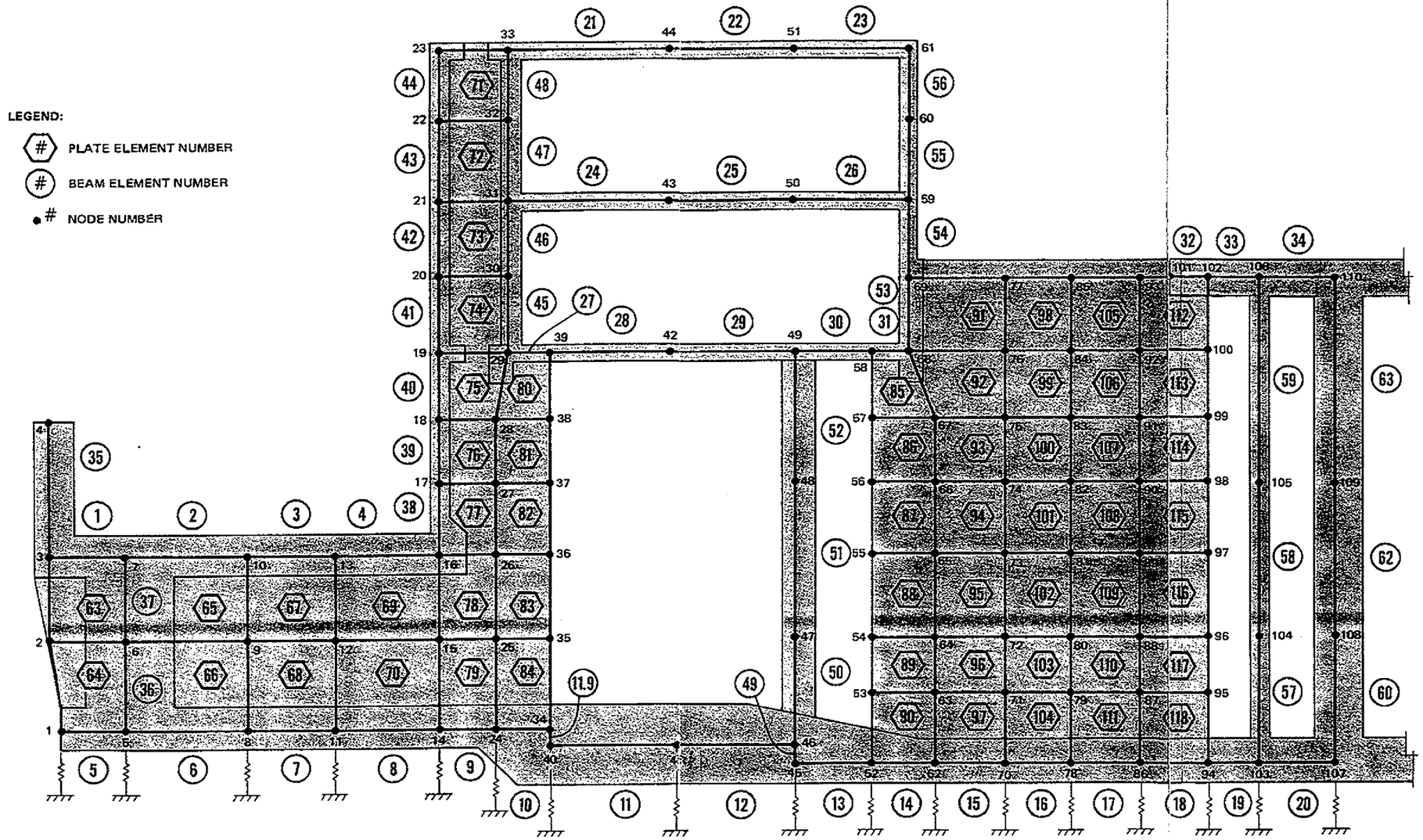

TWO DIMENSIONAL FINITE ELEMENT MATHEMATICAL MODEL OF TYPICAL TRANSVERSE SECTION THROUGH THE SCREEN WELL AREA AND RECIRCULATING WATER PUMP DECK

SAN ONOFRE NUCLEAR GENERATING STATION Units 2 & 3
INTAKE STRUCTURE MATHEMATICAL MODEL FOR EQUIVALENT STATIC LOAD ANALYSIS (Sheet 1 of 3)
Figure 3.7-27

10079-11D-270
13JL6

Amended: April 2009 TL: E047997

Site File Copy

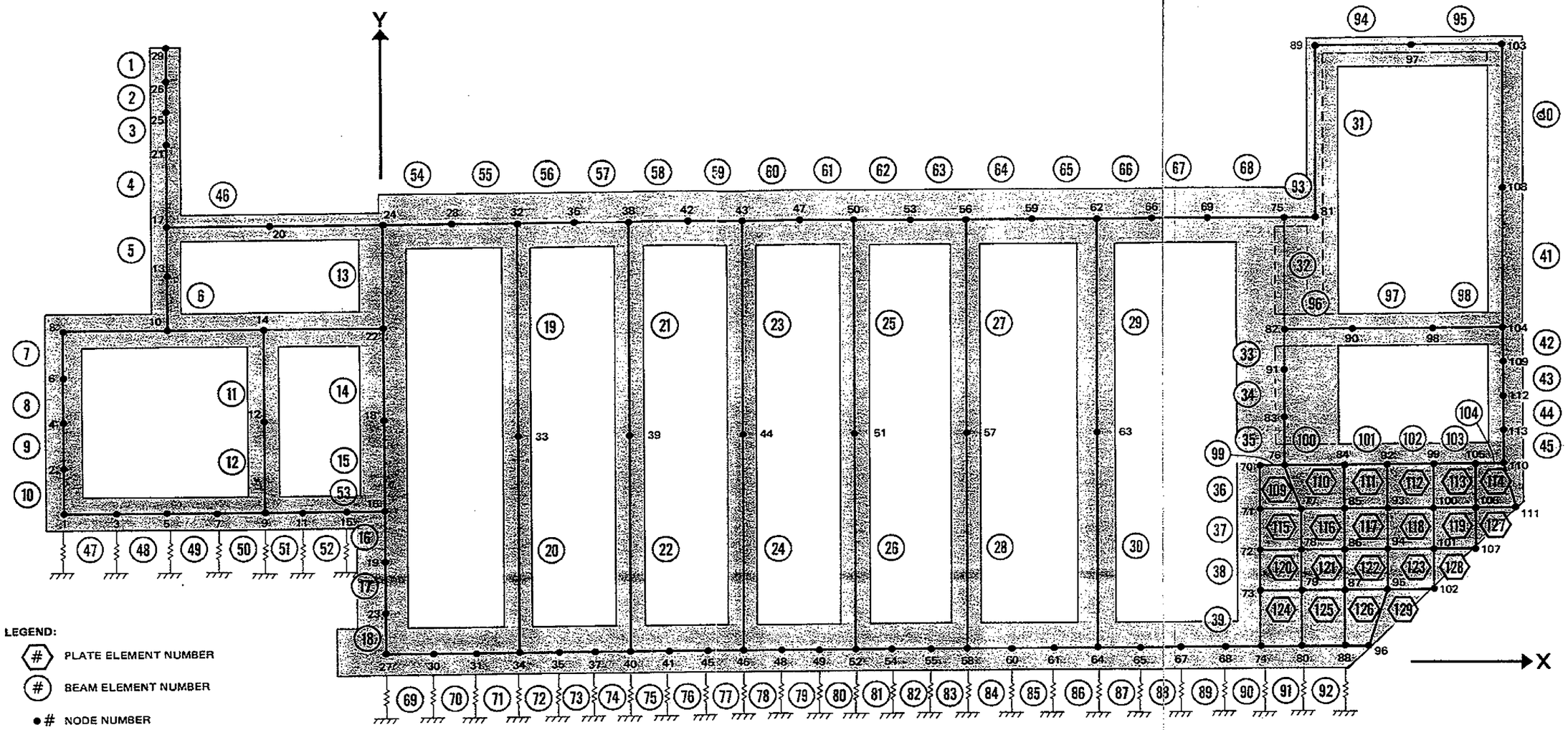

LEGEND:

(#) PLATE ELEMENT NUMBER

(#) BEAM ELEMENT NUMBER

●# NODE NUMBER

NOTE:

SOIL SPRINGS AT HAUNCH SUPPORT OMITTED FOR CLARITY.

TWO DIMENSIONAL FINITE ELEMENT MATHEMATICAL MODEL OF TYPICAL LONGITUDINAL SECTION THROUGH THE SALT WATER COOLING TUNNEL, THE SCREEN WELL AREA, AND PORTIONS OF THE RECIRCULATION SYSTEM

SAN ONOFRE
NUCLEAR GENERATING STATION
Units 2 & 3

INTAKE STRUCTURE
MATHEMATICAL MODEL FOR
EQUIVALENT STATIC LOAD ANALYSIS
(Sheet 2 of 3)

Figure 3.7-27

10079-11D-271

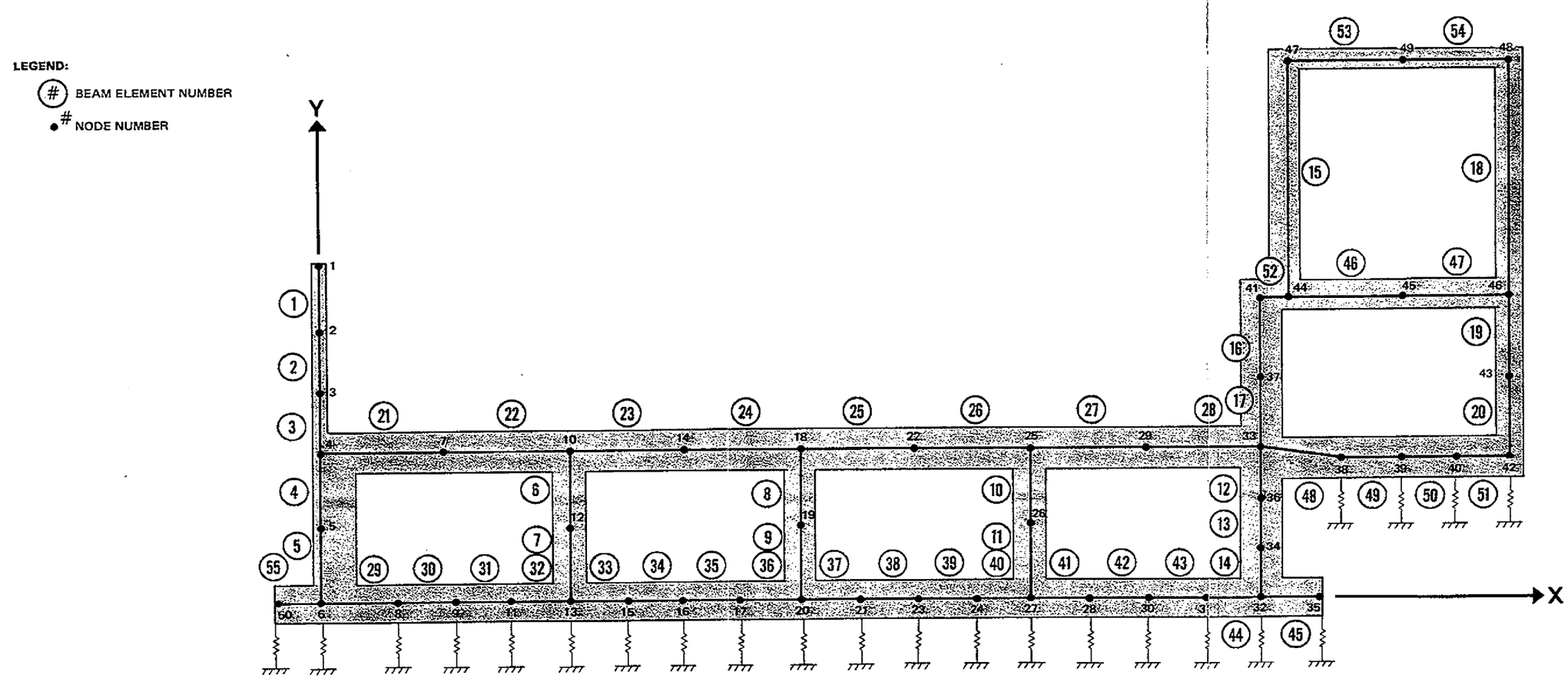

TWO DIMENSIONAL FINITE ELEMENT MATHEMATICAL MODEL OF TYPICAL LONGITUDINAL SECTION THROUGH THE SALT WATER COOLING TUNNEL AND RECIRCULATING WATER PUMP DECK

SAN ONOFRE NUCLEAR GENERATING STATION
Units 2 & 3

INTAKE STRUCTURE
MATHEMATICAL MODEL FOR
EQUIVALENT STATIC LOAD ANALYSIS
(Sheet 3 of 3)

Figure 3.7-27

10079-11D-272
13JL6

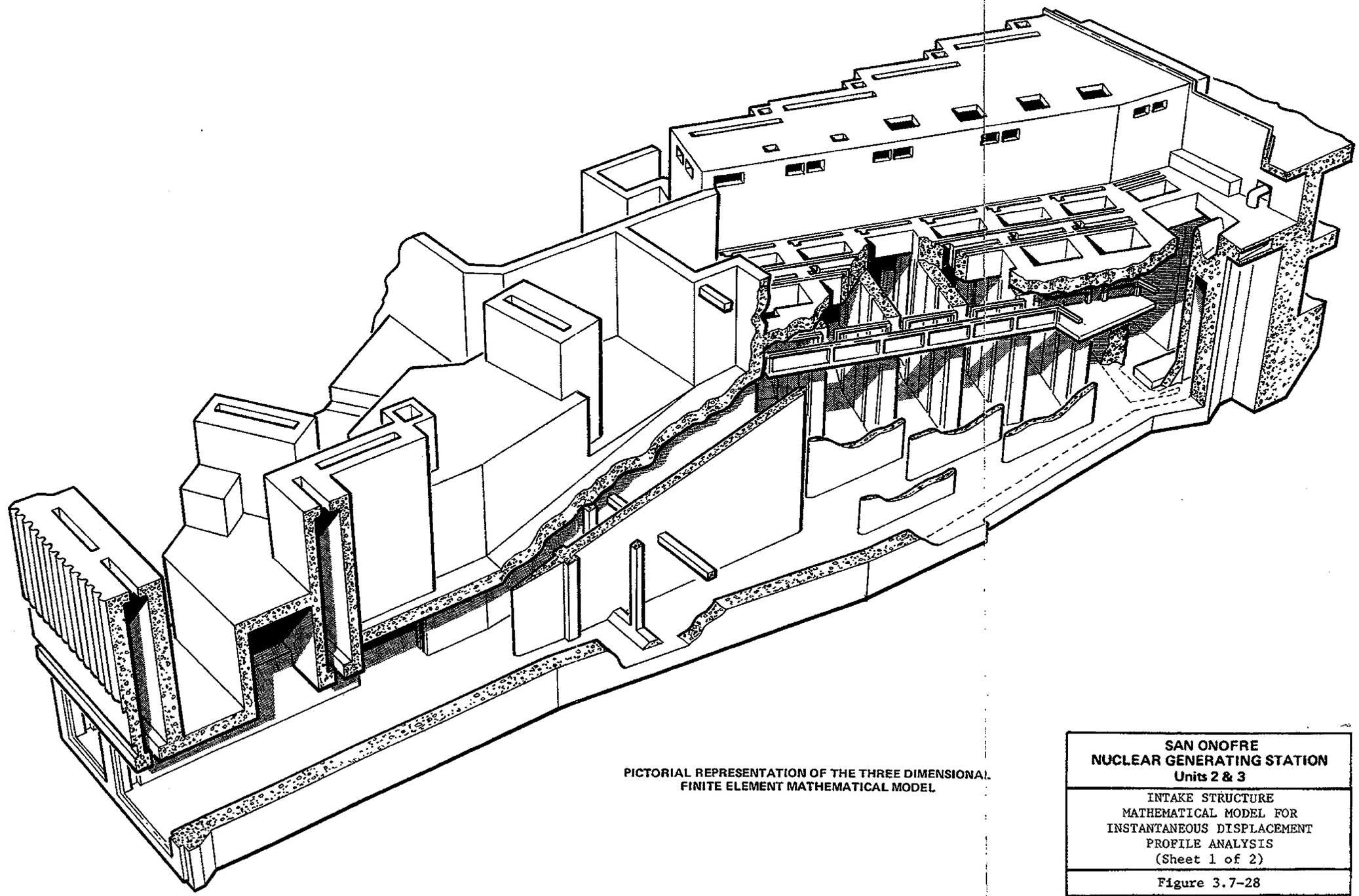

PICTORIAL REPRESENTATION OF THE THREE DIMENSIONAL
FINITE ELEMENT MATHEMATICAL MODEL

10079-11D-253
13JL6

SAN ONOFRE NUCLEAR GENERATING STATION Units 2 & 3
INTAKE STRUCTURE MATHEMATICAL MODEL FOR INSTANTANEOUS DISPLACEMENT PROFILE ANALYSIS (Sheet 1 of 2)
Figure 3.7-28

Site File Copy

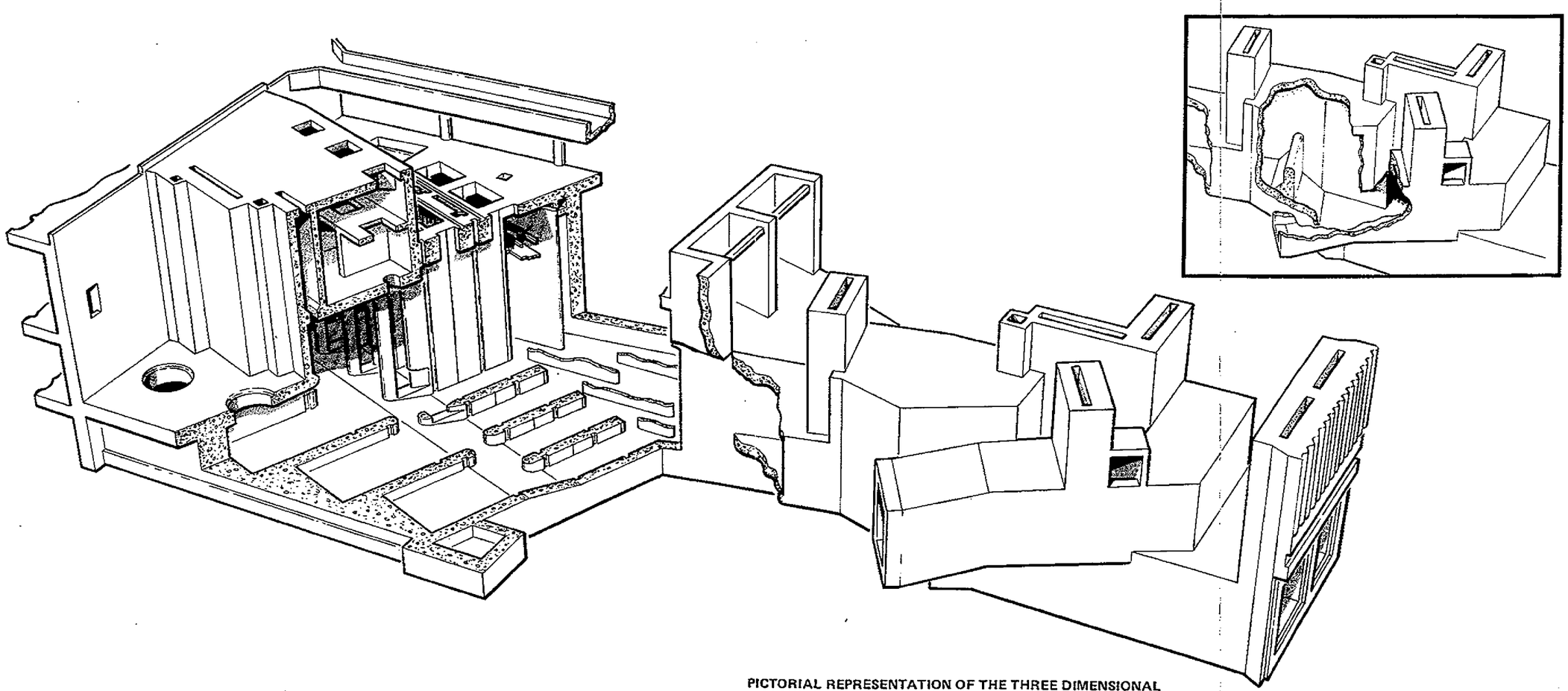

PICTORIAL REPRESENTATION OF THE THREE DIMENSIONAL
FINITE ELEMENT MATHEMATICAL MODEL

SAN ONOFRE NUCLEAR GENERATING STATION Units 2 & 3
INTAKE STRUCTURE MATHEMATICAL MODEL FOR INSTANTANEOUS DISPLACEMENT PROFILE ANALYSIS (Sheet 2 of 2)
Figure 3.7-28

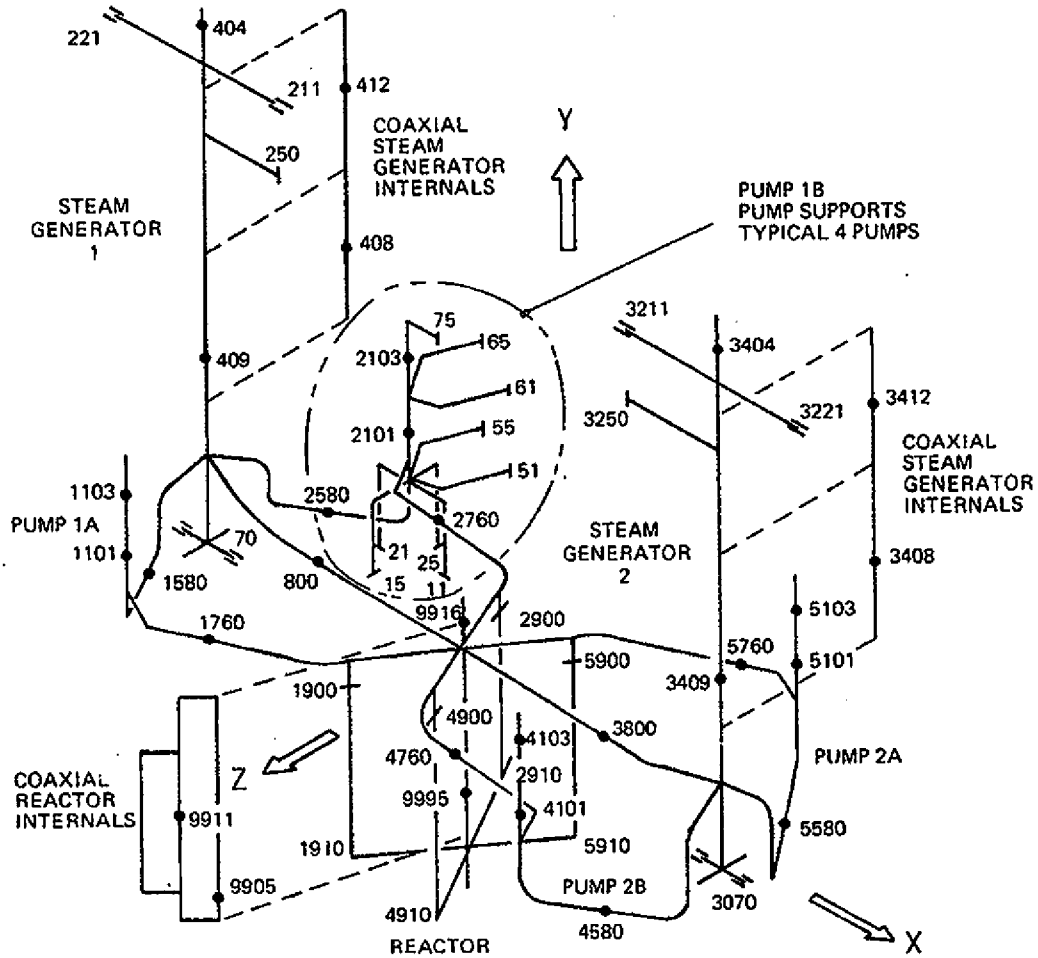

COMPONENT NAME	MASS POINT NUMBER	DEGREES OF FREEDOM
REACTOR	9916, 9911, 9905 9995	X, Y, Z X, Z
STEAM GENERATORS	404, 3404, 412, 3412 409, 3409 408, 3408	X, Y, Z X, Z X, Z
PUMPS	1103, 2103, 4103, 5103 1101, 2101, 4101, 5101	X, Y, Z X, Z
REACTOR COOLANT PIPING	800, 3800 1760, 2760, 4760, 5760 1580, 2580, 4580, 5580	Y, Z X, Y, Z X, Y, Z

COMPONENT NAME	SUPPORT POINT NUMBER	RESTRAINT
REACTOR	1900, 2900, 4900, 5900 1910, 2910, 4910, 5910	FX, FZ FIXED
STEAM GENERATORS	70, 3070 250, 3250 211, 221 3211, 3221	FY, FZ FX FZ FZ
REACTOR COOLANT PUMPS (TYPICAL)	11, 15, 21, 25 51, 55, 61, 65 75	FY FX, FZ FX, FZ

● MASS NODE

SLIDING T (ALLOWS X DIRECTION MOVEMENT ONLY)

SAN ONOFRE
NUCLEAR GENERATING STATION
Units 2 & 3

TYPICAL REACTOR COOLANT SYSTEM
SEISMIC ANALYSIS MODEL

Figure 3.7-29

10079-11D-360
13JL6

Site File Copy

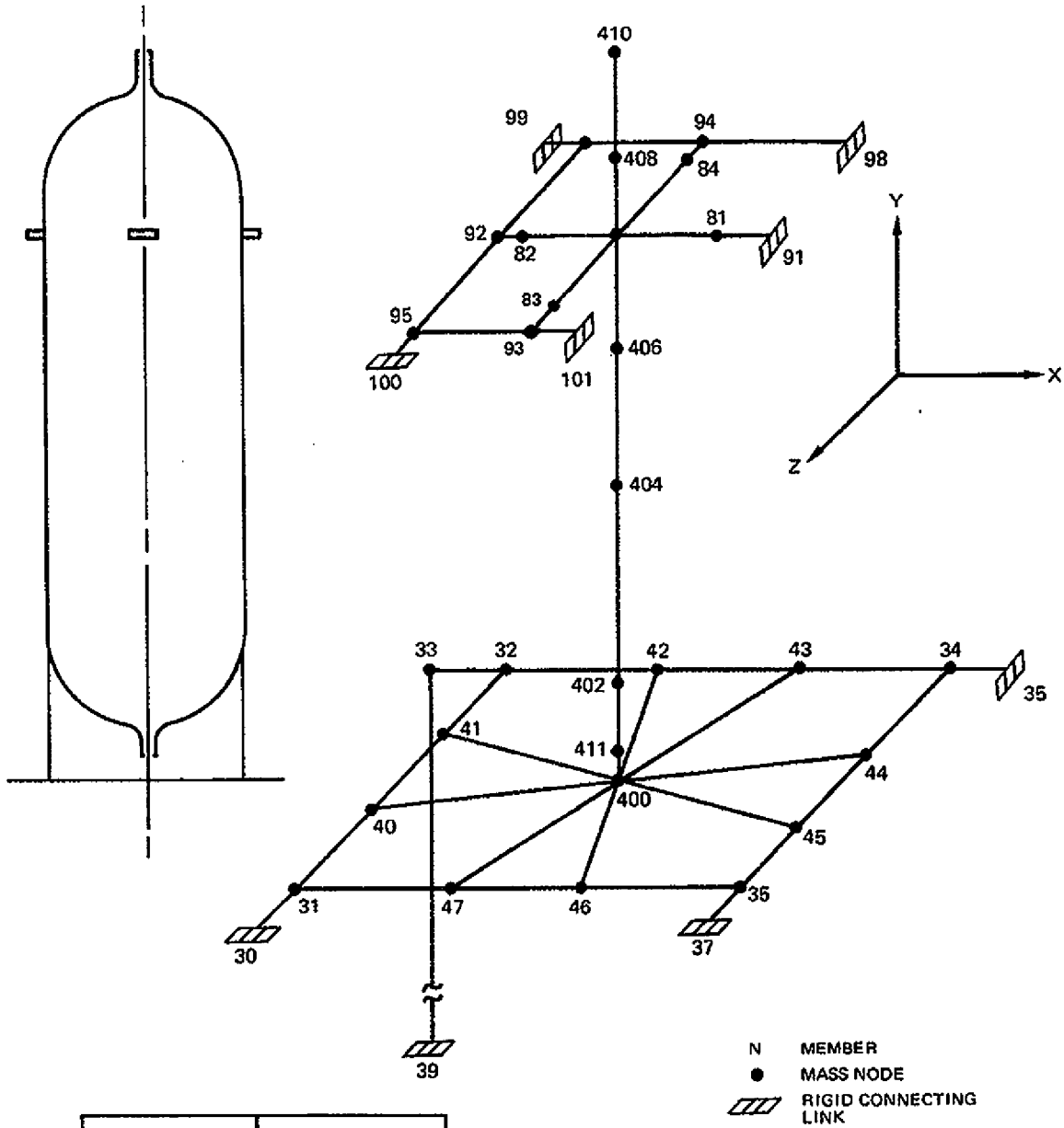

MASS POINT NUMBER	DEGREES OF FREEDOM
402, 404, 406 408	X, Z X, Y, Z

SUPPORT POINT NUMBER	RESTRAINT
81, 82 83, 84 400	Z X FIXED

SAN ONOFRE NUCLEAR GENERATING STATION Units 2 & 3

PRESSURIZER SEISMIC ANALYSIS MODEL

Figure 3.7-30

10079-11D-361
13JL6

Site File Copy

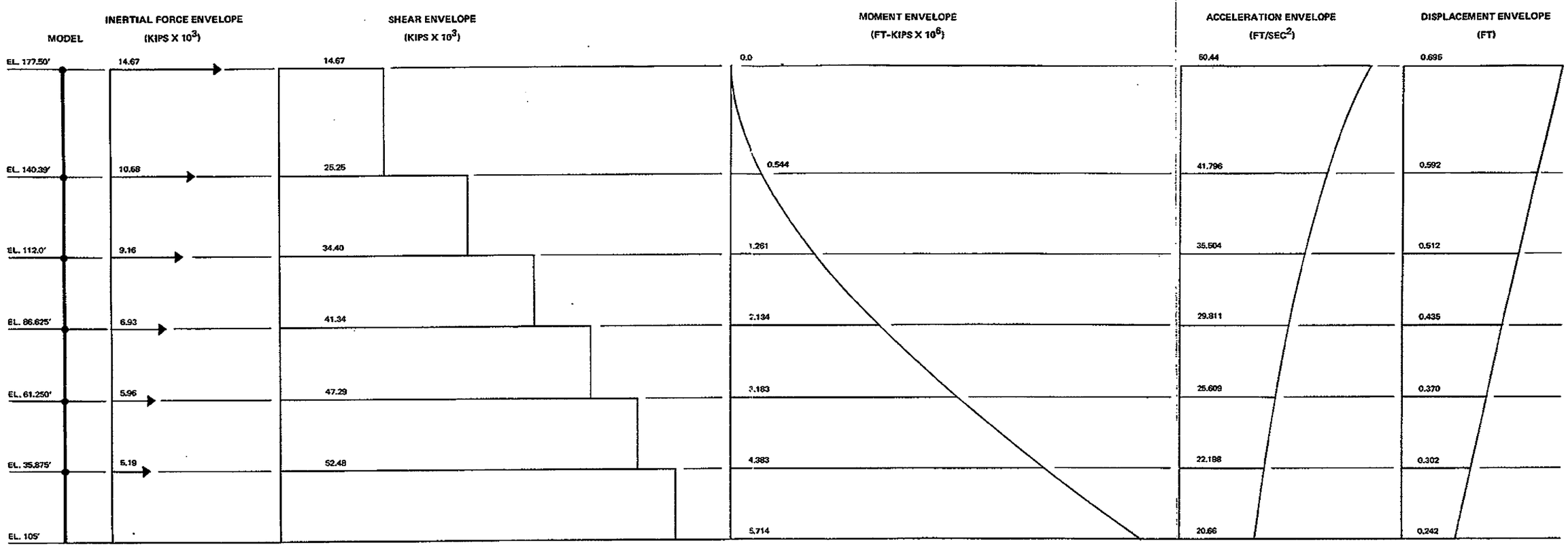

SAN ONOFRE NUCLEAR GENERATING STATION Units 2 & 3
CONTAINMENT SHELL SELECTED TOTAL RESPONSE FROM DBE ANALYSIS
Figure 3.7-31

Site File Copy

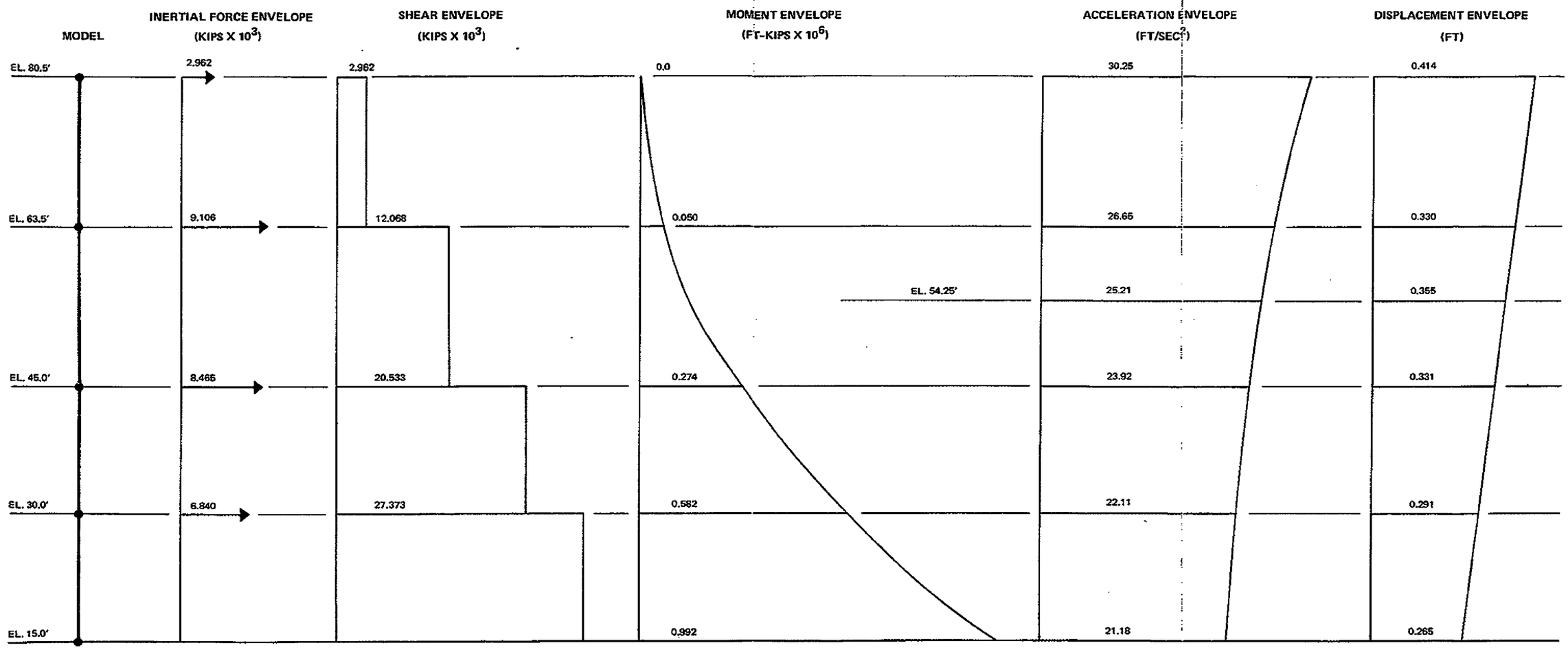

SAN ONOFRE NUCLEAR GENERATING STATION Units 2 & 3
CONTAINMENT INTERNAL STRUCTURE SELECTED TOTAL RESPONSE FROM DBE ANALYSIS
Figure 3.7-32

Site File Copy

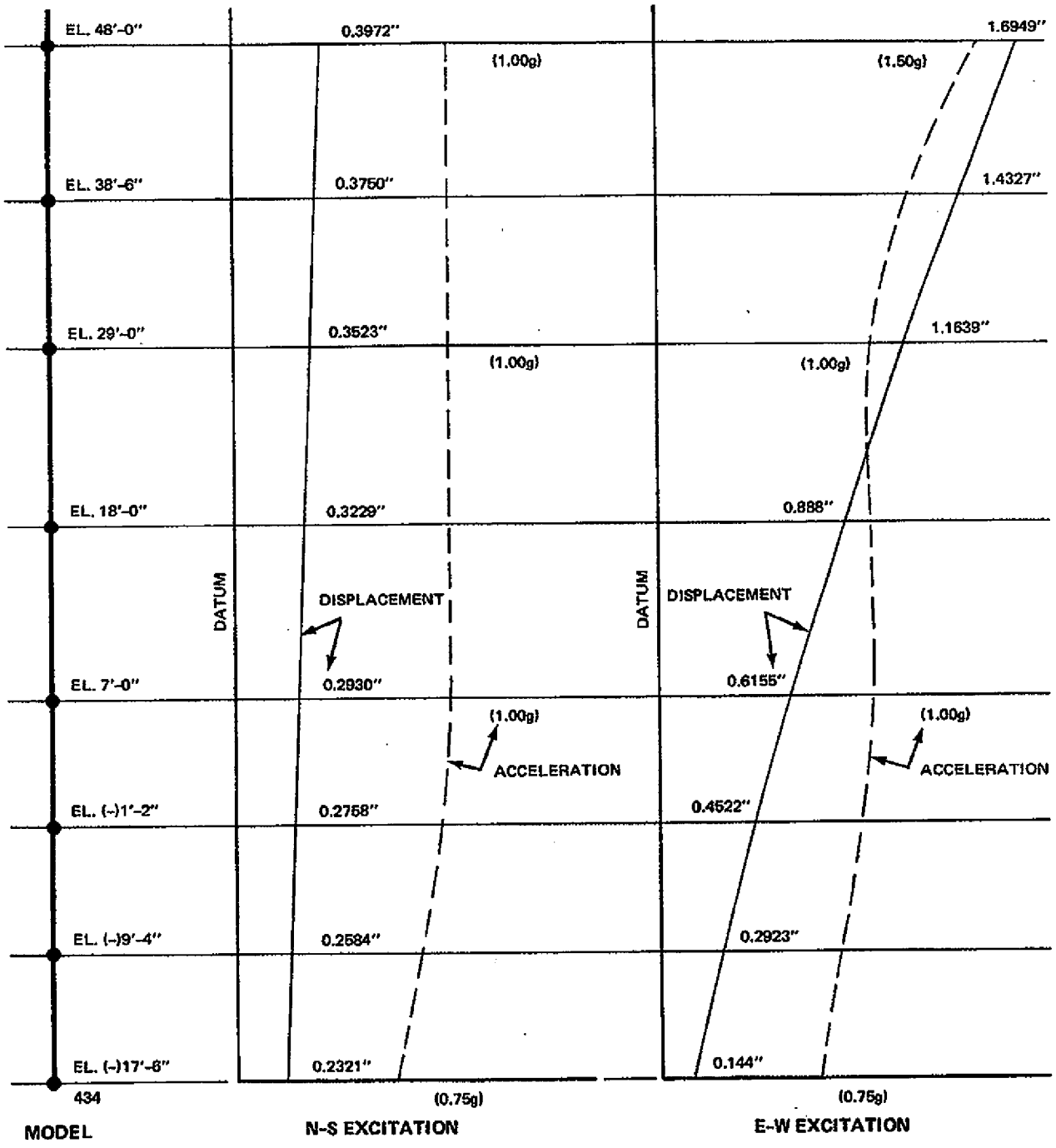

REPRESENTATIVE DISPLACEMENT AND ACCELERATION RESPONSE

SAN ONOFRE NUCLEAR GENERATING STATION Units 2 & 3
SAFETY EQUIPMENT BUILDING SELECTED TOTAL RESPONSE FROM DBE ANALYSIS
Figure 3.7-33

10079-11D-358
13JL6

Site File Copy

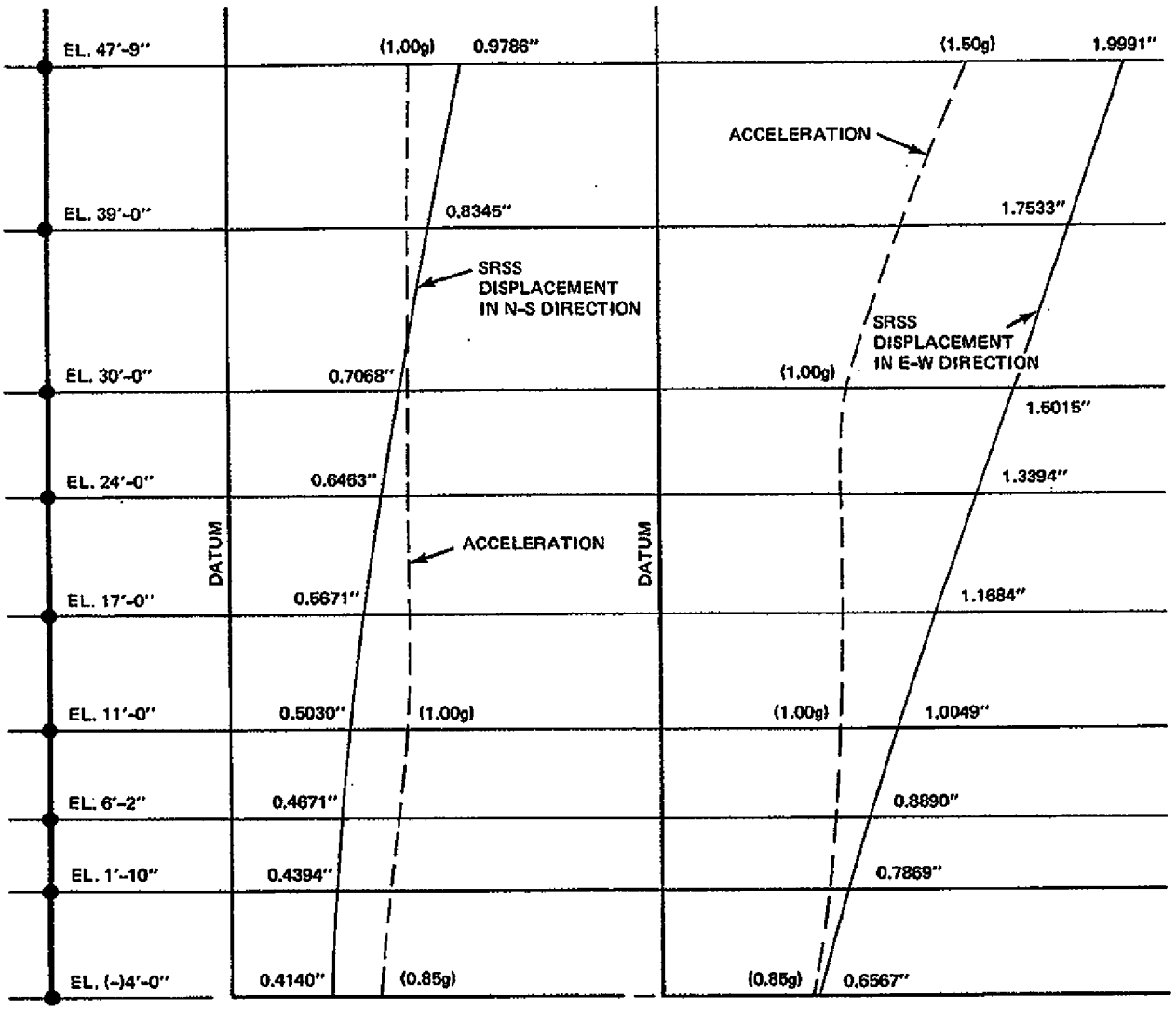

REPRESENTATIVE DISPLACEMENT AND ACCELERATION RESPONSE

SAN ONOFRE NUCLEAR GENERATING STATION Units 2 & 3
ELECTRICAL AND PIPING GALLERY STRUCTURE SELECTED TOTAL RESPONSE FROM DBE ANALYSIS
Figure 3.7-34

10079-11D-359
13JL6

Site File Copy

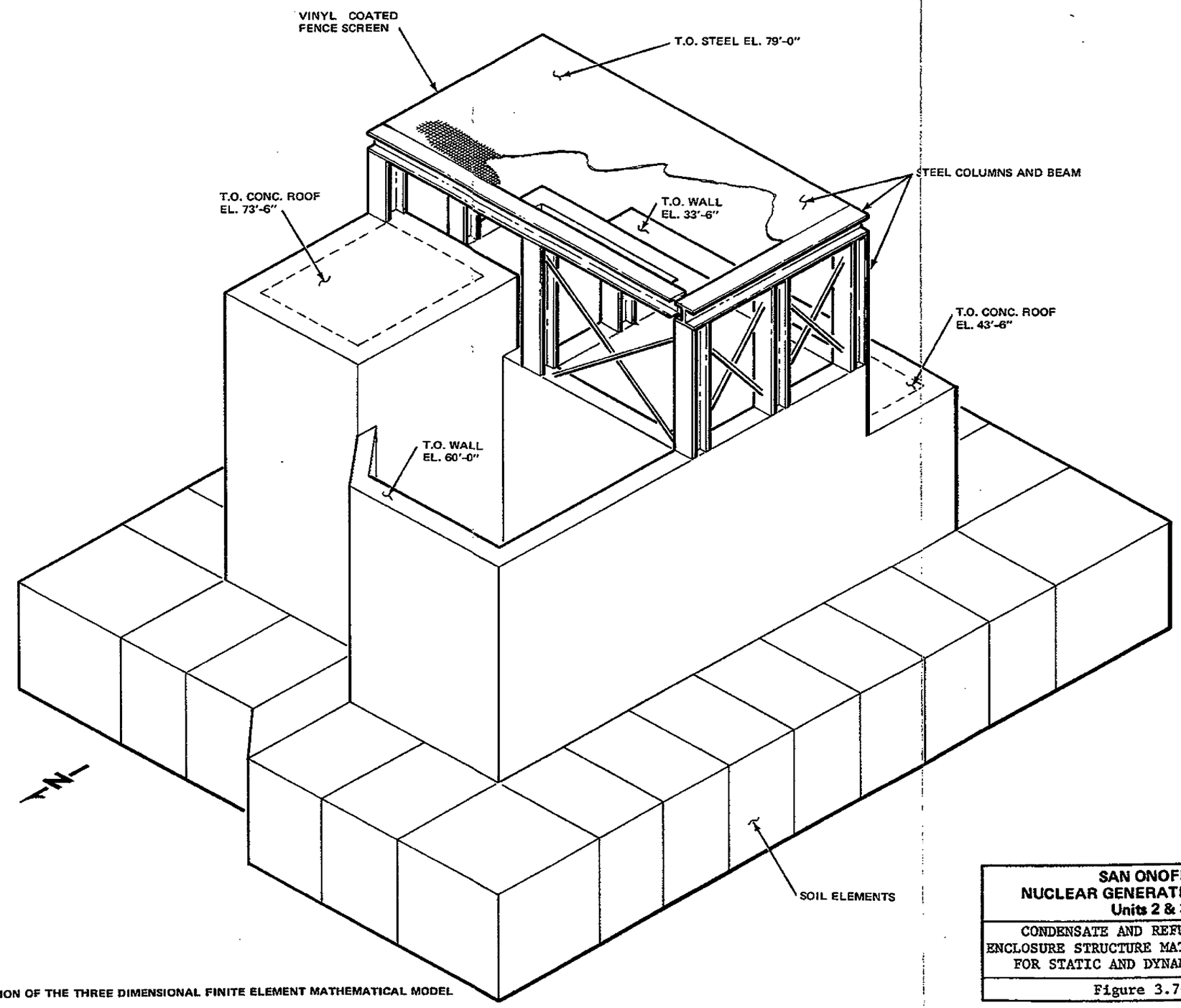

PICTORIAL REPRESENTATION OF THE THREE DIMENSIONAL FINITE ELEMENT MATHEMATICAL MODEL

10079-12A-013
28MR7

SAN ONOFRE NUCLEAR GENERATING STATION Units 2 & 3
CONDENSATE AND REFUELING TANK ENCLOSURE STRUCTURE MATHEMATICAL MODEL FOR STATIC AND DYNAMIC ANALYSES
Figure 3.7-35

Site File Copy

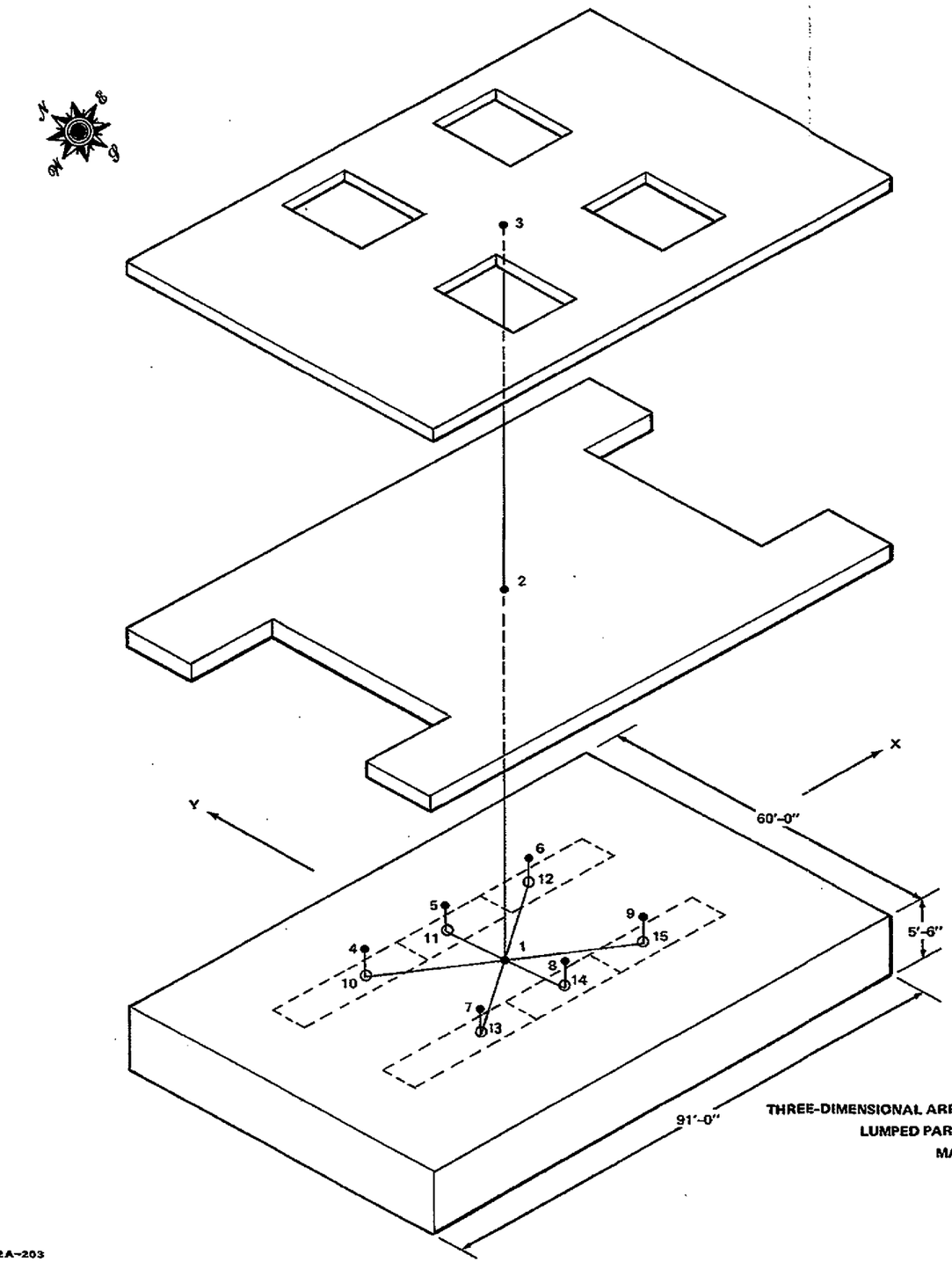

NODE DESCRIPTION SCHEDULE					
NODE NO.	REF. ELEV.	CONNECTING NODES		HORIZONTAL COORDINATES	
		BELOW	ABOVE	X (FT)	Y (FT)
1	27'-9"	–	2	0.00	0.00
2	48'-0"	1	3	0.00	0.00
3	65'-7"	2	–	0.00	0.00
4	34'-9"	10	–	-15.50	11.00
5	34'-0"	11	–	0.00	11.00
6	34'-7"	12	–	16.25	11.00
7	34'-7"	13	–	-16.25	-11.00
8	34'-0"	14	–	0.00	-11.00
9	34'-9"	15	–	15.50	-11.00
10	27'-9"	–	4	-15.50	11.00
11	27'-9"	–	5	0.00	11.00
12	27'-9"	–	6	16.25	11.00
13	27'-9"	–	7	-16.25	-11.00
14	27'-9"	–	8	0.00	-11.00
15	27'-9"	–	9	15.50	-11.00

NOTE:

NODES 10 THROUGH 15 ARE CONSTRAINED TO THE CORRESPONDING DEGREE OF FREEDOM OF THE NODE 1.

THREE-DIMENSIONAL ARRANGEMENT OF MULTI-CONNECTED NODAL POINTS
LUMPED PARAMETER GEOMETRICALLY COUPLED
MATHEMATICAL MODEL

SAN ONOFRE
NUCLEAR GENERATING STATION
Units 2 & 3

DIESEL GENERATOR BUILDING
MATHEMATICAL MODEL FOR
DYNAMIC ANALYSES

Figure 3.7-36

10079-12A-203
285E7

Site File Copy

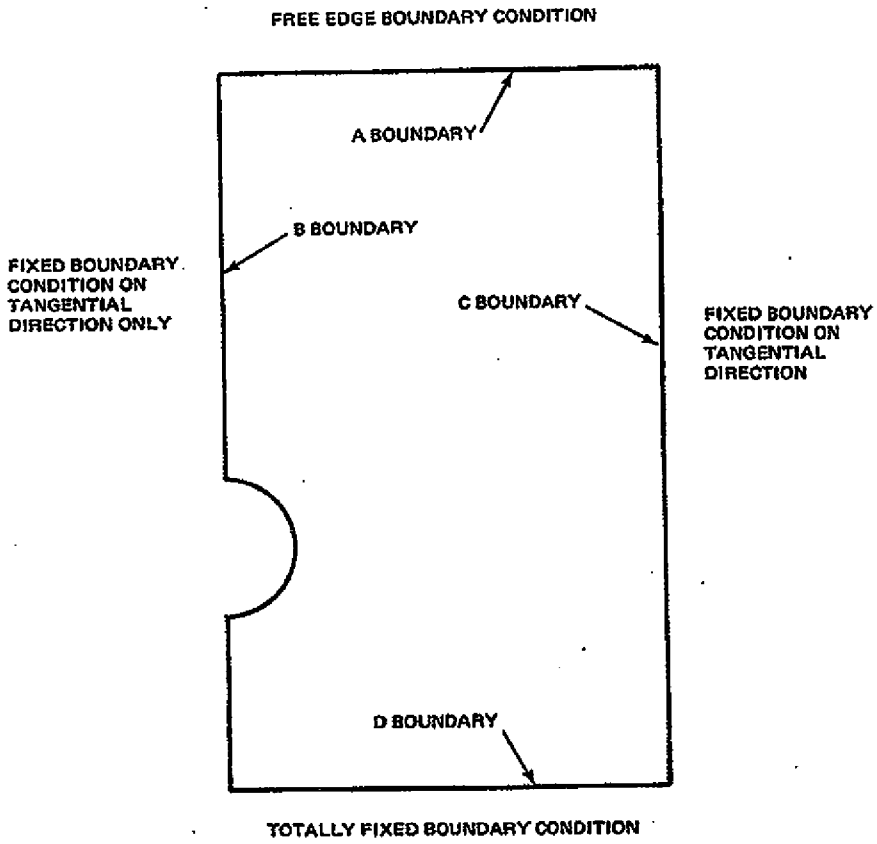

SAN ONOFRE NUCLEAR GENERATING STATION Units 2 & 3
EQUIPMENT HATCH BOUNDARY CONDITIONS FOR FINITE ELEMENT ANALYSIS
Figure 3.8-15

10079-11D-316
21MY6

Site File Copy

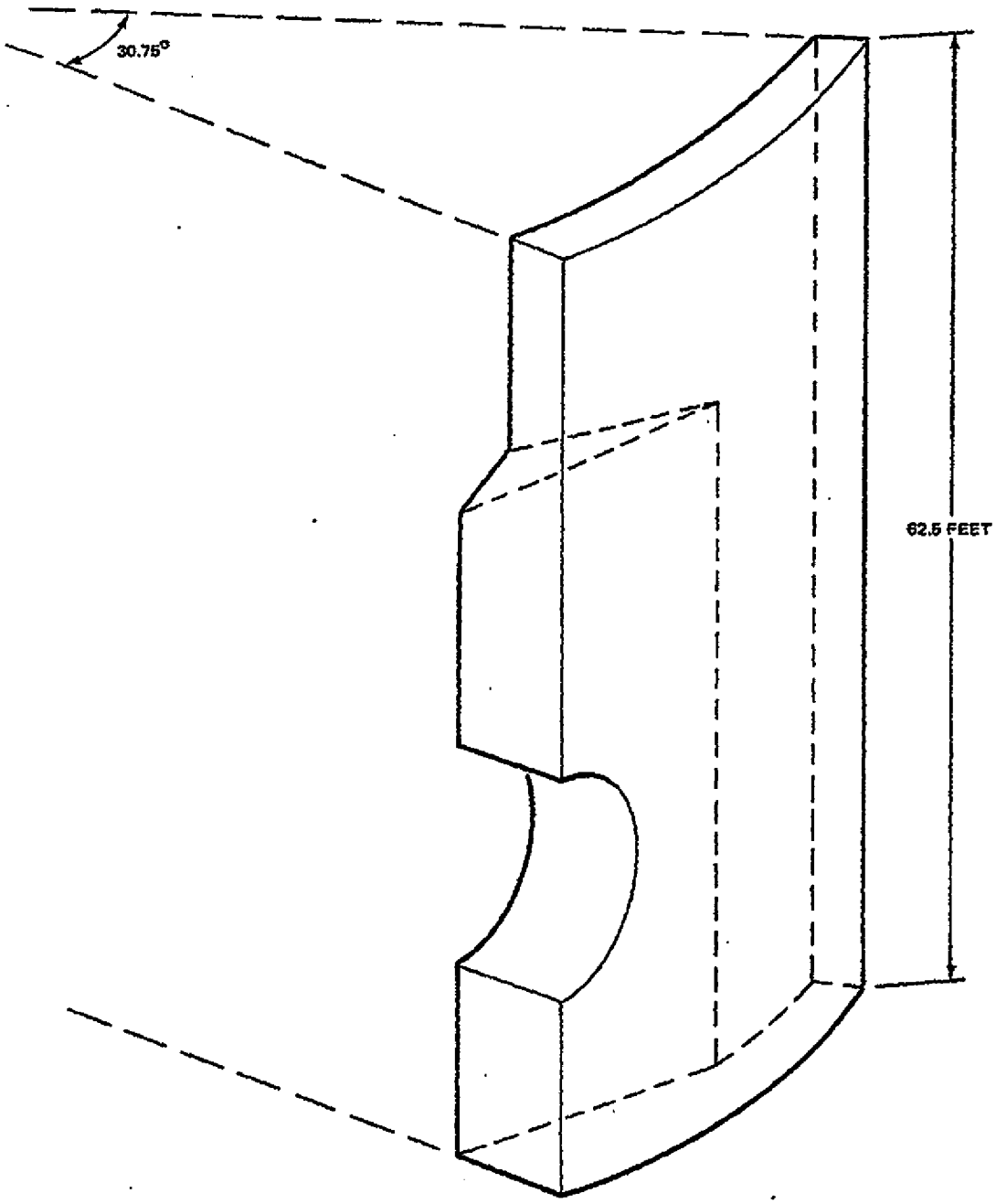

SAN ONOFRE NUCLEAR GENERATING STATION Units 2 & 3 Updated Final Safety Analysis Report
EQUIPMENT HATCH PENETRATION REGION FINITE ELEMENT MODEL GEOMETRY
Figure 3.8-16

Site File Copy

Site File Copy
Site File Copy

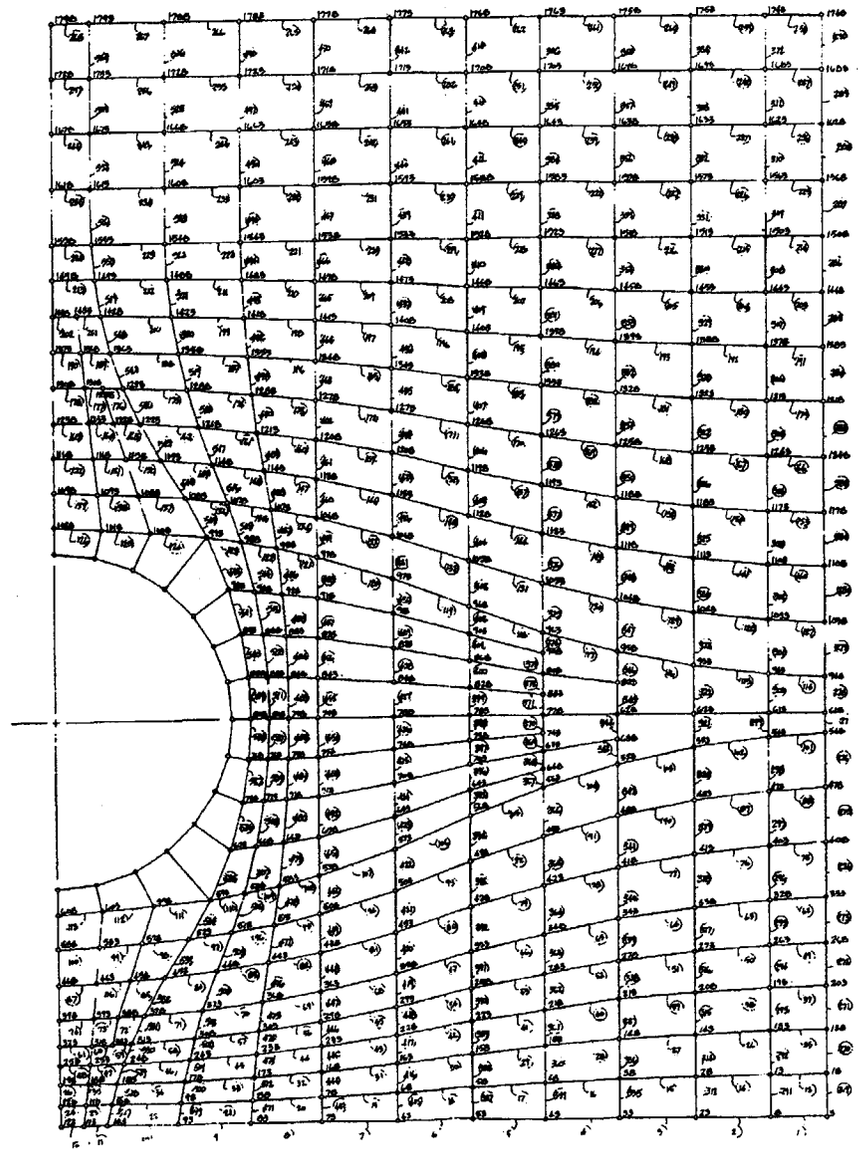

TRUSS ELEMENTS - NODE POINTS

10079-11D-318
21MY6

Updated

SAN ONOFRE NUCLEAR GENERATING STATION Units 2 & 3
EQUIPMENT HATCH FINITE ELEMENT ANALYSIS (Sheet 1 of 4)
Figure 3.8-17

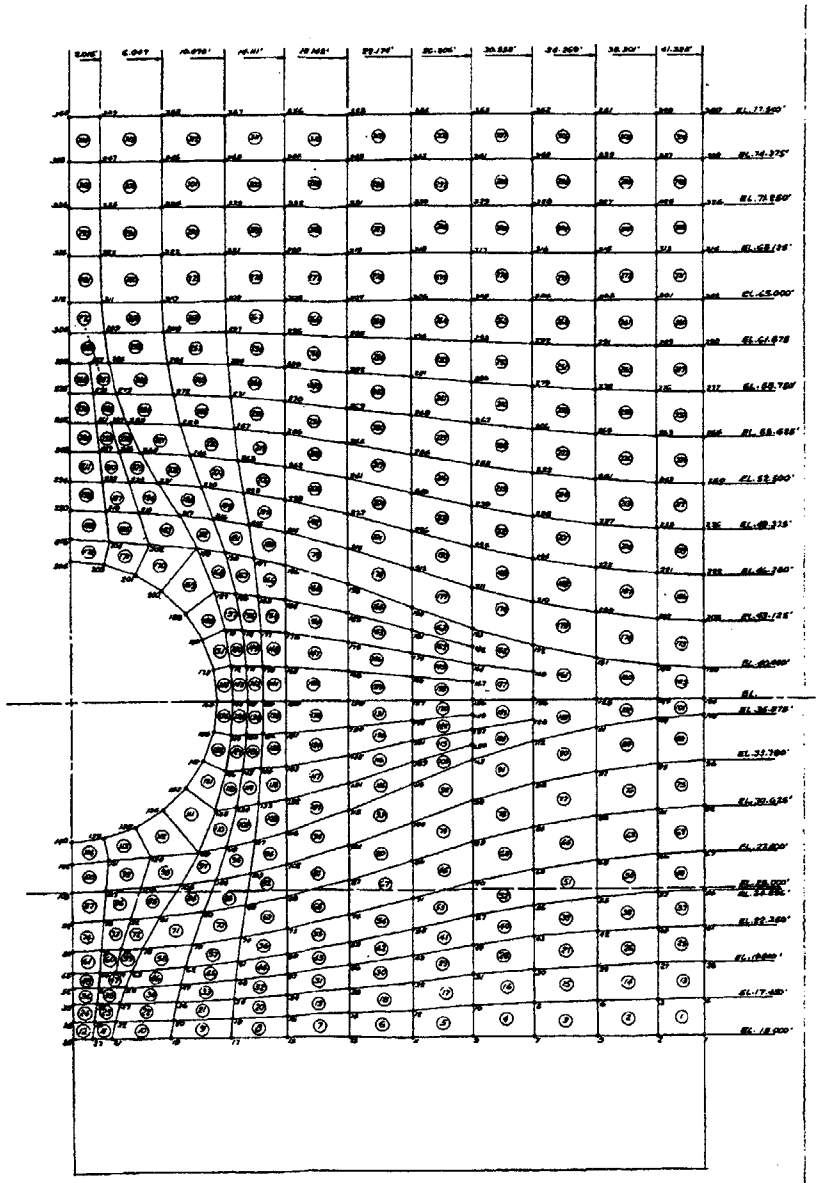

BRICK ELEMENTS - NEW GRID POINTS

Updated

SAN ONOFRE NUCLEAR GENERATING STATION Units 2 & 3
EQUIPMENT HATCH FINITE ELEMENT ANALYSIS (Sheet 4 of 4)
Figure 3.8-17

10079-11D-321
21MY9

Amended: June 2003 TL: E004628

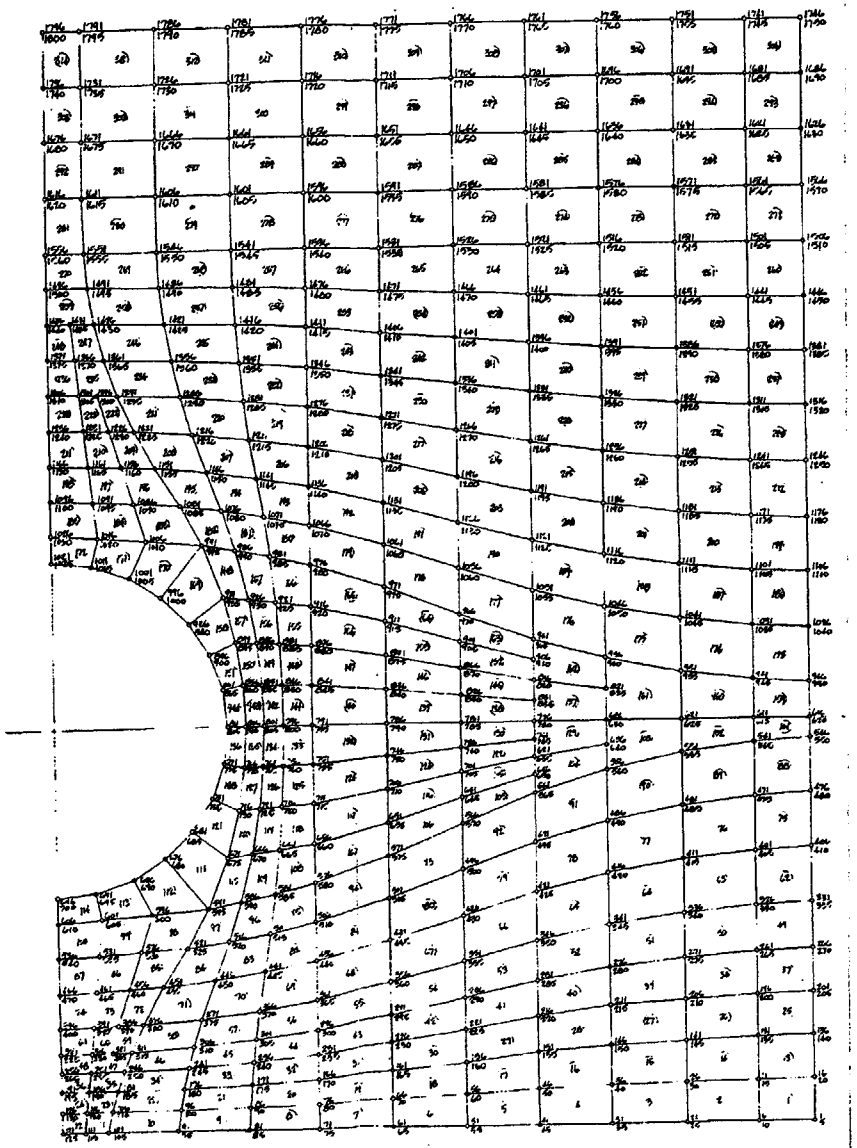

GRID ELEMENTS – THREE DIMENSIONAL NODE POINTS

Updated

SAN ONOFRE NUCLEAR GENERATING STATION Units 2 & 3
EQUIPMENT HATCH FINITE ELEMENT ANALYSIS (Sheet 3 of 4)
Figure 3.8-17

10079-11D-320
21MY6

Amended: June 2003 TL: E004628

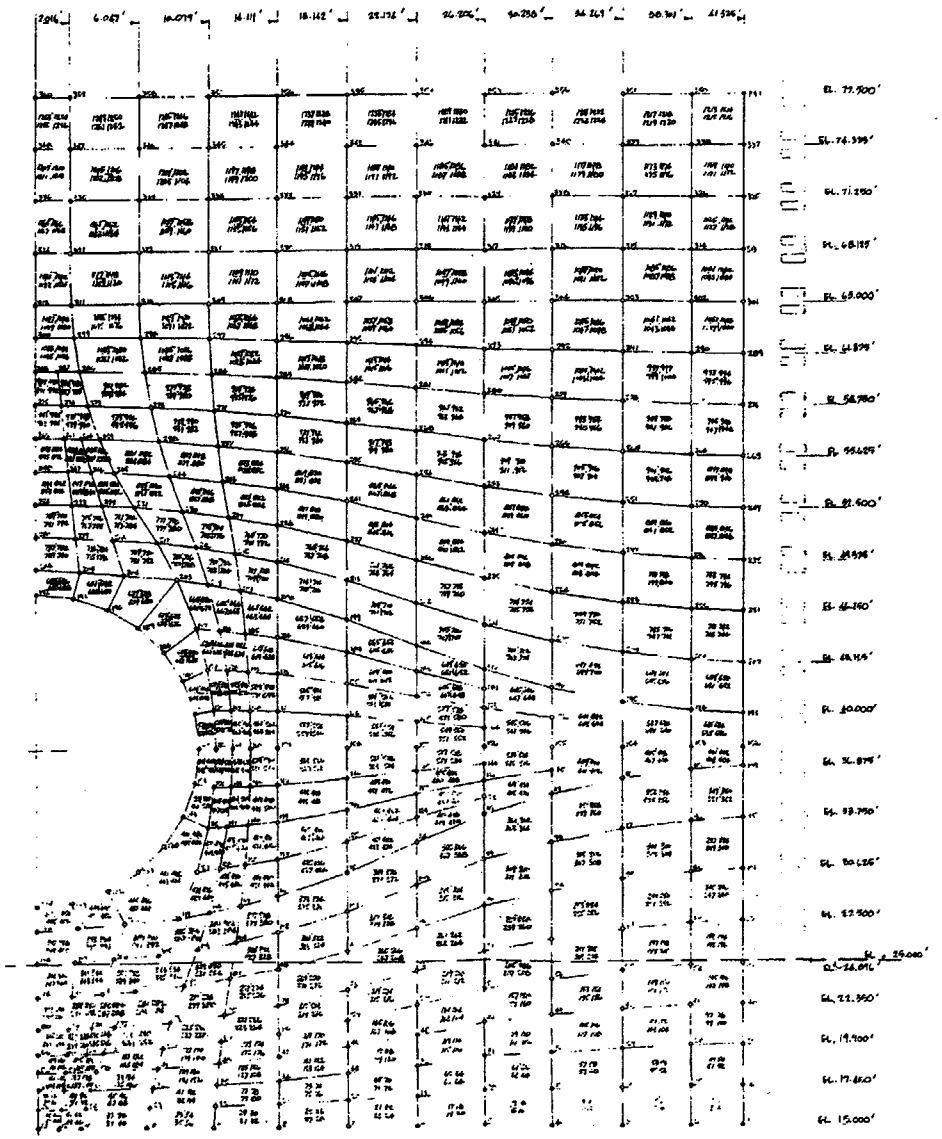

BRICK ELEMENTS - GRID POINTS

Updated

SAN ONOFRE NUCLEAR GENERATING STATION Units 2 & 3
EQUIPMENT HATCH FINITE ELEMENT ANALYSIS (Sheet 2 of 4)
Figure 3.8-17

10079-110-319
21MY6

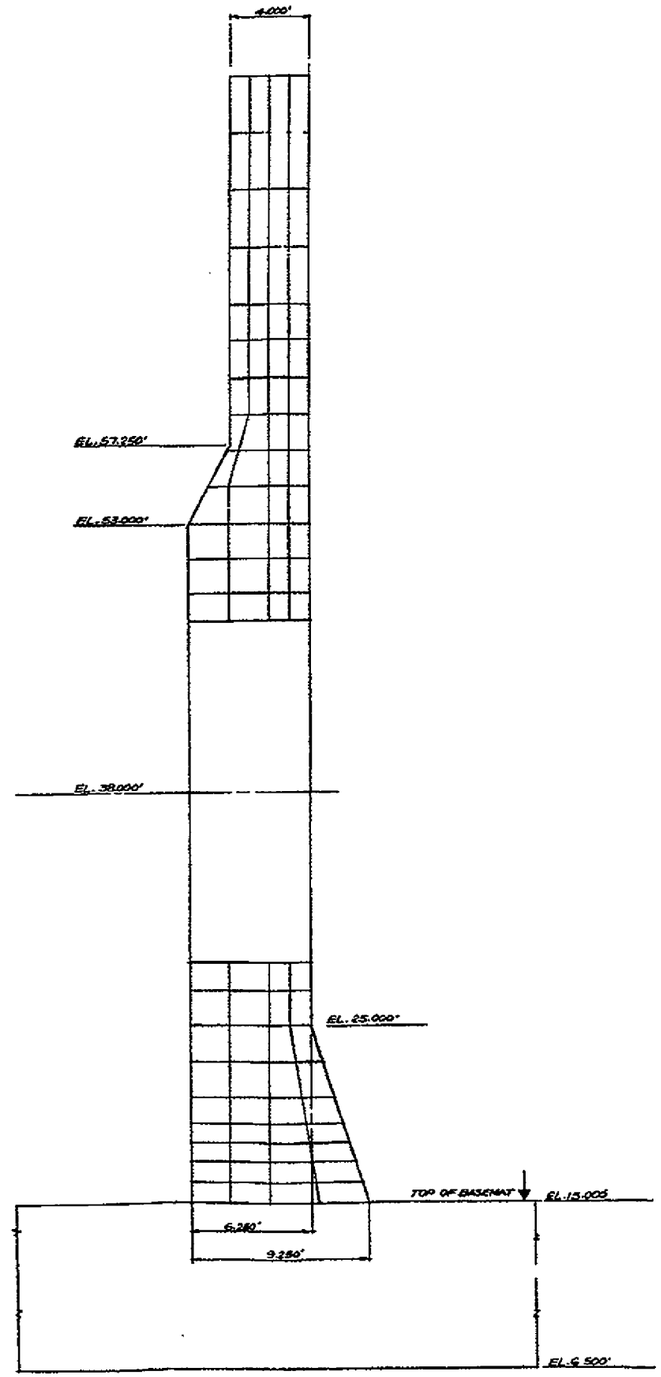

10079-11D-322
21MY6

SAN ONOFRE NUCLEAR GENERATING STATION Units 2 & 3
EQUIPMENT HATCH LAYERED ELEMENTS THROUGH WALL THICKNESS
Figure 3.8-18

Site File Copy

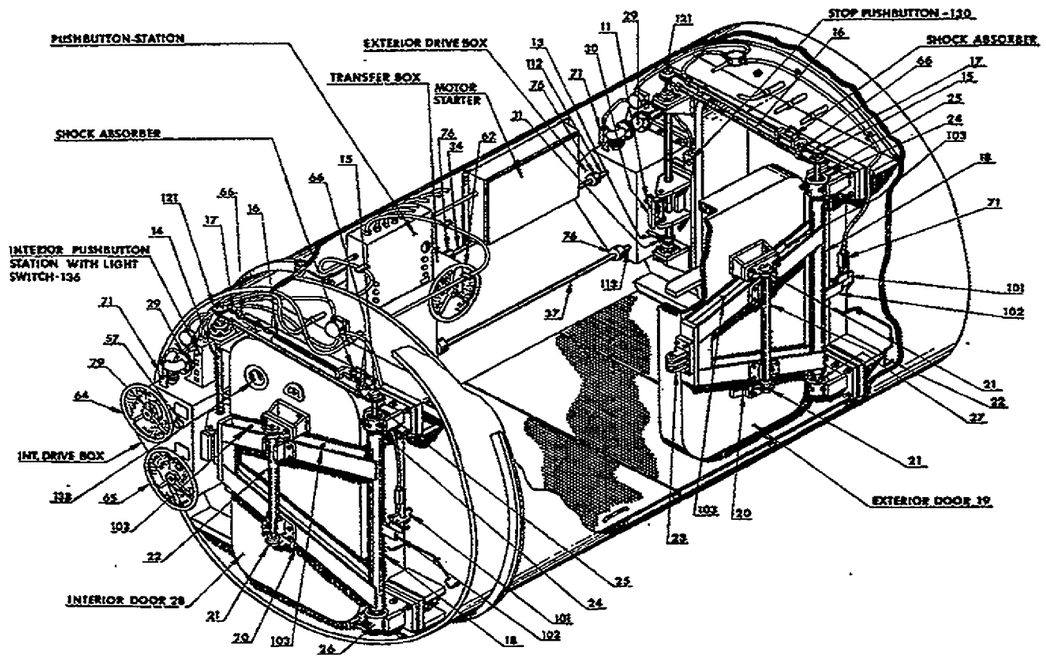

INTERIOR VIEW

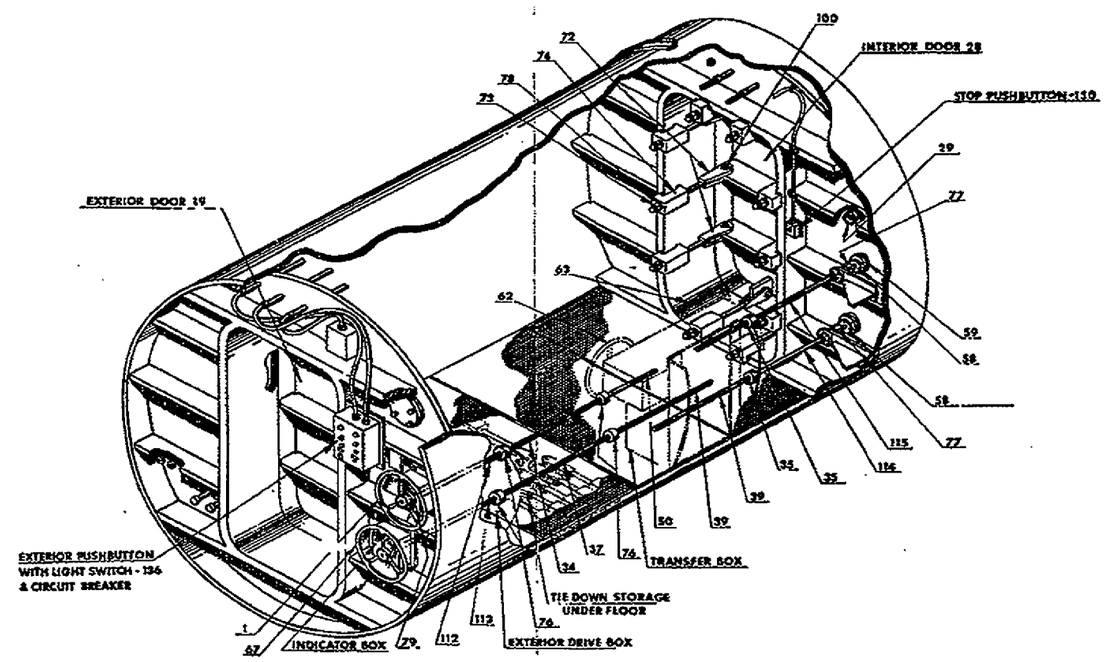

EXTERIOR VIEW

SAN ONOFRE NUCLEAR GENERATING STATION Units 2 & 3
PERSONNEL LOCK EXTERIOR AND INTERIOR VIEW (Sheet 2 of 2)
Figure 3.8-20

Site File Copy

PERSONNEL LOCK PURCHASED PARTS

NO.	DESCRIPTION
1, 62, 63 64, 65, 67	20 IN. DIA HANDWHEEL – "TOMCO" PART NO. 410098 OFFSET TYPE POLISHED RIM – FOR SPECIAL MODIFICATIONS CONTACT CHICAGO BRIDGE & IRON COMPANY
3(a)	SPUR GEAR – 8 PITCH – 2.000 P.D. – 16 TEETH – 1 1/4 FACE – 14 1/2° PRESSURE ANGLE – .875 +.003 –.000 DIA BORE WITH 5/16 SQ KEYWAY – (2) 5/16-18 TAPPED HOLES 90° APART WITH (1) HOLE OVER KEYWAY – 1 5/8 DIA HUB WITH 3/4 HUB PROJECTION.
4(a)	SPUR GEAR – 8 PITCH – 12.000 P.D. – 96 TEETH – 1 1/4 FACE – 14 1/2° PRESSURE ANGLE – 1.500 +.000 –.003 DIA BORE WITH 3/8 SQ KEYWAY (2) 1/2-13 TAPPED HOLES 90° APART WITH (1) HOLE OVER KEYWAY 3 IN. HUB DIA WITH 1 1/8 IN. HUB PROJECTION.
15	SPROCKET 2.000 +.0003 DIA BORE WITH KEYWAY FOR –.000 1/2 SQ KEY, DRILL AND TAP (2) 1/2-13 UNC-2B HOLES 90 DEGREES APART WITH ONE HOLE OVER KEYWAY MARTIN NO. 50516
17 and 49	ROLLER CHAIN 5/8 PITCH RC 50
21	ROLLER PILLOW BLOCK – ADAPTER TYPE FOR 2 IN. DIA SHAFT "SHAFER" NO. 2PA-200F
25	BALL BEARING CARTRIDGE BLOCK FOR 2 3/16 DIA SHAFT LINK BELT NO. C235 OR EQUAL
27	ROLLER BEARING CARTRIDGE BLOCK FOR 2 3/16 DIA SHAFT "SHAFER" NO. 2MA-200
29	EQUALIZING VALVE – 3 IN. DIA JAMESBURY CORP BALL VALVE 3A150F RF MOD. A 150 NO. ANSI-VPS 316.
35	ROLLER CHAIN FLEXIBLE COUPLING, BORE ONE HALF .875 +.003 DIA WITH KEYWAY FOR 3/16 SQ KEY, DRILL –.000 AND TAP (2) 1/4 20 UNC HOLES ONE OVER KEYWAY, ONE 90 DEGREES FROM KEYWAY. BORE OTHER HALF 1. +.003 DIA WITH KEYWAY FOR 1/4 SQ KEY, –.000 DRILL AND TAP (2) 3/8-16 UNC HOLES ONE OVER KEYWAY ONE 90 DEGREES FROM KEYWAY MARTIN NO. 5016.
47	SPROCKET – MARTIN NO. 506515 – 1.000 +.003 DIA BORE –.000
48	RINGFEDER ASSY NO. RFN 7012-1N1
50	DALTON MODEL R-100 TYPE G RIGHT ANGLE DRIVE UNIT TYPE E WITH SPECIAL SHAFT LENGTHS RATIO 1:1 (SAME WITH TYPE G AND SPECIAL)

NO.	DESCRIPTION
52	EXTENSION SPRINGS WIRE SIZE .063 – SPRING DIA. .500 – FREE HEIGHT 2.500 ENDS LOOPED – SPRING RATE 10.4 LBS./IN. MAX EXTENDED LENGTH 4.12 IN. – ASSOCIATED SPRING CORP. NO E500-063-250
53(a)	SPUR GEAR – 10 PITCH – 4.000 P.D. – 40 TEETH – 1 IN. FACE – 14 1/2° P.A. 2 1/8 DIA HUB WITH 2/8 HUB PROJECTION – .875 +.003 DIA BORE WITH 3/16 –.000 KEYWAY AND (2) 5/16-18 TAPPED HOLES WITH (1) HOLE OVER KEYWAY.
54	SPUR GEAR (LEAST EXPENSIVE) 8 PITCH – 4.000 P.D. 32 TEETH – 14 1/2° PRESSURE ANGLE – APPROX. 5/8 FACE – APPROXIMATELY 2/4 HUB DIA. WITH 1 IN. HUB PROJECTION 3/8 DIA. BORE WITH (1) NO 10-32 TAPPED HOLE
55	SPROCKET, LADDER CHAIN BOSTON GEAR NO. CA10
56	LADDER CHAIN – .185 IN. PITCH BOSTON GEAR NO. 1A (HIGH TENSILE & YIELD POINT OF 25 LBS)
58	SHAFT SEAL ASSEMBLIES BY CBI
	118 FLANGE SEALS SAL. SEAL NO. R-304-118
	116 1/2 – 12 UNC HEX. SOC. HD. CAP SCREWS x 0-1 3/4 SA-193 GR B7 (CBI MS 8019)
	119 "O" RINGS PARKER NO 2-224 E740-75 EPDM
60	SPROCKET – MARTIN 50820 – 3/4 BORE – NO KEYWAY SET SCREW
63	CHAIN TIGHTENER – PLAIN SHAFT – LINK BELT NO. C1
69	SPUR GEARS 8 D.P. – 2 IN. P.D. 1 1/4 FACE, 16 TEETH 1 BORE, 14 1/2° D.A. DRILL AND TAP 1 SET SCREW HOLE 5/16-18 UNC
71	LIMIT SWITCH – O.P.D.T. LEVER ACTION – ALLEN BRADLEY NO. 802TMT-W3 WITH 3/4 CONDUIT CONNECTIONS
76	ROLLER CHAIN FLEXIBLE COUPLING, BORE ONE HALF 1. +.003 –.000 DIA WITH KEYWAY FOR 1/4 SQ KEY, DRILL AND TAP (2) 3/8-16 UNC HOLES ONE OVER KEYWAY, ONE 90 DEGREES FROM KEYWAY. BORE OTHER HALF 1.750 +.003 –.000 DIA WITH KEYWAY FOR 3/8 SQ KEY, DRILL AND TAP (2) 3/8-16 UNC HOLES ONE OVER KEYWAY ONE 90 DEGREES FROM KEYWAY – MARTIN NO. 5016
79	SLIP CLUTCH WITH 7 3/4 BORE AND 3/16 KEYWAY, 2 IN. HUB WITH 1/4 KEYWAY HILLIARD NO. LA-1-312
80	SPROCKET, LADDER CHAIN BOSTON GEAR NO. CA60

NO.	DESCRIPTION
94	CLUTCH COUPLING – WARNER ELECTRIC NO PCC-825 PER 1-25565 90 VOLT L.H. HUB – 1 1/8 BORE WITH 1/4 x 1/8 KEYWAY IN BUSHING NO 180-0141, 1 IN. BORE WITH 1/4 x 1/8 KEYWAY IN BUSHING NO 180-0010.
95	SPEED REDUCER. BOSTON GEAR NO. FW32B-150-H4.
96	MOTOR, BOSTON GEAR NO F29008 FACE MOUNTED (NEMA TYPE C) DRIPPROOF, SHUNT WOUND, 1/3 H.P., 1750 R/MIN.
97	D. C. REDUCED VOLTAGE REVERSING STARTER WITH NEMA 4 ENCLOSURE SQUARE D CLASS 7725 TYPE HCG-1 OR EQUAL FOR 1/3 H.P. BOSTON GEAR MOTOR R29008 135V.D.C. VOLTAGE. ARMATURE 2.6 AMPS, 0.330 OHMS, FIELD 0.38 AMPS 242 OHMS – SUPPLY VOLTAGE 105 MIN AND 140 MAX STARTER TO LIMIT INRUSH TO 250% OF FULL CURRENT LOAD. THERMAL UNIT NUMBER B3-70 (AMBIENT TEMPERATURE IS 100 TO 110°F)
121	SPROCKET FOR 2 1/2 DIA SHAFT WITH KEYWAY FOR 5/8 SQ KEY, DRILL AND TAP (2) 5/8-11 UNC-2B HOLES, 90 DEGREES APART WITH ONE HOLE OVER KEYWAY. MARTIN 50616.
	CAM FOLLOWERS MCGILL "CAMROL" NO CF-1-S
	ROD END BEARINGS 3/4 – 16 UNF MALE END – SEALMASTER NO. TRE-12
	ACCORDION SLEEVES – 1 3/4 I.D. – NO LIMIT O.D. – MOVEMENT: MAX 7 1/2 IN. – MIN. 2 IN. – END COLLARS: 1 1/4 ID x 1 IN LG AND 2 7/8 I.D. x 1 IN. LG A & A MANUFACTURING COMPANY.
130	PUSHBUTTON STATION – ALLEN BRADLEY UNIT NO. 800 H – WK2A, NEMA TYPE 4 GENERAL PURPOSE ENCLOSURE 800H-1H24
131	RELAYS – SQUARE D CLASS 8501-125 VDC MODELS GDO-20, GDO-30, GDO-40 AND GDO-60.
132	POTENTIOMETER – OHMITE MODEL "K" NO. 0451 WITH NO. 6533 MOUNT AND NO. 5150 KNOB
133	PILOT LIGHT – ALLEN BRADLEY NO. 800T-G10R WITH LAMP 800T-N31
134	PUSH BUTTON UNIT – ALLEN BRADLEY NO. 800H-WX6A
135	PUSH BUTTON UNIT – ALLEN BRADLEY NO. 800H-WX61A
136	3 WAY SWITCH – ALLEN BRADLEY NO. 800H-JL2A 125 V.C.D.
137	HYDRAULIC CYLINDER – WARCO PRESSURE MASTER. DOUBLE END 2 IN. BORE 3 3/4 IN. STROKE – STD ROD, MODEL NO. C-4052-HH-C WITH VITON SEALS, CUSHIONS TO BE "EXACTAJUST".
138	SIGHT GLASS – PRESSURE NO. 5-1508.

a. MATERIAL IS CAST STEEL 0.20% UNTREATED OR BETTER SUCH AS 1030 OR 1040 SAE WITH BRINELL HARDNESS NUMBER OF 200 OR BETTER.

NO.	DESCRIPTION
7, 38, 40, 112, 115 41, 42, 43, 113, 114 46	7/8 IN. DIA SHAFTS
5	1-1/2 IN. DIA SHAFTS
6	ACTUATOR ARM ASSEMBLY
7	LOCKING PLATE ASSEMBLY
8	VALVE PLATE ASSEMBLY
9	VALVE ROD ASSEMBLY
10	LATCH PLATE ASSEMBLY
11	LATCH ROD ASSEMBLY
12	SWING PLATE ASSEMBLY
13	SWING ROD ASSEMBLY
14	2 IN. DIA SHAFT
16	1 IN. DIA ROD
18	HINGE ASSEMBLY
19	EXTERIOR DOOR ASSEMBLY
20	MOUNTING BRACKET ASSEMBLY
22	CENTER HINGE PIN ASSEMBLY
23	ROLLER ASSEMBLY
24	UPPER HINGE SUPPORT BRACKET ASSEMBLY
26	LOWER HINGE SUPPORT BRACKET ASSEMBLY
28	INTERIOR DOOR ASSEMBLY
30	LATCHING BAR ASSEMBLY
31	CLEVIS PLATE (DOOR SWING)
32	BRACKET ASSEMBLY
33	BRACKET ASSEMBLY (LATCH)
34, 37	1-3/4 IN. DIA SHAFTS
39	1 IN. DIA SHAFTS
44, 45, 61	3/8 IN. DIA SHAFT
51	INTERLOCK ASSEMBLY
57	INDICATOR POINTER
59	SHAFT SEAL PENETRATION
68	3/8 IN. ROD (FOR INTERLOCK)
70	ACTUATOR STOP
72	TIE DOWN ROD ASSEMBLY
73	TIE DOWN NUT

NO.	DESCRIPTION
74	TIE DOWN PAWL
77	RIGID COUPLING
78	TIE DOWN SPHERICAL WASHERS
100	TIE DOWN PIN
101	DOOR STOP BRACKET
102	HINGE DOOR STOP BRACKET
103	DOOR RESTRICTOR BOLT
105	DOOR RESTRICTOR BRACKET
110	SHAFT SEAL RETAINER PLATE
111	SHAFT SEAL BODY
145-C	SHOCK ABSORBER STOP ASSEMBLY

SAN ONOFRE
NUCLEAR GENERATING STATION
Units 2 & 3

PERSONNEL LOCK
EXTERIOR AND INTERIOR VIEW
(Sheet 1 of 2)

Figure 3.8-20

ESCAPE LOCK PURCHASED PARTS

NO.	DESCRIPTION
1, 2, 3, 4, 5, 6	10 IN. DIA WHEEL – 3/4 BORE WITH 3/16 SQ KEYWAY (2) 5/16-18 TAPPED HOLES 90° APART WITH (1) HOLE OVER KEYWAY–TOMCO NO. 11016 OFFSET TYPE
11, 13, 21	SPROCKET-RC NO. 50 CHAIN MARTIN NO. 50B518 3/4 DIA BORE WITH 3/16 SQ KEYWAY – (2) 1/4-20 TAPPED HOLES 90° APART WITH (1) HOLE OVER KEYWAY.
12, 22, 49, 60	ROLLER CHAIN 5/8 PITCH RC NO. 50
25	SPUR GEAR-6,000 P.D. 10 D.P.-60 TEETH 1 FACE-14 1/2° P.A. 2 1/8 DIA HUB-7/8 HUB PROJECTION-3/4 BORE WITH 3/16 SQ KEYWAY – (2) 1/4-20 TAPPED HOLES 90° APART WITH (1) OVER KEYWAY MARTIN NO. C1060
35	SET SCREW COLLAR-BOSTON GEAR NO. SC1001–1 IN. DIA BORE
50	ROLLER BEARING – 1 IN. MCGILL CAMROL NO. CYR–1–S
51	EQUALIZING VALVE – 2 IN. JAMESBURY BALL VALVE NO. 2A150F–36TT CBI MS 967.
52	MITER GEARS – 10 D.P. 2,500 P.D. – 25 TEETH .55 FACE 20° P.A. 2 IN. HUB DIA – MOUNTING DISTANCE 2 7/16-3/4 BORE WITH 3/16 SQ KEYWAY (2) 5/16-18 TAPPED HOLES 90° APART WITH (1) OVER KEYWAY MARTIN M1025
53	ROLLER CHAIN FLEXIBLE COUPLING – MORSE NO.5016 BORE ONE HALF 3/4 DIA WITH 3/16 SQ KEYWAY AND (1) 1/4-20 TAPPED HOLE OVER KEYWAY. BORE OTHER HALF 1-1/4 DIA WITH 1/4 SQ KEYWAY AND (1) 3/8-16 TAPPED HOLE OVER KEYWAY.
54	GEARED FLEXIBLE COUPLING – LINK BELT NO. SG140 BORE BOTH ENDS 3/4 DIA WITH 3/16 SQ KEYWAY AND (1) 1/4-20 TAPPED HOLE OVER KEYWAY
55	SPROCKET – RC NO. 50 MARTIN NO. 50B517 1 7/16 DIA BORE WITH 3/8 SQ KEYWAY. (2) 3/8-16 TAPPED HOLES 90° APART WITH (1) OVER KEYWAY.
56	SPHERICAL BEARING – HEIM NO. LS-30C
57	CARTRIDGE BEARING – SHAFER NO. ZL200
58	SHAFT SEAL ASSEMBLY
	102 – 1/2 – 13 UNC HEX SOC HEAD CAP SCREWS x 0' -1 3/4 SA193 GR B7 (CBI MS 842)
	107 – FLANGE SEALS BAL-SEAL NO. R-304-116
	108 – "O" RINGS – PARKER NO. 2-224-S604-7 SILICONE
61	SPUR GEAR 1,500 P.D. – 10 D.P. – 15 TEETH – 1 FACE – 14 1/2° P.A. – 1 7/32 DIA HUB – 5/8 HUB PROJECTION 3/4 BORE WITH 3/16 SQ KEYWAY – (2) 1/4-20 TAPPED HOLES 90° APART WITH (1) OVER KEYWAY MARTIN NO. S1016
64	LIMIT SWITCH – D.P.D.T. LEVER ACTION – ALLEN BRADLEY NO. 802THT-W1 WITH 3/4 CONDUIT CONNECTIONS

NO.	DESCRIPTION
72	SPROCKET – 12 TOOTH FOR 3/8 PITCH CHAIN 3/4 BORE – MARTIN 35BS12
73	ROLLER CHAIN 3/8 PITCH – MORSE NO. 35
74	SPROCKET – 48 TEETH FOR 3/8 PITCH CHAIN 5/8 BORE MARTIN 35B48
75	5/8 IN. I.D. BEARING BUNTING NO. P64–5
76	SLIP CLUTCH – HILLARD NO. DL2–1–313 WITH 3/4 BORE AND 3/16 KEYWAY HUB TO HAVE 1.375 O.D. WITH KEYWAY FOR 1/8 x 1/2 WOODRUFF KEY
90	SPROCKET 48 TEETH BOSTON NO. KSA48 WITH 5/8 BORE (CBI MODIFIED)
116	ROLLER CHAIN FLEX COUPLING LINK BELT NO. RC5016P 3/4 BORE, BOTH ENDS WITH 3/16 SQ KEYWAY AND (1) 1/4-20 TAPPED HOLE OVER KEYWAY
117	GEARED FLEXIBLE COUPLING FALK NO. 10 G10 NO. S.G. 140 BORE ONE HALF FOR 3/4 DIA SHAFT WITH KEYWAY FOR 3/16 SQ KEY AND HOLE DRILLED AND TAPPED FOR 1/4-20 UNC SET SCREW. BORE OTHER HALF FOR 1 1/4 DIA SHAFT WITH KEYWAY FOR 1/4 SQ KEY AND HOLE DRILLED AND TAPPED FOR 3/8-16 UNC SET SCREW WITH ALEMITES.
121	SPROCKET – MARTIN NO. 50BS20 FOR 1 7/16 DIA SHAFT WITH KEYWAY FOR 3/8 SQ KEY. DRILL AND TAP (2) 3/8-16 UNC. HOLES 90° APART WITH (1) OVER KEYWAY.
	ROD END BEARING – 3/8-24 UNF MALE END HEIM NO. HM-6
	CAM FOLLOWERS – MCGILL "CAMROL" NO. CF–1–S.
	ACCORDION SLEEVES – 1 IN. I.D. – NO LIMIT O.D. MOVEMENT: MAX 2 3/4 MIN. 3/4-END COLLARS: 3/4 I.D. x 3/4 AND 1 15/16 I.D. x 3/4 TEMP: AMBIENT TO 150F – A & A MANUFACTURING COMPANY
	SPROCKET RC NO. 50 – MARTIN NO. 50BS10 – 3/4 DIA BORE WITH 3/16 SQ KEYWAY (2) 1/4-20 TAPPED HOLES 90° APART WITH (1) OVER KEYWAY.
	SPROCKET RC NO. 50 – 40 TEETH – 7.966 P.D. 3/4 DIA BORE WITH 3/16 SQ KEYWAY (2) 1/4-20 TAPPED HOLES 90° APART WITH (1) OVER KEYWAY MARTIN NO. 50B40 ROD END BEARING – 1/2-20 UNF MALE END HEIM NO. HM-8
	MATERIAL IS CAST STEEL 0.20% C. UNTREATED OR BETTER SUCH AS 1030 or 1040 SAE WITH BRINELL HARDNESS NUMBER OF 200 OR BETTER.
7	INTERLOCK ASSEMBLY
8, 10, 14, 16, 17, 18 20, 23, 24, 27, 62, 63	3/4 IN. DIA SHAFTS

NO.	DESCRIPTION
9, 15, 19, 26	1 1/4 IN. DIA SHAFTS
28, 30, 32	ACTUATOR ARM ASSEMBLIES
29, 31, 33	LOCKING PLATE ASSEMBLIES
34	ACTUATOR STOP ASSEMBLY
36	SWING ACTUATING RODS
38	SWING ARM CLEVIS
39, 44, 46	OPERATING ROD ASSEMBLY
40	LATCHING BAR ASSEMBLY
41	ROLLER ASSEMBLY
42	HINGE ASSEMBLY
43, 45, 47	VALVE, LATCH & SWING PLATE ASSEMBLY
48	INDICATOR ASSEMBLY
58	SHAFT SEAL ASSEMBLY
71	RIGID COUPLING
93	INTERIOR DOOR TIEDOWN ASSEMBLY
105, 106	SHAFT SEAL RETAINER PLATES
109	SHAFT SEAL GLAND PLATE

SAN ONOFRE NUCLEAR GENERATING STATION Units 2 & 3

ESCAPE LOCK
EXTERIOR AND INTERIOR VIEW
(Sheet 1 of 2)

Figure 3.8-21

10079-12A-270
30 DEC 7

Site File Copy

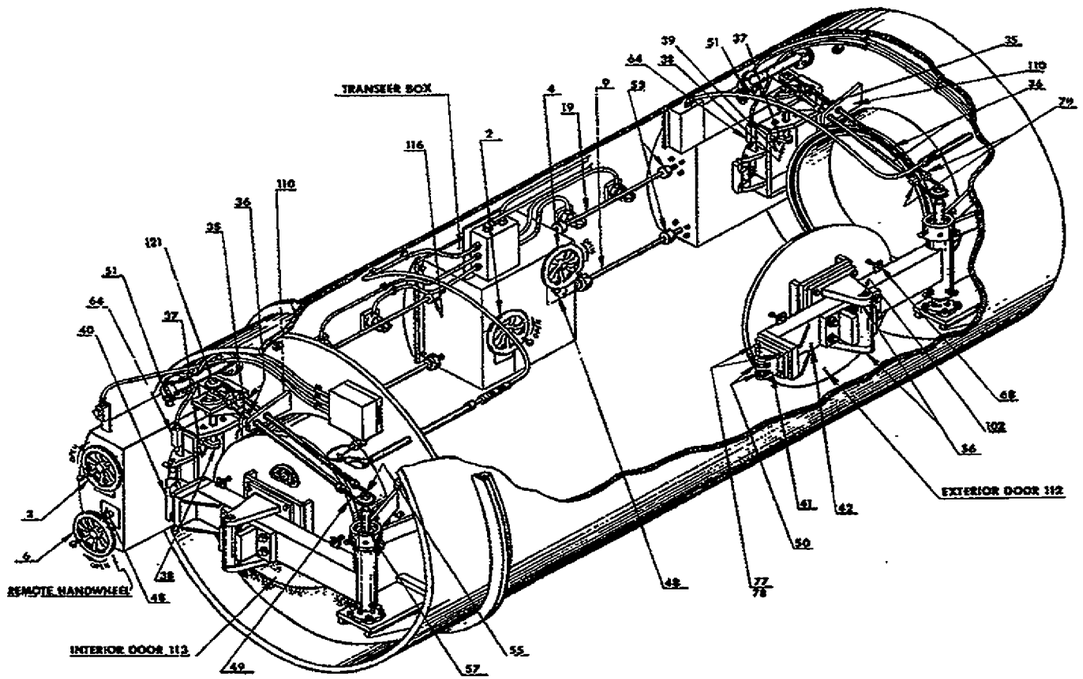

INTERIOR VIEW

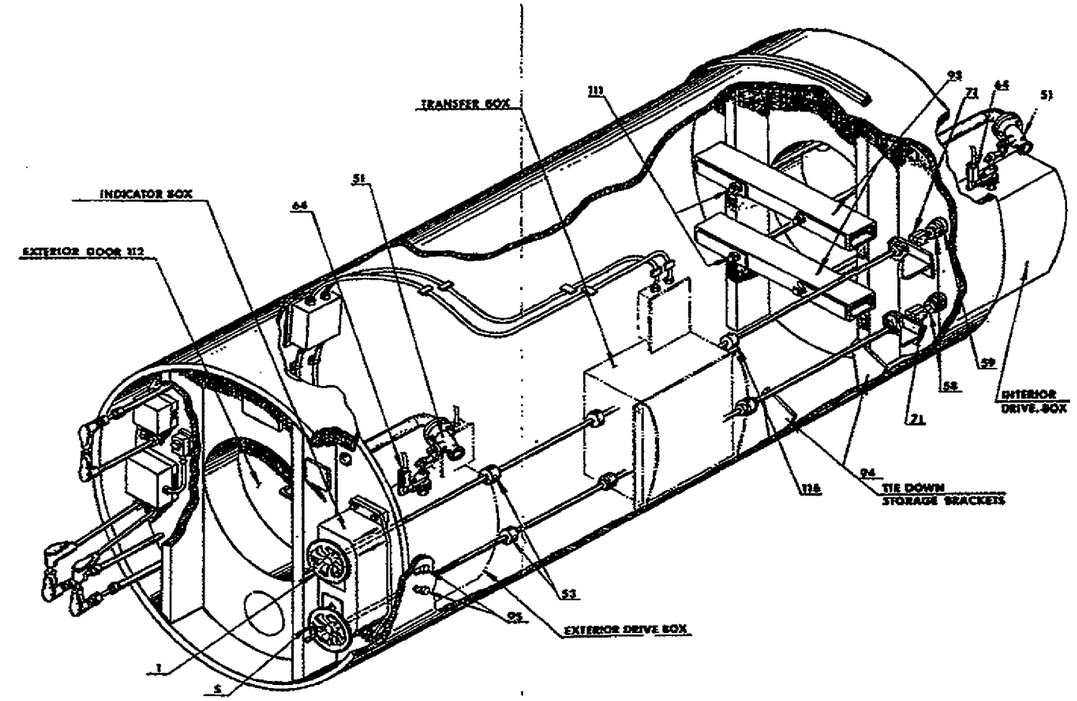

EXTERIOR VIEW

SAN ONOFRE NUCLEAR GENERATING STATION Units 2 & 3
ESCAPE LOCK EXTERIOR AND INTERIOR VIEW (Sheet 2 of 2)
Figure 3.8-21

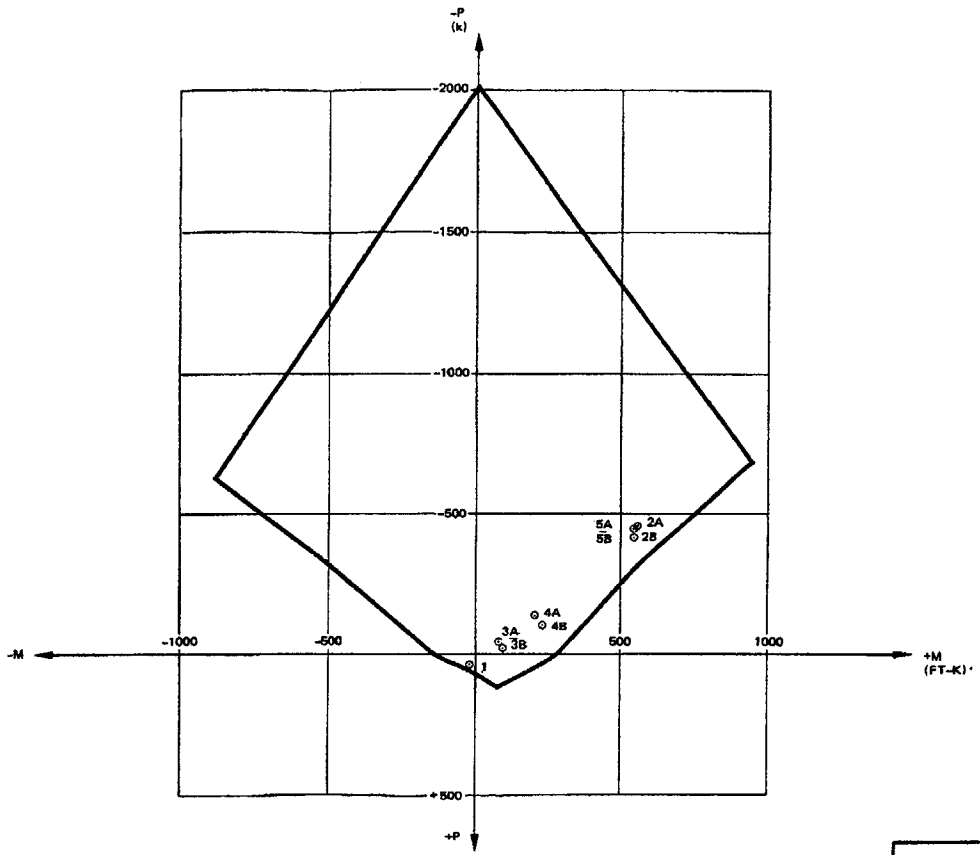

SECTION 1 – MERIDIONAL

GOVERNING LOADING COMBINATIONS:

1. $D + F + T_A + 1.5P$
2. $D + F + T_A + 1.25P \pm 1.25E$
3. $D + F + T_A \pm 1.25E$
4. $D + F + T_A + P \pm E'$
5. $D + F + T_A \pm E'$

NOTES:

1. REFER TO TABLE 3.8-2, SHEET 1, FOR SECTION NUMBER IDENTIFICATION
2. NOTATIONS "A" AND "B" IDENTIFY "PLUS" AND "MINUS" LOAD COMBINATIONS RESPECTIVELY.

Updated

SAN ONOFRE NUCLEAR GENERATING STATION
Units 2 & 3

CONTAINMENT STRUCTURE INTERACTION DIAGRAMS WITH ACTUAL RESULTS OF PRINCIPAL LOAD COMBINATIONS (Sheet 1 of 20)

Figure 3.8-22

10079-11D-277
11MY6

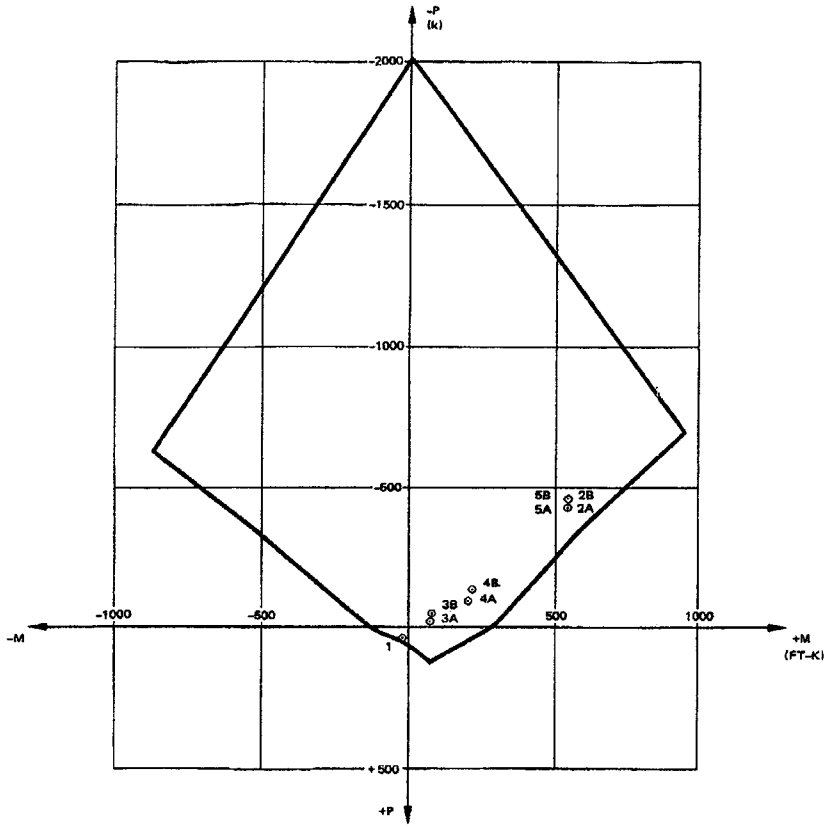

SECTION 1 – HOOP

GOVERNING LOADING COMBINATIONS:

1. $D + F + T_A + 1.5P$
2. $D + F + T_A + 1.25P \pm 1.25E$
3. $D + F + T_A \pm 1.25E$
4. $D + F + T_A + P \pm E'$
5. $D + F + T_A \pm E'$

NOTES:

1. REFER TO TABLE 3.8-2, SHEET 1, FOR SECTION NUMBER IDENTIFICATION
2. NOTATIONS "A" AND "B" IDENTIFY "PLUS" AND "MINUS" LOAD COMBINATIONS RESPECTIVELY.

Updated

SAN ONOFRE NUCLEAR GENERATING STATION Units 2 & 3

CONTAINMENT STRUCTURE INTERACTION DIAGRAMS WITH ACTUAL RESULTS OF PRINCIPAL LOAD COMBINATIONS (Sheet 2 of 20)

Figure 3.8-22

10079-11D-278
11MY6

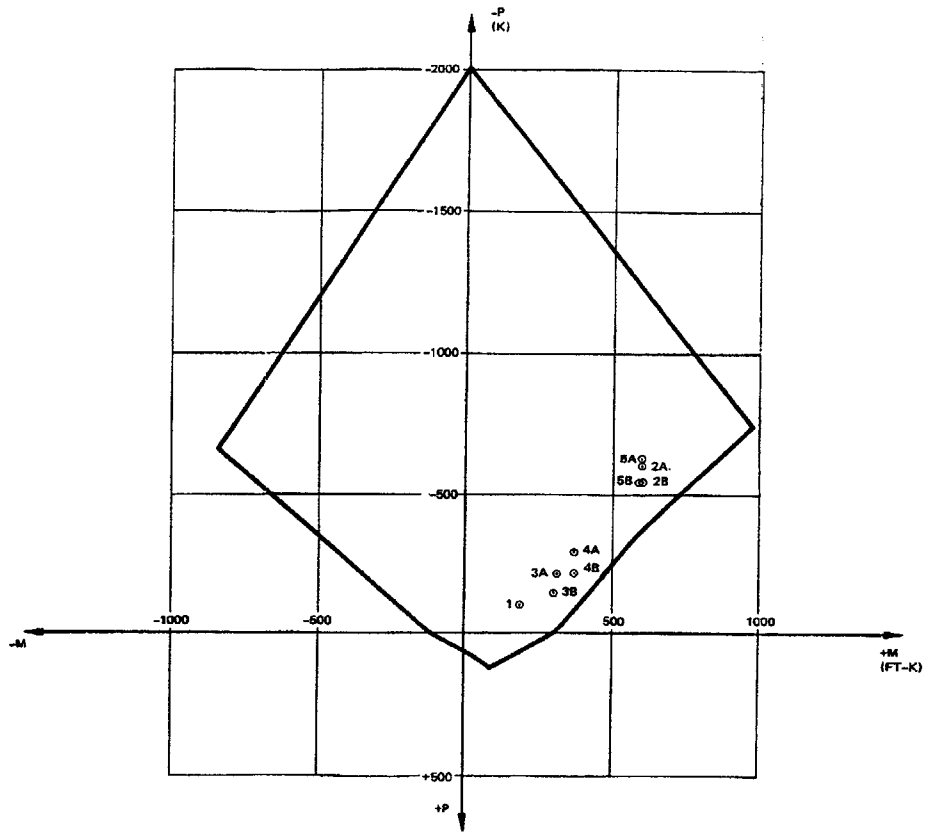

SECTION 2 – MERIDIONAL

GOVERNING LOADING COMBINATIONS:

1. $D + F + T_A + 1.5P$
2. $D + F + T_A + 1.25P \pm 1.25E$
3. $D + F + T_A \pm 1.25E$
4. $D + F + T_A + P \pm E'$
5. $D + F + T_A \pm E'$

NOTES:

1. REFER TO TABLE 3.8-2, SHEET 1, FOR SECTION NUMBER IDENTIFICATION
2. NOTATIONS "A" AND "B" IDENTIFY "PLUS" AND "MINUS" LOAD COMBINATIONS RESPECTIVELY.

Updated

SAN ONOFRE NUCLEAR GENERATING STATION Units 2 & 3

CONTAINMENT STRUCTURE INTERACTION DIAGRAMS WITH ACTUAL RESULTS OF PRINCIPAL LOAD COMBINATIONS (Sheet 3 of 20)

Figure 3.8-22

10079-11D-279
11MY6

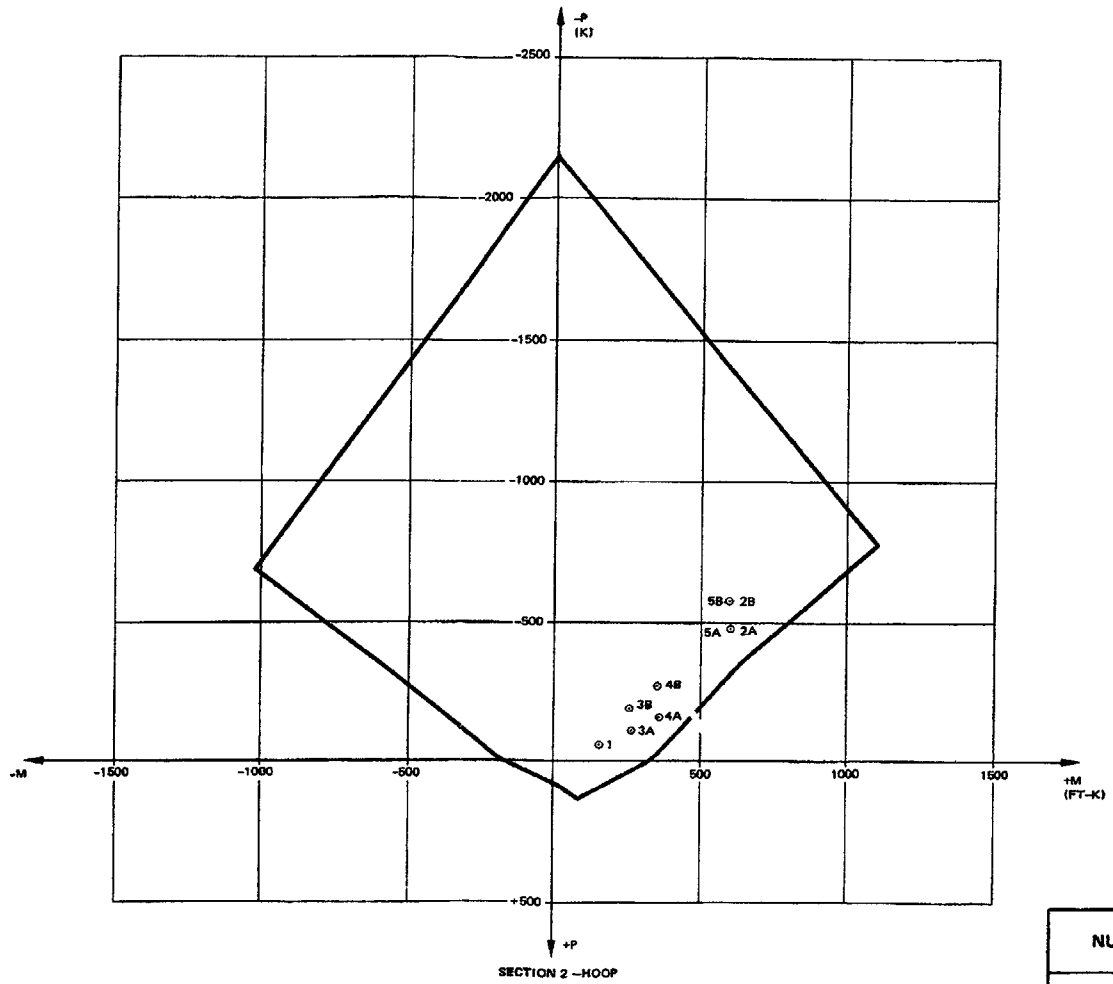

SECTION 2 –HOOP

GOVERNING LOADING COMBINATIONS:

1. $D + F + T_A + 1.5P$
2. $D + F + T_A + 1.25P \pm 1.25E$
3. $D + F + T_A \pm 1.25E$
4. $D + F + T_A + P \pm E'$
5. $D + F + T_A \pm E'$

NOTES:

1. REFER TO TABLE 3.8-2, SHEET 1, FOR SECTION NUMBER IDENTIFICATION
2. NOTATIONS "A" AND "B" IDENTIFY "PLUS" AND "MINUS" LOAD COMBINATIONS RESPECTIVELY.

Updated

SAN ONOFRE NUCLEAR GENERATING STATION Units 2 & 3

CONTAINMENT STRUCTURE INTERACTION DIAGRAMS WITH ACTUAL RESULTS OF PRINCIPAL LOAD COMBINATIONS (Sheet 4 of 20)

Figure 3.8-22

10079-110-280
11MY6

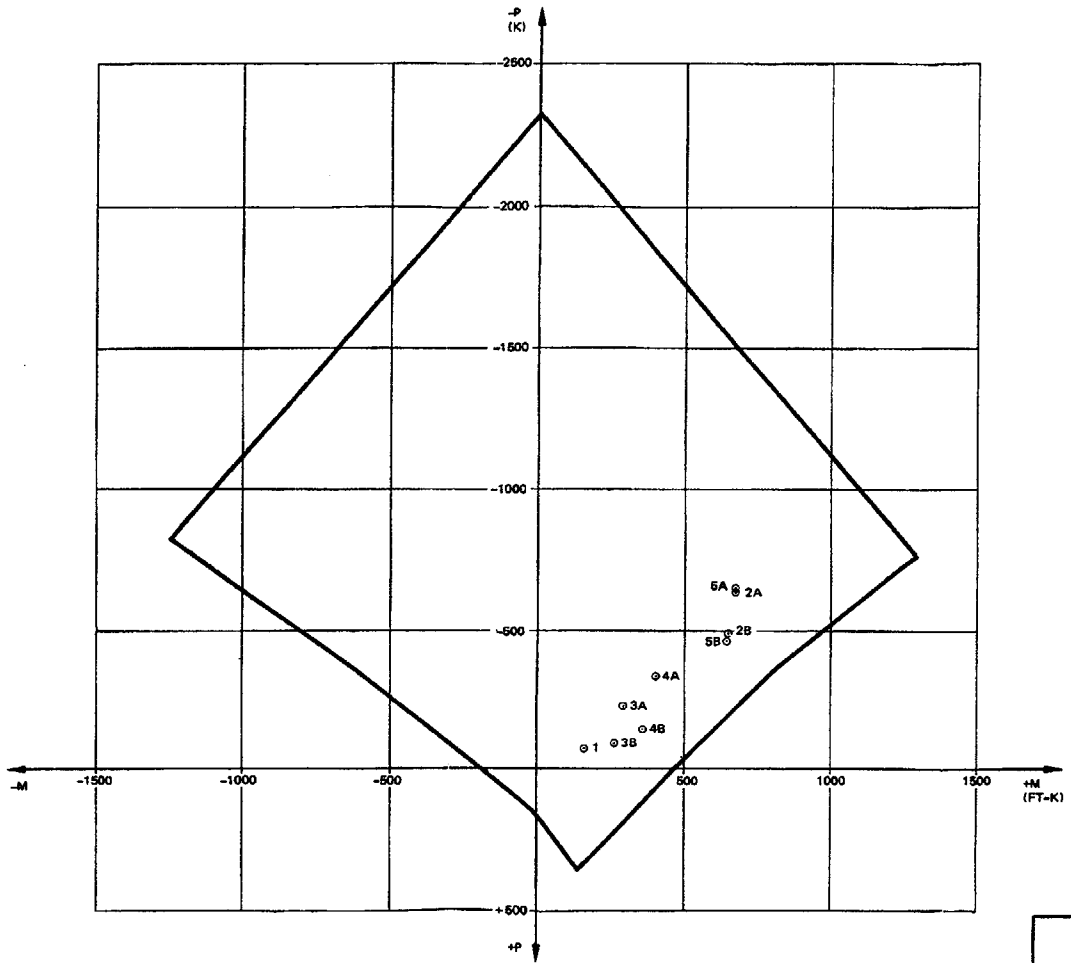

SECTION 3 — MERIDIONAL

GOVERNING LOADING COMBINATIONS:

1. $D + F + T_A + 1.5P$
2. $D + F + T_A + 1.25P \pm 1.25E$
3. $D + F + T_A \pm 1.25E$
4. $D + F + T_A + P \pm E'$
5. $D + F + T_A \pm E'$

NOTES:

1. REFER TO TABLE 3.8-2, SHEET 1 FOR SECTION NUMBER IDENTIFICATION
2. NOTATIONS "A" AND "B" IDENTIFY "PLUS" AND "MINUS" LOAD COMBINATIONS RESPECTIVELY.

Updated

SAN ONOFRE NUCLEAR GENERATING STATION Units 2 & 3

CONTAINMENT STRUCTURE INTERACTION DIAGRAMS WITH ACTUAL RESULTS OF PRINCIPAL LOAD COMBINATIONS (Sheet 5 of 20)

Figure 3.8-22

16079-11D-281
11MY6

Rev: 5

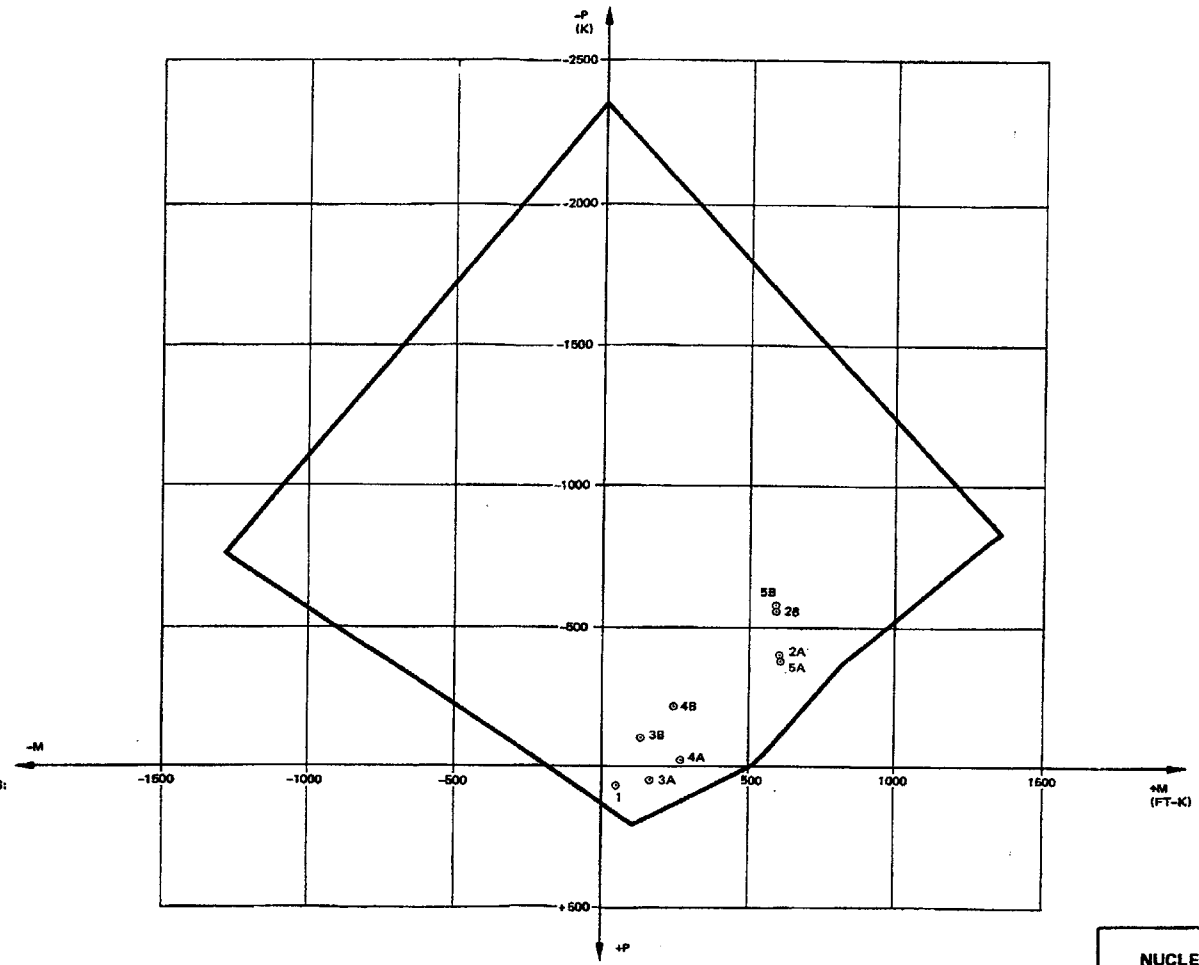

SECTION 3 – HOOP

GOVERNING LOADING COMBINATIONS:

1. $D + F + T_A + 1.5P$
2. $D + F + T_A + 1.25P \pm 1.25E$
3. $D + F + T_A \pm 1.25E$
4. $D + F + T_A + P \pm E'$
5. $D + F + T_A \pm E'$

NOTES:

1. REFER TO TABLE 3.8-2, SHEET 1 FOR SECTION NUMBER IDENTIFICATION
2. NOTATIONS "A" AND "B" IDENTIFY "PLUS" AND "MINUS" LOAD COMBINATIONS RESPECTIVELY.

Updated

SAN ONOFRE NUCLEAR GENERATING STATION Units 2 & 3

CONTAINMENT STRUCTURE INTERACTION DIAGRAMS WITH ACTUAL RESULTS OF PRINCIPAL LOAD COMBINATIONS (Sheet 6 of 20)

Figure 3.8-22

10075-11D-282
11MY4

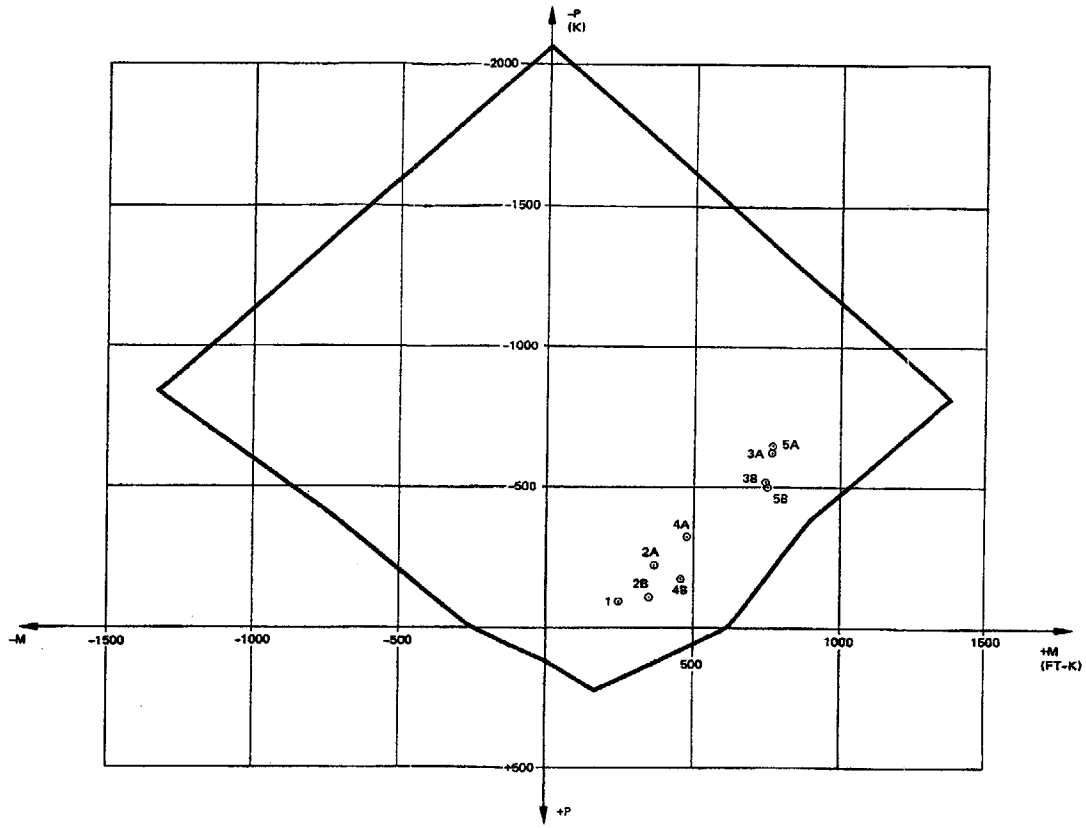

SECTION 4 – MERIDIONAL

GOVERNING LOADING COMBINATIONS:

1. $D + F + T_A + 1.5P$
2. $D + F + T_A + 1.25P \pm 1.25E$
3. $D + F + T_A \pm 1.25E$
4. $D + F + T_A + P \pm E'$
5. $D + F + T_A \pm E'$

NOTES:

1. REFER TO TABLE 3.8-2, SHEET 1, FOR SECTION NUMBER IDENTIFICATION
2. NOTATIONS "A" AND "B" IDENTIFY "PLUS" AND "MINUS" LOAD COMBINATIONS RESPECTIVELY.

Updated

SAN ONOFRE
NUCLEAR GENERATING STATION
Units 2 & 3

CONTAINMENT STRUCTURE
INTERACTION DIAGRAMS
WITH ACTUAL RESULTS OF
PRINCIPAL LOAD COMBINATIONS
(Sheet 7 of 20)

Figure 3.8-22

10079-11D-283
11MY6

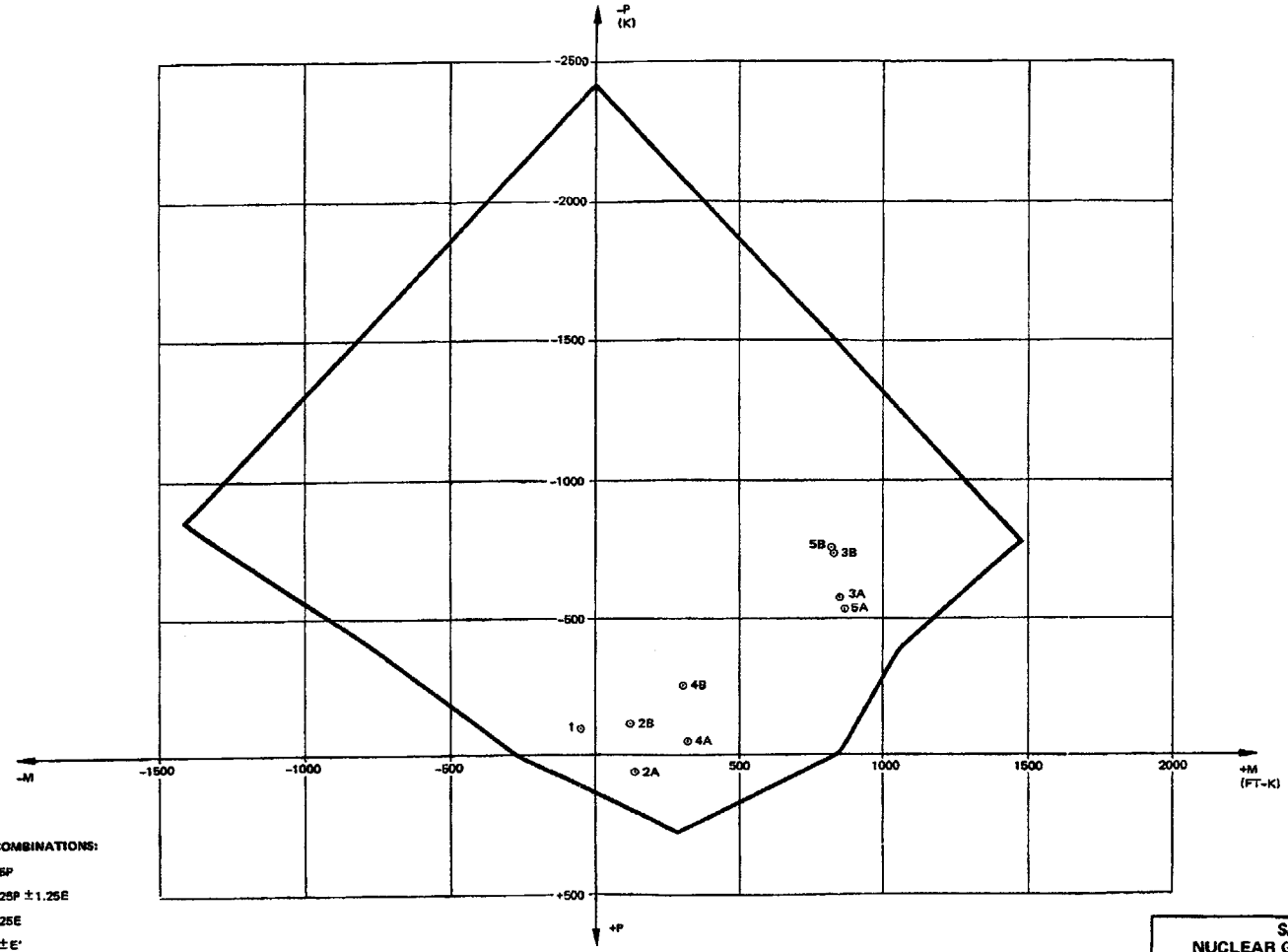

SECTION 4 – HOOP

GOVERNING LOADING COMBINATIONS:

1. $D + F + T_A + 1.5P$
2. $D + F + T_A + 1.25P \pm 1.25E$
3. $D + F + T_A \pm 1.25E$
4. $D + F + T_A + P \pm E'$
5. $D + F + T_A \pm E'$

NOTES:

1. REFER TO TABLE 3.8-2, SHEET 1 FOR SECTION NUMBER IDENTIFICATION
2. NOTATIONS "A" AND "B" IDENTIFY "PLUS" AND "MINUS" LOAD COMBINATIONS RESPECTIVELY.

Updated

SAN ONOFRE NUCLEAR GENERATING STATION Units 2 & 3

CONTAINMENT STRUCTURE INTERACTION DIAGRAMS WITH ACTUAL RESULTS OF PRINCIPAL LOAD COMBINATIONS (Sheet 8 of 20)

Figure 3.8-22

19079-11D-264
11MY6

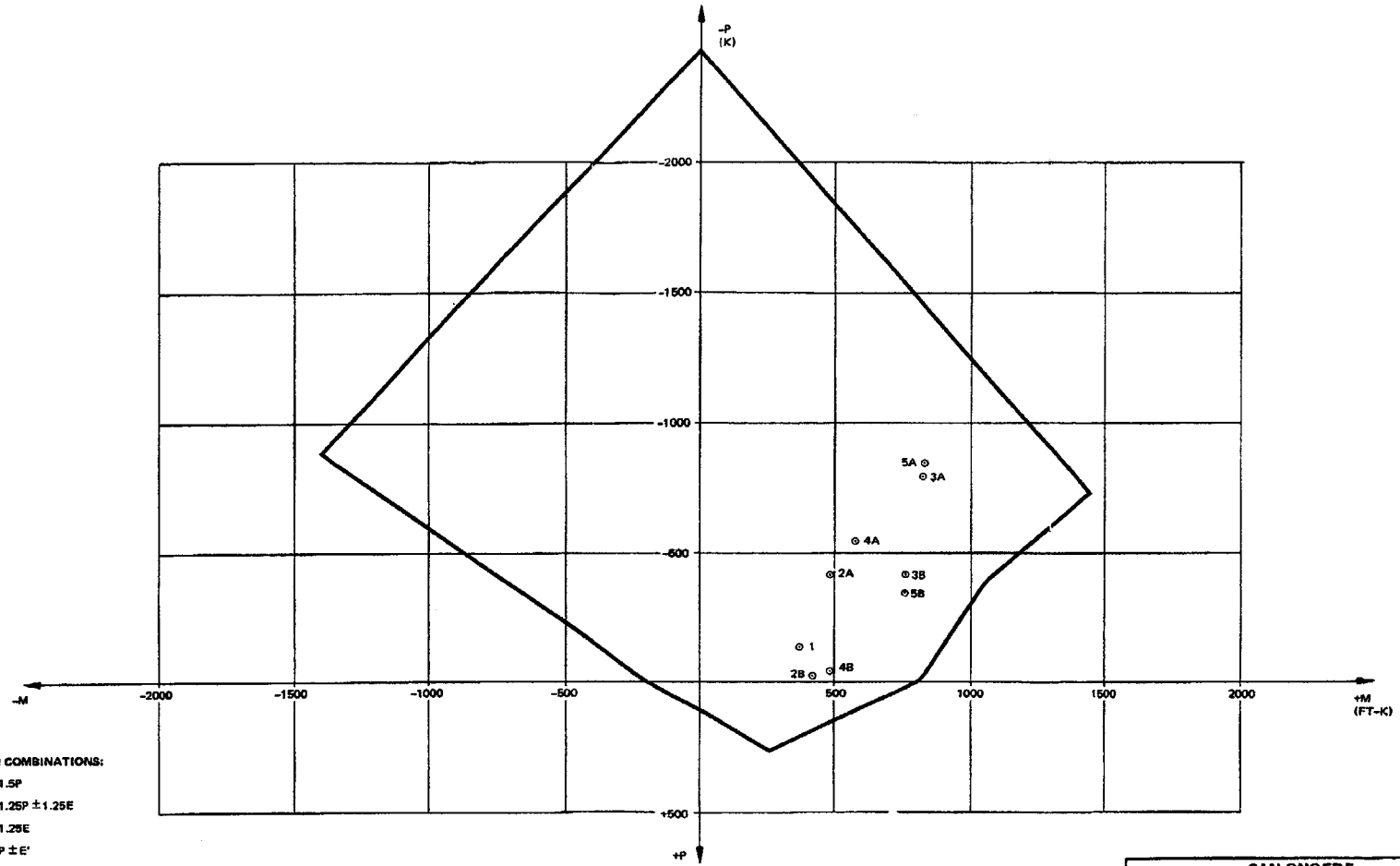

SECTION 5 — MERIDIONAL

GOVERNING LOADING COMBINATIONS:

1. $D + F + T_A + 1.5P$
2. $D + F + T_A + 1.25P \pm 1.25E$
3. $D + F + T_A \pm 1.25E$
4. $D + F + T_A + P \pm E'$
5. $D + F + T_A \pm E'$

NOTES:

1. REFER TO TABLE 3.8-2, SHEET 1, FOR SECTION NUMBER IDENTIFICATION
2. NOTATIONS "A" AND "B" IDENTIFY "PLUS" AND "MINUS" LOAD COMBINATIONS RESPECTIVELY.

Updated

SAN ONOFRE NUCLEAR GENERATING STATION
Units 2 & 3

CONTAINMENT STRUCTURE
INTERACTION DIAGRAMS
WITH ACTUAL RESULTS OF
PRINCIPAL LOAD COMBINATIONS
(Sheet 9 of 20)

Figure 3.8-22

10079-11D-285
11MY6

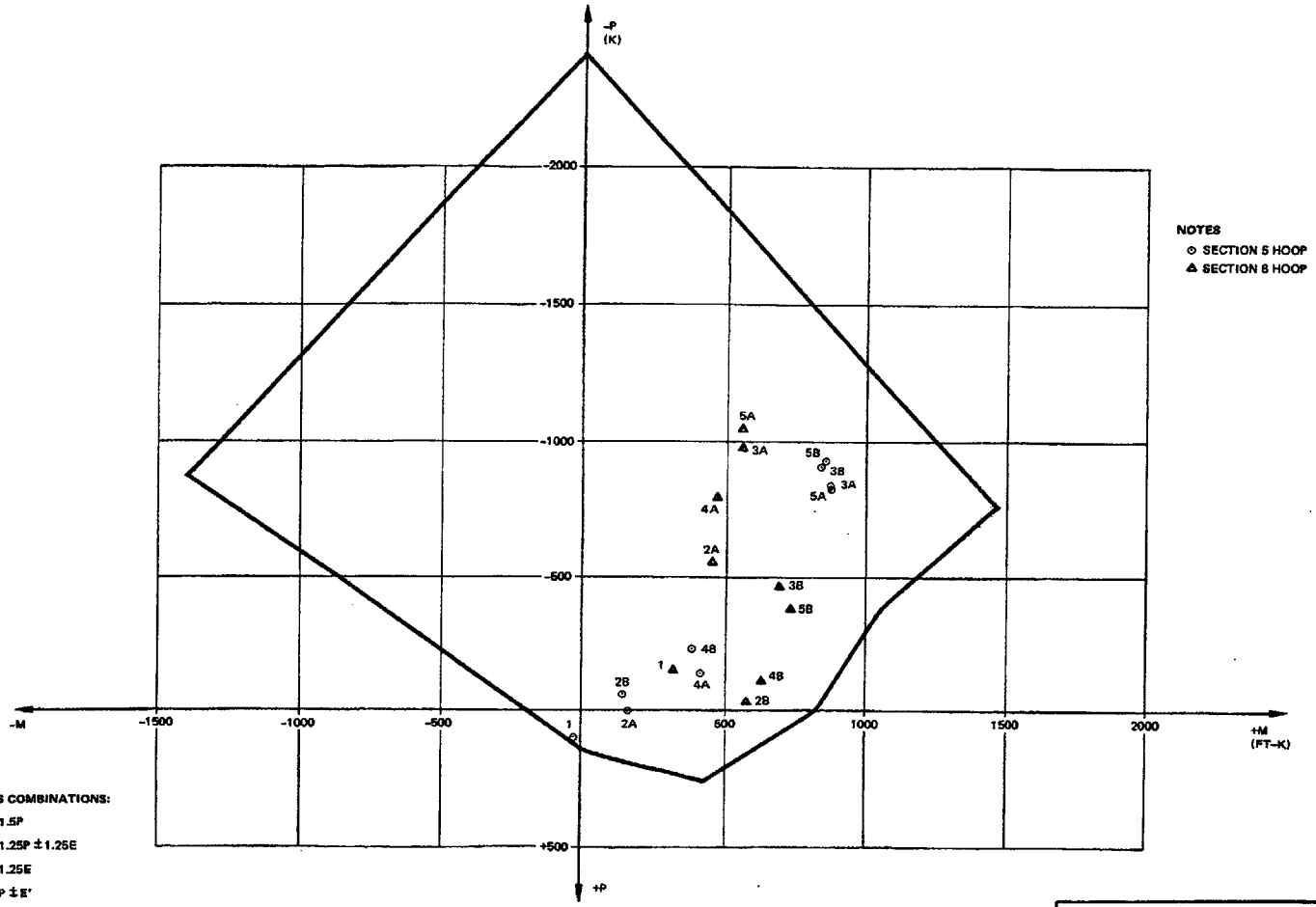

GOVERNING LOADING COMBINATIONS:

1. $D + F + T_A + 1.5P$
2. $D + F + T_A + 1.25P \pm 1.25E$
3. $D + F + T_A \pm 1.25E$
4. $D + F + T_A + P \pm E'$
5. $D + F + T_A \pm E'$

SECTION 5 AND 6 – HOOP

NOTES:

1. REFER TO TABLE 3.8-2, SHEET 1, FOR SECTION NUMBER IDENTIFICATION
2. NOTATIONS "A" AND "B" IDENTIFY "PLUS" AND "MINUS" LOAD COMBINATIONS RESPECTIVELY.

Updated

SAN ONOFRE NUCLEAR GENERATING STATION
Units 2 & 3

CONTAINMENT STRUCTURE INTERACTION DIAGRAMS WITH ACTUAL RESULTS OF PRINCIPAL LOAD COMBINATIONS (Sheet 10 of 20)

Figure 3.8-22

10079-11D-256
11MY6

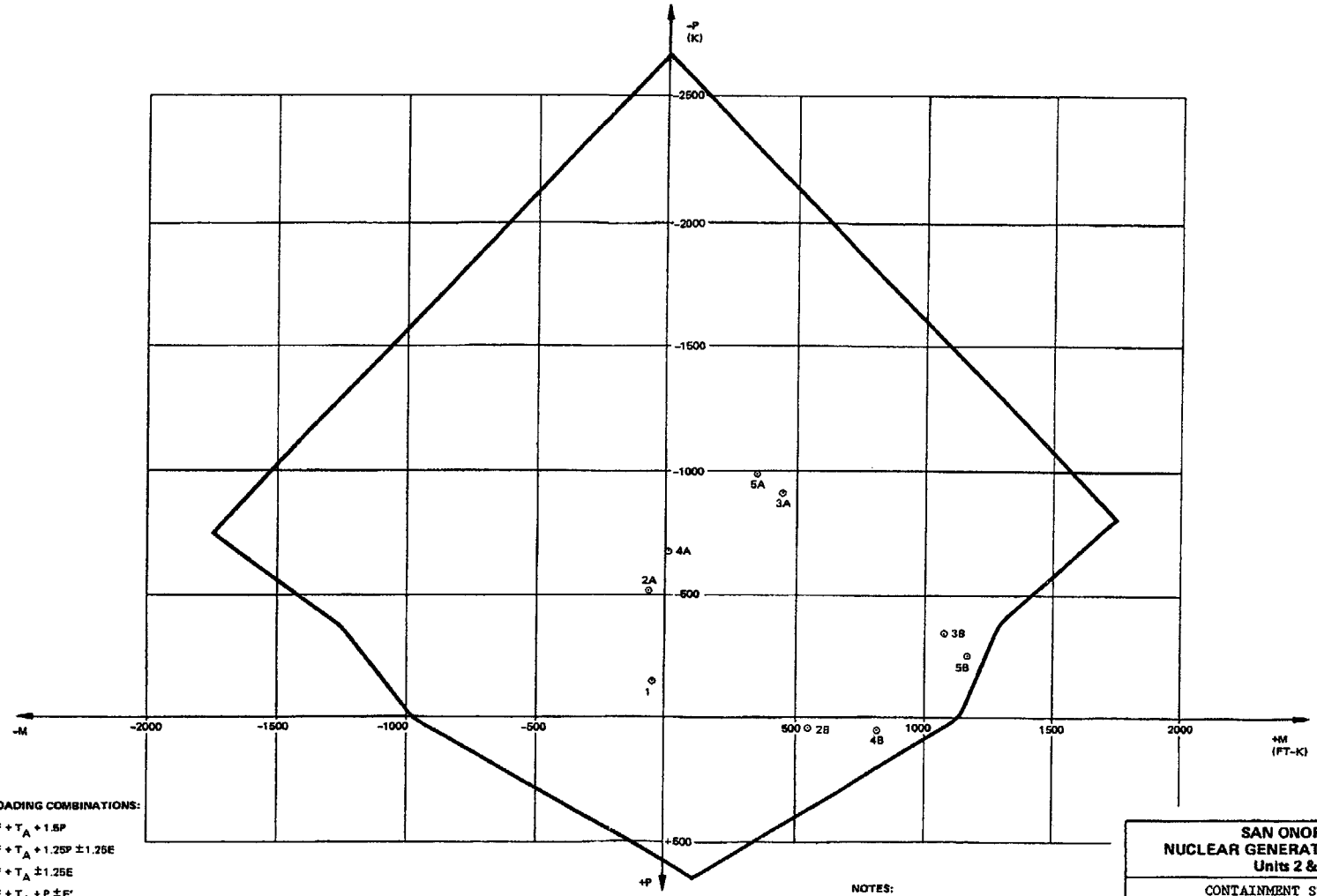

SECTION 6 – MERIDIONAL

GOVERNING LOADING COMBINATIONS:

1. $D + F + T_A + 1.5P$
2. $D + F + T_A + 1.25P \pm 1.25E$
3. $D + F + T_A \pm 1.25E$
4. $D + F + T_A + P \pm E'$
5. $D + F + T_A \pm E'$

NOTES:

1. REFER TO TABLE 3.8-2, SHEET 1, FOR SECTION NUMBER IDENTIFICATION
2. NOTATIONS "A" AND "B" IDENTIFY "PLUS" AND "MINUS" LOAD COMBINATIONS RESPECTIVELY.

Updated

SAN ONOFRE NUCLEAR GENERATING STATION Units 2 & 3

CONTAINMENT STRUCTURE INTERACTION DIAGRAMS WITH ACTUAL RESULTS OF PRINCIPAL LOAD COMBINATIONS (Sheet 11 of 20)

Figure 3.8-22

19079-11D-287
11MY6

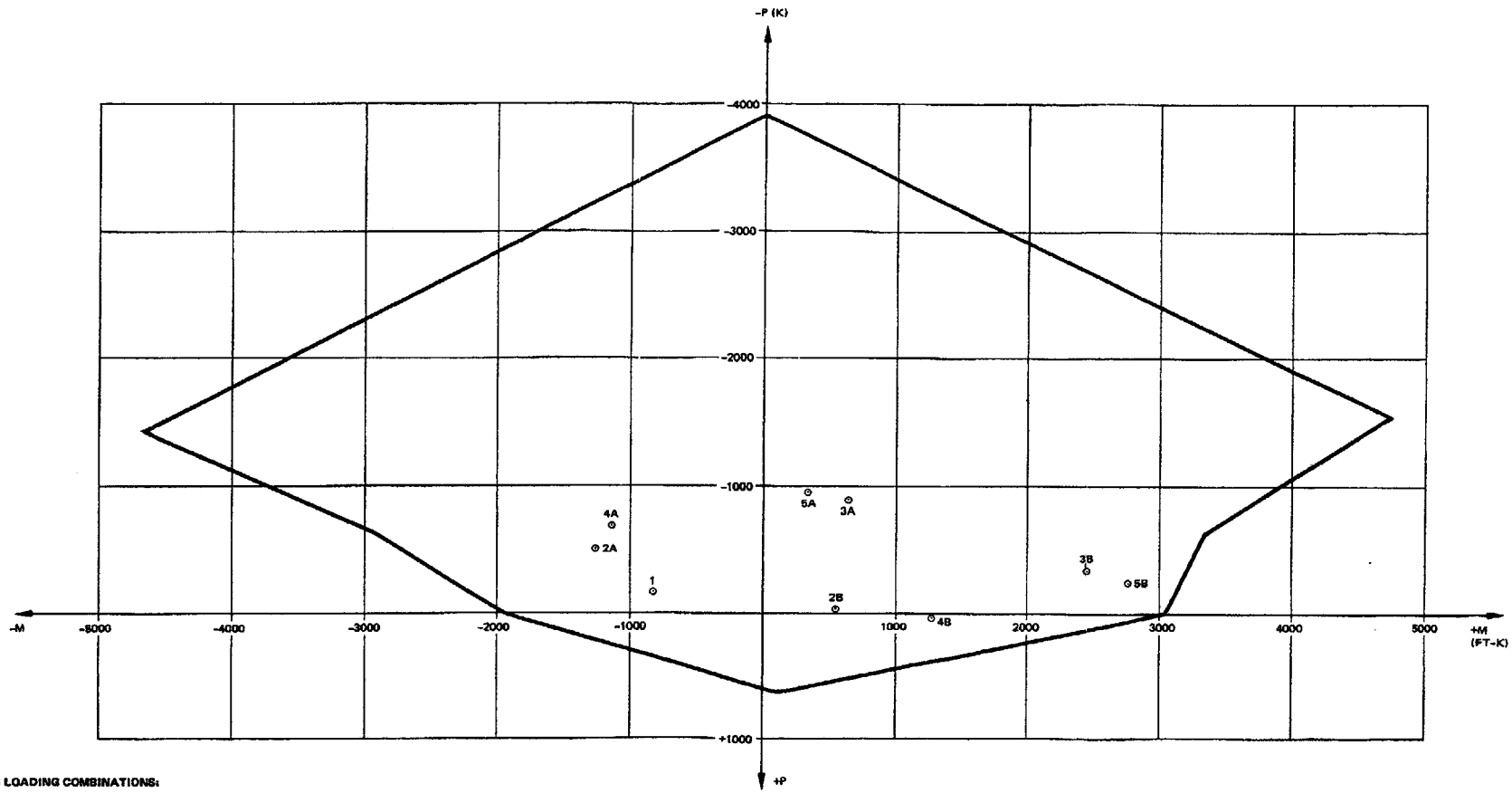

SECTION 7 – MERIDIONAL

GOVERNING LOADING COMBINATIONS:

1. $D + F + T_A + 1.5P$
2. $D + F + T_A + 1.25P \pm 1.25E$
3. $D + F + T_A \pm 1.25E$
4. $D + F + T_A + P \pm E'$
5. $D + F + T_A \pm E'$

NOTES:

1. REFER TO TABLE 3.8-2, SHEET 1, FOR SECTION NUMBER IDENTIFICATION
2. NOTATIONS "A" AND "B" IDENTIFY "PLUS" AND "MINUS" LOAD COMBINATIONS RESPECTIVELY.

Updated

SAN ONOFRE NUCLEAR GENERATING STATION Units 2 & 3

CONTAINMENT STRUCTURE INTERACTION DIAGRAMS WITH ACTUAL RESULTS OF PRINCIPAL LOAD COMBINATIONS (Sheet 12 of 20)

Figure 3.8-22

19079-11D-268
11MY6

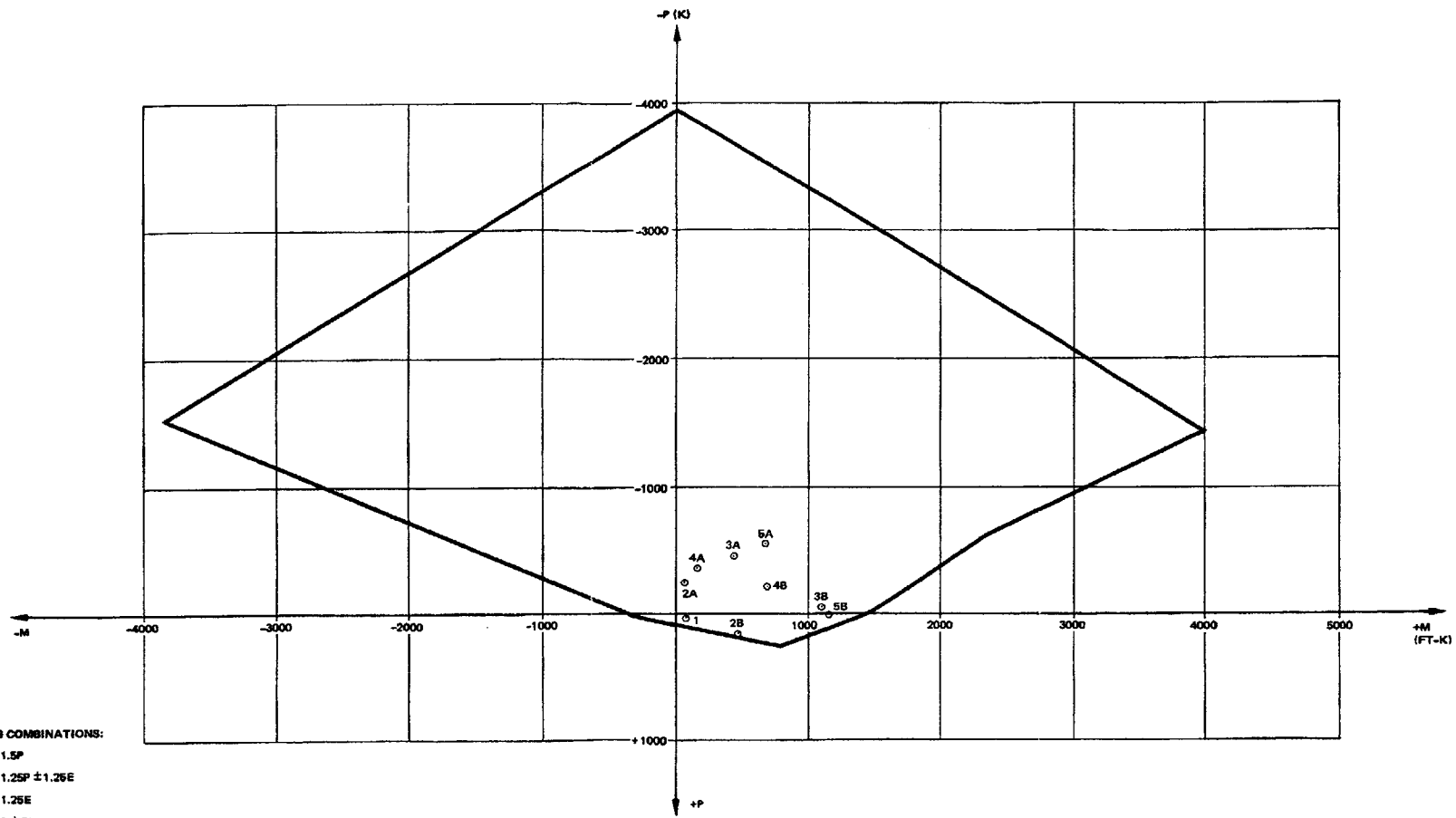

SECTION 7 – HOOP

GOVERNING LOADING COMBINATIONS:

1. $D + F + T_A + 1.5P$
2. $D + F + T_A + 1.25P \pm 1.25E$
3. $D + F + T_A \pm 1.25E$
4. $D + F + T_A + P \pm E'$
5. $D + F + T_A \pm E'$

NOTES:

1. REFER TO TABLE 3.8-2, SHEET 1, FOR SECTION NUMBER IDENTIFICATION
2. NOTATIONS "A" AND "B" IDENTIFY "PLUS" AND "MINUS" LOAD COMBINATIONS RESPECTIVELY.

Updated

SAN ONOFRE NUCLEAR GENERATING STATION
Units 2 & 3

CONTAINMENT STRUCTURE
INTERACTION DIAGRAMS
WITH ACTUAL RESULTS OF
PRINCIPAL LOAD COMBINATIONS
(Sheet 13 of 20)

Figure 3.8-22

10079-110-269

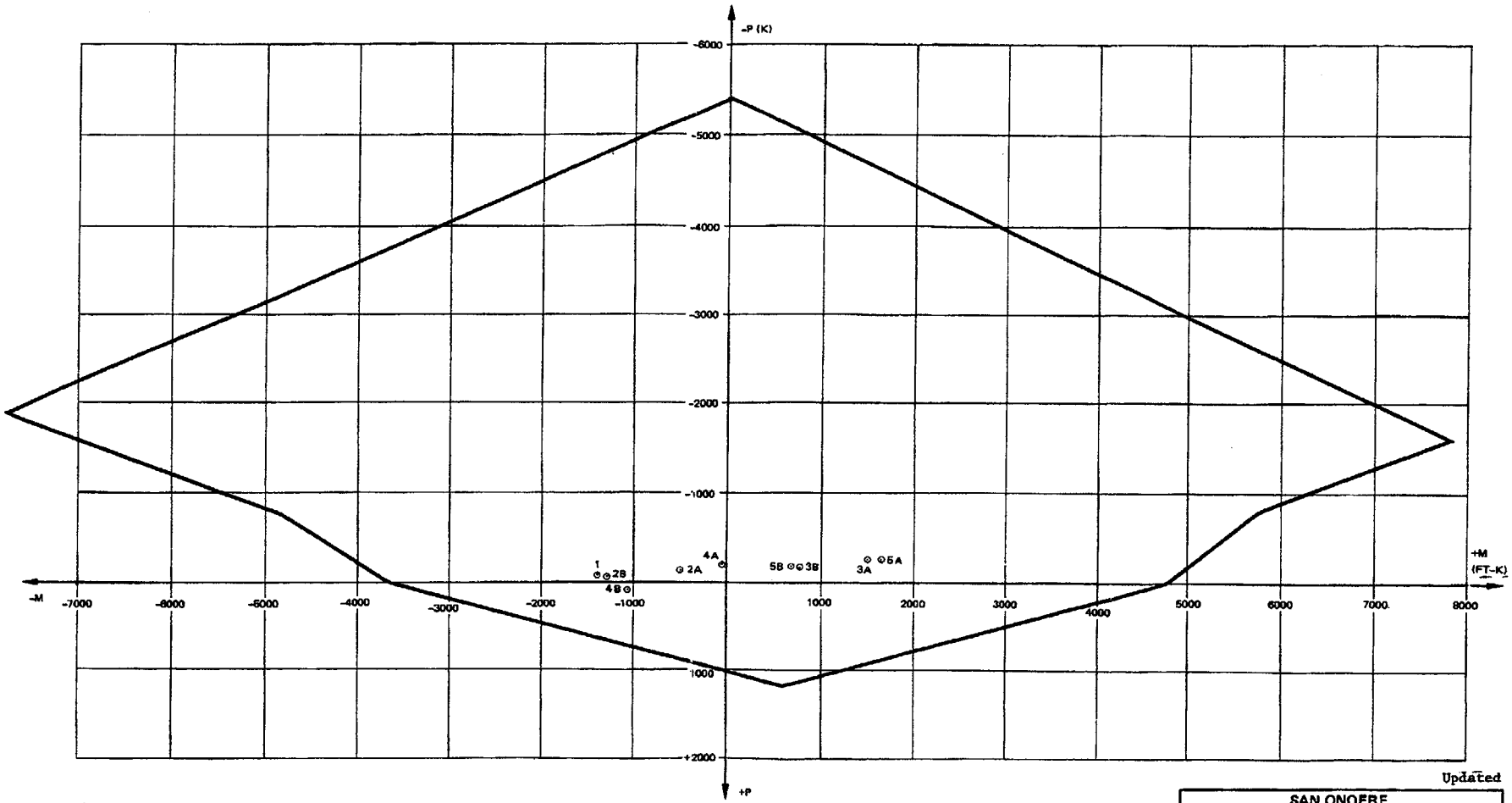

Updated

SECTION 8 – MERIDIONAL

GOVERNING LOADING COMBINATIONS:

1. $D + F + T_A + 1.5P$
2. $D + F + T_A + 1.25P \pm 1.25E$
3. $D + F + T_A \pm 1.25E$
4. $D + F + T_A + P \pm E'$
5. $D + F + T_A \pm E'$

NOTES:

1. REFER TO TABLE 3.8-2, SHEET 1, FOR SECTION NUMBER IDENTIFICATION
2. NOTATIONS "A" AND "B" IDENTIFY "PLUS" AND "MINUS" LOAD COMBINATIONS RESPECTIVELY.

SAN ONOFRE NUCLEAR GENERATING STATION
Units 2 & 3

CONTAINMENT STRUCTURE
INTERACTION DIAGRAMS
WITH ACTUAL RESULTS OF
PRINCIPAL LOAD COMBINATIONS
(Sheet 14 of 20)

Figure 3.8-22

10079-11D-290
11MY6

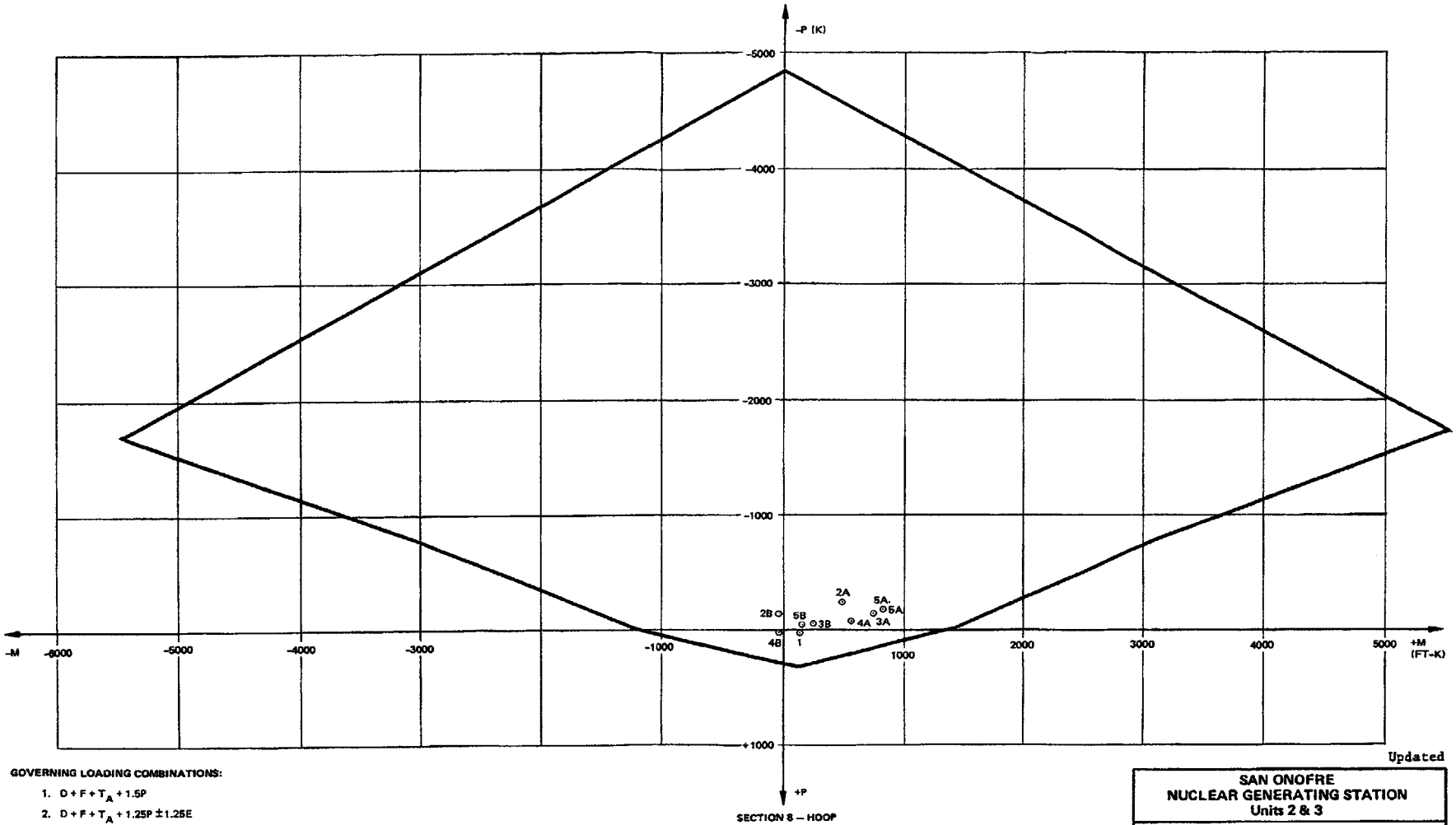

SECTION 8 – HOOP

GOVERNING LOADING COMBINATIONS:

1. $D + F + T_A + 1.5P$
2. $D + F + T_A + 1.25P \pm 1.25E$
3. $D + F + T_A \pm 1.25E$
4. $D + F + T_A + P \pm E'$
5. $D + F + T_A \pm E'$

NOTES:

1. REFER TO TABLE 3.8-2, SHEET 1, FOR SECTION NUMBER IDENTIFICATION
2. NOTATIONS "A" AND "B" IDENTIFY "PLUS" AND "MINUS" LOAD COMBINATIONS RESPECTIVELY.

Updated

SAN ONOFRE NUCLEAR GENERATING STATION
Units 2 & 3

CONTAINMENT STRUCTURE
INTERACTION DIAGRAMS
WITH ACTUAL RESULTS OF
PRINCIPAL LOAD COMBINATIONS
(Sheet 15 of 20)

Figure 3.8-22

10879-11D-291
11MY6

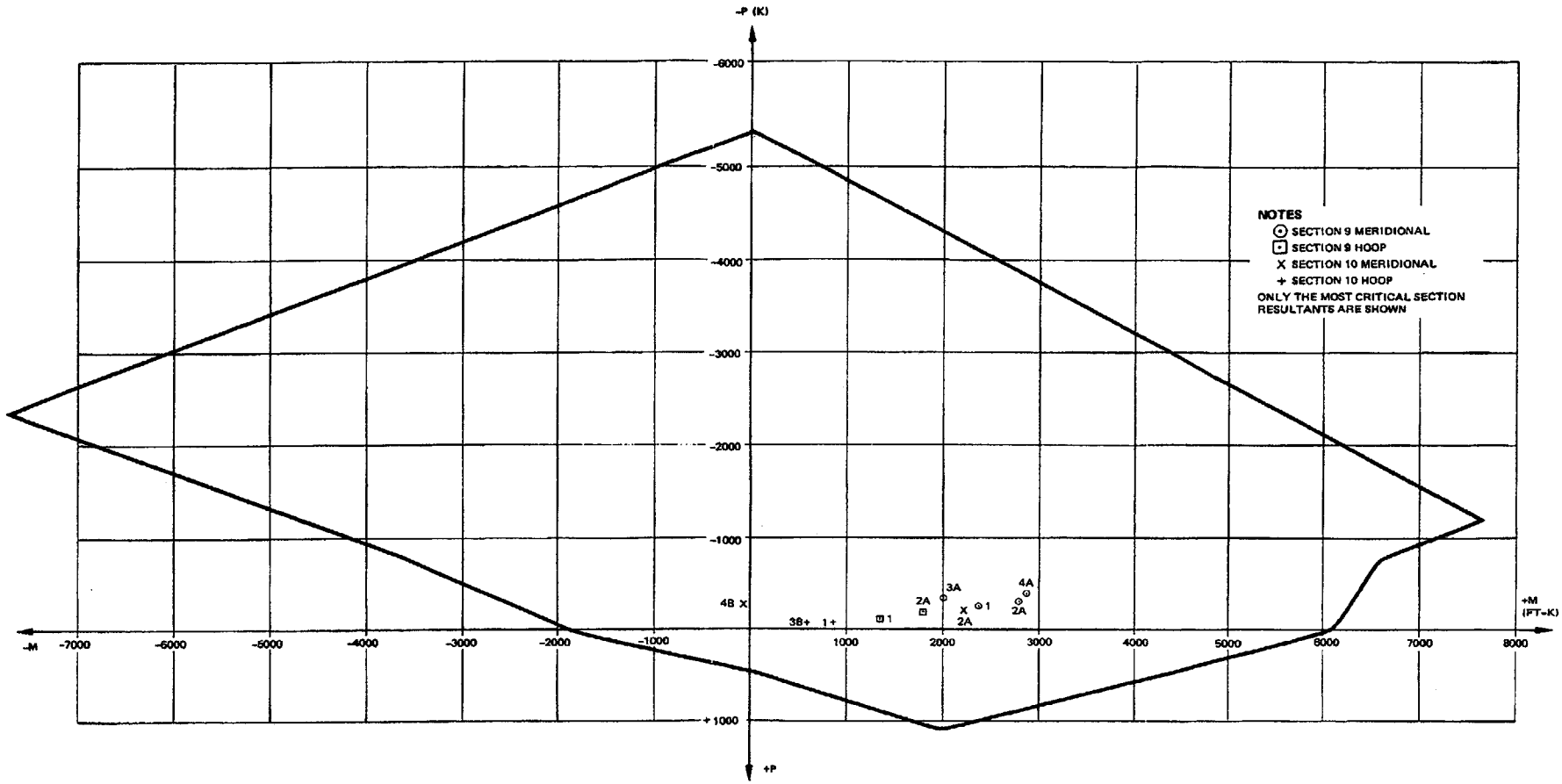

SECTIONS 9 AND 10 – MERIDIONAL AND HOOP

GOVERNING LOADING COMBINATIONS:

1. $D+F+T_A+1.5P$
2. $D+F+T_A+1.25P \pm 1.25E$
3. $D+F+T_A \pm 1.25E$
4. $D+F+T_A+P \pm E'$
5. $D+F+T_A \pm E'$

NOTES:

1. REFER TO TABLE 3.8-2, SHEET 1, FOR SECTION NUMBER IDENTIFICATION
2. NOTATIONS "A" AND "B" IDENTIFY "PLUS" AND "MINUS" LOAD COMBINATIONS RESPECTIVELY

Updated

SAN ONOFRE NUCLEAR GENERATING STATION
Units 2 & 3

CONTAINMENT STRUCTURE INTERACTION DIAGRAMS WITH ACTUAL RESULTS OF PRINCIPAL LOAD COMBINATIONS (Sheet 16 of 20)

Figure 3.8-22

10079-11D-29Z
11MY6

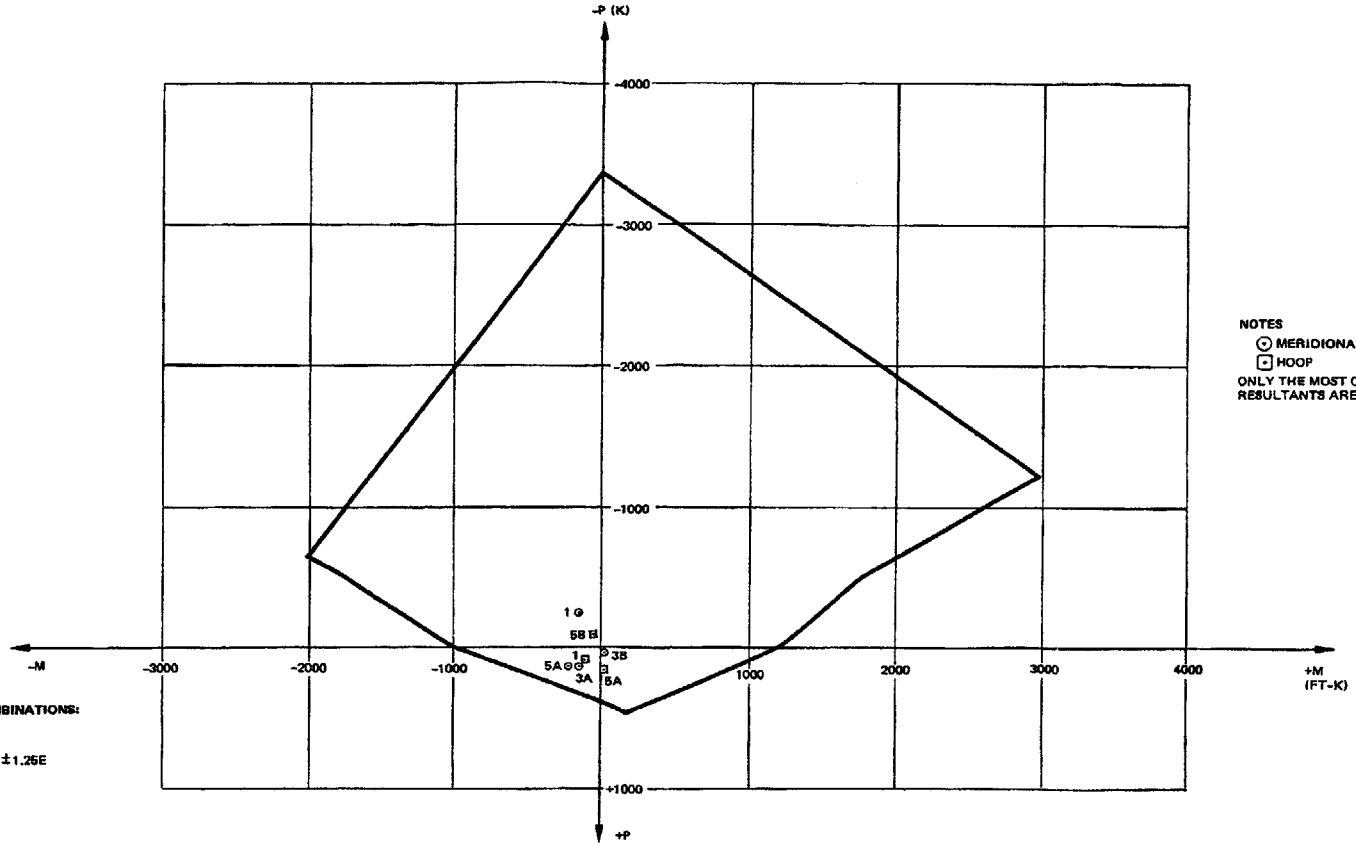

SECTION II – MERIDIONAL AND HOOP

GOVERNING LOADING COMBINATIONS:

1. $D + F + T_A + 1.5P$
2. $D + F + T_A + 1.25P \pm 1.25E$
3. $D + F + T_A \pm 1.25E$
4. $D + F + T_A + P \pm E'$
5. $D + F + T_A \pm E'$

NOTES:

1. REFER TO TABLE 3.8-2, SHEET 1, FOR SECTION NUMBER IDENTIFICATION
2. NOTATIONS "A" AND "B" IDENTIFY "PLUS" AND "MINUS" LOAD COMBINATIONS RESPECTIVELY.

Updated

SAN ONOFRE NUCLEAR GENERATING STATION Units 2 & 3
CONTAINMENT STRUCTURE INTERACTION DIAGRAMS WITH ACTUAL RESULTS OF PRINCIPAL LOAD COMBINATIONS (Sheet 17 of 20)
Figure 3.8-22

10079-11D-293

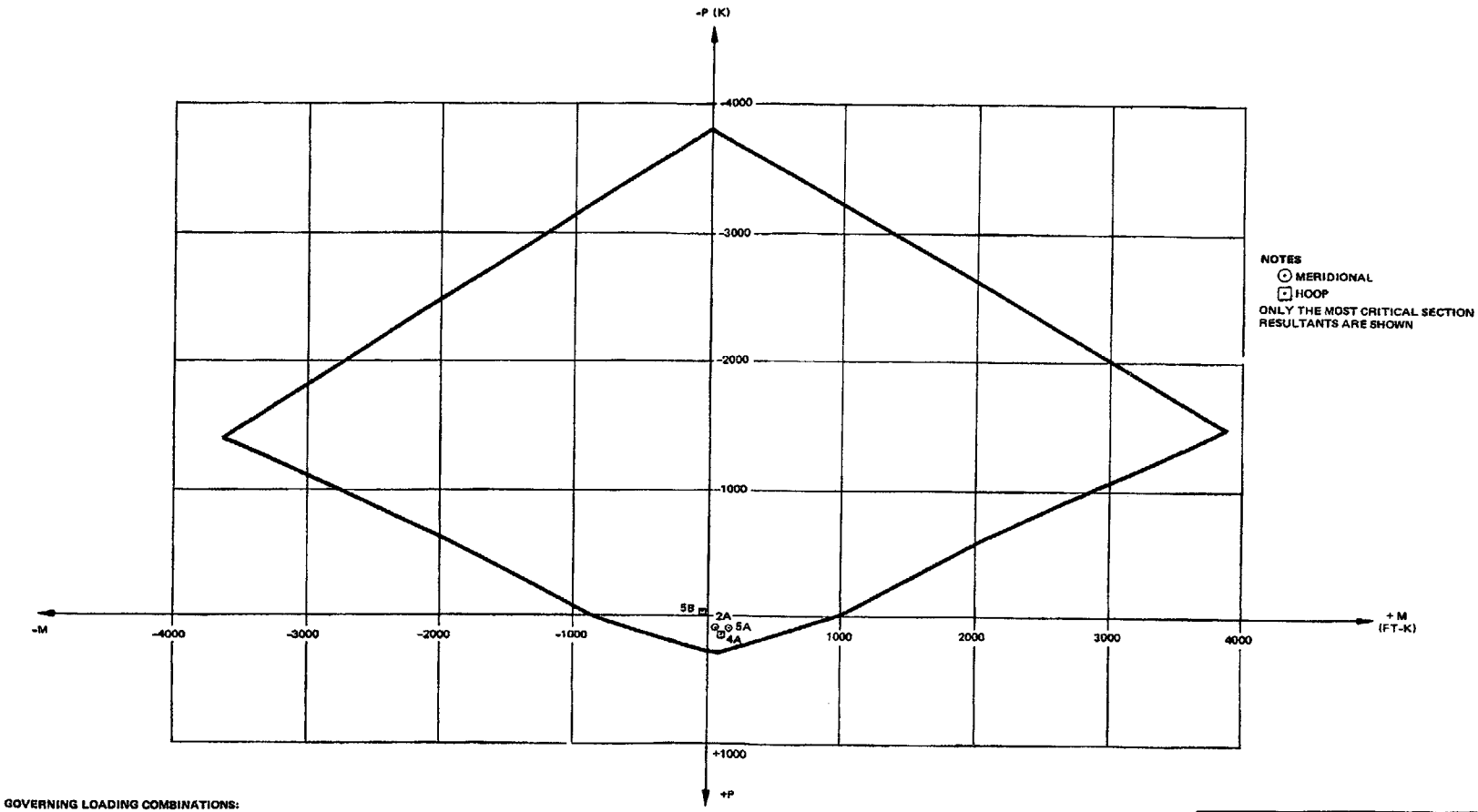

SECTION 12 – MERIDIONAL AND HOOP

GOVERNING LOADING COMBINATIONS:

1. $D + F + T_A + 1.5P$
2. $D + F + T_A + 1.25P \pm 1.25E$
3. $D + F + T_A \pm 1.25E$
4. $D + F + T_A + P \pm E'$
5. $D + F + T_A \pm E'$

NOTES:

1. REFER TO TABLE 3.8-2, SHEET 1; FOR SECTION NUMBER IDENTIFICATION
2. NOTATIONS "A" AND "B" IDENTIFY "PLUS" AND "MINUS" LOAD COMBINATIONS RESPECTIVELY.

Updated

SAN ONOFRE NUCLEAR GENERATING STATION
Units 2 & 3

CONTAINMENT STRUCTURE INTERACTION DIAGRAMS WITH ACTUAL RESULTS OF PRINCIPAL LOAD COMBINATIONS (Sheet 18 of 20)

Figure 3.8-22

10070-11D-294
11MY6

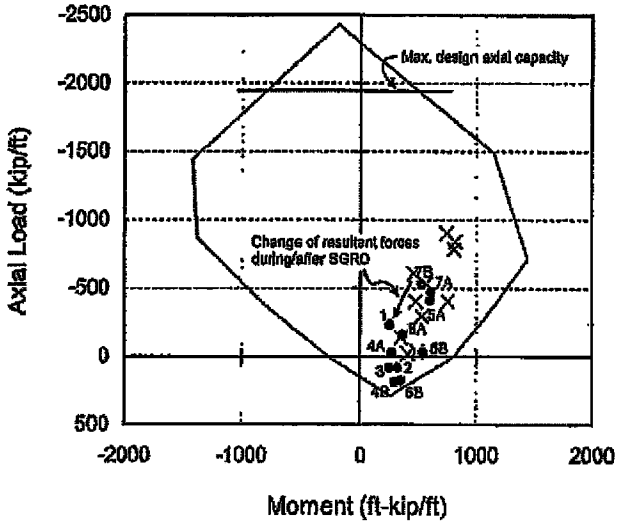

Load Combinations:

1. $D + F + T_0 + (\Delta D + \Delta F)$
2. $D + F + T_A + P + (\Delta D + \Delta F)$
3. $D + F + T_A + 1.5P + (\Delta D + \Delta F)$
4. $D + F + T_A + 1.25P + 1.25E + (\Delta D + \Delta F)$
5. $D + F + T_A + 1.25E + (\Delta D + \Delta F)$
6. $D + F + T_A + P + E' + (\Delta D + \Delta F)$
7. $D + F + T_A + E' + (\Delta D + \Delta F)$

Sign Conventions are:

Axial forces (+) Tension
(–) Compression
Moments (+) Tension on the outside face
(–) Compression on the outside face

X Original loading points
● Updated loading points
A/B: Opposite seismic forces

Interaction Diagram in Meridional Direction for the Restored Opening Area

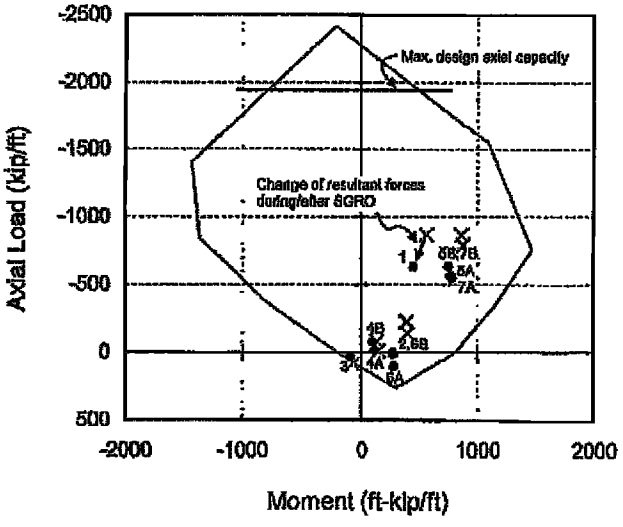

Load Combinations:

1. $D + F + T_0 + (\Delta D + \Delta F)$
2. $D + F + T_A + P + (\Delta D + \Delta F)$
3. $D + F + T_A + 1.5P + (\Delta D + \Delta F)$
4. $D + F + T_A + 1.25P + 1.25E + (\Delta D + \Delta F)$
5. $D + F + T_A + 1.25E + (\Delta D + \Delta F)$
6. $D + F + T_A + P + E' + (\Delta D + \Delta F)$
7. $D + F + T_A + E' + (\Delta D + \Delta F)$

Sign Conventions are:

Axial forces (+) Tension
(–) Compression
Moments (+) Tension on the outside face
(–) Compression on the outside face

X Original loading points
● Updated loading points
A/B: Opposite seismic forces

Interaction Diagram in Hoop Direction for the Restored Opening Area

CONTAINMENT RESTORED CONDITION

CONTAINMENT STRUCTURE INTERACTION DIAGRAMS WITH ACTUAL RESULTS OF PRINCIPAL LOAD COMBINATIONS

Sheet 19 of 20

Figure 3.8-22.

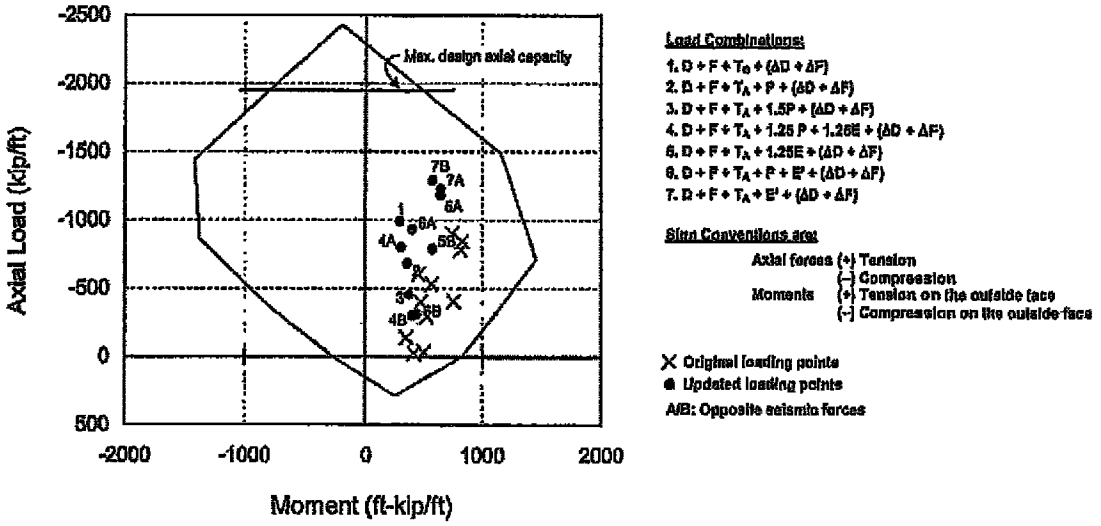

Interaction Diagram in Meridional Direction Adjacent to the Restored Opening Area

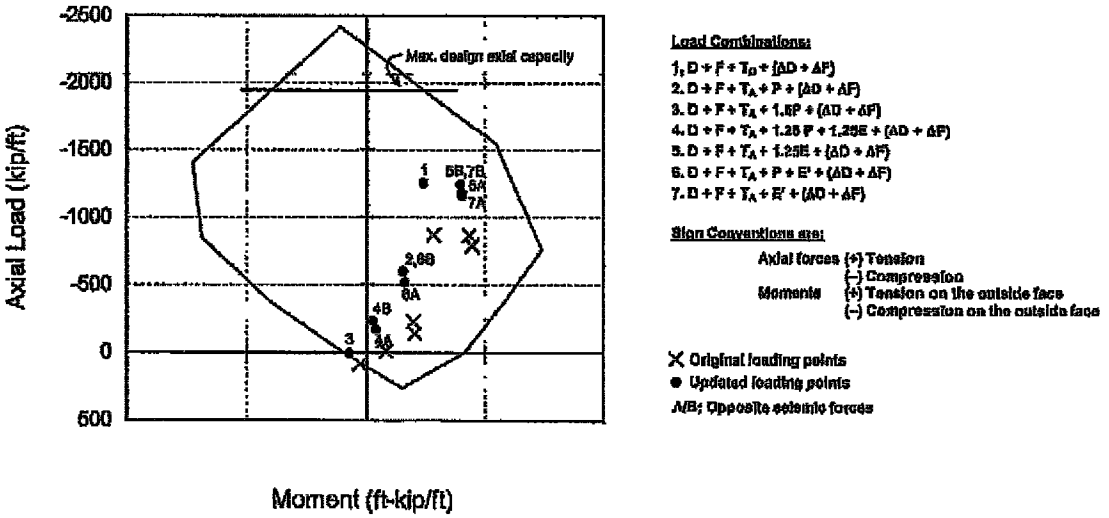

Interaction Diagram in Hoop Direction Adjacent to the Restored Opening Area

CONTAINMENT RESTORED CONDITION

CONTAINMENT STRUCTURE INTERACTION DIAGRAMS WITH ACTUAL RESULTS OF PRINCIPAL LOAD COMBINATIONS

Sheet 20 of 20

Figure 3.8-22

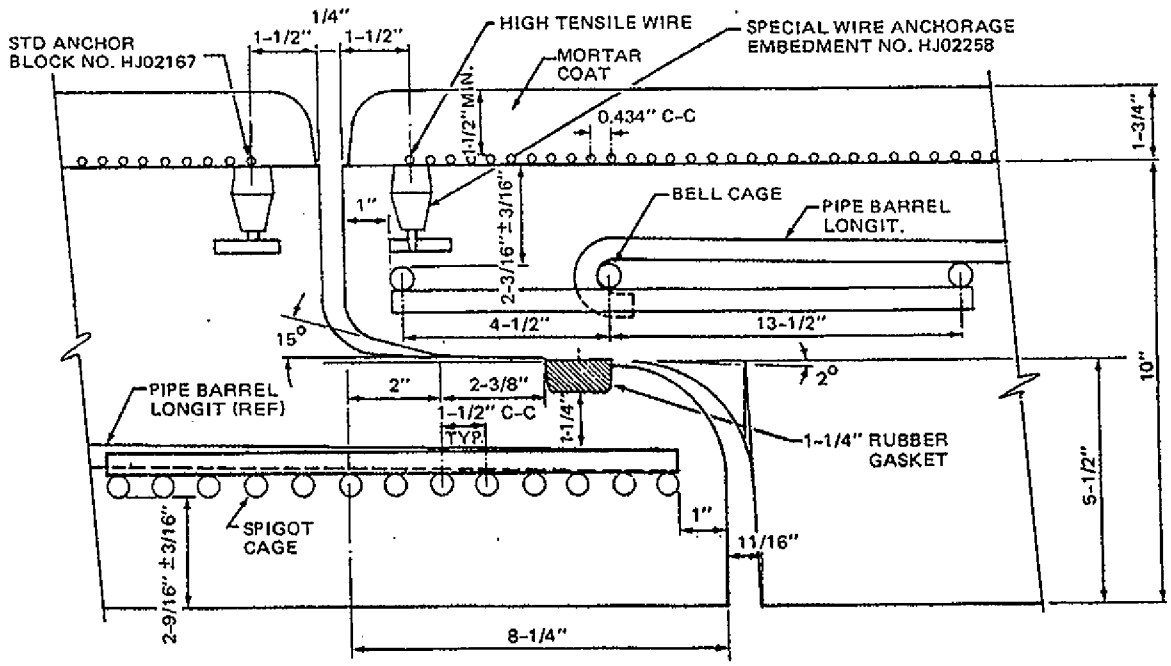

SAN ONOFRE NUCLEAR GENERATING STATION Units 2 & 3
JOINT DETAIL
Figure 3.8-50

10079
29SEP78

Amended: April 2009 TL: E047997

Site File Copy

Figure 3.8-51

FINAL ANALYSIS LOADING COMBINATIONS
OF CONTAINMENT SHELL
(For use with Table 3.8-2)

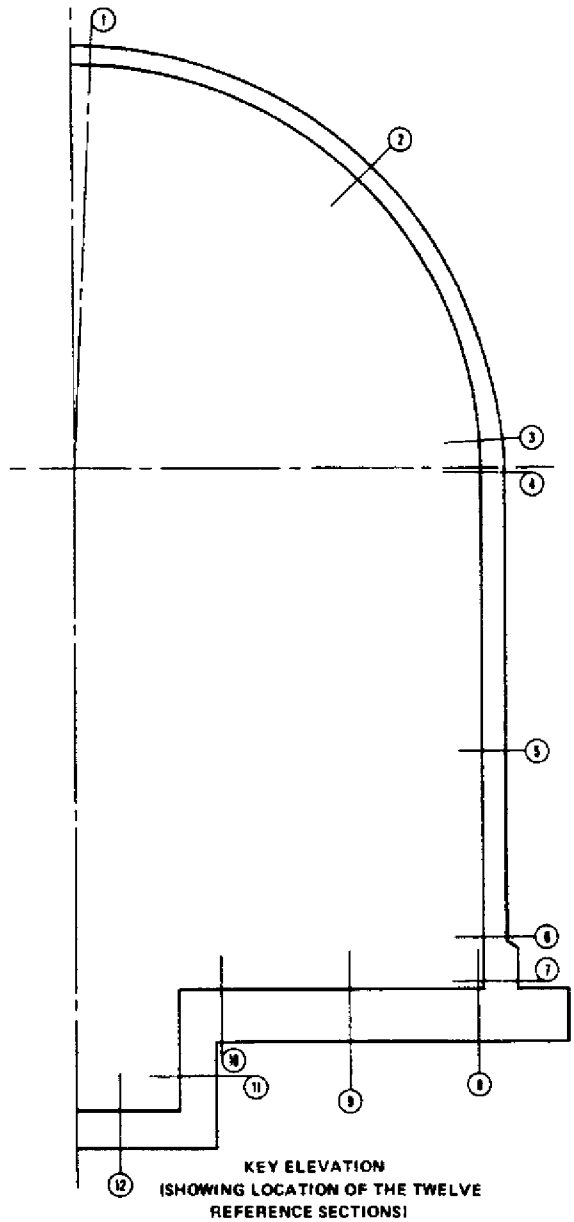

Site File Copy

3.7A APPENDIX 3.7A

SEISMIC RESPONSE SPECTRA

The SONGS design seismic response spectra are provided in the following figures and listed in Table 3.7A-1:

- 3.7A-1 Design Basis Earthquake Vertical Acceleration Response Spectra, Parallel to Hot Leg Reactor Vessel Column Support
- 3.7A-2 Design Basis Earthquake Horizontal Acceleration Response Spectra, Parallel to Hot Leg Reactor Vessel Column Support
- 3.7A-3 Design Basis Earthquake Horizontal Acceleration Response Spectra, Parallel to Hot Leg Reactor Vessel Base Shear Key
- 3.7A-4 Design Basis Earthquake Horizontal Acceleration Response Spectra, Parallel to Hot Leg Reactor Vessel Nozzle Restraint
- 3.7A-5 Design Basis Earthquake Vertical Acceleration Response Spectra, Parallel to Hot Leg Steam Generator Base Support
- 3.7A-6 Design Basis Earthquake Horizontal Acceleration Response Spectra, Parallel to Hot Leg Steam Generator Snubber Support
- 3.7A-7 Design Basis Earthquake Vertical Acceleration Response Spectra, Parallel to Hot Leg RCP Base Support
- 3.7A-8 Design Basis Earthquake Horizontal Acceleration Response Spectra, Parallel to Hot Leg RCP Lower Horizontal Support
- 3.7A-9 Design Basis Earthquake Horizontal Acceleration Response Spectra, Parallel to Hot Leg RCP Upper Horizontal Support
- 3.7A-10 Design Basis Earthquake Horizontal Acceleration Response Spectra, Parallel to Hot Leg RCP Snubber Support
- 3.7A-11 Design Basis Earthquake Vertical Acceleration Response Spectra, Parallel to Hot Leg Pressurizer Base Support
- 3.7A-12 Design Basis Earthquake Horizontal Acceleration Response Spectra, Parallel to Hot Leg Pressurizer Base Support

- 3.7A-13 Design Basis Earthquake Horizontal Acceleration Response Spectra, Parallel to Hot Leg Pressurizer Shear Key Support
- 3.7A-14 Design Basis Earthquake Vertical Acceleration Response Spectra, Perpendicular to Hot Leg Reactor Vessel Column Support
- 3.7A-15 Design Basis Earthquake Horizontal Acceleration Response Spectra, Perpendicular to Hot Leg Reactor Vessel Column Support
- 3.7A-16 Design Basis Earthquake Horizontal Acceleration Response Spectra, Perpendicular to Hot Leg Reactor Vessel Base Shear Key
- 3.7A-17 Design Basis Earthquake Horizontal Acceleration Response Spectra, Perpendicular to Hot Leg Reactor Vessel Nozzle Restraints
- 3.7A-18 Design Basis Earthquake Vertical Acceleration Response Spectra, Perpendicular to Hot Leg Steam Generator Base Support
- 3.7A-19 Design Basis Earthquake Horizontal Acceleration Response Spectra, Perpendicular to Hot Leg Steam Generator Base Support
- 3.7A-20 Design Basis Earthquake Horizontal Acceleration Response Spectra, Perpendicular to Hot Leg Steam Generator Shear Key Support
- 3.7A-21 Design Basis Earthquake Vertical Acceleration Response Spectra, Perpendicular to Hot Leg RCP Base Support
- 3.7A-22 Design Basis Earthquake Horizontal Acceleration Response Spectra, Perpendicular to Hot Leg RCP Lower Horizontal Support
- 3.7A-23 Design Basis Earthquake Horizontal Acceleration Response Spectra, Perpendicular to Hot Leg RCP Upper Horizontal Support
- 3.7A-24 Design Basis Earthquake Horizontal Acceleration Response Spectra, Perpendicular to Hot Leg RCP Snubber Support
- 3.7A-25 Design Basis Earthquake Vertical Acceleration Response Spectra, Perpendicular to Hot Leg Pressurizer Base Support
- 3.7A-26 Design Basis Earthquake Horizontal Acceleration Response Spectra, Perpendicular to Hot Leg Pressurizer Base Support
- 3.7A-27 Design Basis Earthquake Horizontal Acceleration Response Spectra, Perpendicular to Hot Leg Pressurizer Shear Key Support

- 3.7A-28 Operating Basis Earthquake Vertical Acceleration Response Spectra, Parallel to Hot Leg Reactor Vessel Column Support
- 3.7A-29 Operating Basis Earthquake Horizontal Acceleration Response Spectra, Parallel to Hot Leg Reactor Vessel Column Support
- 3.7A-30 Operating Basis Earthquake Horizontal Acceleration Response Spectra, Parallel to Hot Leg Reactor Vessel Base Shear Key
- 3.7A-31 Operating Basis Earthquake Horizontal Acceleration Response Spectra, Parallel to Hot Leg Reactor Vessel Nozzle Restraint
- 3.7A-32 Operating Basis Earthquake Vertical Acceleration Response Spectra, Parallel to Hot Leg Steam Generator Base Support
- 3.7A-33 Operating Basis Earthquake Horizontal Acceleration Response Spectra, Parallel to Hot Leg Steam Generator Snubber Support
- 3.7A-34 Operating Basis Earthquake Vertical Acceleration Response Spectra, Parallel to Hot Leg RCP Base Support
- 3.7A-35 Operating Basis Earthquake Horizontal Acceleration Response Spectra, Parallel to Hot Leg RCP Lower Horizontal Support
- 3.7A-36 Operating Basis Earthquake Horizontal Acceleration Response Spectra, Parallel to Hot Leg RCP Upper Horizontal Support
- 3.7A-37 Operating Basis Earthquake Horizontal Acceleration Response Spectra, Parallel to Hot Leg RCP Snubber Support
- 3.7A-38 Operating Basis Earthquake Vertical Acceleration Response Spectra, Parallel to Hot Leg Pressurizer Base Support
- 3.7A-39 Operating Basis Earthquake Horizontal Acceleration Response Spectra, Parallel to Hot Leg Pressurizer Base Support
- 3.7A-40 Operating Basis Earthquake Horizontal Acceleration Response Spectra, Parallel to Hot Leg Pressurizer Shear Key Support
- 3.7A-41 Operating Basis Earthquake Vertical Acceleration Response Spectra, Perpendicular to Hot Leg Reactor Vessel Column Support
- 3.7A-42 Operating Basis Earthquake Horizontal Acceleration Response Spectra, Perpendicular to Hot Leg Reactor Vessel Column Support

- 3.7A-43 Operating Basis Earthquake Horizontal Acceleration Response Spectra, Perpendicular to Hot Leg Reactor Vessel Base Shear Key
- 3.7A-44 Operating Basis Earthquake Horizontal Acceleration Response Spectra, Perpendicular to Hot Leg Reactor Vessel Nozzle Restraints
- 3.7A-45 Operating Basis Earthquake Vertical Acceleration Response Spectra, Perpendicular to Hot Leg Steam Generator Base Support
- 3.7A-46 Operating Basis Earthquake Horizontal Acceleration Response Spectra, Perpendicular to Hot Leg Steam Generator Base Support
- 3.7A-47 Operating Basis Earthquake Horizontal Acceleration Response Spectra, Perpendicular to Hot Leg Steam Generator Shear Key Support
- 3.7A-48 Operating Basis Earthquake Vertical Acceleration Response Spectra, Perpendicular to Hot Leg RCP Base Support
- 3.7A-49 Operating Basis Earthquake Horizontal Acceleration Response Spectra, Perpendicular to Hot Leg RCP Lower Horizontal Support
- 3.7A-50 Operating Basis Earthquake Horizontal Acceleration Response Spectra, Perpendicular to Hot Leg RCP Upper Horizontal Support
- 3.7A-51 Operating Basis Earthquake Horizontal Acceleration Response Spectra, Perpendicular to Hot Leg RCP Snubber Support
- 3.7A-52 Operating Basis Earthquake Vertical Acceleration Response Spectra, Perpendicular to Hot Leg Pressurizer Base Support
- 3.7A-53 Operating Basis Earthquake Horizontal Acceleration Response Spectra, Perpendicular to Hot Leg Pressurizer Base Support
- 3.7A-54 Operating Basis Earthquake Horizontal Acceleration Response Spectra, Perpendicular to Hot Leg Pressurizer Shear Key Support
- 3.7A-55 Design Basis Earthquake Vertical Acceleration Response Spectra, for Containment Interior Structure Basemat
- 3.7A-56 Design Basis Earthquake Horizontal Acceleration Response Spectra, for Containment Interior Structure Basemat
- 3.7A-57 Design Basis Earthquake Vertical Acceleration Response Spectra, for Containment Interior Structure - Elevation 63'-6"

- 3.7A-58 Design Basis Earthquake Horizontal Acceleration Response Spectra, for Containment Interior Structure - Elevation 63'-6"
- 3.7A-59 Design Basis Earthquake Vertical Acceleration Response Spectra, for Containment Interior Structure - Elevation 80'-6"
- 3.7A-60 Design Basis Earthquake Horizontal Acceleration Response Spectra, for Containment Interior Structure - Elevation 80'-6"
- 3.7A-61 Design Basis Earthquake Vertical Acceleration Response Spectra, for Containment Exterior Shell Basemat
- 3.7A-62 Design Basis Earthquake Horizontal Acceleration Response Spectra, for Containment Exterior Shell Basemat
- 3.7A-63 Design Basis Earthquake Vertical Acceleration Response Spectra, for Containment Exterior Shell - Elevation 177'-6"
- 3.7A-64 Design Basis Earthquake Horizontal Acceleration Response Spectra, for Containment Exterior Shell - Elevation 177'-6"
- 3.7A-65 Operating Basis Earthquake Vertical Acceleration Response Spectra, for Containment Interior Structure Basemat
- 3.7A-66 Operating Basis Earthquake Horizontal Acceleration Response Spectra, for Containment Interior Structure Basemat
- 3.7A-67 Operating Basis Earthquake Vertical Acceleration Response Spectra, for Containment Interior Structure - Elevation 63'-6"
- 3.7A-68 Operating Basis Earthquake Horizontal Acceleration Response Spectra, for Containment Interior Structure - Elevation 63'-6"
- 3.7A-69 Operating Basis Earthquake Vertical Acceleration Response Spectra, for Containment Interior Structure - Elevation 80'-6"
- 3.7A-70 Operating Basis Earthquake Horizontal Acceleration Response Spectra, for Containment Interior Structure - Elevation 80'-6"
- 3.7A-71 Operating Basis Earthquake Vertical Acceleration Response Spectra, for Containment Exterior Shell Basemat
- 3.7A-72 Operating Basis Earthquake Horizontal Acceleration Response Spectra, for Containment Exterior Shell Basemat

- 3.7A-73 Operating Basis Earthquake Vertical Acceleration Response Spectra, for Containment Exterior Shell - Elevation 177'-6"
- 3.7A-74 Operating Basis Earthquake Horizontal Acceleration Response Spectra, for Containment Exterior Shell - Elevation 177'-6"
- 3.7A-75 Design Basis Earthquake Vertical Acceleration Response Spectra, at Node 1 Elevation 9'-0" of Auxiliary Building
- 3.7A-76 Design Basis Earthquake Horizontal Acceleration Response Spectra, at Node 1 Elevation 9'-0" of Auxiliary Building
- 3.7A-77 Design Basis Earthquake Vertical Acceleration Response Spectra, at Node 12 Elevation 85'-0" of Auxiliary Building
- 3.7A-78 Design Basis Earthquake Horizontal Acceleration Response Spectra, at Node 12 Elevation 85'-0" of Auxiliary Building
- 3.7A-79 Operating Basis Earthquake Vertical Acceleration Response Spectra, at Node 1 Elevation 9'-0" of Auxiliary Building
- 3.7A-80 Operating Basis Earthquake Horizontal Acceleration Response Spectra, at Node 1 Elevation 9'-0" of Auxiliary Building
- 3.7A-81 Operating Basis Earthquake Vertical Acceleration Response Spectra, at Node 12 Elevation 85'-0" of Auxiliary Building
- 3.7A-82 Operating Basis Earthquake Horizontal Acceleration Response Spectra, at Node 12 Elevation 85'-0" of Auxiliary Building
- 3.7A-83 Design Basis Earthquake Vertical Acceleration Response Spectra, at Node 12A Elevation 85'-0" of Central Control Area Auxiliary Building
- 3.7A-84 Operating Basis Earthquake Vertical Acceleration Response Spectra, at Node 12A Elevation 85'-0" of Central Control Area Auxiliary Building
- 3.7A-85 Design Basis Earthquake Vertical Acceleration Response Spectra, at Node 1 Elevation 17'-6" of Fuel Handling Building
- 3.7A-86 Design Basis Earthquake Horizontal Acceleration Response Spectra, at Node 1 Elevation 17'-6" of Fuel Handling Building
- 3.7A-87 Operating Basis Earthquake Vertical Acceleration Response Spectra, at Node 1 Elevation 17'-6" of Fuel Handling Building

- 3.7A-88 Operating Basis Earthquake Horizontal Acceleration Response Spectra, at Node 1 Elevation 17'-6" of Fuel Handling Building
- 3.7A-89 Design Basis Earthquake Vertical Acceleration Response Spectra, at Node 6 Elevation 114'-0" of Fuel Handling Building
- 3.7A-90 Design Basis Earthquake Horizontal Acceleration Response Spectra, at Node 6 Elevation 114'-0" of Fuel Handling Building
- 3.7A-91 Operating Basis Earthquake Vertical Acceleration Response Spectra, at Node 6 Elevation 114'-0" of Fuel Handling Building
- 3.7A-92 Operating Basis Earthquake Horizontal Acceleration Response Spectra, at Node 6 Elevation 114'-0" of Fuel Handling Building
- 3.7A-93 Design Basis Earthquake Vertical Acceleration Response Spectra, at Elevation -15'-6" of Safety Equipment Building (Safety Injection Area)
- 3.7A-94 Design Basis Earthquake E-W Horizontal Acceleration Response Spectra, at Elevation -15'-6" of Safety Equipment Building (Safety Injection Area)
- 3.7A-95 Design Basis Earthquake N-S Horizontal Acceleration Response Spectra, at Elevation -15'-6" of Safety Equipment Building (Safety Injection Area)
- 3.7A-96 Design Basis Earthquake Vertical Acceleration. Response Spectra, at Elevation -5'-3" of Safety Equipment Building (Component Cooling Area)
- 3.7A-97 Design Basis Earthquake E-W' Horizontal Acceleration Response Spectra, at Elevation -5'-3" of Safety Equipment Building (Component Cooling Area)
- 3.7A-98 Design Basis Earthquake N-S Horizontal Acceleration Response Spectra, at Elevation -5'-3" of Safety Equipment Building (Component Cooling Area)
- 3.7A-99 Design Basis Earthquake Vertical Acceleration Response Spectra, at Elevation +50'-6" of Safety Equipment Building
- 3.7A-100 Design Basis Earthquake E-W' Horizontal Acceleration Response Spectra, at Elevation +50'-6" of Safety Equipment Building
- 3.7A-101 Design Basis Earthquake N-S Horizontal Acceleration Response Spectra, at Elevation +50'-6" of Safety Equipment Building

TABLE 3.7A-1							
Figure	Controlled Document	Figure	Controlled Document	Figure	Controlled Document	Figure	Controlled Document
3.7A-1	20573	3.7A-27	20599	3.7A-53	20625	3.7A-79	20714
3.7A-2	20574	3.7A-28	20600	3.7A-54	20626	3.7A-80	20713
3.7A-3	20575	3.7A-29	20601	3.7A-55	20627	3.7A-81	20732
3.7A-4	20576	3.7A-30	20602	3.7A-56	20628	3.7A-82	20731
3.7A-5	20577	3.7A-31	20603	3.7A-57	20633	3.7A-83	20738
3.7A-6	20578	3.7A-32	20604	3.7A-58	20634	3.7A-84	20740
3.7A-7	20579	3.7A-33	20605	3.7A-59	20635	3.7A-85	20813
3.7A-8	20580	3.7A-34	20606	3.7A-60	20636	3.7A-86	20812
3.7A-9	20581	3.7A-35	20607	3.7A-61	20637	3.7A-87	20823
3.7A-10	20582	3.7A-36	20608	3.7A-62	20638	3.7A-88	20822
3.7A-11	20583	3.7A-37	20609	3.7A-63	20647	3.7A-89	20924
3.7A-12	20584	3.7A-38	20610	3.7A-64	20648	3.7A-90	20923
3.7A-13	20585	3.7A-39	20611	3.7A-65	20649	3.7A-91	20926
3.7A-14	20586	3.7A-40	20612	3.7A-66	20650	3.7A-92	20925
3.7A-15	20587	3.7A-41	20613	3.7A-67	20655	3.7A-93	20937
3.7A-16	20588	3.7A-42	20614	3.7A-68	20656	3.7A-94	20927
3.7A-17	20589	3.7A-43	20615	3.7A-69	20657	3.7A-95	20932
3.7A-18	20590	3.7A-44	20616	3.7A-70	20658	3.7A-96	20938
3.7A-19	20591	3.7A-45	20617	3.7A-71	20659	3.7A-97	20928
3.7A-20	20592	3.7A-46	20618	3.7A-72	20660	3.7A-98	20933
3.7A-21	20593	3.7A-47	20619	3.7A-73	20669	3.7A-99	20941
3.7A-22	20594	3.7A-48	20620	3.7A-74	20670	3.7A-100	20931
3.7A-23	20595	3.7A-49	20621	3.7A-75	20690	3.7A-101	20936
3.7A-24	20596	3.7A-50	20622	3.7A-76	20689		
3.7A-25	20597	3.7A-51	20623	3.7A-77	20708		
3.7A-26	20598	3.7A-52	20624	3.7A-78	20707		

APPENDIX 3.7C

SOIL-STRUCTURE INTERACTION PARAMETERS

Site File Copy

Site File Copy

APPENDIX 3.7C

SOIL-STRUCTURE INTERACTION PARAMETERS

DEVELOPMENT OF SOIL-STRUCTURE INTERACTION PARAMETERS PROPOSED UNITS 2 AND 3 SAN ONOFRE GENERATING STATION SAN ONOFRE, CALIFORNIA

for

Southern California Edison Company
P. O. Box 800
Rosemead, California 91770

by

WOODWARD-McNEILL & ASSOCIATES
Consulting Engineers and Geologists

31 January 1974
(Final Revision)

APPENDIX 3.7C

TABLE OF CONTENTS

	Page
1.0 INTRODUCTION	1
1.1 Scope	1
1.2 Organization of Report	2
2.0 LABORATORY AND FIELD TESTING	2
2.1 Laboratory Testing	3
2.2 Field Testing	3
2.2.1 General	3
2.2.2 Slab-Response Tests	4
2.2.3 Rayleigh-Wave Tests	5
2.2.4 Attenuation Tests	5
3.0 DISCUSSION AND CONCLUSIONS	5
3.1 Modulus and Damping Parameters	6
3.2 Soil Damping and Spring Constant	6
3.2.1 Soil Damping	7
3.2.2 Spring Constant	8
3.3 Lateral Pressures on Structure Walls	9
3.4 Evaluation of Structural Sliding	10
3.5 Evaluation of Critical Instantaneous Displacement Profile	11
4.0 SUMMARY OF SOIL-STRUCTURE INTERACTION PARAMETERS	12
4.1 Parameters for Dynamic Analyses	12
4.2 Static Analyses Parameters	12
5.0 REVIEW OF THE USE OF RECOMMENDED PARAMETERS	13

TABLE I - DESIGN PARAMETERS

TABLE II - SUMMARY OF DETERMINATION OF STRESSES ON WALLS

TABLE III - CASES STUDIED FOR STRUCTURE SLIDING ANALYSES

FIGURE 1 - SITE PLAN

FIGURE 2 - MODULUS AND DAMPING VS. STRAIN, SAN MATEO FORMATION SAND

FIGURE 3 - INSTRUMENTATION

Amended: April 2009 TL: E047997

TABLE OF CONTENTS

FIGURE 4 - TESTS IN PROGRESS

FIGURE 5 - MAXIMUM SLAB RESPONSE MEASUREMENTS

FIGURE 6 - SOIL DAMPING FOR STRUCTURES (SCHEMATIC)

FIGURE 7 - SHEAR MODULUS DETERMINATION (SCHEMATIC)

FIGURE 8 - EFFECT OF EMBEDMENT ON SPRING CONSTANT

FIGURE 9 - LATERAL PRESSURES DUE TO ADJACENT STRUCTURE

FIGURE 10 - EXAMPLE OF STRUCTURAL SLIDING RESULTS

FIGURE 11 - CRITICAL DISPLACEMENT PROFILE FOR OFFSHORE CONDUIT EXTENDING WEST OF PERMANENT SEA WALL

FIGURE 12 - OBE & DBE INDUCED STRAINS

FIGURE 13 - ESTIMATED SETTLEMENT FOR FOUNDATIONS BEARING ON SAN MATEO FORMATION SANDS

APPENDIX A - SLAB RESPONSE TESTS

APPENDIX B - RAYLEIGH WAVE TESTS

APPENDIX C - ATTENUATION TESTS

APPENDIX D - DAMPING

APPENDIX E - EVALUATION OF SPRING CONSTANT

APPENDIX F - LATERAL PRESSURES ON STRUCTURE WALLS

APPENDIX G - STRUCTURE SLIDING

APPENDIX H - EVALUATION OF CRITICAL INSTANTANEOUS DISPLACEMENT PROFILE

BIBLIOGRAPHY

Amended: April 2009 TL: E047997

DEVELOPMENT OF SOIL-STRUCTURE INTERACTION PARAMETERS, PROPOSED UNITS 2 AND 3 SAN ONOFRE GENERATING STATION SAN ONOFRE, CALIFORNIA

1.0 INTRODUCTION

1.1 Scope

As part of the geotechnical studies for the proposed expansion of the San Onofre Nuclear Generating Station (SONGS) for Units 2 and 3, this report presents the results of field testing and analyses used to develop soil-structure interaction parameters. The field tests were initiated to both confirm the laboratory-derived modulus and damping parameters and set the rules by which those parameters should be used in evaluating soil-structure interaction. The need for this extensive effort is realized when considering the requirements to supply soil-structure interaction parameters for state-of-the-art level structures analyses. These analyses are required to design the Seismic Category 1 structures to withstand the large Design Basis Earthquake (DBE) motions. The SONGS 2 and 3 Category 1 structures exhibit unusual shape and inertia characteristics for which there is no precedence available in the literature or design experience.

The present study can be separated into three basic areas to indicate the specific items considered in detail. These items are listed below:

- field tests - slab response
  R-wave
  attenuation
- lab tests - modulus and damping parameters from previous studies

Amended: April 2009 TL: E047997

- Analytical studies with field and laboratory test results as basic data to develop 5 aspects of soil-structure interaction

  - spring constants and modulus values
  - dampings (hysteretic and spatial)
  - structural sliding
  - most critical instantaneous displacement profile for structural design and interaction between structures
  - consideration of lateral stresses on structural walls

1.2 Organization of Report

The field and laboratory investigations including reference to previous, parallel work pertinent to this study are described in Section 2. Section 3 describes the five aspects of soil-structure interaction considered; Section 4 presents the general soil-structure interaction parameters developed for the SONGS 2 and 3 site. Finally, Section 5 summarizes final review procedures of how parameters are utilized.

The necessary back-up data for the sections described above are assembled in the appendices, as follows:

Appendix A	Slab Response Tests
Appendix B	Rayleigh Wave Tests
Appendix C	Attenuation Tests
Appendix D	Evaluation of Damping
Appendix E	Evaluation of Spring Constant
Appendix F	Evaluation of Stresses on Walls
Appendix G	Evaluation of Structure Sliding
Appendix H	Evaluation of Critical Instantaneous Displacement Profile

2.0 LABORATORY AND FIELD TESTING

The data upon which the analyses reported here are based were derived from both laboratory and field testing. Because

Amended: April 2009 TL: E047997

all Category 1 structures are to be founded on San Mateo Formation Sand, all tests were limited to that material. The laboratory testing was reported in a previous study (Ref. 4) on modulus and damping parameters. The field tests, including slab response measurements were conducted at the site (Fig. 1) and are presented in this report. The paragraphs which follow discuss both the laboratory and field testing.

2.1 Laboratory Testing

The results of tests performed to develop strain-dependent modulus and damping parameters are presented in the 14 October 1971 report entitled, *Elastic and Damping Properties, Laydown Area, San Onofre Nuclear Generating Station* (Ref. 4). The data presented in that report resulted in the development of the strain-dependent modulus and damping curves presented in Fig. 2. These relationships were verified by the field attenuation and Rayleigh-wave tests described below and were used in the detailed analyses of the slab response tests.

2.2 Field Testing

2.2.1 General

All field tests were performed in the Unit 1 laydown area as located on the Site Plan, Fig. 1, due to the flat working area and easy access to the exposed native San Mateo Sand material. Testing was completed between 5 and 12 September 1972, and included a series of three types of tests: slab-response tests, Rayleigh-wave tests, and attenuation tests. These tests are described in detail below.

Amended: April 2009 TL: E047997

2.2.2 *Slab-Response Tests*

The slab-response tests were conducted by setting five concrete slabs of different size, shape, and embedment configurations into transient motion and measuring the intensity and the decay of the response motion. The test slabs ranged from 4 to 10 ft in diameter and 2 to 5 ft in thickness. The sizes and shapes were chosen to evaluate the effects of geometry, scaling and embedment on response. Response measurements were made with velocity-sensing geophones. A typical instrumentation layout is shown in the photograph in Fig. 3a. The slabs were set into transient motion by tensioning a cable and weak link with a crane or tractor until the weak link failed. The intensity of response was controlled by using weak links with tensile load capacities varying from 3 to 16 kips as shown on Fig. 3b. Typical vertical and horizontal response tests using a crane and a tractor are indicated on Figs. 4a and 4b, respectively. For the 105 tests performed, response of the slabs generally ranged from accelerations of 0.2 to 1.0 times the acceleration of gravity over a frequency range of 10 to 100 cycles per second, as indicated from peak response points plotted in Fig. 5. A description of the details of the slab response tests and the test results are presented in Appendix A. Basically, the stiffness was evaluated by the response frequency, and the damping by the decay of the response motion.

Amended: April 2009 TL: E047997

2.2.3 *Rayleigh-Wave Tests*

Rayleigh-wave traverses were performed in two mutually perpendicular, 5-ft deep and about 100-ft long trenches. These tests consisted of measuring the wave length of vibratory input motion at various frequencies. The Rayleigh-wave velocity was calculated from the measured wave length and input frequency and is essentially equal to shear-wave velocity. The measurements were carried out to verify earlier measurements of near-surface shear-wave velocity and estimates of low-strain level shear modulus. The details of Rayleigh-wave tests and the test results are presented in Appendix B.

2.2.4 *Attenuation Tests*

An attenuation test was performed using a vibrating sheepsfoot roller as a source of vibratory energy and monitoring the motion simultaneously at two distances from this source. These measurements yield the hysteretic damping of the soil and were used to verify the laboratory-determined relationship between damping and strain. The details of this test and the test results are presented in Appendix C.

3.0 DISCUSSION AND CONCLUSIONS

The purpose of all testing completed during the present investigation was twofold: (1) to verify the previously determined damping and modulus parameters; and (2) to develop the soil-structure interaction parameters. The paragraphs which follow discuss the verification and the development of the soil-

Amended: April 2009 TL: E047997

structure interaction parameters.

3.1 Modulus and Damping Parameters

The relationship between modulus and strain presented on Fig. 2 was developed from a combination of dynamic laboratory tests and field seismic tests. The verification of the low-strain level value of modulus near the ground surface was of primary concern in the present study. This was accomplished by the measurement of the Rayleigh-wave velocity described above and in Appendix B. Results of the test are presented in Appendix B. They indicate a range of Rayleigh-wave velocities between 850 and 1200 fps, with a velocity of 930 fps as a representative average for the near-surface (upper 15 ft) soils. This range in values is consistent with the shear-wave velocity used to develop the modulus curve on Fig. 2.

The relationship between hysteretic damping and strain presented in Fig. 2 was developed entirely from dynamic laboratory testing. The field verification of this relationship was done by performing attenuation tests in the field as described above and in Appendix C. A comparison of the field results to the laboratory determined curve, as presented in Appendix D, indicates good agreement between the two.

3.2 Soil Damping and Spring Constant

The development of soil damping and spring constant parameters for structures was necessary for the response evaluation of structures at the SONGS 2 and 3 sites. These parameters were developed from a combination of the slab response tests

Amended: April 2009 TL: E047997

and the strain-dependent modulus and damping curves (Fig. 2) as discussed below.

3.2.1 *Soil Damping*

There are basically four tasks involved in the evaluation of soil damping: (1) determination of the manner in which to combine hysteretic and spatial damping; (2) evaluation of the effective radius of the foundation which depends on stress distribution; (3) evaluation of the effect of embedment of the foundation; and (4) evaluation of shape and scaling effects. The details of analyses of field data to evaluate these tasks are presented in Appendix D. In brief, it was found that for the soil conditions at the SONGS 2 and 3 site: (1) total damping could be determined by adding the spatial and hysteretic damping algebraically; (2) an effective radius of about 60% of the actual radius (corresponds to parabolic stress distribution) could be utilized in the theoretical equations to determine a conservative value of geometrical damping for the translational modes (horizontal and vertical) while 80% (corresponds to uniform stress distribution) could be used for rotational modes (rocking and twisting); (3) the effects of embedment are negligible on the amount of damping; and (4) the effects of scaling and shapes (for regular shapes like square or circular) were negligible on the amount of damping.

The general methods of obtaining damping are summarized on Fig. 6 with the general equations included in Table I.

Amended: April 2009 TL: E047997

It is noted that the strain for which the hysteretic damping is calculated should be the seismic induced free-field strain for OBE and DBE analysis, as it would likely dominate over the local strains caused by response of the structure. This should be checked by the method to evaluate strain compatibility suggested in Section 4.2.

3.2.2 *Spring Constant*

There are basically four tasks involved in the evaluation of spring constants: (1) determination of the confinement to be used in the calculation of modulus; (2) evaluation of the effective radius (stress distribution); (3) evaluation of the effect of embedment; and (4) evaluation of the shape and scaling effects. Slab-response tests were carried out in the field to respond to these tasks. Details of analysis-of field data, obtained from these tests, to evaluate these tasks are presented in Appendix E. Task-1 was answered by determining the shear modulus from the strain and confinement-dependent curve (Fig. 2), and then the other tasks were evaluated. If the results of the evaluation of task-2 were consistent with judgment, then the assumption could be considered reasonable. The evaluation of shear modulus for these tests was done by assuming the strain in the soil was accommodated within one radius below the test slab. Therefore, the strain was calculated as the measured response deflection divided by the radius of the foundation and the mean confinement was calculated at an average depth of one-half a radius

Amended: April 2009 TL: E047997

below the foundation as indicated in Fig. 7. Tasks-3 and 4 were answered by field tests of slabs with different embedments and shapes. These tests are also described in Appendix E. In summary, using the task-1 assumption, it was found that: (1) the evaluation of effective radius leads to a correction factor on the theoretical equation consistent with uniform stress distribution (see Table I, factor C_1); (2) the effect of embedment was significant as is indicated on Fig. 8 (correction indicated as C_2); and (3) the effects of shape (for regular shapes) and scaling were negligible.

The general equations for obtaining spring constants are presented in Table I. Also, included in Table I are specific equations for the containment model which was studied separately due to its complex base geometry. As in the case of damping, the strain to be used in the actual structure model should be equal to the seismic induced free-field strain for OBE and DBE analyses. This should be checked by the method suggested in Section 4.2.

3.3 Lateral Pressures on Structure Walls

Three basic pressures must be considered in the evaluation of seismic-induced stresses on structure walls: (1) active pressure acting on the side of the structure tending to move the structure away from the soil; (2) developed passive pressure acting on the opposite side of the structure (due to inertial loads) tending to move the structure into the soil; and (3) pressures due to the proximity of adjacent structures. The

Amended: April 2009 TL: E047997

details of analyses to determine these stresses are presented in Appendix F. The criteria used to determine dynamic lateral soil pressures are based on Mononobe-Okabe method. A summary of the method of evaluation is presented in Table II with a schematic diagram indicating the effects of the proximity of the adjacent structures presented on Fig. 9. Because all sides of the structure could be subjected to both passive and active pressures, all walls should be designed for whichever analysis yields the highest pressure for each wall element as indicated on Table II.

3.4 Evaluation of Structural Sliding

During a large earthquake the horizontal forces developed due to inertial loads from large structures with shallow embedments may be significant and tend to cause structural sliding. The geometry of the Auxiliary Building makes it the most critical Category 1 structure from this standpoint. Therefore, a dynamic finite-element program was utilized to evaluate this problem by constructing the element mesh with very thin elements just below the structure and calculating a time-history of the ratio of the shear and normal stresses in that soil just below the structure to compare with the available frictional resistance. A series of cases were calculated considering various factors as summarized on Table III. The details of the analysis and the results of all cases are presented in Appendix G. The most critical case as indicated on Table III is reported as Fig. 10. For this case the stress ratio is always less than the available frictional resistance ($^2/_3 \tan \phi$) of 0.59; therefore, we conclude that the Auxiliary Building is safe against sliding for DBE-induced loading.

Amended: April 2009 TL: E047997

Based on the results of the analyses performed for the various cases summarized in Table III, several general conclusions can be drawn:

1. The phase relationship between the horizontal and vertical motion does not appear to influence sliding appreciably.

2. Inclusion of rotational inertia does not increase the sliding potential.

3. Sliding forces are largest at the center of the slab and decrease toward the edges.

4. The most critical combination of conditions involves a surface slab (i.e., no embedment) subjected to a combination of horizontal and vertical base motions.

3.5 Evaluation of Critical Instantaneous Displacement Profile

For structures with unusual geometry or small anticipated inertial loading the use of a seismic instantaneous displacement may be critical for design. The critical instantaneous displacement profile (CIDP) is defined as the deflected shape that the structure would assume at an instant during the earthquake which would cause maximum stresses in structural elements. The determination of the CIDP is made using a travelling shear wave finite-element computer program and evaluating the displacement profile along the base of structural elements in the finite-element mesh at every instant in time. The critical profile is found using maximum slope change across the profile (maximum bending) as a criterion. The details of the procedure are presented in Appendix H. An example of results is presented for the Intake Conduit in Fig. 11.

Amended: April 2009 TL: E047997

4.0 SUMMARY OF SOIL-STRUCTURE INTERACTION PARAMETERS

Interaction parameters for both static and dynamic analyses are summarized in the paragraphs which follow.

4.1 Parameters for Dynamic Analyses

Using the procedures outlined in the foregoing sections, the soil-structure interaction parameters can be developed for each Category 1 structure. The actual parameters will depend on the geometry, inertia and embedment of the structure together with the shear modulus and hysteretic damping of the soil. As noted in Fig. 2, the shear modulus and hysteretic damping of the soil are strain dependent. To determine the appropriate value of these parameters, it was necessary to determine the DBE and the OBE induced free-field strains. These strains were evaluated on the basis of finite element analyses as presented in Fig. 12.

4.2 Static Analyses Parameters

The denseness of the San Mateo Sand material indicates that a static spring model analysis is appropriate for the consideration of static deflections of the base mat. Further, by comparing dynamic modulus values for dense sands (Seed and Idriss, 1970) and static reloading modulus values for the same material (Kulhawy, Duncan and Seed, 1969) for the same strain level, it is found that there is essentially no difference. For this reason, it is concluded that the static analyses can be performed using the same stiffness parameters as calculated for dynamic analyses. Strain compatibility should be attained in performing the analysis as described in the following steps:

Amended: April 2009 TL: E047997

1. Choose initial value of modulus for the spring constant equation in Table I as appropriate.

2. Complete analysis calculating the maximum deflection of the foundation.

3. Calculate strain by dividing the deflection from Step 2 by the radius of the foundation.

4. Compare modulus from Fig. 2 corresponding to the strain from Step 3 to the modulus chosen in Step 1.

5. If the values of modulus are different, repeat Steps 1 through 4 until compatibility is attained.

It is important that the net bearing pressure be used as the applied load in calculating strain (i.e., total pressure at the structure subgrade minus pressure due to soil removed between adjacent grade and the structure subgrade). If the net pressure is zero or negative use K_m= 590 (see Fig. 2). For net pressures greater than 10 ksf (approximately equal to the initial overburden removed to attain plant grade at el. +30 ft) the amount of net pressure over 10 ksf should not be included in the calculation of σ_m. Parametric studies using these procedures yielded results for the evaluation of settlement of isolated footings for net loads of up to 10,000 kips and bearing pressures of up to 20 ksf as presented graphically on Fig. 13. These can be used in conjunction with the equation for net allowable bearing capacity as given on Fig. 13 for design of isolated footings. Evaluation of structures should be done by an acceptable mat deflection criterion using the techniques presented above.

5.0 REVIEW OF THE USE OF RECOMMENDED PARAMETERS

Due to the complexity of structures and of the soil structure interaction concepts, interpretation and simplifying assumptions must be made to utilize the general rules for design parameters.

For this reason it is imperative that a detailed review be made by this firm of how all parameters are calculated and used in the analyses completed by Bechtel Corporation. By mutual agreement between Southern California Edison Company, Bechtel Corporation, and Woodward-McNeill & Associates, this review is to consist of at least one working meeting for each major structural analysis with appropriate representation of each company, and should be ultimately followed up with written documentation.

Amended: April 2009 TL: E047997

TABLE I

DESIGN PARAMETERS

Parameters	Mode of Motion: VERTICAL TRANSLATION	HORIZONTAL TRANSLATION	ROCKING	TWISTING
Inertia	m, mass of foundation and machine	m, mass of foundation and machine	I_r, mass moment of inertia about rocking axis	I_t, mass moment of inertia about twist axis
Radius	$r = \sqrt{\frac{BL}{\pi}}$	$r = \sqrt{\frac{BL}{\pi}}$	$r = \sqrt[4]{\frac{BL^3}{3\pi}}$	$r = \sqrt[4]{\frac{BL(B^2 + L^2)}{6\pi}}$
Inertia Ratio	$B_v = \frac{(1-\nu)m}{4\rho r_e^3}$	$B_h = \frac{(7-8\nu)m}{32(1-\nu)\rho r_e^3}$	$B_r = \frac{3(1-\nu)I'_r}{8\rho r_e^5}$	$B_t = \frac{I_t}{\rho r_e^5}$
Effective Inertia for Design	m	m	$I'_r = \eta_r I_r$ See Appendix E for value of η_r	I_t
Stiffness Coefficient	$k_v = \frac{4GrC}{(1-\nu)}$	$k_h = \frac{32(1-\nu)\ GrC}{(7-8\nu)}$	$k_r = \frac{8Gr^3C}{3(1-\nu)}$	$k_t = \frac{16Gr^3C}{3}$
Geometric Damping	$D_v = \frac{0.425}{\sqrt{B_v}}$	$D_h = \frac{0.288}{\sqrt{B_h}}$	$D_r = \frac{0.15}{(1+B_r)\sqrt{B_r}}$	$D_t = \frac{0.50}{1+2B_t}$
General Case $C = C_1\ C_2$	$C_1 = 0.81$ C_2 = See Fig. 8	$C_1 = 1.0$ C_2 = See Fig. 8	$C_1 = 0.66$ C_2 = See Fig. 8	$C_1 = 0.41$ C_2 = See Fig. 8
Containment Structure Value of C	1.08	1.09	0.60	insufficient data

* For rectangular shaped foundations, calculation should be based on equations of pgs. 350 and 351, Richart, Hall and Woods, "Vibrations of Soil and Foundation."

$r_e = 0.6r$ for translation modes

$r_e = 0.8r$ for rotational modes

Note: for square or rectangular footing-

B = width of foundation in plan (parallel to axis of rotation)

L = length of foundation in plan (perpendicular to axis of rotation)

Amended: April 2009 TL: E047997

TABLE II

SUMMARY OF DETERMINATION OF STRESSES ON WALLS

1) Active Pressure on Structure Walls (σ_A) (at-rest condition assumed as a minimum condition)

Case	Equivalent Fluid Pressure Above Water Table (pcf)	Equivalent Fluid Pressure Below Water Table (pcf)
Static (at rest)	45	23*
Seismic** DBE	75	39*
Seismic** OBE or lower	45	23*

Note: * Hydrostatic head should be added.
** These values include static stresses. Seismic lateral stresses should be checked by the inertial load method, presented in 2 below.

2) Passive Pressure Developed on Structure Walls Due to Inertial Loads. (uniform stress assumed)

For Horizontal Translation: $\sigma_p = \frac{C_2 - 1}{C_2}\left(\frac{P}{A}\right)$

For Rocking Rotation : $\sigma_p = \frac{C_2 - 1}{C_2}\left(\frac{4M}{hA}\right)$

where: σ_p = Stress against wall

P = 70% of the maximum total horizontal inertial load

M = 70% of the maximum total inertial moment

A = Area of side of structure

h = Depth of embedment

C_2 = Embedment correction factor (See Fig. 8)

3) Stresses Due to Adjacent Structures (σ_L); See Fig. 9

4) Lateral Stress for Design (σ_T); $\left.\begin{array}{r}\sigma_T = \sigma_A + \sigma_L \\ \sigma_T = \sigma_p + \sigma_L\end{array}\right\}$ Use Whichever is Larger

Amended: April 2009 TL: E047997

TABLE III

CASES STUDIED FOR
STRUCTURE SLIDING ANALYSES

Case No.	Input Motion			Condition			Figure Nos. for Results	Location of Output
	H only	H & V in phase	H & V out of phase	Mass only	Mass plus Inertia	Embedment		
1	✓			✓			G-3	L, C, R
2		✓		✓			G-4	L, C, R
3			✓	✓			G-5	L, C, R
4	✓				✓		G-6	L, C, R
5		✓			✓		G-7	L, C, R
6	✓			✓		✓	G-8	L, C
7		✓		✓		✓	G-9	L, C, R

Where: H = Horizontal
V = Vertical
L = Left end of slab
C = Center of slab
R = Right end of slab

NOTE: Check is for item included; blank is for item not included.

Amended: April 2009 TL: E047997

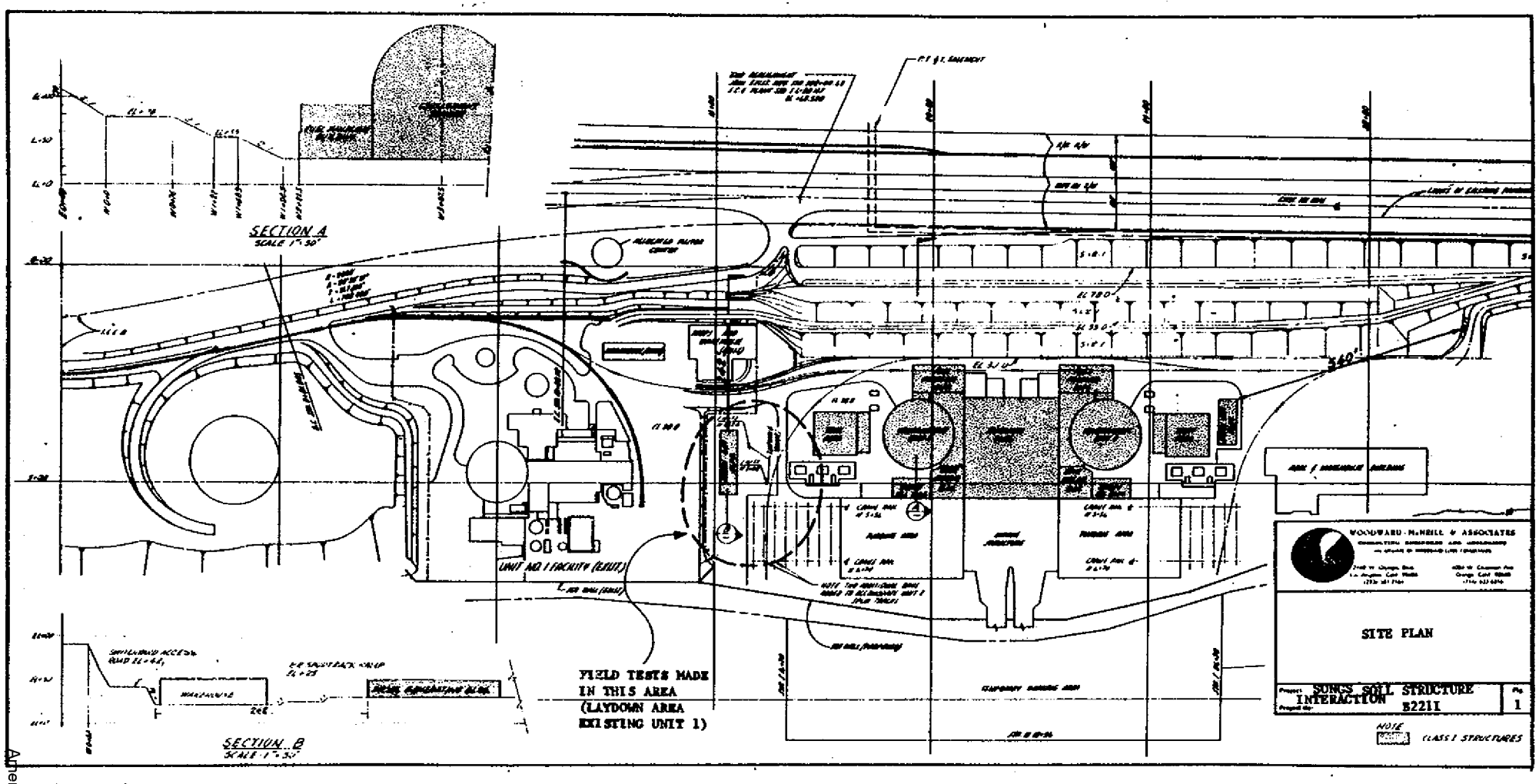

Attended: April 2009 TL: E047997

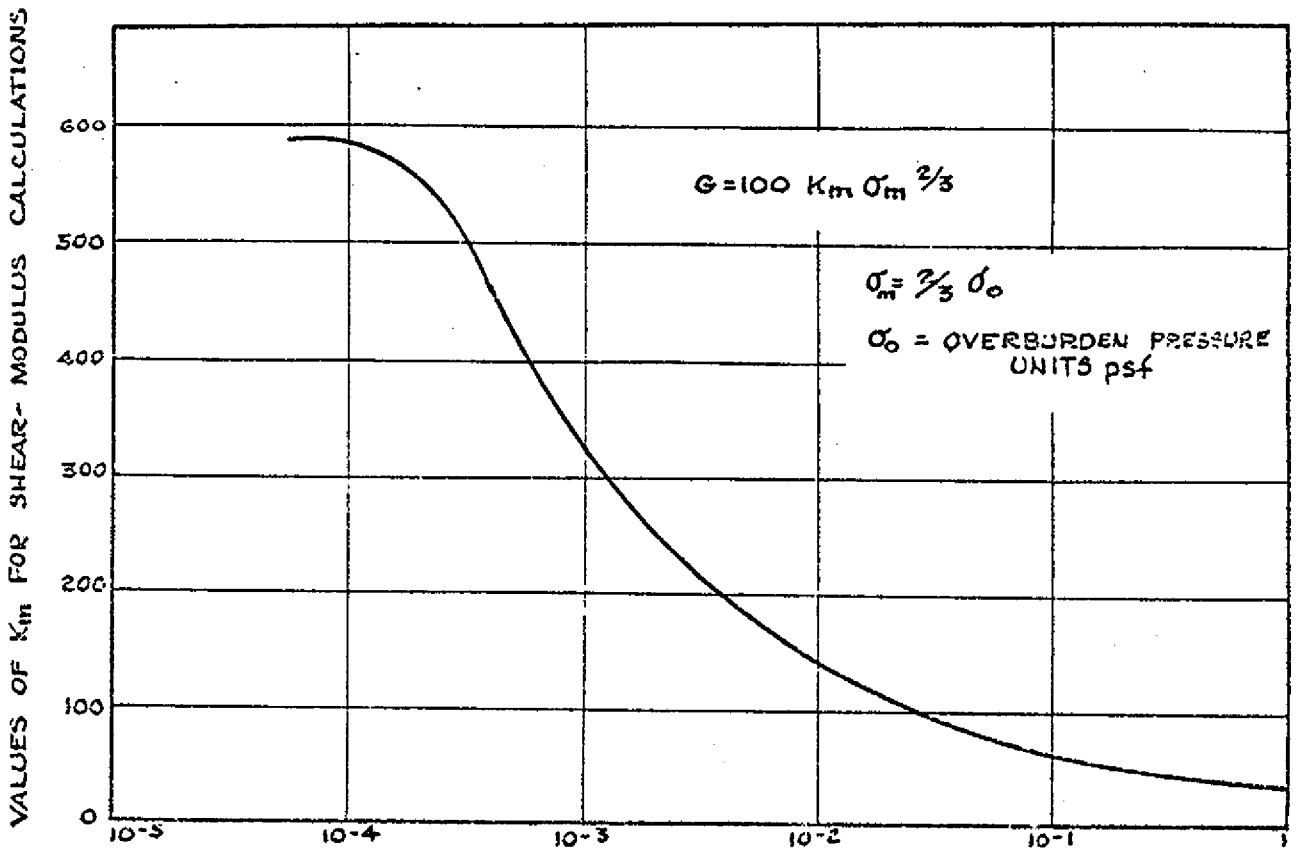

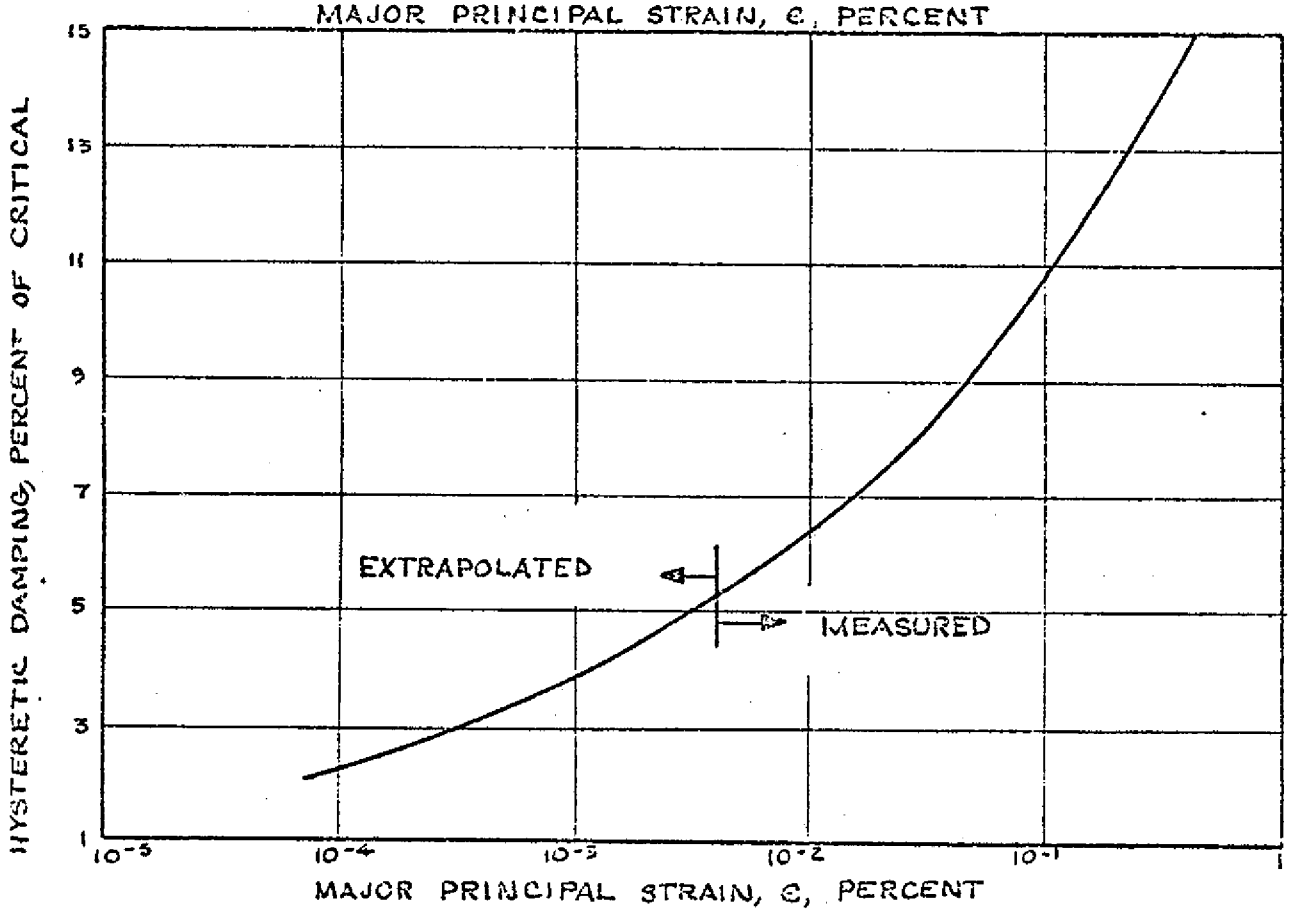

Project: SONGS SOIL STRUCTURE INTERACTION Job Number: E221I	MODULUS AND DAMPING VS STRAIN SAN MATEO FORMATION SAND	Fig. 2

Amended April 2009 DF E047997

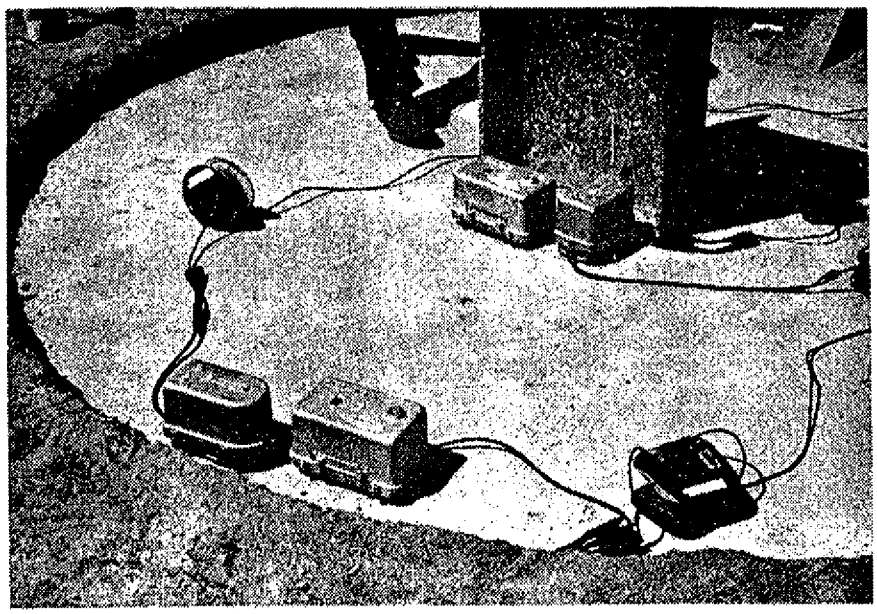

(a) INSTRUMENTATION LAYOUT FOR FOUNDATION RESPONSE TESTS

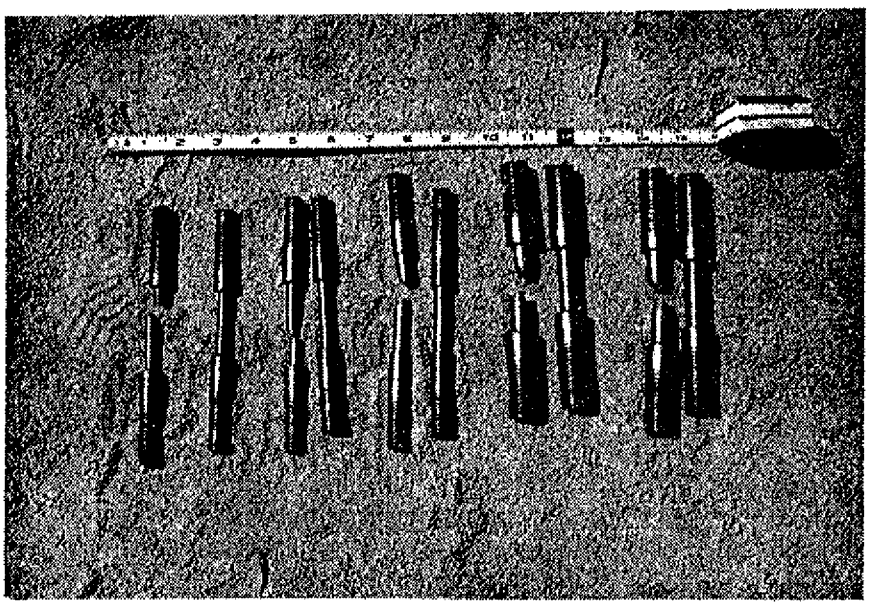

(b) WEAK LINKS USED IN TESTS (3 TO 16 KIPS TENSILE STRENGTH)

Project: SONGS SOILS STRUCTURE INTERACTION Job Number: B221I	INSTRUMENTATION	Fig. 3

Amended: April 2009 TL: E047997

(a) VERTICAL RESPONSE TEST

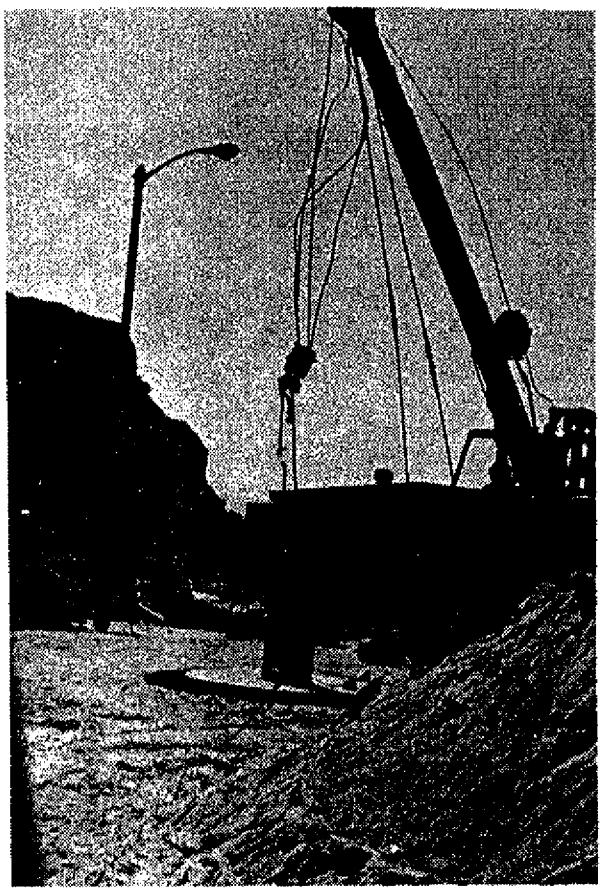

(b) HORIZONTAL RESPONSE TEST

Project: SONGS SOIL STRUCTURE INTERACTION Job Number: B221I	TESTS IN PROGRESS	Fig. 4

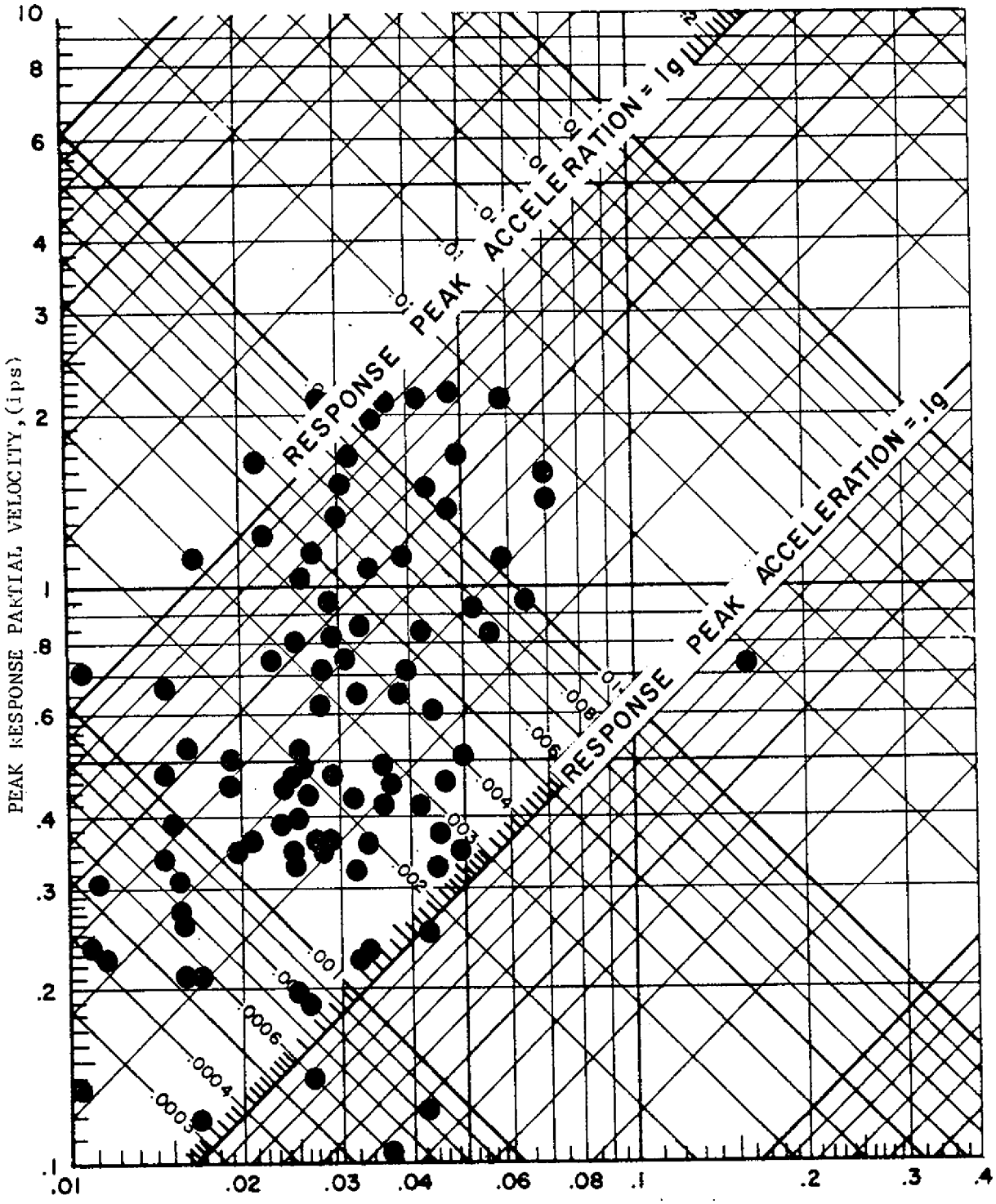

RESPONSE PERIOD OF FOUNDATION (sec)

Project: SONGS SOIL STRUCTURE INTERACTION **Job Number:** B221I	MAXIMUM SLAB RESPONSE MEASUREMENTS	Fig. 5

WOODWARD-McNEILL & ASSOCIATES
Amended: April 2009 TL: E047997

STEP 1

EVALUATE GEOMETRIC DAMPING FROM APPROPRIATE EQUATIONS OF TABLE-1

USE EFFECTIVE RADIUS IN CALCULATION AS INDICATED ON CURVES TO RIGHT

r_e = Effective Radius

r = Structure Radius

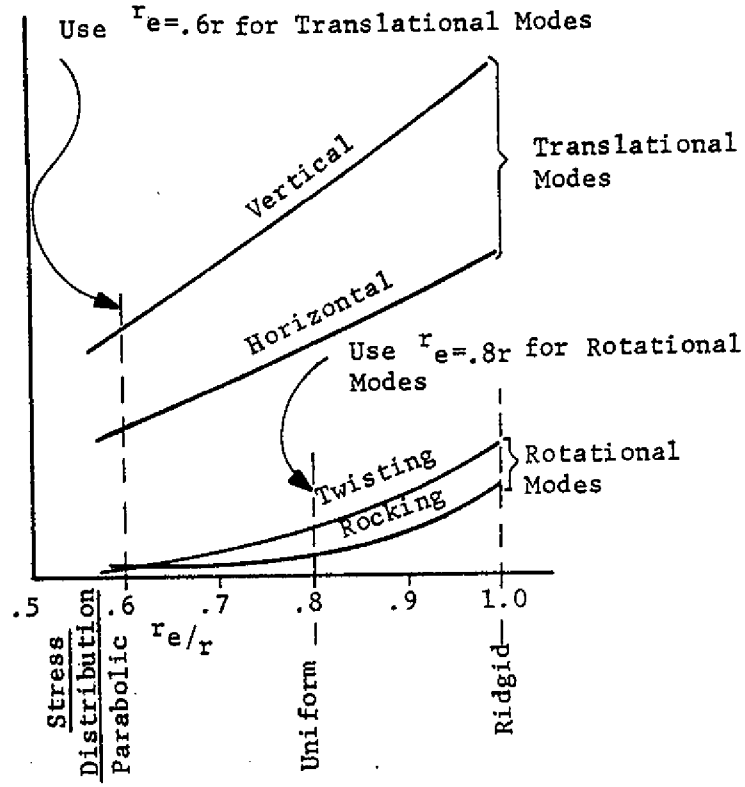

STEP 2

EVALUATE HYSTERETIC DAMPING FROM FIG. 2 USING FREE FIELD EARTHQUAKE INDUCED STRAIN

STEP 3

ADD GEOMETRIC AND HYSTERETIC DAMPING TO OBTAIN CONSERVATIVE ESTIMATE (LOW) OF DAMPING FOR DESIGN

Project: SONGS SOIL STRUCTURE INTERACTION Job Number: B221I	SOIL DAMPING FOR STRUCTURES (SCHEMATIC)	Fig. 6

WOODWARD-McNEILL & ASSOCIATES

O-1

Amended: April 2009 TL: E047997

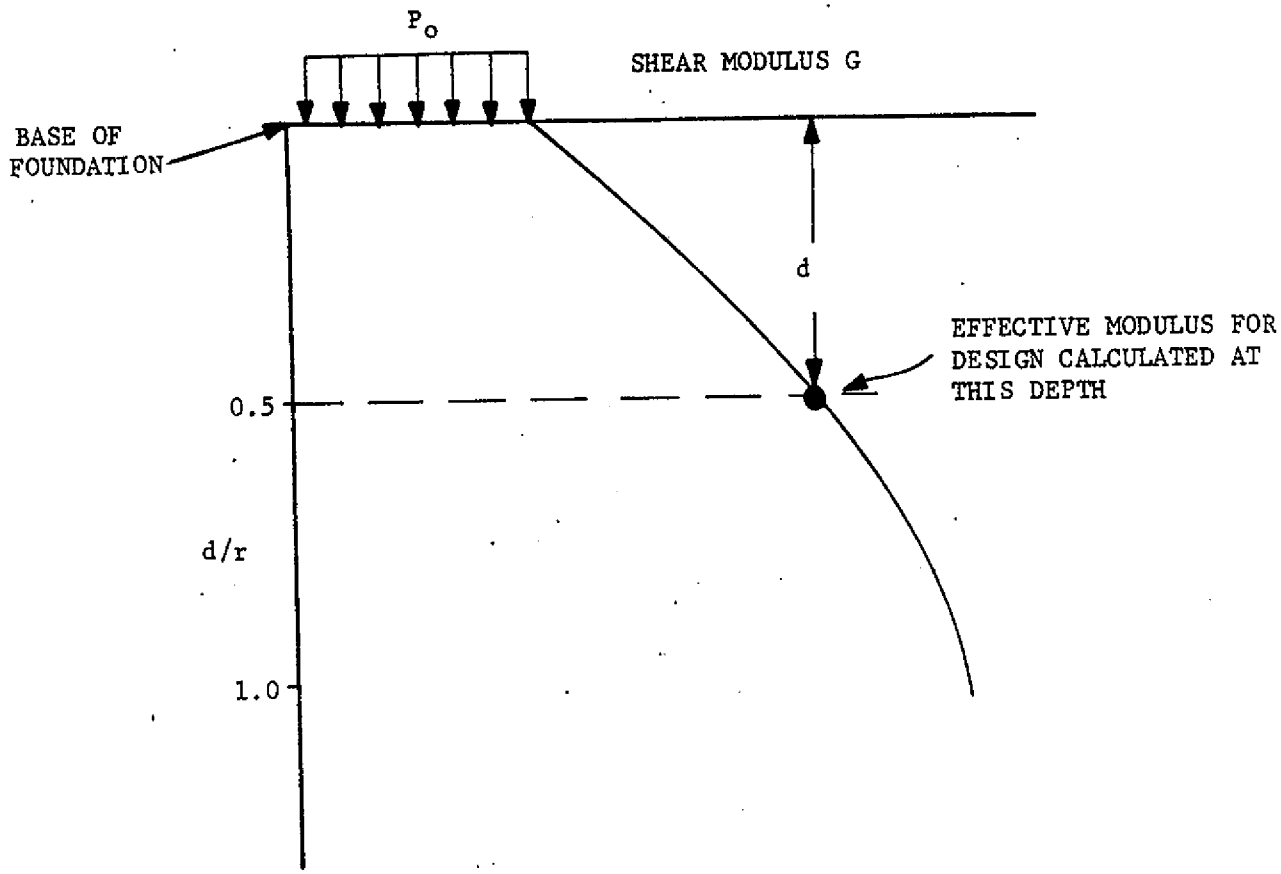

WHERE:

d = Depth below base of foundation

r = Radius of foundation

G = Shear modulus

$\sigma_m = 2(\gamma' d + 0.9 P_o)/3$

P_o = Total bearing pressure

Project: SONGS SOIL STRUCTURE INTERACTION Job Number: B221I	SHEAR MODULUS DETERMINATION (SCHEMATIC)	Fig. 7

WOODWARD-McNEILL & ASSOCIATES

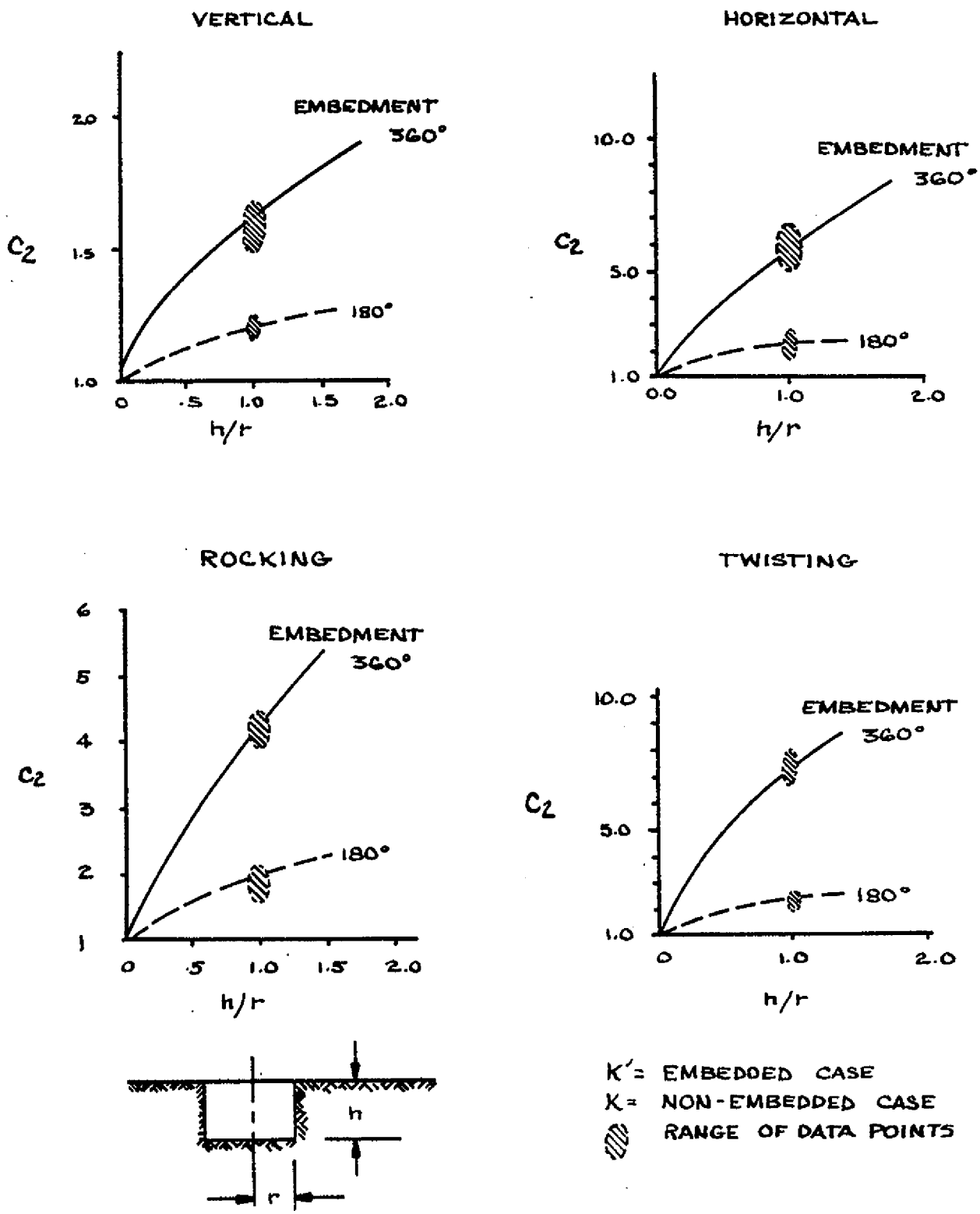

Project: SONGS SOIL STRUCTURE INTERACTION **Job Number:** B221I	EFFECT OF EMBEDMENT ON SPRING CONSTANT	Fig. 8

WOODWARD - McNEILL & ASSOCIATES

LATERAL PRESSURE DUE TO ADJACENT STRUCTURES

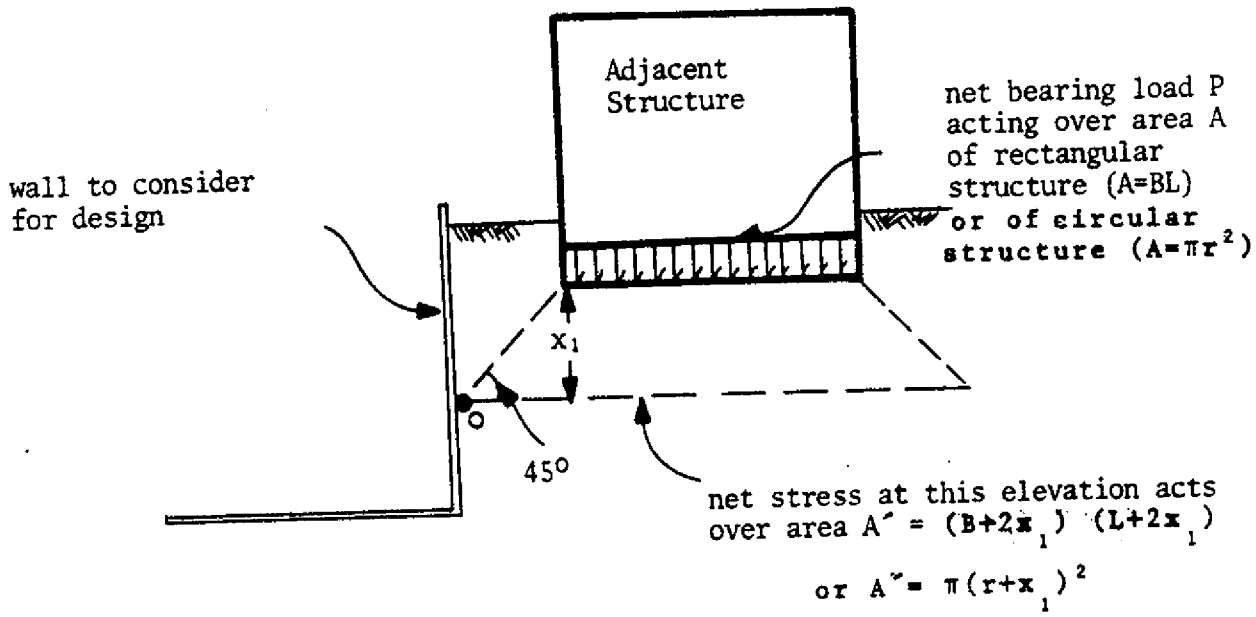

additional lateral pressure on wall $= \frac{A}{A'} \cdot PM$ (uniform)

(applied below point .0)

where: M = 0.34 for Static and OBE condition

M = 0.57 for DBE condition

Notes:

1) The example presented is for a rectangular structure. For circular structures adjust the radius by x_1, to calculate A´.

2) The lateral pressure calculated here should be added to either the active earth pressure or the inertial load for design.

Project: SONGS SOIL STRUCTURE INTERACTION **Job Number:** B221I	LATERAL PRESSURES DUE TO ADJACENT STRUCTURES	Fig. 9

WOODWARD - McNEILL & ASSOCIATES

Amended: April 2009 TL: E047997

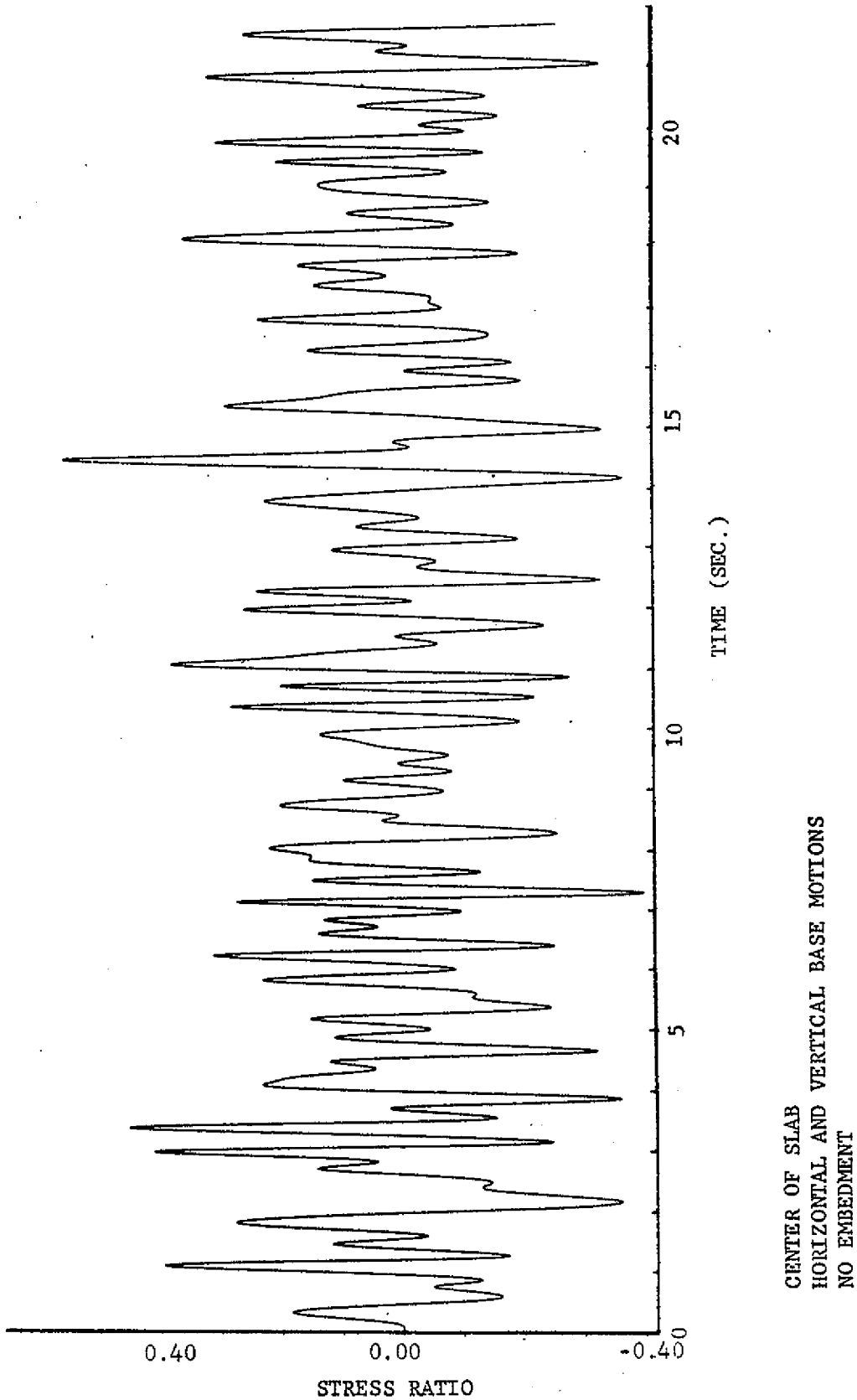

Project: SONGS SOIL STRUCTURE INTERACTION **Job Number:** B221I	EXAMPLE OF STRUCTURAL SLIDING RESULTS	Fig. 10

WOODWARD – McNEILL & ASSOCIATES

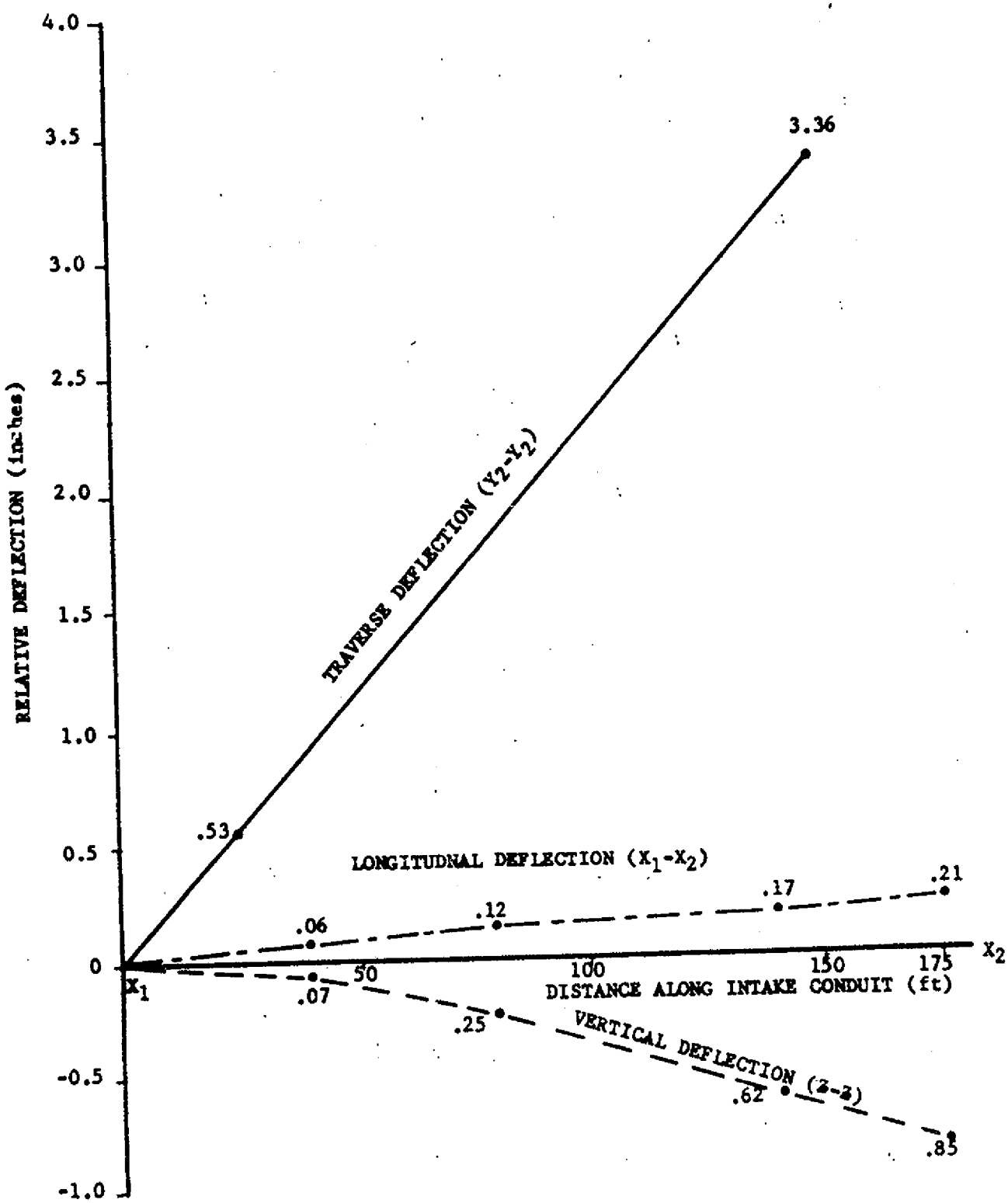

Project: SCE POST ACRS TASK 12 Job Number: B221I	CRITICAL DISPLACEMENT PROFILE FOR OFF-SHORE CONDUIT EXTENDING WEST OF PERMANENT SEA WALL	Fig. 11

WOODWARD - McNEILL & ASSOCIATES

Amended: April 2009 TL: E047997

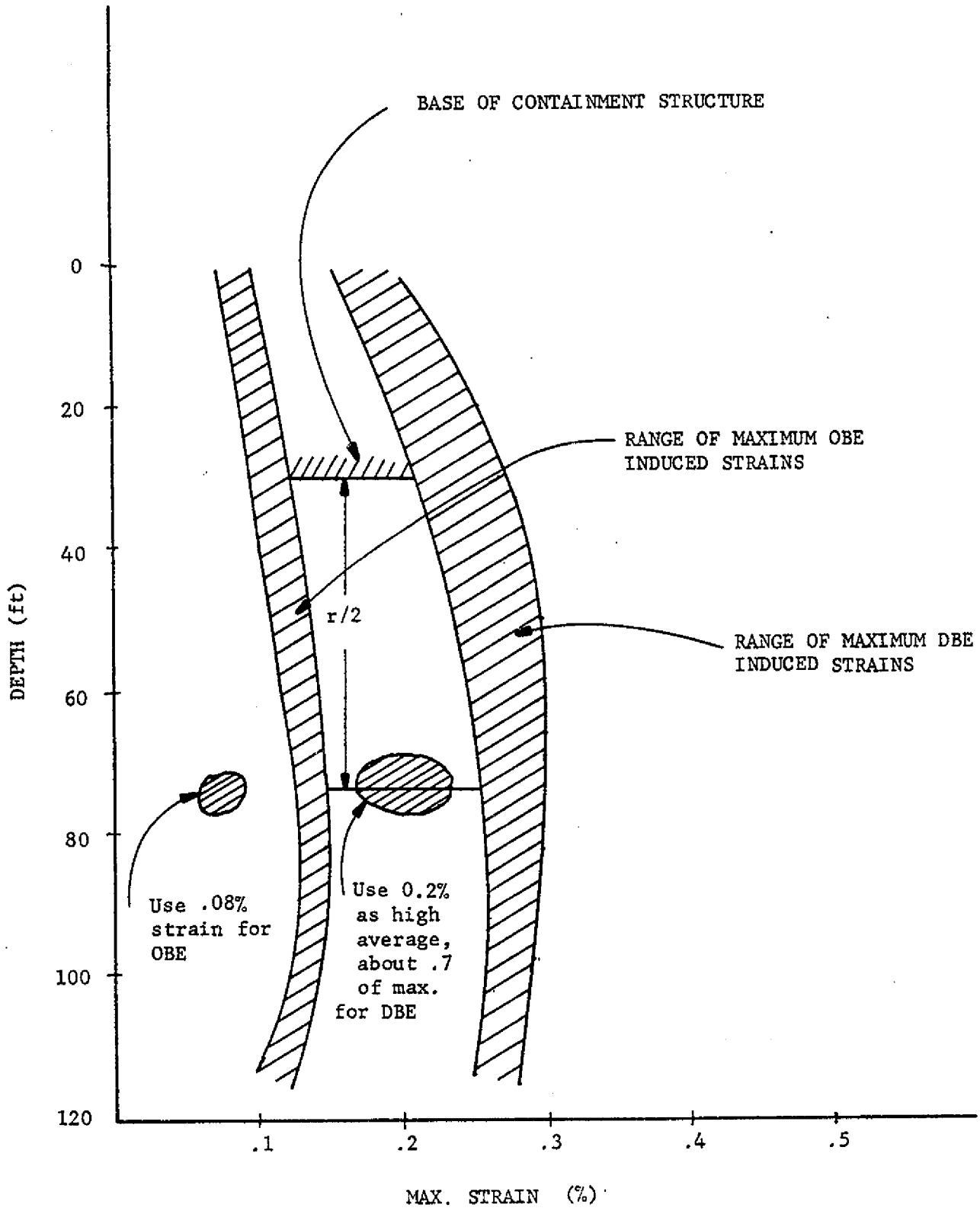

Project: SONGS SOIL STRUCTURE INTERACTION **Job Number:** B221I	OBE & DBE INDUCED STRAINS	Fig. 12

WOODWARD - McNEILL & ASSOCIATES

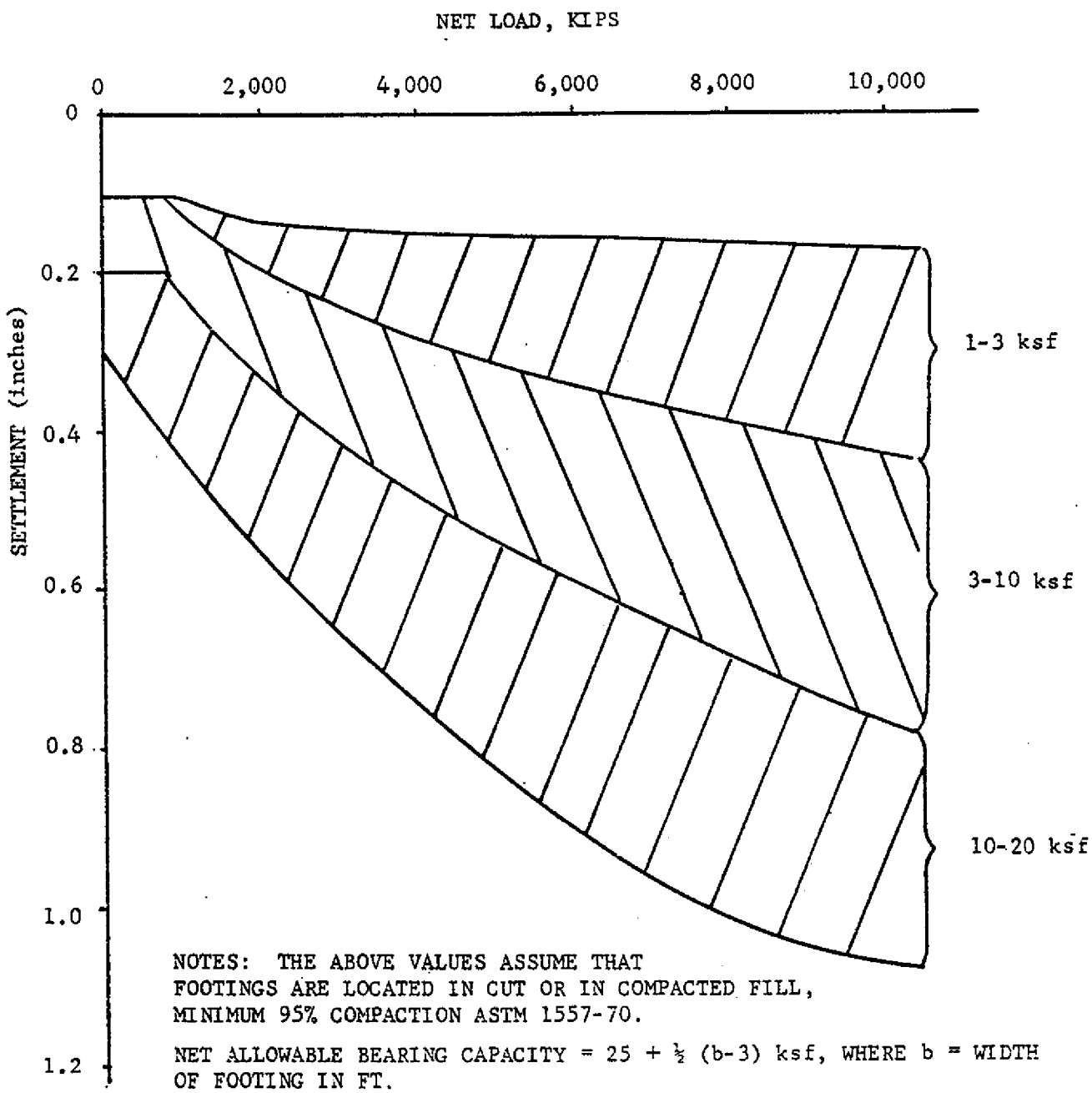

NOTES: THE ABOVE VALUES ASSUME THAT FOOTINGS ARE LOCATED IN CUT OR IN COMPACTED FILL, MINIMUM 95% COMPACTION ASTM 1557-70.

NET ALLOWABLE BEARING CAPACITY = 25 + ½ (b-3) ksf, WHERE b = WIDTH OF FOOTING IN FT.

NET LOAD = TOTAL LOAD-Wt. OF SOIL DISPLACED BETWEEN THE FOOTING BASE AND ADJACENT GRADE OR TOP OF ADJACENT FLOOR SLAB (WHICH EVER IS LESS)

MINIMUM WIDTH OF FOOTING = 3'

DIFFERENTIAL SETTLEMENTS COULD BE UP TO ½ THE VALUE INDICATED ABOVE.

Project: SONGS SOIL STRUCTURE INTERACTION **Job Number:** B221T	ESTIMATED SETTLEMENT FOR FOUNDATIONS BEARING ON SAN MATEO FM. SANDS	Fig. 13

WOODWARD-McNEILL & ASSOCIATES

APPENDIX A

SLAB RESPONSE TESTS

Five test slabs were constructed in the laydown area of Unit 1 between 5 September and 12 September 1972. The various slab configurations are shown on Figs. A-1 and A-2. Slab Nos. 1 and 2 are of similar construction, geometry, and dimensions. Slab No. 1 was constructed above the existing ground surface, while slab No. 2 was fully embedded in the ground. Slab No. 3, shown on Fig. A-2, was constructed below the ground surface. The configuration of this slab was designed to model the basic shape of the proposed containment structure foundation. Slab Nos. 4 and 5 were of smaller dimensions then the other slabs, and were constructed primarily to evaluate scaling and shape effects on slab response.

Test Procedures

It was desired to measure slab response in the horizontal, vertical, twisting, and rocking modes for each slab under various embedment conditions after a transient vibration was input to each slab. Each slab was set into motion by attaching it with a cable to a loader or crane by means of a weak link, as illustrated on Fig. A-3. Vibrations with various amplitudes were induced in the slabs by tensioning a cable between the slab and tractor until it broke at the weak link. The response of the slab to the transient load was measured with horizontally and vertically oriented velocity-sensitive geophones used in conjunction with a CEC 124 Oscillograph recorder. From the response frequency and attenuation characteristics

Amended: April 2009 TL: E047997

of the slab vibrations it is possible to calculate soil stiffness and damping factors, knowing the mass of the slab, its geometry, and the mode of vibration.

Previous research has indicated that embedment characteristics, i.e., depth of slab embedment and the nature of the surrounding soil, affect the slab response. For this reason, slabs Nos. 2 and 3 were tested under various conditions of embedment. Slab No. 2 was first tested with complete embedment below the existing ground surface (in undisturbed soil). The soil around one-half of the slab was then excavated, and the slab was tested again. The remainder of the soil around the slab was then excavated, and the slab was again tested. As it was desired to determine if there were any differences between slab response due to embedment in undisturbed native soils versus compacted backfill native soils, the soil which had been excavated from around slab No. 2 was then backfilled in thin lifts and compacted with hand-held mechanical vibrators. A final set of response tests was then made on this slab. Slab No. 3 was tested with two embedment conditions; (1) non-embedment, and (2) full embedment in compacted backfill of native soils. The various embedment conditions for these slabs are illustrated on Fig. A-4.

Examples of the recorded field test traces for various slabs are presented on Figs. A-5, A-6, A-7 and A-8.

It can be noted in Fig. A-5, which is a record for horizontal input motion, that some vertical motion occurred during this test, i.e., there was some rocking. This occurred to some extent in all horizontal tests. Although coupling did occur between the horizontal and rocking modes, careful interpretation was done in order to determine the dominant form of motion.

Fig. A-8 presents the test record for twisting input motion of slab No. 5. It can be noted on this figure that geophone H_2 registered motion. This is due to the fact that because of the size of the geophone with respect to the slab, it was not possible to center the geophone, as can be seen on the schematic test setup plan shown on Fig. A-8.

A summary of representative frequency response data determined for each mode of motion for each slab is presented in Table A-1.

Amended: April 2009 TL: E047997

TABLE A-1

SUMMARY OF SLAB RESPONSE MEASUREMENTS

Slab No.	Embedment Condition	Representative Frequency Response (cps) F_v	F_h	F_r	F_t
1	Non-embedment	21	20	20	19
2	Full Embedment in Natural Ground	27	50	39	52
2	180° Embedment, Natural Ground	23	30	27	29
2	Non-embedment (slightly undercut)[1]	23	18	17	14
2	Full Embedment in[2] Backfill	--	24	25	36
3	Below Ground Surface, but non-embedded	32	29	32	29
3	Full Embedment in[2] Backfill	(19-24)	(33-37)	39	39
4	Full Embedment	(40-49)	--	(59-67)	(80-90)
5	Full Embedment	(36-48)	--	(59-65)	90

Notes:

[1] During full perimeter excavation, the slab was accidently undercut locally. Therefore results were likely low and were not utilized.

[2] Because of close working conditions and time constraints neither a high nor a uniform degree of compaction was achieved. Therefore results were likely low and were not utilized.

Amended: April 2009 TL: E047997

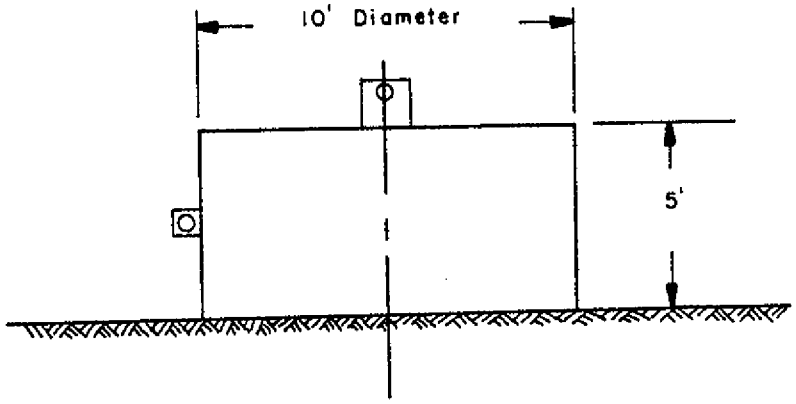

SLAB NO. 1

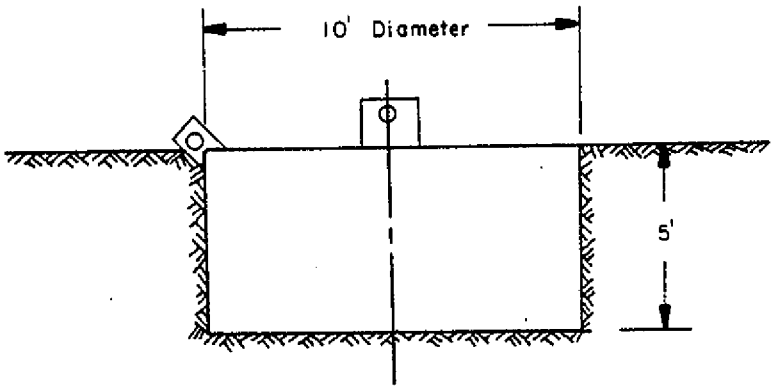

SLAB NO. 2

Project: SONGS Job Number: B221I	TEST SLAB CONFIGURATIONS	Fig. A-1

WOODWARD-McNEILL & ASSOCIATES
Amended: April 2009 TL: E047997

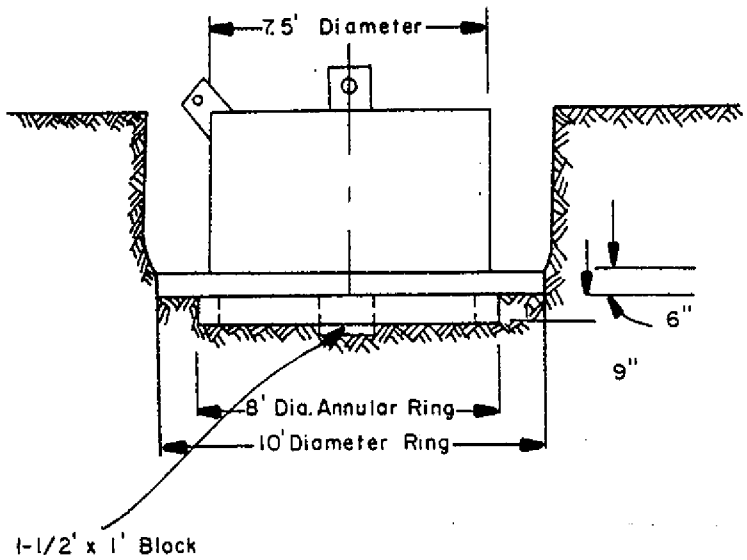

SLAB NO. 3

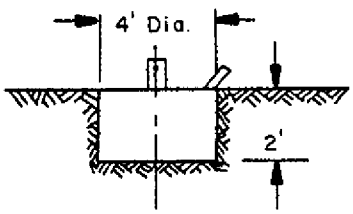

SLAB NO. 4

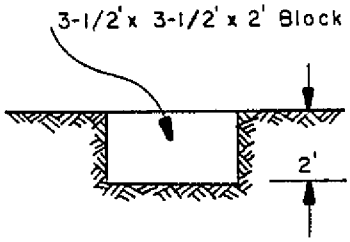

SLAB NO. 5

Project: SONGS Job Number: B221I	TEST SLAB CONFIGURATIONS	Fig. A-2

WOODWARD-McNEILL & ASSOCIATES

Amended: April 2009 TL: E047997

VERTICAL MODE

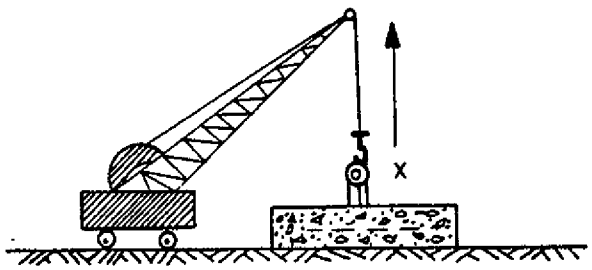

(ELEVATION)

Pull upward with crane using a "weak link" attached to crane cable

HORIZONTAL MODE

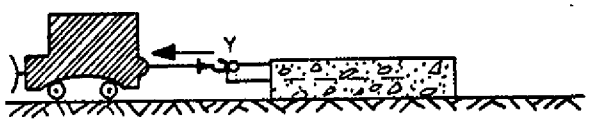

(ELEVATION)

Pull horizontally with cat using "weak link" attached to slab with a cable

ROCKING MODE

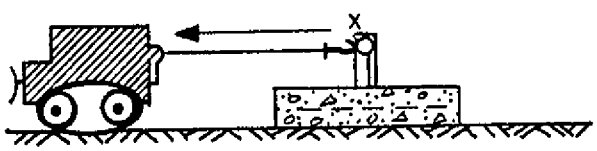

(ELEVATION)

Pull as indicated for the horizontal mode

TWISTING MODE

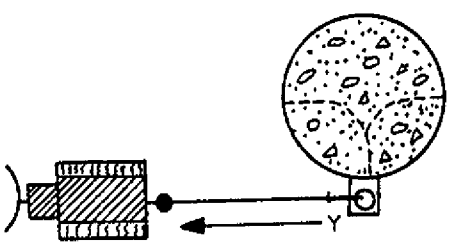

(PLAN)

Pull as indicated for the horizontal mode

Project: SONGS Job Number: B221I	METHODS OF DYNAMIC EXCITATION OF TEST SLABS	Fig. A-3

WOODWARD-McNEILL & ASSOCIATES

Amended: April 2009 TL: E047997

SLAB NO. 2

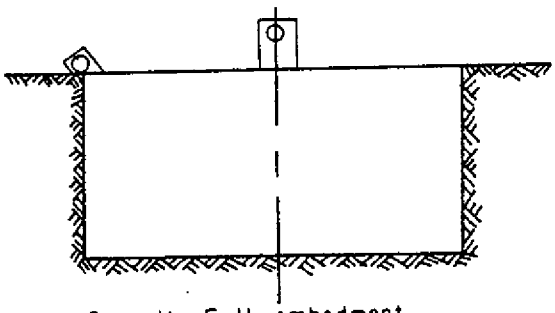

Case 1: Full embedment in natural ground

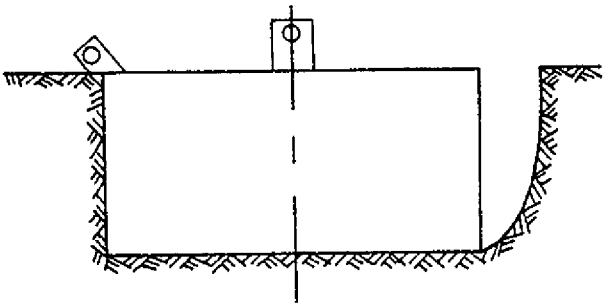

Case 2: Half embedment in natural ground

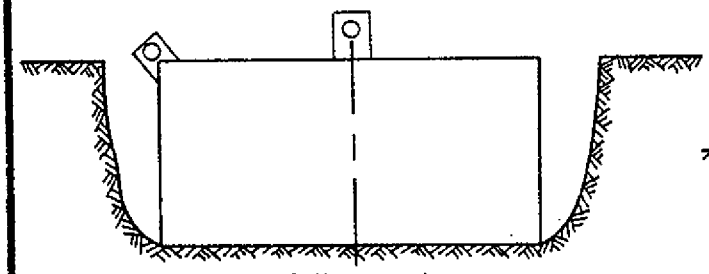

Case 3: Soil around slab excavated

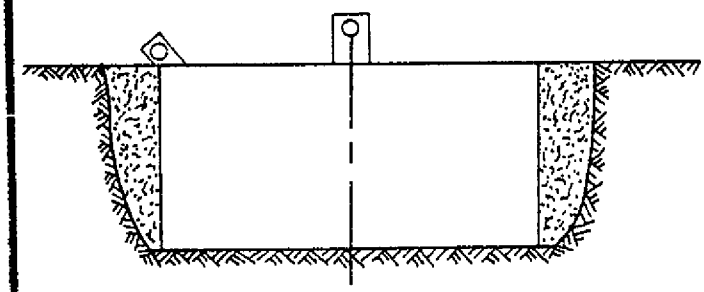

Case 4: Soil backfilled and compacted around slab

SLAB NO. 3

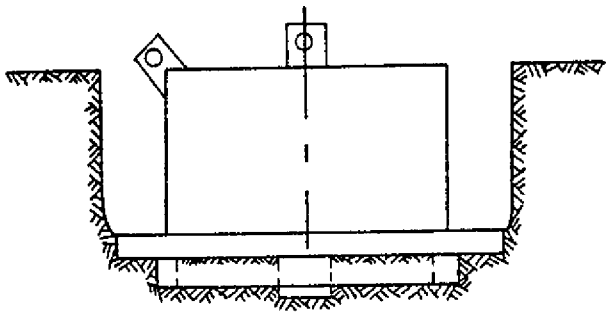

Case 1: Soil around slab excavated

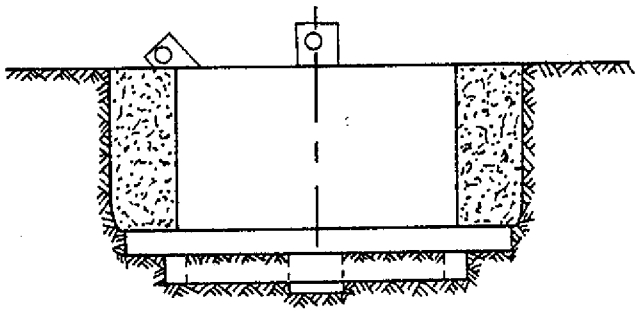

Case 2: Soil backfilled and compacted around slab

Project: SONGS Job Number: B221I	EMBEDMENT CONDITIONS SLABS NO. 2 AND 3	Fig. A-4

WOODWARD-McNEILL ASSOCIATES

Amended: April 2009 TL: E047997

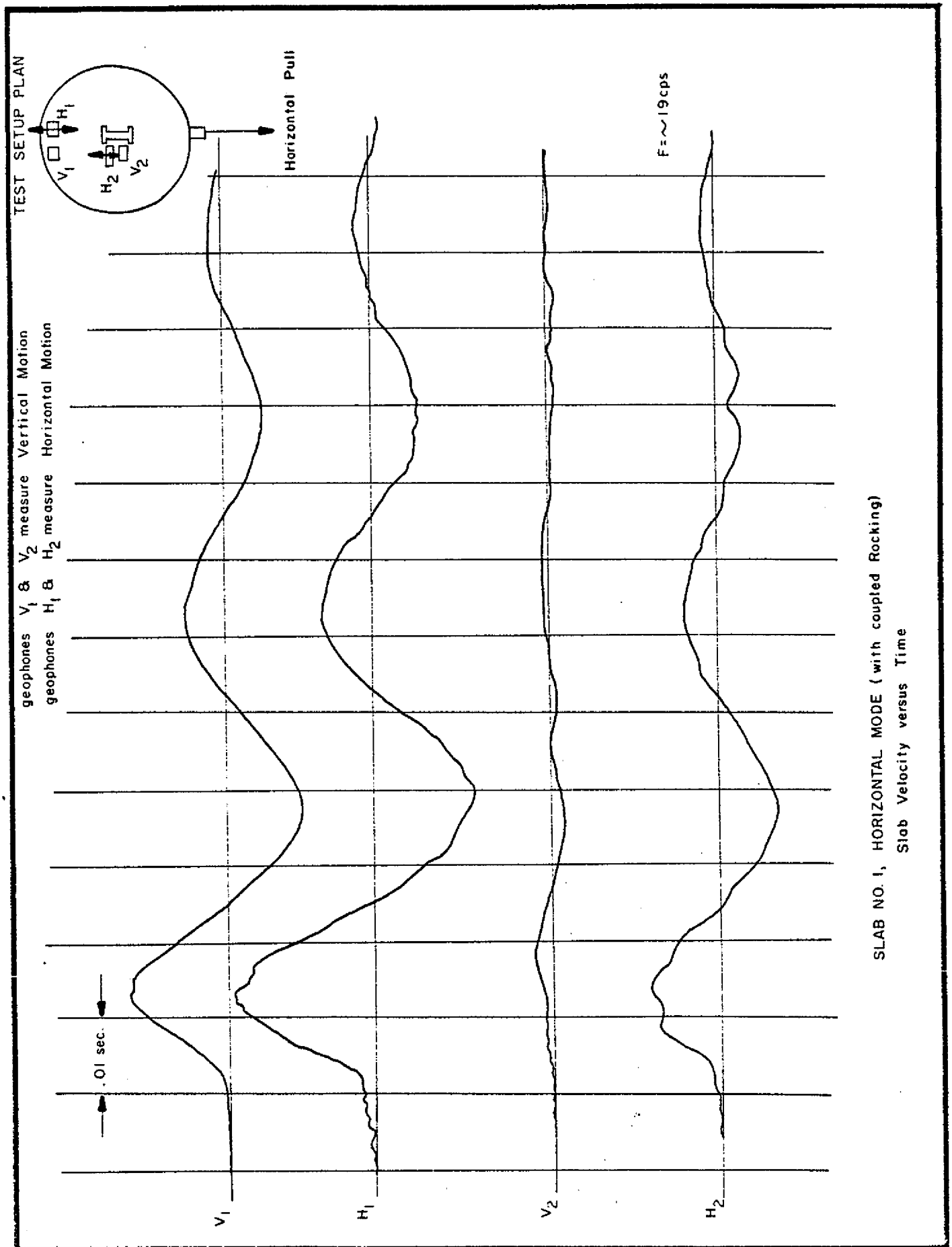

Project: SONGS Job Number: 8221 I	RECORDED DATA, SLAB RESPONSE TEST HORIZONTAL MODE	Fig. A-5

0-1

WOODWARD-McNEILL & ASSOCIATES

Amended: April 2009 TL: E047997

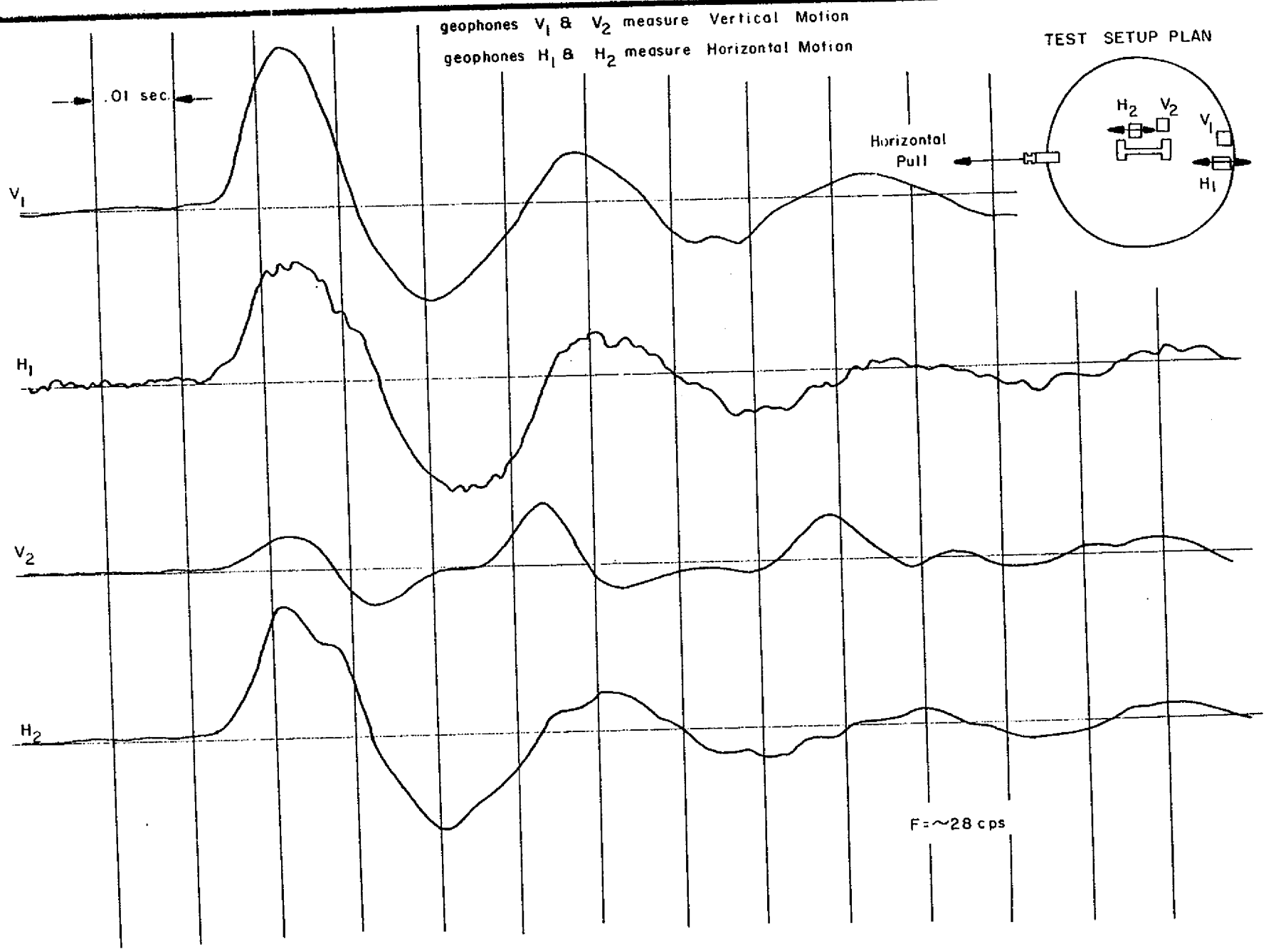

SLAB NO. 2, HALF EMBEDMENT CASE, ROCKING MODE

Slab Velocity versus Time

Project: SONGS

Job Number: B221I

RECORDED DATA, SLAB RESPONSE

TEST ROCKING MODE

WOODWARD-McNEILL & ASSOCIATES

Fig. A-6

Amended: April 2009 TL: E047997

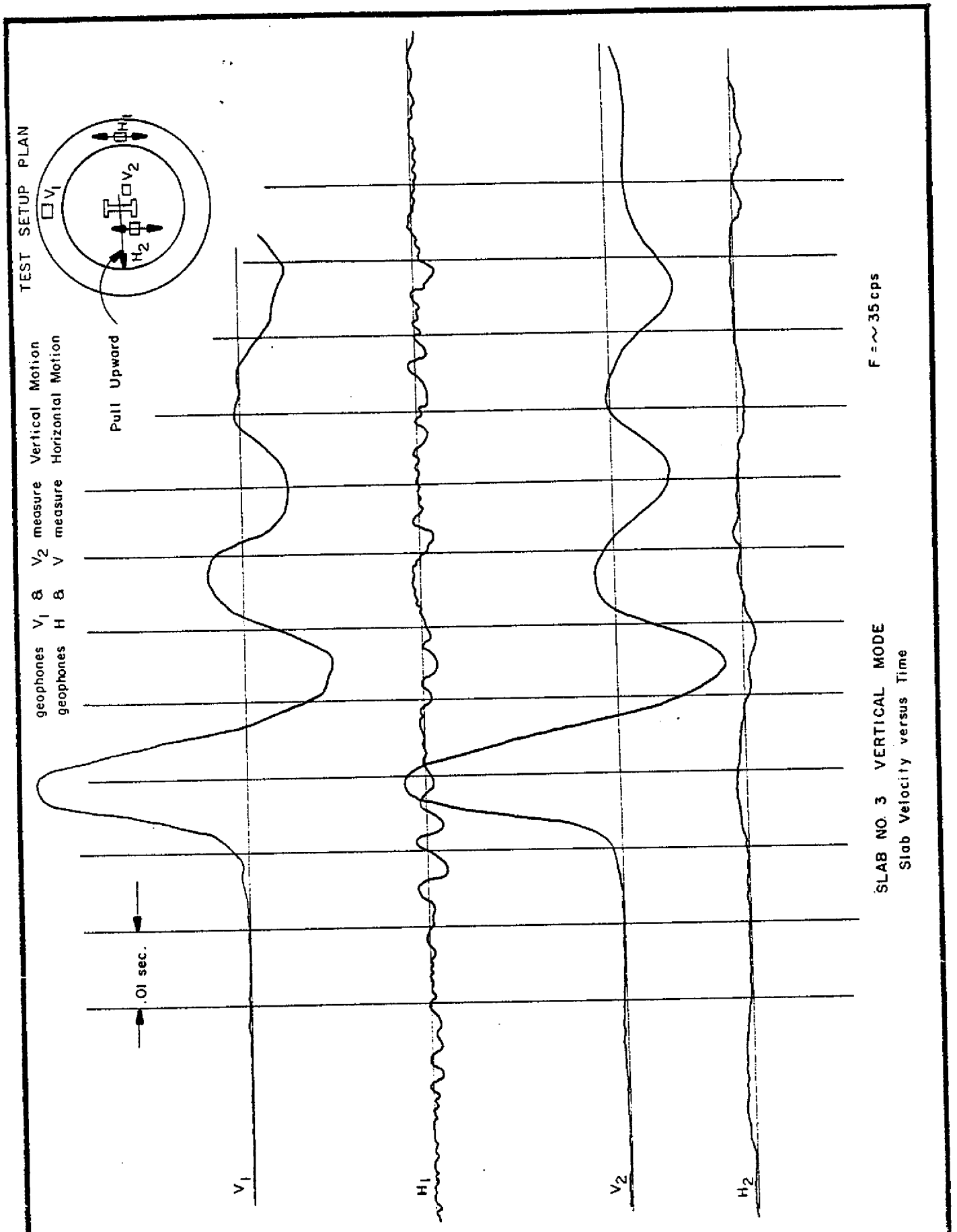

Project: SONGS SOIL STRUCTURE INTERACTION Job Number: B221I	RECORDED DATA, SLAB RESPONSE TEST VERTICAL MODE	Fig. A-7

WOODWARD-McNEILL & ASSOCIATES

Amended: April 2009 TL: E047997

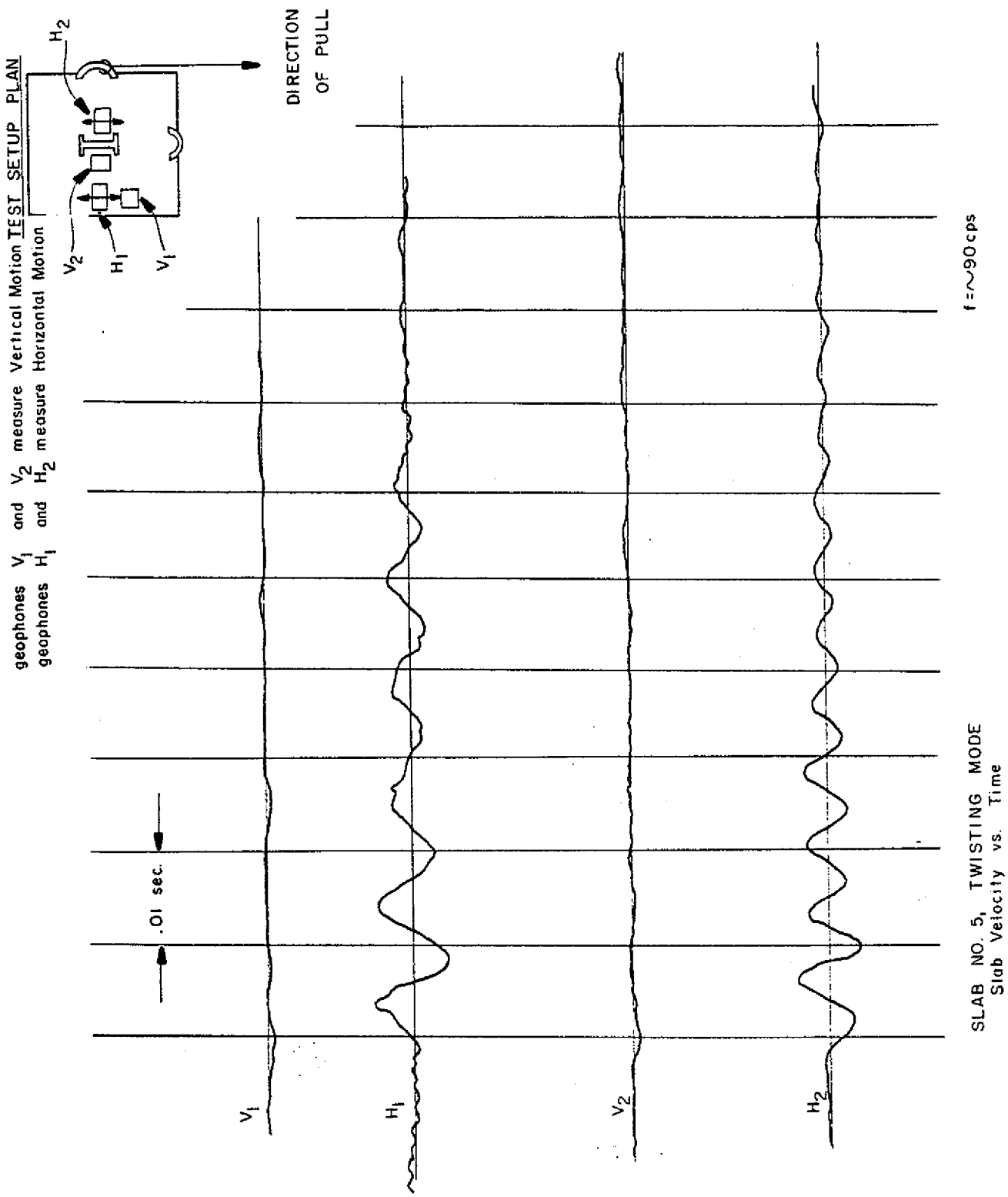

Project: SONGS SOIL STRUCTURE INTERACTION Job Number: B221I	RECORDED DATA, SLAB RESPONSE TEST TWISTING MODE	Fig. A-8

WOODWARD-McNEILL & ASSOCIATES

Amended: April 2009 TL: E047997

APPENDIX B

RAYLEIGH WAVE TESTS

Rayleigh wave traverses were conducted in the laydown area at the site at the locations shown on Fig. B-1. The purpose of performing these traverses was to provide data for the calculation of the Rayleigh wave velocity for the near-surface soil at the site.

Two 5-ft deep trenches were excavated in order to improve coupling between the input source and the subsurface soils and to insure that tests would be made in undisturbed native soil (San Mateo Formation Sand). The first trench was dug parallel to the beach, and the other perpendicular.

For the first two traverses conducted, Rayleigh waves were created by allowing a small electromechanical vibrator to vibrate in the vertical mode in the bottom of the trench. The third traverse utilized a vibrating sheepsfoot roller as the source of the Rayleigh waves. This vibrator produced large amplitude motions which also provided data for the attenuation measurements, described in Appendix C.

The Rayleigh wave motions were sensed with a pair of vertically oriented geophones. The procedure involved two steps: first, setting the two geophones at the same distance from the vibrator, and checking that they are exactly in phase; and second, moving one geophone to a progressively larger distance from the vibrator and measuring the time phase changes at several vibrator frequencies at each new location. An examples of the data recorded in the field is presented in Fig. B-2.

Amended: April 2009 TL: E047997

Appendix B

Page 2

The data are analyzed by using the simple relationship:

$$V_r = \frac{D}{t}$$

Where: V_r = Rayleigh-wave velocity

D = distance between geophones

t = time phase change

The wave length corresponding to each frequency can then be determined by the relationship:

$$\lambda = \frac{D}{tF}$$

Where: λ = wave length

F = frequency

The Rayleigh wave velocity V_r is a property of the near-surface material, and is, for practical purposes, equal to the shear wave velocity for material in this zone. The test averages the soil property to a depth of about 0.5 times the wave length. Thus the high frequencies (short wave lengths) provide properties of only the surface materials; and the low frequencies integrate the properties of surface, near-surface, and deeper materials.

For this site, the Rayleigh wave velocity was found to range from 850 to 1200 fps, with a velocity of 930 fps as a representative average for the near-surface (upper 15 ft) soils. This value was confirmed by direct measurement of surface wave velocity from attenuation tests as discussed in Appendix C.

Amended: April 2009 TL: E047997

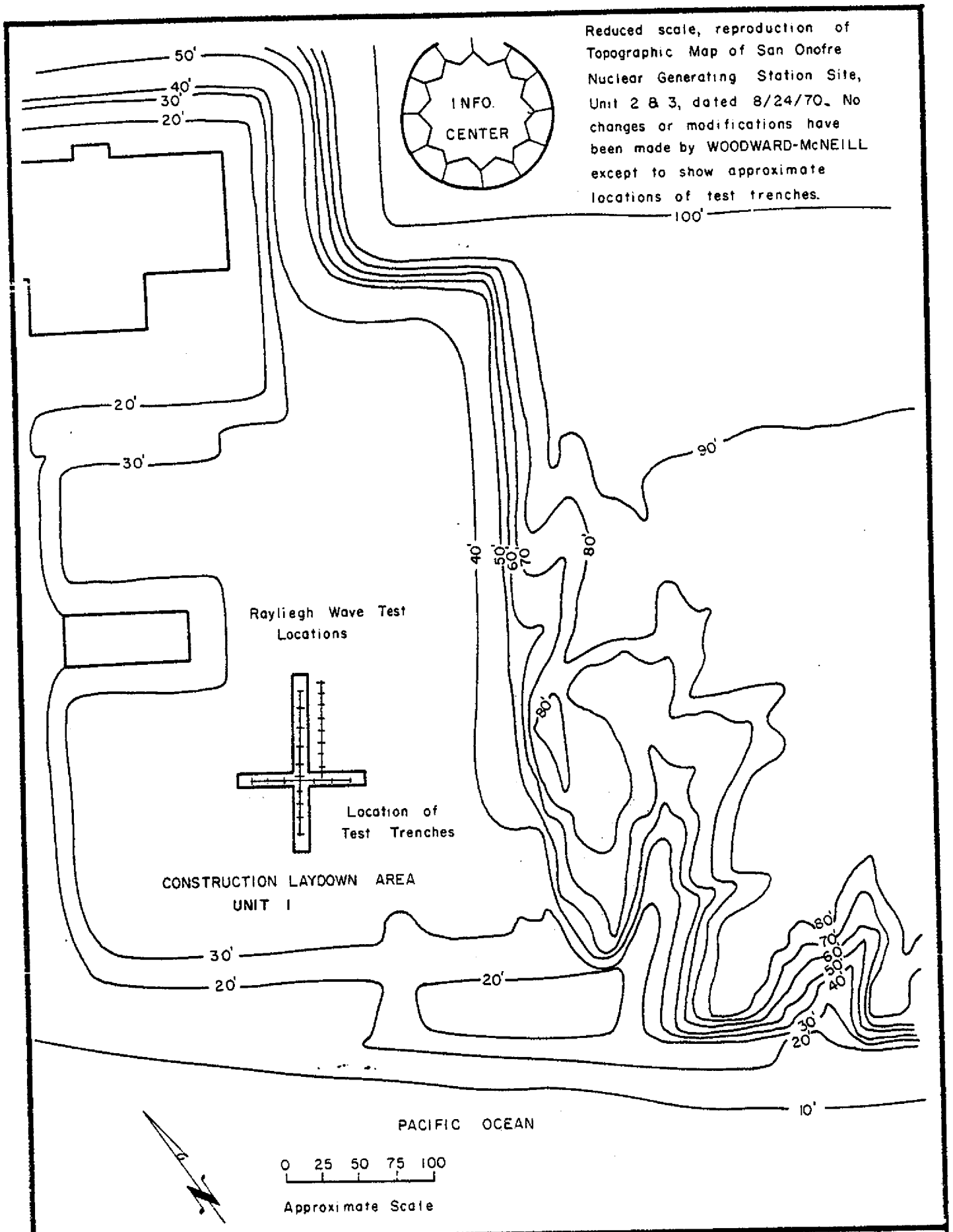

Project: SONGS SOIL STRUCTURE Job Number: B221I	SITE PLAN	Fig. B-1

WOODWARD-McNEILL & ASSOCIATES

Amended: April 2009 TL: E047997

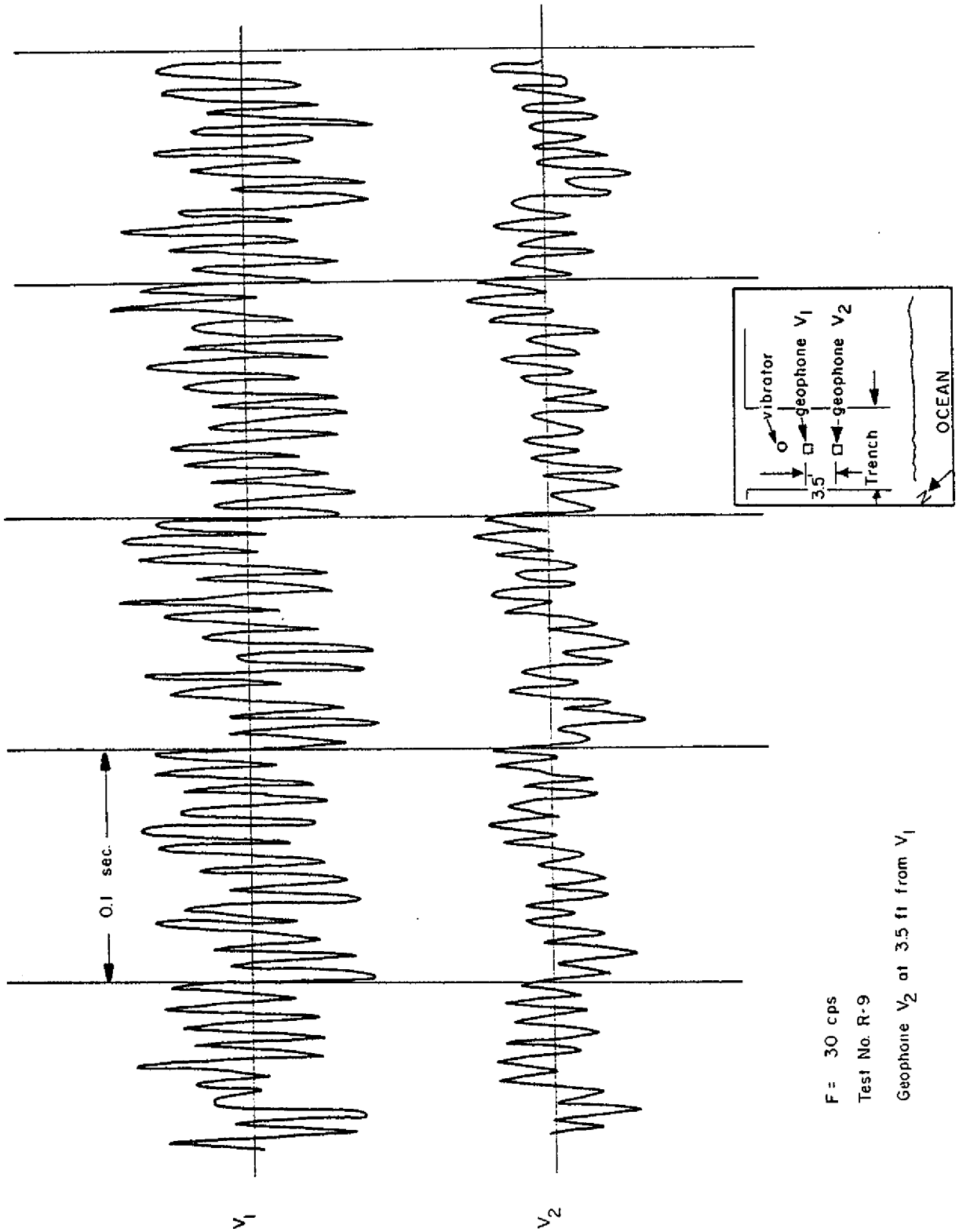

Project: SONGS SOIL STRUCTURE INTERACTION Job Number: B221I	RECORDED DATA, RAYLIEGH WAVE TEST	Fig. B-2

WOODWARD-McNEILL & ASSOCIATES

Amended: April 2009 TL: E047997

APPENDIX C

ATTENUATION TEST

Of the three Rayleigh wave traverses described in Appendix B, the third traverse, which utilized a vibrating sheepsfoot roller as the source of motion, also provided data for wave attenuation measurements. The test was carried out by inducing a large amplitude vibration in the ground and measuring the resulting vibration levels simultaneously with two geophones located on a straight line at different distances from the source. For uniform soils the attenuation of vibrations can be described by the following equation:

$$\frac{A_2}{A_1} = \left(\sqrt{\frac{r_1}{r_2}}\right) e^{-\alpha(r_2 - r_1)}$$

where the terms are defined on Fig. C-1.

The part of the equation under the radical indicates the portion of attenuation due to geometric energy dispersion with distance. The α term in the exponential part of the equation indicates the portion of attenuation due to the frequency-dependent internal damping or hysteresis of the soil.

Since the San Mateo Formation Sand at the site is fairly uniform, this equation should yield an adequate description of the soil damping properties. The results of the evaluation of "α" are presented graphically on Fig. C-2 for the test data shown on Fig. C-1 as well as another test performed with V_2 moved to a distance r_2 = 100 ft from the vibration source. Damping values can be calculated for the range of "α" indicated on Fig. C-2 by the following equation:

Amended: April 2009 TL: E047997

Appendix C

Page 2

$$\frac{D}{1-D^2} = \frac{V\alpha}{2\pi F}$$

where D = damping
V = wave velocity
F = frequency of vibration
α = attenuation constant

This calculation yields a hysteretic damping of 4-1/2 to 7% of critical. These values are comparable to those determined by laboratory tests as outlined in the report entitled *Elastic and Damping Properties, Laydown Area, San Onofre Nuclear Generating Station,* Fig. F-2 and F-3 (Ref. 4).

Amended: April 2009 TL: E047997

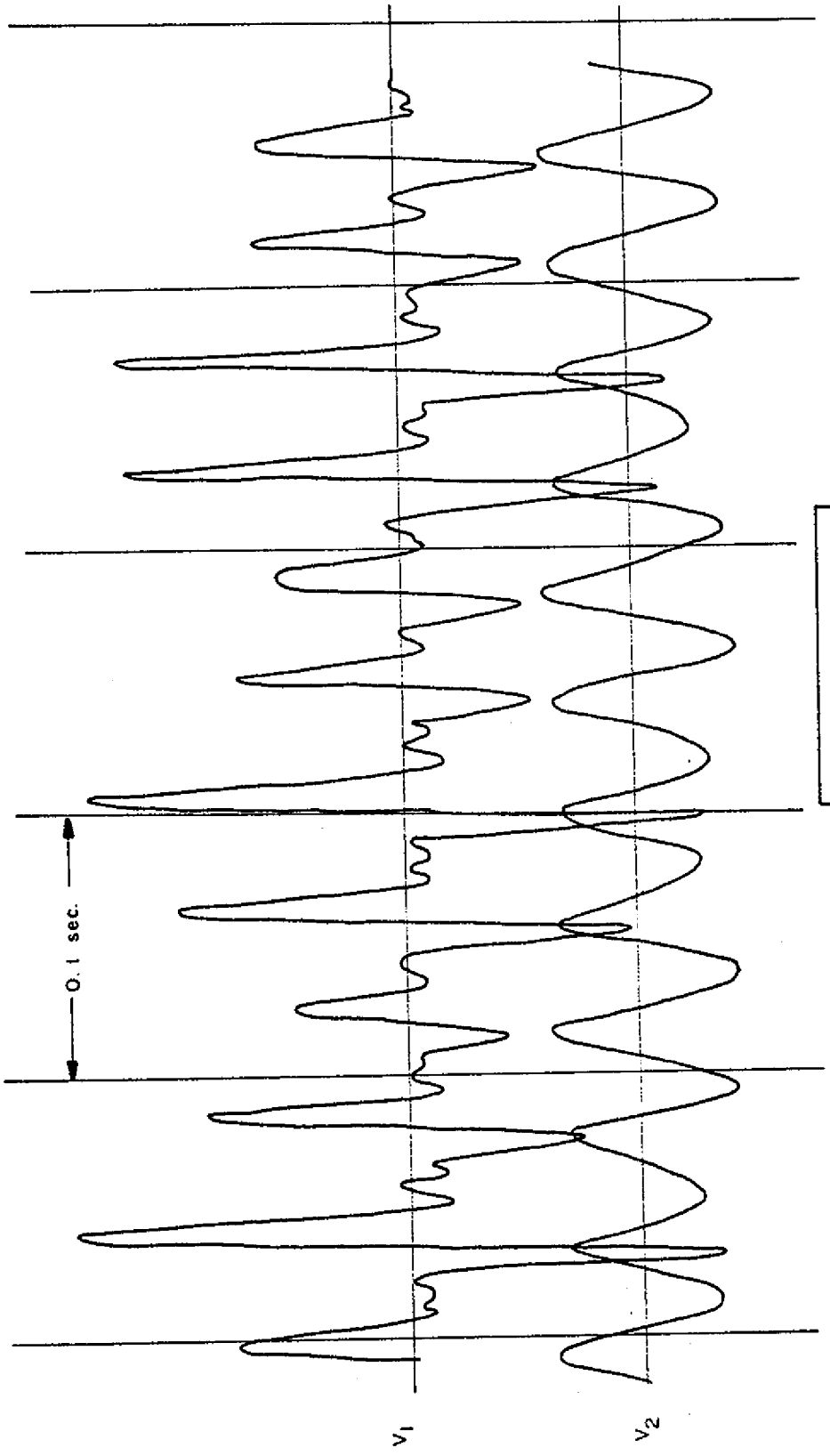

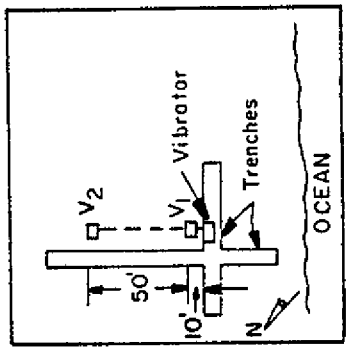

F = 23 cps
Test No. R-14
V_2 at 50 ft. from V_1
r1 = 10'
r2 = 60'
$A_1 \propto V_1$, $A_2 \propto V_2$ } for equal values of frequency

Project: SONGS SOIL STRUCTURE INTERACTION Job Number: B221I	RECORDED FIELD DATA ATTENUATION, TEST	Fig. C-1

WOODWARD-McNEILL & ASSOCIATES

Amended: April 2009 TL: E047997

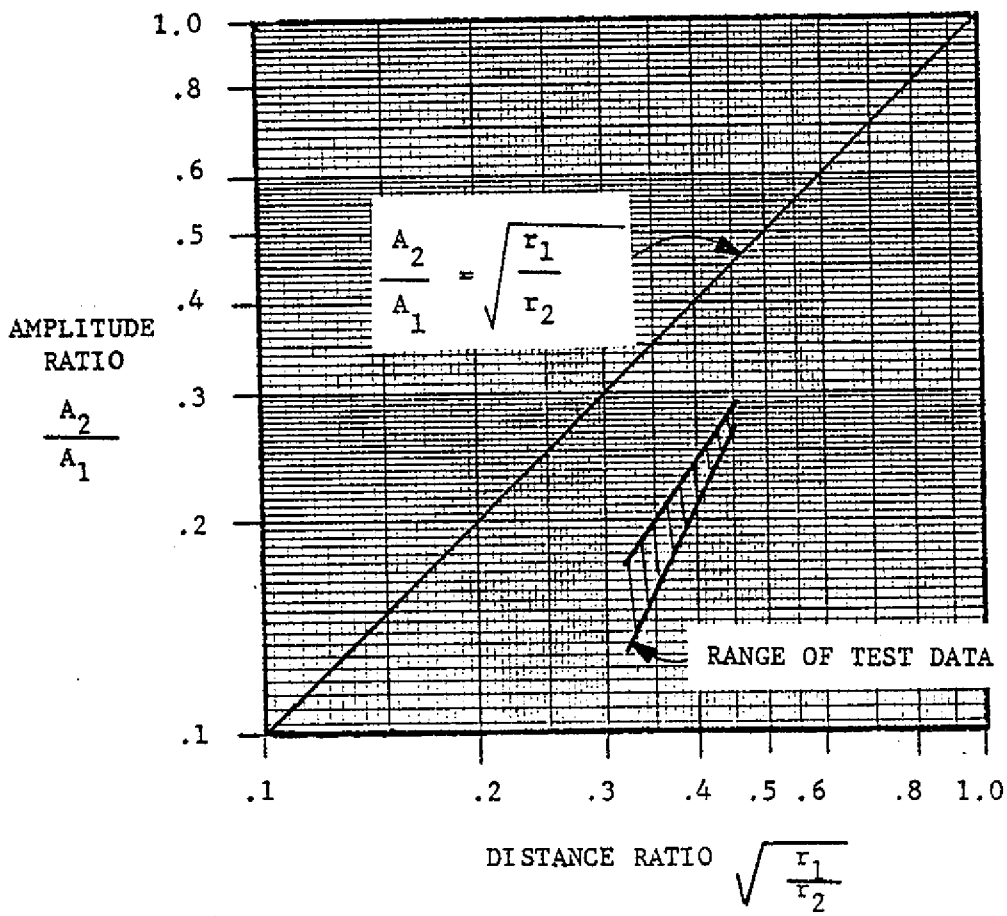

$$\frac{A_2}{A_1} = \sqrt{\frac{r_1}{r_2}}\, e^{-\alpha (r_2 - r_1)}$$

WHERE α = .008 TO .012 FOR THE RANGE OF TEST DATA

DEFINITION OF TERMS

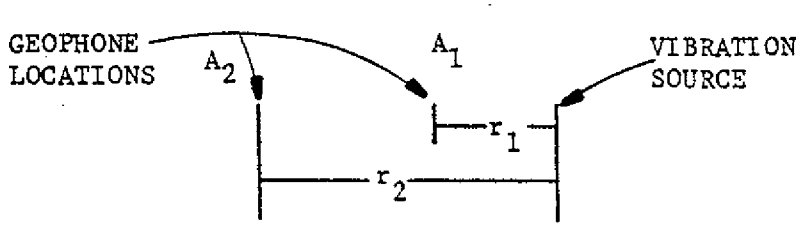

Project: SONGS SOIL STRUCTURE INTERACTION **Job Number:** B221I	RESULTS OF ATTENUATION TESTS	Fig. C-2

WOODWARD-McNEILL & ASSOCIATES

Amended: April 2009 TL: E047997

APPENDIX D

DAMPING

D-1 General

Both hysteretic and spatial damping are of importance for design. Hysteretic damping refers to that portion of the damping influenced by the internal behavior of a soil mass. It is a function of the stress-strain hysteresis of the soil. Spatial, or geometric damping refers to the decay of vibrations with distance from the source of motion. The determination of these quantities is discussed below.

D-2 Hysteretic Damping

The hysteretic damping of the site soils has been calculated from attenuation test results as described in Appendix C, and has been previously studied and reported on in Ref. 4. The data presented in that report were based on dynamic strain-control triaxial test results. A summary plot of the results of those tests is presented on Fig. D-1.

The field tests performed provided supportive data for the laboratory results. The range of results of attenuation tests calculated in Appendix C is indicated on Fig. D-1. These values show general agreement with the laboratory determined curve.

D-3 Spatial Damping

For most dynamic design conditions spatial (geometric) damping is more significant than hysteretic damping. The design equations for the calculation of damping values are presented in Table D-1 (Ref. 16). The effective radius, r_e, in these equations depends on the stress distribution below the slab

Amended: April 2009 TL: E047997

(Ref. 16). Therefore, it is necessary to know the stress distribution beneath the slab. The values of effective radius for the assumed stress distributions are given below (Ref. 16):

Distribution of Contact Pressures	Values of Effective Radius (r_e)
Rigid	$r_e = r$
Uniform	$r_e = .808\ r$
Parabolic	$r_e = .606\ r$

Figures D-2, D-3, and D-4 present the calculated damping curves for geometric damping for the range of effective radius values listed above, as well as the field test results. It should be noted that the field results are for total damping (hysteretic plus geometric). Therefore, the data points could be about 4-1/2 to 7% lower than shown on Figs. D-2, D-3, and D-4. From these results, it can be seen that there is a fairly wide range of results for the translational modes, while the range is relatively narrow for the rotational modes. Based on these results, it is concluded that an effective radius of 0.6 and 0.8 of the actual foundation radius results is a conservative estimate of damping for the translational and rotational modes, respectively.

The scatter in the test-results indicates there is no grouping of test-results according to embedment conditions; therefore, it is concluded that embedment conditions do not appreciably affect damping for this site.

Amended: April 2009 TL: E047997

TABLE D-1

DESIGN PARAMETERS

Parameters	Mode of Motion: VERTICAL TRANSLATION	HORIZONTAL TRANSLATION	ROCKING	TWISTING
Inertia	m, mass of foundation and machine	m, mass of foundation and machine	I_r, mass moment of inertia about rocking axis	I_t, mass moment of inertia about twist axis
Radius	$r = \sqrt{\frac{BL}{\pi}}$	$r = \sqrt{\frac{BL}{\pi}}$	$r = \sqrt[4]{\frac{BL^3}{6\pi}}$	$r = \sqrt[4]{\frac{BL(B^2 + L^2)}{6\pi}}$
Inertia Ratio	$B_v = \frac{(1-\nu)m}{4\rho r_e^3}$	$B_h = \frac{(7-8\nu)m}{32(1-\nu)\rho r_e^3}$	$B_r = \frac{3(1-\nu)I_r'}{8\rho r_e^5}$	$B_t = \frac{I_t}{\rho r_e^5}$
Effective Inertia for Design	m	m	$I_r' = \eta_r I_r$	I_t
Geometric Damping Coefficient	$c_v = \frac{3.4r^2\sqrt{G\rho}}{(1-\nu)}$ $(B_v \geq 0.36)$	$c_h = \frac{18.4(1-\nu)r^2\sqrt{G\rho}}{(7-8\nu)}$ $(B_h \geq 0.17)$	$c_r = \frac{0.80r^4\sqrt{G\rho}}{(1-\nu)(1+B_r\eta_r)}$	$c_t = \frac{2.31r^4\sqrt{G\rho}\sqrt{B_t}}{1 + 2B_t}$
Geometric Damping	$D_v = \frac{0.425}{\sqrt{B_v}}$	$D_h = \frac{0.288}{\sqrt{B_h}}$	$D_r = \frac{0.15}{(1+B_r)\sqrt{B_r}}$	$D_t = \frac{0.50}{1+2B_t}$

Note : for square or rectangular foundation - B = width of foundation in plan (parallel to axis of rotation)

L = length of foundation in plan (perpendicular to axis of rotation)

Ref. 16

Amended: April 2009 TL: E047997

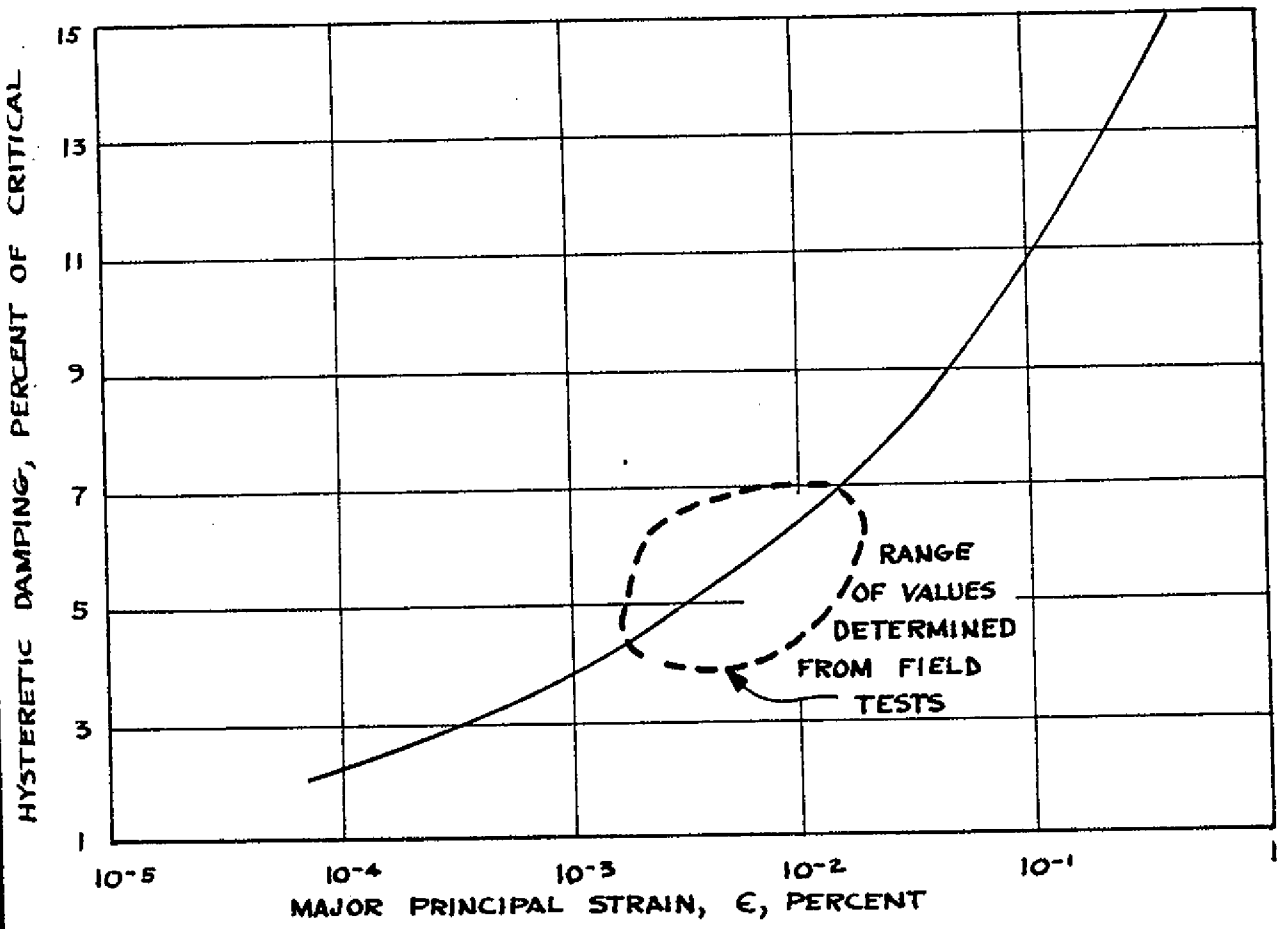

Project: SONGS SOIL STRUCTURE INTERACTION Job Number:	VALUES OF HYSTERETIC DAMPING	Fig. D-1

WOODWARD - McNEILL & ASSOCIATES

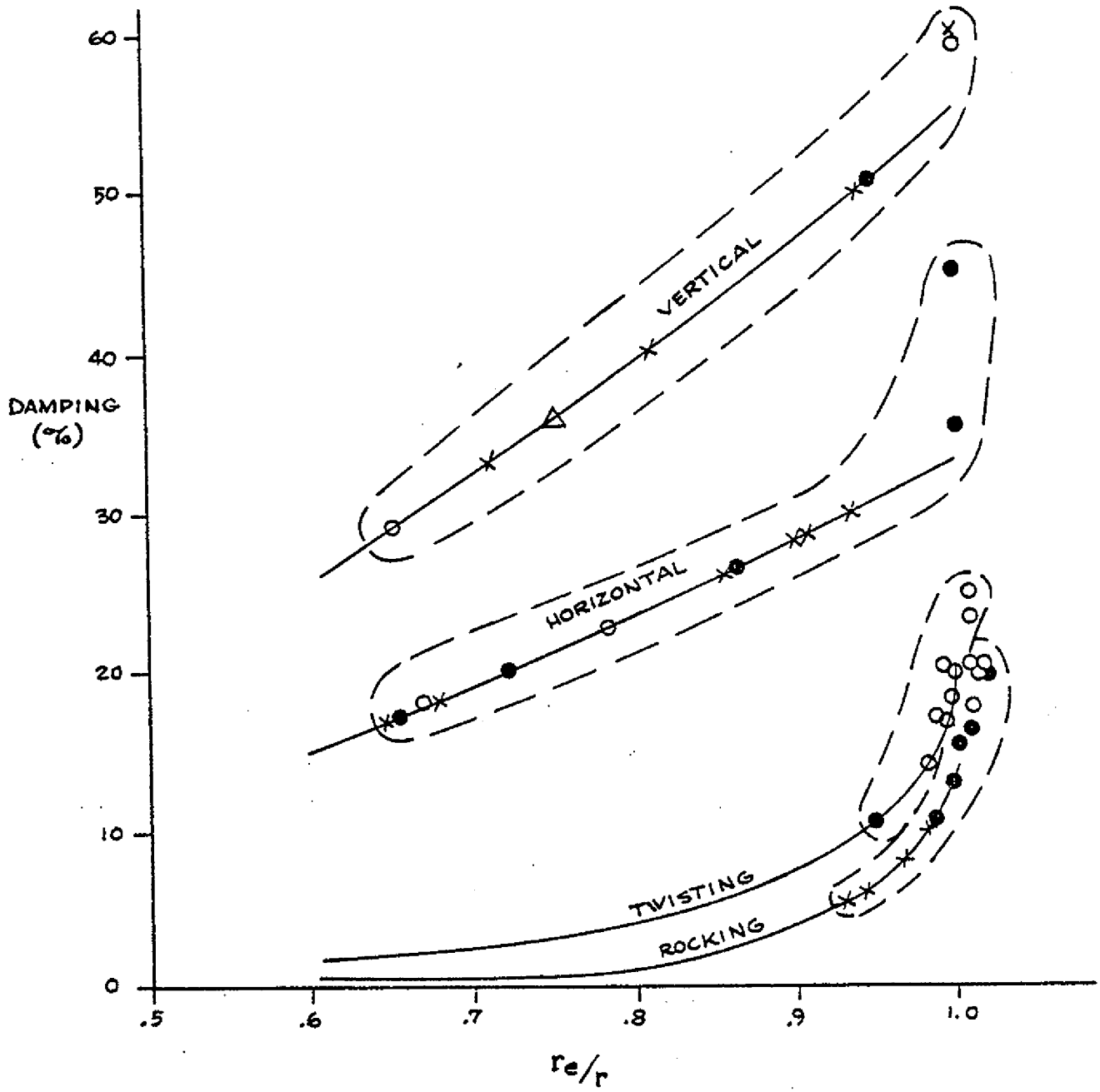

r_e = EFFECTIVE RADIUS
r = ACTUAL RADIUS
— = CALCULATED

SYMBOL	SLAB NO.
● X	1 & 2
O	2A
△	2C

Project: SONGS SOIL STRUCTURE INTERACTION Job Number: B221I	DAMPING VERSUS EFFECTIVE RADIUS	Fig. D-2

WOODWARD-McNEILL & ASSOCIATES

Amended: April 2009 TL: E047997

SLAB NO. 3

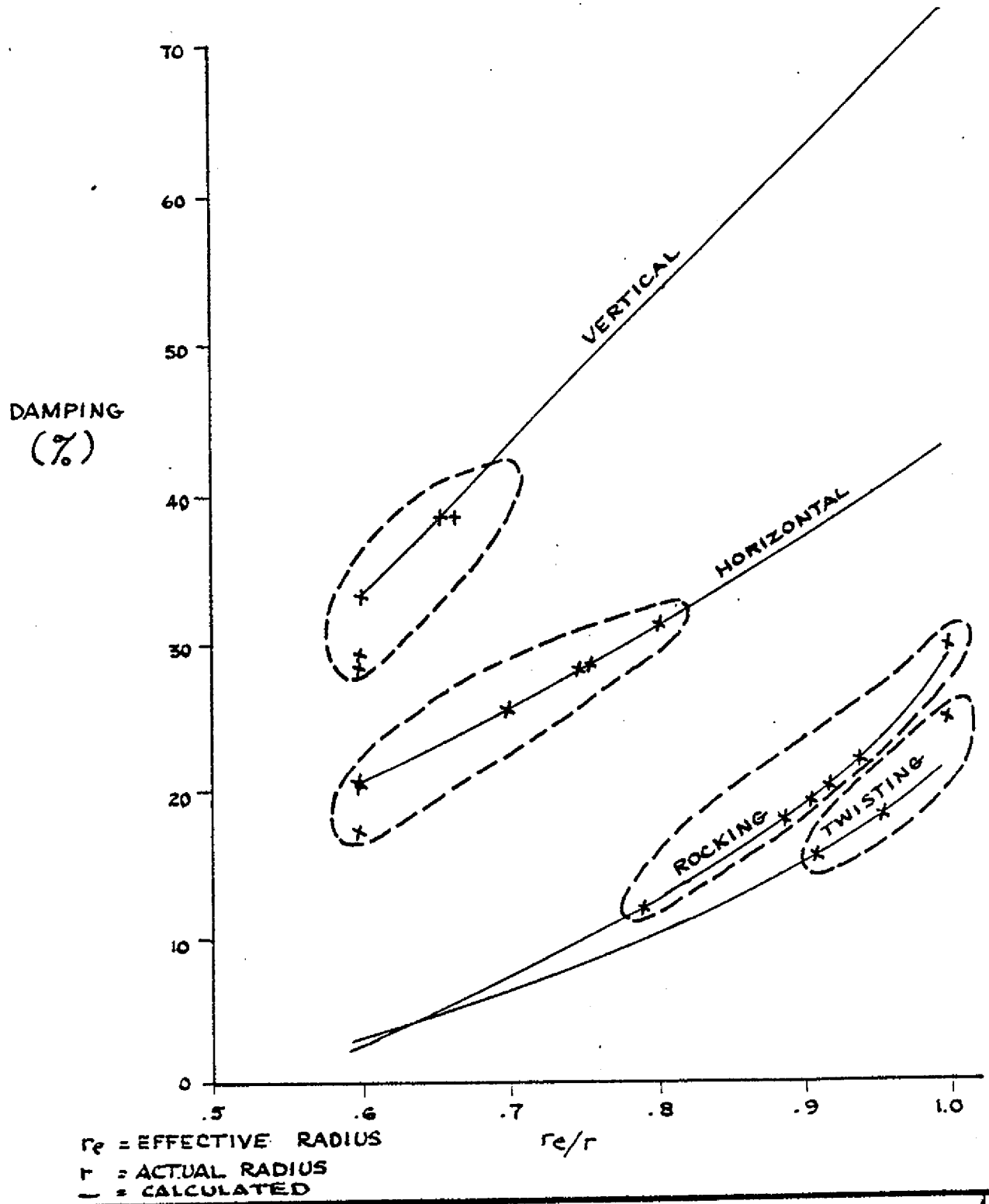

Project: SONGS SOIL STRUCTURE INTERACTION Job Number: 3221I	DAMPING VERSUS EFFECTIVE RADIUS SLAB NO. 3	Fig. D-3

WOODWARD – McNEILL & ASSOCIATES

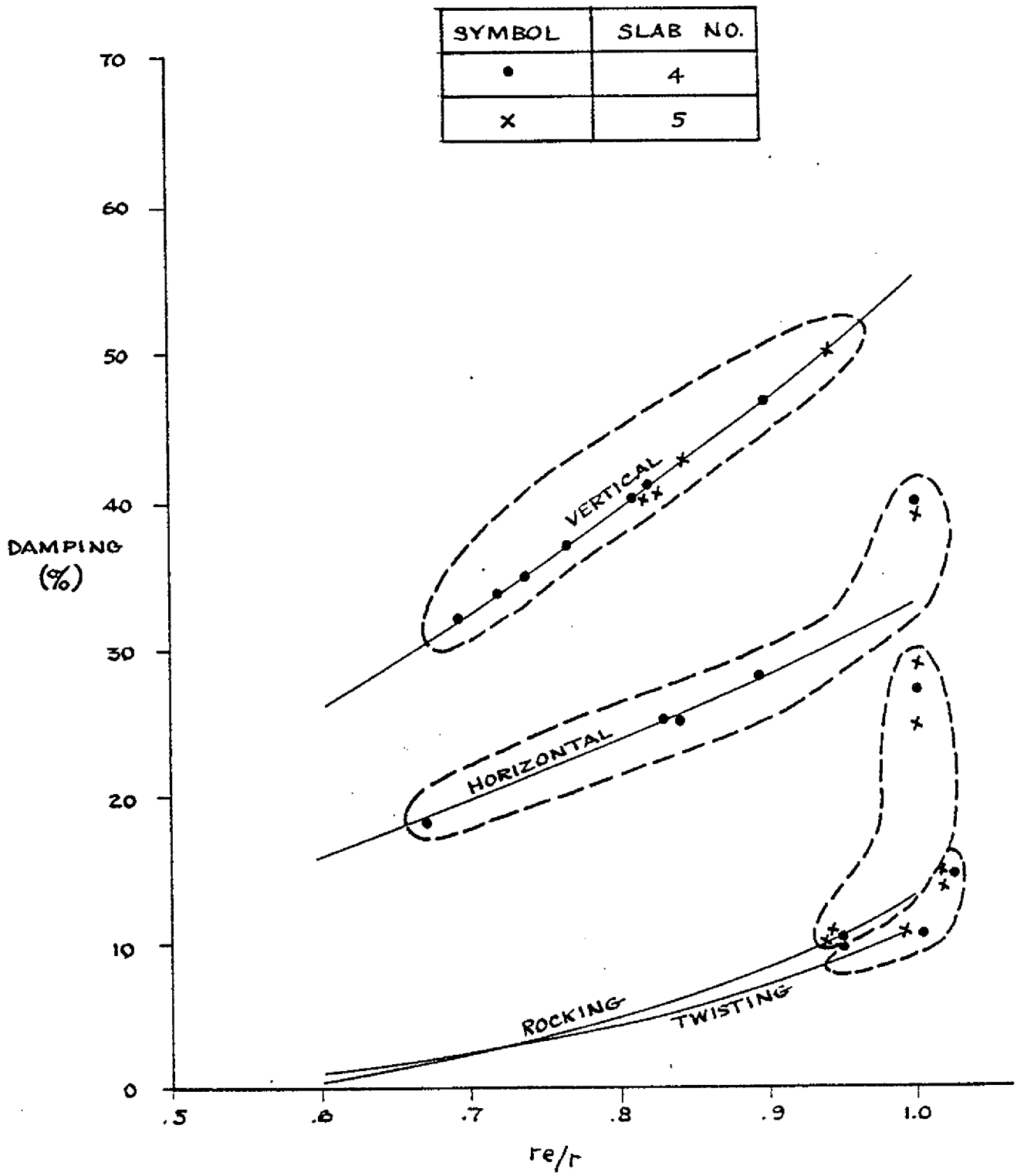

r_e = EFFECTIVE RADIUS
r = ACTUAL RADIUS
— = CALCULATED

Project: SONGS SOIL STRUCTURE INTERACTION **Job Number:** B221I	DAMPING VERSUS EFFECTIVE RADIUS SLAB NO. 4 AND 5	Fig. D-4

WOODWARD - McNEILL & ASSOCIATES

Amended: April 2009 TL: E047997

APPENDIX E

EVALUATION OF SPRING CONSTANTS

E-1 Introduction

The choice of an appropriate soil stiffness (of spring constant K), is fundamentally important to dynamic foundation design because its value is the most significant unknown in the determination of fundamental frequency, and it governs the static displacement of the foundation and the maximum amplitude of dynamic motion. The field tests performed on the Laydown Area at the site (Unit 1) provided information required to evaluate the compatibility of structural response calculations with data previously presented in the materials report (Ref. 4). In addition, because of the unique geometry of some of the proposed structure foundations, for which analytical solutions are not available, these tests were performed to develop adjustment factors for existing solutions and to determine the effects of various embedment conditions on structural response.

Whereas damping values were determined by analysis of the attenuation of vibrations after each slab was set into motion (as described in Appendix D), the evaluation of spring constants was made by analyzing frequency response of each slab.

The previous values given for spring constants (see Appendix H, Ref. 4) have been further studied and refined and are reported on in this report. Figure E-4 of that report has been included in this report as Fig. E-1, for ease of reference,

Amended: April 2009 TL: E047997

because it has been used for the determination of effective Shear Modulus.

E-2 Shear Modulus Determination

In order to evaluate spring constants for the soil-structure systems at the site, it is necessary to determine shear modulus values (G) for each test pad. Since G varies with strain (see Fig. E-1), it is necessary to determine the strain developed in the soil during dynamic loadings. In the field tests performed for this study, the slabs were set into transient motion, which produced a displacement and corresponding strain in the supporting soils. Based on our experience, we have assumed that the strain is accommodated within a depth of one radius below the slab, and that an average shear modulus can be calculated at a depth of half the radius below the base of the slab. Based on our previous work at this site, we have determined that for the San Mateo Formation Sand, the shear modulus should be calculated according to the following equation:

$$G = 100\ K_m\ (\sigma_m)^{2/3}$$

where $\sigma_m = \frac{2}{3}\ (x\gamma' + mp)$

where K_m = strain dependent parameter as determined from Fig. E-1
x = depth below base
γ' = effective unit weight
m = stress reduction factor
p = net bearing pressure

Amended: April 2009 TL: E047997

Figure E-2 presents the relationship between confinement (σ_m), strain (ε), and shear modulus (G) for the soils at the site. The values determined for each test slab are also shown on the figure.

E-3 Basic Equations

Analytical solutions have been developed for the calculation of spring constants for the vertical, horizontal, rocking, and twisting modes of motion of a rigid circular footing resting on an elastic half space (Ref. 16). These relations are presented in Table E-1.

In terms of frequency response, the basic relationship between undamped natural frequency (F_n) and stiffness is given by:

$$F_n = \frac{1}{2\pi}\sqrt{\frac{\text{stiffness}}{\text{inertia}}}$$

Where stiffness = k_v, k_h, k_r, or k_t

inertia = m_v, m_h, I_r, or I_t

The undamped natural frequency (F_n) and damped natural frequency (F_d), which is measured in our field tests, are related as given below:

$$F_d = F_n\sqrt{1-D^2}$$

Where D = damping factor

It can be seen by review of the damping factors determined from the field tests (Appendix D) that F_n and F_d are approxi-

TABLE E-1

DESIGN PARAMETERS

Parameters	Mode of Motion: VERTICAL TRANSLATION	HORIZONTAL TRANSLATION	ROCKING	TWISTING
Inertia	m, mass of foundation and machine	m, mass of foundation and machine	I_r, mass moment of inertia about rocking axis	I_t, mass moment of inertia about twist axis
Radius	$r = \sqrt{\frac{BL}{\pi}}$	$r = \sqrt{\frac{BL}{\pi}}$	$r = \sqrt[4]{\frac{BL^3}{3\pi}}$	$r = \sqrt[4]{\frac{BL(B^2 + L^2)}{6\pi}}$
Inertia Ratio	$B_v = \frac{(1-\nu)m}{4\rho r^3}$	$B_h = \frac{(7-8\nu)m}{32(1-\nu)\rho r^3}$	$B_r = \frac{3(1-\nu)I'_r}{8\rho r^5}$	$B_t = \frac{I_t}{\rho r^5}$
Effective Inertia for Design	m	m	$I'_r = \eta_r I_r$	I_t
Stiffness Coefficient	$k_v = \frac{4Gr}{(1-\nu)}$	$k_h = \frac{32(1-\nu)Gr}{(7-8\nu)}$	$k_r = \frac{8Gr^3}{3(1-\nu)}$	$k_t = \frac{16Gr^3}{3}$
Stress Distribution	rigid	uniform	rigid	rigid

Note: for square or rectangular foundation - B = width of foundation in plan (parallel to axis of rotation)

L = length of foundation in plan (perpendicular to axis of rotation)

Amended: April 2009 TL: E047997

mately equal. Table E-2, below, presents equations for spring constants as a function of frequency.

TABLE E-2

Motion	Spring Constant
Vertical and Horizontal	$k_{v,h} = 4\pi^2 F^2 m$
Rocking	$k_r = 4\pi^2 F^2 I_r$
Twisting	$k_t = 4\pi^2 F^2 I_t$

Where m = mass of slab

I_r = moment of inertia in Rocking Mode

I_t = moment of inertia in Twisting Mode

From the equations of Tables E-1 and E-2, spring constants can be calculated for each slab as a function of G and F, respectively. These relationships are presented in Table E-3 below:

Amended: April 2009 TL: E047997

TABLE E-3
$k=f(G,F)$

Motion	SLABS 1 & 2 Spring Constant k		SLAB 3 Spring Constant k		SLABS 4 & 5 Spring Constant k	
	$k=XGC$	$k=YF^2$	$k=XGC$	$k=YF^2$	$k=XGC$	$k=YF^2$
Vertical	$k_v=30.8GC$	$k_v=72.4F^2$	$k_v=30.8GC$	$k_v=42.4F^2$	$k_v=12.1GC$	$k_v=4.65F^2$
Horizontal	$k_h=25GC$	$k_h=72.4F^2$	$k_h=25GC$	$k_h=42.4F^2$	$k_h=9.7GC$	$k_h=4.65F^2$
Rocking	$k_r=512GC$	$k_r=1040F^2$	$k_r=512GC$	$k_r=390F^2$	$k_r=32.4GC$	$k_r=10.9F^2$
Twisting	$k_t=665GC$	$k_t=905F^2$	$k_t=665GC$	$k_t=330F^2$	$k_t=42.7GC$	$k_t=9.3F^2$

where $C = C_1 \times C_2 \times C_3 \times C_4$ = correction factor

C_1 = Empirical Correction Factor
C_2 = Embedment Correction Factor
C_3 = Scaling Correction Factor
C_4 = Shape Correction Factor

These correction factors are discussed in the sections which follow.

E-4 Empirical Correction Factor-C_1

The value of C_1 is determined by comparing the theoretical value of k (based on k = XGC, Table E-3) with the value of k determined from actual frequency response measurements obtained in the field ($k = YF^2$) from a circular slab on the ground surface (slab - 1). From this comparison, values for the empirical correction factor, C_1, were calculated for each mode. These values are presented below:

Mode	Empirical Correction Factor - C_1
Vertical	0.81
Horizontal	1.0
Rocking	0.66
Twisting	0.41

The values for C_1 presented above are probably due to the actual stress distributions. For the vertical mode, theoretical values are consistent to a rigid base stress distribution (Table E-1). Field tests indicated that a correction factor of .81 should be applied, which is consistent to a uniform stress distribution (r_e = .808r).

For the horizontal mode field tests, the values calculated from measured frequency agreed with the theoretical values; therefore C_1 equals 1.0. For this mode, uniform stress distribution is consistent to the theoretical equation (Table E-1).

For the rotational modes, stiffness is proportional to radius to the third power, therefore for uniform stress distribution where r_e = .81r, $r_e^3 = 0.53r^3$. The values determined for C_1 for the rocking and twisting modes were 0.66 and 0.41, respectively, which are reasonably close to the calculated values of 0.53

E-5 Embedment Correction Factor - C_2

Because there is relatively little data available which describe the effect of embedment on stiffness, field tests were

performed for this purpose. Test-results for Slab No. 2 (embedded) were compared with those for Slab No. 1 (non-embedded), and the results plotted as a graph of slab embedment to radius ratio (h/r) versus spring constant ratio $\left(\frac{k \text{ embedded}}{k \text{ non-embedded}}\right)$. The values of k were calculated from frequency response data according to the equations of Table E-3. These graphs are presented on Figs. E-3, E-4, E-5 and E-6. It should be noted that these curves are based on one set of data points (at h/r=1.0), and the shape of the curves has been estimated from previous work by Kaldjian (1968). From the data of Figs. E-3 through E-6 an embedment correction factor, C_2, is determined as a function of the degree of embedment.

E-6 Scaling Correction Factor-C_3

To evaluate the effects of scaling, tests were made on circular slabs 4 to 10 ft in diameter as shown in Appendix A (Slabs 4 and 2, respectively). The ratio of frequency responses for two slabs of similar geometry but different size is given by:

$$\frac{F_2}{F_1} = \sqrt{\frac{k_2 \; m_1}{m_2 \; k_1}}$$

Where m = mass or inertia
k = stiffness

For the two slabs tested to evaluate the effects of scaling, a calculation was made of the theoretical frequency response

Amended: April 2009 TL: E047997

ratio for each mode of vibration. Taking into account the difference in shear modulus for the two slabs, these calculations indicate that the response of the 10 ft diameter slab (No. 2) should have a frequency of 65 to 70% of that of the 4 ft diameter slab (No. 4) for all modes, A review of the frequency response test-results presented in Appendix A indicates that the ratio of the measured responses for these slabs did not deviate appreciably from the theoretical ratio calculated for each case. This indicates that a scaling correction factor (C_3) of 1.0 can be used for engineering analysis.

E-7 Shape Correction Factor - C_4

A number of tests were made on slabs with various shape-characteristics in order to determine differences in responses. Two of the slabs (Nos. 4 and 5) had approximately the same mass, thickness, inertia, and embedment conditions. The significant difference between the two was in their shapes. One was circular (No. 4) while the other was square (No. 5). A review of the test-results presented in Appendix A, Table A-1, indicates that there was no appreciable difference in measured frequency response; therefore, it is concluded that a correction factor (C_4) of 1.0 for foundation shape can be utilized for engineering design for normal shaped foundations (i.e., circular, square, rectangular).

Tests were also made on slabs to evaluate the effects on response of the special foundation shape of the proposed containment structures for Units 2 and 3. Slab No. 3, shown in Appendix A, was constructed for this purpose. Tests were made on this slab and compared to the theoretical calculation for a slab with the same overall dimensions, but of uniform geometry (cylindrical). For the shape of the containment structure, the overall correction factors presented on the following table were determined:

Mode	Correction Factor-C
Vertical	1.075
Horizontal	1.09
Rocking	0.60
Twisting	N.A.

It should be noted that the correction factors presented above take into account not only the correction for the complex shape of the foundation, but also the unique embedment conditions of the containment structure (see Appendix A, Fig. A-4) and the empirical correction factor. The scaling correction factor was assumed to be 1.0 as discussed in Section E-6 above.

E-8 Special Consideration for Rocking Mode Inertia

Table E-4 presents design equations for stiffness calculations. For the rocking mode, the effective inertia for the rocking mode is given as a function of η_r and B_r. For the

Amended: April 2009 TL: E047997

slabs tested in this study η_r was not significantly greater than 1.0; however for design, the value of η_r should be calculated and the moment of inertia adjusted by η_r as indicated from Fig. E-7.

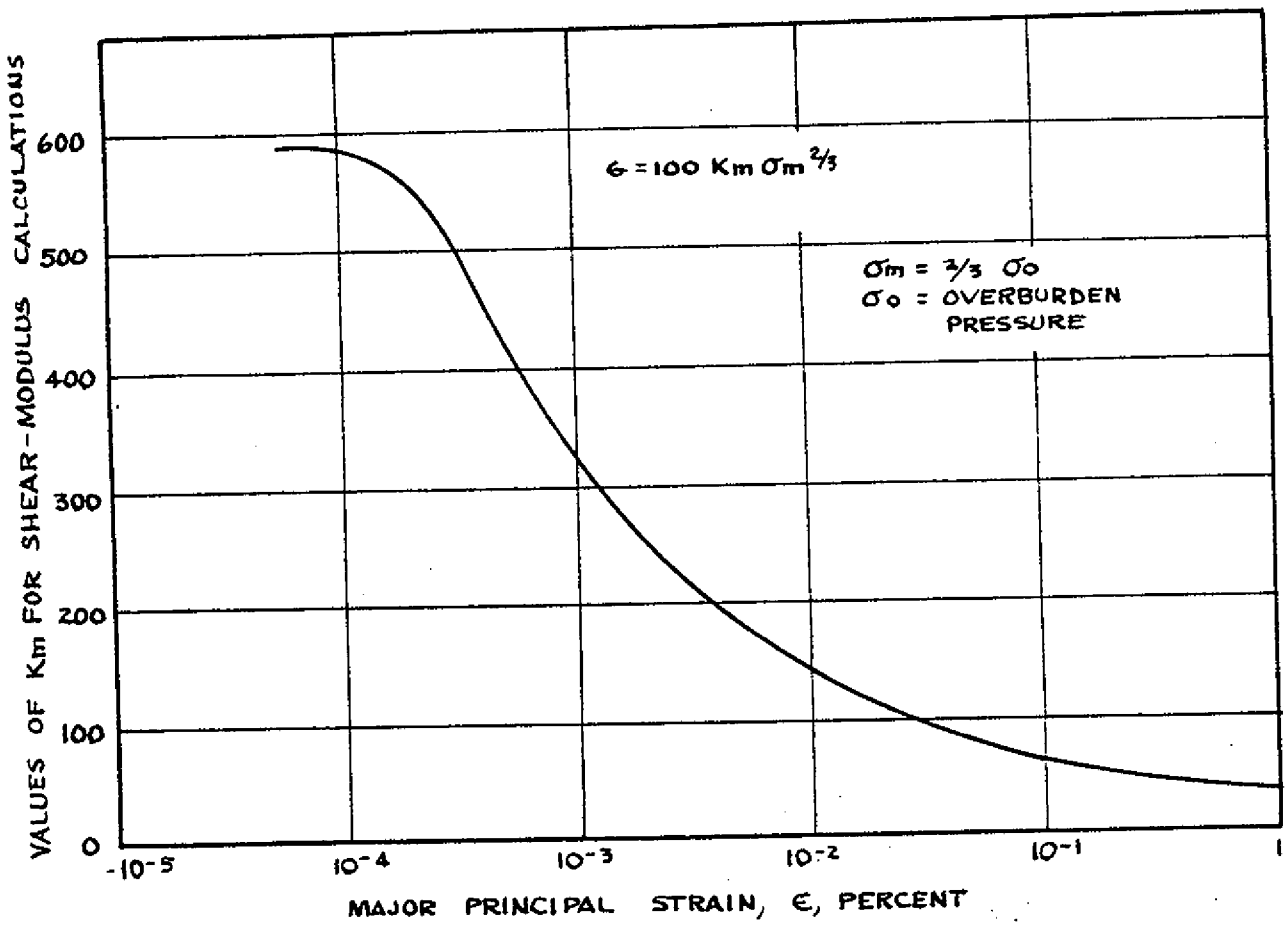

Project: SONGS SOIL STRUCTURE INTERACTION **Job Number:** B221I	RECOMMENDED MODULUS VALUES	Fig. E-1

WOODWARD - McNEILL & ASSOCIATES

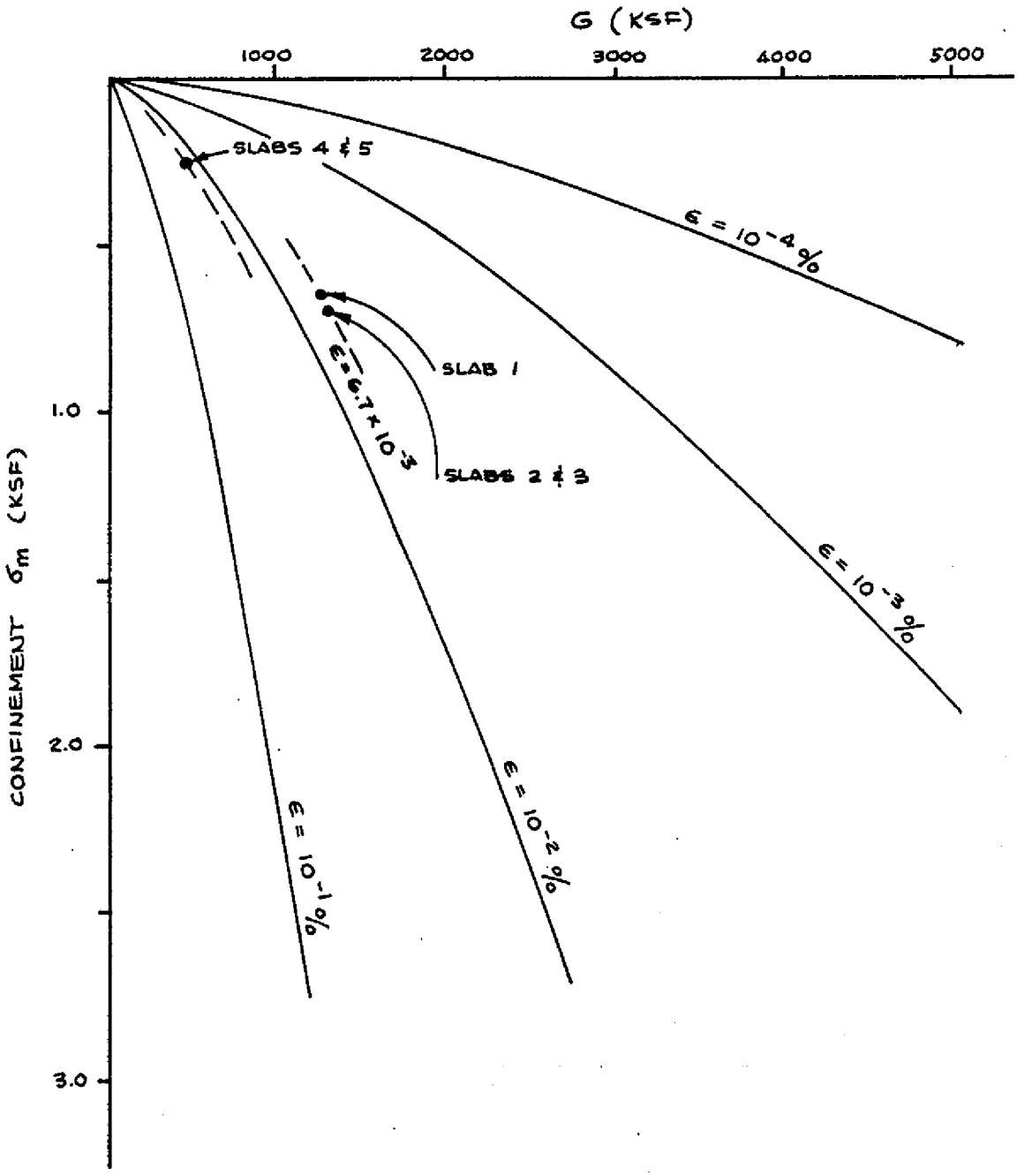

SAN MATEO SAND

$G = 100\ K_m\ (\sigma_m)^{2/3}$ PSF

$\sigma_m = 2/3$ (OVERBURDEN)

Project: SONGS SOIL STRUCTURE INTERACTION Job Number: B221I	SHEAR MODULUS FOR TEST SLABS	Fig. E-2

Amended: April 2009 TL: E047997

VERTICAL MODE

Note: Shape of curve estimated from previous work by Koldjian (1968)

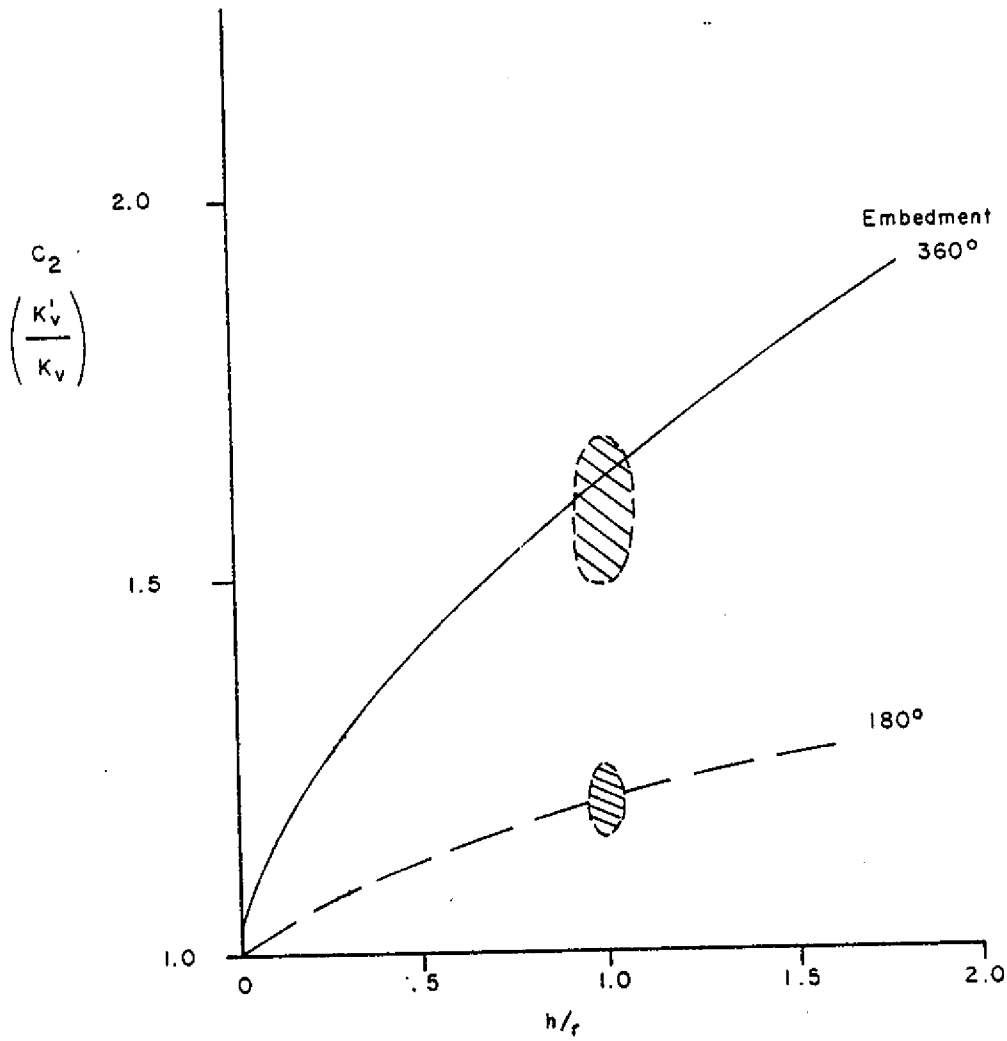

K' = embedded case

K = non-embedded case

C_2 = embedment correction factor

= range of data points

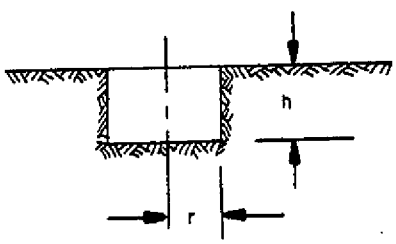

Project: SONGS SOIL STRUCTURE INTERACTION Job Number: B221I	EFFECT OF EMBEDMENT ON SPRING CONSTANT VERTICAL MODE	Fig. 3-3

WOODWARD-McNEILL & ASSOCIATES

Amended: April 2009 TL: E047997

HORIZONTAL MODE

Note: Shape of curve estimated from previous work by Kaldjian (1968)

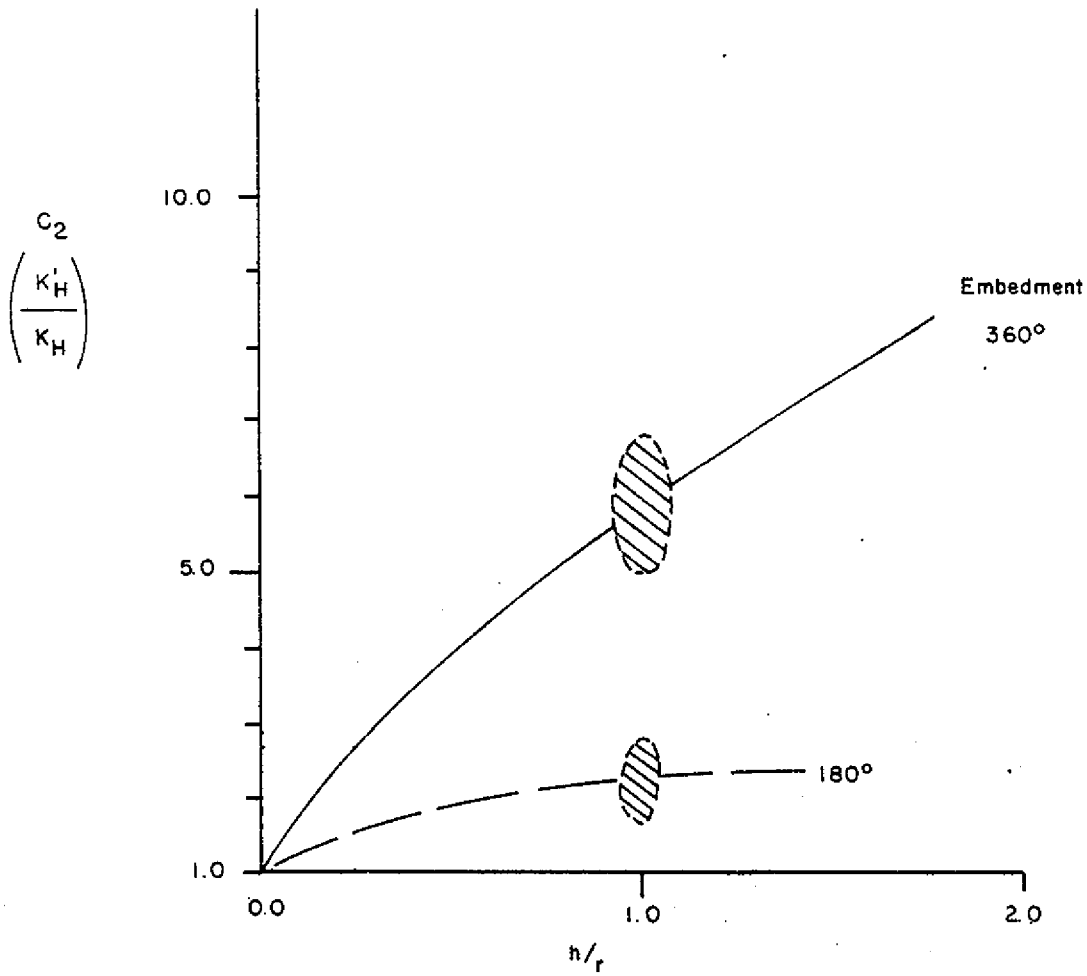

C_2 = embedment correction factor

K' = embedded case

K = non-embedded case

= range of data points

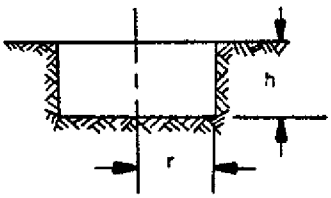

Project: SONGS SOIL STRUCTURE INTERACTION Job Number B221I	EFFECT OF EMBEDMENT ON SPRING CONSTANT, HORIZONTAL MODE	Fig. E-4

Amended: April 2009 TL: E047997

ROCKING MODE

Note: Shape of curve estimated from previous work by Kaldjian (1968)

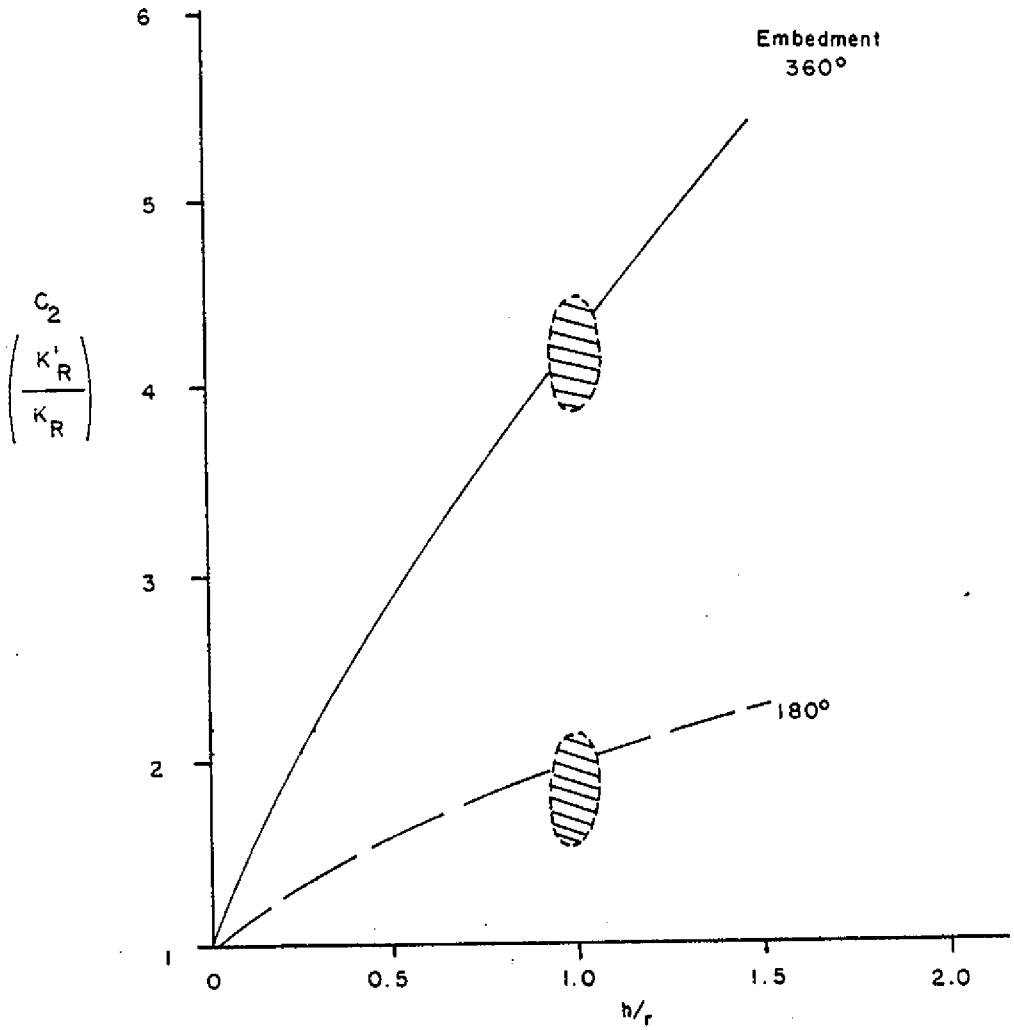

C_2 = embedment correction factor

K' = embedded case

K = non-embedded case

= range of data points

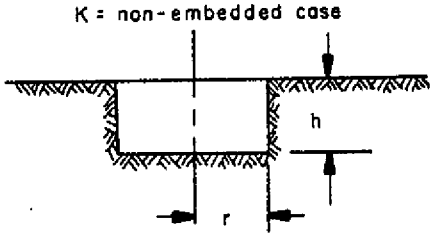

Project: SONGS SOIL STRUCTURE INTERACTION Job Number: B221I	EFFECT OF EMBEDMENT ON SPRING CONSTANT ROCKING MODE	Fig. E-5

WOODWARD-McNEILL & ASSOCIATES

Amended: April 2009 TL: E047997

TWISTING MODE

Note: Shape of curve estimated from previous work by Kaldjian (1968)

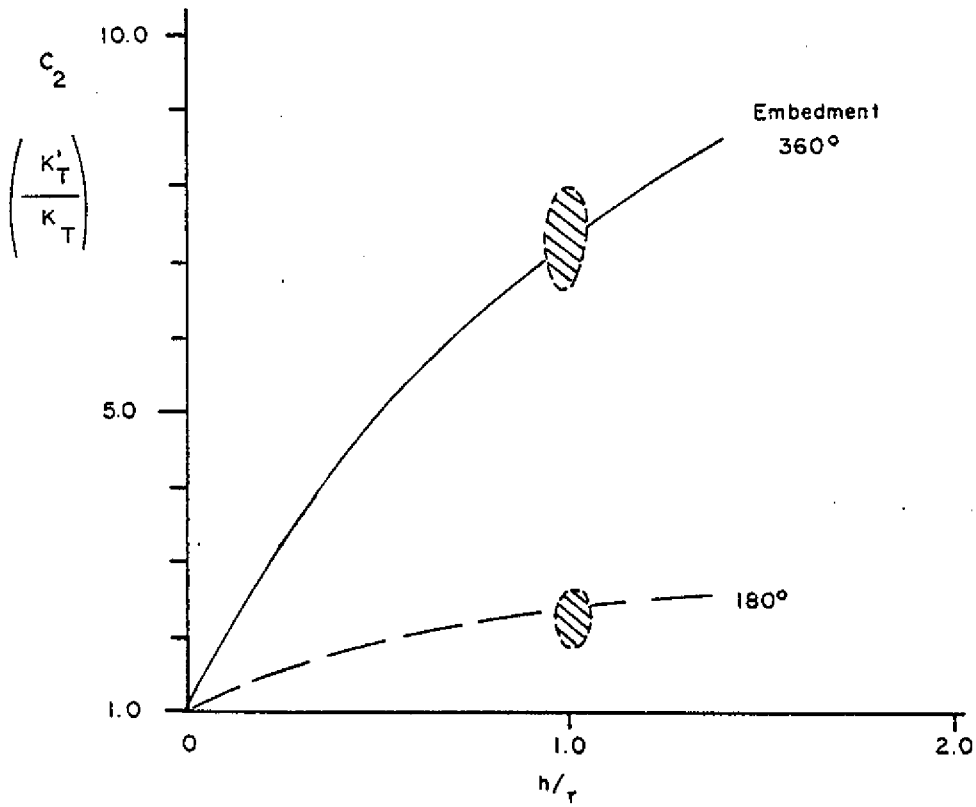

C_2 = embedment correction factor

K' = embedded case

K = non-embedded case

= range of data points

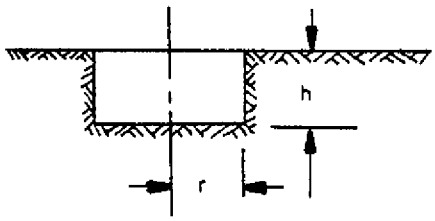

Project: SONGS SOIL STRUCTURE INTERACTION Job Number: B221I	EFFECT OF EMBEDMENT ON SPRING CONSTANT, TWISTING MODE	Fig. E-6

WOODWARD-McNEILL & ASSOCIATES

Amended: April 2009 TL: E047997

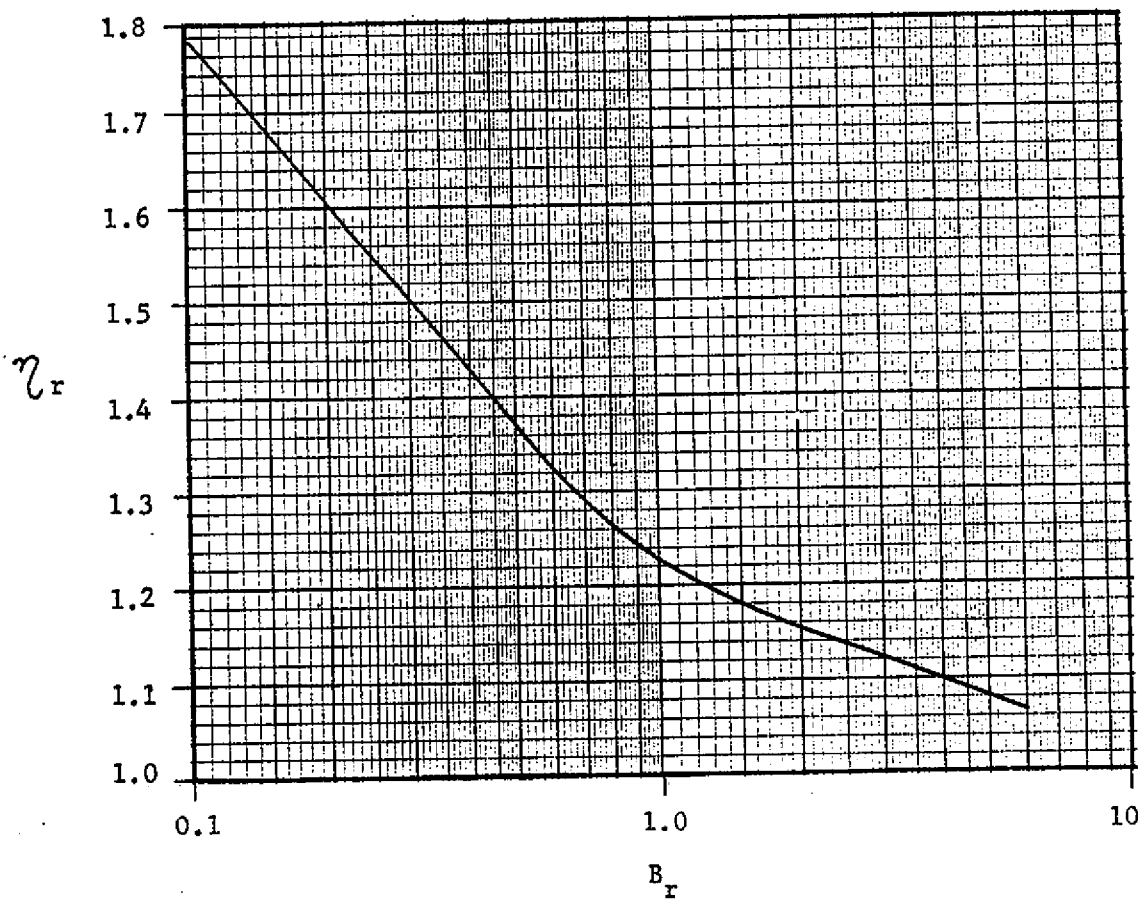

Project: SONGS SOIL STRUCTURE INTERACTION **Job Number:** B221I	INERTIAL EFFECTS ON ROCKING MODE (η_r vs B_r)	**Fig.** E-7

WOODWARD – McNEILL & ASSOCIATES

APPENDIX F

LATERAL PRESSURES ON STRUCTURE WALLS

F-1 General

Structures at the site will be constructed in the San Mateo Formation Sand. Field measurements indicate that the in-situ density of this material is on the order of 100% relative compaction as determined by ASTM D1557-70, and a dry density of about 120 pcf. Backfill will be compacted to a minimum of 95% relative compaction above the water table and 100% compaction below the water table. Laboratory tests indicate the soil has an angle of internal friction of 41.5^0 and an effective cohesion of 750 psf, however in the spirit of conservatism the cohesion has been neglected for this analysis.

Three conditions causing lateral stresses on walls are discussed. The first, described by Seed and Whitman (1970), is a force-equilibrium analysis for which the critical angle of slope of the base of the wedge is determined to obtain maximum (active) earth pressure on walls. The second involves the calculation of lateral (passive) pressures mobilized due to inertial loads. The third involves the calculation of additional lateral pressures due to nearby structures. It is expected that during an earthquake the structure would be acted upon by both the active stress component on the side of the structure that at an instant in time was tending to move away from the soil, and by the passive stress component on the opposite side of the structure which was tending to move into the soil. Both conditions

Amended: April 2009 TL: E047997

should be analyzed to evaluate the most critical stress for each wall element. The lateral stress caused by a nearby structure should then be added to the larger of these two stresses for design. Details of these techniques of analysis are presented in the following sections of this appendix.

F-2 Lateral Earth Pressures

The at-rest earth-pressure coefficient is considered applicable for evaluation of static stresses in the San Mateo Formation Sand against rigid side walls of structures. This coefficient (k_o) is obtained from the expression: $k_o = 1 - \sin \phi$ (Jaky, 1944). For the San Mateo Formation Sand this calculation yields $k_o = 0.34$. For the dynamic DBE and OBE loading conditions a wedge analysis approach was used to determine seismic earth pressure coefficients. The steps involved in this procedure are presented in Attachment F-1. The equivalent fluid pressures determined from these analyses are presented in Table F-1 below.

It should be noted that for static calculation, the at-rest earth-pressure coefficient was used, because of the assumption that the structures will be essentially rigid.

F-3 Lateral Stresses Due to Inertial Loading

The equivalent fluid pressures presented in the preceding section will act on one side of the structure during earthquake loading while stresses due to inertial loads will act on the opposite side, as the structure moves differentially with respect

to the soil. Calculations should be made of both stresses, and the larger value used for design for each element of the wall.

The stress due to inertial loading can be determined as follows:

For Horizontal Translation,

$$\sigma_p = \frac{(C_2 - 1)\ P}{C_2\ A} \quad \text{(uniform stress distribution).}$$

For Rocking Rotation,

$$\sigma_p = \frac{(C_2 - 1)\ 4M}{C_2 hA}$$

where σ_p = Stress against wall

P = 70% of the maximum total horizontal inertial load

M = 70% of the maximum total inertial moment

A = Area of side of structure

h = Depth of embedment

C_2 = Embedment correction factor (see Appendix E)

In the spirit of conservatism it has been assumed that walls parallel to the direction of earthquake induced pressures do not contribute to the resistance to the induced motion, i.e., all the stress is concentrated on the wall perpendicular to the direction of motion. An explanation of the equations presented above is given in Attachment F-2.

F-4 Lateral Loads Due to Adjacent Structures

For the special case of walls close to adjacent structures,

additional load should be considered in design to take into account the pressure caused by the bearing load of the adjacent structure. Our recommendations for determination of how much additional load to consider for this circumstance is presented on Fig. F-1.

TABLE F-1

Lateral Earth Pressures
San Mateo Sand

Case	Equivalent Fluid Pressure Above Water Table (pcf)	Equivalent Fluid Pressure Below Water Table (pcf)
Static (at-rest)	45	23*
Seismic** DBE	75	39*
Seismic** OBE or lower	45	23*

Note: * Hydrostatic head should be added.
** These values include static stresses. Seismic lateral stresses should be checked by the inertial load method, presented in Section F-3.

Amended: April 2009 TL: E047997

ATTACHMENT F-1

Wedge Analysis -- Active Earthpressures due to Earthquake Loading.

ACTIVE PRESSURE -- Horizontal Acceleration = $K_h g$
Vertical Acceleration = $K_v g$

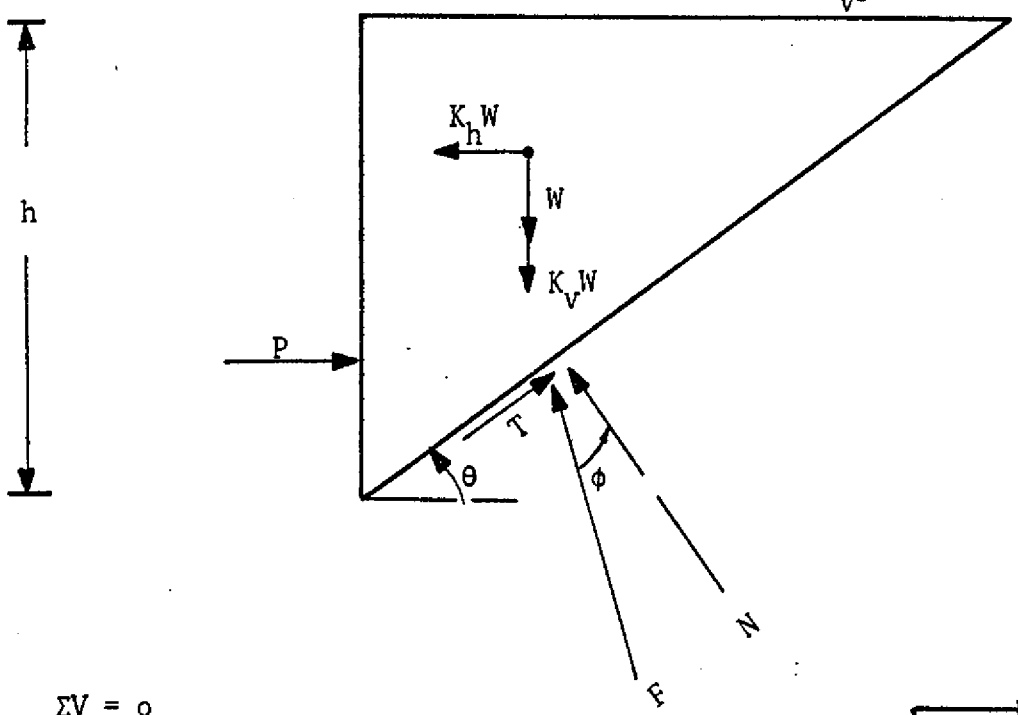

$\Sigma V = o$

$\Sigma H = o$

(1) $W + W K_v = F \cos(\Theta - \phi)$

$$F = \frac{W(1+K_v)}{\cos(\theta - \phi)}$$

(2) $P = WK_h + F \sin(\Theta - \phi)$

$$= WK_h + \frac{W(1+K_v) \sin(\theta - \phi)}{\cos(\theta - \phi)}$$

$$= W\left[K_h + (1+K_v)\tan(\Theta - \phi)\right]$$

$$= \tfrac{1}{2}\gamma h^2 \cot\Theta \left[K_h + (1+K_v)\tan(\Theta - \phi)\right]$$

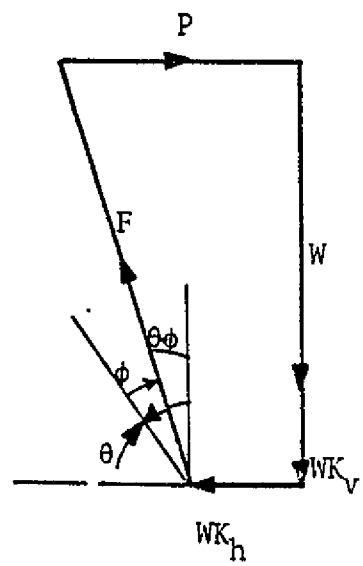

$P = 1/2 \quad \gamma h^2 K$

Where,

$$K = \cot \Theta \quad \left[K_h + (1+K_v) \tan (\Theta - \phi)\right]$$

K_{AE} is the maximum value at $\Theta = \Theta$ critical

$$K_{AE} = \cot \Theta_{cr} \left[K_h + (1+K_v) \tan (\Theta_{cr} - \phi)\right]$$

The values of K_{AE} calculated for upward and downward assumed vertical seismic coefficients for DBE and OBE conditions, are presented below. The resulting equivalent fluid pressures are presented in Table F-1.

Earthquake Loading	K_{AE} (due to ↑ K_v)	Θ_{cr}	K_{AE} (due to ↓ K_v)	Θ_{cr}
DBE K_h = .47g K_v = .31g	0.57	27	0.56	49
OBE K_h = .2g K_v = .13g	0.29	56	0.33	59

Amended: April 2009 TL: E047997

ATTACHMENT F-2

Explanation of Inertial Loading Equations
Presented in Section F-3

For a structure on the gound surface:

$$K_{BASE} = K' \; C_1 \quad \text{(See Appendix E)}$$

For an embedded structure:

$$K_{TOTAL} = K' \; C_1 \; C_2 \quad \text{(See Appendix E)}$$

$$\therefore \quad K_{SIDES} = K_{TOTAL} - K_{BASE} = K'C_1 \; (C_2-1)$$

$$P_{TOTAL} = K_{TOTAL} \; \delta$$

$$P_{SIDES} = K_{SIDES} \; \delta$$

$$= K'C_1 \; (C_2-1) \; \delta$$

$$= \frac{K'C_1 \; (C_2-1) \; P_{TOTAL}}{K_{TOTAL}}$$

$$= \frac{K'C_1 \; (C_2-1) \; P_{TOTAL}}{K'C_1 \; C_2}$$

$$P_{SIDES} = \frac{(C_2-1) \; P_{TOTAL}}{C_2}$$

$$\sigma_{SIDES} = \frac{P_{SIDES}}{A_{SIDES}}$$

$$\therefore \quad \sigma_{SIDES} \quad \frac{(C_2-1)}{C_2} \; \frac{P_{TOTAL}}{A_{SIDES}} \quad \text{(horizontal translation)}$$

Amended: April 2009 TL: E047997

Attachment F-2
Page 2

$$P_{TOTAL} = \frac{M}{X}$$

$$\therefore \quad \sigma_{SIDES} = \frac{(C_2-1)}{C_2} \frac{M}{AX} \text{ (Rocking Rotation)}$$

Definition of Terms :

K_{BASE} = Soil stiffness along base of structure

K' = Uncorrected stiffness

K_{SIDES} = Soil stiffness on sides of structure

K_{TOTAL} = Overall soil stiffness

C_1 = Empirical correction factor (See Appendix E)

C_2 = Embedment correction factor (See Appendix E)

P_{SIDES} = Horizontal inertial load on sides of structure

P_{TOTAL} = Total horizontal inertial load

δ = Deflection of structure

A_{SIDES} = Area of Wall

M = Total inertial moment

X = Distance from center of base mat to center of gravity

Amended: April 2009 TL: E047997

LATERAL PRESSURE DUE TO ADJACENT STRUCTURES

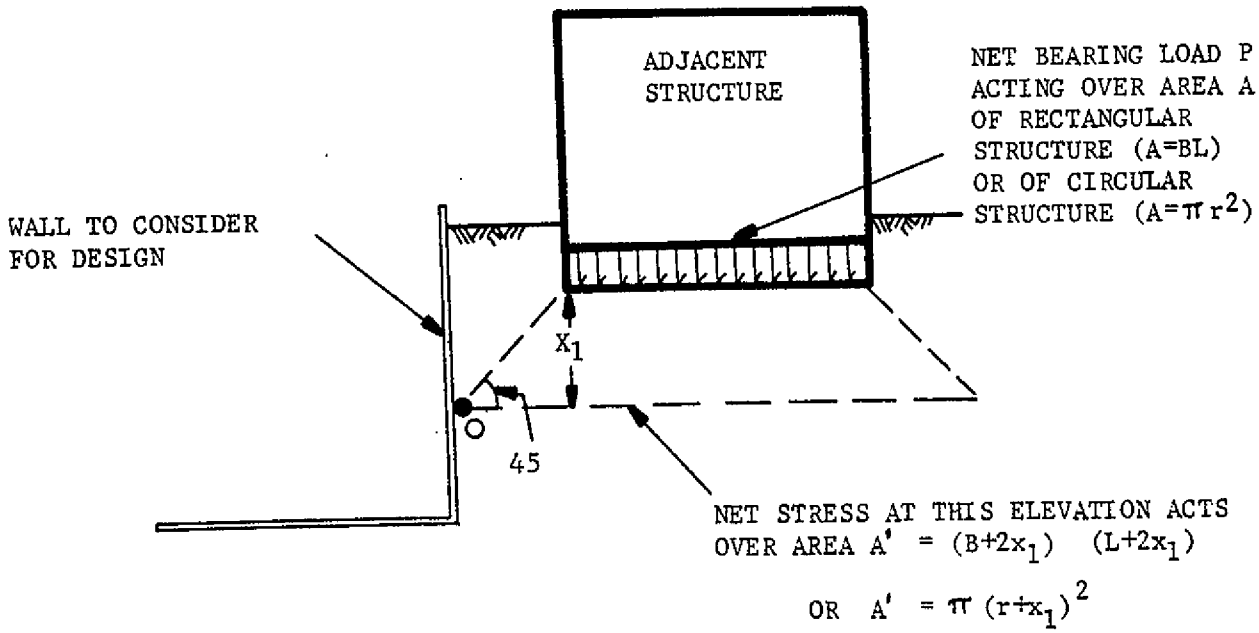

ADDITIONAL LATERAL PRESSURE ON WALL $= \frac{A}{A'} \cdot PM$ (UNIFORM)

(APPLIED BELOW POINT .0)

WHERE: M = 0.34 FOR STATIC AND OBE CONDITION

M = 0.57 FOR DBE CONDITION

NOTES:

1. THE EXAMPLE PRESENTED IS FOR A RECTANGULAR STRUCTURE. FOR CIRCULAR STRUCTURES ADJUST THE RADIUS BY x_1, TO CALCULATE A'.

2. THE LATERAL PRESSURE CALCULATED HERE SHOULD BE ADDED TO EITHER THE ACTIVE EARTH PRESSURE OR THE INERTIAL LOAD FOR DESIGN.

Project: SONGS SOIL STRUCTURE INTERACTION **Job Number:** 3221I	LATERAL PRESSURES DUE TO ADJACENT STRUCTURES	Fig. F-1

WOODWARD-McNEILL & ASSOCIATES

APPENDIX G

STRUCTURE SLIDING

G-1 Introduction

During an earthquake horizontal forces are developed between a slab and the supporting soil which may cause the slab to slide with respect to the soil. Normally, if the slab is supporting building loads and the earthquake motion is not large, the frictional resistance mobilized between the slab and the soil is enough to prevent sliding. However, if a large earthquake input is considered, the possibility of potential sliding should be investigated. The auxiliary building has a proposed mat-foundation which has a fairly large flat area in contact with soil with little or no embedment. As the design base motion for the structure is a very strong motion, it is considered essential that a study of potential sliding between mat foundation and the supporting soil be made.

Though the analyses presented here were done for the specific case of the auxiliary building, some general conclusions can be drawn from the results of these analyses.

G-2 Evaluation of Potential Sliding Ratio

Consider a soil-element just below a slab. In the static condition, a vertical stress σ_{ys}, due to the load from the slab, is acting on this element. Normal and shear stresses would be induced in this soil element due to the effect of the imposed

Amended: April 2009 TL: E047997

base motion on the slab-soil system. These stress conditions can be represented as shown below:

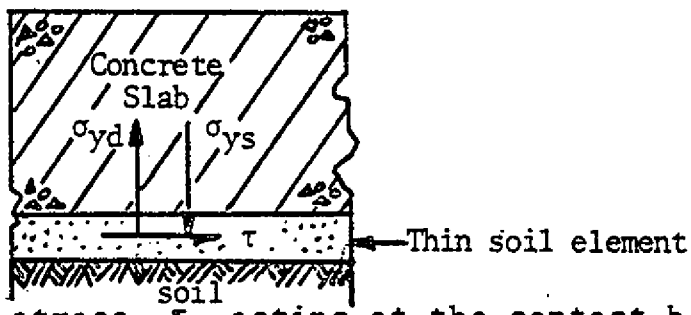

Thus, the shear stress, τ, acting at the contact between the slab and the soil, can be taken as the dynamically induced shear stress in the thin soil element just below the slab and the net normal stress can be obtained by evaluating $\sigma_n=(\sigma_{yd}-\sigma_{ys})$. The ratio of τ/σ_n can then be easily evaluated. This ratio can be taken as a measure of friction mobilized during the imposed base motion. So long as this friction is smaller than the available angle of friction between the concrete and soil, no sliding would be anticipated. A time-history of τ/σ_n would indicate if the mobilized friction exceeds the available friction at any time, and if so, for how long.

G-3 Analyses for Auxiliary Building

In order to study potential sliding of the mat-foundation of the auxiliary building during the ground motions, a two-dimensional finite-element model was prepared to incorporate interaction between foundation and the underlying soil. The soil deposit was assumed to be 120 ft thick and to be resting on a rigid base. This layer extended far enough horizontally

Amended: April 2009 TL: E047997

from the edges of the foundation so as to minimize the influence of restrained vertical boundaries. The finite-element representation of the soil-foundation system is shown on Fig. G-1.

The mat foundation for the auxiliary building is 230' X 220' in size as shown on Fig. G-2 from Bechtel. The total normal load on the soil is about 3500 psf. In representing this foundation in the finite-element mesh, a concrete block was assumed to have appropriate thickness to represent this normal pressure.

In order to obtain the base motion which would yield a response time-history, at 30 ft depth below the ground surface which was the same as the DBE, a top-down analysis using wave propagation techniques was conducted. From this analysis, an acceleration time-history of 80 sec. duration at a depth of 120 ft was obtained. Because of core limitation of the available computer storage, appropriate sections, which govern the response spectral characteristics, were selected from this time-history to give a 22 sec. duration acceleration time-history. This 22 sec. motion was used as the base motion.

To study sliding at the contact between the foundation and the soil, normal and shear stresses were obtained in thin layers close to the contact. We feel that these stresses reasonably represent the stresses at the contact between the soil and the foundation. The ratio of the dynamic shear stress and the total normal stress at any instant was considered to

be a measure of the potential sliding. If this ratio exceeded the value $\delta = \frac{2}{3} \tan \phi$ where δ is the angle of friction between soil and concrete, sliding is indicated. Thus, a time-history of the ratio τ/σ_n was obtained at three different locations in the foundation. A study of the time-history of τ/σ_n ratio at these three locations would indicate not only the potential sliding but also the phase differences between these points; i.e., whether these points would slide simultaneously or at different times. These time-histories were obtained for all cases studied, and are presented in this report.

Similar analyses were done using a finite-element model in which the vertical dimension of the slab was selected to give the same rotational inertia as that of the actual structure. In addition to the above, influences of a nominal embedment of 5 ft as well as of combined horizontal and vertical base motions were studied. Table G-1 presents a tabulation of the various cases studied. The resulting time-histories of τ/σ_n are presented on Figs. G-3 through G-9.

G-4 Results of Analyses

On the basis of the results of the cases studied, the following observations are made.

a) The maximum potential sliding develops at the center of the slab. (Fig. G-3, (a), (b), and (c))

b) The effect of embedment is to reduce the potential sliding, i.e., the maximum value of the stress ratio is smaller for embedded slabs than for slabs with no-embedment. (Figs. G-4 (a) and G-9 (a))

Amended: April 2009 TL: E047997

c) The influence of prescribed vertical motion (i.e., 2/3 the horizontal motion) with the horizontal motion was to increase the potential sliding. (Fig. G-3 (b) and G-4 (b))

d) The maximum potential for sliding was not significantly influenced when the horizontal and vertical motions were out of phase. (Figs. G-4 (b) and G-5 (b))

e) Inclusion of the rotational inertia in modeling the slab for the analysis did not increase the sliding potential. (Figs. G-4 (b) and G-6 (b))

f) From all the cases studied, the maximum potential for sliding was obtained for non-embedded slabs subjected to horizontal and vertical inphase motions simultaneously. The corresponding stress ratio (τ/σ_n) was found to be 0.57. The time-history for this case is presented on Fig. G-10.

g) The available friction between the slab and soil is 2/3 (tan 41.5^0) = 0.59. As this is larger than the mobilized friction (0.57) no sliding is anticipated. Furthermore, the peak value of 0.57 occurs only for a short duration during the time-history of stress ratio. The average value of stress ratio is about 2/3 of the peak value. Thus the average mobilized friction is considerably smaller than the available friction.

TABLE G-1

CASES STUDIED FOR
STRUCTURE SLIDING ANALYSES

Case No.	Input Motion			Condition			Figure Nos. for Results	Location of Output
	H only	H & V in phase	H & V out of phase	Mass only	Mass plus Inertia	Embedment		
1	✓			✓			G-3	L, C, R
2		✓		✓			G-4	L, C, R
3			✓	✓			G-5	L, C, R
4	✓				✓		G-6	L, C, R
5		✓			✓		G-7	L, C, R
6	✓			✓		✓	G-8	L, C
7		✓		✓		✓	G-9	L, C, R

Where: H = Horizontal
V = Vertical
L = Left end of slab
C = Center of slab
R = Right end of slab

NOTE: Check is for item included; blank is for item not included.

Amended: April 2009 TL: E047997

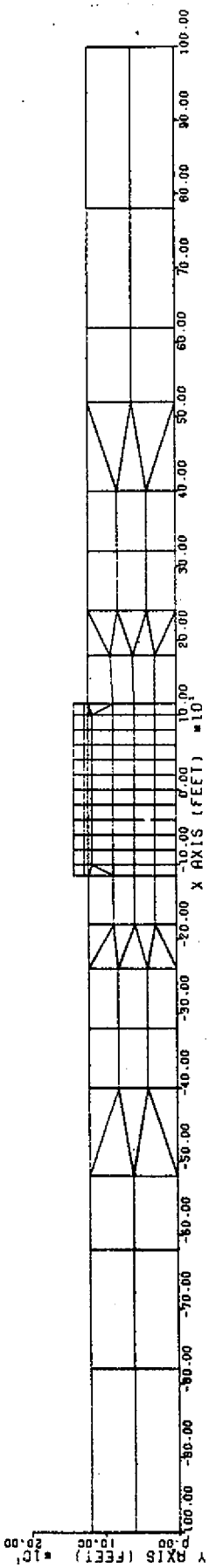

FINITE ELEMENT MESH

Project: SONG SOIL STRUCTURE INTERACTION **Job Number** B221I	FINITE ELEMENT MESH	Fig. G-1

WOODWARD - McNEILL & ASSOCIATES

Amended: April 2009 TL: E047997

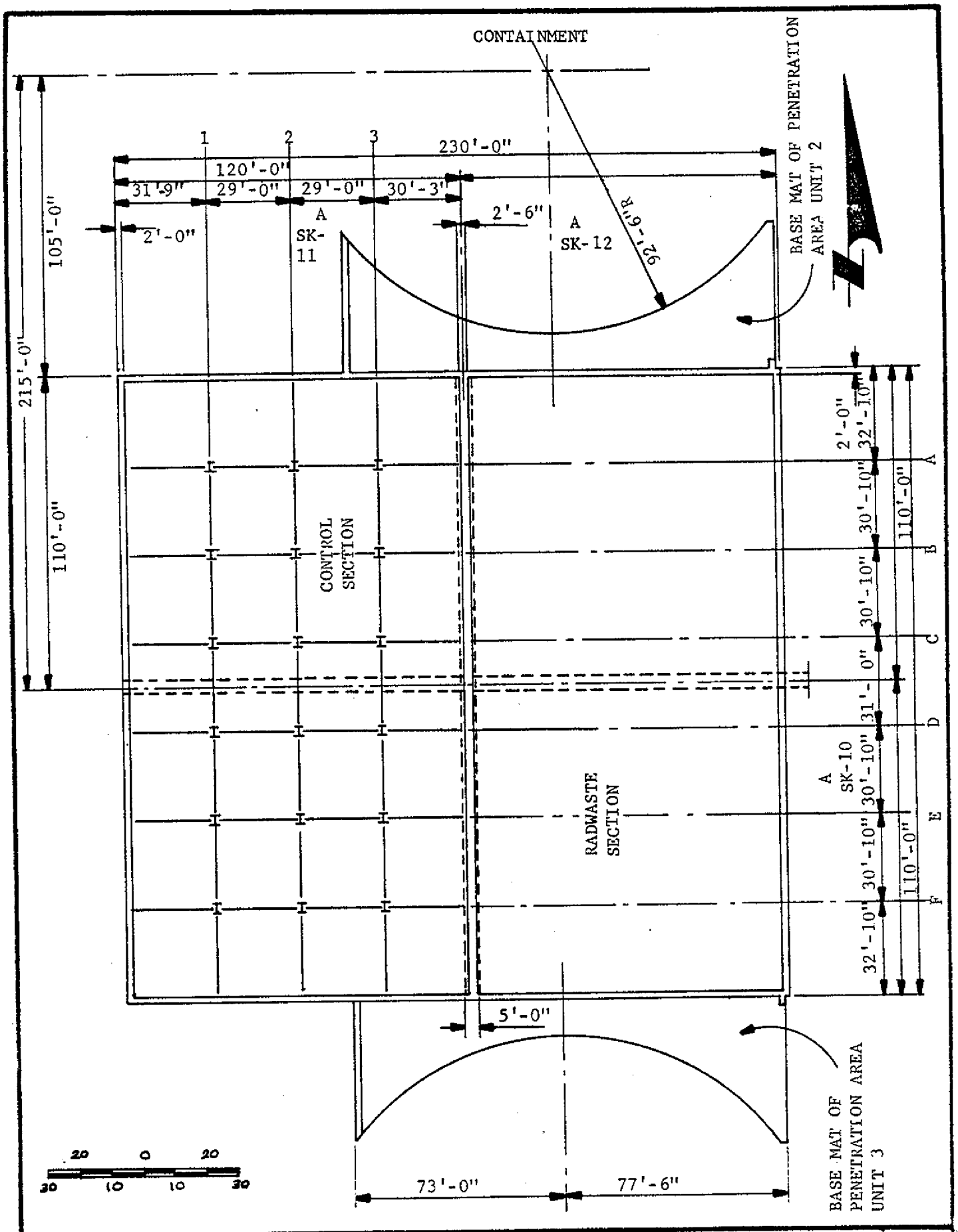

Project: SONGS SOIL STRUCTURE INTERACTION **Job Number:** B221I	AUXILIARY BUILDING PLAN	Fig. G-2

WOODWARD - McNEILL & ASSOCIATES

Amended: April 2009 TL: E047997

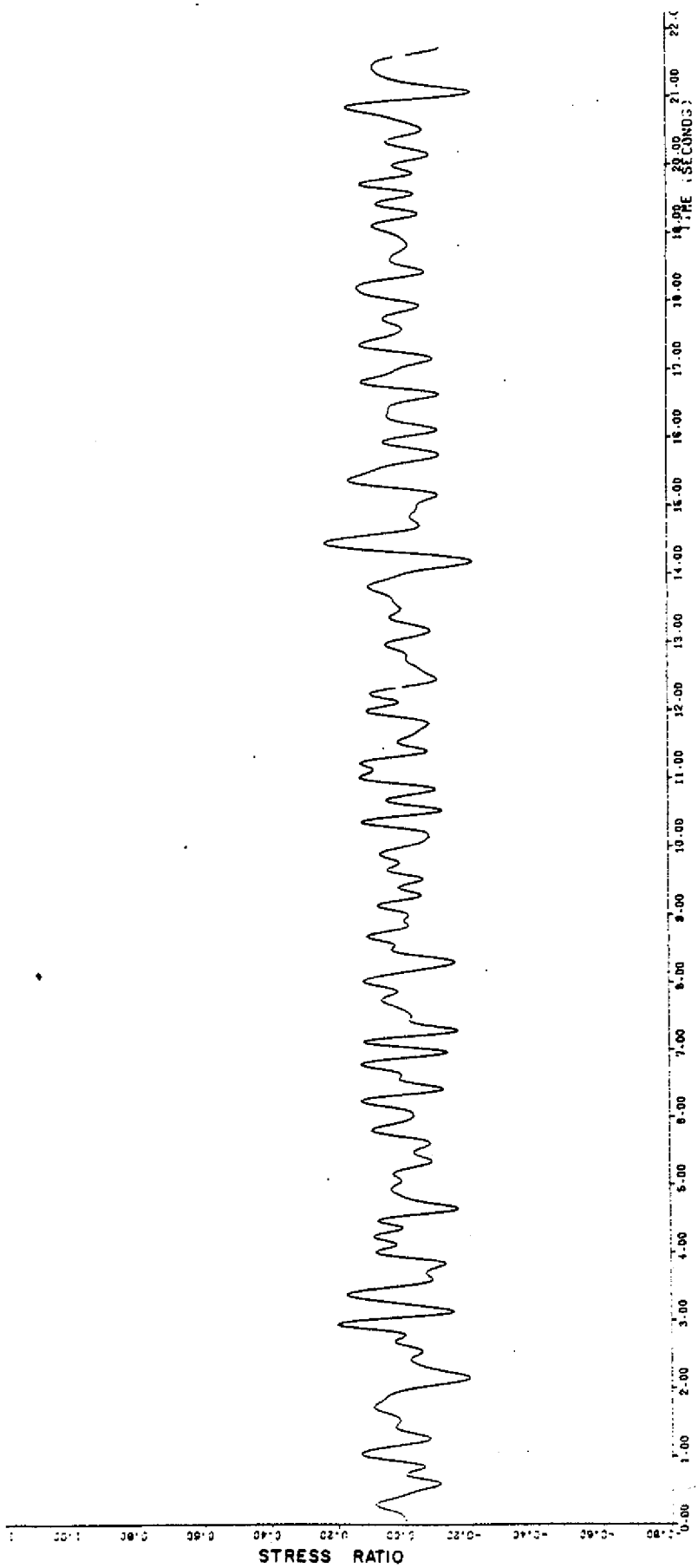

Project: SONGS SOIL STRUCTURE INTERACTION **Job Number:** B221I	NO EMBEDMENT-LEFT END OF SLAB HORIZONTAL BASE MOTION ONLY	Fig. G3a

WOODWARD-McNEILL & ASSOCIATES

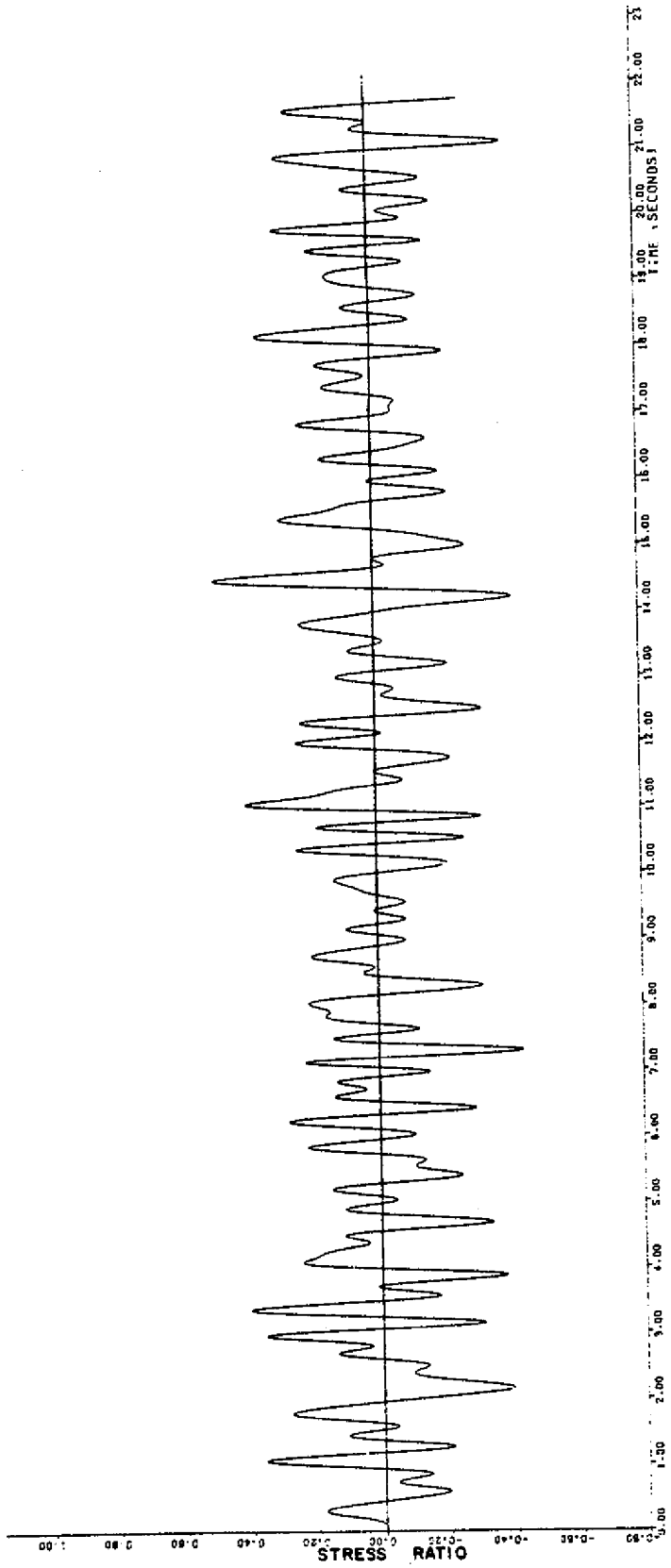

Project: SONGS SOIL STRUCTURE INTERACTION **Job Number:** B221I	NO EMBEDMENT-CENTER OF SLAB HORIZONTAL BASE MOTION ONLY	Fig. G3b

WOODWARD-McNEILL & ASSOCIATES

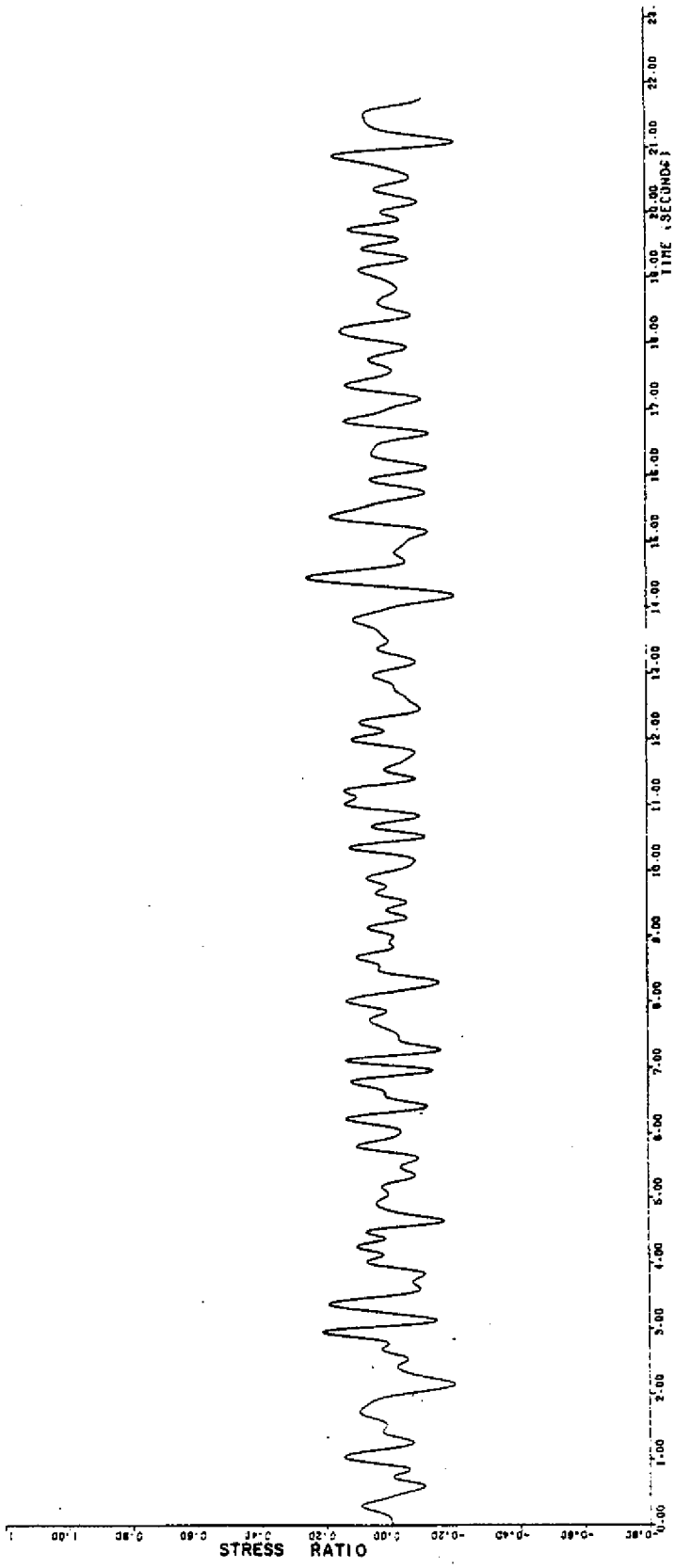

Project: SONGS SOIL STRUCTURE INTERACTION **Job Number:** B221I	NO EMBEDMENT-RIGHT END OF SLAB HORIZONTAL BASE MOTION ONLY	Fig. G3c

WOODWARD-McNEILL & ASSOCIATES

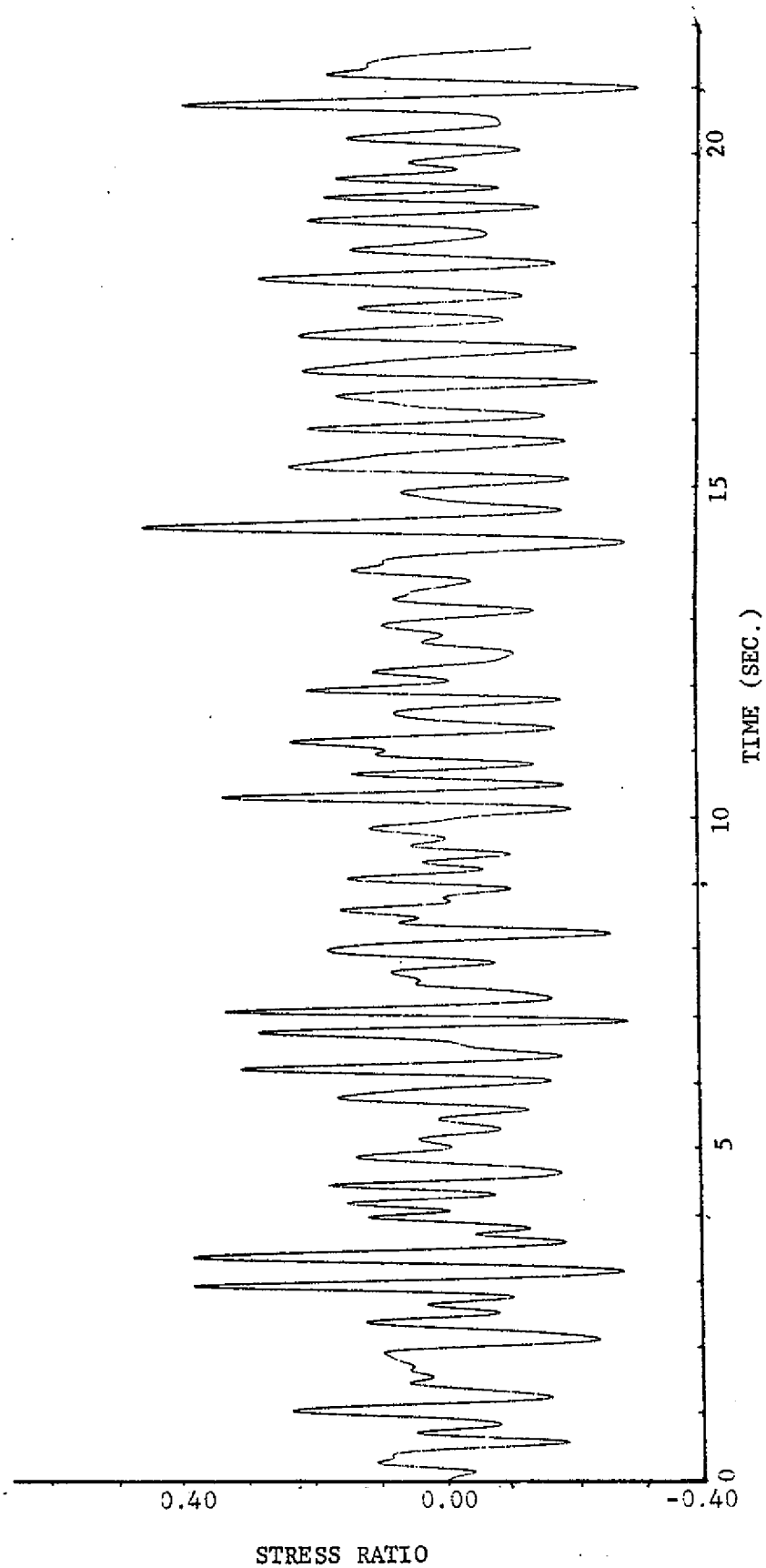

Project: SONGS SOIL STRUCTURE INTERACTION **Job Number:** B221I	NO EMBEDMENT LEFT EDGE OF SLAB HORIZONTAL AND VERTICAL BASE MOTIONS	**Fig.** G-4 a

WOODWARD - McNEILL & ASSOCIATES

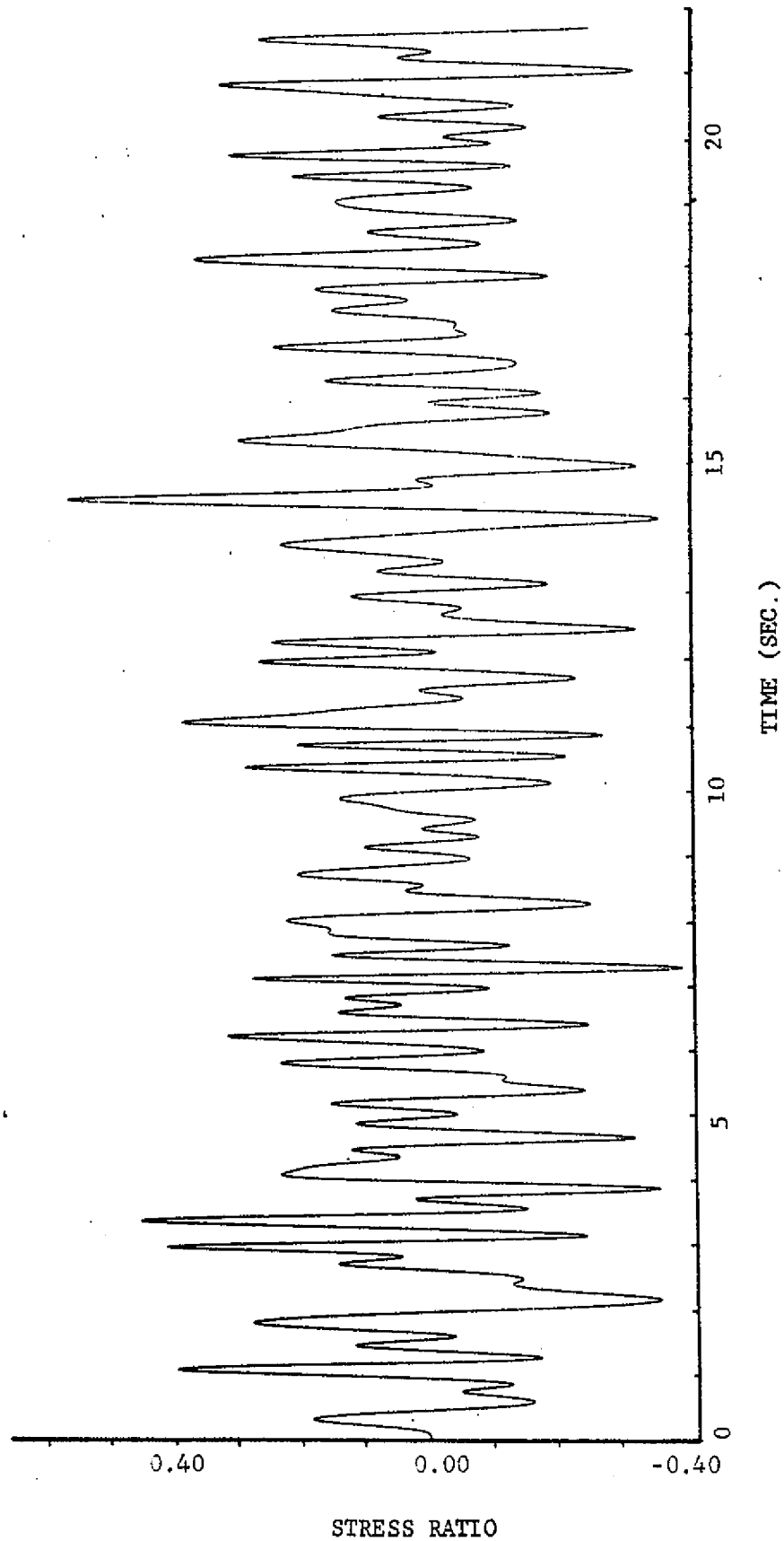

Project: SONGS SOIL STRUCTURE INTERACTION **Job Number:** B221I	NO EMBEDMENT CENTER OF SLAB HORIZONTAL AND VERTICAL BASE MOTIONS	Fig. G-4b

WOODWARD - McNEILL & ASSOCIATES

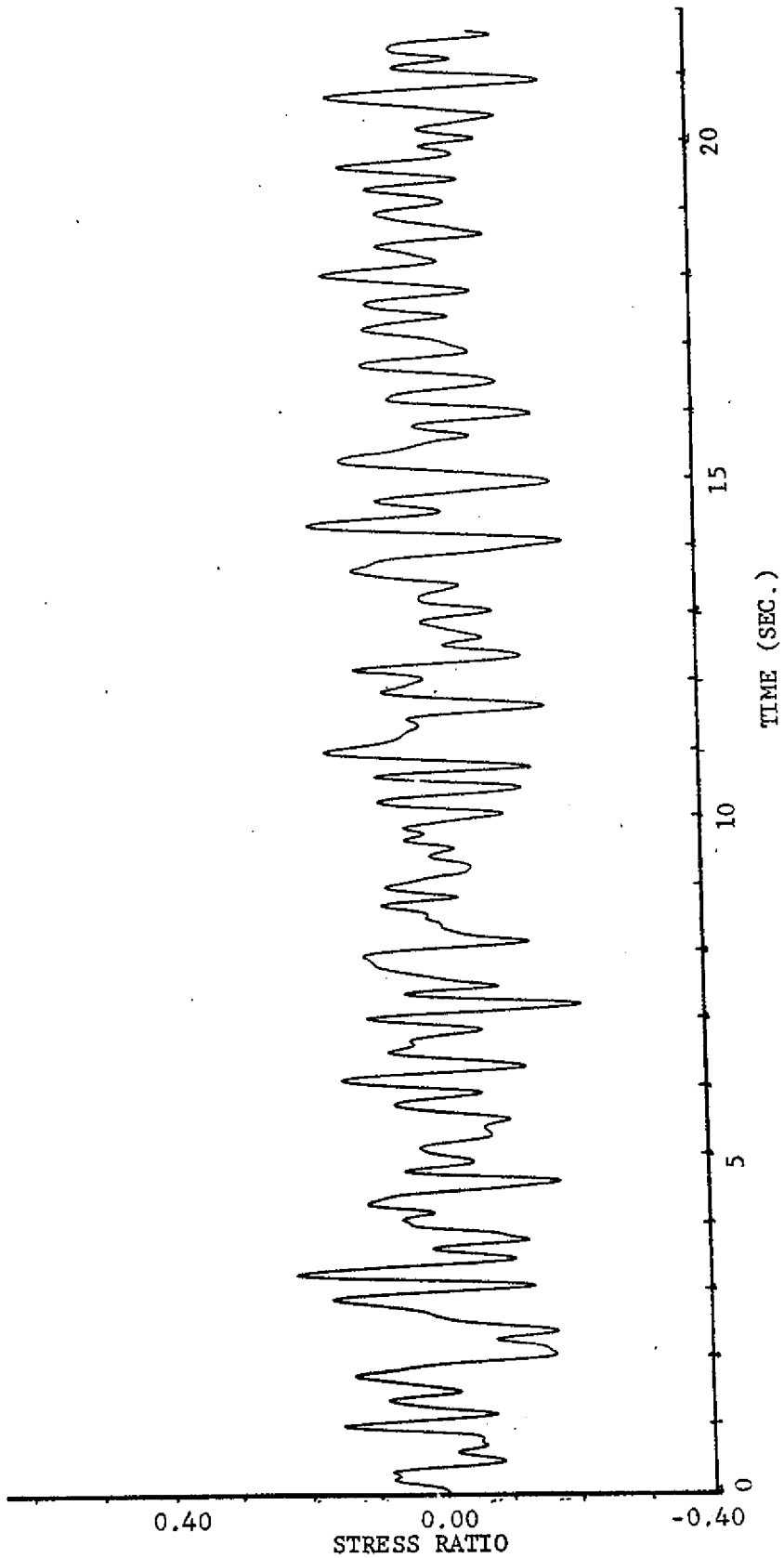

Project: SONGS SOIL STRUCTURE INTERACTION **Job Number:** B221I	NO EMBEDMENT RIGHT EDGE OF SLAB HORIZONTAL AND VERTICAL BASE MOTIONS	**Fig.** G-4c

WOODWARD – McNEILL & ASSOCIATES

Amended: April 2009 TL: E047997

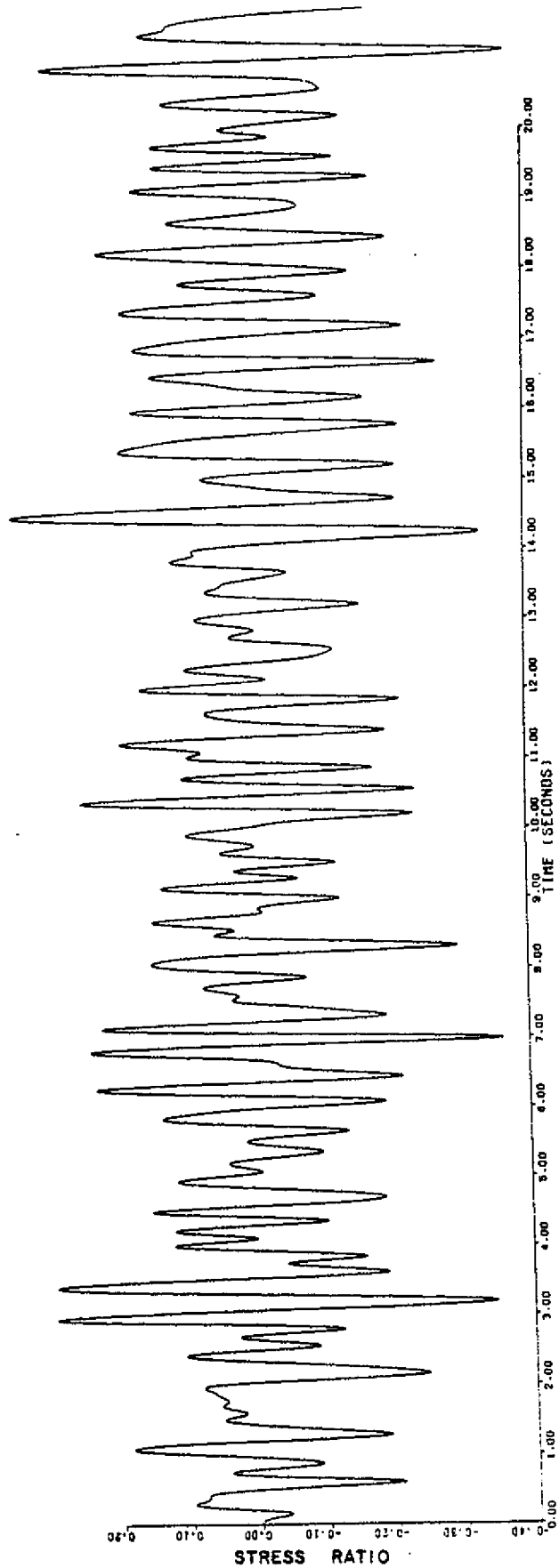

Project: SONGS SOIL STRUCTURE INTERACTION **Job Number:** B221I	NO EMBEDMENT-LEFT END OF SLAB HORIZONTAL AND VERTICAL (OUT OF PHASE) BASE MOTIONS	Fig. G5a

WOODWARD-McNEILL & ASSOCIATES

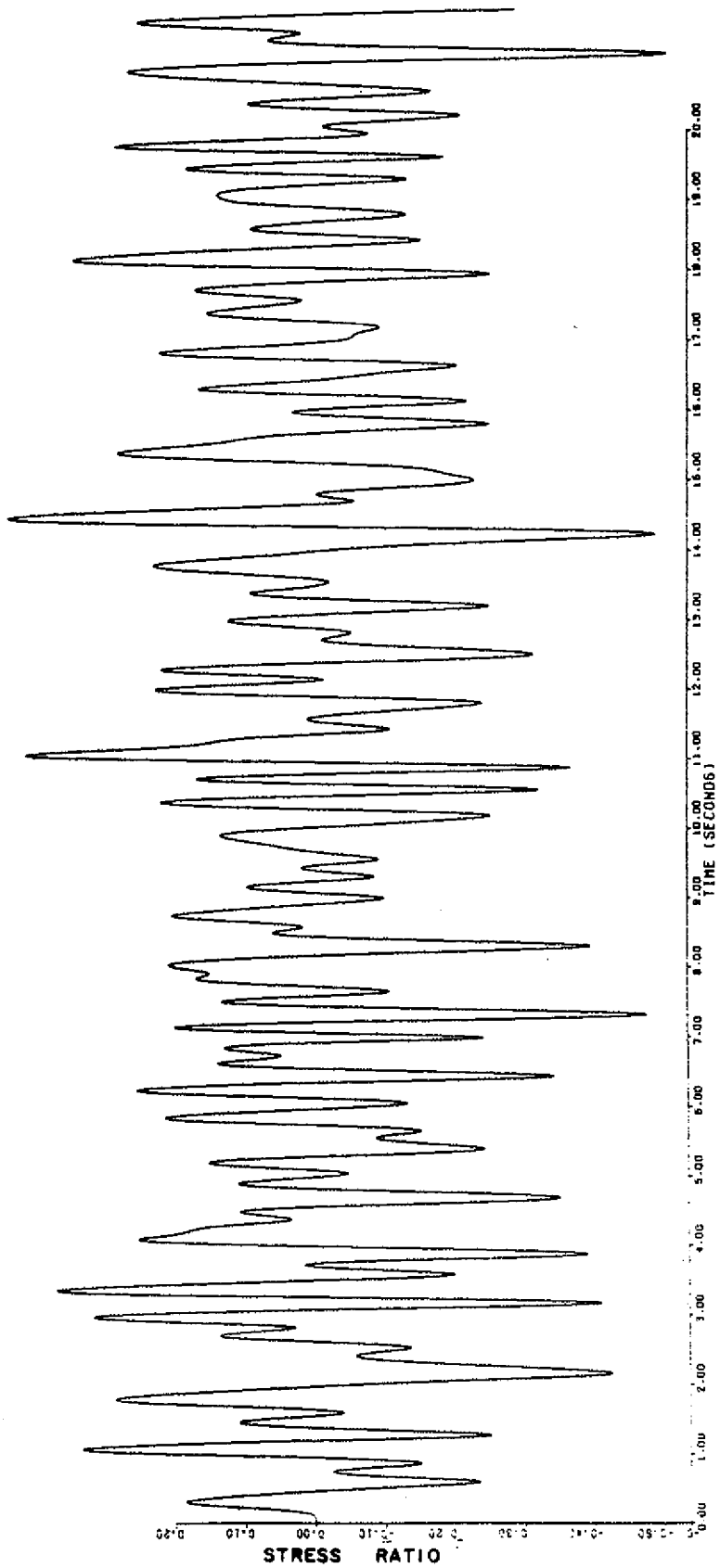

Project: SONGS SOIL STRUCTURE INTERACTION **Job Number:** B221I	NO EMBEDMENT-CENTER OF SLAB HORIZONTAL AND VERTICAL (OUT OF PHASE) BASE MOTION	Fig. G5b

WOODWARD-McNEILL & ASSOCIATES

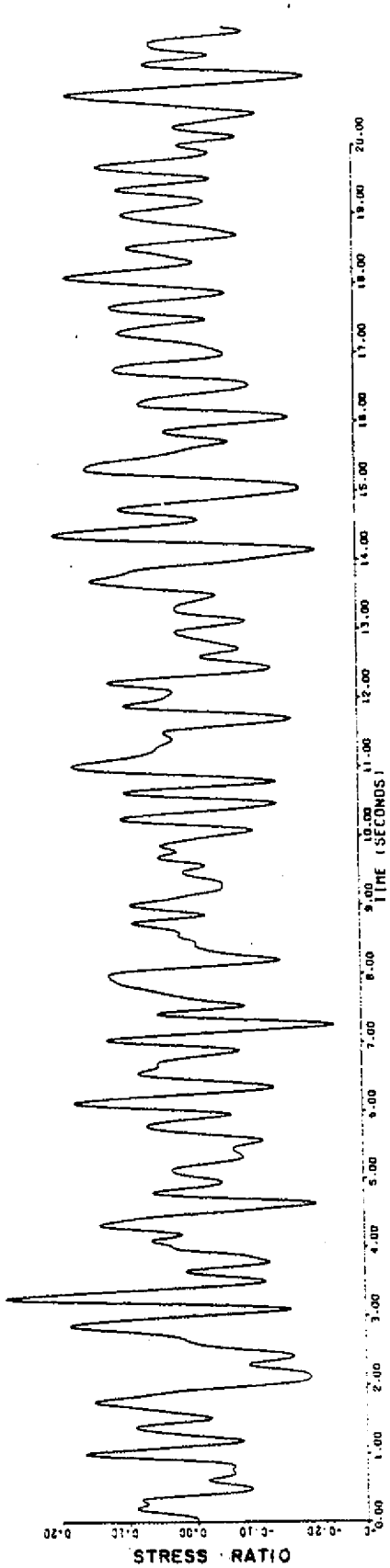

Project: SONGS SOIL STRUCTURE INTERACTION **Job Number:** B221I	NO EMBEDMENT-RIGHT END OF SLAB HORIZONTAL AND VERTICAL (OUT OF PHASE) BASE MOTIONS	Fig. G5c

WOODWARD-McNEILL & ASSOCIATES

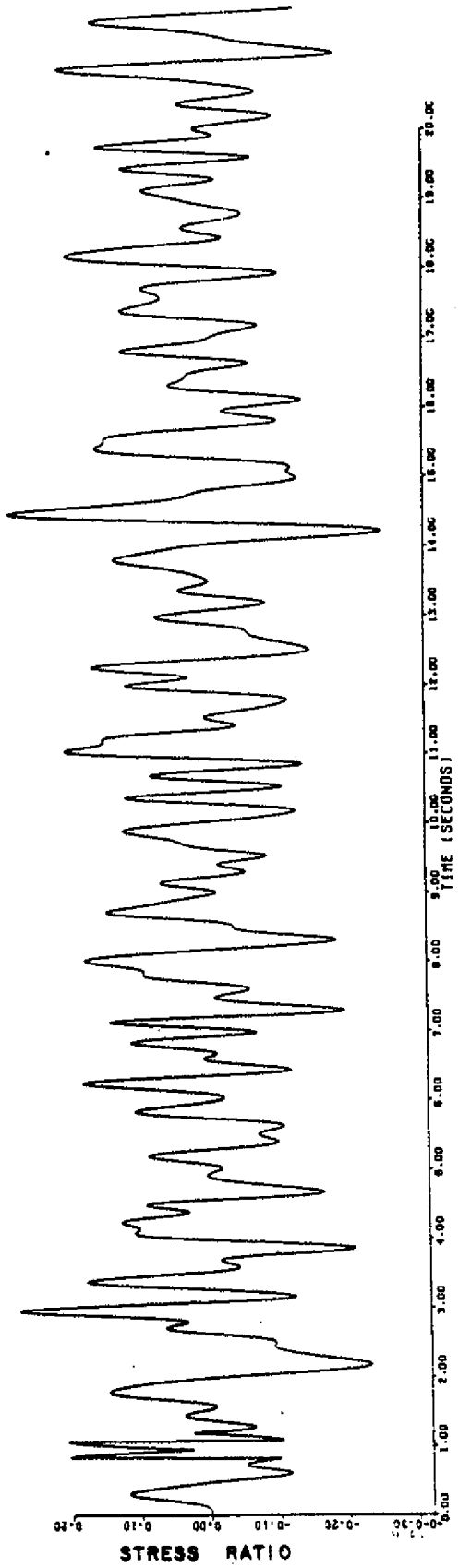

Project: SONGS SOIL STRUCTURE INTERACTION **Job Number:** B221I	NO EMBEDMENT-ROTATIONAL INERTIA INCLUDED LEFT END OF SLAB HORIZONTAL BASE MOTION ONLY	Fig. G6a

WOODWARD-McNEILL & ASSOCIATES

Amended: April 2009 TL: E047997

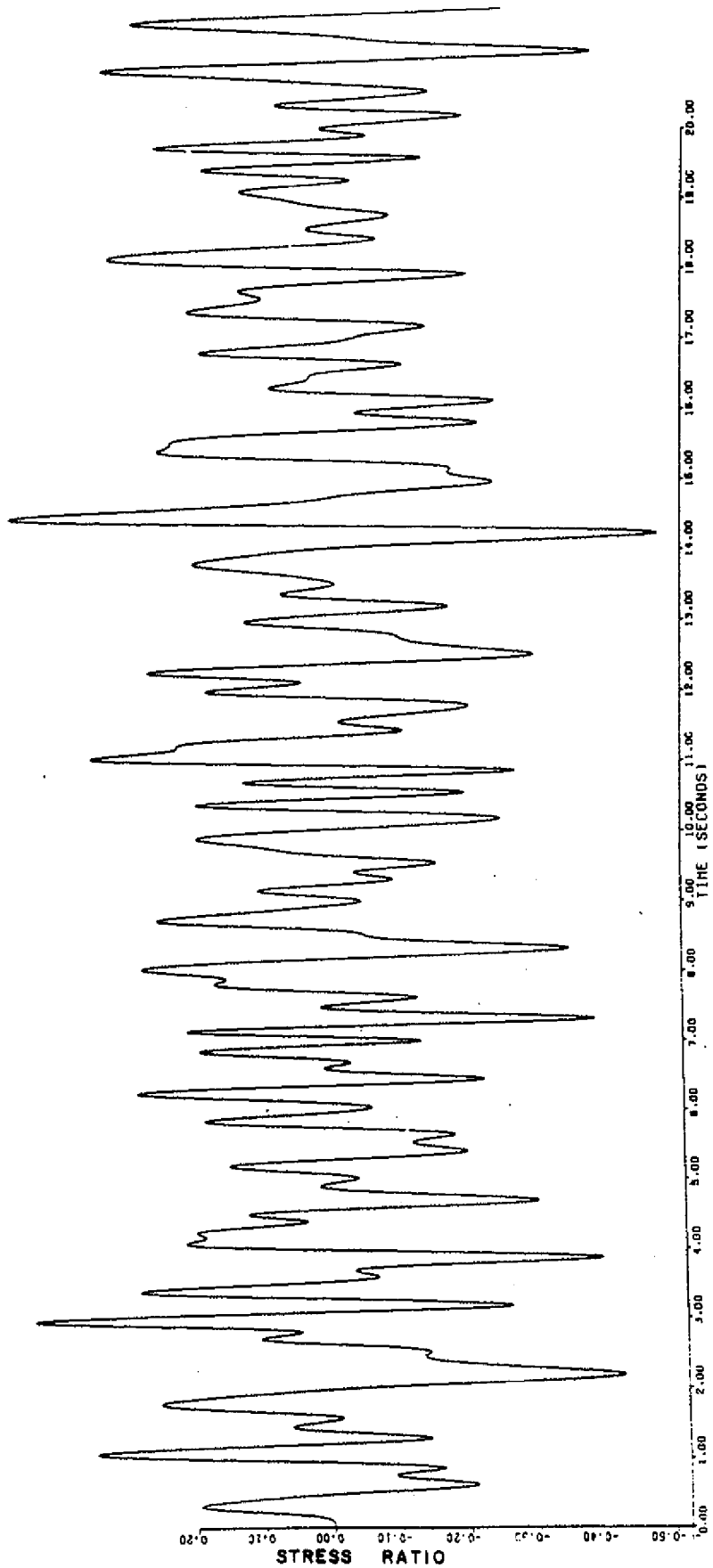

Project: SONGS SOIL STRUCTURE INTERACTION **Job Number:** B221I	NO EMBEDMENT-ROTATIONAL INERTIA INCLUDED CENTER OF SLAB HORIZONTAL BASE MOTION ONLY	Fig. G6b

WOODWARD-McNEILL & ASSOCIATES

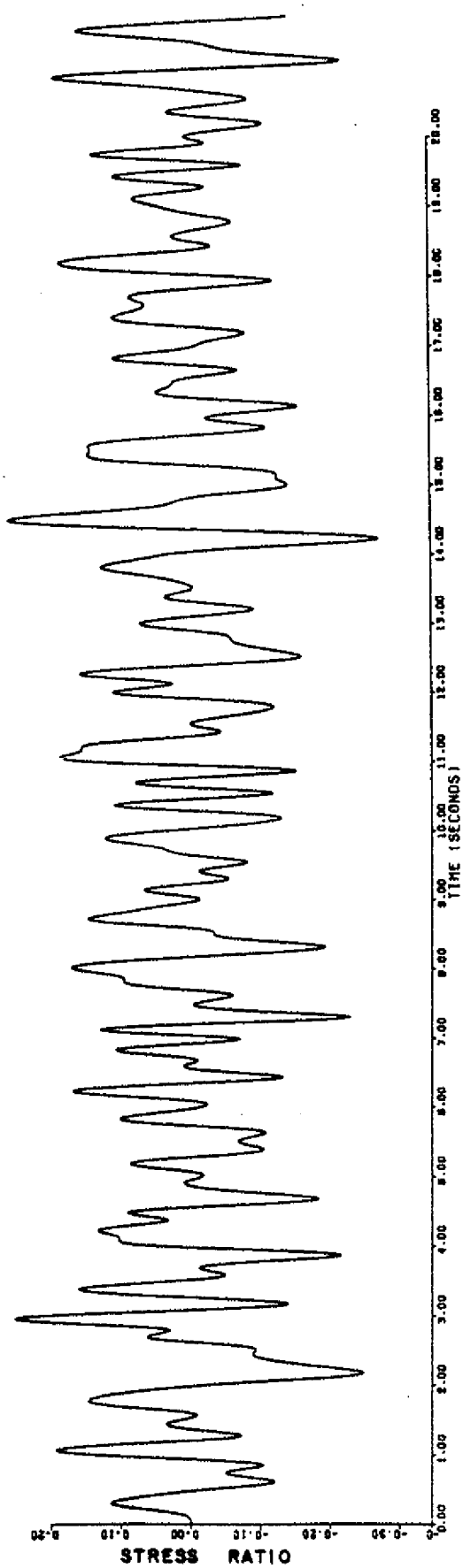

Project: SONGS SOIL STRUCTURE INTERACTION **Job Number:** B221I	NO EMBEDMENT-ROTATIONAL INERTIA INCLUDED RIGHT END OF SLAB HORIZONTAL BASE MOTION ONLY	Fig. G6c

WOODWARD-McNEILL & ASSOCIATES

Amended: April 2009 TL: E047997

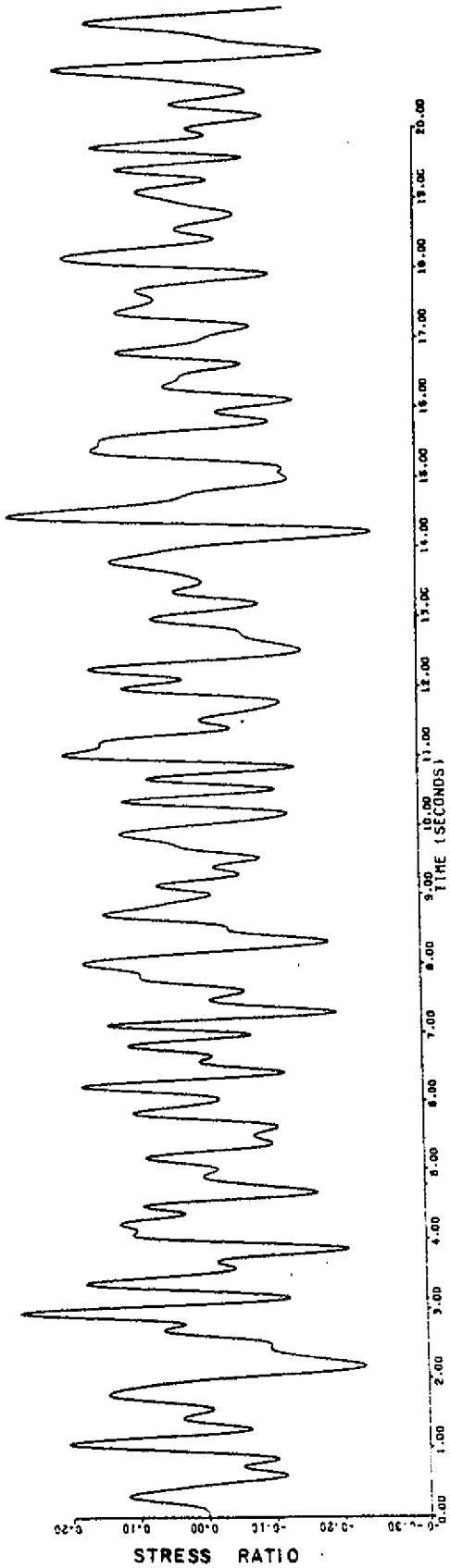

Project: SONGS SOIL STRUCTURE INTERACTION **Job Number:** B221I	NO EMBEDMENT-ROTATIONAL INERTIA INCLUDED LEFT END OF SLAB HORIZONTAL AND VERTICAL BASE MOTIONS	Fig. G7a

WOODWARD-McNEILL & ASSOCIATES

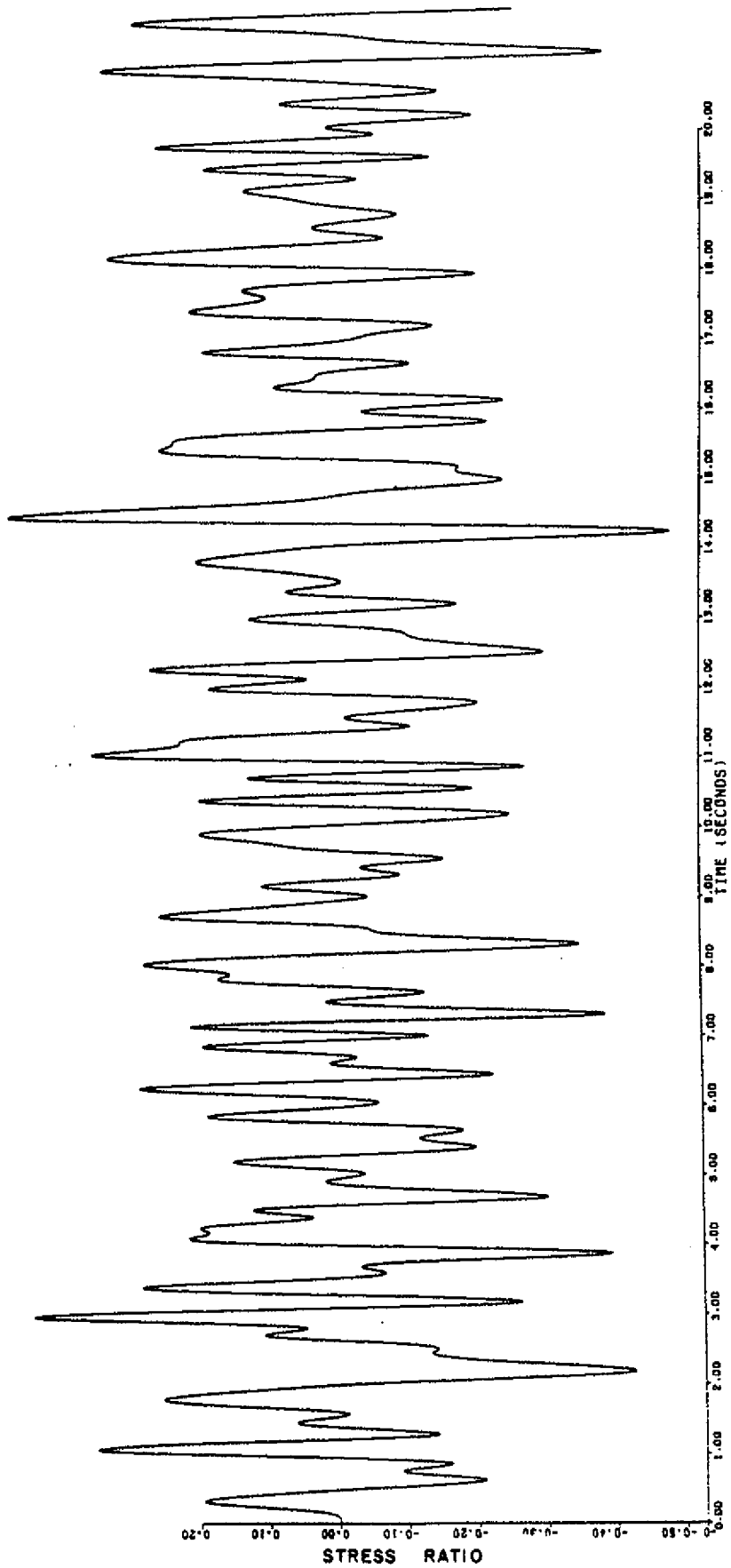

Project: SONGS SOIL STRUCTURE INTERACTION **Job Number:** 3221I	NO EMBEDMENT-ROTATIONAL INERTIA INCLUDED CENTER OF SLAB HORIZONTAL AND VERTICAL BASE MOTIONS	Fig. G7b

WOODWARD-McNEILL & ASSOCIATES

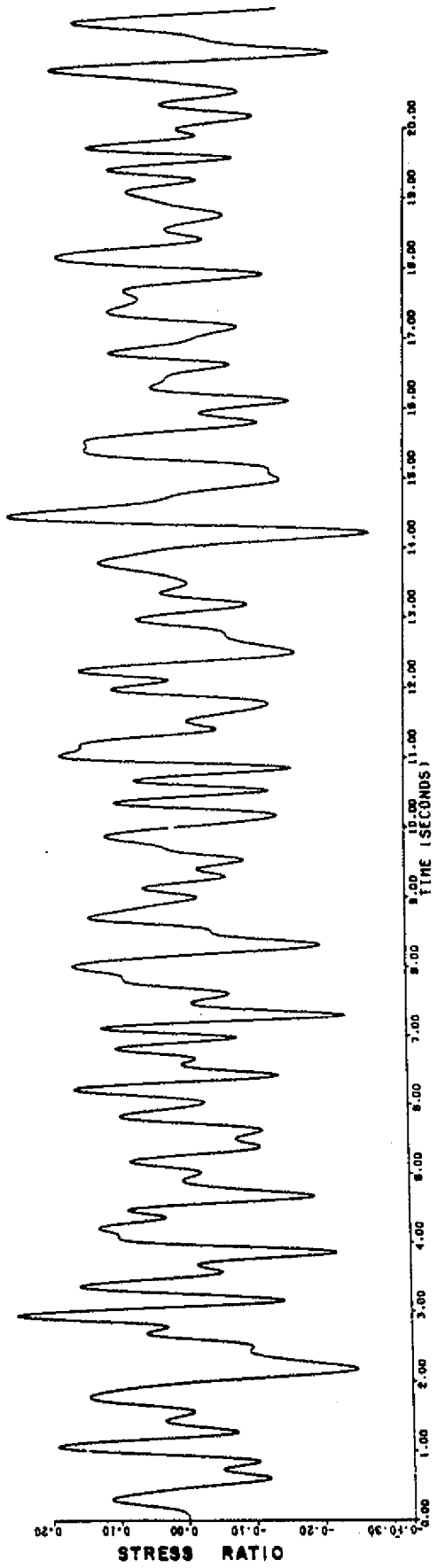

Project: SONGS SOIL STRUCTURE INTERACTION **Job Number:** B221I	NO EMBEDMENT ROTATIONAL INERTIA INCLUDED RIGHT END OF SLAB HORIZONTAL AND VERTICAL BASE MOTIONS	**Fig.** G7c

WOODWARD - McNEILL & ASSOCIATES

Amended: April 2009 TL: E047997

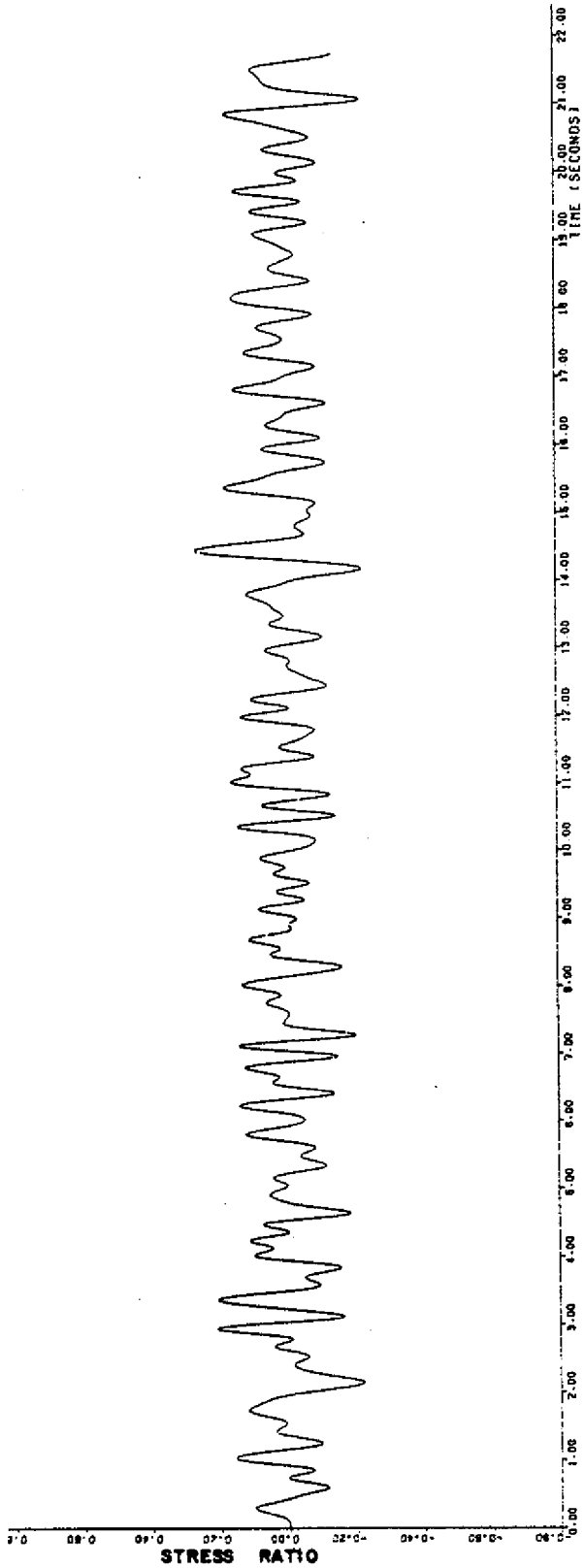

Project: SONGS SOIL STRUCTURE INTERACTION **Job Number:** B221I	EMBEDDED SLAB LEFT END OF SLAB HORIZONTAL BASE MOTION ONLY	Fig. G8a

WOODWARD-McNEILL & ASSOCIATES

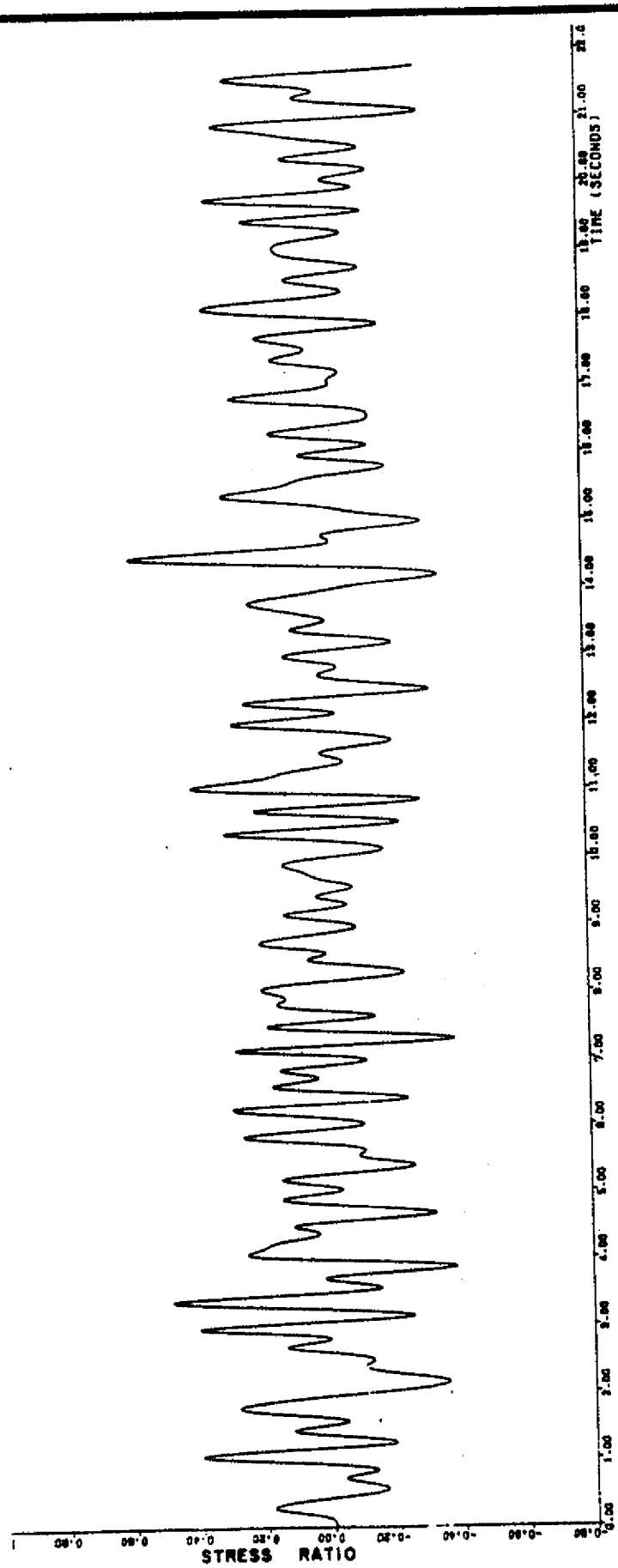

Project: SONGS SOIL STRUCTURE INTERACTION **Job Number:** B221I	EMBEDDED SLAB CENTER OF SLAB HORIZONTAL BASE MOTION ONLY	Fig. G8b

WOODWARD-McNEILL & ASSOCIATES

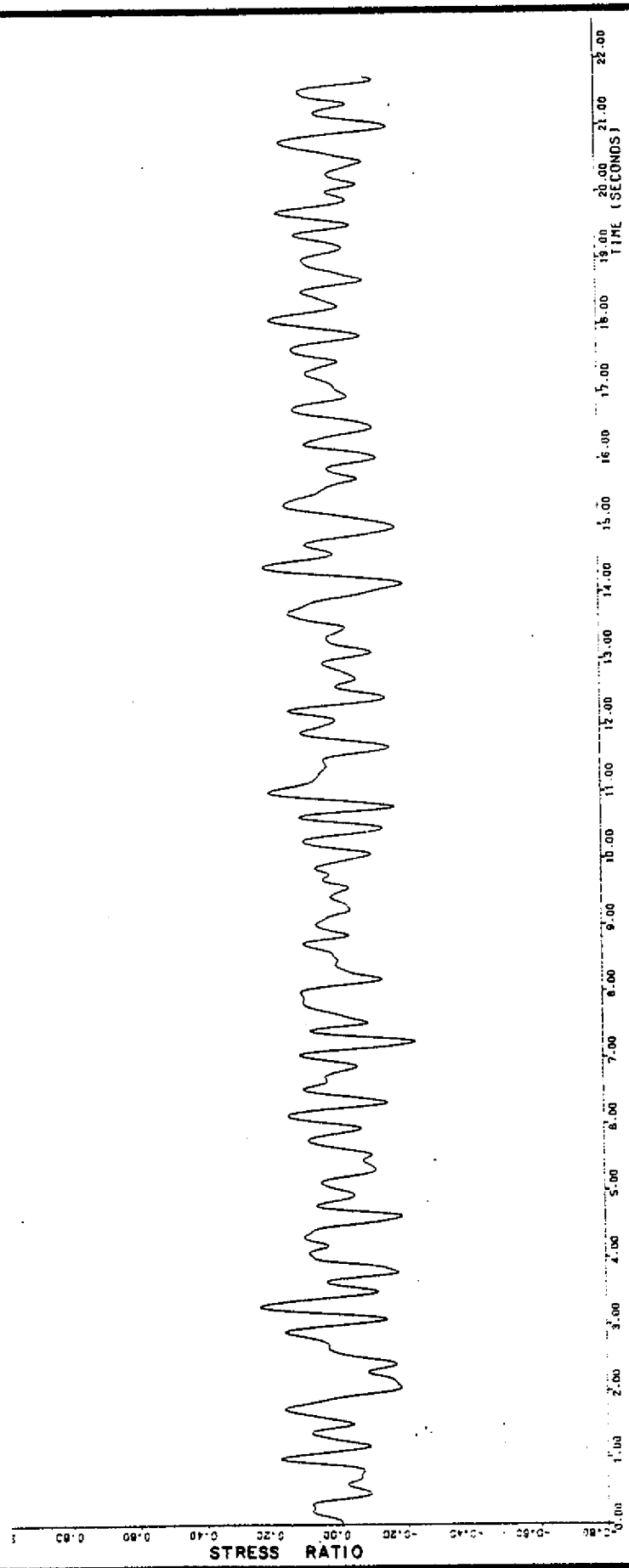

Project: SONGS SOIL STRUCTURE INTERACTION **Job Number:** B221I	EMBEDDED SLAB LEFT END OF SLAB HORIZONTAL AND VERTICAL BASE MOTIONS	**Fig.** G9a

WOODWARD – McNEILL & ASSOCIATES

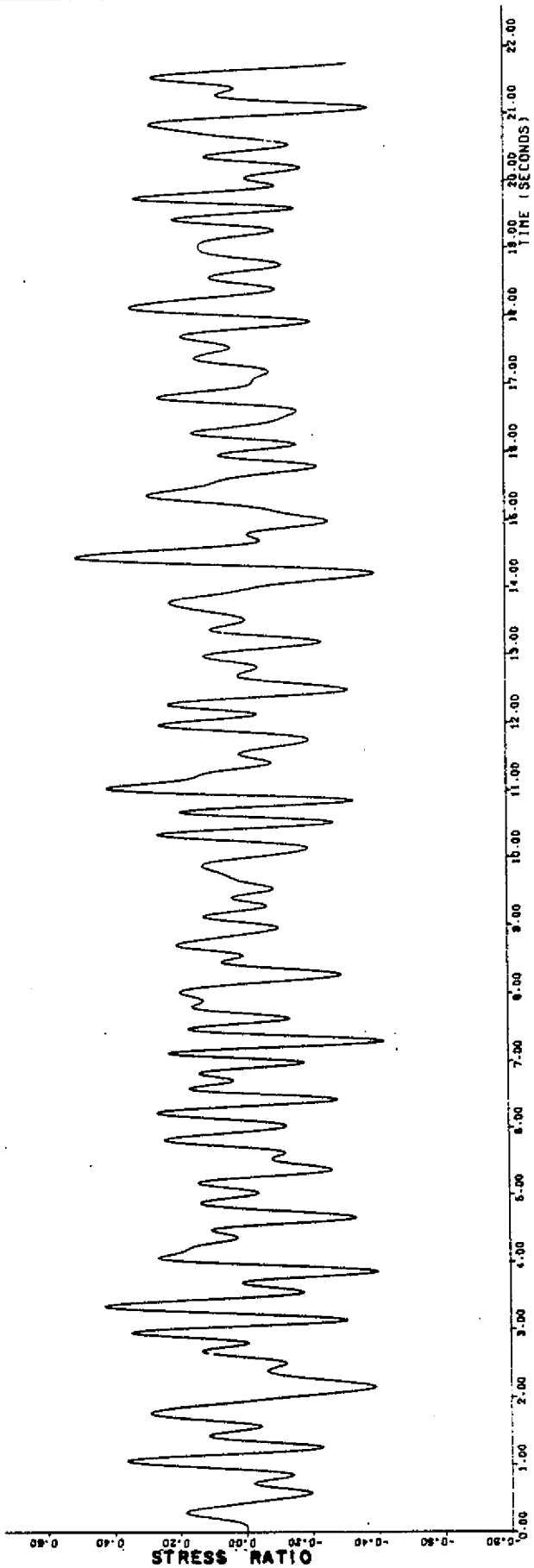

Project: SONGS SOIL STRUCTURE INTERACTION **Job Number:** B221I	EMBEDDED SLAB CENTER OF SLAB HORIZONTAL AND VERTICAL BASE MOTIONS	Fig. G9b

WOODWARD – McNEILL & ASSOCIATES

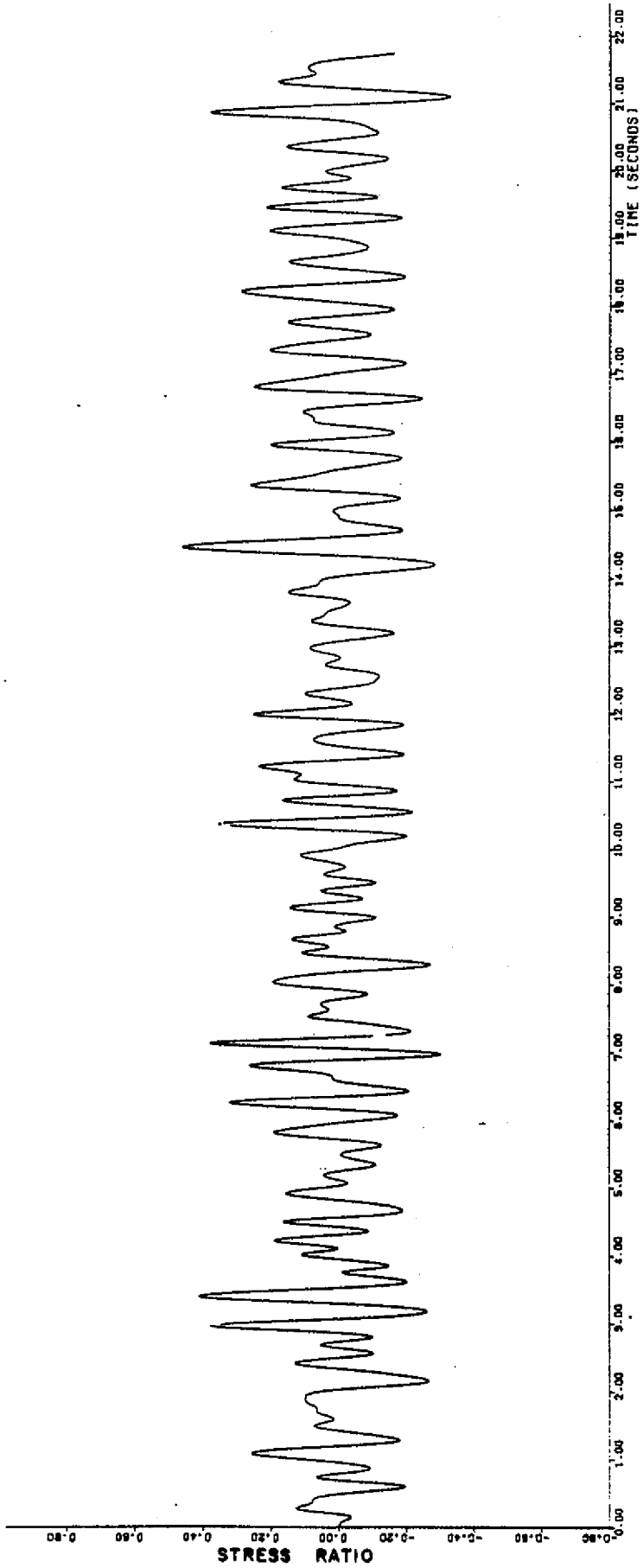

Project: SONGS SOIL STRUCTURE INTERACTION **Job Number:** B221I	EMBEDDED SLAB RIGHT END OF SLAB HORIZONTAL AND VERTICAL BASE MOTIONS	**Fig.** G9c

WOODWARD - McNEILL & ASSOCIATES

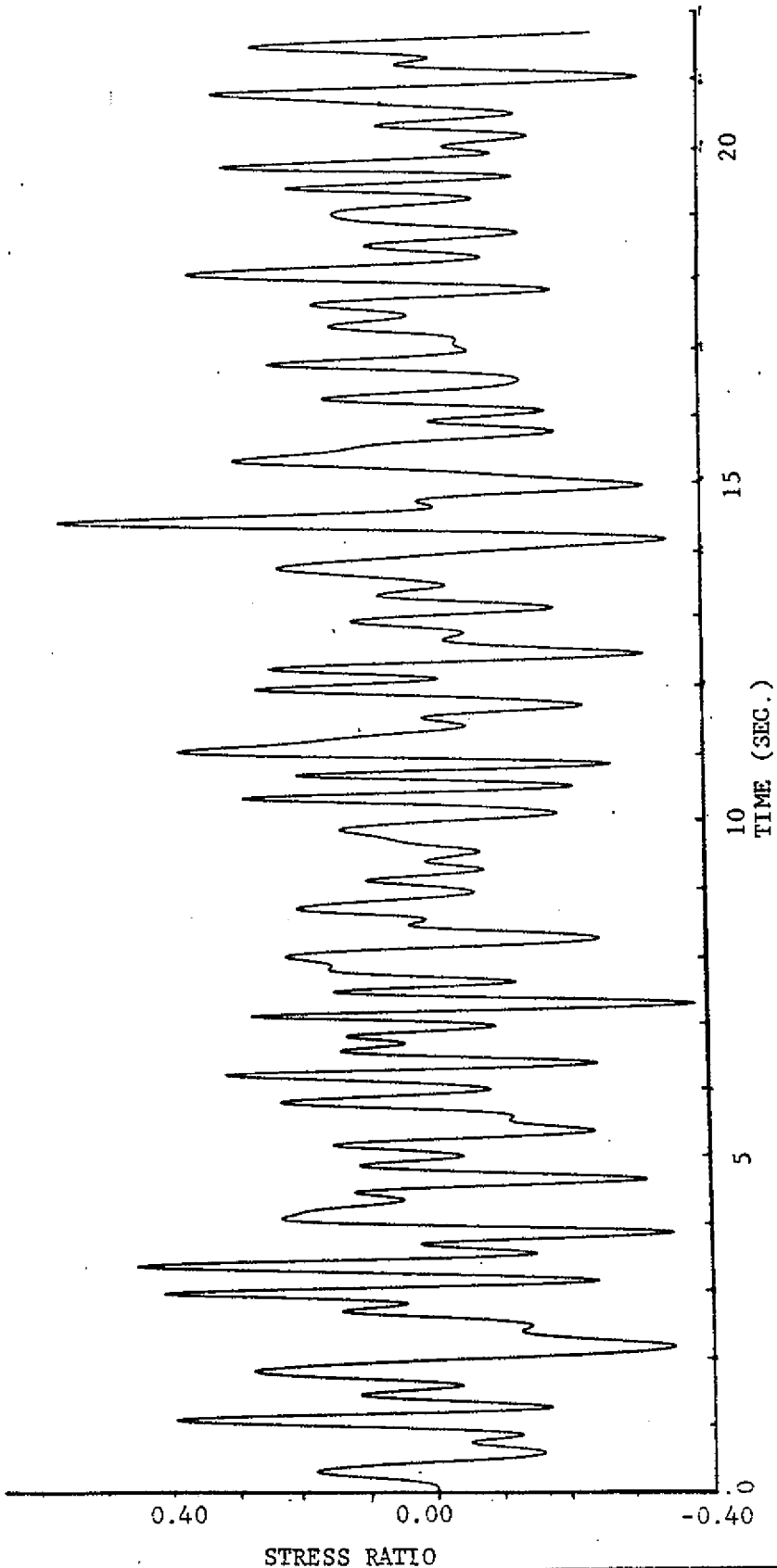

Project: SONGS SOIL STRUCTURE INTERACTION **Job Number:** B221I	NO EMBEDMENT CENTER OF SLAB HORIZONTAL AND VERTICAL BASE MOTIONS	Fig. G-10

WOODWARD - McNEILL & ASSOCIATES

APPENDIX H

EVALUATION OF CRITICAL INSTANTANEOUS DISPLACEMENT PROFILE

H-1 General

Determination of the DBE induced critical instantaneous displacement profile was done so that a pseudo-static calculation of stresses in a structure could be facilitated. This was done for structures grouped into either of two categories:

(1) Structures with complicated geometry and difficult to model.

(2) Structures below ground with the same mass or inertia as the displaced soil, for which response modeling is not appropriate for dynamic analysis.

The method of analysis is outlined in the following five (5) steps:

(1) Select appropriate section(s) of structure for modeling.

(2) Make suitable finite-element model(s) to represent actual soil-structure configuration(s).

(3) Determine dynamic properties of soil and structure for computer program input.

(4) Input the DBE time-history to the model and obtain and plot displacement time-history output at selected nodal points.

(5) Input the output from Step 4 into another computer program to obtain the critical instantaneous displacement profile(s) based on a maximum differential slope criteria.

These steps will be discussed in more detail in the section that follows.

H-2 Analysis

The computer program to study dynamic response of earth structures subjected to single travelling wave inputs was developed

Amended: April 2009 TL: E047997

at the University of California, Berkeley in 1967. DBE earthquake wave motions were input, propagating along the base of the finite-element model. A schematic diagram of the analysis is shown in Fig. H-1(a) through (c).

Procedures involved for this analysis are described below:

(1) Determine a representative cross-section of the structure to be studied. This is shown schematically by the shaded elements presented in Fig. H-1a.

(2) The configuration is then divided into suitable number of finite-elements. The mesh- consisting of these elements is extended to a sufficient distance to eliminate the influence of fixed vertical boundaries on the response value in the vicinity of the location of interest. Nodal points 1 through 5 represent five select points, at which displacement time-histories are desired at the base of the structure.

(3) Dynamic properties of soil are obtained as well as properties of concrete. These properties include Young's modulus of the soil at the strain level of interest and the equivalent modulus of structural elements, assuming a solid structure. The structural element modulus values are chosen by consideration of section modulus of the structure and/or judgment. Then properties are input to the computer program.

(4) Output from the computer program consists of vertical and horizontal displacement time-histories of the five selected nodal points at interface of the soil-structure system. Typical displacement-time histories of the five points are shown in Fig. H-1b. Delay time, t_i, is time required for wave front movement from one point to the next, and is expressed by the equation:

$$t_i = \frac{X_i}{V_s} \quad , i = 1, 2, 3, 4.$$

Where X_i = distance between two adjacent points.

t_i = time required for wave front movement from one point to the next point.

V_s = shear wave velocity.

(5) To determine the most critical bending conditions of the system during DBE earthquake motion, the displacement time-histories are input into another computer program in the sequence described in Step 4 and Fig. H-1b to obtain instantaneous displacement profiles corresponding to maximum slope change of any two adjacent points. The typical result of the computer output for horizontal displacement is presented schematically in Fig. H-1c.

BIBLIOGRAPHY

1. Barneich, J. A., Johns, D. H., and McNeill, R. L. (1974). "Soil Structure Interaction Parameters for Aseismic Design of Nuclear Power Stations," Pre-print 2182, ASCE National Meeting on Water Resources Engineering, Los Angeles, Jan. 1974.

2. Clough, R. W., and Chopra, A. K. (1966) "Earthquake Stress Analysis in Earth Dams," Journal of the Engineering Mechanics Division, ASCE, Vol. 92, No. EM2, Proc. Paper 4793, April, pp. 197-212.

3. Duncan, J. M., and Chang, C. Y. (1970) "Nonlinear Analysis of Stress and Strain in Soils," Journal of the Soil Mechanics and Foundations Division, ASCE, Vol. 96, No. SM5, September.

4. "Elastic and Damping Properties, Laydown Area, San Onofre Nuclear Generating Station," Report by Woodward-McNeill & Associates, dated 14 October 1971, presented as "Material Property Studies, San Onofre Nuclear Generating Station," PSAR, Amendment 11, Appendix 2E.

5. Hardin, B. O., and Drnevich, V. P. (1972) "Shear Modulus and Damping in Soils: Design Equations and Curves," Journal of the Soil Mechanics and Foundations Division, ASCE, Vol. 98, No. SM7, Proc. Paper 9006, July, pp. 667-692.

6. Idriss, I. M., Dezfulian, H., and Seed, H. B. (1969) "Computer Programs for Evaluating the Seismic Response of Soil Deposits with Non-Linear Characteristics Using Equivalent Linear Procedures," Research Report, Geotechnical Engineering, University of California, Berkeley.

7. Idriss, I. M., and Seed, H. B. (1974) "Seismic Response by Variable Damping Finite Elements," Journal of the Geotechnical Engineering Division, ASCE, Vol. 100, No. GT1, January.

8. Idriss, I. M., Lysmer, J., Hwang, R., and Seed, H. B. (1972) "Computer Programs for Evaluating the Seismic Response of Soil Structures by Variable Damping Finite Elements," Report, Earthquake Engineering Research Center, University of California, Berkeley, August.

9. Kaldjian, M. J. (1969) "Discussion of Design Procedures for Dynamically Loaded Foundations," by R. V. Whitman and F. E. Richart Jr., Paper No. 5569, Journal of the Soil Mechanics and Foundations Division, Proc. Paper, ASCE, Vol. 95, No. SM1, January.

Amended: April 2009 TL: E047997

10. Kulhawy, R. H., Duncan, J. M., and Seed, H. B. (1969) "Finite Element Analyses of Stresses and Movements in Embankments During Construction," Report No. TE 69-4, Office of Research Services, University of California, Berkeley.

11. Lysmer, J., Seed, H. B., and Schnabel, P. B. (1970) "Influence of Base Rock Characteristics on Ground Response," Earthquake Engineering Research Center Report No. EERC 70-7, University of California, Berkeley, November.

12. McNeill, R. L., and Mathur, J. N. (1973) "Soil Structure Interaction--A State of the Art Review," Presented at the Structural Engineers Association of Southern California Convention, San Diego, California, 1973.

13. McNeill, R. L. (1969) "Machine Foundations--The State of the Art," Proc. 7th International Conference on Soil Mechanics and Foundation Engineering, Mexico City, Mexico, August, 1969.

14. Newmark, N. M., and Hall, W. J. (1969) "Seismic Design Criteria for Nuclear Reactor Facilities," Proceedings, 3rd World Conference on Earthquake Engineering, Vol. II, Santiago, Chile.

15. Newmark, N. M., and Rosenblueth, E., "Fundamentals of Earthquake Engineering," Prentice Hall, 1971.

16. Richart, R. E., Jr., Hall, J. R., and Woods, R. D. (1970) "Vibrations of Soil and Foundations," Prentice Hall Inc., New York.

17. Schnabel, P., Seed, H. B., and Lysmer, J. (1971), "Modification of Seismograph Records for Effects of Local Soil Conditions," Earthquake Engineering Research Center, University of California, Berkeley, December.

18. Seed, H. B., and Idriss, I. M. (1970) "Soil Moduli and Damping Factors for Dynamic Response Analyses," Earthquake Engineering Research Center, Report No. EERC 70-10, University of California, Berkeley, December.

19. Seed, H. B., and Idriss, I. M. (1969) "Rock Motion Accelerograms for High Magnitude Earthquakes," Earthquake Engineering Research Center Report No. EERC 69-7, University of California, Berkeley, April.

20. Seed, H. B., Idriss, I. M., and Kiefer, R. W. (1969) "Characteristics of Rock Motions During Earthquakes," Journal of the Soil Mechanics and Foundations Division, ASCE, Vol. 95, No. SM5, September.

21. Seed, H. B. and Whitman, R. V. (1970) "Design of Earth Retaining Structures for Dynamic Loads", ASCE Specialty Conference on Lateral Stresses in the Ground and Design of Earth Retaining Structures, Cornell University, Ithaca, New York.

Amended: April 2009 TL: E047997

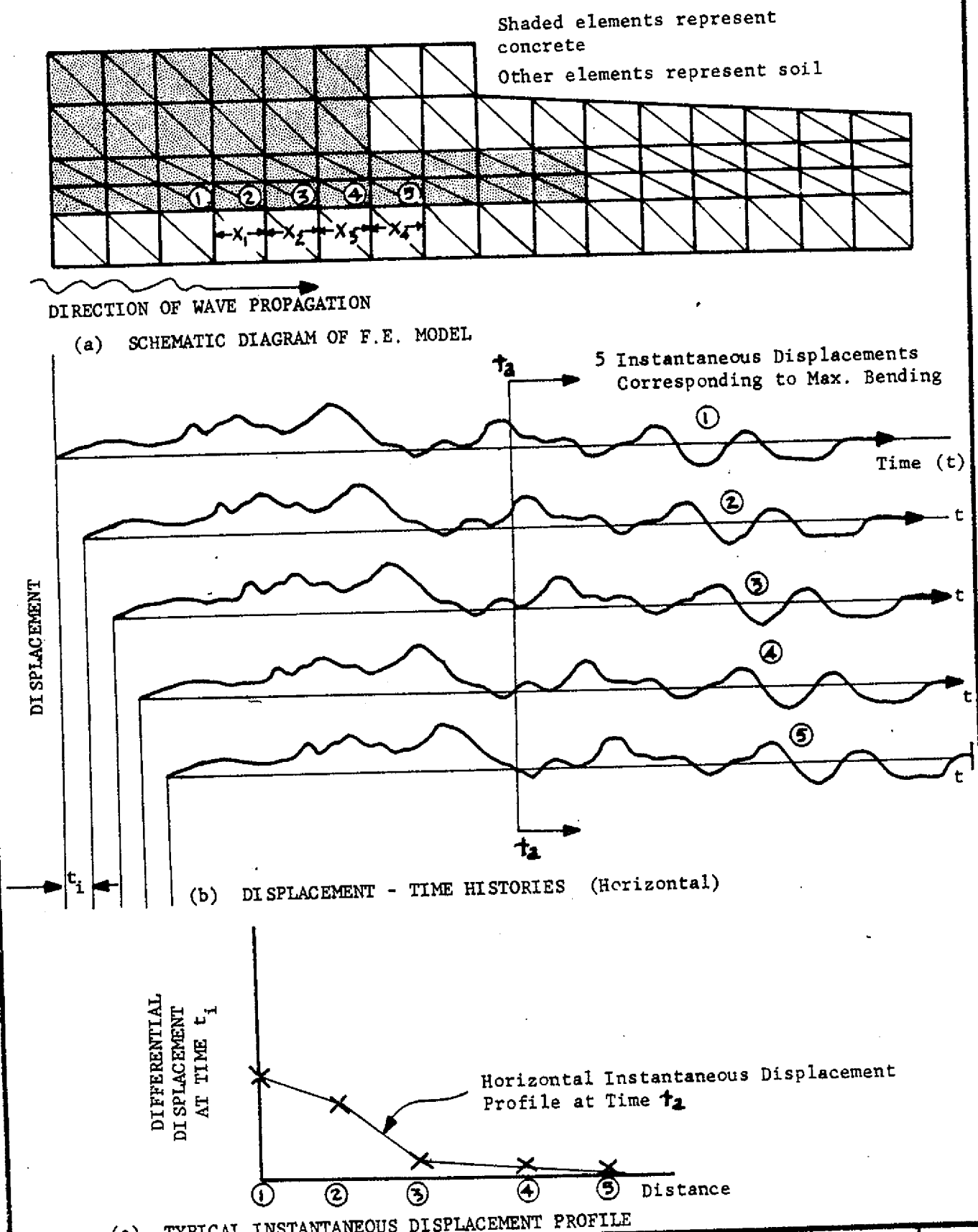

Project: SONGS SOIL STRUCTURE INTERACTION **Job Number:** B221I	SUMMARY OF PROCEDURE FOR DETERMINATION OF INSTANTANEOUS DISPLACEMENT PROFILE	Fig. H-1

WOODWARD - McNEILL & ASSOCIATES

Amended: April 2009 TL: E047997

3.8A APPENDIX 3.8A

VISUAL INSPECTION CRITERIA FOR STRUCTURAL STEEL AND MISCELLANEOUS METAL WELDING TO MEET DESIGN REQUIREMENTS

3.8A.1 INTRODUCTION

This appendix provides the acceptance criteria used for visual inspection of the welding of structural steel and miscellaneous metals during original construction that was performed in accordance with AWS D1.1-72. These criteria reflect the design requirements consistent with engineering approval specified in AWS D1.1-72, Sections 1.1.2, 3.1.4, 3.7.4, and 3.7.5. They also include welding of light gage material in HVAC ductwork whose classification is not specifically covered by AWS D1.1-72.

The visual inspection criteria for structural steel and miscellaneous metal welding performed to maintain structures is considered in the SCE Welding Program. The criteria is consistent with the design criteria presented in this appendix and provides the SCE engineering approval specified in AWS D1.1-1994, Sections 1.1.3, 3.1.5, 3.7.4 and 3.7.5.

3.8A.2 CLASSIFICATION OF WELD JOINTS

The following classification of weld joints satisfy the design intent. In addition, this classification of weld joints are based upon suitability for service in accordance with the following categories.

3.8A.2.1 Category A Joints
are part of the main building frame and carry the principal design loads.

3.8A.2.2 Category B Joints
are connections between the main building frame and miscellaneous metals.

3.8A.2.3 Category C Joints
are not part of the main building frame but rather provide auxiliary support or framing for systems, components, and equipment. These joints are within the miscellaneous metal category and include, but are not limited to, pipe supports beyond the scope of ASME, stairways, embedments, instrument supports, electrical raceway and supports, and HVAC duct supports.

3.8A.2.4 Category D Joints
are not part of the building frame or auxiliary support system, but rather perform a passive or inactive function. These joints are within the miscellaneous metal category and include, but are not limited to, doors, windows, hatch covers and frames, ledger angles, handrails, and gratings.

3.8A.2.5 Category E Joints
are limited to those welds, used in ductwork welding of thin gage stainless steel, whose classification is not specifically covered by AWS D1.1.

3.8A.2.6 Category F Joints
are limited to those welds, used in ductwork welding of thin gage carbon steel, whose classification is not specifically covered by AWS D1.1-72.

Acceptance criteria for visual examination of weldments made to maintain structures is contained in the SCE Welding Program. The acceptance criteria coincides with the requirements of the latest edition of AWS D1.1 and is not applied based on a differentiation between weld joint categories. The SCE Welding Program additionally provides for examination techniques and surface finish requirements. The requirements for flared-bevel groove welds is consistent with figure 3.8A-1.

3.8A.3 ACCEPTANCE CRITERIA

Weld joints were categorized during original construction. The acceptance criteria used during original construction was based on the type of joint and its suitability for the purpose. In addition to the requirements stated below pertaining to the overall weld, the cover pass (final weld layer) of all welds was required to be free of slag or any other foreign deposits that might interfere with the proper visual inspection of welds. Prior to visual inspection, the surfaces of welds and adjacent base metal were cleaned by chipping or pneumatic gun, exercising care that the finished weld was not damaged.

3.8A.3.1 Category A Joints
were considered acceptable when the following requirements were met:

A. The weld met or exceeded specified size requirements. Either or both fillet weld legs could exceed design size by 1/8-inch for welds up to and including 5/16-inch fillet, and 1/4-inch for welds larger than 5/16-inch fillet. Welds were permitted to be longer than specified. Continuous welds could be accepted in place of intermittent welds.

B. A fillet weld in any single continuous weld was permitted to underrun the nominal fillet size required by 1/16-inch (1.6 mm) or less without correction, provided that the undersize portion of the weld did not exceed 10% of the length of the weld. On web-to-flange welds on girders, no underrun was permitted at the ends for a length equal to twice the width of the flange.

C. The weld was permitted to contain a maximum of 5% by surface area of unaligned, unclustered porosity.

D. Convexity height could not exceed 1/8-inch. Rollover not exceeding 1/8-inch was acceptable provided the toe or fusion line of the weld remained visible for inspection. Butt weld reinforcement was not permitted to exceed 1/8-inch.

E. The weld could have an underfilled crater, provided the underfill depth did not exceed 1/32-inch and the crater had a smooth contour blending gradually with the adjacent weld and base metal without acute notches.

F. Undercut not exceeding 1/32-inch in depth was acceptable when oriented parallel to the longitudinal axis of the base metal and for joints that traversed 50% base metal width were acceptable provided the undercut did not exceed 0.01-inch in depth.

G. There were no cracks in the weld.

H. Thorough fusion was found to exist between weld metal and base metal, except as permitted in paragraph 3.8A.3.1, item D.

I. The following provisions and acceptance criteria were applied to flare-bevel groove welds in which the flared Profile results from the shape of the member being welded and was not specifically provided to achieve weld penetration. An application of this type of welding existed along the rounded edges of structural tubing welded against a flat steel surface.

1. The flared-bevel was filled with weld metal deposited flush as a minimum with the other surface. When welding unistrut members to flat surfaces, a 1/8" reinforcement was required.

2. A partially filled weld applied when the partial depth term, W, was given in the welding symbol as indicated in figure 3.8A-1. The partial depth refers to the weld dimension from the inner tangent point to the finished weld surface. Such weld dimension was not readily measured in completed welds; accordingly, the perpendicular width of the weld surface, B, as tabulated in figure 3.8A-1, was used instead as the acceptance criteria for weld size. The underfill, U, by itself was not a governing indicator of weld size and shall not be scrutinized provided that the minimum surface width, B, was verified.

3. Flush welds applied when W was not specified. For design purposes, these welds were considered to have a penetration equal to at least 0.45 times the flare radius, R, which is equivalent to a minimum effective throat of 0.30 R. Refer to figure 3.8A-1 for a definition of weld penetration and effective throat.

4. Additional outer fillet weld was provided only when specified in design drawings.

5. This type of flare-bevel groove weld was considered equivalent to fillet welds and were accepted on the basis of visual examination without any volumetric weld examination or inspection of the root pass, unless specified in the design drawings. For full penetration flare-bevel groove welds, inspection of the root pass remained as a requirement.

J. Arc strikes outside the area of permanent welds were avoided on base metals. Arc strikes were ground to blend with the adjoining surface. The area after blending met all the criteria within this category.

3.8A.3.2 Category B Joints
were accepted based upon the same criteria as applied to Category A joints.

3.8A.3.3 Category C Joints
were accepted when the following requirements were met:

A. All conditions described as acceptable in paragraph 3.8A.3.1, items B, C, D, G, H and I were acceptable for Type C joints.

B. Undercut (underfill) not exceeding 1/32-inch could be accepted for the full length of the weld. Undercut not exceeding 1/16-inch could be accepted provided it was wider than it is deep and did not have an acute intersection at its root. The accumulative length of 1/16-inch undercut could not exceed 50% of the weld length. For members welded from both sides, the cumulative undercut depth or length was not permitted to exceed the criteria.

C. Underfilled groove weld craters were accepted provided the depth of underfill was 1/16-inch or less. Underfilled single-pass fillet weld craters were accepted provided the crater length is less than 10%, of the weld length. On multi-pass fillet welds, a crater depth of 1/16-inch or less were accepted.

D. Burn-through was not permitted. However, minor burn-through not exceeding 1/4-inch in length was permitted for "unistrut" members which were welded along their length to obtain continuity with an associated structural member. This was provided so that an equivalent length of fillet weld was added to compensate for welds weakened by burn-through. This deviation was limited to one burn-through per 1 foot of weld length.

E. The weld met or exceeded specified size requirements. Welds were permitted to be longer than specified. Continuous welds were acceptable in place of intermittent welds.

F. Weld splatter was not required to be removed prior to repainting. However, removal of weld splatter, if required by other nonwelding design requirements, remained in force.

G. Arc strikes were acceptable provided that the craters (1) did not contain cracks (as determined by visual examination) and (2) the maximum size did not exceed the 3/8-inch plan or the 1/16-inch profile. Arc strikes were required to be free of foreign deposits which might interfere with the performance of proper visual inspection.

H. The weld could contain a maximum of 5% slag, by surface area, on the finished weld, provided that slag deposits did not interfere with the performance of proper visual inspection.

NOTE: Undercut on a member which provided auxiliary support or framing for systems, components, and equipment, and which was welded to a main member, was required to meet the requirements of a Category C joint as defined in 3.8A.3.3, item A above. Such members included, but were not limited to, pipe support members (beyond the scope of ASME), instrument support members, electrical raceway support members and HVAC duct support members. Undercut on a main member of the same weld joint was required to meet the requirements of a Category A joint.

3.8A.3.4 Category D Joints
were accepted when the following requirements were met:

A. All of the conditions described as acceptable in paragraph 3.8A.3.1, items A, B, D, G, H, and I.

B. All of the conditions described as acceptable in paragraph 3.8A.3.3, item C.

C. Porosity or slag inclusions were not a criterion for rejection.

D. Undercut was not permitted to not exceed 50% of the material thickness.

3.8A.3.5 Category E Joints
were accepted when the following requirements were met:

A. All conditions described as acceptable in paragraph 3.8A.3.1, items A, B, C, D, G, H, I, and paragraph 3.8A.3.4, item D, were acceptable for Category E joints.

B. Faying surfaces were not permitted to exceed a 3/16-inch gap between the parts to be joined. The leg of the fillet weld size was increased by the amount of the separation.

C. Abutting parts to be joined by butt welds were carefully aligned and misalignment could not exceed the thickness of the thinner material being welded as measured from the highest abutting member. In no case was more than 1/8-inch misalignment permitted as a departure from the theoretical alignment.

D. The butt weld profile was required to be convex; the reinforcement or crowning could not exceed 1/8-inch. The welded joint for ductwork was required to develop complete penetration for a minimum of 80%, of the length of the welded joint.

E. Corner welds used to seal ductwork were designated partial penetration welds. Such welds did not require full fusion and weld reinforcement greater than the material

thickness verified the adequacy of the weld, provided the toes of the weld had complete fusion.

F. The face of fillet welds were permitted to be slightly convex, flat, or slightly concave. Convexity shall not exceed 1/8-inch. Concavity could not reduce the weld throat beyond that required for weld size. Fillet weld size was as required by structural calculations, with minimum sizes as indicated in Table 3.8A-1.

G. Turning vanes and turning vane rails, damper stops, runners, and other nonstructural components, which were determined to be of light gage material and were welded to heavier gage ductwork, were welded with a fillet weld as required by design drawings. The fillet welds were permitted to exceed the profile and convexity limits as previously described and were considered acceptable for this application. Minor burn-through could not be avoided and was permitted up to 1/4-inch in length provided the equivalent length of fillet welds were added to compensate for welds weakened by burn-through.

H. Burn-through on partial penetration welds was permitted and leaktight integrity was maintained. Metal flow on the inside of the duct was permitted provided it was fused completely with the parent metal and metal thickness was not reduced by greater than 50%.

I. Scratching of metal in fit-up and isolated arc strikes were required to be removed only to the extent necessary to remove sharp burrs. The intent of this stipulation was to limit excess grinding of base metal, provided it did not exceed 50% of the base metal thickness in isolated areas.

J. Distortion caused by welding longitudinal seams was not permitted to exceed 2% of the nominal diameter measured from the cross-sectional cord of the distorted area. Temporary distortions larger than this were accommodated, provided it was demonstrated that the final in-place tolerances did not exceed the 2% value.

3.8A.3.6 Category F Joints

were accepted when the following requirements are met:

A. All conditions described as acceptable in paragraph 3.8A.3.5, items A through J were considered for Category F joints except as limited below:

1. Isolated porosity for carbon steel was not cause for rejection provided the extent of such porosity would not impact the adequacy of the epoxy coating to be subsequently applied. An average of one pinhole per 2 linear feet of weld length was considered acceptable without additional rework. Clustered porosity was not permitted to exceed 1% of the weld area, provided that the clusters are filled after the first epoxy coat with an approved epoxy filler (Valspar 46X2900 or 46X1900) per manufacturer's recommendations. Otherwise, the clustered porosity was required to be repaired by rewelding.

2. For carbon steel, intermittent minor joint gaps, including roll-over which accompany the welding relief provided in paragraph 3.8A.3.5, items A through J, was limited to the extent that such area would not impact the adequacy of the epoxy coating to be subsequently applied. Such areas were repaired by rewelding, or corrected using an epoxy filler (Valspar 46X2900 or 46X1900) per manufacturer's recommendations, to the extent that the epoxy coating integrity was assured.

Table 3.8A-1

MINIMUM FILLET WELD SIZE

Base Metal thickness of thicker part joined (T)		Minimum size of fillet weld*		
in.	mm	in.	mm	
T ≤ 1/4	T ≤ 6.4	1/8	3	
1/4 < T ≤ 1/2	6.4 < T ≤ 12.7	3/16	5	single-pass
1/2 < T ≤ 3/4	12.7 < T ≤ 19.0	1/4	6	weld must
3/4 < T	19.0 < T	5/16	8	be used

* The weld size should not exceed the thickness of the thinner part joined without Weld Engineering and Engineering approval. For this exception, particular care should be taken to provide sufficient preheat to ensure weld soundness.

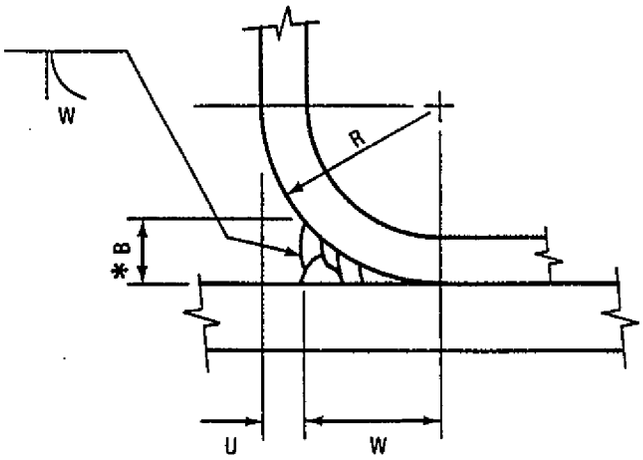

(INCHES)

W	1/4	5/16	3/8
B	3/16	1/4	1/4

MINIMUM R = 3/4 IN.

(A) PARTIALLY FILLED WELD

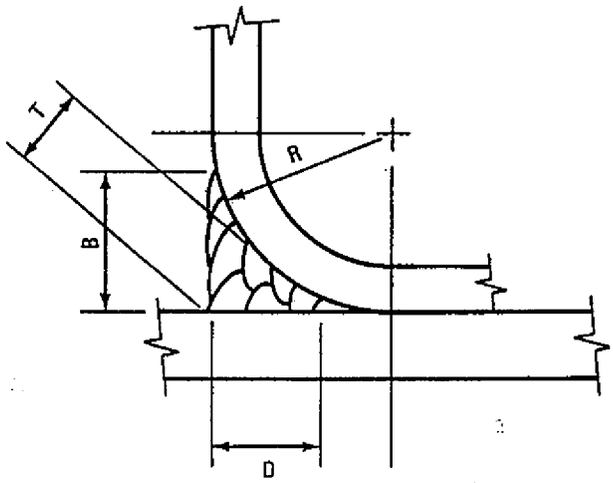

D ⩾ 0.45 R (PENETRATION)
T ⩾ 0.30 R (EFFECTIVE THROAT)
B ≈ R ± 1/8"

(B) FLUSH WELD

* MEASURED PERPENDICULAR TO FLAT SURFACE, BUT FINISHED WELD NEED NOT BE PERPENDICULAR TO FLAT SURFACE:

SAN ONOFRE NUCLEAR GENERATING STATION Units 2 & 3
WELDS ALONG PRE-EXISTING FLARED EDGES
Figure 3.8A-1

Site File Copy

Site File Copy

3B APPENDIX 3B

A FUNCTIONAL EVALUATION OF THE COMPONENTS OF THE SYSTEMS SHARED BY THE TWO-UNITS

3B.1 INTRODUCTION

Systems and components shared by Units 2 and 3 are discussed in this appendix. Shared structures are discussed in Chapter 1.

3B.2 EVALUATION

Table 3B-1 indicates those systems that are shared between Units 2 and 3. A brief description of the function of each system is given in this table, and the extent of sharing is also indicated. The last column of the table shows the UFSAR (DSAR) chapter that provides a detailed description of the related system and evaluates the implications of sharing between units

Table 3B-1
SUMMARY OF SHARED SYSTEMS (Sheet 1)

System	Function	Shared Components	Refer to DSAR Chapter
Domestic water system	Supplies water for typical domestic use and for emergency eyewash and shower stations throughout the plant	Entire system	9
Control Room/Command Center Habitability Systems	Provides adequate protection to permit access and occupancy of the Control Room/Command Center.	Entire System	6 and 9
Auxiliary building HVAC system	A heating, ventilating, and air conditioning (HVAC) system circulates air through the building. A standby VAC system is in place if needed.	Entire System	9
Auxiliary support building normal chilled water system	Provides cooling water supply for the auxiliary building.	Entire System	9

Table 3B-1
SUMMARY OF SHARED SYSTEMS (Sheet 2)

System	Function	Shared Components	Refer to DSAR Chapter
Telephone system	Onsite and offsite telephone communications	Entire system	9
VHF communications system	Communications link between control room and U.S. Marine Corps Headquarters Fire Station	Entire system	9
Public address and intercom systems	Intraplant paging and inter-office communications	Entire system	9
Emergency evacuation alarm	Evacuation of exclusion area	Entire system	9
Offsite power system	Source of ac power	Switchyard, including offsite power grid	8
Normal lighting system	Lights all required plant areas	Entire system	9
Emergency lighting system	Personnel evacuation lighting	Entire system	9
Fire protection system	Detects and extinguishes fires in all plant areas	Entire system	9
UHF radio system	Onsite communications	Entire system	9
Security system	Monitors plant access	Entire system	13
Miscellaneous liquid waste system	Collects and processes miscellaneous radioactive liquid wastes.	Entire system	11

Table 3B-1
SUMMARY OF SHARED SYSTEMS (Sheet 3)

System	Function	Shared Components	Refer to DSAR Chapter
Solid waste management system	Collects and prepares radioactive solid wastes and solidifies concentrated radioactive liquid wastes for offsite disposal	Entire system	11
Meteorological monitoring and display system	Collection and display of onsite meteorological data	Entire system	2
Personnel monitoring system	Determination of actual radiation exposure of employees	Entire system	12
Area radiation monitoring system	Continuously monitors radiation levels in potentially radioactive areas throughout the plant	Portions of system in common plant areas	12
Biological sampling system	Detects the quantity of radioactive plant releases entering the human food chain	Entire system	None
Environmental radiation monitoring system	Monitors the offsite radiation level resulting from plant releases	Entire system	None

Table 3B-1
SUMMARY OF SHARED SYSTEMS (Sheet 4)

System	Function	Shared Components	Refer to DSAR Chapter
Sump and drain system	Collects and discharges area leakage	Portion of system in common plant areas	9
Oily Waste Holding Sumps and system (subset of Sumps and Drains)	Provides for collection of various oil waste streams between the two units and common equipment.	Holding sumps and some minor piping runs.	9
Sanitary waste system	Collects and processes plant sanitary wastes	Entire system	9
Control Room/Command Center	Monitors Units 2 and 3 and common support systems	Shared space	1
Digital dispatch security monitoring system	Station status telemetering	Monitoring panel	None

Table 3B-1

SUMMARY OF SHARED SYSTEMS (Sheet 5)

System	Function	Shared Components	Refer to DSAR Chapter
UPS System	Provide Uninterruptible Power Supply to plant security systems	The UPS system of a unit supply power to security systems of both units	8
800 Mhz UHF	Establish offsite communication	Receives signal keying power from Fire Detection Power Distribution Panel which can be aligned to receive power from Units 2 or 3	3
12 kV Ring Bus	Supplies Cold and Dark systems.	Entire System	8
Backup Generators	Backup 12 kV Ring Bus and other equipment.	1500 kW and 500 kW Diesel Generators	8
Saltwater Dilution System	Dilute effluents to the Pacific Ocean.	Entire System	9

3C APPENDIX 3C

COMPUTER PROGRAMS USED IN STRUCTURAL ANALYSIS

Subsections 3C.1 through 3C.13 in Appendix 3C identify the computer software and their validation problems used in San Onofre's Units 2 and 3 initial structural design and analysis. Each subsection addresses specific software and describes its validation process. The Appendix's contents include the historical information developed during San Onofre's original design to address structural analysis. The test cases documented in the various subsections for each application confirmed the software's validity in order to determine the plants' design basis. Once a software's validity is established, the test case's results remain the same. Hence, there is no need to update a particular subsection.

Similar structural analysis conducted for recent plant modifications or to confirm structural adequacy employs software validated using the SONGS procedure SO123-XXIV-5.1, "EC&FS Software Quality Assurance." Such software is typically PC based and represents considerable improvements in applicability and ease of use. Appendix 3C has been expanded to list software currently being used at SONGS.

3C.1 FINITE ELEMENT COMPUTER PROGRAM (FINEL)

3C.1.1 DESCRIPTION

FINEL is a two-dimensional, static, small displacement, bilinear-elastic, finite-element computer program. FINEL is an improved version of the original FINEL code developed under the direction of Dr. E. L. Wilson at the University of California at Berkeley in 1962 under National Science Foundation grant G18986.

The primary purpose of this program is to perform plane or axisymmetric stress analysis of reinforced concrete structures. The program allows for concrete cracking and reinforcement yielding. This is done by a series of successive elastic iterations in which the stiffness matrix is modified to account for the nonlinear effect of cracking or yielding of each element. Loading includes concentrated, pressure, displacement (no inclined roller), thermal, inertial and, for axisymmetric problems, centrifugal forces.

In addition to analysis of reinforced concrete structures, FINEL can perform linear stress analysis on structures that can be modeled as plane stress, plane strain, or axisymmetric problems with axially symmetric material properties; i.e., isotropic in the plane (radial plane for axisymmetric problems), with the same or different properties normal to the plane.

FINEL has been used extensively to analyze reinforced concrete containment vessels.

Two types of material behavior are incorporated into FINEL:

A. Ductile

The stress-strain curve is bilinear in compression and in tension. This type of material behavior is used to model reinforcing steel and the liner plate material.

B. Brittle

The stress-strain curve is bilinear in compression and fractures (cracks) in tension. This type of material behavior is used to represent concrete and the foundation media.

3C.1.2 VALIDATION

Demonstration of the applicability and validity of the FINEL program is achieved through the comparison of the results obtained using the program with experimental and/or manually calculated solutions.

Eight test problems, outlined in paragraphs 3C.1.2.1 through 3C.1.2.8, were used in this demonstration, the results of which show that the FINEL solutions are essentially identical to experimental and/or manually calculated solutions.

3C.1.2.1 FINEL Example 1, Cracking Analysis of a Prestressed Concrete Reactor Vessel (PCRV)

The purpose of this test problem is to compare the results obtained from the FINEL program with the results obtained from both experimental and analytical investigation of the cracking of a cylindrical PCRV subjected to internal pressurization. A pictorial representation of the PCRV under investigation is shown in figure 3C.1-1.

The finite element idealization used in the FINEL analysis is shown in figure 3C.1-2. The zoning is obtained from the zoning used in reference 1 by subdividing each element into four elements. Since reference 1 used a quadratic element, while FINEL uses a linear element, the two zonings will have the same order of accuracy. Another difference between the analysis of reference 1 and the FINEL analysis is the assumed cracking criteria. Reference 1 used the following maximum strain criteria:

$$\varepsilon_{crack} = \frac{500 \text{ lb/in.}^2}{E} = 0.000116$$

(incorrectly reported as 0.00015 in reference 1)

The FINEL program used the following maximum stress criteria:

$$T_{crack} = 500 \text{ lb/in.}^2$$

Also, reference 1 reduced the shear stiffness to zero once an element cracked, while a shear stiffness reduction factor of 0.5 was used in the FINEL analysis.

The loading steps applied to the FINEL model of the PCRV are given in table 3C.1-1. Other parameters used are:

Young's Modulus = E = 4.3×10^6 lb/in.^{2}

Poisson's Ratio = v = 1/3

Cracking Stress = T_{crack} = 500 lb/in.^{2}

Table 3C.1-1

LOADING STEPS FOR FINEL MODEL (FINEL Example 1)

Step	Longitudinal Prestress (lbs)	Circumferential Prestress (lb/in.^{2})	Internal Pressure (lb/in.^{2})	No. of Iterations Required for Convergence
1	760,000	620	0	1
2	760,000	620	500	4
3	760,000	620	575	6
4	760,000	620	625	5
5	760,000	620	675	5
6	760,000	620	725	10

The cracking patterns calculated by reference 1 (v = 1/3) and the FINEL analysis are shown in figure 3C.1-3. Agreement is very good, taking into account the difference in the load-deformation curves; i.e., similar patterns, with the cracks from reference 1 growing more rapidly with increased load.

Load deformation curves for a point on the PCRV from references 1 and 2 and the FINEL analysis are shown in figure 3C.1-4. The numerical results of reference 1 and the FINEL analysis accurately predict the load at which significant cracking begins.

However, after significant cracking occurs, both the results of reference 1 and the FINEL analysis underestimate the deformation. Therefore, it is apparent that after significant cracking has occurred, a more accurate stiffness formulation is needed to predict the deformations of a PCRV. The fact that the results of the FINEL analysis agree more closely with the results of reference 1 where v = 0 than to reference 1 where v = 1/3 is due to the different failure criteria assumed. Reference 1 used a maximum strain criteria and FINEL uses a maximum stress criteria.

The results of this investigation indicate that the FINEL program can accurately predict loads at which significant cracking is initiated in a PCRV. As the load is increased above the point where significant cracking occurs, the results are only approximate. A more accurate stiffness for-

mulation is needed to accurately predict the behavior of a PCRV after significant cracking has occurred.

3C.1.2.2 FINEL Example 2, Analysis of a Simply Supported Beam

The purpose of this test problem is to compare the results obtained from the FINEL program with the results obtained from both experimental and analytical investigations of the cracking of a simply supported beam. A pictorial representation of the characteristics of the simply supported beam under investigation is shown in figure 3C.1-5.

The finite element mesh used in reference 3 and in the FINEL analysis is shown in figure 3C.1-6. The FINEL analysis requires a finer mesh because it used linear displacement elements while reference 2 used quadratic displacement elements.

The material properties of the concrete and reinforcing steel and the loading history used in the FINEL analysis are given in tables 3C.1-2 and 3C.1-3.

This problem solution was not continued beyond the yield point of the reinforcing steel due to an error in the FINEL program which has since been corrected.

The cracking patterns obtained from reference 3 and FINEL are shown in figure 3C.1-7. The load-deflection curves from references 3 and 4 and the FINEL analysis are shown in figure 3C.1-8. The load deflection curve obtained from the FINEL analysis shows very good agreement with the experimental results. The cracked region grows faster in the FINEL analysis and more slowly in reference 3, since the FINEL and reference 3 load-deflection curves show different gradients (stiffnesses).

Table 3C.1-2

MATERIAL PROPERTIES OF THE CONCRETE AND REINFORCING STEEL USED FOR FINEL VERIFICATION
(FINEL Example 2)

Property	Concrete	Steel
E	4.3×10^6 lb/in.^{2}	29×10^6 lb/in.^{2}
V	0.15	0.29
T_{yield}	-4,820 lb/in.^{2}	±44,900 lb/in.^{2}
E_{yield}	0.	0.
T_{crack}	+546 lb/in.^{2}	-----
E_{crack}	1.0 lb/in.^{2}	-----
Shear stiffness reduction factor for once cracked concrete	0.5	-----

Table 3C.1-3

LOADING HISTORY USED FOR THE FINEL VERIFICATION
(FINEL Example 2)

Load, P (lb)	Number of Cycles At Load for Convergence
1	1
8,700	4
20,000	4
28,000	1
31,200	4
31,300	1[a]

[a] Reinforcing steel yielded

3C.1.2.3 FINEL Example 3, Analysis of an End-Loaded Cantilever

The analysis of an end-loaded cantilever prismatic beam is performed to test the constant strain finite elements. The results are compared to theory. The beam geometry and finite-element mesh are illustrated in figure 3C.1-9. The problem is treated by a plane stress analysis, and the mesh contains 119 nodes and 96 quadrilateral constant strain elements.

The deflections and stress results from the FINEL program are compared with the hand calculations in tables 3C.1-4 and 3C.1-5. The theoretical linear strain variation across the depth of the beam is represented by discrete constant strain "steps" due to these finite elements. The differences in results are largely due to this feature of the constant strain elements.

3C.1.2.4 FINEL Example 4, Analysis of an Axially Constrained Hollow Cylinder with a Distributed Pressure Loading

The purpose of this test problem is to compare the response of an axially constrained hollow cylinder to internal pressure, determined using FINEL, with an analytical solution of the same problem. The finite-element model is illustrated in figure 3C.1-10. Nodal points are free to move only in the radial direction, modeling the conditions of axisymmetry and plane strain.

The closed-form solution is based upon Roark Formulas for Stress and Strain.[5] A summary comparison between the closed-form and FINEL solutions is given in table 3C.1-6.

Table 3C.1-4

DEFLECTION RESULTS FROM FINEL VERIFICATION USING AN END-LOADED CANTILEVER (FINEL Example 3)[a]

Node	Deflections	
	FINEL	Hand Calculations
25	0.0182	0.0169
46	0.0652	0.0630
67	0.1338	0.1316
88	0.2176	0.2160
116	0.3417	0.3413

[a] Flexural deflections only are computed here.

Table 3C.1-5

STRESS RESULTS FROM FINEL VERIFICATION USING AN END-LOADED CANTILEVER (FINEL Example 3)[a]

Node	Deflections	
	FINEL	Hand Calculations
a	63.132	64.5833
b	54.048	56.2500
c	46.107	57.9170
d	38.087	39.5830
e	30.069	31.2500
f	22.050	22.9170
g	14.032	14.5830
h	6.004	6.2500

[a] Computed at center of outer elements to correspond to output from computer.

3C.1.2.5 FINEL Example 5, Analysis of an Axially Constrained Hollow Cylinder with a Linear Temperature Gradient

The purpose of this test problem is to compare the response of an axially constrained hollow cylinder to a radially varying temperature gradient, determined using FINEL, with a closed-form solution to the same problem. The finite-element model is illustrated in figure 3C.1-11. The conditions of axisymmetry and plane strain are imposed by using the axisymmetric quadrilateral element and restraining all nodes against axial displacement. The temperature is illustrated in figure 3C.1-12.

The closed form solution is based on Timoshenko, Elasticity[6] and Manson, Thermal Stress.[7] A summary comparison between the closed-form and FINEL solutions is given in table 3C.1-7.

3C.1.2.6 FINEL Example 6, Analysis of an Axially Constrained Hollow Cylinder with a Nonlinear Temperature Gradient

The purpose of this test problem is to compare the response of an axially restrained hollow cylinder to a radially varying temperature gradient, determined using FINEL, with a closed-form solution to the same problem. The finite-element model is illustrated in figure 3C.1-13. The conditions of axisymmetry and plane strain are imposed by using the axisymmetric quadrilateral element and restraining all nodes against axial displacement. The bilinear temperature gradient is illustrated in figure 3C.1-14.

Table 3C.1-6
SUMMARY COMPARISON, FINEL EXAMPLE 4

Element	r (ft)	Tangential Stress (k/ft^2)		Axial Stress (k/ft^2)		Radial Stress (k/ft^2)	
		Analytical[(a)] Solution	FINEL Solution	Analytical[(a)] Solution	FINEL Solution	Analytical[(a)] Solution	FINEL Solution
1	65.19	17.79	17.79	4.212	4.212	-0.95	-0.95
2	65.56	17.69	17.69	4.212	4.212	-0.84	-0.84
3	65.94	17.58	17.58	4.212	4.212	-0.73	-0.73
4	66.31	17.48	17.48	4.212	4.212	-0.63	-0.63
5	66.69	17.38	17.38	4.212	4.212	-0.53	-0.53
6	67.06	17.28	17.28	4.212	4.212	-0.43	-0.43
7	67.44	17.18	17.18	4.212	4.212	-0.33	-0.33
8	67.81	17.08	17.08	4.212	4.212	-0.24	-0.23
9	68.19	16.99	16.99	4.212	4.212	-0.14	-0.14
10	68.56	16.89	16.89	4.212	4.212	-0.05	-0.05

[(a)] Based on Roark Formulas for Stress and Strain[(5)]

Table 3C.1-7
SUMMARY COMPARISON, FINEL EXAMPLE 5

Element	r (ft)	Tangential Stress (k/ft^2)		Axial Stress (k/ft^2)		Radial Stress (k/ft^2)	
		Analytical[(a)] Solution	FINEL Solution	Analytical[(a)] Solution	FINEL Solution	Analytical[(a)] Solution	FINEL Solution
1	65.19	-78.34	-78.33	-77.96	-77.96	-0.22	-0.23
2	65.56	-60.67	-60.66	-60.68	-60.68	-0.62	-0.62
3	65.94	-43.10	-43.09	-43.40	-43.40	-0.91	-0.91
4	66.31	-25.63	-25.62	-26.12	-26.12	-1.10	-1.10
5	66.69	-8.26	8.25	-8.84	-8.84	-1.19	-1.19
6	67.06	9.01	9.02	-8.44	-8.44	-1.18	-1.18
7	67.44	26.19	26.20	-25.72	-25.72	-1.08	-1.08
8	67.81	43.27	43.28	-43.00	-43.00	-0.88	-0.88
9	68.19	60.26	60.27	-60.28	-60.28	-0.59	-0.59
10	68.56	77.16	77.17	-77.56	-77.56	-0.21	-0.21

[(a)] Based on formula given in Timoshenko, Elasticity[(6)] and Manson, Thermal Stress[(7)]

Table 3C.1-8
SUMMARY COMPARISON, FINEL EXAMPLE 6

Element	r (ft)	Tangential Stress (k/ft^2)		Axial Stress (k/ft^2)		Radial Stress (k/ft^2)	
		Analytical[(a)] Solution	FINEL Solution	Analytical[(a)] Solution	FINEL Solution	Analytical[(a)] Solution	FINEL Solution
1	65.19	-385.68	-383.29	-442.35	-441.72	-1.25	-1.10
2	65.56	-199.73	-197.38	-258.09	-257.47	-2.94	-2.76
3	65.93	-51.93	-68.07	-110.92	-128.89	-3.57	-3.49
4	66.31	-16.09	-13.58	-75.24	-74.61	-3.73	-3.70
5	66.68	19.54	22.06	-39.56	-38.92	-3.68	-3.66
6	67.06	54.98	57.50	-3.88	-3.24	-3.44	-3.41
7	67.43	90.22	92.75	31.80	32.45	-3.00	-2.98
8	67.81	125.27	127.81	67.47	68.14	-2.37	-2.35
9	68.19	160.14	162.68	103.15	103.82	-1.56	-1.54
10	68.56	194.82	197.37	138.83	139.51	-0.56	-0.54

[(a)] Based on formula given in Timoshenko, Elasticity[(6)] and Manson, Thermal Stress[(7)]

The closed form solution is based on Timoshenko, Elasticity[6] and Manson, Thermal Stress.[7] A summary comparison between the closed-form and FINEL solutions is given in table 3C.1-8.

3C.1.2.7 FINEL Example 7, Analysis of a Deep Elastic Panel

The purpose of this test problem is to compare the response of a deep elastic panel subjected to a uniformly distributed load determined using FINEL with a closed-form solution to the same problem. The finite element model is illustrated in figure 3C.1-15.

Due to the symmetry of the actual problem, only half of the panel has been modeled. Appropriate boundary conditions are applied to the nodal points along the axis of symmetry.

Boundary conditions along axis X = 0

Θ rotation = 0

X displacement = 0

The closed-form solution is based on Timoshenko, Elasticity.[8] The stress results from FINEL represent the centroidal value for each plate element. Therefore, in order to obtain stress values at locations more suitable for comparison with the theoretical solution, a graphical extrapolation of the results obtained from the FINEL analysis is necessary to establish stress values at nodal points along the axis of symmetry. Figure 3C.1-16 illustrates the approach used to establish the stress levels at nodal points 1 and 61.

The results from the FINEL solution for the stresses at the nodal points located at the top and bottom of the panel along the axis of symmetry were compared to those from the manually calculated solution as shown in table 3C.1-9.

The magnitude of the error reflects the use of graphical extrapolation in conjunction with a relatively coarse mesh of constant strain elements.

This verification problem demonstrates the performance of the constant strain finite elements to solve an elasticity problem where shear effects are significant. These results confirm the known limitations of this type of element.

3C.1.2.8 FINEL Example 8, Analysis of a Deep Elastic Panel (Finer Mesh Size)

The purpose of this test problem is to compare the response of a deep elastic panel subjected to a uniformly distributed load determined using FINEL with a closed-form solution to the same problem. The problem is identical to the one presented in paragraph 3C.1.2.7 except that the mesh size of the finite model has been reduced. The actual mesh size of the finite-element model is shown in figure 3C.1-17.

Table 3C.1-9

COMPARISON OF RESULTS FOR A DEEP ELASTIC PANEL
(FINEL Example 7)

Node	Stress (k/in.^{2})	
	FINEL	Hand Calculation
Node 61	-52.0	-48.8
Node 1	146.0	126.8

The closed-form solution is based on Timoshenko, Elasticity.[8] For comparison purposes, the FINEL results at the nodal points located at the top and bottom of the panel along the axis of symmetry are extrapolated from the centroidal plate element results along the diagonal away from these nodal points using the following cubic polynomial curve fit algorithm.[9]

$$4 = (a_o + x\ (a_1 + x\ (a_2 = a_3 x)))$$

The results from the FINEL solution for the stress at the points of interest were compared to those from the manually calculated solution as shown in table 3C.1-10.

This verification problem demonstrates the performance of the constant strain finite elements to solve an elasticity problem where shear effects are significant. These results confirm the known limitations of this type of element.

3C.1.3 EXTENT OF APPLICATION

FINEL is used to perform the cracked-section analysis of the containment structure, based on an axisymmetric analysis. The program performs a design check of the structure for which all geometric and design parameters are known.

Table 3C.1-10

COMPARISON OF RESULTS FOR THE DEEP ELASTIC PANEL
(FINEL Example 8)

Node	Stress	
	FINEL	Hand Calculation
21	-51.185	-48.8
1	137.925	126.8

3C.1.4 REFERENCES

1. Zienkiewicz, O. C., Owen, D. R. J., Phillips, D. V., and Nayak, G. C., "Finite Element Methods in the Analysis of Reactor Vessels," Nuclear Engineering and Design, Vol 20, No. 507, 1972.

2. Sozen, M. A. and Paul, S. L., "Structural Behavior of a Small-Scale Prestressed Concrete Reactor Vessel," Nuclear Engineering and Design, Vol 8, No. 403, 1968.

3. Suidan, M. and Schnobrich, W. C., "Finite Element Analysis of Reinforced Concrete," Journal of the Structural Division, ASCE, Vol 99, No. ST10, pp 2109-2122, October 1973.

4. Burns, N. H. and Siess, C. P., "Load Deformation Characteristics of Beam-Column Connections in Reinforced Concrete," Structural Research Series No. 234, Civil Engineering Studies, University of Illinois, Urbana-Champaign, Illinois, January 1962.

5. Roark, Raymond, Formulas for Stress and Strain, Fourth Edition, McGraw-Hill, p 308, 1965.

6. Timoshenko and Goodier, Theory of Elasticity, Third Edition, McGraw-Hill, p 448, 1970.

7. Manson, Thermal Stress and Low Cycle Fatigue, McGraw-Hill, pp 28-29, 1960.

8. Timoshenko and Goodier, Theory of Elasticity, Third Edition, McGraw-Hill, pp 538-545, 1970.

9. Connor and Will, "Computer Aided Teaching of the Finite Element Displacement Method," MIT Research Report 69-23, p 196, February 1969.

3C.2 AXISYMMETRIC SHELL AND SOLID COMPUTER PROGRAM (ASHSD)

3C.2.1 DESCRIPTION

The ASHSD program is capable of both static and dynamic elastic analysis of structural systems idealized by either axisymmetric shell or axisymmetric solid finite-elements or by a combination thereof.

The ASHSD code is also capable of handling both axisymmetric and asymmetric loadings.

This program is a refinement of the original ASHSD code by S. Ghosh, developed at the University of California at Berkeley under the direction of Dr. E. L. Wilson and published for National Science Foundation Research Project GK4395.[1] The present program is modified by

Bechtel Power Corporation for the special purpose of static and dynamic analysis of nuclear containment structures. The modified program has the following features:

A. The original shell element used by the code is entirely replaced with a new shell finite-element that uses an interaction stiffness allowing analysis of layered shells. A complete discussion of the theory is given in Theory of Anisotropic Shells by S. A. Ambartsumyan.[2]

B. Since shell layers may be bonded or unbonded from each other, it is possible to describe concrete shells in their actual geometric form. For example, it is possible to describe liner plate, concrete, reinforcing steel, and post-tensioning steel in their real spatial locations.

C. Post-tension forces may be applied to the shell by subjecting only the unbonded post-tensioning elements to a pseudo-thermal loading.

D. Isotropic and orthotropic elastic constants are possible for both shell and solid elements. For example, the orthotropic material properties may be used to describe the different stiffnesses of reinforcing steel in the hoop and meridional directions.

E. Nonuniform axisymmetric or asymmetric thermal gradients through the wall thickness may be imposed.

F. Eigenvectors and eigenvalues may be computed by the program.

G. Three dynamic response routines are available in the program. They are:

   1. Arbitrary dynamic loading or earthquake, base excitation using an uncoupled (modal) technique

   2. Arbitrary dynamic (loading or earthquake), base excitation using a coupled (direct integration) technique

   3. Response spectrum nodal analysis for absolute and square-root-of-the-sum-of-the-squares displacements and element stresses.

H. The coupled time-history solution has the capability to allow an arbitrary damping matrix.

The program uses an extended Ritz technique of seeking a stationary value of an energy integral. Hamilton's variational principle is used to derive the equations of motion such as Lagrange's equations involving the total kinetic and potential energies of the system. If the program is used for only the static analysis, the kinetic energy being absent, the problem is governed by the principle of minimum potential energy.

Any arbitrary loading is approximated by the cosine terms of a Fourier series with a finite number of terms. For each Fourier component, the stiffness and mass matrices and the corresponding load vectors are formed. These are consistent with the assumed sinusoidal displacement field. After solving for the response of all the Fourier terms, their contributions are summed up to obtain the total response.

3C.2.2 VALIDATION

Eight test problems, outlined in paragraphs 3C.2.2.1 through 3C.2.2.8, demonstrate applicability and validity of the ASHSD program. Results of the problems for various loadings demonstrate that ASHSD results are essentially identical to the results obtained by hand calculations or those obtained by the closed-form analytical results available in technical literature.

3C.2.2.1 ASHSD Example 1, Closed Cylinder Under Internal Pressure

This test example demonstrates the membrane state of stress of a closed cylinder subjected to a uniformly distributed internal pressure. Because of symmetry, a finite-element idealization of one-half of the cylinder and the appropriate boundary conditions is used. The numerical data required for the ASHSD program input also are described. Refer to figure 3C.2-1.

For the purpose of illustrating the layered shell feature of the ASHSD program, a second test case is undertaken. The thickness of the closed cylinder used in the above example is divided into three layers as shown in figure 3C.2-2.

The longitudinal and circumferential forces for all node points of the two ASHSD program runs are listed in table 3C.2-1. The theoretical values for the membrane stress resultants are calculated to be PR/2 (=27,000 lb/in.) and PR (=54,000 lb/in.), respectively. As noted in table 3C.2-1, the results from both analyses compare with the theoretical values.

Table 3C.2-1

TABULATION OF MEMBRANE STRESS RESULTANTS, ASHSD EXAMPLE 1

Node Point	Shell		Layered Shell	
	Longitudinal Force (lb/in)	Circumferential Force (lb/in)	Longitudinal Force (lb/in)	Circumferential Force (lb/in)
1	27,000.0	54,004.0	27,000.0	54,004.0
2	27,000.0	54,005.0	27,000.0	54,005.0
3	27,000.0	54,008.0	27,000.0	54,008.0
4	27,000.0	54,012.0	27,000.0	54,012.0
5	27,000.0	54,015.0	27,000.0	54,015.0
6	27,000 0	54,012.0	27,000.0	54,012.0
7	27,001.0	53,999.0	27,001.0	53,999.0
8	27,001.0	53,968.0	27,001.0	53,968.0

9	27,001.0	53,912.0	27,001.0	53,912.0
10	27,000.0	53,829.0	27,000.0	53,829.0
11	26,999 0	53,731.0	26,999.0	53,731.0
12[a]	26,997.0	53,654.0	26,997.0	53,654.0
13[a]	26,994.0	53,674.0	26,994.0	53,674.0
14[a]	26,989 0	53,912.0	26,989.0	53,912.0
15[a]	26,984.0	54,532.0	26,984.0	54,532.0
16[a]	27,111.0	55,724.0	27,111.0	55,724.0

[a] Results for node points 12 through 16 are influenced by the boundary conditions at node point 16.

3C.2.2.2 ASHSD Example 2, Cylindrical Shell Under Internal Pressure

This test example illustrates the use of arbitrary static loading conditions. A sketch of the cylinder and the applied pressure is shown in figure 3C.2-3. Since there is a plane of symmetry, only one-half of the cylinder need be considered. The finite-element model, boundary conditions, and the relevant input data are described in figure 3C.2-4.

Figure 3C.2-5 shows a comparison of ASHSD radial displacements and analytically obtained displacements found in Theory of Plates and Shells.[3]

A comparison of ASHSD longitudinal moments and those obtained from Theory of Plates and Shells[3] is shown in figure 3C.2-6.

Both the radial displacements and the longitudinal moments check with analytical solutions obtained from Theory of Plates and Shells.

3C.2.2.3 ASHSD Example 3, Spherical Dome, Dead Load Analysis

This test example demonstrates the dead load analysis feature of the ASHSD program. It considers a spherical dome of constant thickness under its own weight, as shown in figure 3C.2-7. The axisymmetric finite-element model and pertinent shell data are described in figure 3C.2-8.

The exact analytical solutions obtained from Applied Elasticity[4] for longitudinal and circumferential forces are compared to the ASHSD finite-element results in figures 3C.2-9 and 3C.2-10, respectively.

With the exception of forces near the shell boundary, all forces away from the boundary have excellent agreement between the two solutions.

3C.2.2.4 ASHSD Example 4, Cylindrical Shell Subjected to an Internal Pressure and a Uniform Temperature Rise

This test example demonstrates the use of arbitrary static load and thermal load conditions. A short circular cylindrical shell, clamped at both ends, is subjected to an internal pressure and a uniform temperature rise, as shown in figure 3C.2-11. Because of symmetry, one-half of the cylinder is used in this finite-element model, which is shown in figure 3C.2-12. For the purpose of imputing the thermal coefficient of expansion of this isotropic shell, it is required to identify the shell material as orthotropic.

A comparison of ASHSD longitudinal moments and the theoretical solutions reported in Thin Elastic Shells[5] is displayed in figure 3C.2-13.

The finite-element model has approximately the same complexities as the examples demonstrating membrane stresses and displacements. Inasmuch as the moment involves higher-order effects, better correlation between the finite-element result and the theoretical solution is accomplished using a larger number of elements.

3C.2.2.5 ASHSD Example 5, Asymmetric Bending of Cylindrical Shell

This test example illustrates the use of higher harmonics for asymmetric loading cases. The cylindrical shell analyzed is a short, wide cylinder, as shown in figure 3C.2-14. The finite-element idealization of the cylinder and other pertinent data are illustrated in figure 3C.2-15. At each end of the cylinder, moments of the form $M = M_o \cos n\Theta$ were input for harmonics n = 0, 2, 5, 20.

Figures 3C.2-16 through 3C.2-19 show the theoretical results per Analysis of Unsymmetric Bending of Shells[6] and ASHSD results for element longitudinal bending moments and radial displacements for harmonic number n = 0, 2, 5, and 20, respectively.

As noted in figures 3C.2-16 through 3C.2-19, the results obtained from the ASHSD program are in good agreement with that reported in Analysis of Unsymmetric Bending of Shells.[6]

3C.2.2.6 ASHSD Example 6, Isotropic Disk, Axisymmetric Solids

This test example illustrates the use of the ASHSD solid elements to evaluate the stress distribution in axisymmetric structures. The structural problem consists of a 2-inch thick isotropic disk with a 10-inch inner radius and a 20-inch outer radius supported at the outer top edge. The finite-element model and the applied load are shown in figure 3C.2-20. The disk is divided into 10 quadrilateral solid elements having 22 node points.

The radial and axial displacements for all node points, obtained from the ASHSD computer run and Finite-Element Stress Analysis of Axisymmetric Solids with Orthotropic, Temperature-Dependent Material Properties,[7] are tabulated in table 3C.2-2. The radial, axial, and tangential stresses for all elements obtained from these same sources are tabulated in table 3C.2-3.

3C.2.2.7 ASHSD Example 7, Rotating Disk, Axisymmetric Solids

This test example demonstrates the use of the ASHSD solid elements to evaluate the stress distribution within an axisymmetric solid resulting from the centrifugal force as the body rotates about its axis of symmetry. The problem consists of a 1-inch thick disk with a 10-inch radius. The disk is divided into 10 quadrilateral solid elements having 22 nodal points. The centrifugal force was idealized by a set of equivalent inertia forces applied at each nodal point. The finite-element model is shown in figure 3C.2-21 and the equivalent inertial forces in table 3C.2-4.

Since the thickness of the disk was small in comparison with its radius, the variation of radial and tangential stresses over the thickness was neglected, making the problem two-dimensional.

Table 3C.2-2

TABULATION OF RADIAL AND AXIAL DISPLACEMENTS, ASHSD EXAMPLE 6 (Sheet 1 of 2)

Node Point	Radial Displacement		Axial Displacement	
	ASHSD	Analytical[a]	ASHSD	Analytical[a]
1	1.86526	1.865246	1.70644×10^{-3}	1.596941×10^{-3}
2	1.74648	1.746466	1.42706×10^{-4}	4.343421×10^{-5}
3	1.65210	1.652084	1.32770×10^{-4}	4.377285×10^{-5}
4	1.57633	1.576314	1.58635×10^{-4}	8.014718×10^{-5}
5	1.51518	1.515166	1.77255×10^{-4}	1.095182×10^{-4}
6	1.46573	1.465718	1.90285×10^{-4}	1.334706×10^{-4}
7	1.42579	1.425777	1.99601×10^{-4}	1.538673×10^{-4}
8	1.39368	1.393668	2.06398×10^{-4}	1.718854×10^{-4}
9	1.36810	1.368085	2.11214×10^{-4}	1.880642×10^{-4}
10	1.34802	1.348000	2.07829×10^{-4}	1.961813×10^{-4}
11	1.33263	1.332815	0.0	0.0
12	1.86526	1.865266	2.54113×10^{-2}	2.530175×10^{-2}
13	1.74648	1.746486	2.69750×10^{-2}	2.687561×10^{-2}
14	1 65210	1.652105	2.69850×10^{-2}	2.689533×10^{-2}
15	1.57633	1.576336	2.69591×10^{-2}	2.688047×10^{-2}
16	1.51518	1.515188	2.69405×10^{-2}	2.687260×10^{-2}
17	1.46573	1.465740	2.69275×10^{-2}	2.687051×10^{-2}
18	1.42579	1.425800	2.69181×10^{-2}	2.687228×10^{-2}
19	1.39368	1.393691	2.69113×10^{-2}	2.687674×10^{-2}

[a] Finite-Element Stress Analysis of Axisymmetric Solids with Orthotropic, Temperature-Dependent Material Properties.[7]

Table 3C.2-2

TABULATION OF RADIAL AND AXIAL DISPLACEMENTS, ASHSD
EXAMPLE 6 (Sheet 2 of 2)

Node Point	Radial Displacement		Axial Displacement	
	ASHSD	Analytical[a]	ASHSD	Analytical[a]
20	1.36810	1.368108	2.69065×10^{-2}	2.688331×10^{-2}
21	1.34802	1.348023	2.69099×10^{-2}	2.689816×10^{-2}
22	1.33263	1.332637	2.71177×10^{-2}	2.711740×10^{-2}

The radial and tangential stresses for all node points, obtained from the ASHSD computer run and Theory of Elasticity,[8] are tabulated in table 3C.2-5.

3C.2.2.8 ASHSD Example 8, Free Vibration of a Cylindrical Shell

This test example demonstrates the use of the ASHSD program to compute eigenvalues and eigenvectors for a thin elastic shell. The problem considered the free-vibration of a simply-supported (hinged at both ends) circular cylindrical shell. In order to obtain both symmetric and antisymmetric vibrating modes along the generator of the cylinder, the entire cylindrical shell was used for the free-vibration analysis. See figure 3C.2-22 for a pictorial representation of the computer model.

The first eight natural frequencies of the cylinder as obtained by the ASHSD program were compared with the results in Sing-Chih Tang's Response of a Finite Tube To Moving Pressure[9] as shown in table 3C.2-6.

3C.2.3 EXTENT OF APPLICATION

The ASHSD program is used in performing the preliminary static analysis of the containment structure for various loads. The results of these analyses are employed in arriving at the design section parameters for the cracked section analysis performed using the FINEL program. The ASHSD program is also used for dynamic modal analysis of the containment structure.

Table 3C.2-3
TABULATION OF RADIAL, AXIAL, AND TANGENTIAL STRESSES, ASHSD EXAMPLE 6

Element Number	Radial Stress		Axial Stress		Tangential Stress	
	ASHSD	Analytical[a]	ASHSD	Analytical[a]	ASHSD	Analytical[a]
1	-87.71	-88.0	0.74	1.0	154.6	154.0
2	-67.55	-68.0	-0.08	0.0	134.2	134.0
3	-52.04	-52.0	-0.08	0.0	118.7	118.0
4	-39.86	-40.0	-0.06	0.0	106.5	106.0
5	-30.10	-30.0	-0.04	0.0	96.8	97.0
6	-22.18	-22.0	-0.03	0.0	88.8	89.0
7	-15.65	-16.0	-0.03	0.0	82.3	82.0
8	-10.21	-10.0	-0.02	0.0	76.9	77.0
9	-5.63	-6.0	-0.02	0.0	72.3	72.0
10	-1.74	-2.0	-0.13	0.0	68.4	68.0

(a) Finite-Element Stress Analysis of Axisymmetric Solids with Orthotropic, Temperature-Dependent Material Properties.[7]

Table 3C.2-4

TABULATION OF INERTIA AND NODE POINT FORCES
ASHSD EXAMPLE 7

(1)	(2)	(3)	(4)	(5)
Node Point	Mass[(a)] ($lb/s^2/in.$)	R (in.)	Inertia Forces (lbs)	(4)/R Node Pt. Force (lb/in.)
1,12	2.8075×10^{-5}	0.0	0.	0.
2,13	1.1230×10^{-4}	1.0	2.527	2.527
3,14	2.2460×10^{-4}	2.0	10.107	5.535
4,15	3.3690×10^{-4}	3.0	22.741	7.580
5,16	4.4920×10^{-4}	4.0	40.428	10.107
6,17	5.6150×10^{-4}	5.0	63.169	12.634
7,18	6.7380×10^{-4}	6.0	90.963	15.161
8,19	7.8610×10^{-4}	7.0	123.811	17.687
9,20	8.9840×10^{-4}	8.0	161.612	20.214
10,21	1.0107×10^{-3}	9.0	204.667	22.741
11,22	5.3343×10^{-4}	10.0	120.022	12.002

[(a)] A factor 2 π as been dropped for the mass listed in column (2).

Table 3C.2-5

TABULATION OF RADIAL AND TANGENTIAL STRESSES
ASHSD EXAMPLE 7

Element Number	Radial Stress σ_r ($lb/in.^2$)		Tangential Stress σ_Θ ($lb/in.^2$)	
	ASHSD	Analytical[(a)]	ASHSD	Analytical[(a)]
1	199.80	199.74	199.80	200.00
2	196.00	195.74	198.00	198.10
3	187.20	187.73	194.00	194.28
4	175.40	175.71	188.20	188.56
5	159.50	159.70	180.50	180.93
6	139.50	139.67	171.00	171.39
7	115.50	115.64	159.50	159.94
8	87.48	87.61	146.20	146.59
9	55.46	55.57	131.00	131.33
10	19.42	19.52	113.40	114.16

[(a)] Theory of Elasticity.[(8)]

Table 3C.2-6

COMPARISON OF NATURAL FREQUENCIES (RAD/S)
FOR A SIMPLY SUPPORTED CYLINDRICAL SHELL
ASHSD EXAMPLE 8

Mode	ASHSD	Ref based on Hermann-Mirsky's Equation		
		More Exact Theory[(a)]	Approximate Theory[(b)]	Elementary Theory[(c)]
1	8,419	8,369	8,369	11,238
2	10,985	10,937	10,938	11,240
3	11,181	11,141	11,143	11,250
4	11,274	11,216	11,220	11,276
5	11,388	11,291	11,297	11,332
6	11,549	11,399	11,408	11,432
7	11,766	11,564	11,577	11,595
8	11,792	11,807	11,827	11,840

(a) More Exact Theory: Considering axial inertia, rotatory inertia, and shear deformation
(b) Approximate Theory: Considering axial inertia
(c) Elementary Theory: Disregarding axial inertia

3C.2.4 REFERENCES

1. Ghosh, S. and Wilson, E. L., "Dynamic Stress Analysis of Axisymmetric Structures Under Arbitrary Loading," College of Engineering, University of California at Berkeley, California, EERC 69-10, September 1969.

2. Ambartsumyan, S. A., "Theory of Anisotropic Shells," F-118, National Aeronautics and Space Administration, Washington, D.C., 1961.

3. Timoshenko, S. P. and Woinowsky, S., Theory of Plates and Shells, 2nd Edition, McGraw-Hill, New York, N.Y., 1959.

4. Wang, C. T., Applied Elasticity, McGraw-Hill, New York, N.Y., 1953.

5. Kraus, H., Thin Elastic Shells, John Wiley, New York, N.Y., 1967.

6. Budiansky, B. and Radkowski, P. P., "Numerical Analysis of Unsymmetric Bending of Shells," AIAA Journal, Vol 1, No. 8, August 1963.

7. Wilson, E. L., and Jones, R. M., "Finite-Element Stress Analysis of Axisymmetric Solids with Orthotropic, Temperature-Dependent Material Properties," Aerospace Corp., Report No. TR-0158 (S3816-22)-1, September 1967.

8. Timoshenko, S. P. and J. N. Goodier, Theory of Elasticity, Second Edition, McGraw-Hill, 1951.

9. Tang, Sing-Chih, "Response of a Finite Tube to Moving Pressure", Journal of the Engineering Mechanics Division, ASCE, June 1967.

3C.3 SYMBOLIC MATRIX INTERPRETIVE SYSTEM PROGRAM (SUPER SMIS)

3C.3.1 DESCRIPTION

SUPER SMIS is a general-purpose program that is used to solve practically any problem in which matrix analysis is applicable. A common application of the SUPER SMIS program is the solution of static and dynamic structural problems.

This program is an improved version of the original Symbolic Matrix Interpretive System (SMIS) program developed at the University of California at Berkeley in 1963.[1] The present program handles about 60 operations, including:

A. General matrix manipulations such as matrix addition, multiplication, and inversion

B. General element stiffness routines for plate or three-dimensional beam and truss elements and for a constant-strain, triangular-plate finite element

C. Element stiffness routine for the three-dimensional beam includes axial, torsional, bending, and shearing stiffness and computation of a consistent element mass matrix

D. Eigenvalue and eigenvector capability

E. Element stress routines for finding the forces for each of the element types

F. Acceptability of matrices generated by other programs as input to the SUPER SMIS program

G. Uncoupled (normal mode) time-history response analysis of dynamic systems

H. Coupled time-history response analysis of dynamic systems

I. Steady-state response analysis of uncoupled systems

The coupled time-history response analysis uses a Newmark-Beta direct-integration technique which allows the solution of coupled or uncoupled systems of equations.[2] This, for example, allows the analysis of systems using any arbitrary damping matrix. It also may be used in the analysis of systems having different excitations at different support points. The system may be treated as having either displacement boundary conditions or as a free-free system with base displacement time-history excitations.

3C.3.2 VALIDATION

Applicability and validity of the SUPER SMIS program are demonstrated in the six test problems outlined in paragraphs 3C.3.2.1 through 3C.3.2.6. In each test problem, the solutions are obtained using SUPER SMIS and some other analytical or computer program technique, then the results are compared. In each example, the comparison of results is in good agreement.

3C.3.2.1 SUPER SMIS Example 1, Lumped Mass-Response Spectrum and Time-History Analyses

This example demonstrates the accuracy of the Plane Frame Element, the Response Spectrum Analysis feature, and the Time-History Analysis feature of SUPER SMIS. The results obtained from SUPER SMIS are compared with those obtained from ICES-DYNAL.

A typical containment shell was modelled with eight lumped masses as shown in figure 3C.3-1. For the two-dimensional plane frame analysis, one degree of translation and one degree of rotation are assigned to each node. The input acceleration spectra and associated time dependent forcing function were taken from BC-TOP-4, Revision 1.[3] The zero period ground acceleration is 0.13g and the 2% damping curve is used.

The results obtained from SUPER SMIS and ICES-DYNAL are tabulated in tables 3C.3-1 and 3C.3-2. A plot of the absolute acceleration is shown in figure 3C.3-2.

3C.3.2.2 SUPER SMIS Example 2, Eigenvalue Analysis of Space Frame

This problem demonstrates the ability of SUPER SMIS in handling tridimensional elements using consistent mass. The natural frequencies are calculated using SUPER SMIS and ICES-DYNAL.

The eigenvalue analysis model used in the demonstration is illustrated in figure 3C.3-3. Each nodal point is assumed to have six degrees of freedom.

Table 3C.3-1

NATURAL FREQUENCIES (Hz), SUPER SMIS EXAMPLE 1

Mode	SUPER SMIS	ICES-DYNAL
1	10.509	10.520
2	30.506	30.538
3	43.131	43.177

Table 3C.3-2

DISPLACEMENT (RMS), SUPER SMIS EXAMPLE 1

Nodal Point	Translation		Rotation	
	SUPER SMIS	ICES-DYNAL	SUPER SMIS	ICES-DYNAL
1	0.000387	0.000395	0.000022	0.000021
2	0.000732	0.000730	0.000025	0.000025
3	0.001179	0.001176	0.000028	0.000028
4	0.001689	0.001684	0.000030	0.000030
5	0.002221	0.002215	0.000032	0.000032
6	0.002714	0.002706	0.000033	0.000033
7	0.003269	0.003260	0.000034	0.000034
8	0.003747	0.003737	0.000035	0.000035

The natural frequency results obtained from SUPER SMIS and ICES-DYNAL programs are summarized in table 3C.3-3.

3C.3.2.3 SUPER SMIS Example 3, Force Distribution in the Tri-Dimensional Space Truss

The purpose of this problem is to check the tri-dimensional truss element in SUPER SMIS. Results are compared with manual calculations for a statically determinant three-dimensional truss.

The basic geometry of the statically determinant three-dimensional truss is shown in figure 3C.3-4. Joint 2 was loaded as shown. The resulting member forces are summarized in table 3C.3-4.

3C.3.2.4 SUPER SMIS Example 4, Constant Strain Triangle Stiffness Matrix

The purpose of this example is to verify the stiffness matrix for the constant strain triangle finite element in SUPER SMIS. Results from SUPER SMIS are compared with hand calculations.

The basic geometry of the constant strain triangle is shown in figure 3C.3-5. The stiffness matrix for the conStant strain triangle given in Theory of Matrix Structural Analysis[4] was used for comparison.

Table 3C.3-3

COMPARISON OF NATURAL FREQUENCIES IN RAD/S AS COMPUTED BY SUPER SMIS AND ICES-DYNAL (SUPER SMIS EXAMPLE 2)

Mode	SMIS	ICES-DYNAL
1	11.142	11.141
2	21.904	21.897
3	33.809	33.810
4	40.026	40.001
5	48.298	48.273
6	95.982	96.009

Table 3C.3-4

COMPARISON OF MEMBER FORCES AS COMPUTED BY SUPER SMIS AND MANUAL CALCULATIONS (SUPER SMIS EXAMPLE 3)

Member No.	Axial Force by Manual Calcs (Comp is +)	Axial Force by SMIS (Comp is +)
1	776.23957	776.240
2	-1723.76043	-1723.76
3	-388.11978	-388.120
4	600.00000	600.000
5	-1500.00000	-1500.00
6	750.00000	750.000

Since the nodal ordering and degree-of-freedom ordering are different for the SUPER SMIS and Przemieniecki constant strain triangles, the Przemieniecki stiffness matrix was manipulated by hand to give the same ordering as used in SUPER SMIS. Parameters of the example problem were then used in the hand calculations to obtain the global stiffness matrix and were compared with the results of SUPER SMIS.

The stiffness matrices obtained by hand calculations and by SUPER SMIS are tabulated in table 3C.3-5.

3C.3.2.5 SUPER SMIS Example 5, Force Distribution in Two-Dimensional Planar Truss

The purpose of this example is to demonstrate the ability of SUPER SMIS to handle the two-dimensional truss element. Results are compared with a manual solution for the same problem.

The basic geometry of the statically determinant two-dimensional truss is shown in figure 3C.3-6. Two separate analyses are performed. The first analysis assumes a horizontal force applied at node 4 while the second assumes a vertical force applied at node 4. The resulting member forces for these two analyses are shown in tables 3C.3-6 and 3C.3-7 along with the corresponding values derived from manual calculations.

3C.3.2.6 SUPER SMIS Example 6, Multistory Building Time History Analysis

This example illustrates the accuracy of the Time-History analysis features of the SUPER SMIS program. The building being analyzed and results of response for use in comparison are taken from Introduction to Structural Dynamics.

The two-story steel frame structure used for this analysis is shown in figure 3C.3-7. The weights of the roof, first floor, and walls are also included along with the moments of inertia of the structural members, the equivalent lumped masses, the elastic stiffness coefficients, and the condition of dynamic equilibrium. A sinusoidal forcing function with a frequency of 4π radians/s is used. The initial displacements are both assumed to be zero while initial velocities are assumed to be -6.2832 in./s. A comparison of the results obtained from the SMIS program and the results from Introduction to Structural Dynamics[5] are shown in table 3C.3-8 and figures 3C.3-8 and 3C.3-9.

3C.3.3 EXTENT OF APPLICATION

The SUPER SMIS program is used in the dynamic analysis of lumped-parameter and consistent mass models of Seismic Category I structures.

Table 3C.3-5

COMPARISON OF STIFFNESS MATRICES OBTAINED BY SUPER SMIS AND MANUAL CALCULATIONS (SUPER SMIS EXAMPLE 4)

Stiffness Matrix Obtained by Manual Calculations[3]						
$[K] = 10^6 *$	0.474218	-0.595943	0.121724	0.098901	0.148351	-0.247253
	-0.595943	1.470837	-0.874894	0.197802	-0.741758	0.543956
	0.121724	-0.874894	0.753170	-0.296703	0.593407	-0.296703
	0.098901	0.197802	-0.296703	0.210482	0.013948	-0.224429
	0.148351	-0.741758	0.593407	0.013948	1.627430	-1.641377
	-0.247253	0.543956	-0.296703	-0.224429	-1.641377	1.865807

Stiffness Matrix Obtained by SUPER SMIS for the Constant Strain Triangle Finite Element:

$$[K] = 10^6 * \begin{vmatrix} 0.474218 & -0.595943 & 0.121724 & 0.098901 & 0.143352 & -0.247253 \\ -0.595943 & 1.470837 & -0.874894 & 0.197802 & -0.741758 & 0.543956 \\ 0.121724 & -0.874894 & 0.753170 & -0.296703 & 0.593407 & -0.296703 \\ 0.098901 & 0.197802 & -0.296703 & 0.210482 & 0.013948 & -0.224429 \\ 0.148352 & -0.741758 & 0.593407 & 0.013948 & 1.627430 & -1.641378 \\ -0.247253 & 0.543956 & -0.296703 & -0.224429 & -1.641378 & 1.865807 \end{vmatrix}$$

Table 3C.3-6

TABULATION OF MEMBER FORCES FOR TWO-DIMENSIONAL PLANAR TRUSS SUBJECTED TO A HORIZONTAL LOAD (SUPER SMIS EXAMPLE 5)

Member No.	Manual Calculations Axial Force (Comp is +)	SMIS Axial Force (Comp is +)
1	-7.50000	-7.50000
2	-2.50000	-2.50000
3	-3.90512	-3.90512
4	3.90512	3.90512
5	-3.90512	-3.90512
6	3.90512	3.90512
7	5.00000	5.00000

Table 3C.3-7

TABULATION OF MEMBER FORCES FOR TWO-DIMENSIONAL PLANAR TRUSS SUBJECTED TO A VERTICAL LOAD
(SUPER SMIS EXAMPLE 5)

Member No.	Hand Calculations Axial Force (Comp is +)	SMIS Axial Force (Comp is +)
1	-6.25000	-6.25000
2	-2.08333	-2.08333
3	9.76281	9.76281
4	3.25427	3.25427
5	-3.25427	-3.25427
6	3.25427	3.25427
7	4.16667	4.16667

Table 3C.3-8

COMPARISON OF NATURAL FREQUENCIES AS COMPUTED BY SUPER SMIS AND BIGGS
(SUPER SMIS EXAMPLE 6)

	Angular Frequency (rad/s)	
SMIS	9.1929	23.5206
BIGGS	9.0000	23.5000

3C.3.4 REFERENCES

1. Wilson, E. L., "Symbolic Matrix Interpretive System," University of California at Berkeley, California, April 1, 1963.

2. Chan, S. D., Cox, H. L., and Benfield, W. A., "Transient Analysis of Forced Vibrations of Complex Mechanical Systems," Journal of the Royal Aeronautical Society, London, England, 66, pp 457-960, 1962.

3. "Seismic Analysis of Structures and Equipment for Nuclear Power Plants," Bechtel Power Corporation, BC-TOP-4, Revision 1, September 1972.

4. Przemieniecki, J. S., Theory of Matrix Structural Analysis, McGraw-Hill, New York, N.Y., pp 83-86, 1968.

5. Biggs, J. M., Introduction to Structural Dynamics, McGraw-Hill, New York, N.Y., pp 249-253, 1964.

3C.4 SPECTRA COMPUTER PROGRAM (SPECTRA)

3C.4.1 DESCRIPTION

The SPECTRA program is an improved version of the original SPECTRA code developed by the California Institute of Technology.[1]

The program computes and plots spectral values of displacement, velocity, and acceleration from an accelerogram time-history digitized at equal time intervals. The computation is based on a closed-form recurrence algorithm for a ramp function. There is no practical limit on the number of periods and damping values for which this computation can be performed.

The computed spectra represent the maximum response of a series of variable frequency, single-degree-of-freedom oscillators subjected to a single support motion represented by the acceleration time history. The program solves the equations of motion for each oscillator, scans the time history of each response, and selects the corresponding maximum values.

3C.4.2 VALIDATION

Three test problems were used to demonstrate the applicability and validity of the SPECTRA program. In each test problem the solutions are obtained using SPECTRA and various analytical techniques, then the results are compared. In each example the comparison of results are in good agreement.

3C.4.2.1 Test Problem I - Symmetrical Triangular Pulse, Undamped System

This problem tested the program by assuming an undamped single degree of freedom oscillator (see figure 3C.4-1) whose support acceleration time history varies like an isosceles triangle. Figure 3C.4-2 gives a pictorial representation of the forcing function used. The pulse duration is 5 seconds and various oscillator natural frequencies were used. The basic[2] equation used to find the dynamic load factor (DLF) is given as follows.

$$DLF = -\omega \int_{o}^{t} f_a(\tau) \sin \omega (t-\tau) \, d\tau$$

where:

ω = natural circular frequency $(K/M)^{1/2}$

$f_a(t)$ = time function for support acceleration

t = time

τ = time variable

K = system stiffness

M = system mass

The data used for comparison was taken from Biggs, Introduction to Structural Dynamics.[2] The results of the SPECTRA response spectra are tabulated in table 3C.4-1 and are pictorially represented in figure 3C.4-3.

3C.4.2.2 Test Problem 2 - Symmetrical Sinusoidal Pulse, Undamped System

This problem tested the program by assuming an undamped single-degree-of-freedom oscillator (figure 3C.4-1) whose support acceleration time history was sinusoidal. The equation for finding the dynamic load factor is given in paragraph 3C.4.2.1 while the equation for the forcing function is given as follows:

$$f_a(t) = \sin\Omega t \qquad 0 \leq \Omega t \leq 2$$

Again the data used for comparison was taken from reference 2.

The results of the SPECTRA response spectra are tabulated in table 3C.4-2 and are pictorially represented in figure 3C.4-4.

3C.4.2.3 Test Problem 3 - Symmetrical Sinusoidal Pulse, Damped System

This problem tested the program by assuming a damped single-degree-of-freedom oscillator (see figure 3C.4-5) with damping of 1%, 2%, 3%, and 10% of critical. The sinusoidal support motion had the same frequency as the undamped oscillator in Test Problem 2. The basic equation used to find the dynamic load factor (DLF) is given as follow:[2]

$$DLF = -\omega_d \int_0^t f_a(\tau) e^{\beta_{(t-\tau)}} \sin \omega_d (t-\tau) \, d\tau$$

where:

ω_d = natural circular damped frequency

β = damping coefficient (C/2M)

$f_a(t)$ = time function for support acceleration

t = time

τ = time variable

Table 3C.4-1

UNDAMPED SYSTEM WITH SYMMETRIC TRIANGULAR PULSE LOAD

td/T	T	u_{max}	DLF[(a)]
0.2	25.	9.624	0.61
0.4	12.5	4.352	1.10
0.6	8.333	2.448	1.39
0.8	6.25	1.489	1.50
1.0	5.0	0.955	1.51
1.2	4.167	0.636	1.45
1.4	3.571	0.435	1.35
1.6	3.125	0.304	1.23
1.8	2.778	0.217	1.11
2.0	2.500	0.158	0.998
2.2	2.273	0.125	0.96
2.4	2.083	0.112	1.02
2.6	1.923	0.102	1.09
2.8	1.786	0.092	1.14
3.0	1.667	0.082	1.17
3.2	1.563	0.072	1.16
3.4	1.471	0.063	1.15
3.6	1.389	0.054	1.10
3.8	1.316	0.046	1.05
4.0	1.25	0.040	1.01

(a) $(DLF)_{max} = \left(\frac{2\pi}{T}\right)^2 u_{max}$

Table 3C.4-2

UNDAMPED SYSTEM WITH SYMMETRICAL SINUSOIDAL PULSE LOAD

Ω/ω	T	u_{max}	DLF[(a)]
0.25	0.25	0.002	1.26
0.50	0.50	0.011	1.74
0.75	0.75	0.056	3.93
1.00	1.00	1.591	62.81
1.25	1.25	0.156	4.28
1.50	1.50	0.118	2.07
1.75	1.75	0.128	1.65
2.00	2.00	0.088	0.87
2.25	2.25	0.102	0.79
2.50	2.50	0.103	0.65
2.75	2.75	0.121	0.63
3.00	3.00	0.148	0.65

(a) $(DLF)_{max} = \left(\frac{2\pi}{T}\right)^2 u_{max}$

At resonant response, where $\omega_d = \Omega$, the free vibration response disappears from the equation for the DLF. Furthermore, for small damping $\omega_d \approx w$ which further simplifies the equation for the DLF such that:

$$DLF_{max} = \omega/2\beta$$

The results of SPECTRA output and the calculated results for DLF are tabulated in table 3C.4-3. The results are very good for damping of 3%, 5%, and 10%; good for damping of 2% and poor for damping of 1%. The latter two cases are not disturbing in view of the fact that the forcing function lasts only three cycles. More cycles are needed for the solution to converge on the maximum response.

3C.4.3 EXTENT OF APPLICATION

The SPECTRA program is used for Seismic Category I structures to generate floor response spectra, computed from time-history motions at various floor or other locations.

Table 3C.4-3

DAMPED SYSTEM WITH SINUSOIDAL SUPPORT ACCELERATION[a]

B/ω	u_{max}	$(DLF)_{SPECTRA}$[b]	$(DLF)_{rigorous}$
0.01	0.906	35.8	50
0.02	0.582	23.0	25
0.03	0.412	16.3	16.67
0.05	0.253	9.99	10.0
0.10	0.127	5.01	5.0

[a] The support motion lasts about three cycles ($19.95/2\pi \approx 3$)

[b] $(DLF)_{SPECTRA} = \left(\frac{2\pi}{T}\right)^2 u_{max}$

3C.4.4 REFERENCES

1. Nigam, N. C. and Jennings, P. C., "Digital Calculation of Response Spectra from Strong-Motion Earthquake Records," Earthquake Engineering Research Laboratory, California Institute of Technology, Pasadena, California, June 1968.

2. Biggs, John M., Introduction to Structural Dynamics, McGraw-Hill, 1964.

3C.5 STRUCTURAL ANALYSIS PROGRAM (SAP)

3C.5.1 DESCRIPTION

The Structural Analysis Program (SAP) is a finite-element computer program that is used to perform linear, elastic analysis of three-dimensional structural systems. SAP is an improved version of SAP IV, a recognized computer code in the public domain, which was originally developed in 1969 by Dr. E. L. Wilson and his associates at the University of California at Berkeley.[1] Applications may be simple simulations involving one or two modeling elements, or they may be large and complex simulations. The program is capable of performing static analysis, modal extractions, and dynamic steady-state, time-history, or spectral-response analysis on structures composed of any combination of the following modeling elements:

- Boundary
- Truss

- Beam
- Curved beam
- Plane strain
- Membrane (plane stress)
- Simple plate
- Shell
- Thick shell
- Brick
- Axisymmetric ring

Static loads which may be considered include nodal forces, distributed pressures, differential temperatures, and boundary movements. The static solution is obtained using the Gaussian elimination technique with modifications to take advantage of matrix sparsity. Modal extraction may be carried out on a condensed system using the Ritz reduction and Jacobi, the Householder-QR algorithm, or on the full system using Subspace Iteration or Determinant Search methods. Dynamic analysis capabilities include seismic response spectrum or time-history, time-history nodal forces, and steady-state frequency response. Time-history dynamic analysis may be performed by modal superposition or direct integration. Multiple static or dynamic load cases for a given structural model may be analyzed in a single computer run.

3C.5.2 VALIDATION

Applicability and validity of the SAP program are demonstrated in the 35 test problems outlined in paragraphs 3C.5.2.1 through 3C.5.2.35. In each of the test problems, solutions are obtained by using the SAP program and some other analytical or computer program technique; then the results are compared. As will be noted, in all cases the solutions compare favorably and are essentially identical. The various analytical or computer program techniques used in the comparisons are extensively referenced within the test problems; they are collectively listed in the references for this appendix.

The following is a brief description of each independent computer program which was used for the comparison runs.

EASE was developed by Engineering Analysis Corporation and is marketed through Control Data Corporation. EASE has a library of finite elements available for use in performing static analysis of linear elastic structures.

NASTRAN was developed for the National Aeronautics and Space Administration. NASTRAN is a large scale finite-element program with capabilities for static analysis, dynamic analysis, piece-wise linear analysis, heat transfer analysis, etc. NASTRAN is available through a variety of computer service bureaus and a version supplied by Univac is available on Bechtel's Univac computer.

DYNAL was developed by McDonnell Douglas Automation Company. DYNAL has a library of finite elements available for use in performing dynamic analysis.

STARDYNE was developed by Mechanics Research, Inc., and is marketed by Control Data corporation. STARDYNE is a series of compatible digital computer programs with a library of finite elements available for performing both static and dynamic analysis.

STRUDL was originally developed at MIT as part of the integrated Civil Engineering System. A Univac supplied version of STRUDL is available on Bechtel's Univac computer. STRUDL has an extensive library of finite elements available for both static and dynamic analysis.

STRUDL-DYNAL was developed by McDonnell Douglas Automation Company. STRUDL-DYNAL was developed by a merger of McAuto's STRUDL and DYNAL programs into one program capable of both static and dynamic analysis. STRUDL-DYNAL has an extensive library of finite elements.

Table 3C.5-1 provides a subject index of the various features of the SAP program with a cross-reference to the program verification example number in which that feature is tested.

Table 3C.5-1
SAP PROGRAM VERIFICATION (Sheet 1 of 4)

Subject	SAP Example
Node Data	1 to 35
Cartesian coordinates	1 to 35
Cylindrical coordinates	10,11,13
New origin	
Multi-point constraints	
Kinematic Reduction	16,17,20,21,22,23,26,35
Boundary Element	1,8,12
Direction vectors	1,8
Translation loading	1,8,12
Rotational loading	
Scale loading	
Method 1 of orientation	1,8,12
Method 2 of orientation	1,8,12
Method 3 of orientation	1,8
Translation stiffness	1,8,12
Rotational stiffness	1,8
Truss Element	1,8
Acceleration loading	1,8
Temperature differential loading	1,8
Scale load	1,8
Beam Element	1,2,8,15,16,17,18,19,20 to 35
Shear areas	1,8,17,18,20,21,22,23,27,35
Fixed-end forces	1,8
Span loads	1,8
Acceleration load	1,8
Temperature differential load	1,8
Surface temperature differential load	1,8
Scale load	1,8
Member releases	1,8
k reference node	1,8,16,19,24,25,26
Angle of inclination method	17,18,20,22,23,27,35
Curved Beam Element	15
Member releases	
Segments	

Table 3C.5-1
SAP PROGRAM VERIFICATION (Sheet 2 of 4)

Subject	SAP Example
Membrane Element (Plane Stress)	3
Beta angle	
Temperature dependent properties	
Acceleration loading	3
Temperature differential loading	3
Pressure loading	3
Scale load	3
Simple Plate Element	2,4
Stress reference plane	2,4
Acceleration load	4
Temperature differential loading	4
Pressure load	4
Scale load	4
Membrane properties	2
Plate properties	
Shell properties	4
Shell Element	7,9,10
Isotropic properties	7,9,10
Orthotropic properties	
Stress reference plane	9
Acceleration load	9
Temperature differential loading	9
Surface temperature differential load	7,9
Pressure load	9,10
Scale load	
Thick shell	13
Acceleration load	13
Temperature differential load	13
Surface pressure load	13
Hydrostatic load	13
Scale load	

Table 3C.5-1
SAP PROGRAM VERIFICATION (Sheet 3 of 4)

Subject	SAP Example
Brick Element	11,12
Acceleration load	11
Temperature differential load	11
Surface pressure load	11,12
Hydrostatic load	11
Scale load	
Plane Strain Element	6
Temperature dependent materials	
Beta angle	
Acceleration load	6
Temperature differential load	6
Pressure load	
Scale load	
Ring Element	5,14
Beta angle	
Temperature dependent materials	
Acceleration load	5
Temperature differential load	5
Pressure load	14
Scale load	
Nodal or Joint Loads	1,2,4,5,6,8,9,11,12,13,14,15
Masses	
Translational	26,35
Rotational	35
Singularities Check	
Lumping Process Cards	
Modal Extraction	16 to 23,26,27,35
Ritz reduction + Jacobi	16
Kinematic reduction + HQR	16,17,20,21,22,23,26,35
Determinant search	16,18,19
Subspace iteration	27
Composite Modal Damping	

Table 3C.5-1
SAP PROGRAM VERIFICATION (Sheet 4 of 4)

Subject	SAP Example
Response Spectrum	19
Time History	20,21,22,23,24,25,35
Seismic or ground motions by closed form	21,35
Seismic or ground motions by numerical integration	20
Forcing function by closed form	22
Forcing function by numerical integration	23
Arrival times	
Method 1 of function input	22,23,24
Method 2 of function input	20,21,25
Initial modal conditions	
Rotational ground motion	35
Checkpoint Restart	28 to 34
No.2	28
No.3	29
No.4	30
No.5	31
No.8	32
No.9	33
No. 10	34
General Element	
Loading Combinations	1,8
Beam Selective Output	1,8
Method 3 of Time-History Function Input	
Steady-State Response	26
Direct Integration	24,25
Forcing function	24
Seismic or ground motion	25
Arrival times	

3C.5.2.1 SAP Example 1 (Figure 3C.5-1)

A plane frame subjected to various static loads. Results compared to within a few percent of results from the Univac STRUDL program.

3C.5.2.2 SAP Example 2 (Figure 3C.5-2)

A space frame, composed of beam and membrane elements, subjected to static loads. Results agreed to within a few percent of results from the EASE program.

3C.5.2.3 SAP Example 3 (Figure 3C.5-3)

A flat plate, composed of plane stress elements, subjected to various in- plane static loads. Results agreed to within 5% for all significant values for both displacements and stresses when compared with the results from the NASTRAN program.

3C.5.2.4 SAP Example 4 (Figure 3C.5-4)

A flat plate, composed of plate elements, subjected to various static loads. Results agreed to within a few percent of the result from the NASTRAN program and results for pressure load also agreed with results from the journal of the engineering mechanics division of the American Society of Civil Engineers.[(2)]

3C.5.2.5 SAP Example 5 (Figure 3C.5-5)

A cylindrical section, composed of axisymmetric ring elements, subjected to various static loads. The results compared to within 5% of the results from the NASTRAN program, at points away from the fixed boundary at the base.

3C.5.2.6 SAP Example 6 (Figure 3C.5-6)

A cross-section of a dam or retaining wall, composed of plane strain elements, subjected to various static loads. The results agreed to within 5% of the results from the STRUDL program.

3C.5.2.7 SAP Example 7 (Figure 3C.5-7)

A flat plate, composed of shell elements, subjected to a temperature gradient loading. Results agreed exactly with results determined by a hand calculation.

3C.5.2.8 SAP Example 8 (Figure 3C.5-1)

A plane frame (same as one in SAP Example 1) subjected to various static loads. Results compared to within a few percent of results from the STRUDL program.

3C.5.2.9 SAP Example 9 (Figure 3C.5-8)

A flat plate, composed of shell elements, subjected to various static loads. Results compared to within 5% of results from the NASTRAN program, except for a larger deviation near the supports or boundaries. Temperature gradient loading was checked separately in SAP Example 7.

3C.5.2.10 SAP Example 10 (Figure 3C.5-9)

A hyperbolic cooling tower, composed of shell elements, subjected to static loads. Results showed excellent agreement when compared with results from selected references[(3)(4)]

3C.5.2.11 SAP Example 11 (Figure 3C.5-10)

A segment of a cylinder, composed of brick elements, subjected to various static loads. Results agreed to within a few percent of results from the STARDYNE program.

3C.5.2.12 SAP Example 12 (Figure 3C.5-11)

The area surrounding a circular penetration in a cylinder was modeled using brick elements and subjected to static loads. Results agreed to within a few percent of results from selected references. Some deviation of results for bending moments was noted, but this was probably due to the use of only one element across the thickness.

3C.5.2.13 SAP Example 13 (Figure 3C.5-12)

The same problem run in SAP Example 11 was rerun using thick shell elements. Results agreed to within 10% of the results from the SAP brick element run or the STARDYNE run, except for the stress results for the pressure loading where some deviation occurred in the vicinity of the loads. This deviation was probably due to the modeling difference.

3C.5.2.14 SAP Example 14 (Figure 3C.5-13)

A segment of a cylinder, composed of axisymmetric ring elements, subjected to a static pressure load. Results agreed exactly with results from hand calculations.

3C.5.2.15 SAP Example 15 (Figure 3C.5-14)

A frame, composed of beam and curved beam elements, subjected to various static loads. Results agreed to within a few percent of results from the STARDYNE program.

3C.5.2.16 SAP Example 16 (Figure 3C.5-15)

A multistory plane frame, composed of beam elements, for which a modal analysis was performed by three methods.

- Ritz Reduction and Jacobi
- Kinematic Reduction and HQR
- Determinant Search

Results agreed to within a few percent of results from the DYNAL program.

3C.5.2.17 SAP Example 17 (Figure 3C.5-16)

A one-story space frame, composed of beam elements, for which a modal analysis by kinematic reduction and HQR was performed. The results agreed to within a few percent of results from the DYNAL program.

3C.5.2.18 SAP Example 18 (Figure 3C.5-16)

A one-story space frame, composed of beam elements, for which a modal analysis by determinant search was performed. Results agreed to within a few percent of results from the DYNAL program.

3C.5.2.19 SAP Example 19 (Figure 3C.5-15)

A multistory plane frame, composed of beam elements, for which a modal analysis by determinant search was performed and a dynamic response by the response spectrum analysis was made. Results agreed to within a few percent of results from the DYNAL program.

3C.5.2.20 SAP Example 20 (Figure 3C.5-16)

A one-story space frame, composed of beam elements, for which a modal analysis by kinematic reduction and HQR was performed and a dynamic response for time-history analysis for ground motion by numerical integration was made. Results generally agreed to within a few percent (with some variation up to 10%) of results from the DYNAL program.

3C.5.2.21 SAP Example 21 (Figure 3C.5-16)

A one-story space frame, composed of beam elements, for which a modal analysis by kinematic reduction and HQR was performed and a dynamic response for time-history analysis for ground motion by closed form solution was made. Results agreed to within a few percent of results from the DYNAL program.

3C.5.2.22 SAP Example 22 (Figure 3C.5-16)

A one-story space frame, composed of beam elements, for which a modal analysis by kinematic reduction and HQR was performed, and a dynamic response for time-history analysis for forcing functions by closed form solution was made. Results agreed to within a few percent of results from the DYNAL program.

3C.5.2.23 SAP Example 23 (Figure 3C.5-16)

A one-story space frame, composed of beam elements, for which a modal analysis by kinematic reduction and HQR was performed, and a dynamic response for time-history analysis for forcing functions by numerical integration was made. Results agreed to within a few percent of results from the DYNAL program.

3C.5.2.24 SAP Example 24 (Figure 3C.5-15)

A multistory plane frame, composed of beam elements, for which a dynamic response for a time-history analysis for forcing functions by direct integration was made. Results agreed to within a few percent of result from the DYNAL program.

3C.5.2.25 SAP Example 25 (Figure 3C.5-15)

A multistory plane frame, composed of beam elements, for which a dynamic response for a time-history analysis for ground motion by direct integration was made. Results agreed to within a few percent of results from the DYNAL program.

3C.5.2.26 SAP Example 26 (Figure 3C .5-17)

A multistory space frame, composed of beam elements, for which a dynamic analysis for a steady-state response for harmonic loads was made. Results agreed to within a few percent of results from the STARDYNE and NASTRAN programs.

3C.5.2.27 SAP Example 27 (Figure 3C.5-16)

A one-story space frame, composed of beam elements, for which a modal analysis by subspace iteration was performed. Results agreed to within a few percent of results from the DYNAL program.

3C.5.2.28 SAP Example 28 (Figure 3C.5-1)

The same problem run in SAP Example 1 was run to check the checkpoint/restart No. 2 feature. Results agreed exactly with results in SAP
Example 1.

3C.5.2.29 SAP Example 29 (Figure 3C.5-1)

The same problem run in SAP Example 1 was run to check the checkpoint/restart No. 3 feature. Results agreed exactly with results in SAP
Example 1.

3C.5.2.30 SAP Example 30 (Figure 3C.5-1)

The same problem run in SAP Example 1 was run to check the checkpoint/restart No. 4 feature. Results agreed exactly with the results in SAP Example 1.

3C.5.2.31 SAP Example 31 (Figure 3C.5-16)

The same problem run in SAP Example 27 was run to check the checkpoint/restart No. 5 feature. Results agreed exactly with the results in SAP Example 27.

3C.5.2.32 SAP Example 32 (Figure 3C.5-16)

The same problem run in SAP Example 27 was run to check the checkpoint/restart No. 8 feature. The results agreed exactly with the results in SAP Example 27.

3C.5.2.33 SAP Example 33 (Figure 3C.5-1)

The same problem run in SAP Example 1 was run to check the checkpoint/restart No. 9 feature. The results agreed exactly with the results in SAP Example 1.

3C.5.2.34 SAP Example 34 (Figure 3C.5-15)

The same problem run in SAP Example 19 was run to check the checkpoint/ restart No. 10 feature. The results agreed exactly with the results in SAP Example 19.

3C.5.2.35 SAP Example 35 (Figure 3C.5-18)

A multistory plane frame, composed of beam elements, for which a modal analysis by kinematic reduction and HQR was performed and a dynamic response for time-history analysis for ground motion (including rotational ground motion) by closed form solution was made. Results for the time-history response agreed to within a few percent of results from the DYNAL program and results from the SRSS of the modal responses agreed to within 2% for displacements and 10% for forces.

3C.5.3 EXTENT OF APPLICATION

The SAP program is used to perform static stress and dynamic spectral response and time-history analyses of Seismic Category I structures and substructures; e.g., static stress analysis of the containment equipment hatch.

3C.5.4 REFERENCES

1. Wilson, E. L., "SAP - A General Structural Analysis Program," University of California at Berkeley, California, September 1970.

2. Hermann, L. R., "Finite-Element Bending Analysis for Plates," Journal of The Engineering Mechanics Division of The American Society of Civil Engineers, Vol 93, No. EM5, October 1967.

3. "Pressure Vessel and Piping 1972 Computer Programs Verification," The American Society of Mechanical Engineers, pp 22-1 through 22-4, 1972.

4. Chan, A. S. L and Firmin, A., "The Analysis of Cooling Towers by the Matrix Finite-Element Methods," The Aeronautical Journal of the Royal Aeronautical Society, October 1970.

3C.6 STRUCTURAL DESIGN LANGUAGE PROGRAM (ICES/STRUDL-II)

3C.6.1 DESCRIPTION

The ICES/STRUDL-II program is a subsystem of the Integrated Civil Engineering System (ICES), which is a series of problem-oriented computer programs written at Massachusetts Institute of Technology.

The ICES/STRUDL-II program is a finite-element computer program that is used to perform linear, elastic analysis of three-dimensional structural systems. Applications may be simple simulations involving one or two modeling elements, or they may be large and complex simulations. The program is capable of performing static analysis, modal extractions, and dynamic steady-state, time-history, or spectral-response analyses on structures composed of any combination of the following modeling elements:

- Boundary
- Truss
- Beam
- Plane strain
- Plane stress (membrane)
- Plate bending (triangular and quadrangular)
- Bending (triangular)
- Shallow shell (triangular and rectangular)
- Tri-dimensional (brick)

3C.6.2 VALIDATION

The ICES/STRUDL-II computer program is a recognized computer code in the public domain and has had sufficient use to justify its applicability and validity.

3C.6.3 EXTENT OF APPLICATION

The ICES/STRUDL-II program is one of several computer programs used to perform static stress analysis of Seismic Category I structures and substructures other than the containment structure.

3C.7 COUPLED STIFFNESS MATRIX PROGRAM (COPK)

3C.7.1 DESCRIPTION

The computer code COPK was developed at Bechtel Power Corporation. It computes the equivalent system stiffness matrix of a shear-wall type of building. The lumped parameter model representation consists of a three-dimensional system of nodal points linked to one another through multiple connectivities effected by the shear walls. The nodal points are arbitrarily located at the center of mass of the masses tributary to each floor level, and motion is defined with respect to these points. For buildings exhibiting eccentricity between centers of mass and centers of resistance, this formulation results in a simple diagonal mass matrix and a geometrically coupled stiffness matrix that accounts for all eccentricities. The stiffness matrix is developed by evaluating the local stiffness matrices of the wall resisting elements and by summing and transforming those stiffnesses with reference to the global coordinates originating at each node.

COPK computes the stiffness matrix within the limitations imposed by a lumped parameter model formulation.

3C.7.2 VALIDATION

Applicability and validity of the COPK program are demonstrated in the four test problems outlined below in paragraphs 3C.7.2.1 through 3C.7.2.4. In each of the test problems, solutions are obtained using the COPK program and either manual calculations or other computer programs and then the results are compared. Comparison of the results show good agreement and therefore substantiate the validity of the computer program with one exception. In test example 4 (table 3C.7-4) the vertical response of reference node 2 is not in close agreement. Examination of this response shows that this response is of a secondary nature; i.e., approximately 2% of the principal response, and therefore this discrepancy is not considered significant.

3C.7.2.1 COPK Example 1, Arithmetic Check of Basic Stiffness Matrix

This problem demonstrates the accuracy of the basic formulation of the stiffness matrix of the COPK Program for axial, shear, flexural, and torsional stiffness characteristics. Figure 3C.7-1 presents the stiffness formulation as developed by the COPK program, while figure 3C.7-2 presents the results of the manual calculation for the same problem.

3C.7.2.2 COPK Example 2, Arithmetic Check of Stiffness Matrix Using Arbitrary Coordinate Location

This problem demonstrates the independence of the stiffness matrix formulation from the selection of the location of the Global Coordinate system.

The same structural assemblage as used in example 1 was used in this analysis. Figure 3C.7-3 represents the results of this analysis and can be readily compared to the results of the manual calculations shown in figure 3C.7-2.

3C.7.2.3 COPK Example 3, Transformation of Stiffness Matrix to Arbitrary Reference Nodal Points

This problem demonstrates the accuracy of the stiffness transformation characteristics of the COPK program. Figure 3C.7-4 represents the results of both the manual calculations and the COPK solution for a different structural assemblage than used in the previous two examples.

3C.7.2.4 COPK Example 4, Deflection Check of a Structural Assemblage

This problem demonstrates the accuracy of system deflections obtained from the COPK generated stiffness matrix loaded into the SUPER SMIS program (section 3C.3). Figures 3C.7-5 and 3C.7-6 and table 3C.7-1 represent the structural assemblage used for the condition of geometrically symmetric cross-sections, while figures 3C.7-7 and 3C.7-8 and table 3C.7-3 represent the structural assemblage used for the condition of geometrically nonsymmetric cross-section. Tables 3C.7-2 and 3C.7-4 present the results obtained using the COPK generated stiffness matrix and those obtained from the SAP program.

3C.7.3 EXTENT OF APPLICATION

The COPK program is used to calculate the geometrically coupled stiffness matrix of the Category I structures other than the containment, which is used as input for the SUPER SMIS (section 3C.3) in performing the subsequent dynamic analysis of the structure.

Table 3C.7-1
SECTIONAL PROPERTIES (COPK)

Connecting	Elem. No.	Av_x (ft^2)	Av_y (ft^2)	A_z (ft^2)	I_x (ft^4)	I_y (ft^4)	I_z (ft^4)	Lower Node				Upper Node			
								No.	x	y	z	No.	x	y	z
RN 1	1	102.8	102.8	231.	0.57088×10^5	0.57088×10^5	0.8500×10^5	4	45.	-34.35	0	5	45.	-34.25	30
	2	58.3	58.3	70.	5.833	0.28583×10^5	0.1	6	40.	36.	0	7	40.	36.	30
To	3	274.2	279.6	329.	0.49362×10^6	0.73774×10^6	0.1	8	-19.6	0	0	9	-19.6	0	30
	4	680.0	462.4	1,344.	0.46476×10^7	0.79986×10^7	0.88881×10^7	10	0	0	0	11	0	0	30
RN 2															
RN 2	5	58.3	58.3	70.	0.28583×10^5	5.833	0.1	12	0	70	30	13	0	70	60
	6	134.3	131.7	158.	0.0673×10^5	0.16437×10^6	0.1	14	-8	-36.	30	15	-8.	-36.	60
To	7	153.	43.3	226.	0.27963×10^5	0.21260×10^6	0.80752×10^5	16	-30.	34.	30	17	-30.	34.	60
	8	502.5	353.1	1,011.	0.35203×10^7	0.60487×10^7	0.67284×10^7	18	0	0	30	19	0	0	60
RN 3															

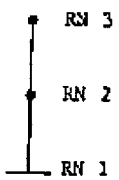

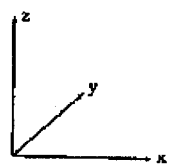

RN	x	y	z
1	20.	20.	0
2	60	30	30
3	-40.	-30.	60

Table 3C.7-2

HORIZONTAL (-Y) FORCE APPLIED AT RN 2:

	Deflection at RN 2		Deflection at RN 3	
	COPK	SAP (Beam)	COPK	SAP (Beam)
Δ_x	3233	3233	-3003	-3002
Δ_y	-25833	-25833	-15973	-15974
Δ_z	584	584	485	-485
Θ_x	17	17	17	17
Θ_y	0	0	0	0
Θ_z	-104	-104	104	104

VERTICAL (-Z) FORCE APPLIED AT RN 3:

	Deflection at RN 2		Deflection at RN 3	
	COPK	SAP (Beam)	COPK	SAP (Beam)
Δ_x	-445	-445	-1847	-1847
Δ_y	485	-485	2224	-2224
Δ_z	-463	-463	-12637	-12638
Θ_x	32	32	84	84
Θ_y	-30	-30	-64	-64
Θ_z	0	0	0	0

Table 3C.7-3
SECTIONAL PROPERTIES

Connecting	Elem. No.	Av_x (ft^2)	Av_y (ft^2)	A_z (ft^2)	I_x (ft^4)	I_y (ft^4)	I_z (ft^4)	Lower Node				Upper Node			
								No.	x	y	z	No.	x	y	z
RN 1	1	510.	238	880	3.397×10^6	4.800×10^6	5.346×10^6	4	0	0	0	5	0	0	30
	2	255	57.8	360	3.206×10^4	4.000×10^5	1.000×10^5	6	-30	40	0	7	-30	40	30
TO	3	100	60.0	180	5.602×10^4	3.201×10^4	-	8	-60	-10	0	9	-60	-10	30
	4	76.5	50.0	150	8.017×10^3	5.941×10^4	-	10	20	-30	0	11	20	-30	30
RN 2															
RN 2	5	510	238	880	3.175×10^6	4.577×10^6	5.737×10^6	12	50	-533	30	13	50	-533	60
	6	125	-	150	28.12	1.250×10^5	-	14	-30	30	30	15	-30	30	60
TO	7	-	50.	60	8000.	11.25	-	16	-60	-10	30	17	-60	-10	60
	8	76.5	50.	150	8017.	5.941×10^4	-	18	20	-30	30	19	20	-30	60
RN 3															

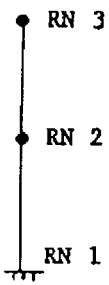

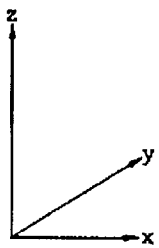

RN	x	y	z
1	20	20	0
2	60	30	30
3	-40	-30	60

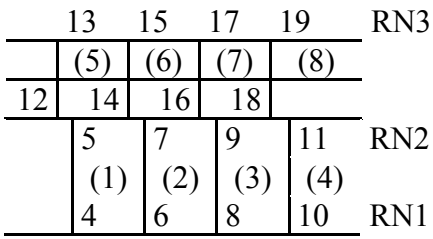

Table 3C.7-4

HORIZONTAL (-Y) FORCE APPLIED AT RN 2:

	Deflection at RN 2		Deflection at RN 3	
	COPK	SAP (Beam)	COPK	SAP (Beam)
Δ_x	4144	4187	-6999	-7073
Δ_y	-54782	-54393	-36978	-36428
Δ_z	628	650	-855	-833
Θ_x	23	23	22	23
Θ_y	-2	-1	-2	-1
Θ_z	-185	-186	-185	-186

VERTICAL (-Z) FORCE APPLIED AT RN 3:

	Deflection at RN 2		Deflection at RN 3	
	COPK	SAP (Beam)	COPK	SAP (Beam)
Δ_x	-549	-480	-2545	-2555
Δ_y	-855	-833	-3147	-2589
Δ_z	-91	-341	-15923	-17216
Θ_x	57	56	96	62
Θ_y	-36	-32	-96	-106
Θ_z	0	0	0	0

3C.7.4 REFERENCES

1. Roark, R. J., Formulas for Stress and Strain, Fourth Edition, McGraw Book Company, 1965.

3C.8 REINFORCING STEEL DESIGN FOR CONCRETE STRUCTURES PROGRAM (RESCOS)

3C.8.1 DESCRIPTION

The computer code RESCOS was developed by Bechtel Power Corporation. It is a "direct-design" computer program, which can be used in the design of reinforcing steel required in reinforced concrete structures. Reinforcement for members under flexural and axial load is proportioned in accordance with the American Concrete Institute (ACI) Standard 318-71[(1)] for strength design provisions and ACI Standard 318-63[(2)] for working stress provisions. Shear reinforcement for reinforced and prestressed concrete members subjected to transverse shear, is determined in accordance with the provisions of the ACI Standard 318-71.

3C.8.2 VALIDATION

Demonstration of the applicability and validity of the RESCOS program is achieved through the comparison of the results obtained using the program with manually calculated solutions based on the provisions of ACI Standards 318-63 and 318-71. Fifteen test problems were used in this demonstration, the results of which show that the RESCOS solutions are substantially identical to the results obtained by manual calculation procedures. The features verified by the 15 test cases are the following:

A. Tensile axial load at centerline for SD (strength design)

B. Compressive axial load at centerline for SD

C. Pure flexural force for SD without As' (compressional steel)

D. Pure flexural force for SD with As'

E. Flexural plus tensile axial force for SD without As'

F. Flexural plus tensile axial force for SD with As'

G. Flexural plus compressive axial force for SD without As'

H. Flexural plus compressive axial force for SD with As'

I. Tensile axial load at centerline for WSD (working stress design)

J. Compressive axial load at centerline for WSD

K. Pure flexural force for WSD

L. Flexural plus tensile axial force for WSD

M. Flexural plus compressive axial force for WSD

N. Shear reinforcement design

O. Shear reinforcement design for prestressed numbers

Table 3C.8-1 gives a summary of the physical parameters used in the program verification as well as a tabulation of the results obtained by the RESCOS program and the manual calculations.

3C.8.3 EXTENT OF APPLICATION

The RESCOS program is used in the reinforced concrete design of Seismic Category I structures.

3C.8.4 REFERENCES

1. "Building Code Requirements for Reinforced Concrete," ACI Standard 318-71, American Concrete Institute, Detroit, Michigan, 1971.

2. "Building Code Requirements for Reinforced Concrete," ACI Standard 318-63, American Concrete Institute, Detroit, Michigan, 1963.

Table 3C.8-1
COMPARISON OF RESULTS FOR RESCOS
PROGRAM VERIFICATION (Sheet 1 of 2)

Problem	Physical Parameters						Miscellaneous	Loads		Assumptions	Results[a]	
	d(in.)	d'(in.)	b(in.)	t(in.)	f'c(k/in.^{2})	f_y(k/in.^{2})		P(kips)	M(ft-kip)		Manual Calculation	RESCOS
1						60		500		As = A_s'	4.63 in.^{2}	4.63 in.^{2}
2					4	60		-500			0	0
3	24	2	12	26	4	40			366		5.76 in.^{2}	5.76 in.^{2}
4	14	2.5	12		5	60			252		4.86 in.^{2}	4.86 in.^{2}
										A_s'	0.72 in.^{2}	0.74 in.^{2}
5	17.5	2.5	10		4	60		30	100		1.644 in.^{2}	1.65 in.^{2}
6	24	2	12	26	3	40		25	500		9.10 in.^{2}	9.10 in.^{2}
										A_s'	0.39 in.^{2}	0.39 in.^{2}
7	20		12	22	4	60		40	160		1.73 in.^{2}	1.73 in.^{2}
8	20	2	12	22	4	60		88	352		4.84 in.^{2}	4.84 in.^{2}
										A_s'	1.71 in.^{2}	1.81 in.^{2}
9	20	2	12	22	40	60		100		As = A_s'	2.08 in.^{2}	2.08 in.^{2}
							Fs=24 k/in.^{2}					
							Fc=1.8 k/in.^{2}					
							n=8					
10	20		12	22	3	40	fs=20 k/in.^{2}	-400		As = A_s'	1.97 in.^{2}	1.97 in.^{2}
							fc=1.35 k/in.^{2}					
							n=9.2					
11	26	2	13.5	28	3	60	fs=24 k/in.^{2}		210		4.56 in.^{2}	4.56 in.^{2}
							fc=1.35 k/in.^{2}			A_s'	1.51 in.^{2}	1.51 in.^{2}
							n=9.2					

[a] All results are A_s unless noted otherwise.

Table 3C.8-1
COMPARISON OF RESULTS FOR RESCOS
PROGRAM VERIFICATION (Sheet 2 of 2)

Problem	Physical Parameters						Miscellaneous	Loads		Assumptions	Results[a]	
	d(in.)	d'(in.)	b(in.)	t(in.)	f'c(k/in.^{2})	f_y(k/in.^{2})		P(kips)	M(ft-kip)		Manual Calculation	RESCOS
12	16	2	10.5	18	3	40	e'=7"	N=17.8 (Tension)	76		3.72 in.^{2}	3.71 in.^{2}
							Fs= 20 k/in.^{2}			A_s'	0.82 in.^{2}	0.82 in.^{2}
							Fc=1.35 k/in.^{2}					
							n=9.2					
13	21	2	11.5	23			e'=9.5 in.	N=26.7 (comp)	98		2.57 in.^{2}	2.57 in.^{2}
							fs- 20 k/in.^{2}					
							n=9.2					
14	24	3	13	28	3	40		Vu-87.3	251	Av at spacing	No. 3 at 4.02 in.	No. 3 at 4.02 in.
										Av at spacing	-	No. 4 at 7.31 in.
										Av at spacing	-	No. 5 at 11.33 in.
15	17	5	12	22	4	60	e'=5 in.	Vu=110	460	Av at spacing	No. 3 at 4.03 in.	No. 3 at 4.03 in.
							fpe=0.55 k/in.^{2}	Vp=20				
							fd=0.15 k/in.^{2}	Vd=50.5				
							fpc=0.08 k/in.^{2}	Vi=103.5				

3C.9 OPTIMUM CONCRETE DESIGN PROGRAM (OPTCON)

3C.9.1 DESCRIPTION

OPTCON is a recently developed computer code (by Bechtel Power Corporation) for reinforced concrete design of nuclear containments. In this code, different stress and strain limitations are incorporated in accordance with reference 1. Furthermore, thermal gradients are considered in a manner similar to that given in reference 2 and included in design. Finally, optimum design is obtained using an iterative process.

Reference 1 requires that nuclear containments be designed for both service load and factored load conditions. For this reason, both of these methods are included in the computer program. Furthermore, the ultimate strength design provisions of references 3 and 4 have been incorporated so that the program may be used in the design of conventional structures.

3C.9.2 VALIDATION

The solutions to individual load cases in the OPTCON program have been demonstrated to be substantially identical to the results obtained by the RESCOS program. Details of the validation test cases are provided in reference 5.

3C.9.3 EXTENT OF APPLICATION

OPTCON is used in the reinforced concrete design of Seismic Category I structures.

3C.9.4 REFERENCES

1. ASME Boiler and Pressure Vessel Code, Section III, Division 2, American Society of Mechanical Engineers, New York, N.Y., January 1, 1975.

2. Gurfinkel, G., Thermal Effects in Walls of Nuclear Containments - Elastic and Inelastic Behavior, Proceedings of the First International Conference on Structural Mechanics in Reactor Technology (SMIRT), Berlin, Germany, Vol 5 - Part J, September 1971.

3. "Building Code Requirements for Reinforced Concrete," ACI Standard 318-71, American Concrete Institute, Detroit, Michigan, 1971.

4. "Building Code Requirements for Reinforced Concrete," ACI Standard 318-63, American Concrete Institute, Detroit, Michigan, 1963.

5. Kohli, T. D. and Gurbuz, O., Optimum Design of Reinforced Concrete for Nuclear Containments, Including Thermal Effects, Proceedings of the ASCE Specialty Conference on Structural Design of Nuclear Plant Facilities, New Orleans, Louisiana, December 8-12, 1975.

3C.10 CE-639-2 COMPUTER PROGRAM

3C.10.1 DESCRIPTION

The CE-639-2 computer program was developed at Bechtel Power Corporation. It computes forces and pressures caused by post-tensioned tendons on a dome. The shape of the dome can be a hemisphere, sphere-torus, sphere-cone, cone, or spheroid. Tendons may lie in one, two, or three directions. This program takes account of the frictional losses due to curvature and wobble using the concept of equivalent friction coefficient. The change in the prestressing forces due to seating of the anchorages is also taken into account.

User specifies the parallels on which the prestressing load is to be computed. The program evenly distributes nodal points along each parallel. The output is given for these points, printing the normal, the hoop, and the meridional pressures. It also prints the horizontal and the vertical components of the meridional pressure.

3C.10.2 VALIDATION

Since neither experimental data nor general analytical techniques are available in open literature, a general, approximate method for establishing the equivalent force distributions of the post-tensioning system was developed to validate the acceptability of CE-639-2. This approximate theory was developed in conjunction with the list of references attached.[(1)(2)(3)] Results obtained using this procedure were compared with the results obtained using CE-639-2. Precise accuracy of CE-639-2 could not be determined owing to the approximate nature of the alternate method; however, the results do show good agreement and therefore substantiate the validity of the computer program.

3C.10.2.1 CE-639-2 Example Problem 1, Equivalent Force Distribution for a Hemispherical Dome

Figures 3C.10-1 and 3C.10-2 pictorially represent the data used in the program verification for a hemispherical dome configuration. Table 3C.10-1 tabulates the results of the two procedures. In general, the agreement between the values obtained by the two methods is good.

3C.10.2.2 CE-639-2 Example Problem 2, Equivalent Force Distribution for a Sphere-Torus Dome

Figures 3C.10-3 and 3C.10-4 pictorially represent the data used in the program verification for a sphere-torus dome configuration. Table 3C.10-2 tabulates the results of the two procedures. In general, the agreement between the values obtained by the two methods is good.

3C.10.3 EXTENT OF APPLICATION

The CE-639-2 program is used as input for the FINEL computer program section 3C.1.

Table 3C.10-1
TABULATION OF RESULTS FOR HEMISPHERICAL DOME (Sheet 1 of 2)

Point	Computation By	Normal Pressure (lb/in.^{2})	Hoop Pressure (lb/in.^{2})	Meridional Pressure (lb/in.^{2})	H-Force (lb/in.)	V-Force (lb/in.)
31	CE-639-2	-101.981	10.366[a]	51.351[a]	2751.76	-2444.20
	Alternate	-102.133	10.308	51.395	2754.55	-2444.61
35	CE-639-2	-106.170	0.565	50.655[a]	2714.92	-2409.85
	Alternate	-104.779	0.611[a]	49.904	2674.68	-2373.72
50	CE-639-2	-108.803	0.840[a]	53.753[a]	2452.30	-2559.26
	Alternate	-107.166	1.116	52.799	2409.48	-2510.93
57	CE-639-2	- 55.350	0.	8.932[a]	346.42	-424.36
	Alternate	- 55.350	0.	8.856	343.46	-420.73
73	CE-639-2	- 56.064	0.	9.084[a]	295.54	-427.88
	Alternate	- 56.064	0.	8.970	293.04	-424.22
107	CE-639-2	- 57.179	11.51	10.949[a]	296.50	-512.96
	Alternate	- 56.841	11.093[a]	10.788	292.20	-505.28
121	CE-639-2	-120.437	3.352	62.968[a]	1380.53	-2904.33
	Alternate	-113.650	2.925[a]	59.129	1297.34	-2726.29
142	CE-639-2	- 61.515	33.503	20.869[a]	348.54	-949.51
	Alternate	- 58.510	33.963[a]	19.728	329.78	-897.40

[a] C-E's 639-2 verification analysis uses different sign conventions for these intermediate results.

Table 3C.10-1
TABULATION OF RESULTS FOR HEMISPHERICAL DOME (Sheet 2 of 2)

Point	Computation By	Normal Pressure (lb/in.^{2})	Hoop Pressure (lb/in.^{2})	Meridional Pressure (lb/in.^{2})	H-Force (lb/in.)	V-Force (lb/in.)
157	CE-639-2	-56.324	0.	9.090[a]	-107.34	403.19
	Alternate	-56.324	0.	9.012	-106.42	399.74
200	CE-639-2	-61.036	36.940	7.337	-53.26	313.66
	Alternate	-56.533	37.396[a]	6.709[a]	-48.70	286.80
276	CE-639-2	-54.799	7.900[a]	8.871[a]	0.	318.72
	Alternate	-54.441	7.882	8.741	-16.41	313.69
342	CE-639-2	-54.518	0.084[a]	8.798[a]	-16.23	297.59
	Alternate	-54.028	0.	8.644	0.	293.30

Table 3C.10-2
TABULATION OF RESULTS FOR SPHERE-TORUS (Sheet 1 of 2)

Point	Computation By	Normal Pressure (lb/in.^{2})	Hoop Pressure (lb/in.^{2})	Meridional Pressure (lb/in.^{2})	H-Force (lb/in.)	V-Force (lb/in.)
7	CE-639-2	-98.630	8.181[(a)]	24.360	1,752.87	-592.80
	Alternate	-98.144	8.094	24.190	1,738.74	-585.99
8	CE-639-2	-99.357	5.142[(a)]	26.761	1,927.49	-652.95
	Alternate	-98.942	5.087	26.557	1,908.88	-643.34
10	CE-639-2	-99.734	1.722	27.819	2,004.19	-678.82
	Alternate	-99.222	1.686	27.554	1,980.58	-667.50
12	CE-639-2	-98.630	8.181	24.360	1,752.88	-592.80
	Alternate	-98.144	8.094	24.190	1,738.74	-585.99
21	CE-639-2	-101.294	9.709	44.806	2,840.98	-2,143.87
	Alternate	-100.289	9.580	44.426	2,817.27	-2,122.63
24	CE-639-2	-104.353	0.591	46.207	2,930.50	-2,209.18
	Alternate	-102.557	0.916	45.306	2,873.07	-2,164.67
52	CE-639-2	-107.194	2.335	56.755	2,589.17	-2,701.99
	Alternate	-103.379	2.429	54.706	2,496.51	-2,601.62
343	CE-639-2	-27.277	0	4.402	-15.55	-140.95
	Alternate	-27.277	0	4.364	-30.25	-137.30
352	CE-639-2	-28.413	11.125	4.432	-15.66	141.90
	Alternate	-27.139	11.025	4.207	-29.15	132.34

Table 3C.10-2
TABULATION OF RESULTS FOR SPHERE-TORUS (Sheet 2 of 2)

Point	Computation By	Normal Pressure (lb/in.^{2})	Hoop Pressure (lb/in.^{2})	Meridional Pressure (lb/in.^{2})	H-Force (lb/in.)	V-Force (lb/in.)
361	CE-639-2	-43.522	17.785	5.283	-18.67	169.16
	Alternate	-27.893	26.921	3.322	-23.02	104.51
371	CE-639-2	-28.431	11.125	4.432	-15.66	141.90
	Alternate	-27.139	11.025	4.207	-29.15	132.34
380	CE-639-2	-27.277	0.	4.402	-15.55	140.95
	Alternate	-27.277	0.	4.364	-30.25	137.30
601	CE-639-2	-26.972	0.039	4.353	-4.11	106.92
	Alternate	-26.801	0.	4.288	0.	105.57
612	CE-639-2	-27.841	9.986	4.642	0.	114.12
	Alternate	-26.865	9.886	4.580	0.	112.76
626	CE-639-2	-23.440	19.260	4.509	0.	110.88
	Alternate	-26.634	25.794	5.932	0.	146.05
639	CE-639-2	-27.841	9.986	4.642	0.	114.12
	Alternate	-26.865	9.886	4.580	0.	112.76
650	CE-639-2	-26.972	0.039	4.353	-4.11	106.92
	Alternate	-26.801	0	4.288	0.	105.57

3C.10.4 REFERENCES

1. Godfrey, D. A., "Evaluation of Prestressed Post-Tensioned Forces on the Shallow Dome of Containment Structures", Nuclear Engineering and Design 10, 325-338, 1969.

2. Lin, T. Y., Design of Prestressed Concrete, John Wiley, 1963.

3. Lipschutz, M. M., Differential Geometry, Schaum's Outline Series, McGraw-Hill, 1969.

3C.11 ICES/STRUDL 11

The ICES/STRUDL-II computer program provides the ability to specify characteristics of problems - framed structures and three-dimensional solid structures, perform analyses - static and dynamic, reduce and combine results.

Analytic procedures in the pertinent portions of ICES/STRUDL-II apply to framed structures. Framed structures are two- or three-dimensional structures composed of slender, linear members that can be represented by properties along a centroidal axis. Such a structure is modeled with joints, including support joints, and members connecting the joints. A variety of force conditions on members or joints can be specified. The member stiffness matrix is computed from beam theory. The total stiffness matrix of the modeled structures is obtained by appropriately combining the individual member stiffnesses.

The stiffness analysis method of solution treats the joint displacements as unknowns. The solution procedure provides results for joints and members. Joint results include displacements and reactions and joint loads as calculated from member end forces. Member results are member end forces and distortions. The assumptions governing the beam element representation of the structure are as follows: linear, elastic, homogeneous, and isotropic behavior, small deformation, plane sections remain plane, and no coupling of axial, torque, and bending.

The program is used to define the dynamic characteristics of the structural models used in the dynamic seismic analyses of the reactor coolant system components. The natural frequencies and mode shapes of the structural models and the influence coefficients which relate member end forces and moments and support reactions to unit displacements are calculated. The influence coefficients are calculated for each dynamic degree-of-freedom of each mass point and for each degree-of-freedom of each support point at which relative motion is imposed. In addition, stiffness coefficients are calculated which relate the forces corresponding to those joint degrees-of-freedom for which mass is specified to the imposed displacements corresponding to those (support) joint degrees-of-freedom at which relative motion will be specified during subsequent seismic response calculations. As appropriate, these data are stored for later use in response spectra or time-history seismic response calculations.

ICES/STRUDL-II is a program which is in the public domain and has had sufficient use to justify its applicability and validity. The version of the program in use at C-E was developed by the McDonnell Automation Company/Engineering Computer International and is run on the IBM-360 computer system.

3C.12 TMCALC

The C-E program TMCALC solves the differential equations of motion for a singly or multiply excited multidegree-of-freedom linear structural system. The program accepts separate independent, time varying inputs at each boundary point in the system at which motions due to a seismic event may be imposed, or where a load forcing function may be imposed. The input excitations are provided in digitized form and are assumed to vary linearly between input time steps. The solution of the equations of motion in normal mode coordinates employs a closed form integration process.

The inputs to TMCALC consist of:

A. Eigenvalues (natural frequencies) and eigenvectors (mode shapes)

B. A stiffness matrix that relates mass point degrees-of-freedom to boundary point degrees-of-freedom

C. Mass and damping matrices

D. Digitized time-history records that define the excitation in terms of motions at the boundary points of the structural system or
forces at mass points

The output from TMCALC consists of digitized time-history records of the absolute accelerations and relative displacements for each mass point and boundary point dynamic degree-of-freedom of the structural system.

The program was developed by C-E in 1970 and is used on the CDC-7600 computer at C-E.

The program is used to calculate the dynamic response of structural models used in the dynamic seismic analysis of the reactor coolant system major components, and in the dynamic analysis of linear structural systems subjected to time varying load forcing functions, such as thrust from postulated pipe ruptures.

To demonstrate the applicability and validity of the TMCALC program, the solutions to test problems were obtained and shown to be substantially identical to the results obtained by hand calculations.

One such problem is shown here for the purposes of illustration. The satisfactory agreement between the program results and the theoretical solution indicates the reliability of TMCALC.

Figure 3C.12-1 is a lumped mass, shear beam representation of a uniform beam with the given properties, subjected to different, arbitrary motions at each of the two supports, as shown. The closed form solution to the equation of motion for this structure can be found using standard integration techniques.[1] From this closed form solution for the equation of the multiply excited system shown in figure 3C.12-1, maximum values of relative displacement, velocity, and acceleration were derived. These solutions are shown in table 3C.12-1 along with the corresponding results from program TMCALC. Differences can be seen to be less than 1%. The respective times at which these maxima occurred are identical.

Table 3C.12-1

SOLUTION TO TMCALC

Response	Theoretical	TMCALC
u	4.8000 in.	4.8002 in.
|	15.2000 in./s	15.2037 in./s
ü	67.1132 in./s^2	67.1172 in./s^2

3C.12.1 REFERENCES

1. Przemieniecki, J. S., Theory of Matrix Structural Analyses, Chapter 13, McGraw-Hill Book Company, New York, N. Y., 1968.

3C.13 FORCE

The computer program FORCE calculates the internal forces and moments at designated locations in a linear elastic structural system, at each time step, due to the time-history of relative displacements of the system mass points and boundary points. The program also selects the maximum value of each component of force or moment at each designated location, and the items at which they occur, over the entire duration of the specified dynamic event. The input to FORCE consists of the following:

A. A matrix of influence coefficients computed by the ICES/STRUDL-II program, which relate the displacements of the mass point and support point dynamic degree-of-freedom to the reaction forces and moments at the designated location

B. The time-history of the relative displacements of the mass point and support point dynamic degrees-of-freedom as calculated by the program TMCALC.

The program forms appropriate linear combinations of the relative displacements at each time step and performs a complete loads analysis of the deformed shape of the structure at each time step over the entire duration of the specified dynamic event.

The program was developed by C-E in 1970 and is used on the CDC-7600 computer.

The program is used to calculate the time dependent reactions in structural models subjected to dynamic excitation which are analyzed by the TMCALC program.

To demonstrate the validity of the FORCE program, results for test cases were obtained and shown to be substantially identical to those obtained for an equivalent analysis using the public domain program STRUDL.[1] Such test case is shown for purposes of illustration. Figure 3C.13-1 is a lumped mass multiple-degree-of-freedom model of a uniform beam that has been defined to have mass and differential boundary excitation. The arbitrary differential support motion and mass point responses chosen for this example are shown in table 3C.13-1. The matrix of influence coefficients and the arbitrary mass point and differential support point motions are inputs to the program to calculate the support reactions and internal shear forces and bending moments indicated in figure 3C-2. These results and those found by performing a stiffness analysis using the STRUDL program are shown in table 3C.13-2. Results can be seen to be substantially identical.

Table 3C.13-1

MASS AND SUPPORT POINT MOTIONS

t	Y15	Y20	Y25	Y30
0.00	-0.10	0.05	0.27	0.31
0.01	-0.16	-0.21	0.47	0.54
0.02	-0.28	0.02	0.36	0.21
0.03	0.19	0.31	-0.17	.29

Table 3C.13-2

STRUDL AND FORCE RESULTS

Load	STRUDL	FORCE
RIO	3,105,000	3,105,000
M10	139,600,000	139,600,000
R30	-1,906,000	-1,906,000
M30	75,990,000	75,990,000
V40	890,400	890,400
M40	32,540,000	32,540,000

3C.13.1 REFERENCES

1. ICES/STRUDL-II, The Structural Design Language Engineers Users Manual, MIT Press, Cambridge, Massachusetts, 1968.

3C.14 RISA-3D

3C.14.1 DESCRIPTION

RISA-3D is a general purpose, three-dimensional, structural analysis and design program for microcomputers based on the linear elastic stiffness method for the solution of the model. The program utilizes finite element solution methods, and has static and dynamic analysis options. Analysis, including deflection and stresses, can be performed on structures constructed of any material or combination of materials. RISA-3D's dynamic analysis includes frequencies and mode shapes and response spectra analysis. Load combinations may be defined using the results from the static and dynamic analyses.

RISA-3D includes extensive graphics which include zoom windowing, display of loads and magnitudes, display of the structure from any angle, deflected shape display and animation, and the display of moment, shear, and axial diagrams. Graphics can be viewed at any time by pressing a key or mouse button.

RISA-3D was developed and provided by RISA Technologies in Lake Forrest, California.

3C.15 SAP90 / SAP2000

3C.15.1 DESCRIPTION

SAP90 and SAP2000 are structural analysis programs for microcomputers. The programs utilize various types of finite elements and has static analysis and dynamic analysis options. The finite element library consists of a FRAME element, a SHELL element, an ASOLID element, and a SOLID element. Loading options allow for gravity, thermal and prestress conditions in addition to nodal loadings with specified forces or displacements. Dynamic loading can be in the form of a base acceleration response spectrum, or time varying loads and base accelerations. Load combinations may be defined using the results from the static and dynamic analyses.

SAP90 / SAP2000 was developed and provided by Computers and Structures, Inc. in Berkeley, California.

3C.16 ANSYS

3C.16.1 DESCRIPTION

The ANSYS program is a finite-element computer program that is used to perform linear and nonlinear analysis of three dimensional structural systems. Applications may be simple simulations involving one or two modeling elements, or they may be large and complex simulations. The program is capable of performing static analysis, modal extractions, and time history, or spectral-response analyses on structures composed of any of the following modeling elements:

- Boundary
- Truss
- Beams
- Plane strain
- Plane stress
- Axisymmetric
- Plates
- Solids

3C.16.2 VALIDATION

The ANSYS computer code is a recognized computer code in the public domain and has had sufficient use to justify its applicability and validity. Installation is verified on the SONGS computer network.

3C.16.3 EXTENT OF APPLICATION

The ANSYS program is one of several computer programs used to perform stress analysis of Seismic Category I structures, and substructures and components.

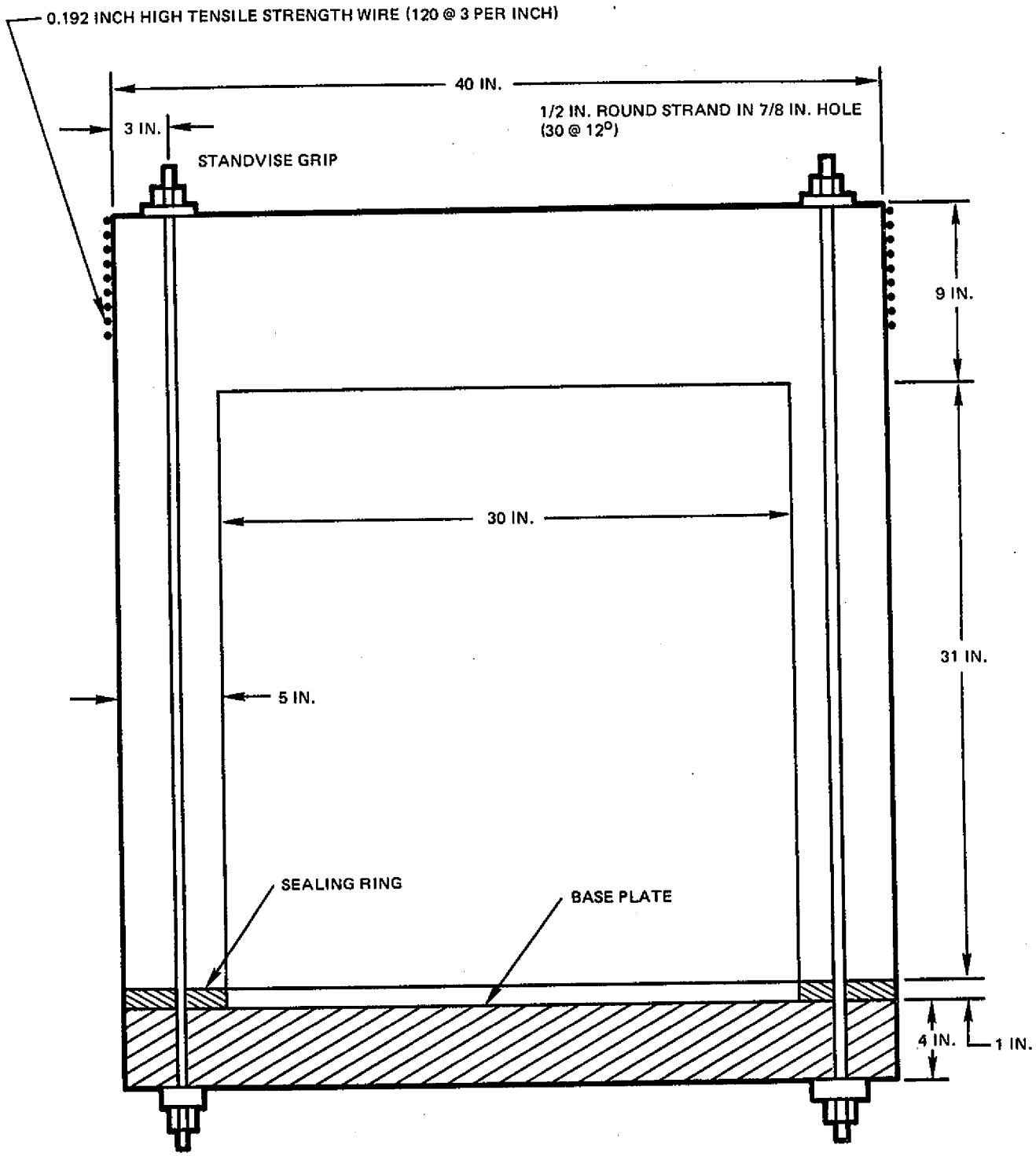

Updated

SAN ONOFRE NUCLEAR GENERATING STATION Units 2 & 3
LONGITUDINAL SECTION OF THE PCRV (FINEL EXAMPLE 1)
Figure 3C.1-1

10079-11D-1329

Amended: April 2009 TL: E047997

Site File Copy

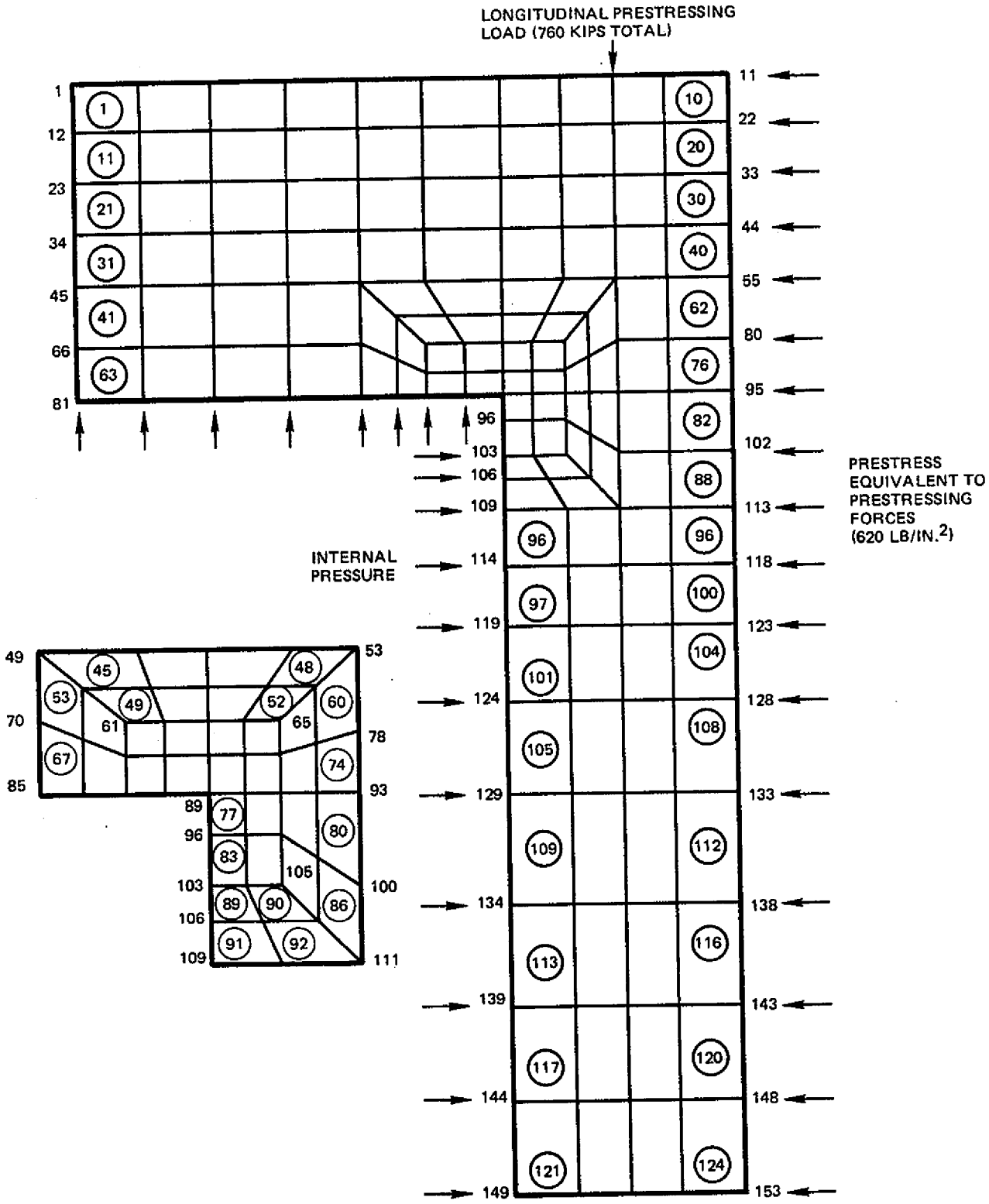

Updated

SAN ONOFRE NUCLEAR GENERATING STATION Units 2 & 3

FINITE ELEMENT IDEALIZATION OF PCRV (FINEL EXAMPLE 1)

Figure 3C.1-2

10079-11D-1330

Amended: April 2009 TL: E047997

Site File Copy

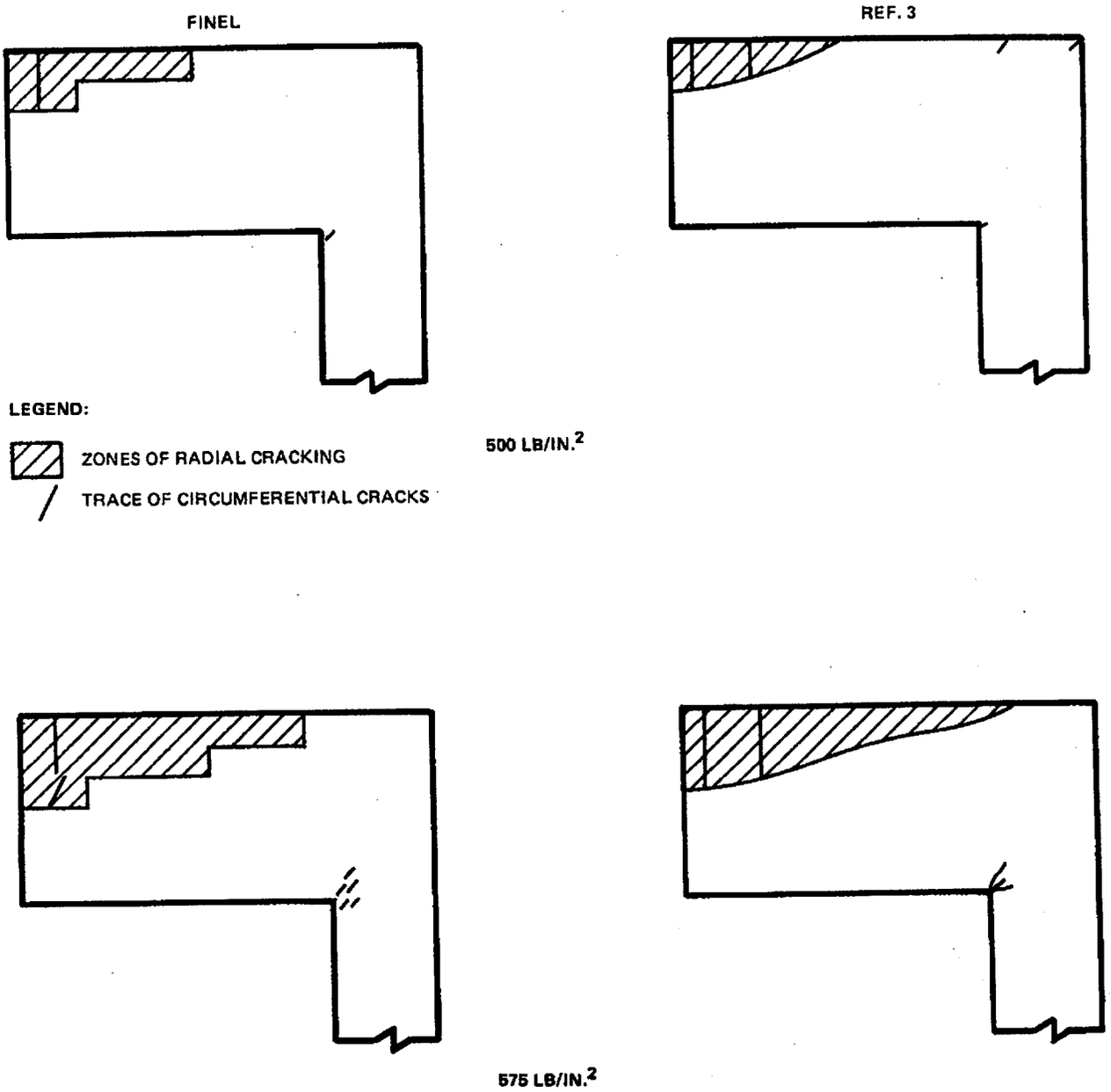

Updated

SAN ONOFRE NUCLEAR GENERATING STATION Units 2 & 3
REGIONS OF CRACKING (FINEL EXAMPLE 1) (Sheet 1 of 3)
Figure 3C.1-3

Amended: June 2003 TL: E004628

10079-11D-1331

Site File Copy

Amended: April 2009 TL: E047997

Site File Copy

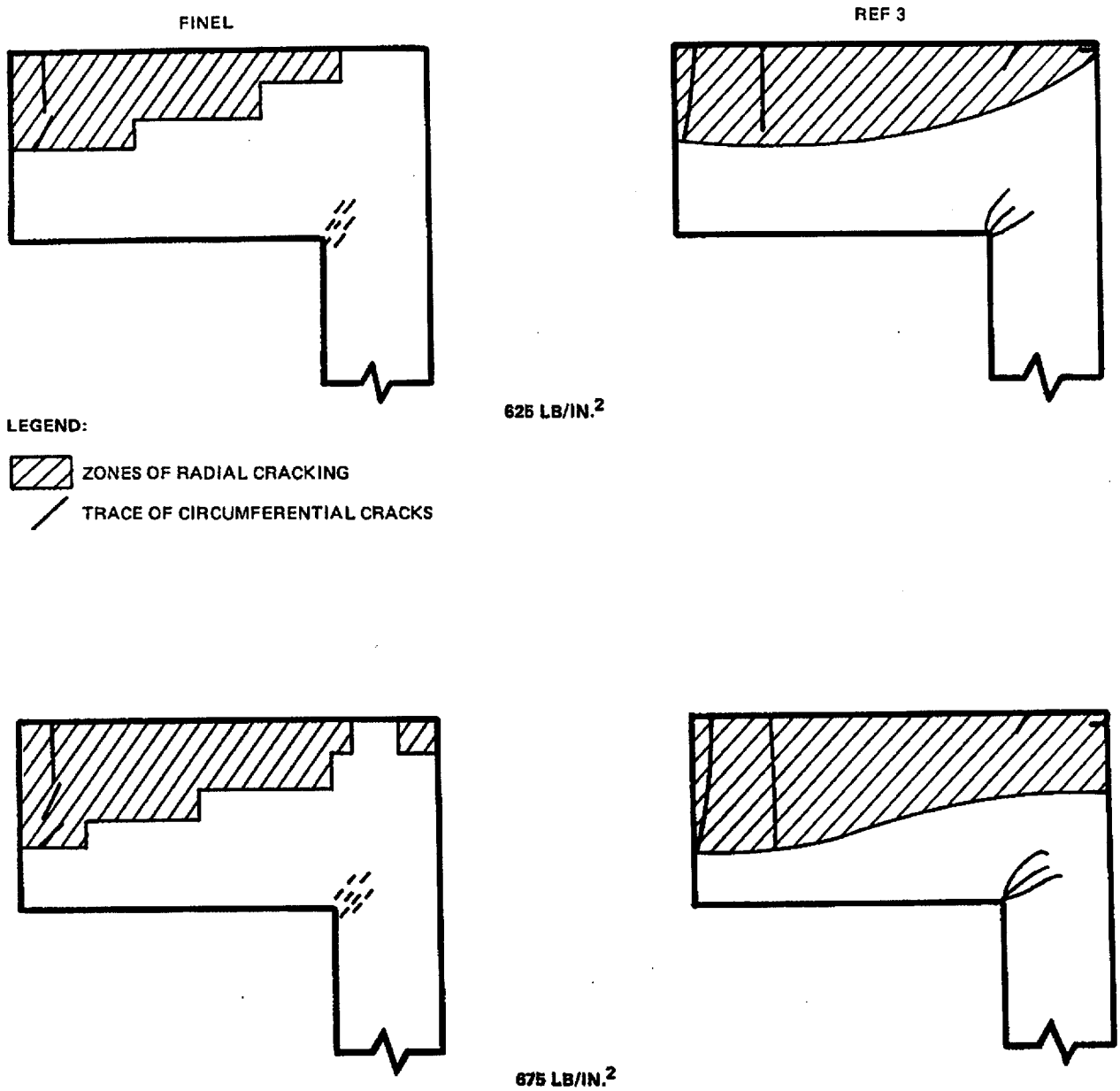

Updated

SAN ONOFRE NUCLEAR GENERATING STATION Units 2 & 3
REGIONS OF CRACKING (FINEL EXAMPLE 1) (Sheet 2 of 3)
Figure 3C.1-3

Amended: June 2003 TL: E004628

10079-11D-1332

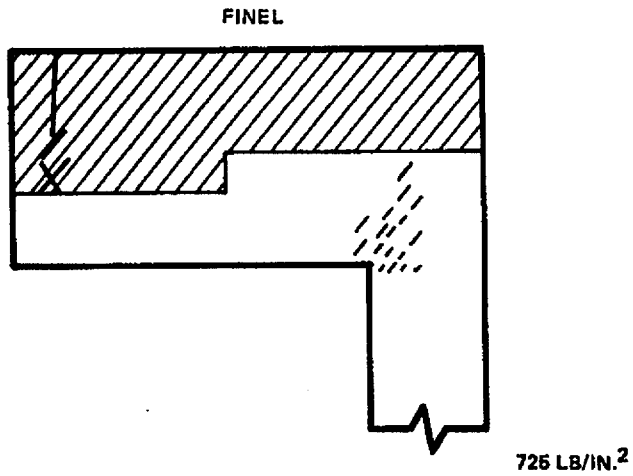

LEGEND:

ZONES OF RADIAL CRACKING

TRACE OF CIRCUMFERENTIAL CRACKS

Updated

SAN ONOFRE NUCLEAR GENERATING STATION Units 2 & 3
REGIONS OF CRACKING (FINEL EXAMPLE 1) (Sheet 3 of 3)
Figure 3C.1-3

Amended: June 2003 TL: E004628

10079-11D-1333

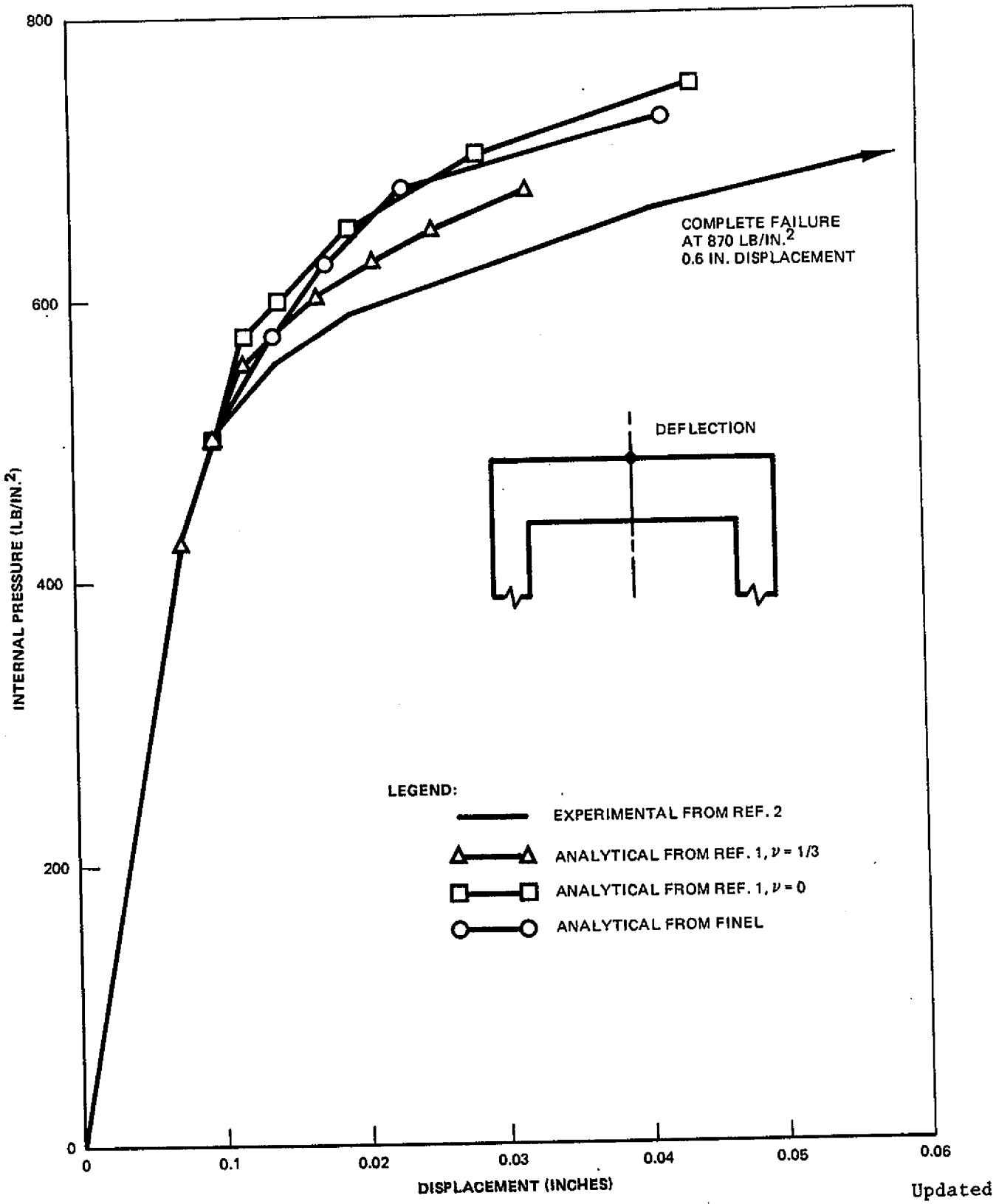

Updated

SAN ONOFRE
NUCLEAR GENERATING STATION
Units 2 & 3

LOAD-DEFORMATION CURVES FROM FINEL VERIFICATION USING A PCRV (FINEL EXAMPLE 1)

Figure 3C.1-4

10079-11D-1334

Amended: April 2009 TL: E047997

Site File Copy

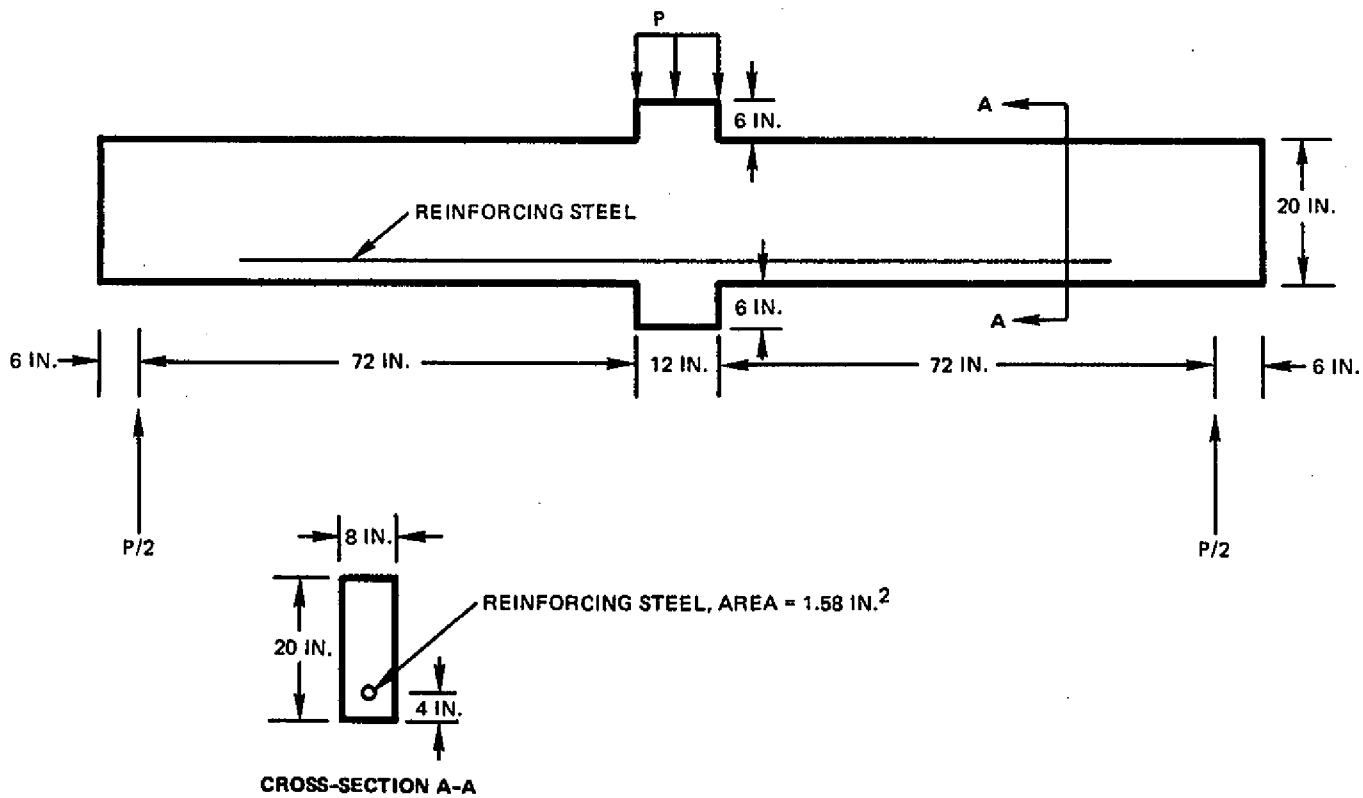

Updated

SAN ONOFRE NUCLEAR GENERATING STATION Units 2 & 3
EXPERIMENTAL BEAM DIMENSIONS (FINEL EXAMPLE 2)
Figure 3C.1-5

10079-11D-1335

Amended: April 2009 TL: E047997

Site File Copy

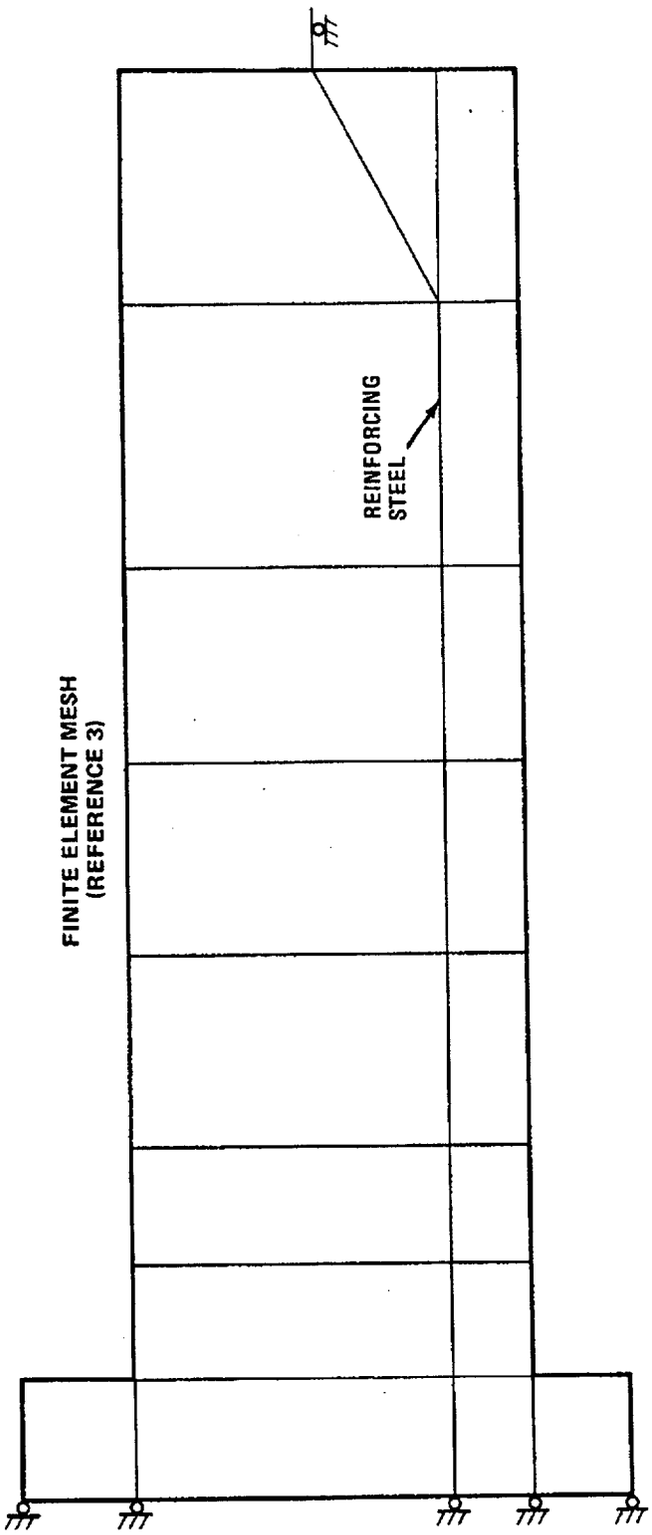

Updated

SAN ONOFRE NUCLEAR GENERATING STATION Units 2 & 3
FINITE-ELEMENT MESH (FINEL EXAMPLE 2) (Sheet 1 of 2)
Figure 3C.1-6

Amended: June 2003 TL: E004628

Site File Copy

Amended: April 2009 TL: E047997

Site File Copy

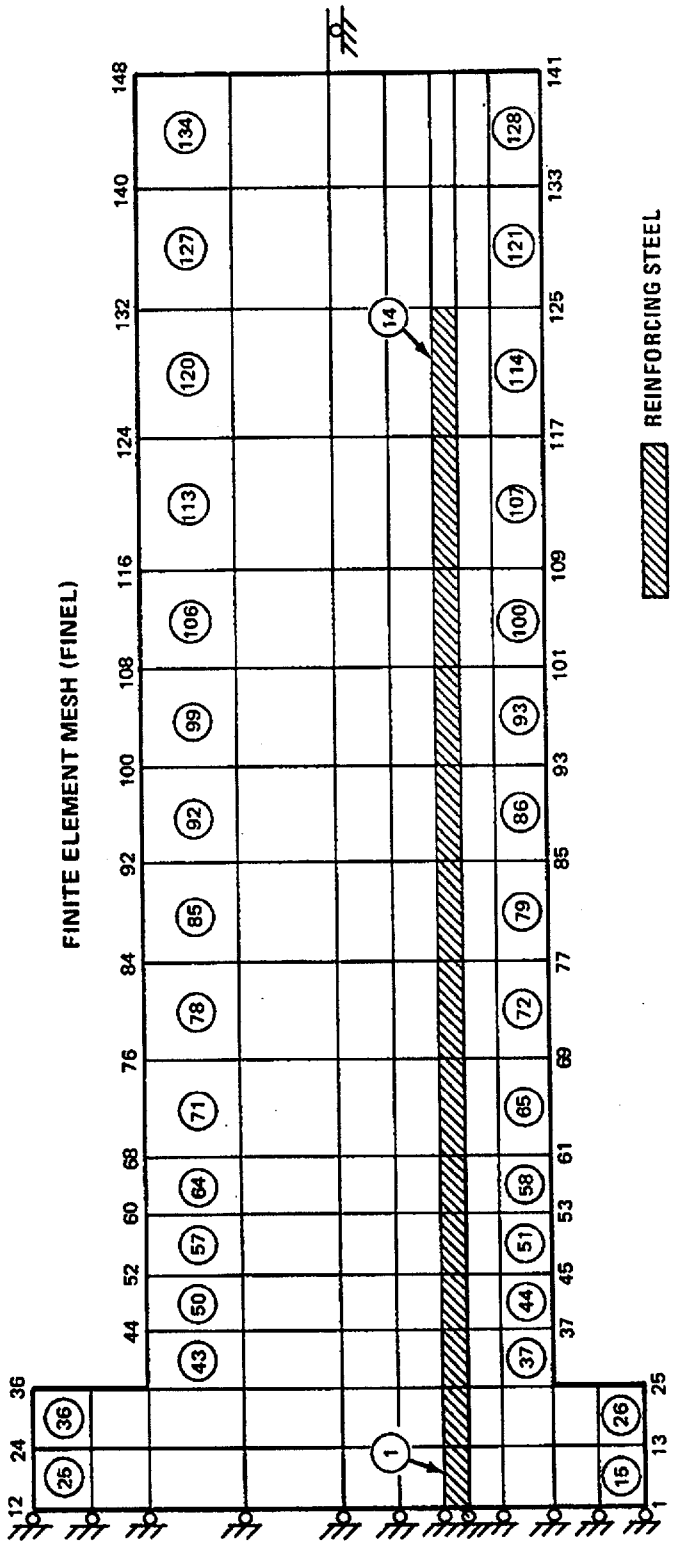

Updated

SAN ONOFRE NUCLEAR GENERATING STATION Units 2 & 3
FINITE-ELEMENT MESH (FINEL EXAMPLE 2) (Sheet 2 of 2)
Figure 3C.1-6

Amended: June 2003 TL: E004628

LEGEND:

BOUNDARY OF CRACKED REGION, REF. 3

CRACKED REGION, FINEL

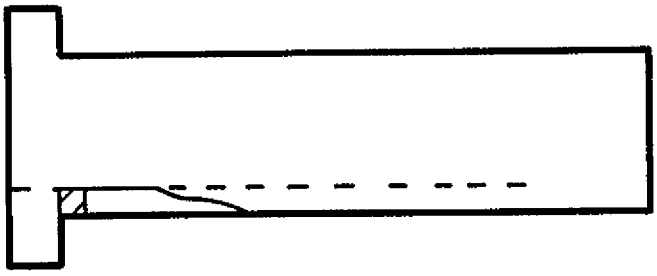

FINEL – 8.7 KIPS REF. 3 – 8.0 KIPS
(NO CRACKING IN FINEL BELOW 8.7 KIPS)

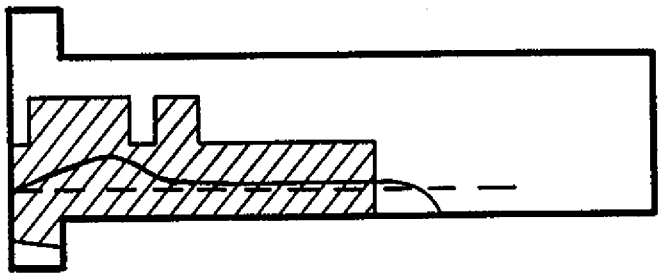

FINEL AND REF. 3 – 28.0 KIPS

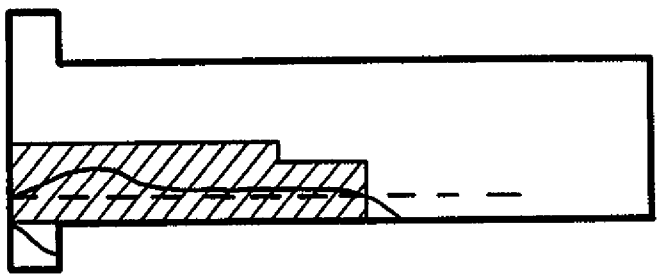

FINEL AND REF. 3 – 20.0 KIPS

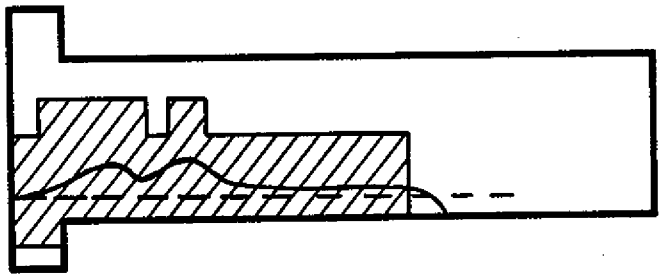

FINEL AND REF. 3 – 31.2 KIPS

Updated

SAN ONOFRE NUCLEAR GENERATING STATION Units 2 & 3
REGIONS OF CRACKING (FINEL EXAMPLE 2)
Figure 3C.1-7

10079-11D-1338

Amended: April 2009 TL: E047997

Site File Copy

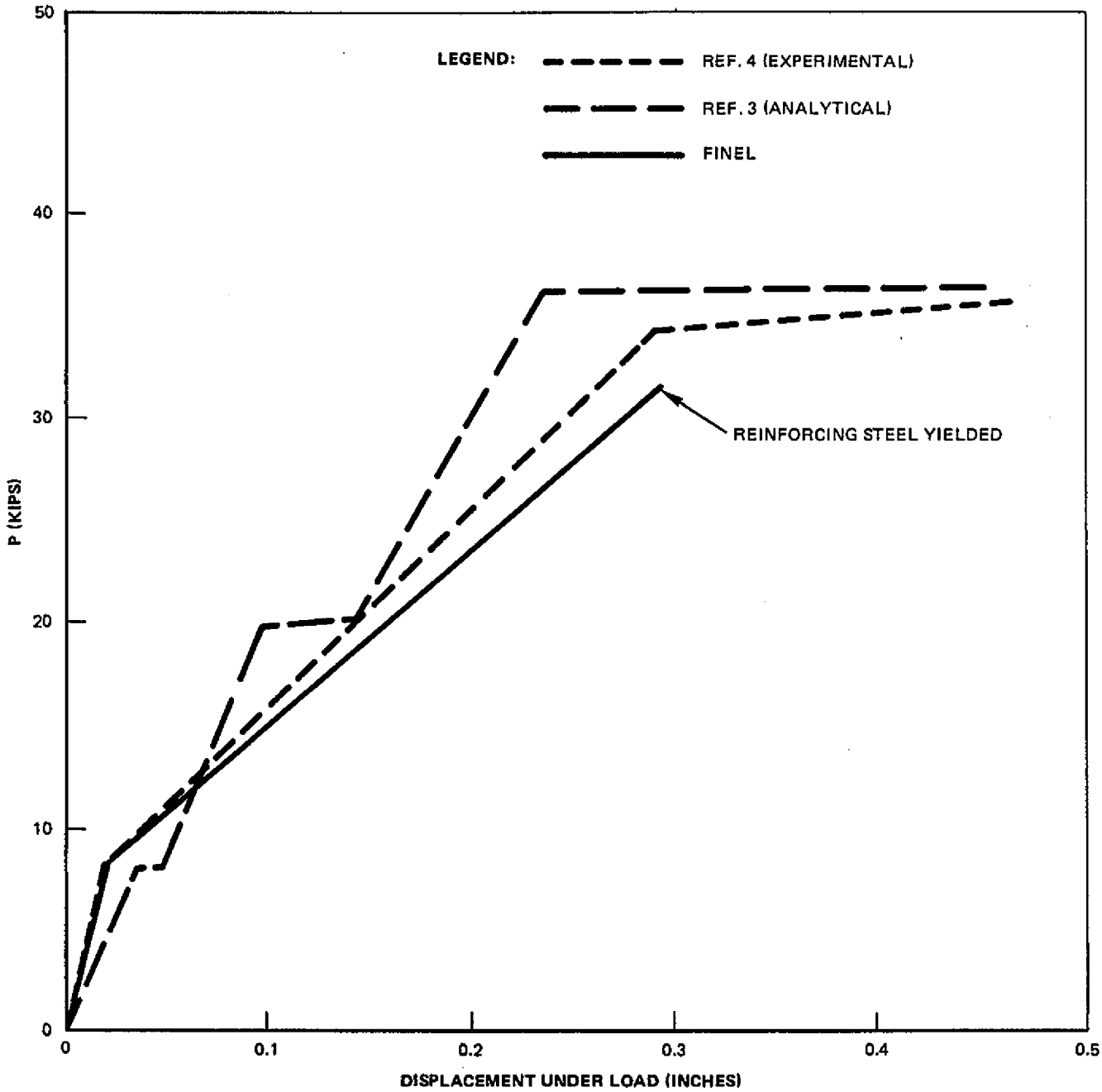

SAN ONOFRE NUCLEAR GENERATING STATION Units 2 & 3
LOAD-DISPLACEMENT CURVES FROM FINEL VERIFICATION USING A SIMPLY SUPPORTED BEAM (FINEL EXAMPLE 2)
Figure 3C.1-8

10079-11D-1340
250G6

Amended: April 2009 TL: E047997

Site File Copy

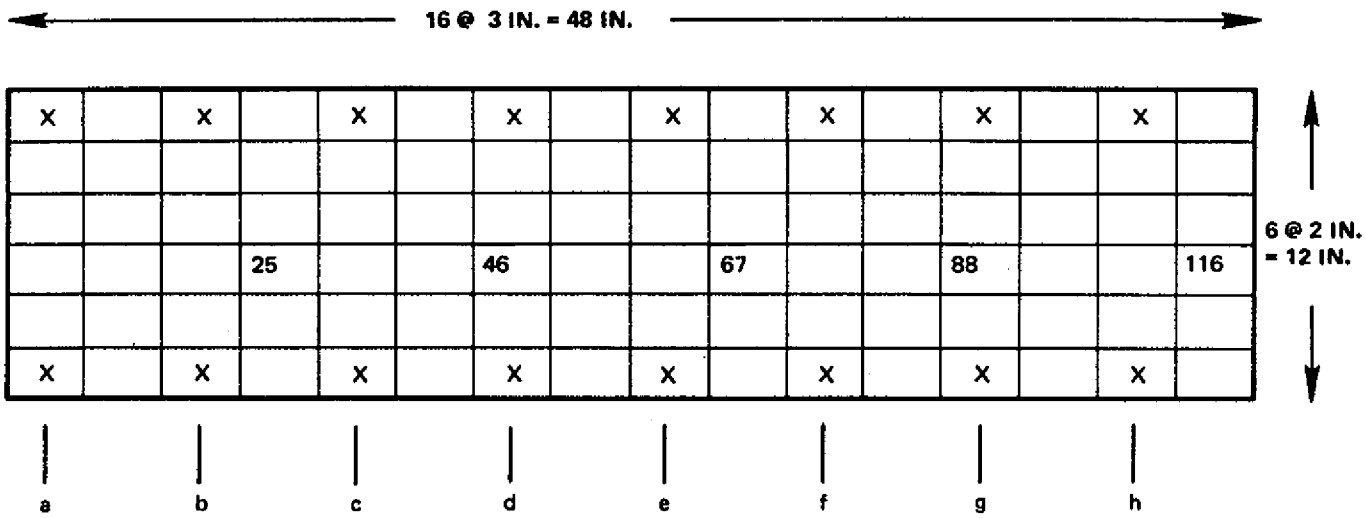

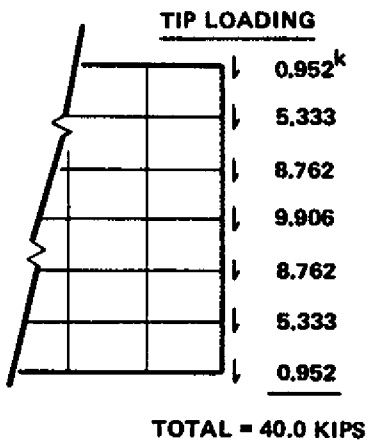

NUMERICAL DATA:

ELASTIC MODULUS
E = 30,000 K/IN.^{2}

POISSON'S RATIO
ν = 0.25

MOMENT OF INERTIA
1 = 144 IN.^{4}

CROSS SECTIONAL AREA
A = 12 IN.^{2}

Updated

SAN ONOFRE NUCLEAR GENERATING STATION
Units 2 & 3

BEAM GEOMETRY AND FINITE-ELEMENT MESH (FINEL EXAMPLE 3)

Figure 3C.1-9

10078-11D-1341

Amended: April 2009 TL: E047997

Site File Copy

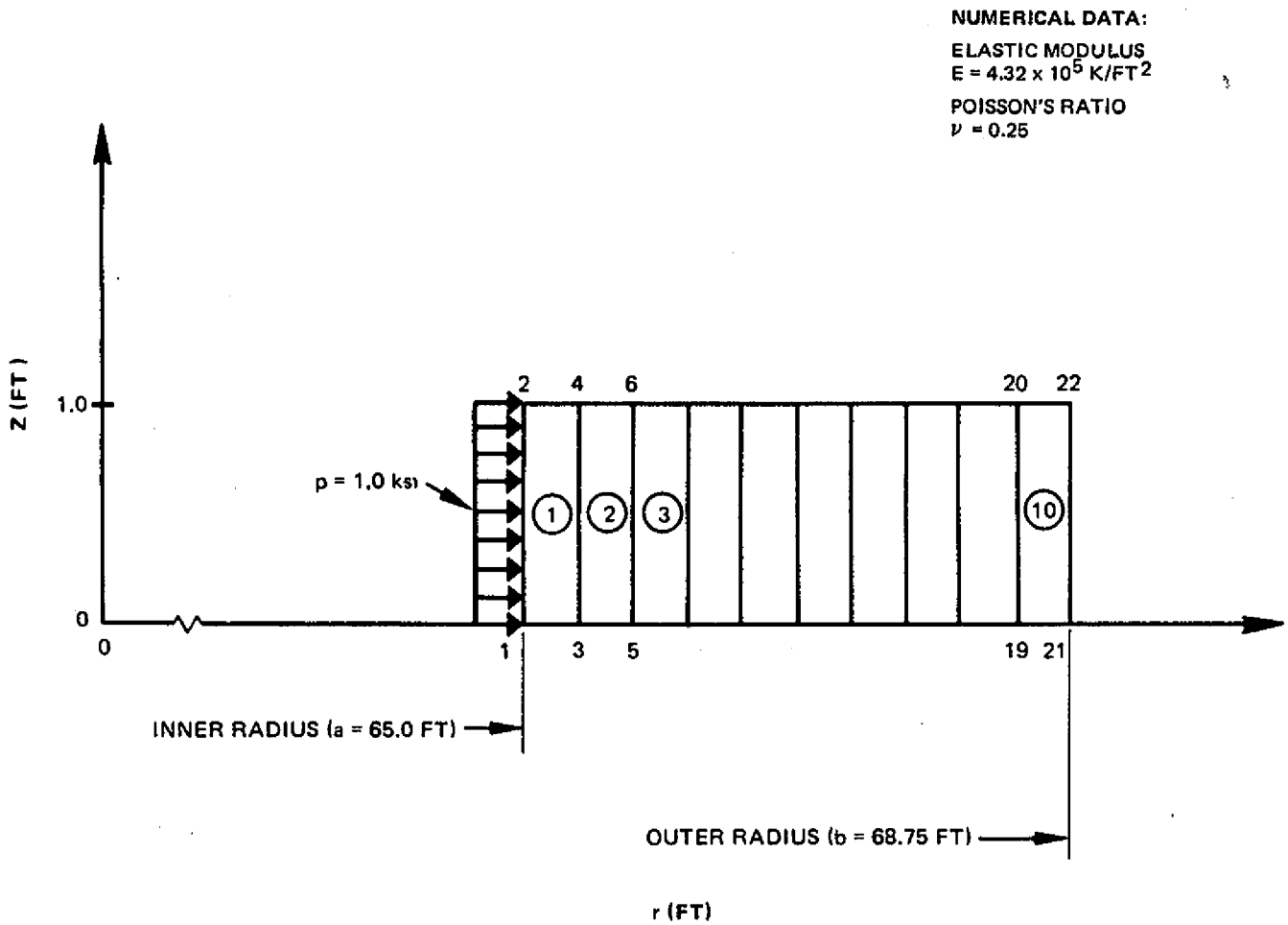

Updated

SAN ONOFRE NUCLEAR GENERATING STATION Units 2 & 3
FINITE-ELEMENT MODEL (FINEL EXAMPLE 4)
Figure 3C.1-10

10079-11D-1342

Amended: April 2009 TL: E047997

Site File Copy

NUMERICAL DATA:

ELASTIC MODULUS
$E = 4.32 \times 10^5$ K/FT^2

POISSON'S RATIO
$\nu = 0.25$

COEFFICIENT OF
THERMAL EXPANSION
$\alpha = 6 \times 10^{-6}$ FT/FT/^{o}F

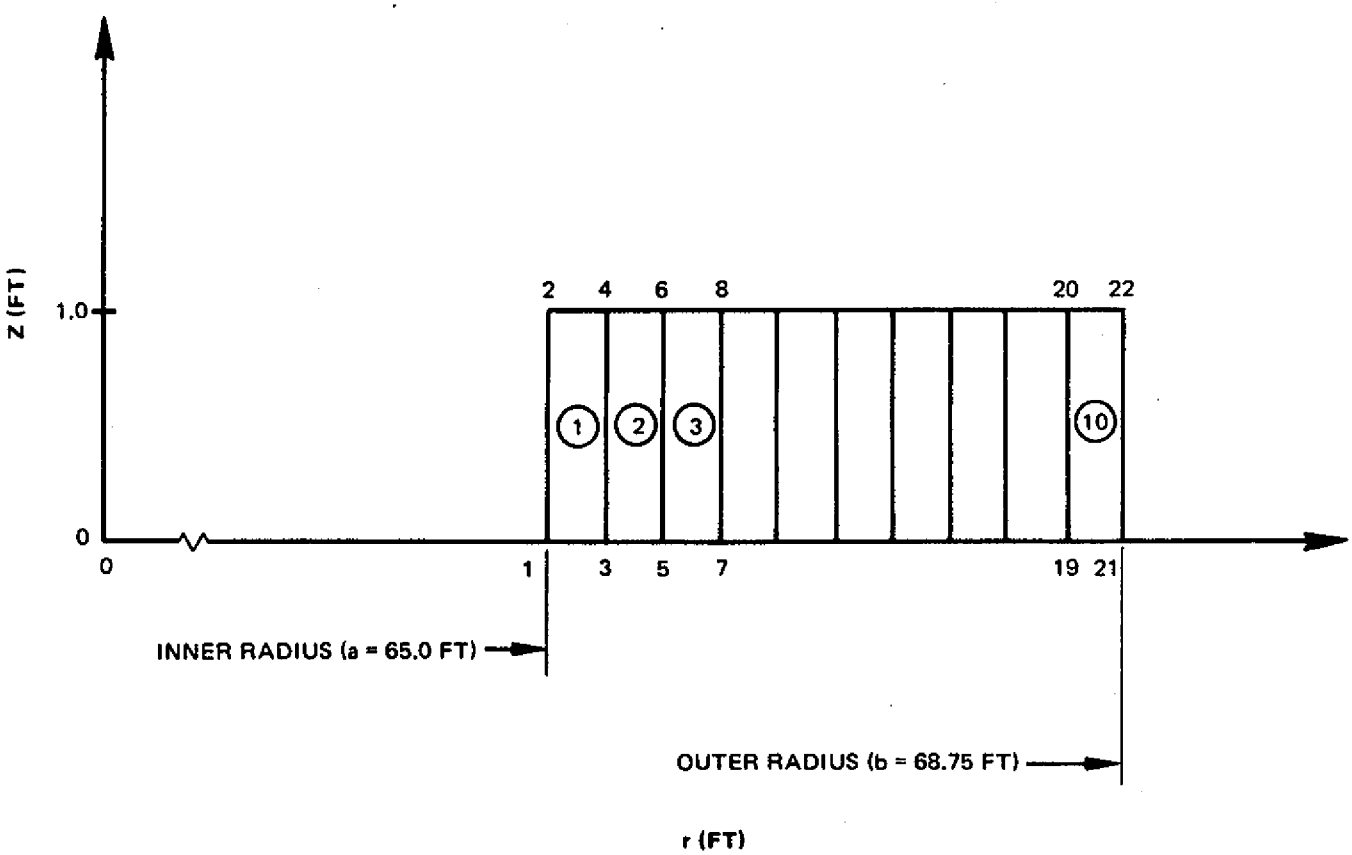

Updated

SAN ONOFRE NUCLEAR GENERATING STATION Units 2 & 3
FINITE-ELEMENT MODEL (FINEL EXAMPLE 5)
Figure 3C.1-11

10079-11D-1344

Amended: April 2009 TL: E047997

Site File Copy

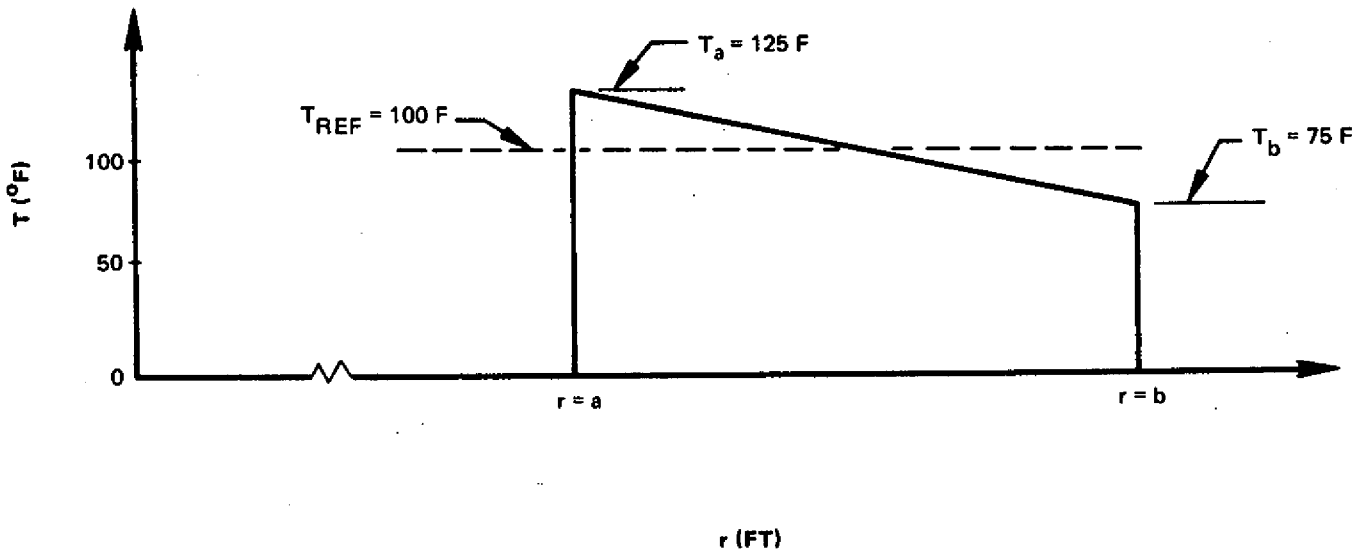

Updated

SAN ONOFRE NUCLEAR GENERATING STATION Units 2 & 3
TEMPERATURE DISTRIBUTION (FINEL EXAMPLE 5)
Figure 3C.1-12

10079-11D-1343

Amended: April 2009 TL: E047997

Site File Copy

NUMERICAL DATA:

ELASTIC MODULUS
$E = 4.32 \times 10^5$ K/FT^2

POISSON'S RATIO
$\nu = 0.25$

COEFFICIENT OF
THERMAL EXPANSION
$\alpha = 6 \times 10^{-6}$ FT/FT/$^\circ$F

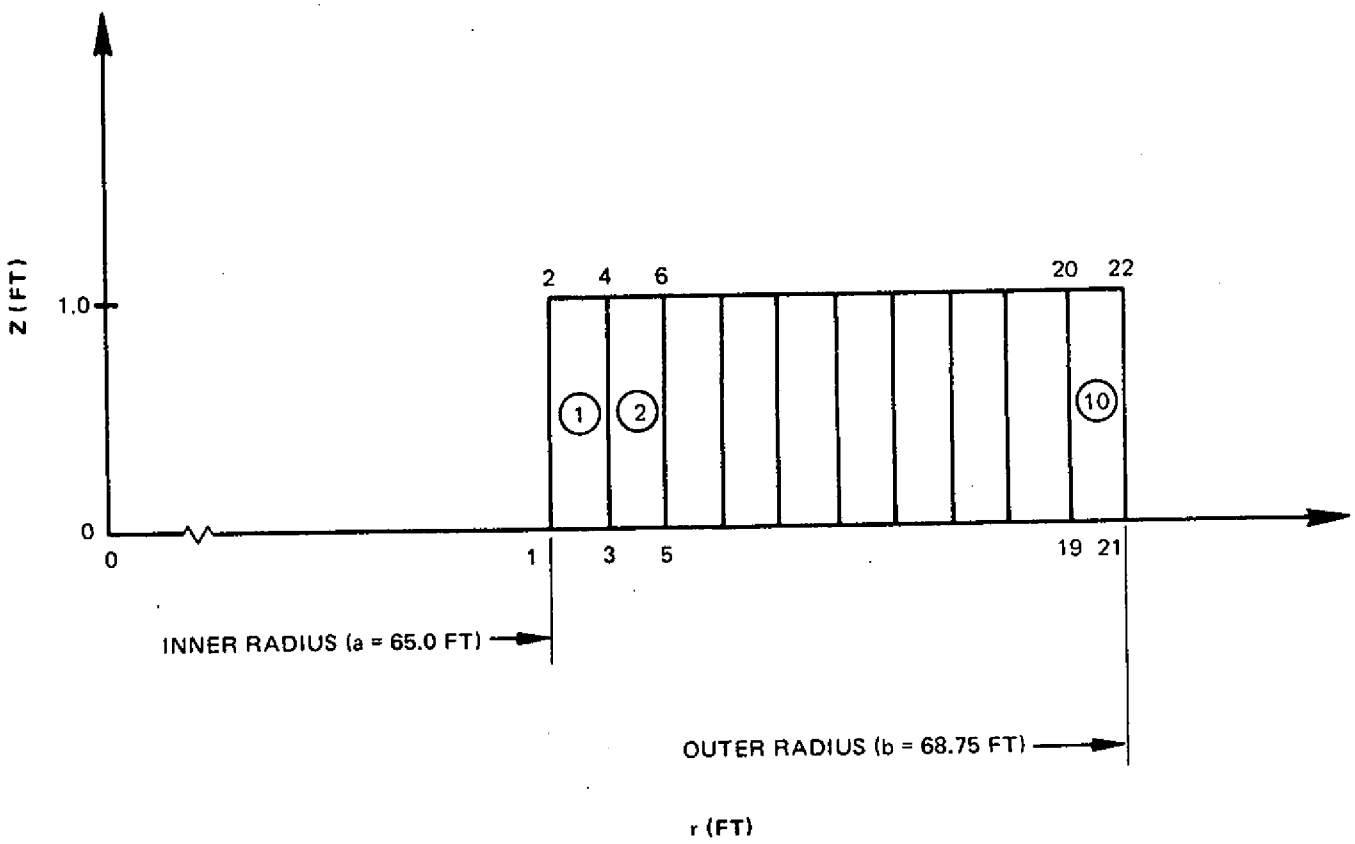

Updated

SAN ONOFRE NUCLEAR GENERATING STATION Units 2 & 3
FINITE-ELEMENT MODEL (FINEL EXAMPLE 6)
Figure 3C.1-13

10079-11D-1345

Amended: April 2009 TL: E047997

Site File Copy

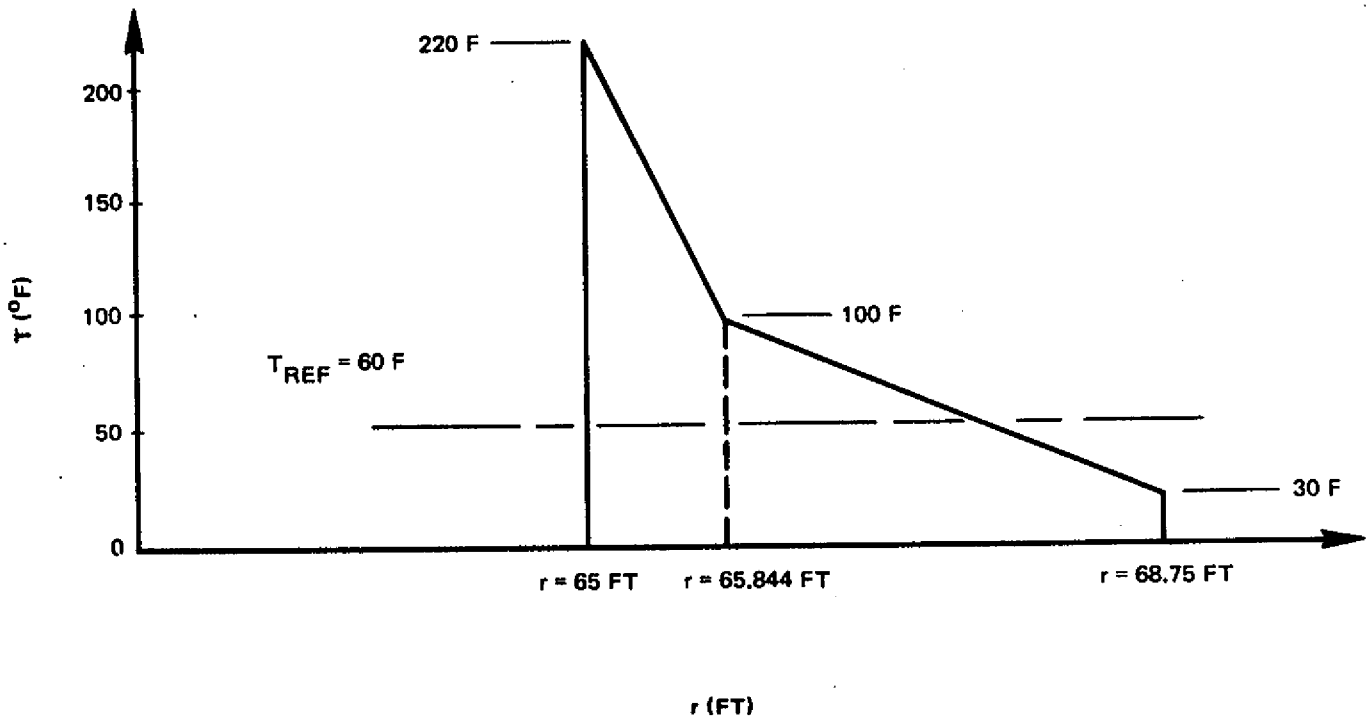

Updated

SAN ONOFRE NUCLEAR GENERATING STATION Units 2 & 3
BILINEAR TEMPERATURE GRADIENT (FINEL EXAMPLE 6)
Figure 3C.1-14

10079-11D-1346

Amended: April 2009 TL: E047997

Site File Copy

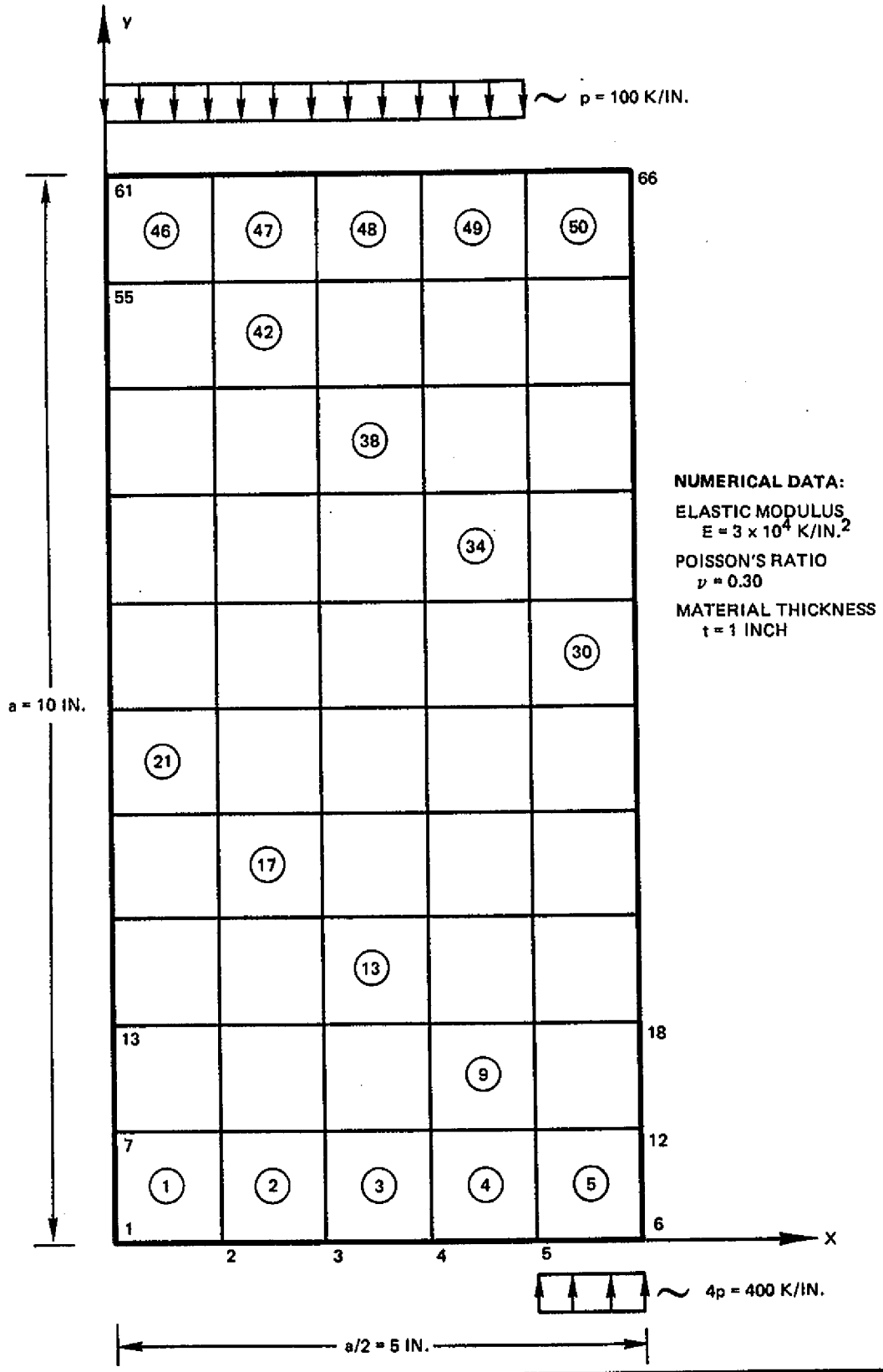

Updated

SAN ONOFRE NUCLEAR GENERATING STATION Units 2 & 3

DEEP ELASTIC PANEL LAYOUT (FINEL EXAMPLE 7)

Figure 3C.1-15

10079-11D-1347

Amended: April 2009 TL: E047997

Site File Copy

FINEL RESULTS

PLATE ELEMENT	(STRESS K/IN.^{2})
30	-1.19
34	-2.86
38	-6.28
42	-20.07
46	-40.15
EXTRAPOLATED VALUE @ NODE 61	-52.0 ←
25	-2.14
19	-12.03
13	-12.38
7	35.51
1	106.48
EXTRAPOLATED VALUE @ NODE 1	146.0 ←

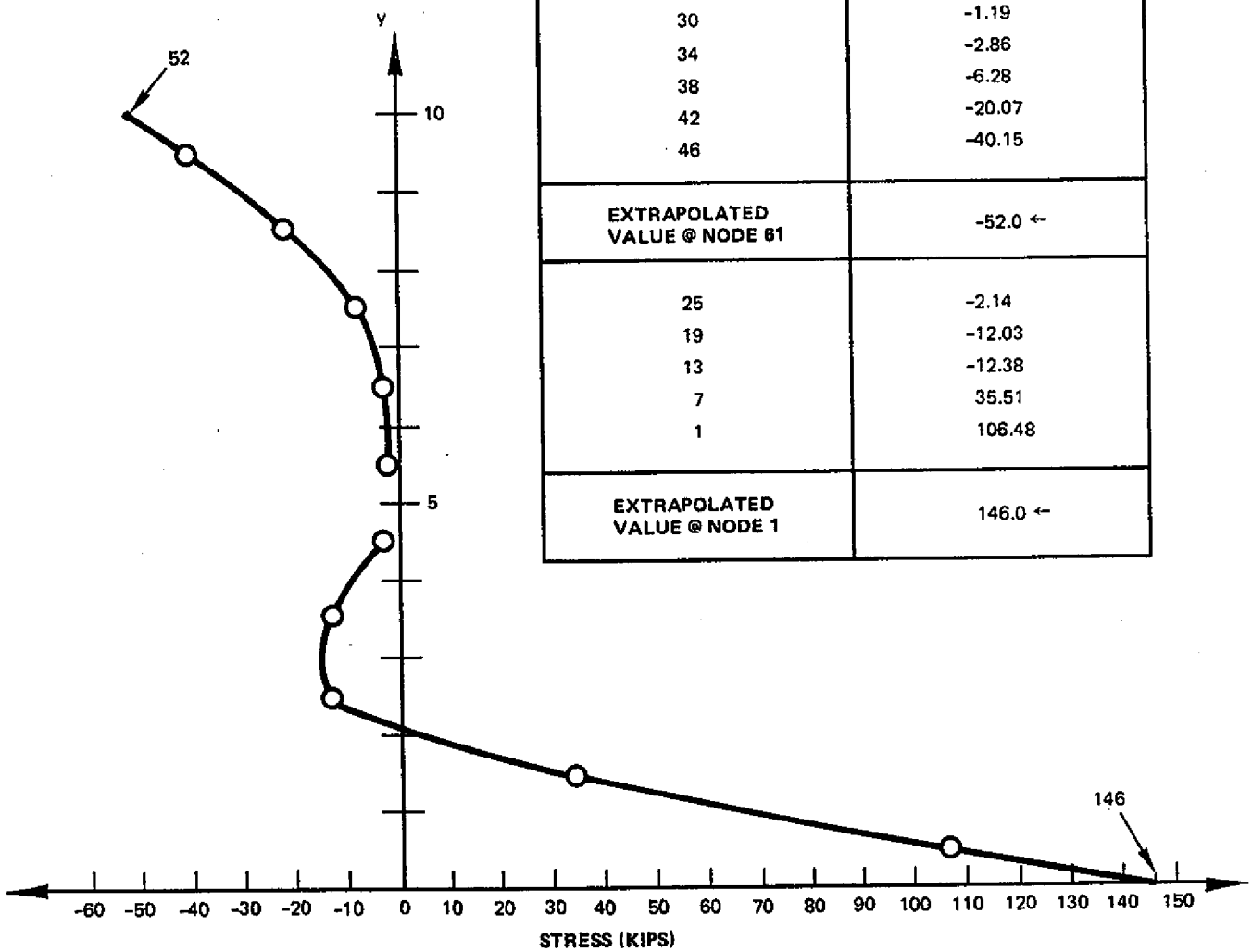

Updated

SAN ONOFRE NUCLEAR GENERATING STATION Units 2 & 3

EXTRAPOLATIONS FOR CORNER STRESSES (FINEL EXAMPLE 7)

Figure 3C.1-16

10079-11D-1348

Amended: April 2009 TL: E047997

Site File Copy

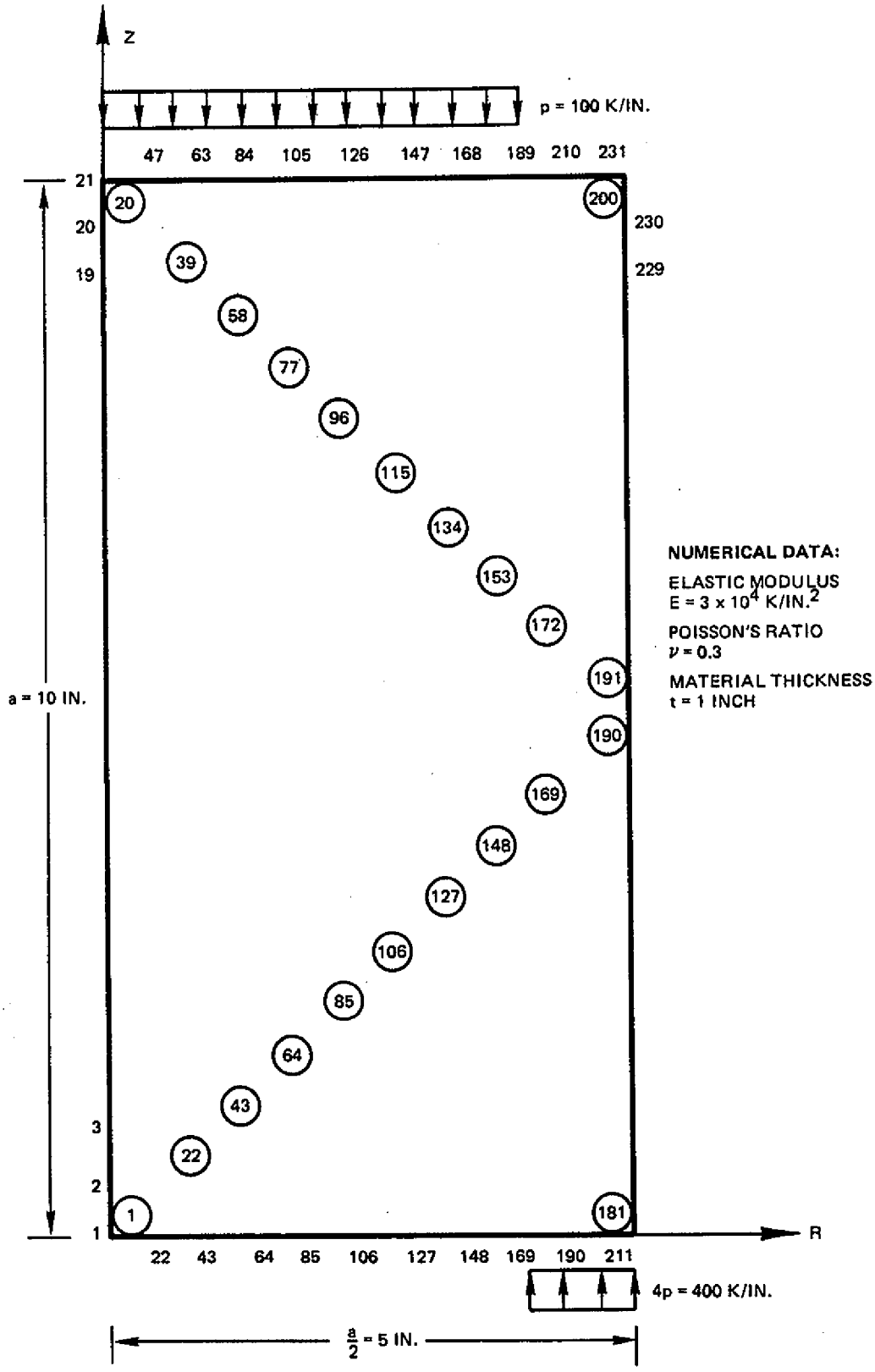

SAN ONOFRE NUCLEAR GENERATING STATION Units 2 & 3
DEEP ELASTIC PANEL LAYOUT (FINEL EXAMPLE 8)
Figure 3C.1-17

10079-11D-1349

Amended: April 2009 TL: E047997

Site File Copy

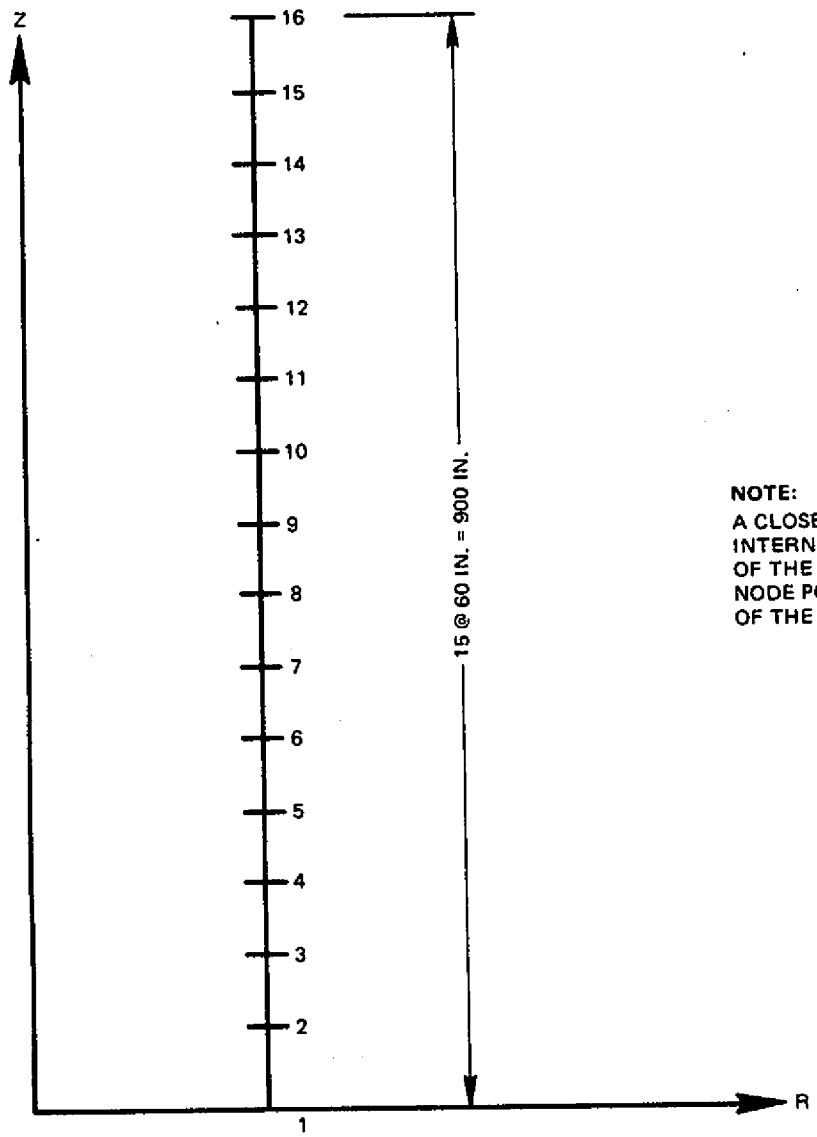

NOTE:
A CLOSED CYLINDER SUBJECTED TO INTERNAL PRESSURE p. ONE-HALF OF THE CYLINDER IS ANALYZED. NODE POINT 1 IS AT THE MIDDLE OF THE CYLINDER.

BOUNDARY CONDITIONS, NODE 1:

Z DISPL = 0
θ DISPL = 0
ROTATION IN R-Z PLANE = 0

BOUNDARY CONDITIONS, NODE 16:

θ DISPL = 0

NUMERICAL DATA

MATERIAL: CONCRETE

E = 4.030508×10^6/IN.^{2}
t = 36 IN. (THICKNESS)
R = 900 IN. (RADIUS)
ν = 0.17 (POISSON'S RATIO)
p = 60/IN.^{2} (INTERNAL PRESSURE)
L = 1,800 IN. (LENGTH OF CYLINDER)
N = 27,000 LB/IN. (AN EQUIVALENT NODE LOAD APPLIED AT NODE 16).

Updated

SAN ONOFRE NUCLEAR GENERATING STATION Units 2 & 3

FINITE-ELEMENT MODEL, SINGLE-LAYER SHELL THICKNESS (ASHSD EXAMPLE 1)

Figure 3C.2-1

10079-11D-1350

Amended: April 2009 TL: E047997

Site File Copy

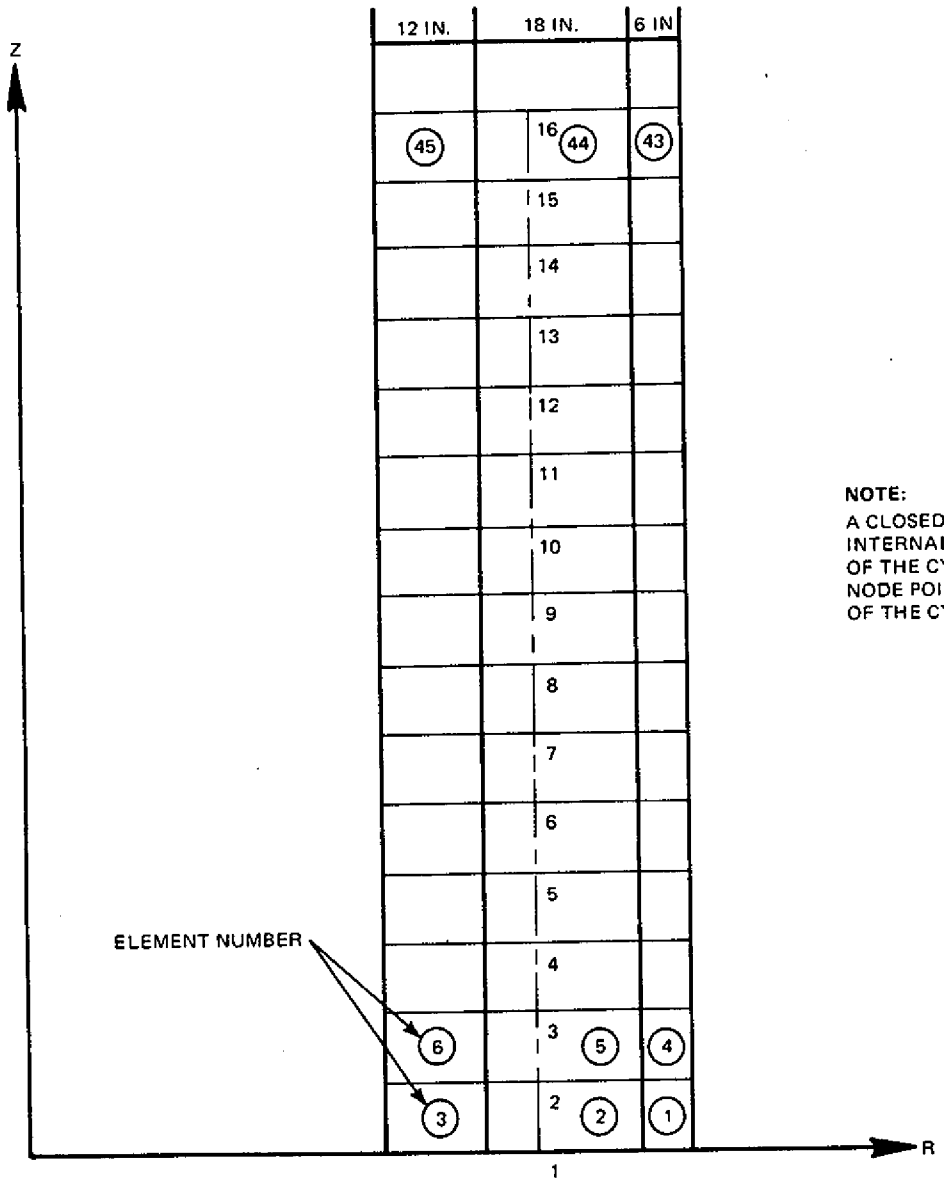

NOTE:
A CLOSED CYLINDER SUBJECTED TO INTERNAL PRESSURE, p. ONE-HALF OF THE CYLINDER IS ANALYZED. NODE POINT 1 IS AT THE MIDDLE OF THE CYLINDER.

BOUNDARY CONDITIONS NODE 1:

Z DISPL = 0
θ DISPL = 0
ROTATION IN R-Z PLANE = 0

BOUNDARY CONDITIONS NODE 16:

θ DISPL = 0

NUMERICAL DATA

MATERIAL: CONCRETE
E = 4.030508×10^6/IN.^{2}
t = 36 IN. (THICKNESS)
R = 900 IN. (RADIUS)
ν = 0.17 (POISSON'S RATIO)
p = 60/IN.^{2} (INTERNAL PRESSURE)
L = 1,800 IN. (LENGTH OF CYLINDER)
N = 27,000 FT/IN. (AN EQUIVALENT NODE LOAD APPLIED AT NODE 16)

Updated

SAN ONOFRE NUCLEAR GENERATING STATION Units 2 & 3

FINITE-ELEMENT MODEL, THREE-LAYER SHELL THICKNESS (ASHSD EXAMPLE 1)

Figure 3C.2-2

10079-11D-1351

Amended: April 2009 TL: E047997

Site File Copy

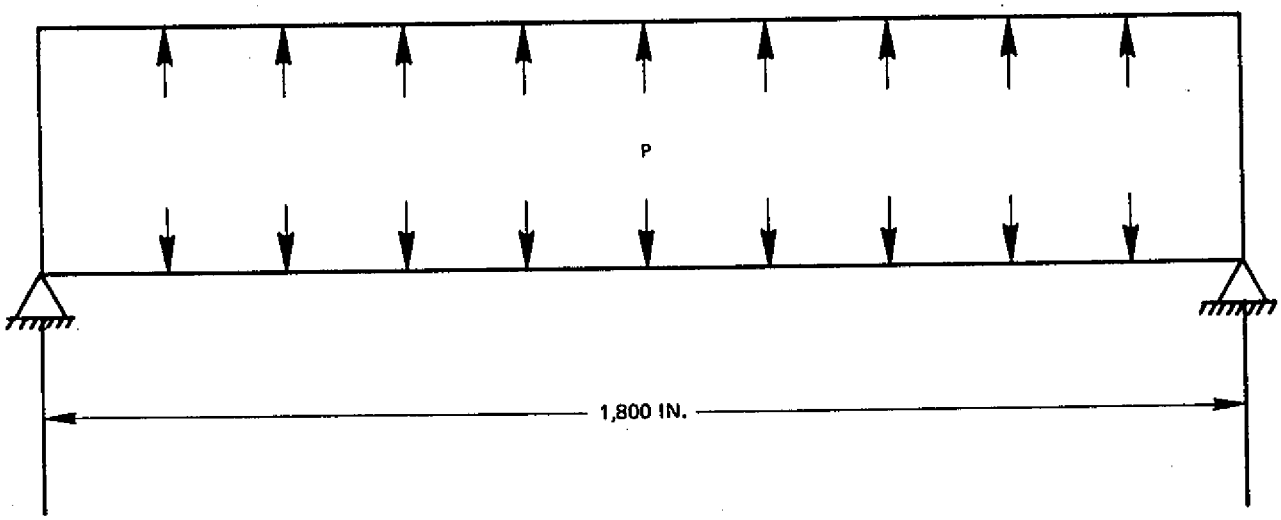

Updated

SAN ONOFRE NUCLEAR GENERATING STATION Units 2 & 3
SIMPLY SUPPORTED CYLINDER (ASHSD EXAMPLE 2)
Figure 3C.2-3

10079-11D-1352

Amended: April 2009 TL: E047997

Site File Copy

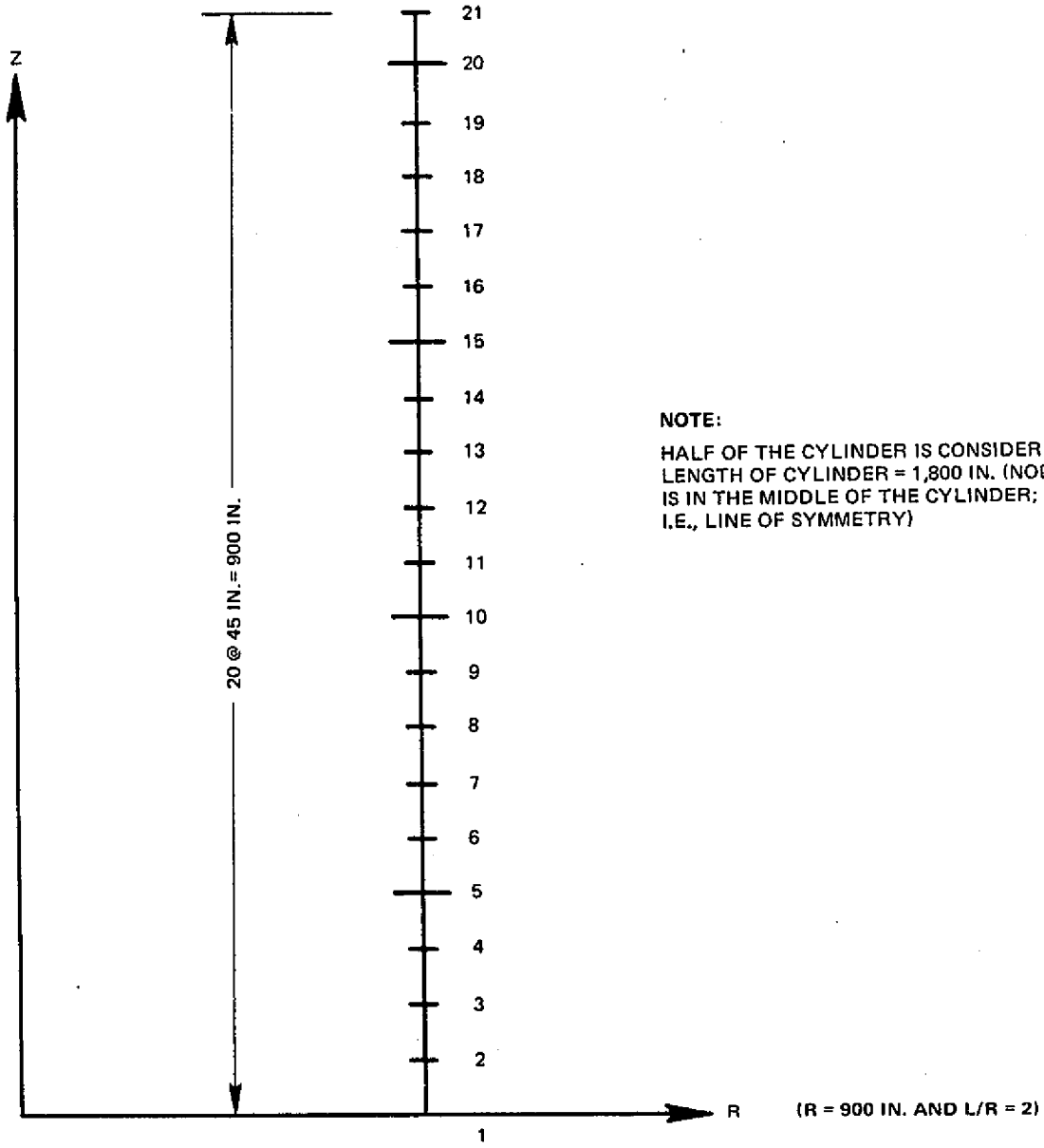

NOTE:

HALF OF THE CYLINDER IS CONSIDERED. LENGTH OF CYLINDER = 1,800 IN. (NODE 1 IS IN THE MIDDLE OF THE CYLINDER; I.E., LINE OF SYMMETRY)

BOUNDARY CONDITIONS, NODE 1:

Z DISPL = 0
θ DISPL = 0
ROTATION IN R-Z PLANE = 0

BOUNDARY CONDITIONS, NODE 21:

R DISPL = 0
θ DISPL = 0

NUMERICAL DATA

MATERIAL – CONCRETE
E = 4,030,508/IN.^{2}
t = 36 IN.
R = 900 IN.
ν = 0.17
p = 60/IN.^{2}

Updated

SAN ONOFRE NUCLEAR GENERATING STATION Units 2 & 3

FINITE-ELEMENT MODEL, SIMPLY SUPPORTED CYLINDER (ASHSD EXAMPLE 2)

Figure 3C.2-4

10079-11D-1353

Amended: April 2009 TL: E047997

Site File Copy

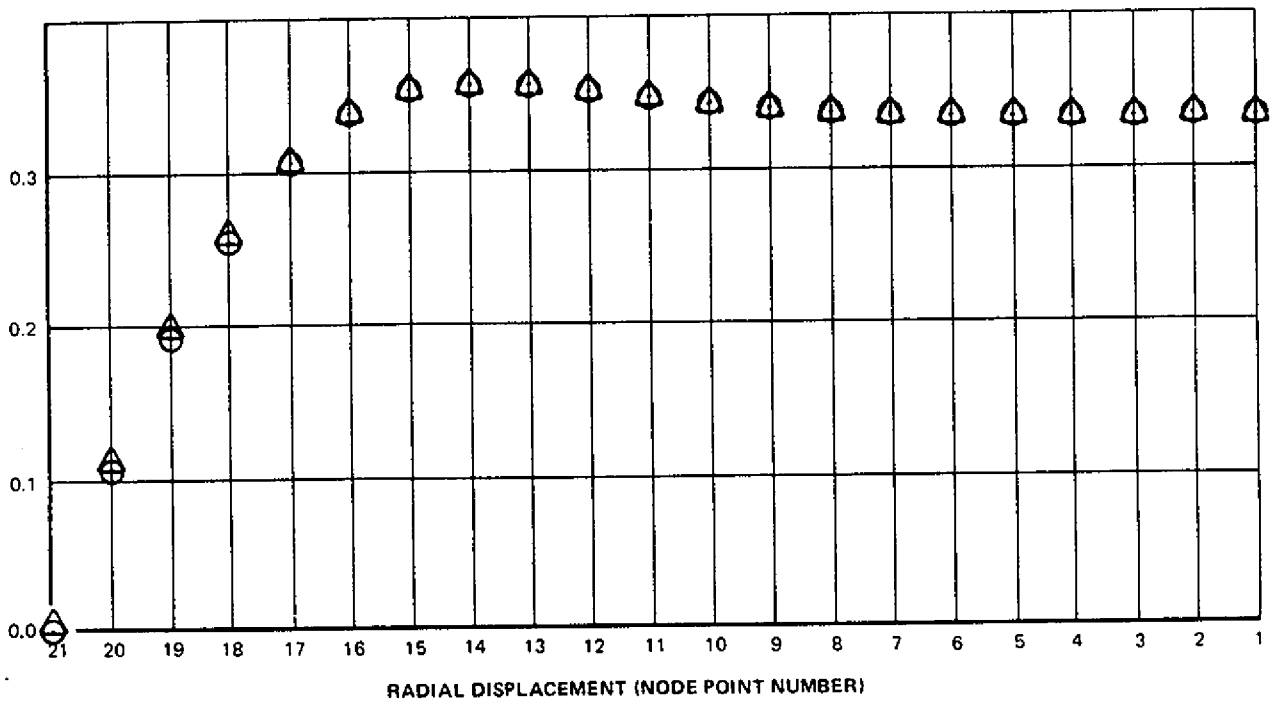

LEGEND:
⊙ ASHSD
△ ANALYTICAL, PER THEORY OF PLATES AND SHELLS (3)

Updated

SAN ONOFRE NUCLEAR GENERATING STATION Units 2 & 3

COMPARISON OF ASHSD RADIAL AND ANALYTICALLY OBTAINED DISPLACEMENTS (ASHSD EXAMPLE 2)

Figure 3C.2-5

10079-11D-1354

Amended: April 2009 TL: E047997

Site File Copy

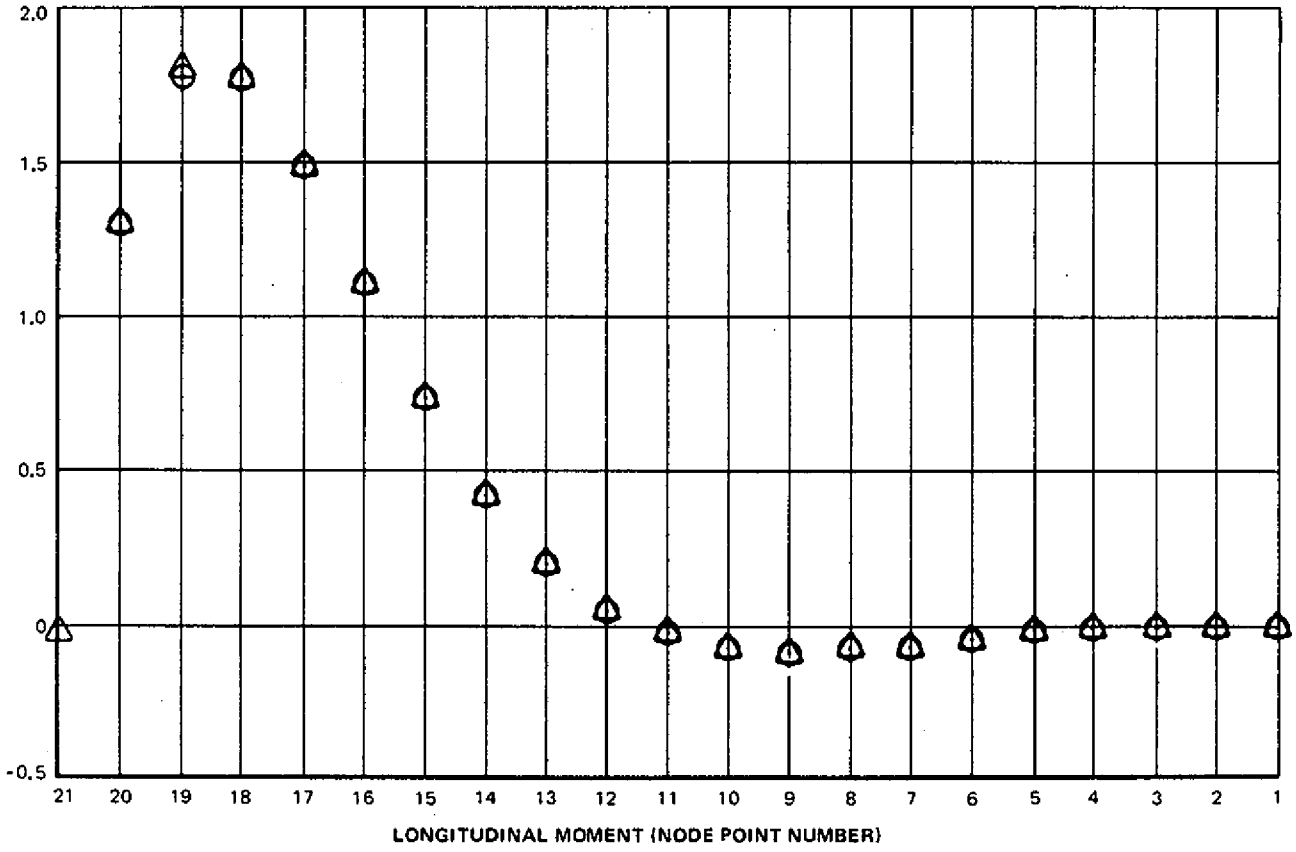

LEGEND:
⊙ ASHSD
△ ANALYTICAL, PER THEORY OF PLATES AND SHELLS[3]

Updated

SAN ONOFRE NUCLEAR GENERATING STATION Units 2 & 3
COMPARISON OF ASHSD LONGITUDINAL AND ANALYTICALLY OBTAINED MOMENTS (ASHSD EXAMPLE 2)
Figure 3C.2-6

10079-11D-1385
250C6

Amended: April 2009 TL: E047997

Site File Copy

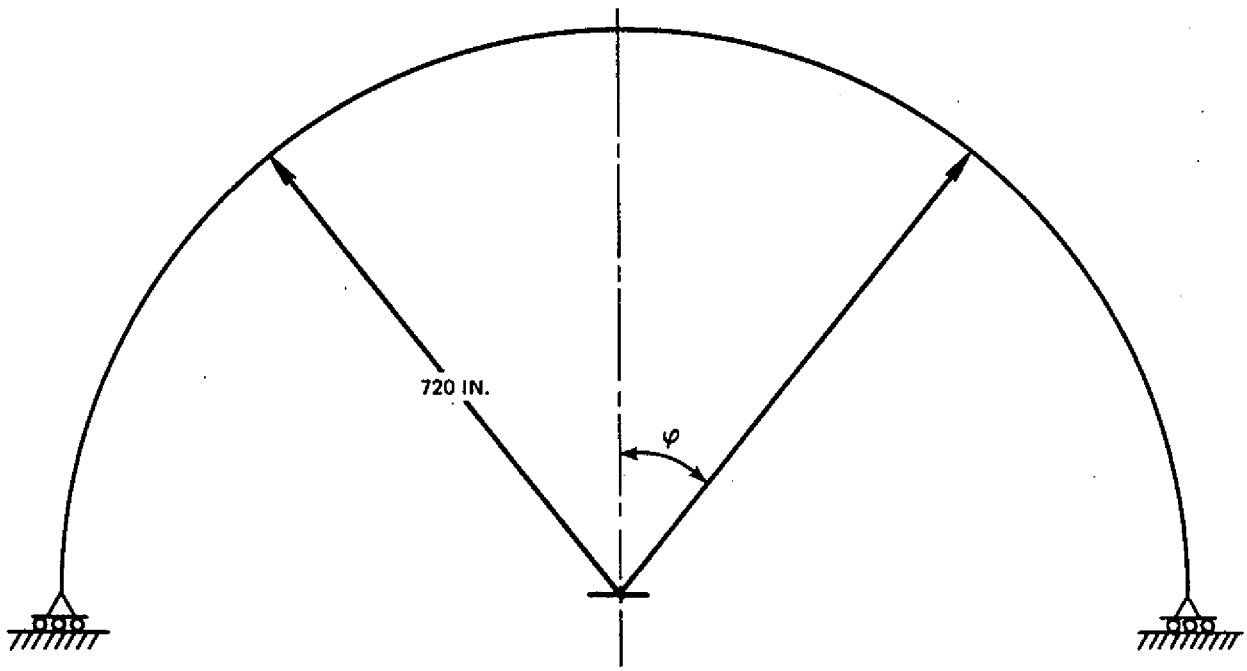

Updated

SAN ONOFRE NUCLEAR GENERATING STATION Units 2 & 3
SPHERICAL DOME (ASHSD EXAMPLE 3)
Figure 3C.2-7

10079-11D-1356

Amended: April 2009 TL: E047997

Site File Copy

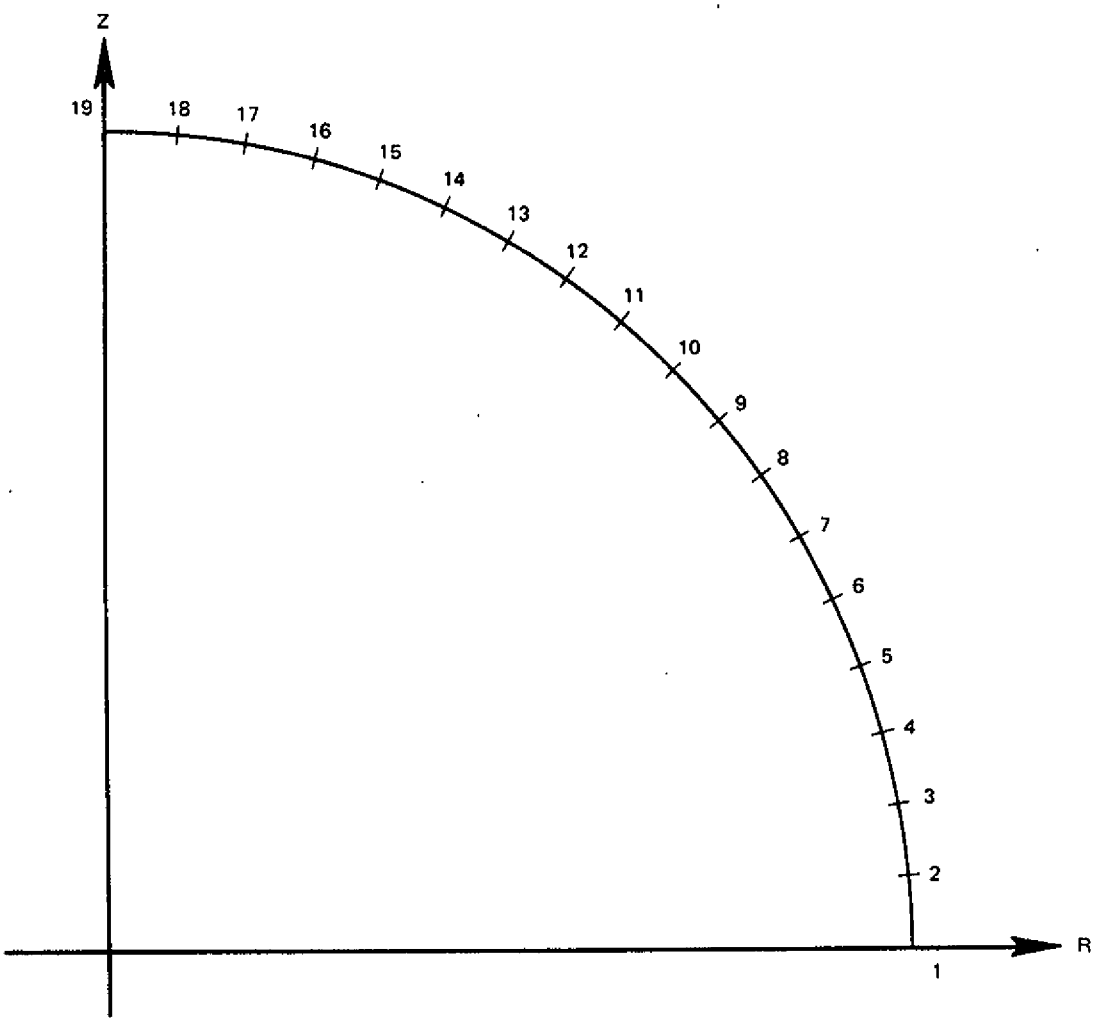

BOUNDARY CONDITIONS, NODE 1:

Z DISPL = 0

BOUNDARY CONDITIONS, NODE 19:

R DISPL = 0

ROTATION IN R-Z PLANE = 0

NUMERICAL DATA

MATERIAL: CONCRETE

E = 4,030,508/IN.^{2}

t = 36 IN.

R = 720 IN.

ν = 0.17

SPECIFIC WEIGHT OF CONCRETE = 150 LB/FT^3

MASS DENSITY OF CONCRETE:

$$\frac{150}{386.4 \times 1728} = 2.246 \times 10^{-4} \ \frac{\text{LB SEC}^2}{\text{IN.}^4}$$

Updated

SAN ONOFRE NUCLEAR GENERATING STATION Units 2 & 3
FINITE-ELEMENT MODEL, SPHERICAL DOME, DEAD LOAD ANALYSIS (ASHSD EXAMPLE 3)
Figure 3C.2-8

10079-11D-1357

Amended: April 2009 TL: E047997

Site File Copy

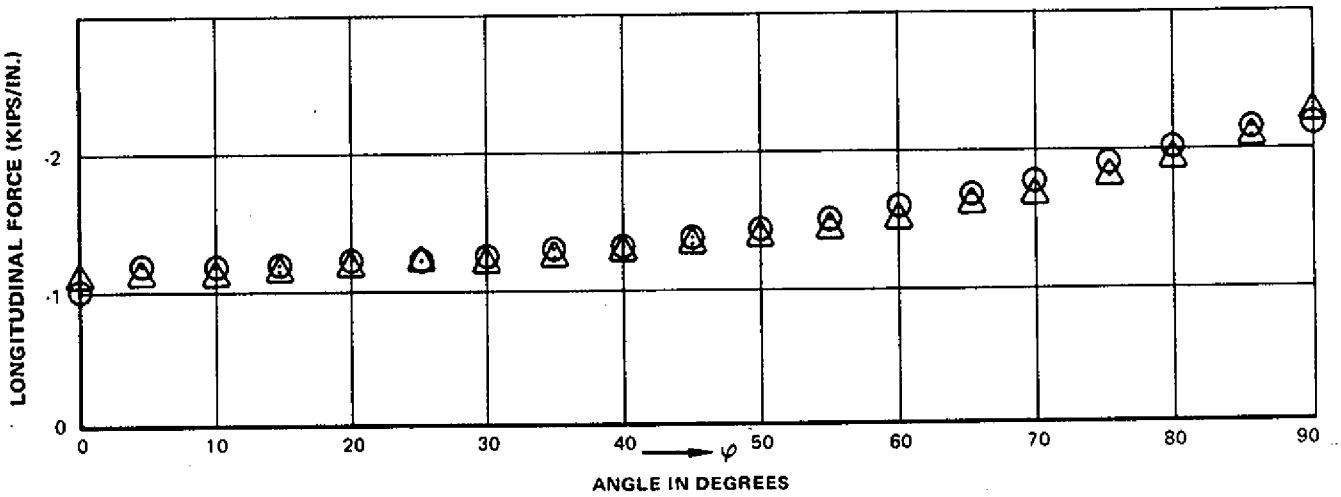

LEGEND:
⊙ ASHSD
△ ANALYTICAL, PER APPLIED ELASTICITY[4]

Updated

SAN ONOFRE NUCLEAR GENERATING STATION Units 2 & 3

COMPARISON OF ASHSD AND ANALYTICALLY OBTAINED LONGITUDINAL FORCES (ASHSD EXAMPLE 3)

Figure 3C.2-9

10079-11D-1358

Amended: April 2009 TL: E047997

Site File Copy

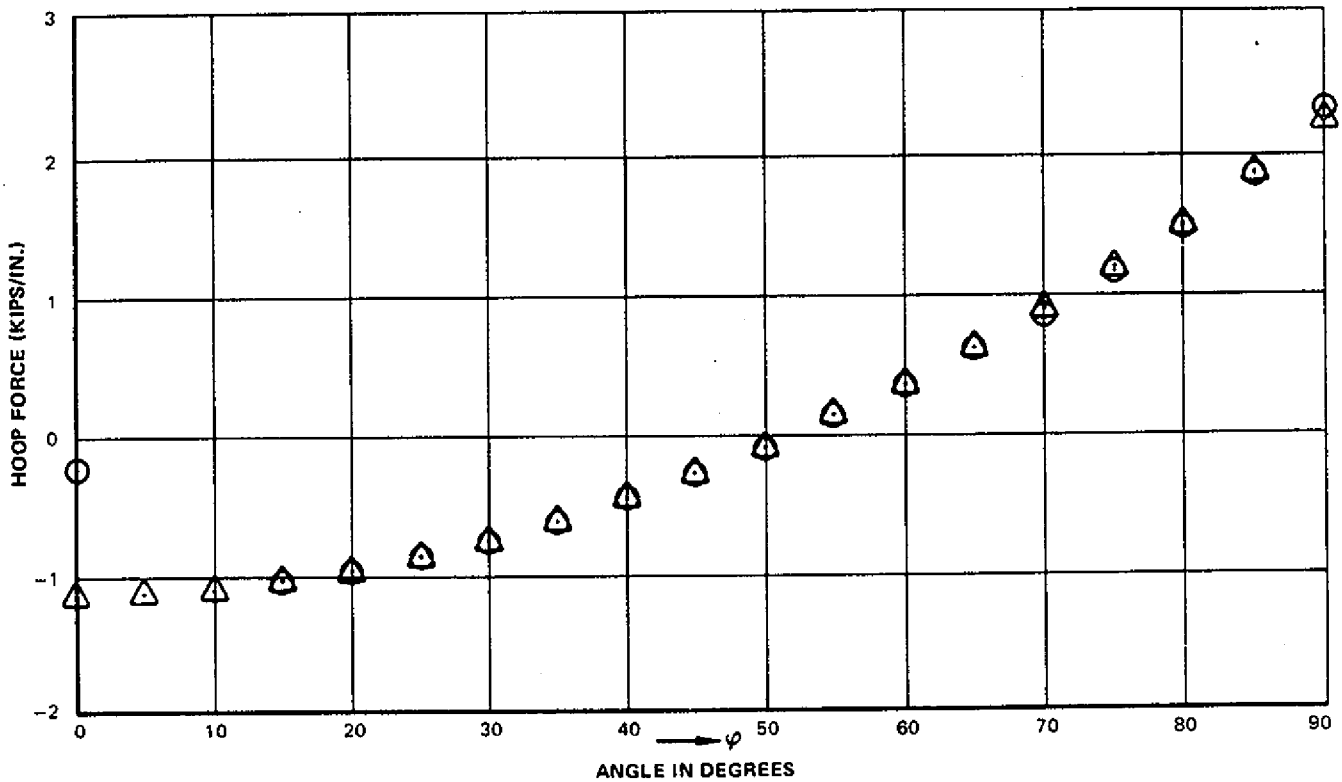

LEGEND:
⊙ ASHSD
△ ANALYTICAL, PER APPLIED ELASTICITY[4]

Updated

SAN ONOFRE
NUCLEAR GENERATING STATION
Units 2 & 3

COMPARISON OF ASHSD AND ANALYTICALLY OBTAINED CIRCUMFERENTIAL FORCES (ASHSD EXAMPLE 3)

Figure 3C.2-10

10079-11D-1359

Amended: April 2009 TL: E047997

Site File Copy

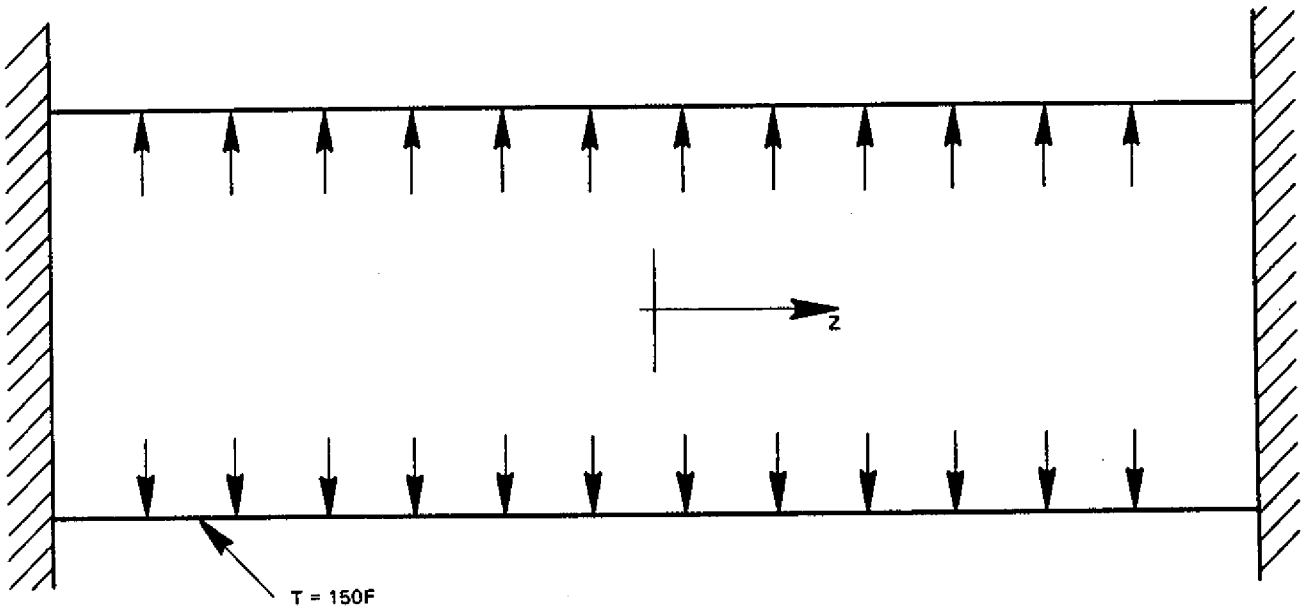

NUMERICAL DATA

MATERIAL – CONCRETE

E	=	4,030,508/IN.^{2}
ν	=	0.17
α	=	$55 \times 10^{-7}/^{o}F$
t	=	30 IN.
R	=	600 IN.
L	=	1,200 IN.
p	=	60/IN.^{2}
T	=	150 F
R/t	=	20
L/R	=	2
R/t	=	20

Updated

SAN ONOFRE NUCLEAR GENERATING STATION Units 2 & 3
PRESSURIZED, UNIFORMLY HEATED, CIRCULAR CYLINDRICAL SHELL WITH CLAMPED ENDS (ASHSD EXAMPLE 4)
Figure 3C.2-11

10079-11D-1360

Amended: April 2009 TL: E047997

Site File Copy

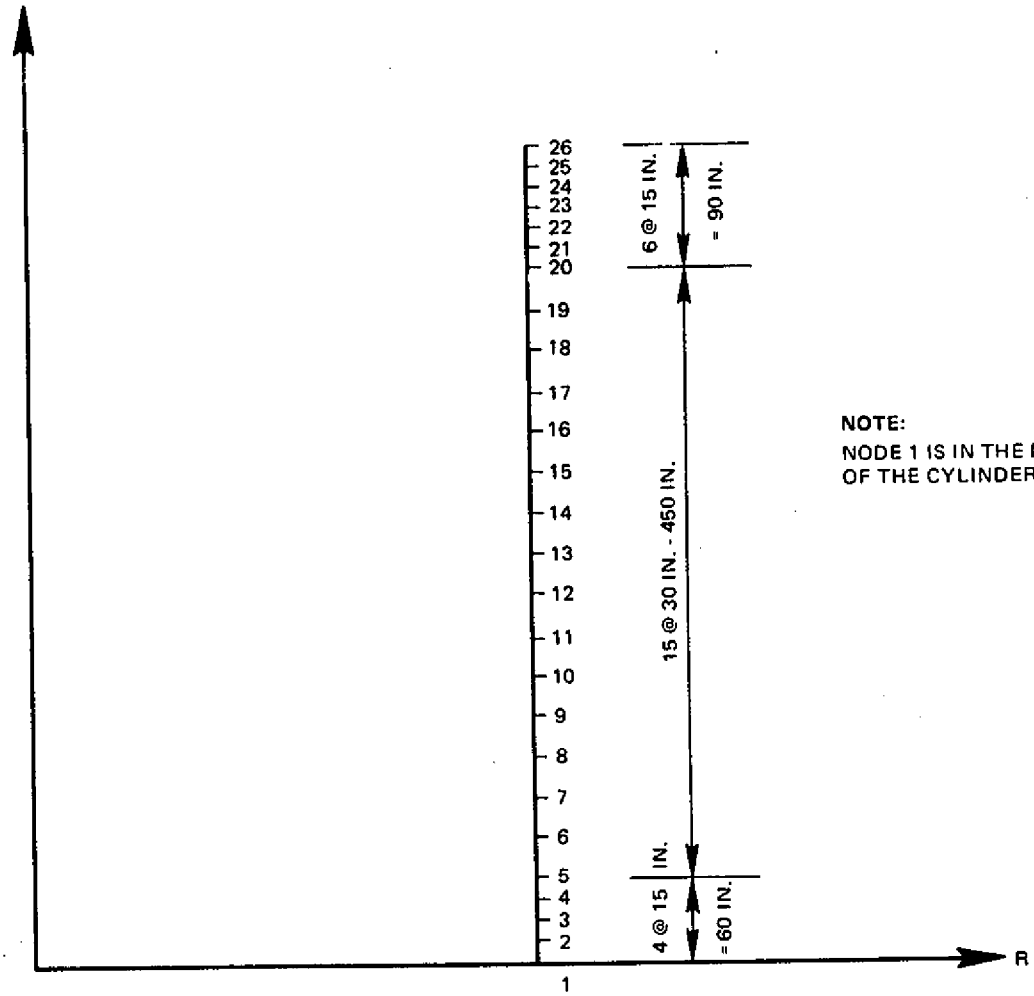

NOTE:
NODE 1 IS IN THE MIDDLE OF THE CYLINDER

BOUNDARY CONDITIONS, NODE 1:

Z DISPL = 0
θ DISPL = 0
ROTATION IN R-Z PLANE = 0

BOUNDARY CONDITIONS, NODE 26:

R DISPL = 0
Z DISPL = 0
θ DISPL = 0

ROTATION IN R-Z PLANE = 0

Updated

SAN ONOFRE NUCLEAR GENERATING STATION Units 2 & 3
FINITE-ELEMENT MODEL (ASHSD EXAMPLE 4)
Figure 3C.2-12

10079-11D-1361

Amended: April 2009 TL: E047997

Site File Copy

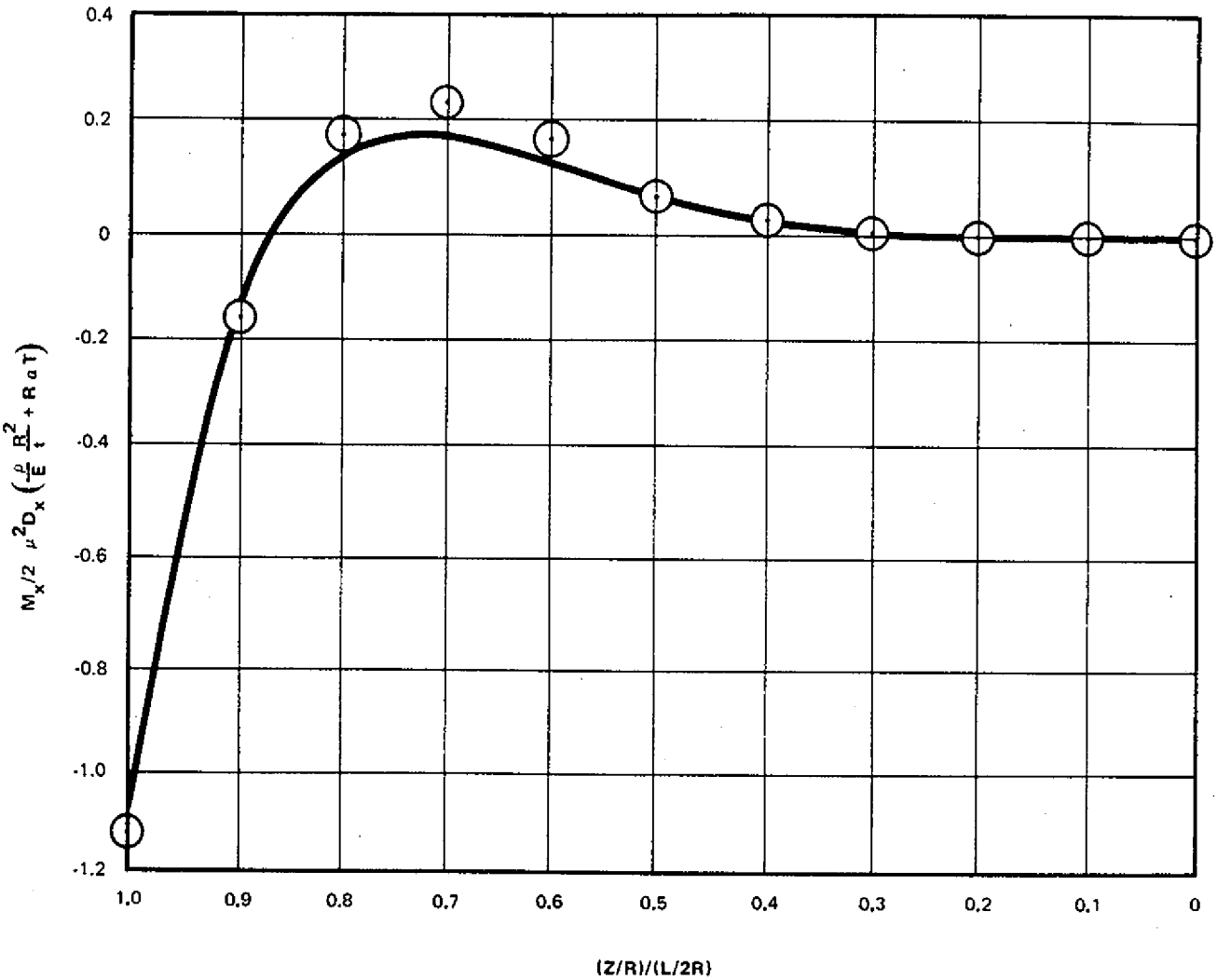

$$\mu = \left(\frac{3(1-\nu^2)}{R^2T^2}\right)^{1/2}$$

$$D_x = \frac{Et^3}{12(1-\nu^2)}$$

LEGEND:
- ⊙ ASHSD
- ▬ ANALYTICAL PER THIN ELASTIC SHELLS [5]

Updated

SAN ONOFRE NUCLEAR GENERATING STATION Units 2 & 3

COMPARISON OF ASHSD LONGITUDINAL MOMENTS AND ANALYTICALLY OBTAINED (ASHSD EXAMPLE 4)

Figure 3C.2-13

10079-11D-1362

Amended: April 2009 TL: E047997

Site File Copy

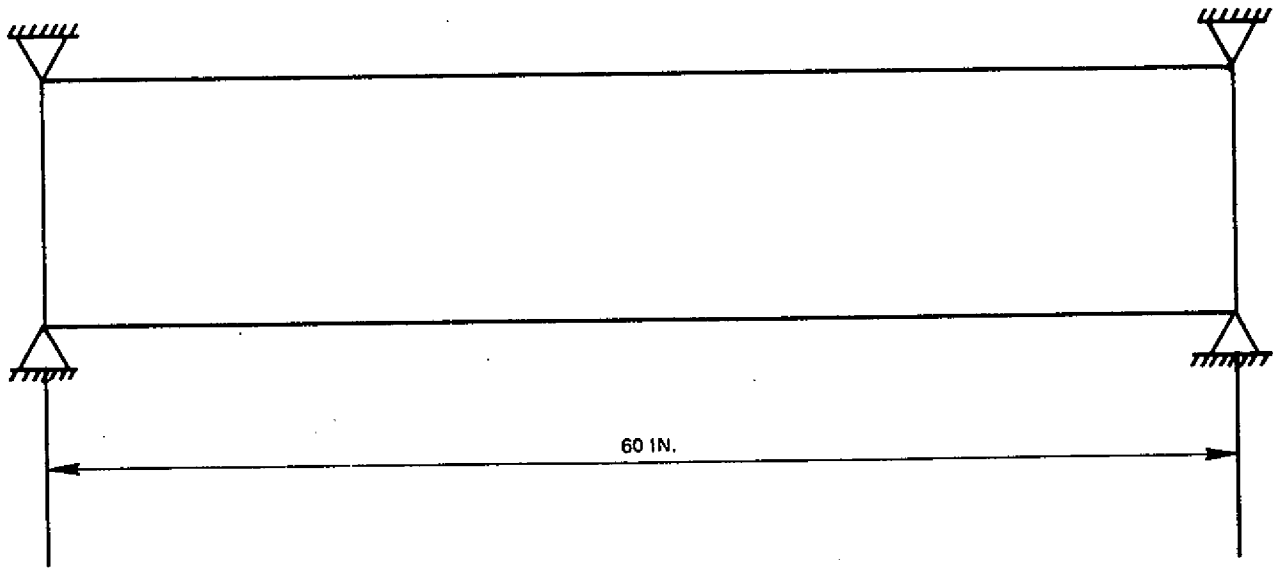

Updated

SAN ONOFRE NUCLEAR GENERATING STATION Units 2 & 3
SHORT, WIDE CYLINDER (ASHSD EXAMPLE 5)
Figure 3C.2-14

10079-11D-1363

Amended: April 2009 TL: E047997

Site File Copy

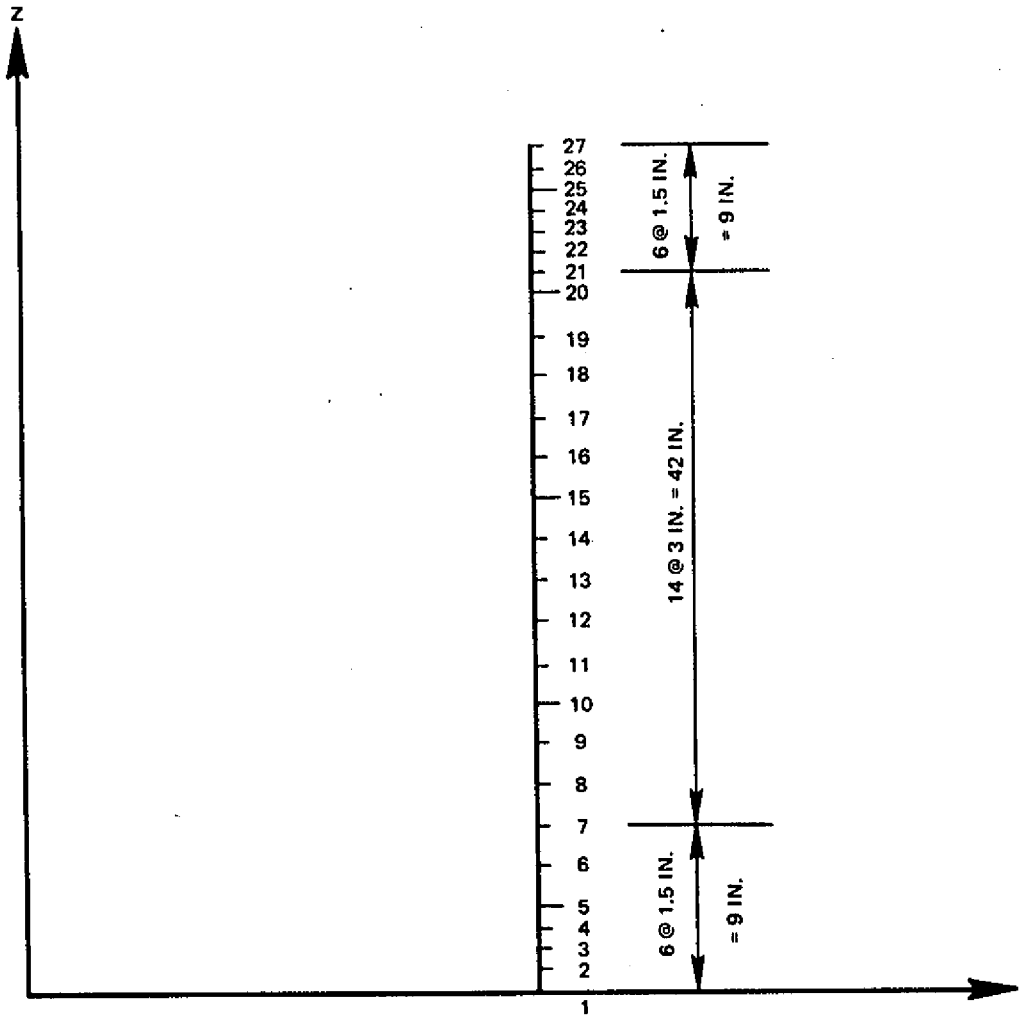

NUMERICAL DATA

MATERIAL: STEEL

$E = 29 \times 10^6/\text{IN.}^2$

$t = 1.25$ IN.

$R = 60.0$ IN.

$\nu = 0.3$

$L = 60.0$ IN.

$L/R = 1$

$R/t = 48$

$$M_o = \frac{Et^2}{100\,(1-\nu^2)} = 497{,}939.66 \text{ LB} - \text{IN./IN.}$$

Updated

SAN ONOFRE NUCLEAR GENERATING STATION Units 2 & 3
FINITE-ELEMENT MODEL; SHORT, WIDE CYLINDER (ASHSD EXAMPLE 5)
Figure 3C.2-15

10079-11D-1364

Amended: April 2009 TL: E047997

Site File Copy

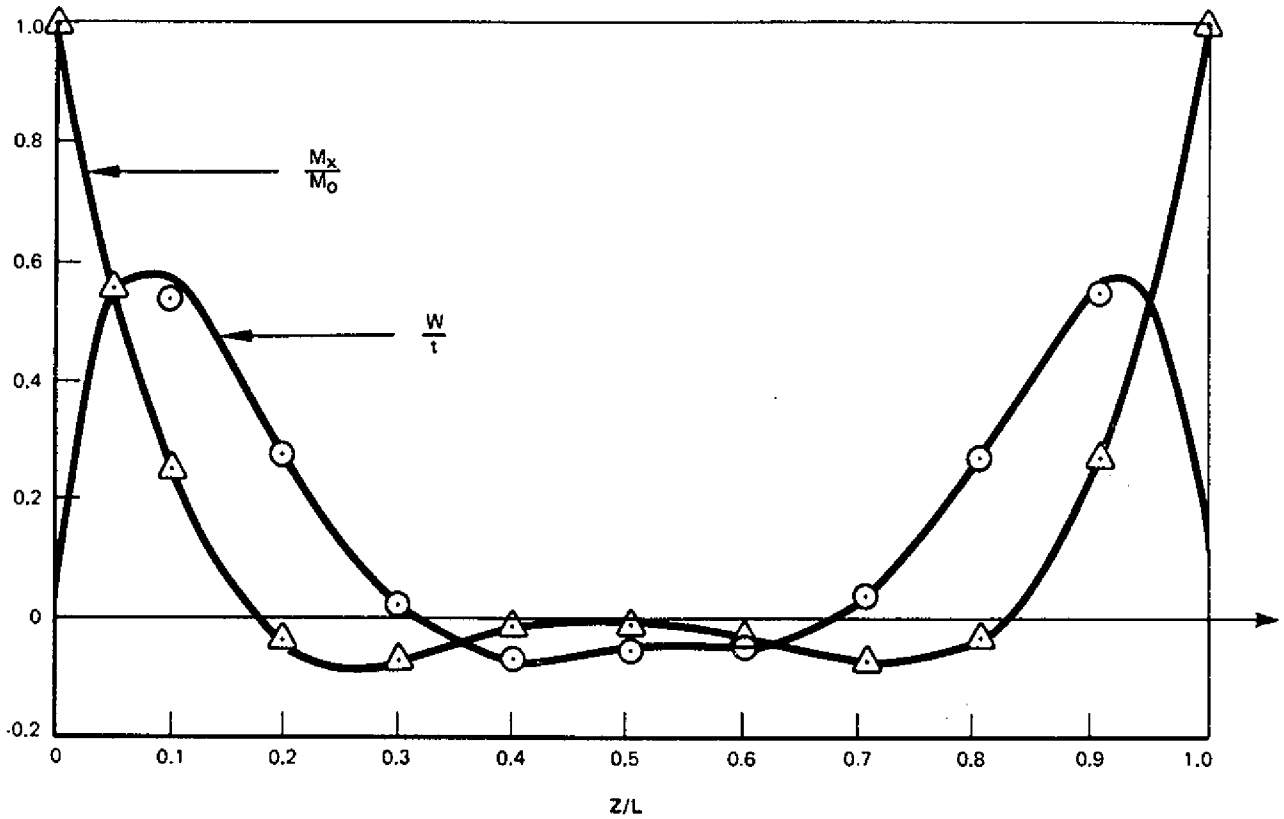

LEGEND:

- ⊙ ASHSD (RADIAL DISPLACEMENT W)
- △ ASHSD (LONGITUDINAL MOMENT M_x)
- ▬ ANALYTICAL, PER NUMERICAL ANALYSIS OF UNSYMMETRIC BENDING OF SHELLS[6]

Updated

SAN ONOFRE NUCLEAR GENERATING STATION Units 2 & 3
LONGITUDINAL BENDING MOMENT AND RADIAL DISPLACEMENT, HARMONIC n = 0 (ASHSD EXAMPLE 5)
Figure 3C.2-16

10079-11D-1365

Amended: April 2009 TL: E047997

Site File Copy

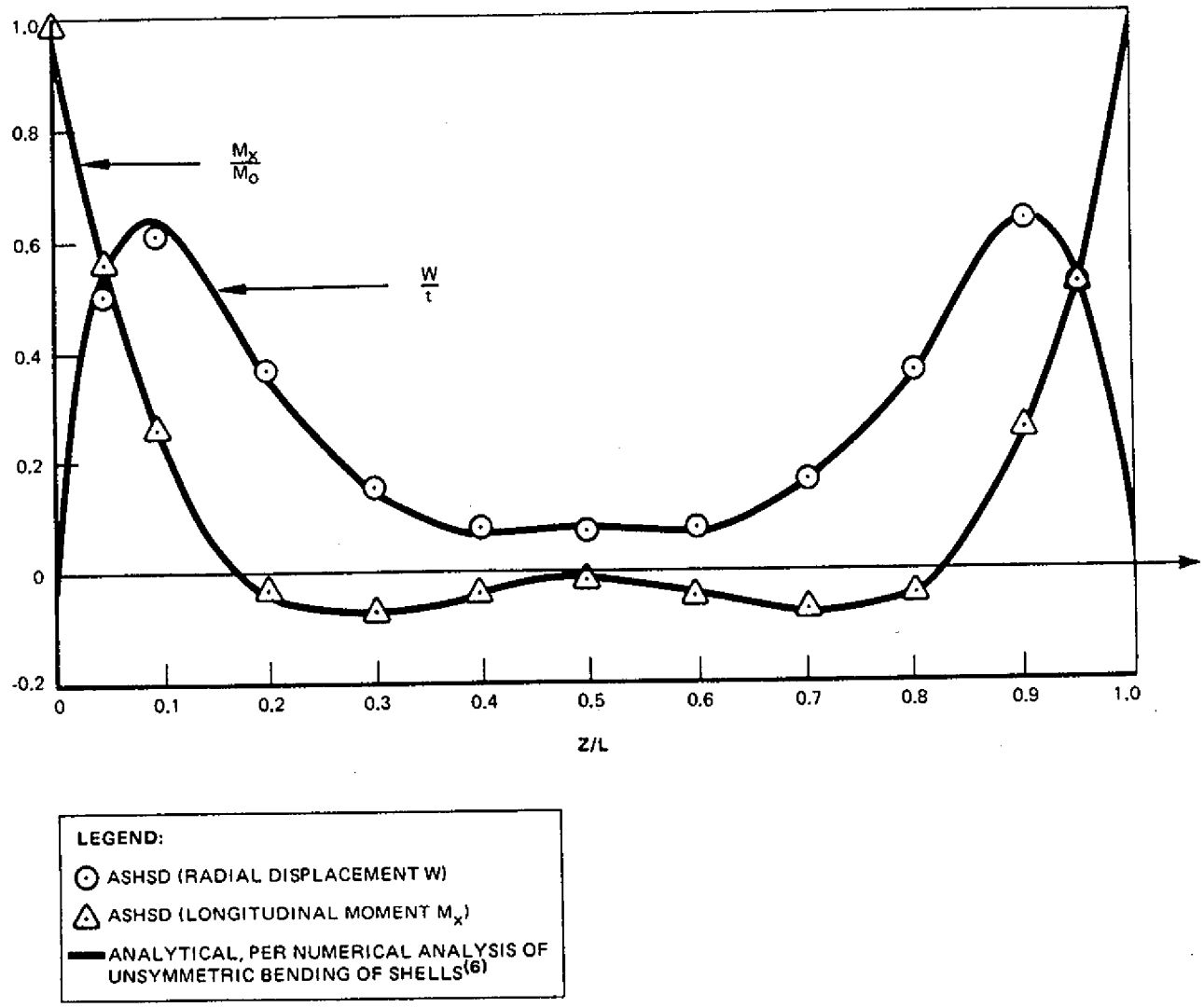

Updated

SAN ONOFRE NUCLEAR GENERATING STATION Units 2 & 3
LONGITUDINAL BENDING MOMENT AND RADIAL DISPLACEMENT, HARMONIC n = 2 (ASHSD EXAMPLE 5)
Figure 3C.2-17

10079-11D-1366

Amended: April 2009 TL: E047997

Site File Copy

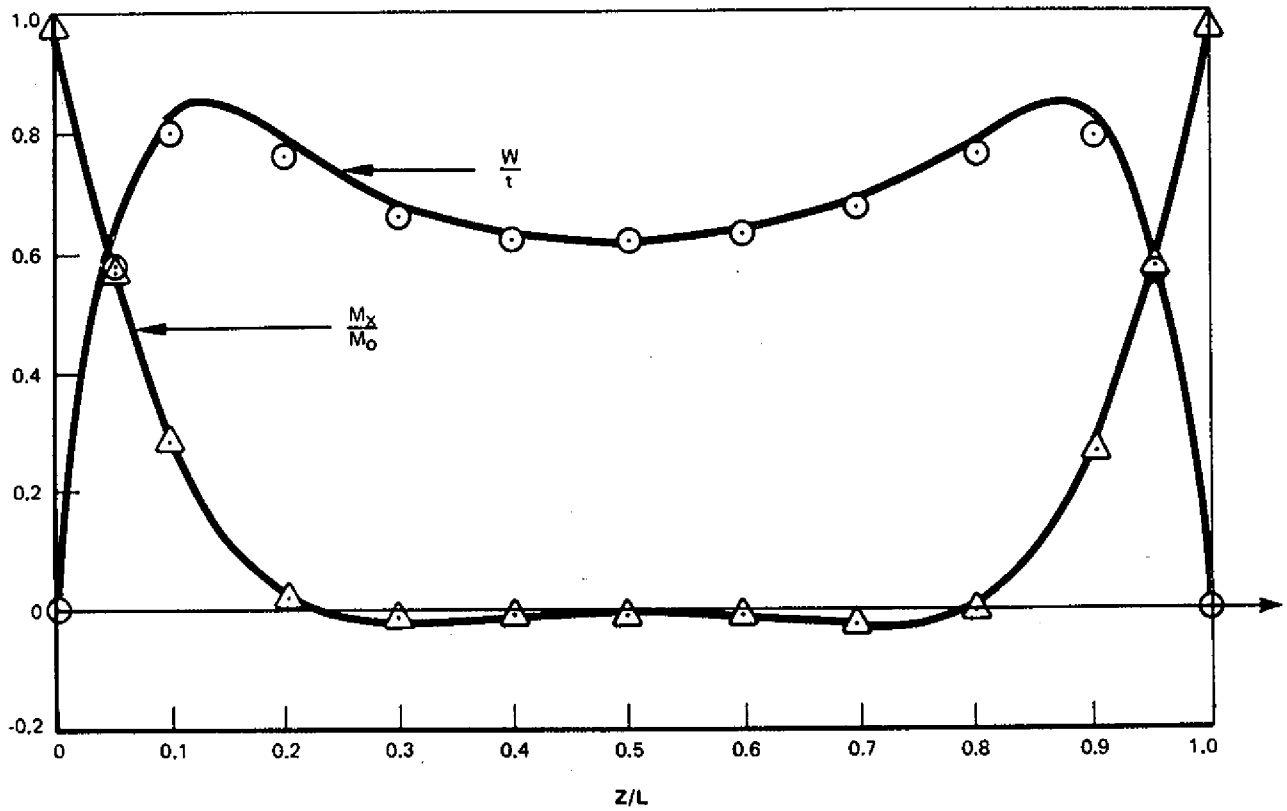

LEGEND:

- ⊙ ASHSD (RADIAL DISPLACEMENT W)
- △ ASHSD (LONGITUDINAL MOMENT M_x)
- ▬ ANALYTICAL, PER NUMERICAL ANALYSIS OF UNSYMMETRIC BENDING OF SHELLS[6]

Updated

SAN ONOFRE NUCLEAR GENERATING STATION Units 2 & 3
LONGITUDINAL BENDING MOMENT AND RADIAL DISPLACEMENT, HARMONIC n = 5 (ASHSD EXAMPLE 5)
Figure 3C.2-18

10079-11D-1367

Amended: April 2009 TL: E047997

Site File Copy

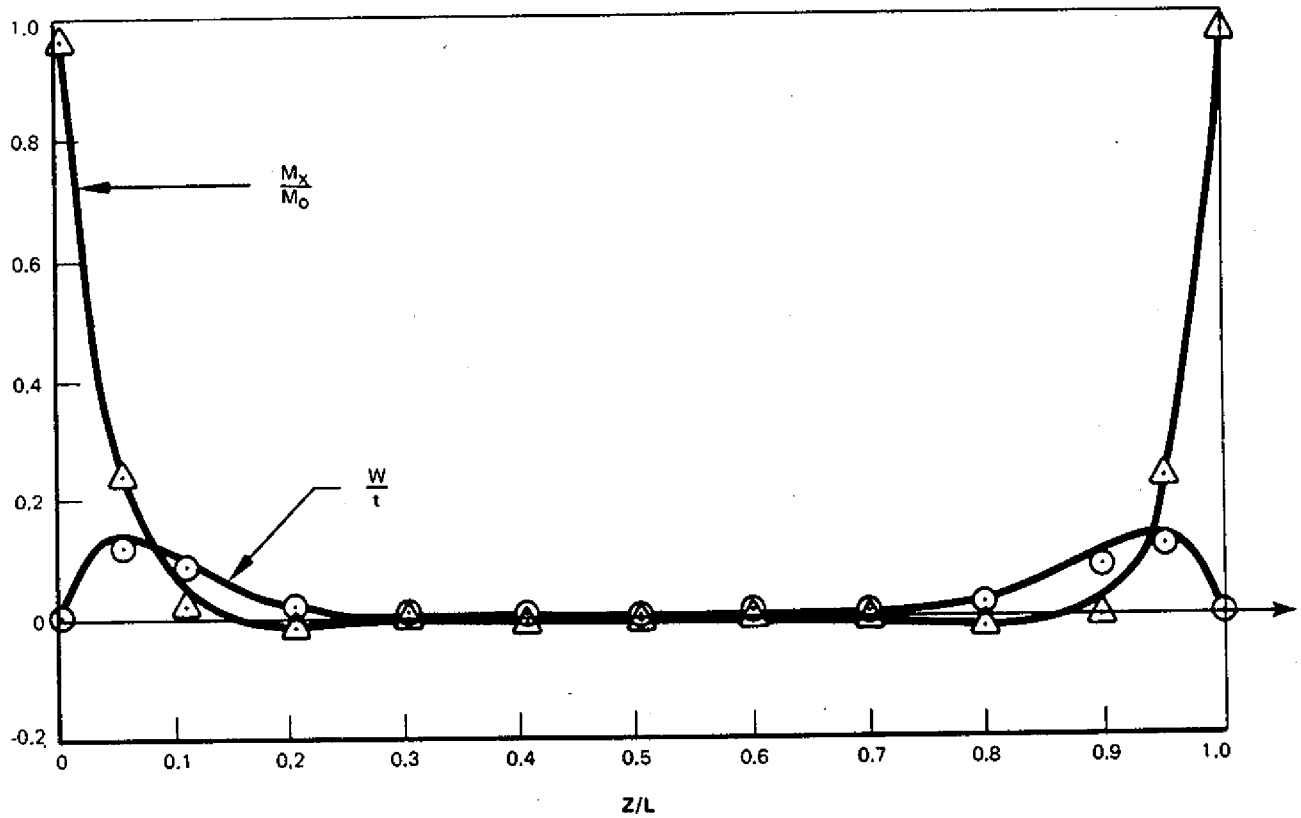

LEGEND:

- ⊙ ASHSD (RADIAL DISPLACEMENT W)
- △ ASHSD (LONGITUDINAL MOMENT M_x)
- ▬ ANALYTICAL, PER NUMERICAL ANALYSIS OF UNSYMMETRIC BENDING OF SHELLS[6]

Updated

SAN ONOFRE NUCLEAR GENERATING STATION Units 2 & 3
LONGITUDINAL BENDING MOMENT AND RADIAL DISPLACEMENT, HARMONIC n = 20 (ASHSD EXAMPLE 5)
Figure 3C.2-19

10079-11D-1368

Amended: April 2009 TL: E047997

Site File Copy

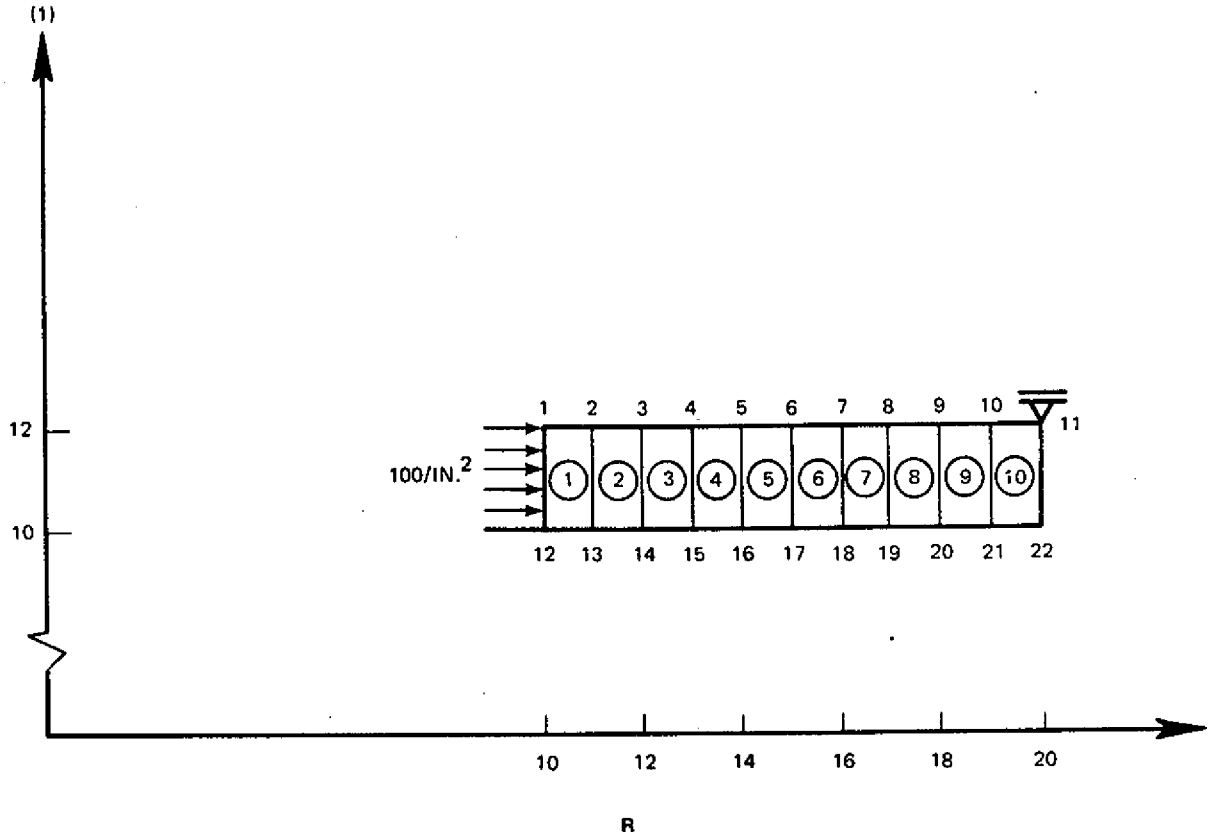

Updated

SAN ONOFRE NUCLEAR GENERATING STATION Units 2 & 3
FINITE-ELEMENT MODEL AND APPLIED LOAD (ASHSD EXAMPLE 6)
Figure 3C.2-20

10079-11D-1369

Amended: April 2009 TL: E047997

Site File Copy

BOUNDARY CONDITIONS:

NODE 1: R–DISPLACEMENT = 0
θ–DISPLACEMENT = 0

NODE 12: R–DISPLACEMENT = 0
θ–DISPLACEMENT = 0
Z–DISPLACEMENT = 0

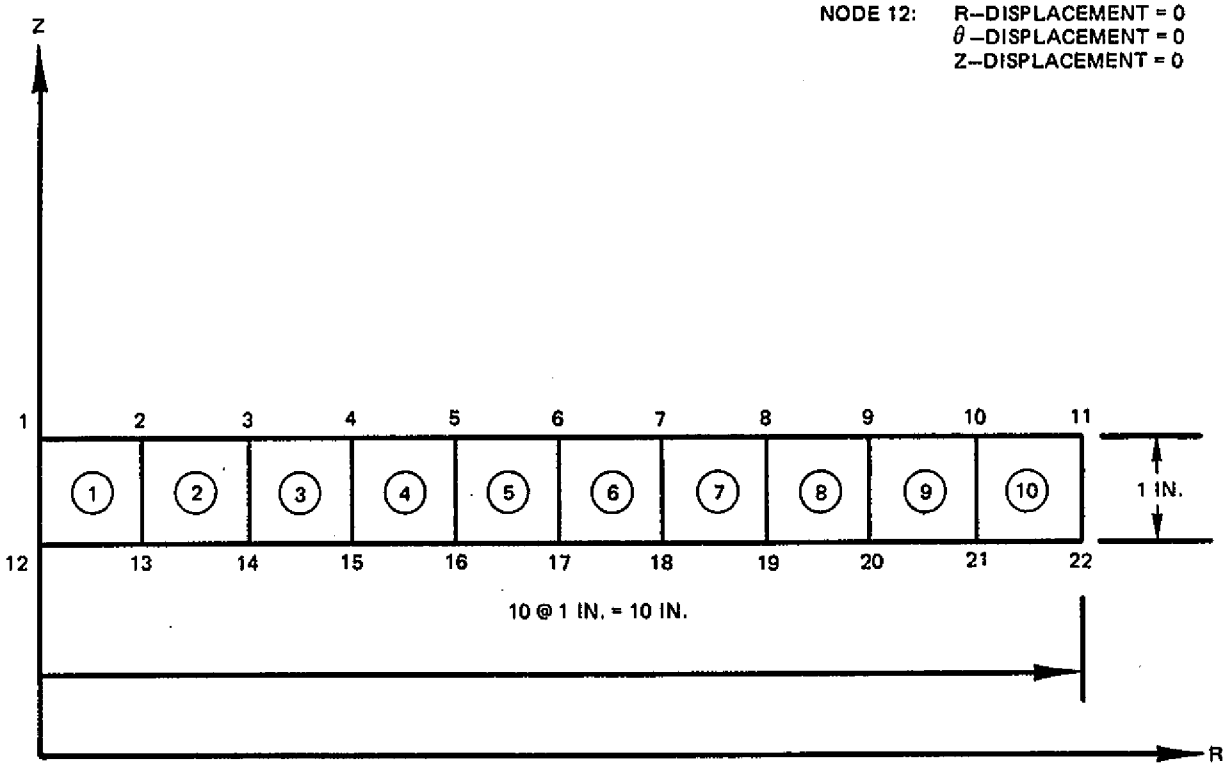

NUMERICAL DATA:

MATERIAL – CONCRETE

E = 4030508 LB/IN.^{2}

ν = 0.17

ρ = 2.246 x 10^{-4} LB-S^2/IN.^{4}

ω = ANGULAR VELOCITY OF ROTATING DISK = 150 RAD/S

R = 10 IN.

Updated

SAN ONOFRE NUCLEAR GENERATING STATION Units 2 & 3
FINITE ELEMENT MODEL (ASHSD EXAMPLE 7)
Figure 3C.2-21

10079-11D-1370

Amended: April 2009 TL: E047997

Site File Copy

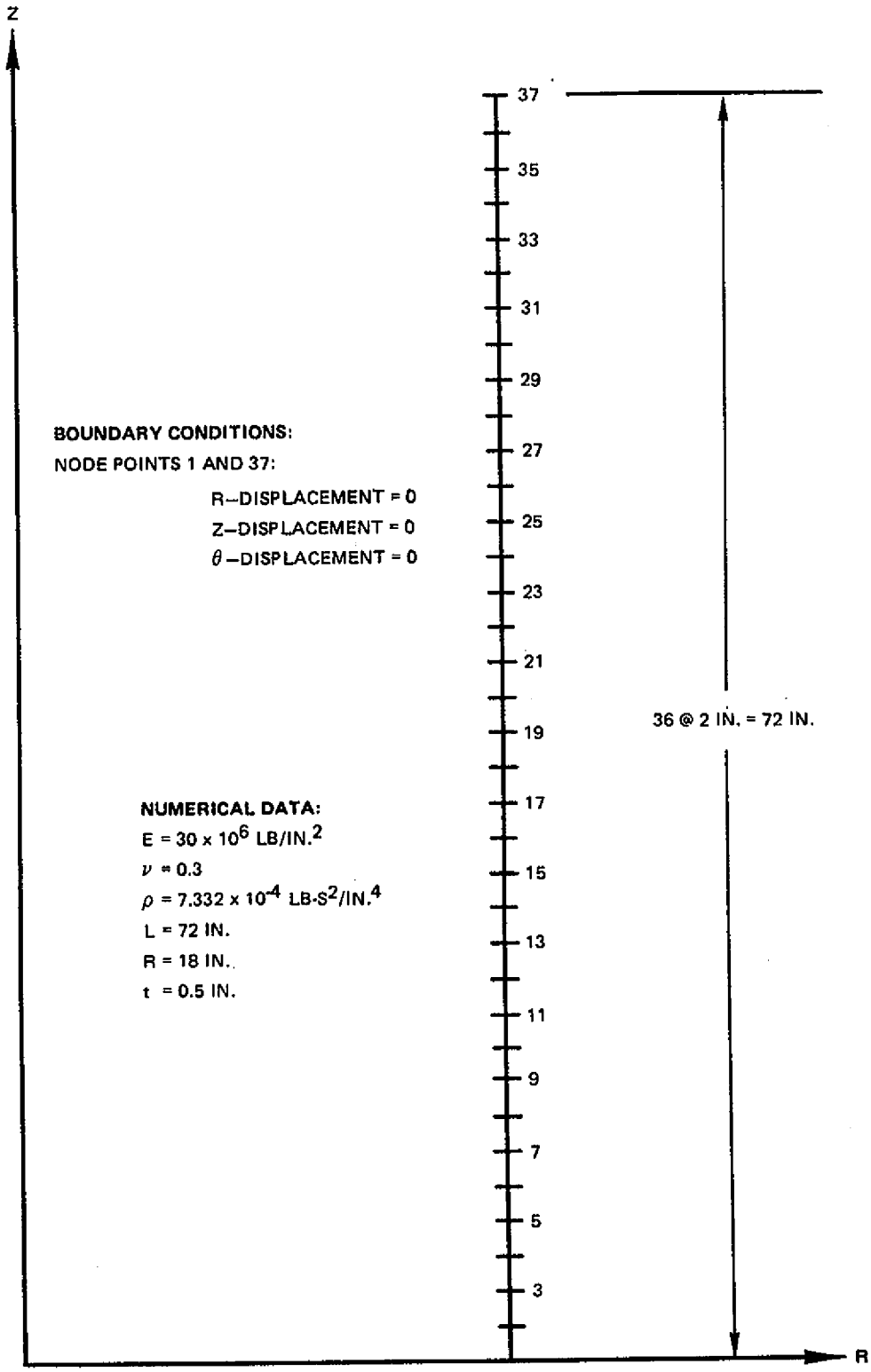

BOUNDARY CONDITIONS:

NODE POINTS 1 AND 37:

R–DISPLACEMENT = 0

Z–DISPLACEMENT = 0

θ–DISPLACEMENT = 0

NUMERICAL DATA:

$E = 30 \times 10^6$ LB/IN.^{2}

$\nu = 0.3$

$\rho = 7.332 \times 10^{-4}$ LB-S^2/IN.^{4}

L = 72 IN.

R = 18 IN.

t = 0.5 IN.

Updated

SAN ONOFRE NUCLEAR GENERATING STATION Units 2 & 3

FINITE ELEMENT MODEL (ASHSD EXAMPLE 8)

Figure 3C.2-22

10079-11D-1371

Amended: April 2009 TL: E047997

Site File Copy

MODEL

NUMERICAL DATA

MASS POINTS	M_i (a) (K-sec^2/ft)	M_{ii} (b) (K-sec^2/ft)	ℓ_i (c) (ft)	A_i (d) (ft^2)	A_i (e) (ft^2)	I_i (f) (ft^4)
8	15	2,000				
			12.0	420	180	60,000
7	35	5,000				
			13.0	710	310	110,000
6	170	155,000				
			11.0	1,970	830	1,240,000
5	105	64,000				
			11.0	1,970	830	1,240,000
4	120	80,000				
			12.0	2,420	1,330	1,270,000
3	185	71,000				
			10.5	2,420	1,330	1,270,000
2	200	126,000				
			9.0	2,330	1,580	1,200,000
1	140	100,000				
			13.5	2,330	1,420	380,000

a. LUMPED MASS AT POINT i
b. MASS MOMENT OF INERTIA AT POINT i
c. LENGTH OF ELEMENT i
d. CROSS-SECTION AREA OF ELEMENT i
e. SHEAR AREA OF ELEMENT i
f. MOMENT OF INERTIA OF ELEMENT i

ADDITIONAL PARAMETERS

1. ELASTIC MODULUS E = 617,000 K/FT^2
2. POISSON'S RATIO ν = 0.167

Updated

SAN ONOFRE NUCLEAR GENERATING STATION Units 2 & 3

LUMPED-MASS MODEL (SUPER SMIS EXAMPLE 1)

Figure 3C.3-1

10079-11D-1372

Amended: April 2009 TL: E047997

Site File Copy

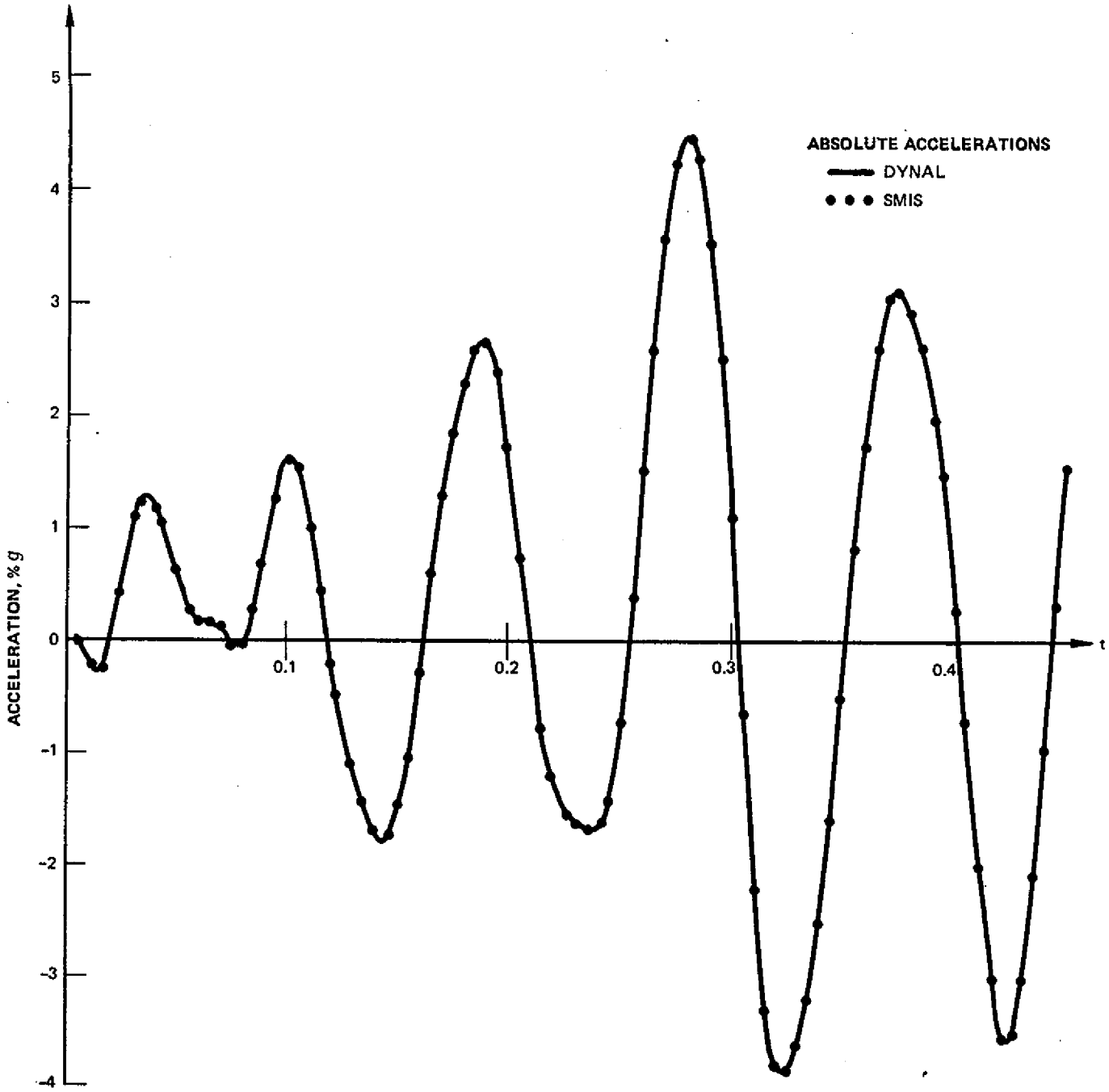

Updated

SAN ONOFRE NUCLEAR GENERATING STATION Units 2 & 3
ABSOLUTE ACCELERATION (SUPER SMIS EXAMPLE 1)
Figure 3C.3-2

10079-11D-1373
250C6

Amended: April 2009 TL: E047997

Site File Copy

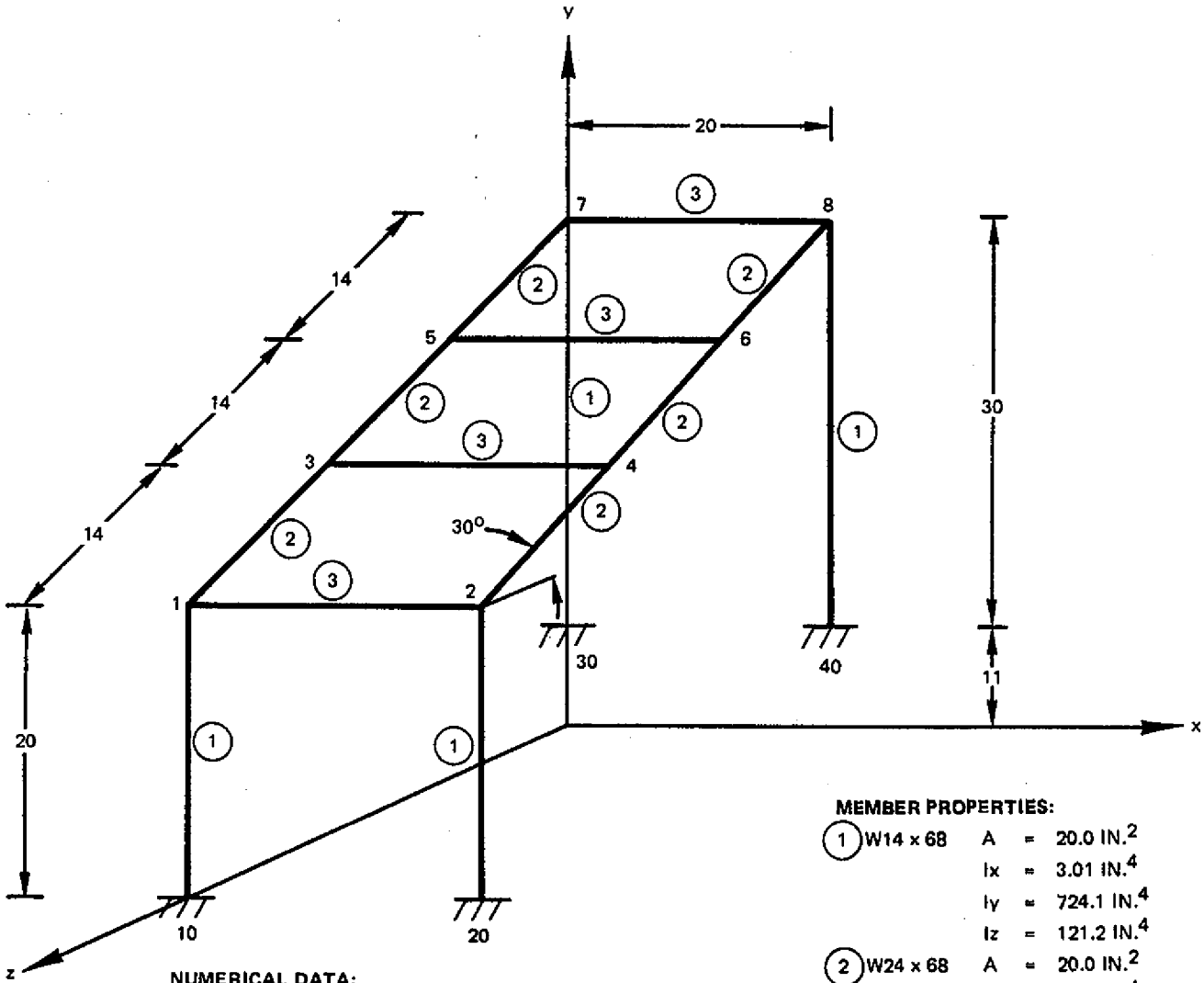

NUMERICAL DATA:

ELASTIC MODULUS $E = 30 \times 10^6$ LB/IN^2

MODULUS OF RIGIDITY $G = 11.5 \times 10^6$ LB/IN.^{2}

POISSON'S RATIO $\nu = 0.31$

MASS DENSITY $\rho = 0.000735 \frac{\text{LB-S}^2}{\text{IN.}^4}$

MEMBER PROPERTIES:

(1)	W14 x 68	A	=	20.0 IN.^{2}
		Ix	=	3.01 IN.^{4}
		Iy	=	724.1 IN.^{4}
		Iz	=	121.2 IN.^{4}
(2)	W24 x 68	A	=	20.0 IN.^{2}
		Ix	=	1.97 IN.^{4}
		Iy	=	153.1 IN.^{4}
		Iz	=	1814.5 IN.^{4}
(3)	W14 x 34	A	=	10.0 IN.^{2}
		Ix	=	0.603 IN.^{4}
		Iy	=	339.2 IN.^{4}
		Iz	=	21.3 IN.^{4}

Updated

SAN ONOFRE
NUCLEAR GENERATING STATION
Units 2 & 3

EIGENVALUE ANALYSIS MODEL
(SUPER SMIS EXAMPLE 2)

Figure 3C.3-3

10079-11D-1374
25066

Amended: April 2009 TL: E047997

Site File Copy

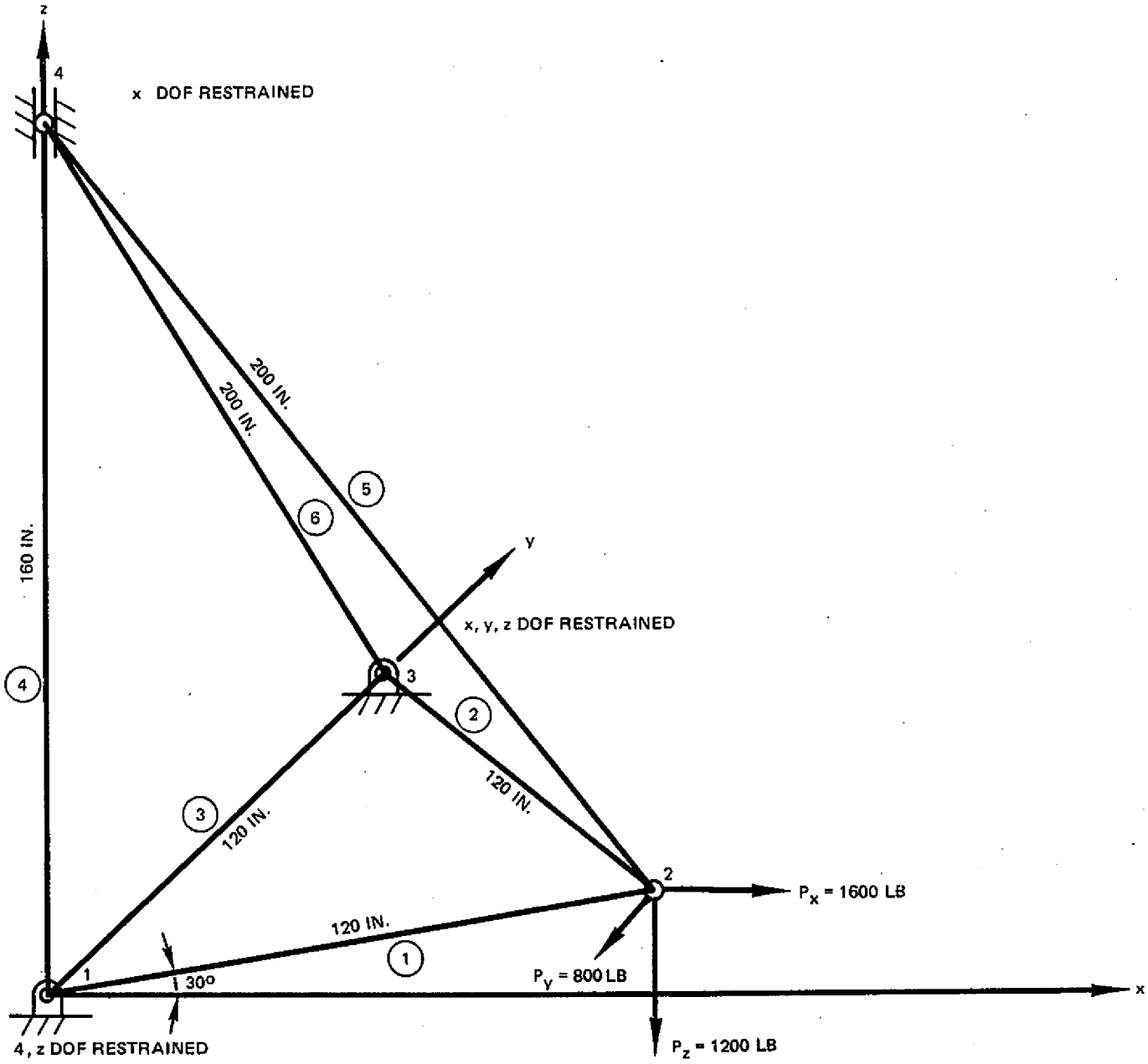

PROBLEM PARAMETERS

MODULUS OF ELASTICITY = $E = 29 \times 10^6$ LB/IN.^{2}

MEMBER NO.	AREA (IN.^{2})
1	2.00
2	2.00
3	2.00
4	6.00
5	4.00
6	4.00

Updated

SAN ONOFRE NUCLEAR GENERATING STATION Units 2 & 3

TRI-DIMENSIONAL SPACE TRUSS (SUPER SMIS EXAMPLE 3)

Figure 3C.3-4

10079-11D-1375

Amended: April 2009 TL: E047997

Site File Copy

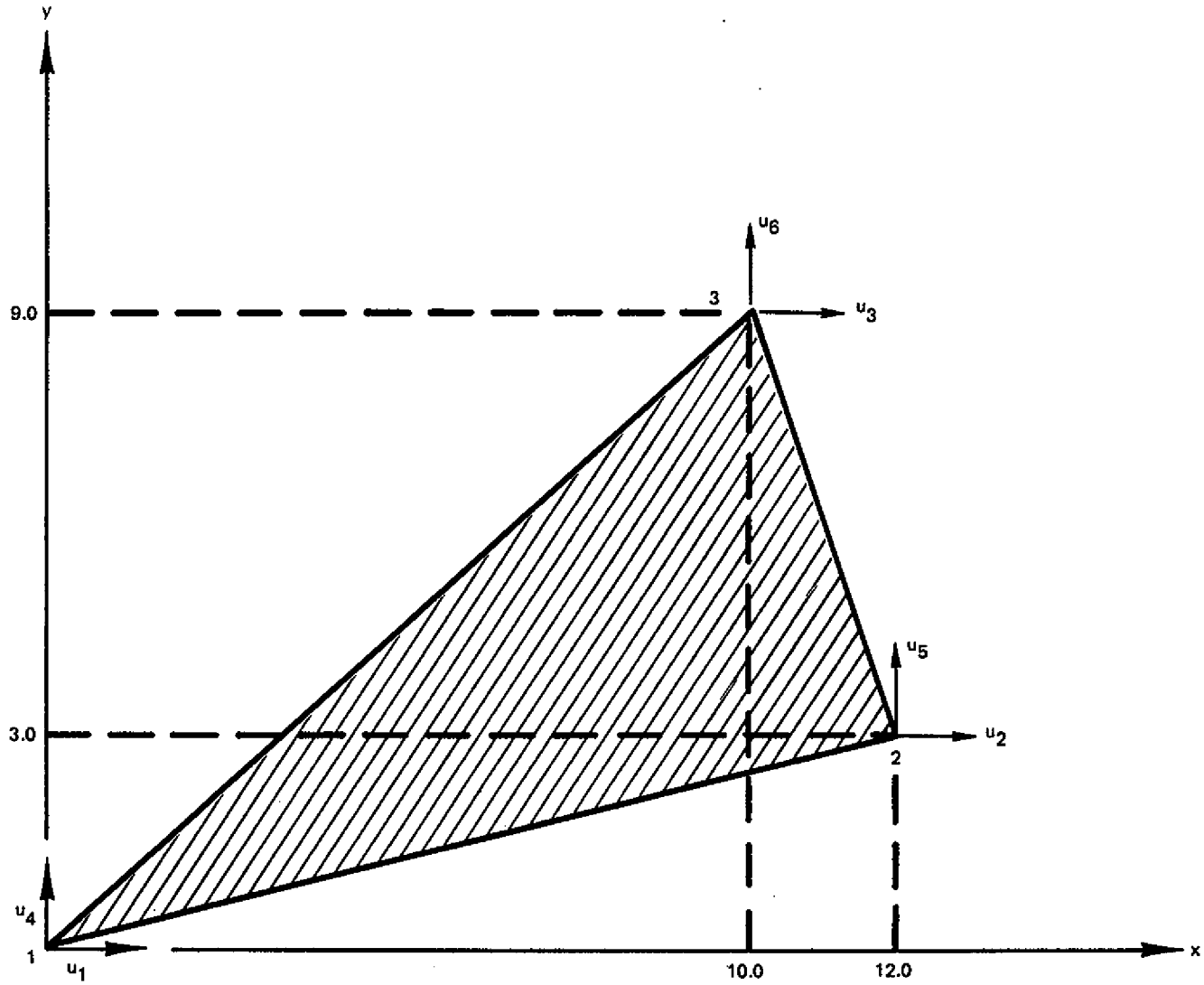

PROBLEM PARAMETERS

THICKNESS = t = 0.060 IN.

MODULUS OF ELASTICITY = $E = 30 \times 10^6$ LB/IN.^{2}

POISSON'S RATIO = $\nu = 0.30$

$$\text{AREA} = A = \frac{(x_2 - x_1)(y_3 - y_1) - (x_1 - x_3)(y_1 - y_2)}{2}$$

$$A = \frac{(12)(9) - (-10)(-3)}{2}$$

$$A = 39.0 \text{ IN.}^2$$

Updated

SAN ONOFRE NUCLEAR GENERATING STATION Units 2 & 3
CONSTANT STRAIN TRIANGLE (SUPER SMIS EXAMPLE 4)
Figure 3C.3-5

10079-11D-1376

Amended: April 2009 TL: E047997

Site File Copy

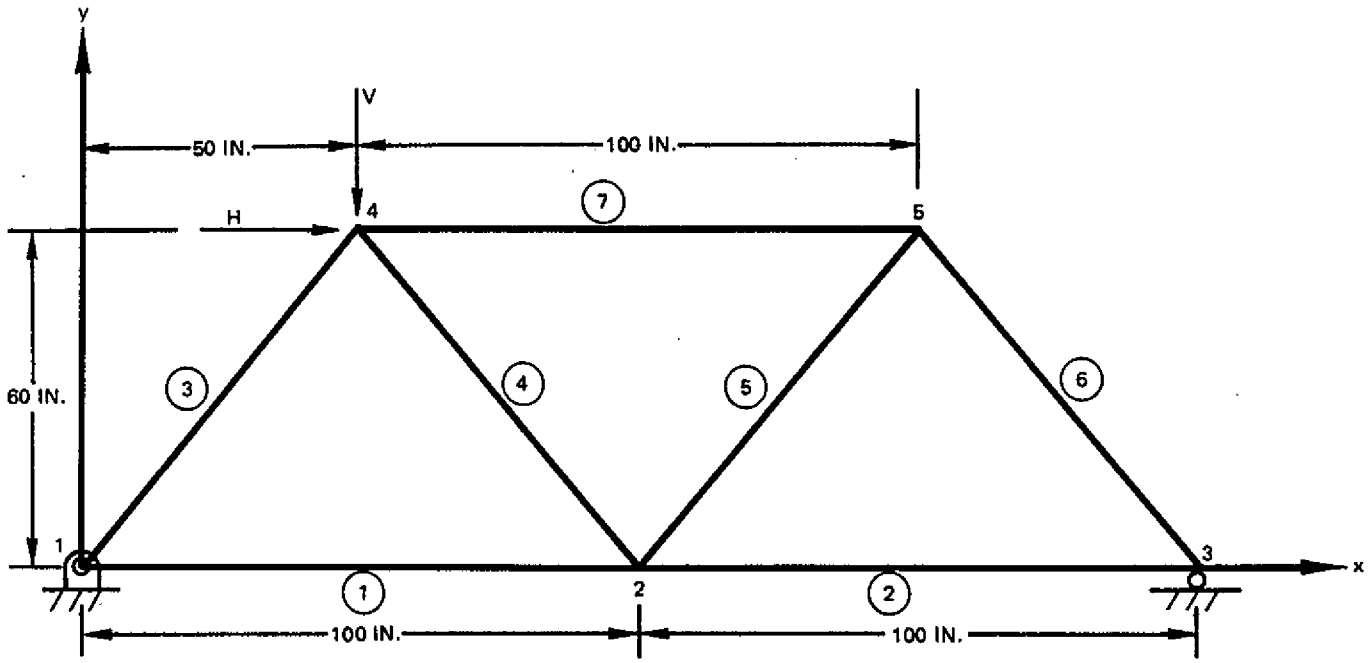

MEMBER PROPERTIES:

MEMBER NO.	AREA (IN.^{2})
1	4.0
2	4.0
3	7.5
4	7.5
5	7.5
6	7.5
7	4.0

E = 27 x 10^6/LB/IN.^{2}

FOR HORIZONTAL LOADING: H = 10 LB

FOR VERTICAL LOADING: V = 10 LB

Updated

SAN ONOFRE
NUCLEAR GENERATING STATION
Units 2 & 3

TWO-DIMENSIONAL PLANAR TRUSS
(SUPER SMIS EXAMPLE 5)

Figure 3C.3-6

10079-11D-1377
250C6

Amended: April 2009 TL: E047997

Site File Copy

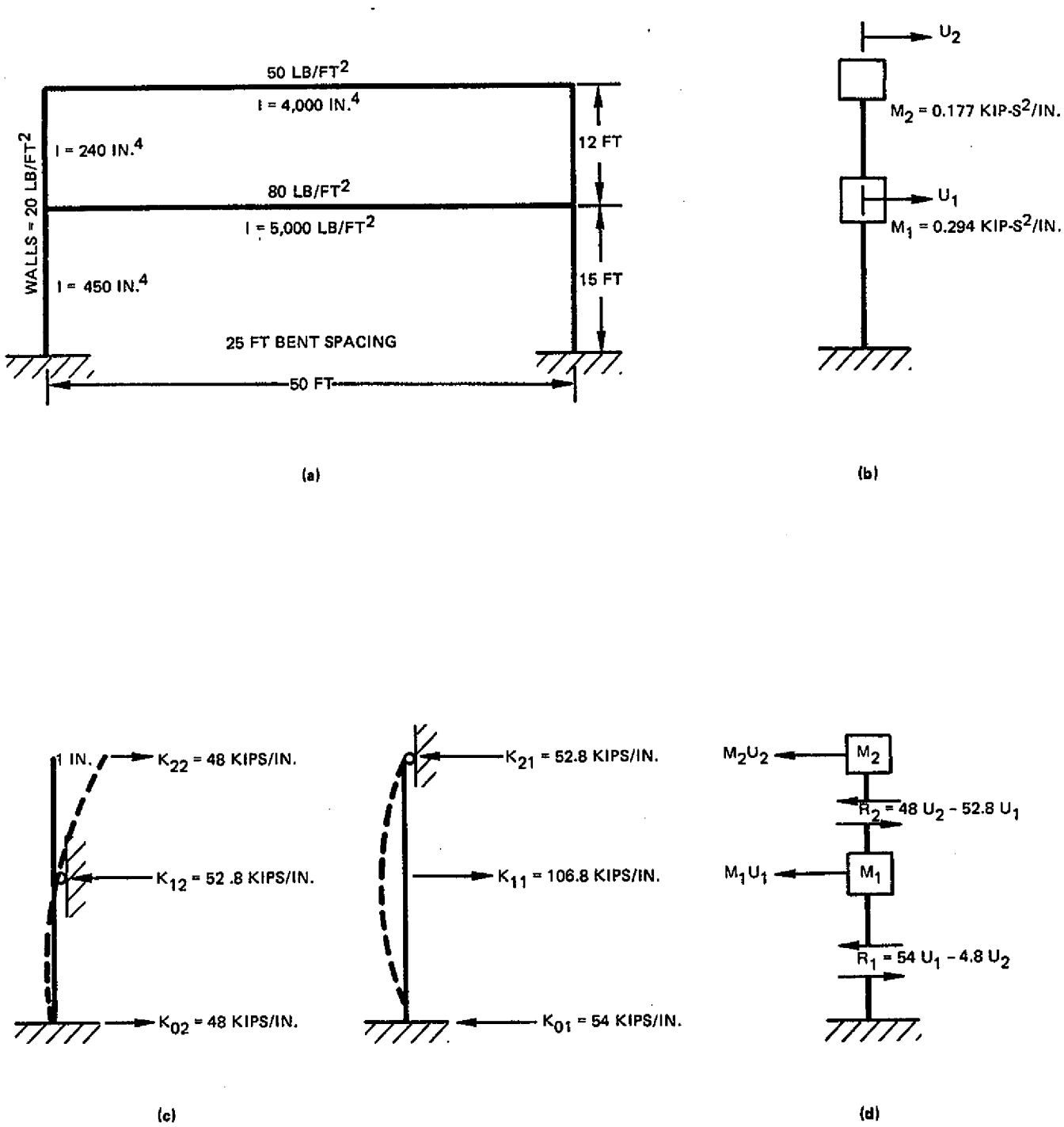

Updated

SAN ONOFRE NUCLEAR GENERATING STATION Units 2 & 3
MULTISTORY BUILDING TIME-HISTORY ANALYSIS (SUPER SMIS EXAMPLE 6)
Figure 3C.3-7

10079-11D-1378

Amended: April 2009 TL: E047997

Site File Copy

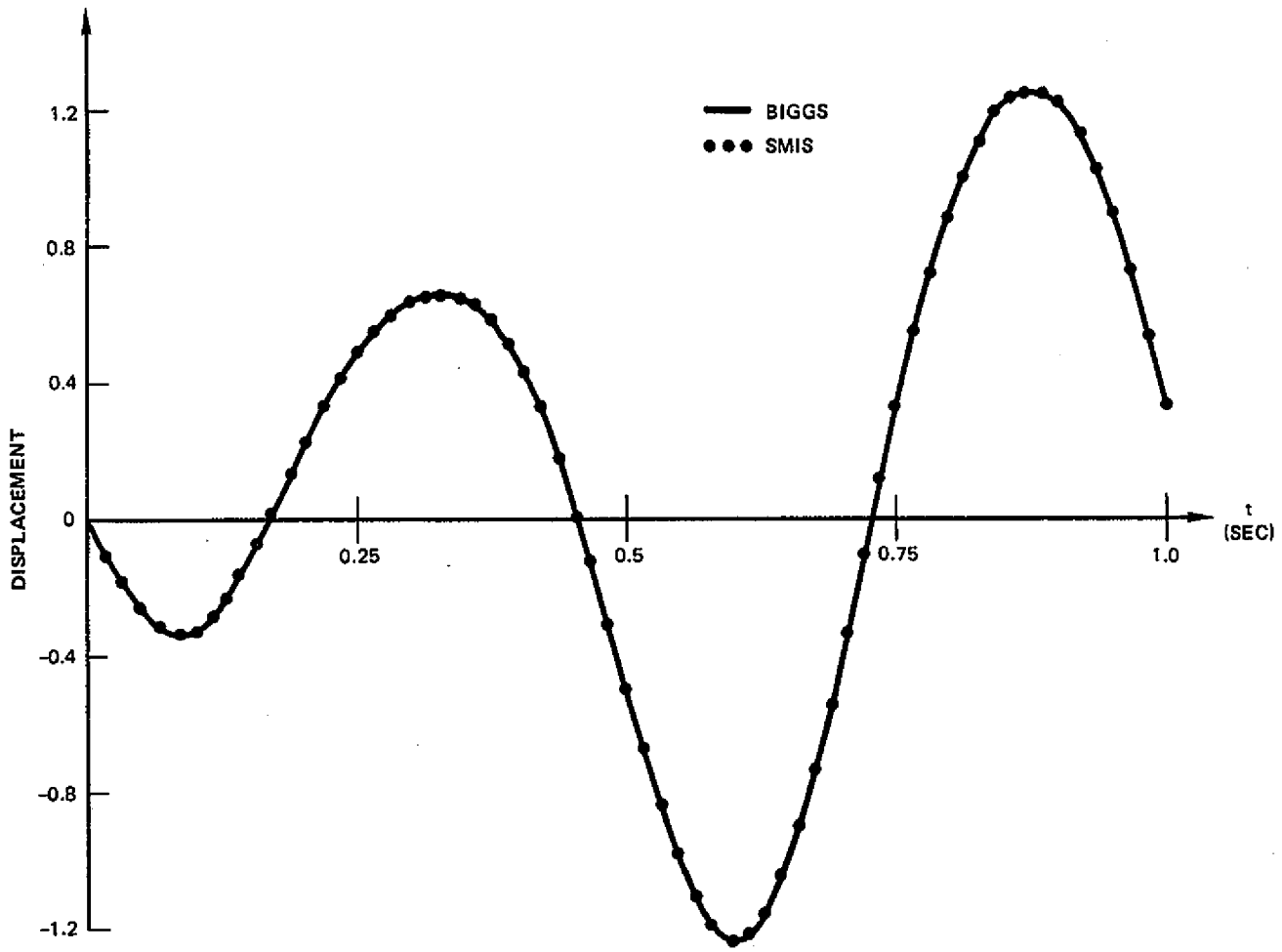

Updated

SAN ONOFRE NUCLEAR GENERATING STATION Units 2 & 3
FIRST FLOOR DISPLACEMENT RESPONSE (SUPER SMIS EXAMPLE 6)
Figure 3C.3-8

10079-11D-1379

Amended: April 2009 TL: E047997

Site File Copy

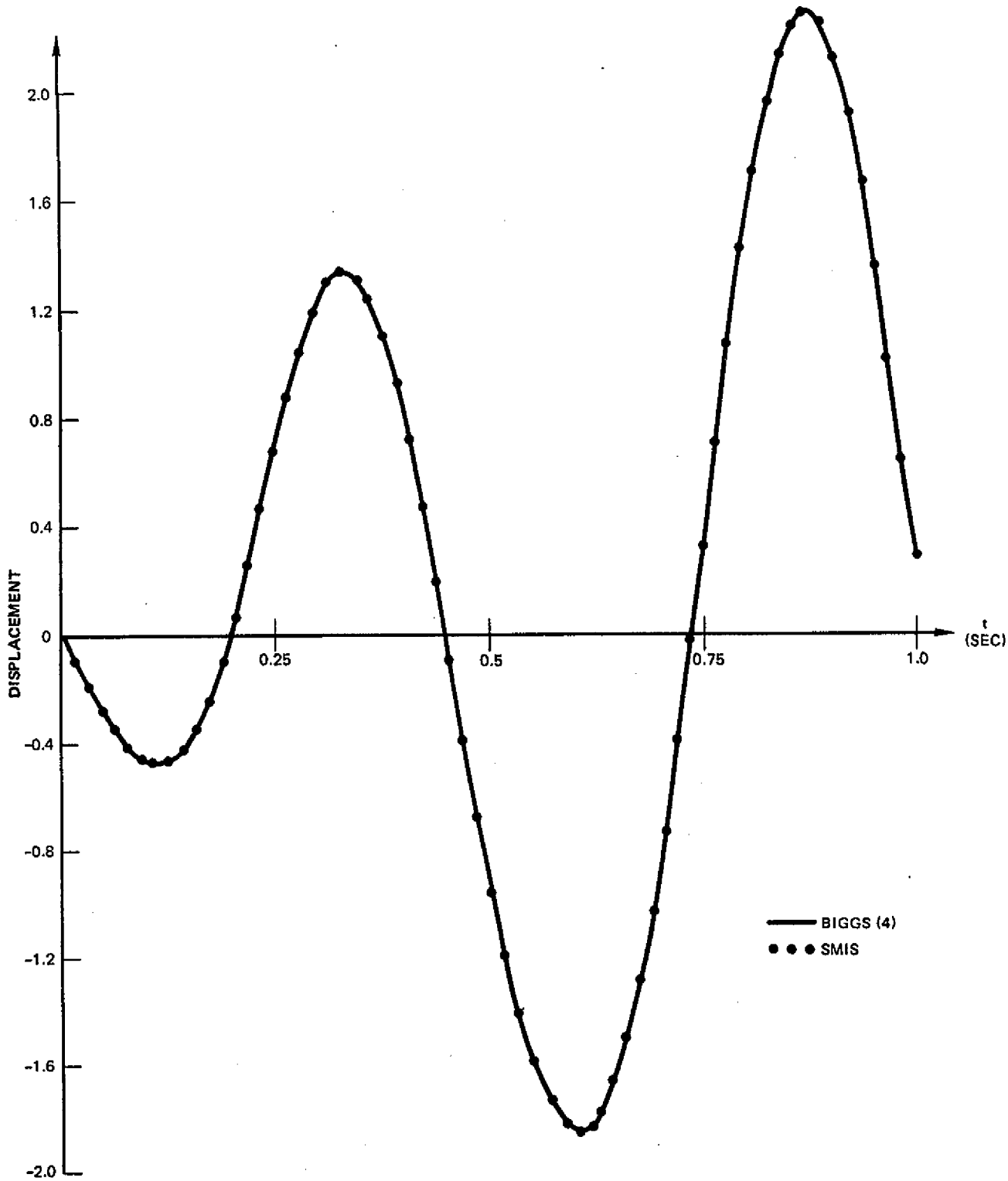

Updated

SAN ONOFRE NUCLEAR GENERATING STATION Units 2 & 3
SECOND FLOOR DISPLACEMENT RESPONSE (SUPER SMIS EXAMPLE 6)
Figure 3C.3-9

10079-11D-1380

Amended: April 2009 TL: E047997

Site File Copy

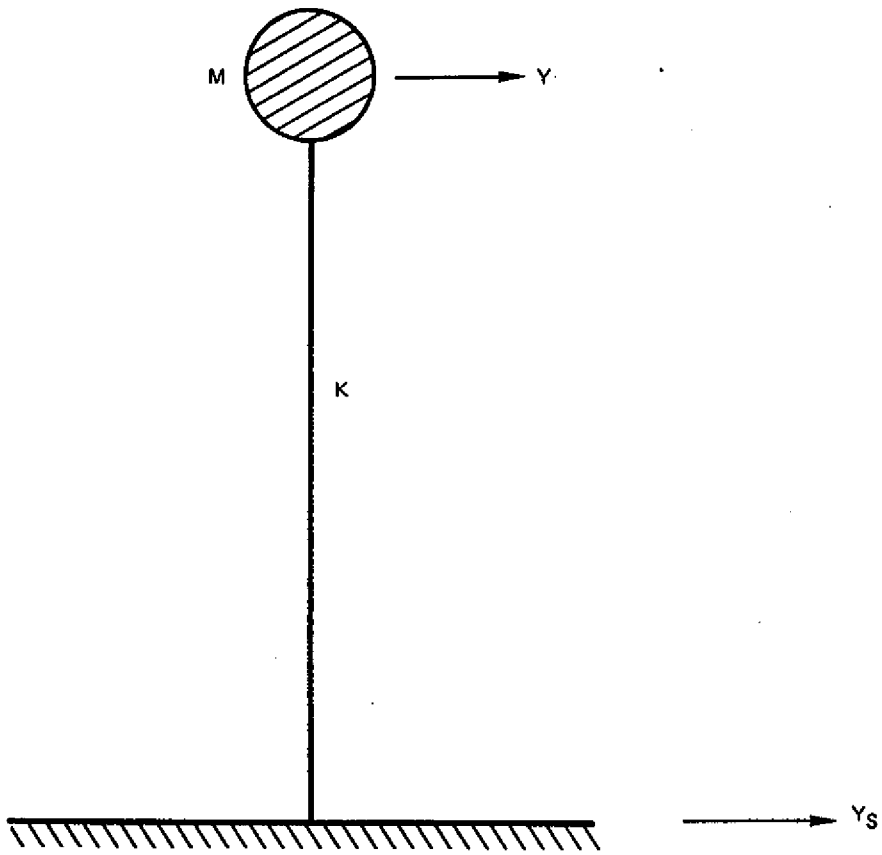

Updated

SAN ONOFRE NUCLEAR GENERATING STATION Units 2 & 3
SINGLE-DEGREE-OF-FREEDOM OSCILLATOR SUBJECTED TO SUPPORT ACCELERATION
Figure 3C.4-1

10079-11D-1381
250C6

Amended: April 2009 TL: E047997

Site File Copy

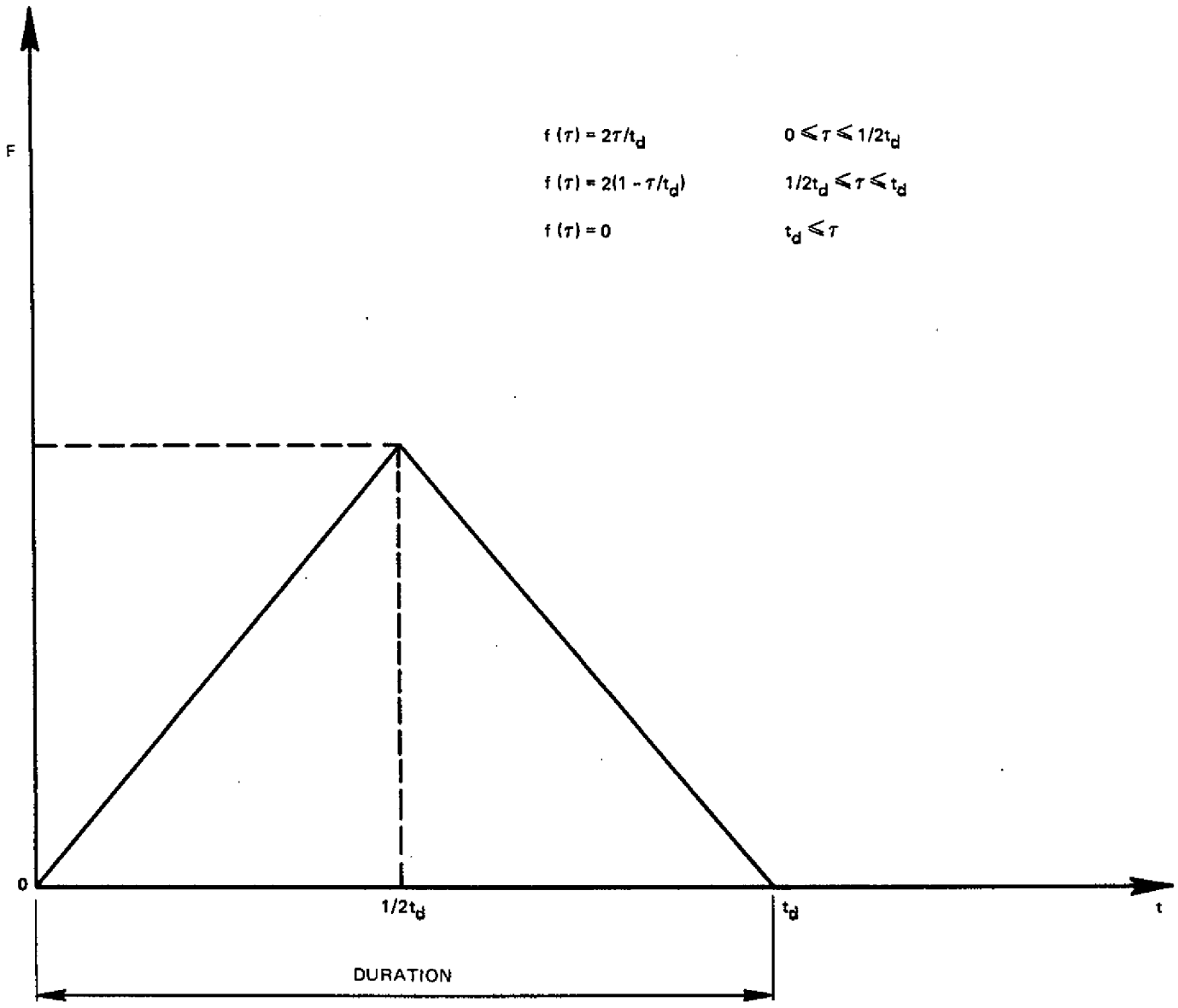

NUMERICAL DATA

PULSE DURATION t_d	=	5.00 SECONDS
TIME INTERVAL Δt	=	0.05 SECOND

Updated

SAN ONOFRE NUCLEAR GENERATING STATION Units 2 & 3
SYMMETRICAL TRIANGULAR PULSE LOAD
Figure 3C.4-2

10079-11D-1382

Amended: April 2009 TL: E047997

Site File Copy

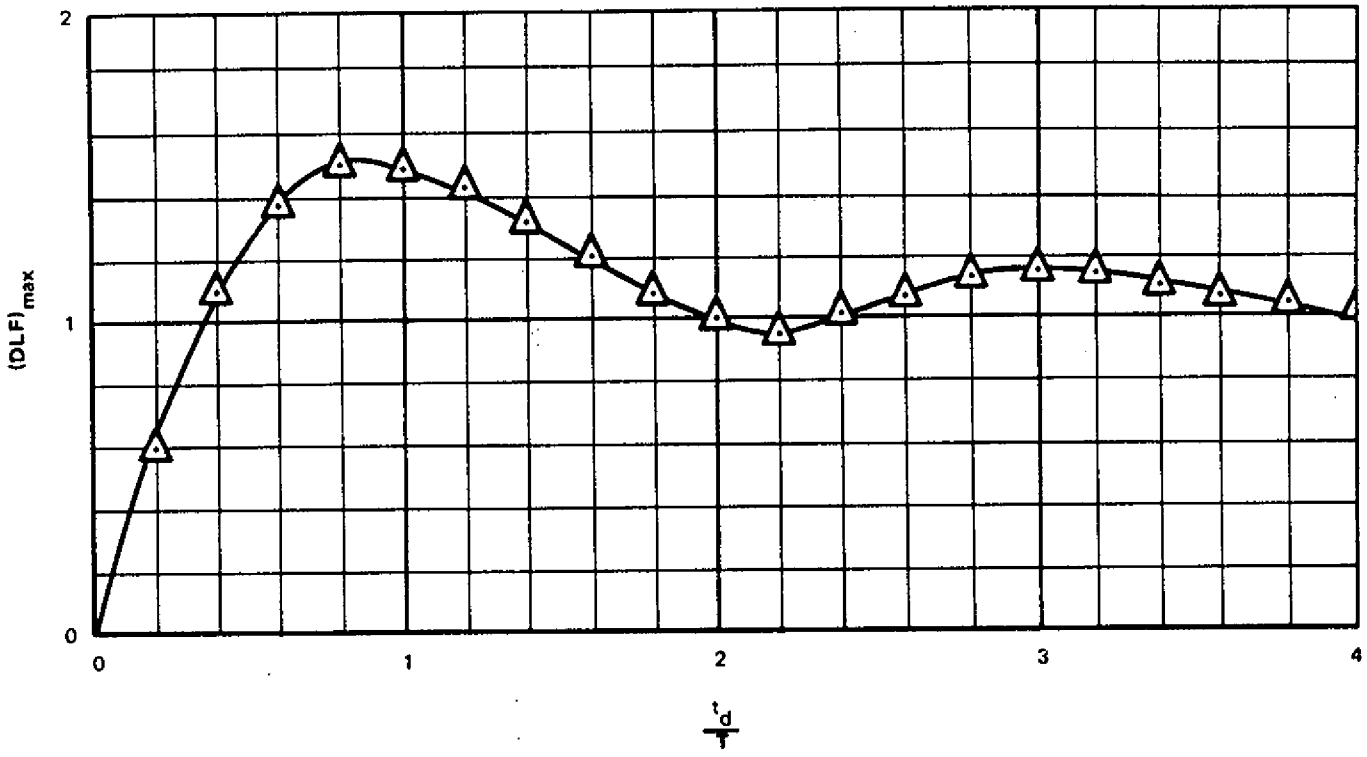

LEGEND:
△ SPECTRA
— ANALYTICAL PER INTRODUCTION TO STRUCTURAL DYNAMICS (2)

DYNAMIC LOAD FACTOR FOR SYMMETRIC TRIANGULAR PULSE LOAD, UNDAMPED SYSTEM

Updated

SAN ONOFRE NUCLEAR GENERATING STATION Units 2 & 3
RESPONSE SPECTRA COMPARISON (SPECTRA EXAMPLE 1)
Figure 3C.4-3

10079-11D-1383

Amended: April 2009 TL: E047997

Site File Copy

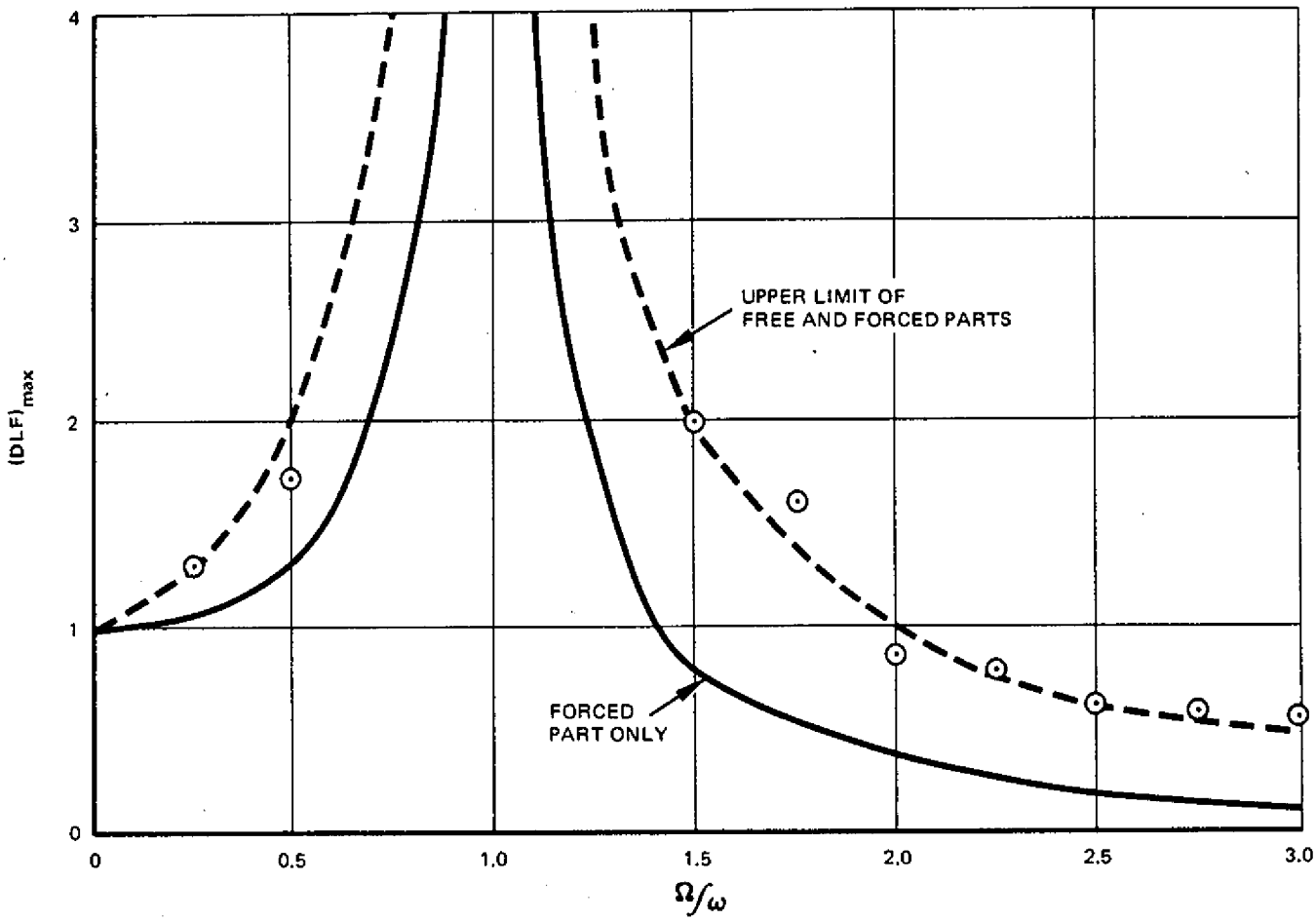

LEGEND
⊙ SPECTRA (IN THE SPECTRA RUN THE FREQUENCY OF THE FORCING FUNCTION Ω IS 2π)
ANALYTICAL PER INTRODUCTION TO STRUCTURAL DYNAMICS[2]

MAXIMUM DYNAMIC LOAD FACTOR FOR SINUSOIDAL PULSE LOAD, Sin Ωt, UNDAMPED SYSTEMS

Updated

SAN ONOFRE NUCLEAR GENERATING STATION Units 2 & 3
RESPONSE SPECTRA COMPARISON (SPECTRA EXAMPLE 2)
Figure 3C.4-4

10079-11D-1384

Amended: April 2009 TL: E047997

Site File Copy

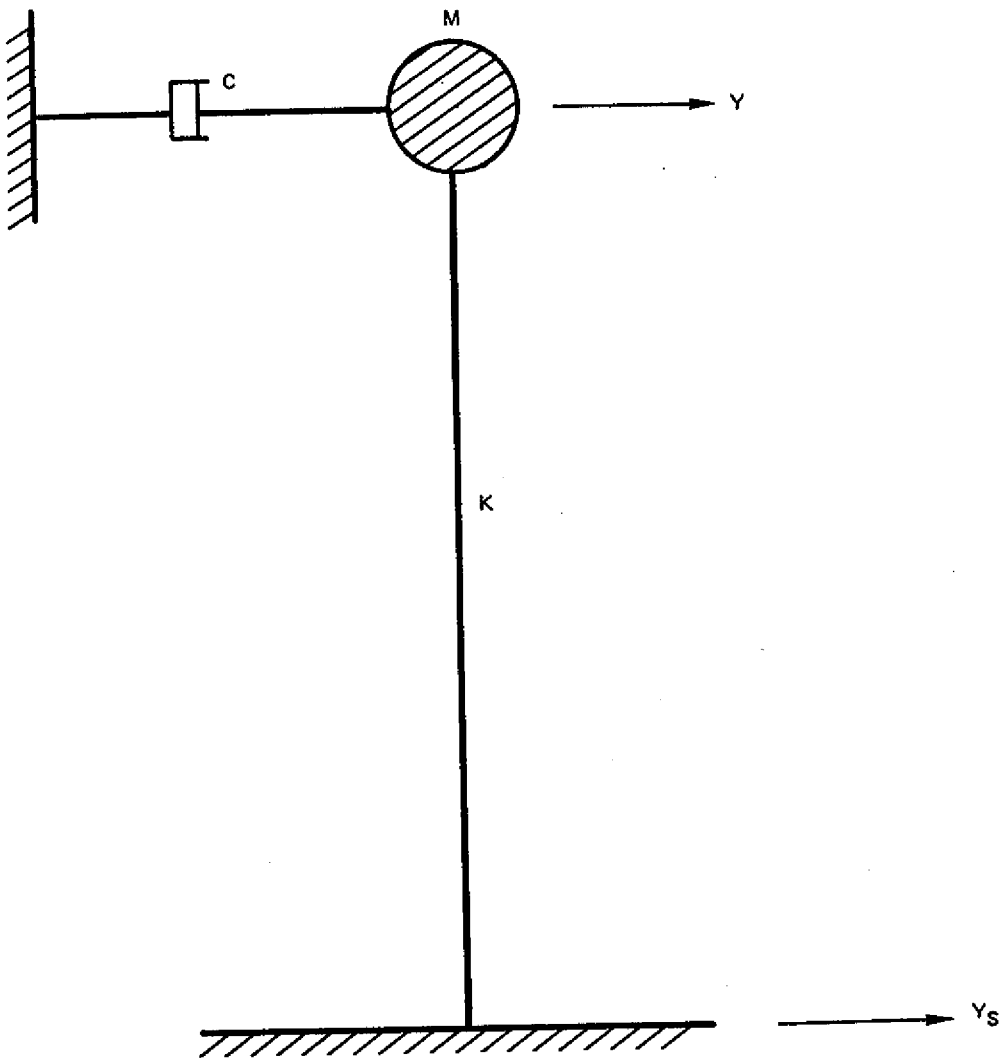

Updated

SAN ONOFRE NUCLEAR GENERATING STATION Units 2 & 3
DAMPED SINGLE-DEGREE-OF-FREEDOM OSCILLATOR SUBJECTED TO SUPPORT ACCELERATION
Figure 3C.4-5

10079-11D-1385

Amended: April 2009 TL: E047997

Site File Copy

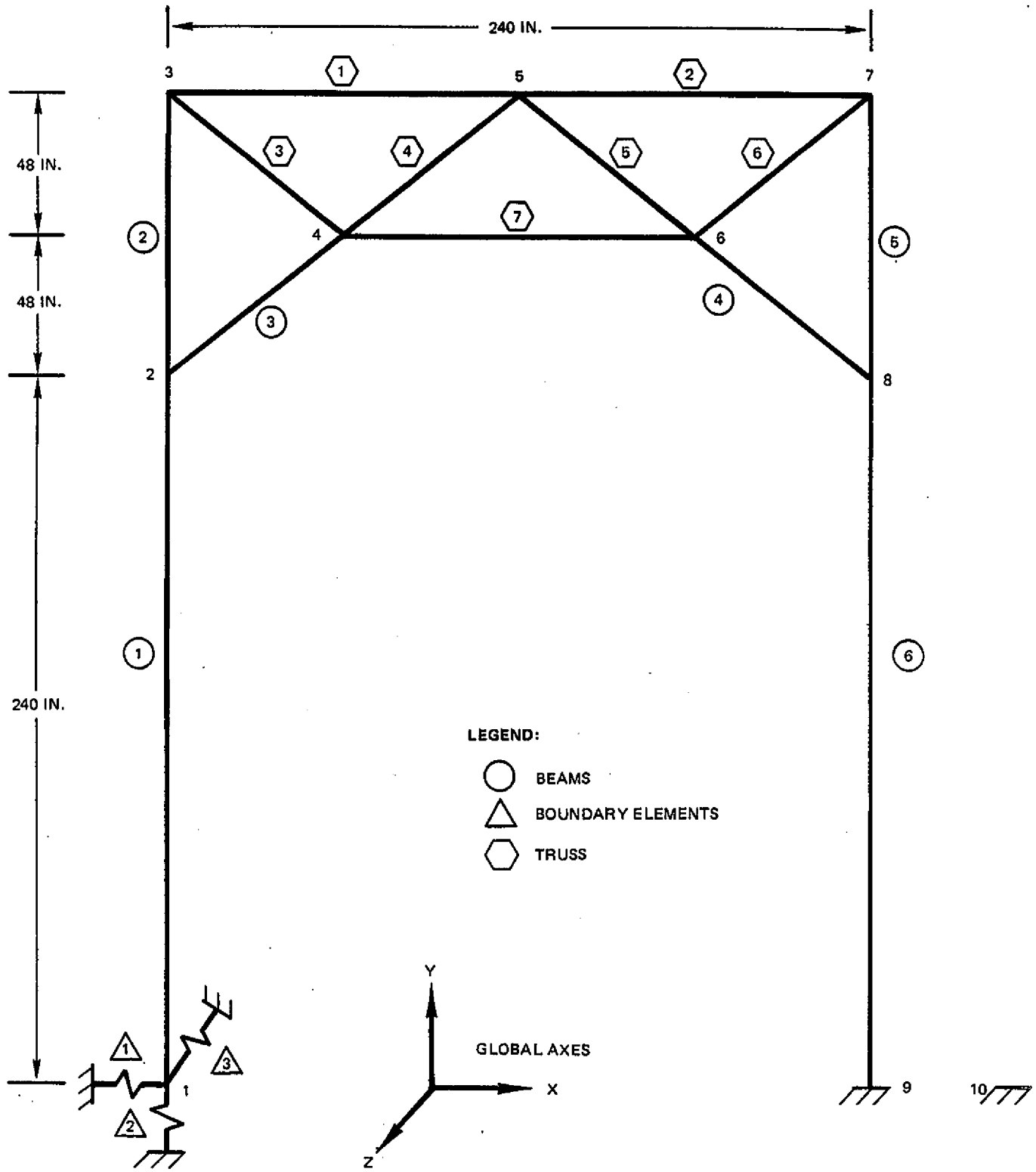

Updated

SAN ONOFRE NUCLEAR GENERATING STATION Units 2 & 3
PLANE FRAME COMPOSED OF BEAM, TRUSS AND BOUNDARY ELEMENTS (SAP EXAMPLES 1, 8, 28, 29, 30, AND 33)
Figure 3C.5-1

10079-11D-1386
250C6

Amended: April 2009 TL: E047997

Site File Copy

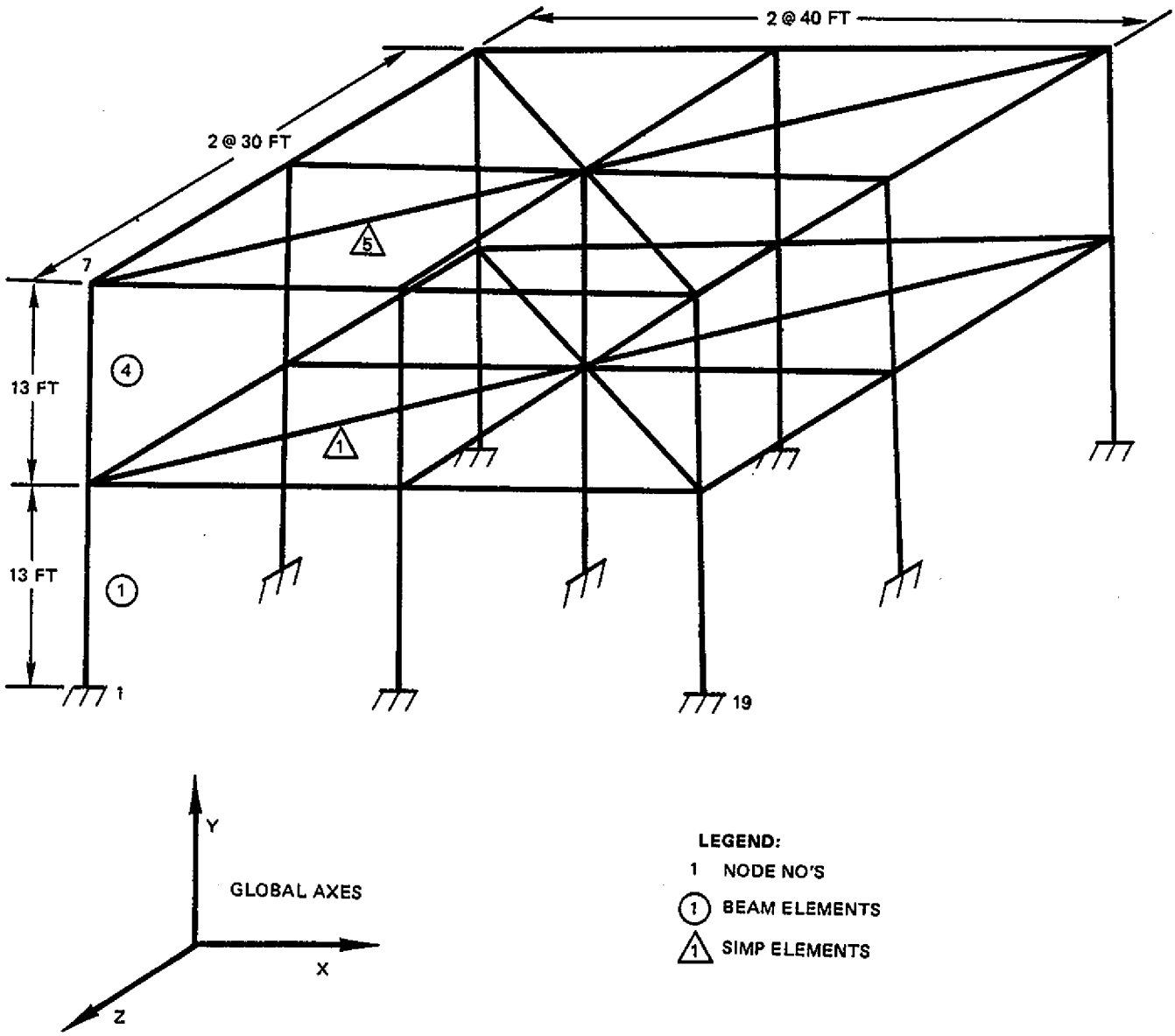

Updated

SAN ONOFRE NUCLEAR GENERATING STATION Units 2 & 3
TWO-STORY 3-DIMENSIONAL SPACE FRAME COMPOSED OF BEAM AND MEMBRANE ELEMENTS (SAP EXAMPLE 2)
Figure 3C.5-2

10079-11D-1387
250C6

Amended: April 2009 TL: E047997

Site File Copy

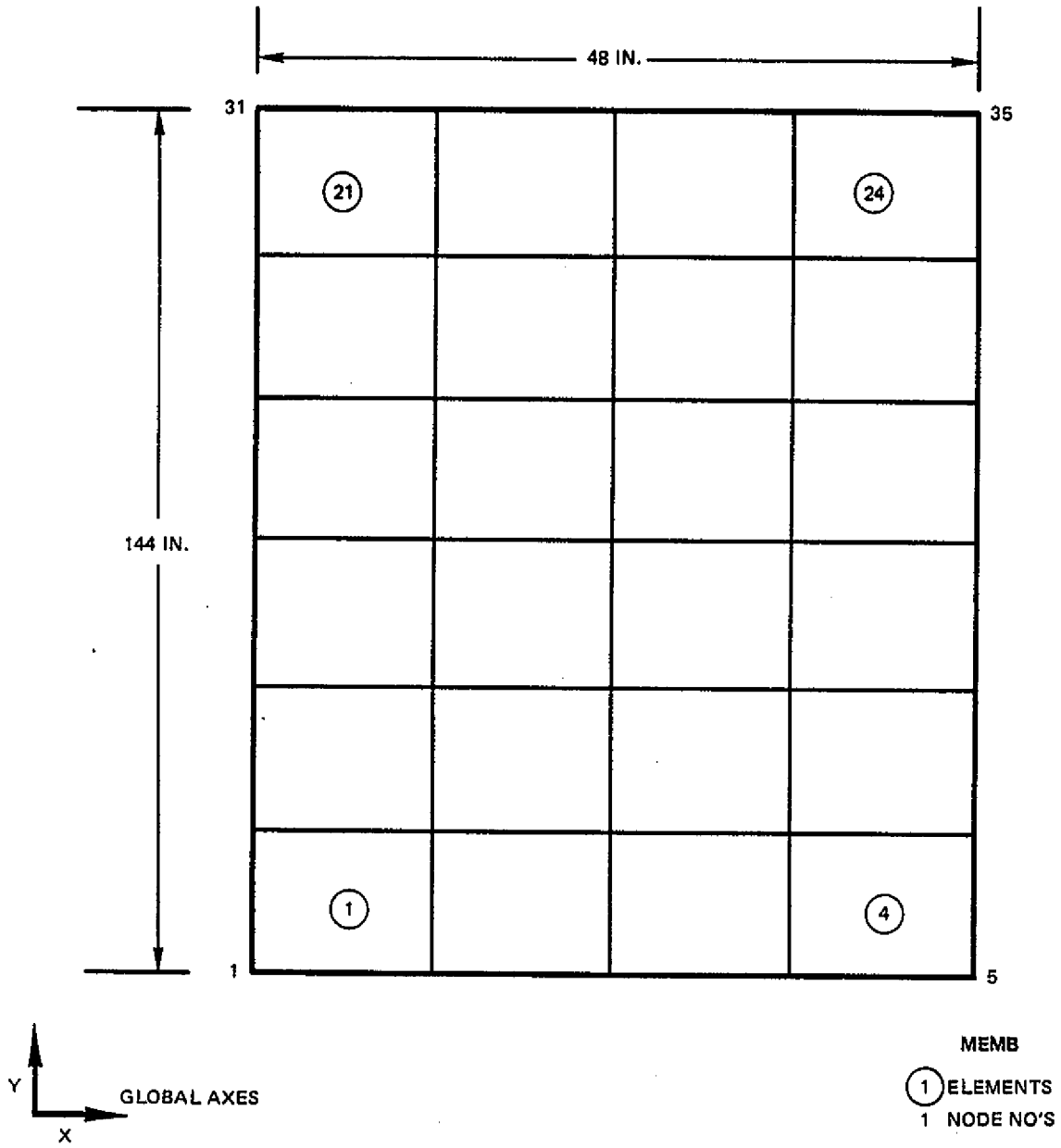

SAN ONOFRE NUCLEAR GENERATING STATION Units 2 & 3
FLAT PLATE SUBJECTED TO IN-PLANE LOADING (SAP EXAMPLE 3)
Figure 3C.5-3

10079-11D-1388
250C6

Amended: April 2009 TL: E047997

Site File Copy

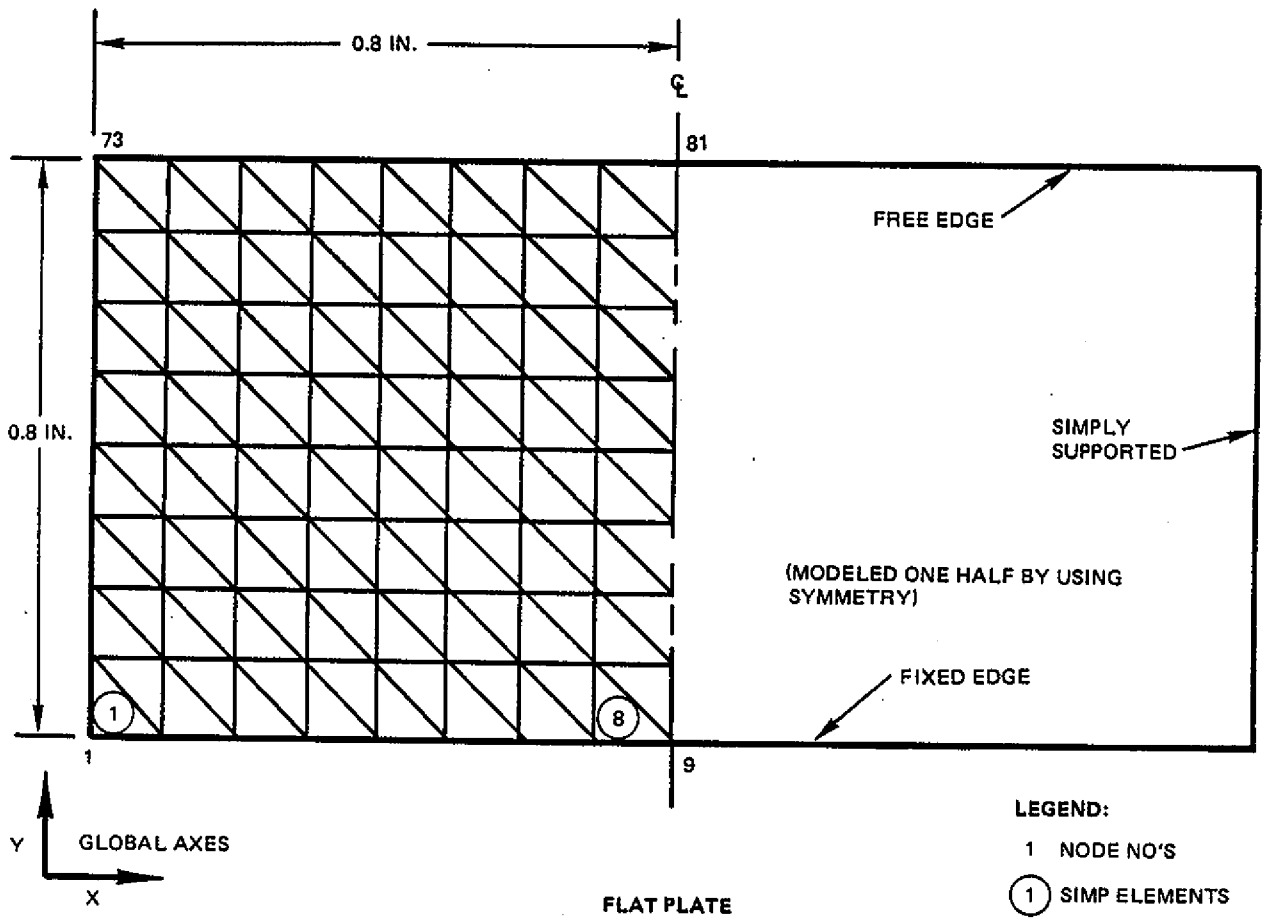

FLAT PLATE

Updated

SAN ONOFRE NUCLEAR GENERATING STATION Units 2 & 3
FLAT PLATE SUBJECTED TO OUT-OF-PLANE LOADING (SAP EXAMPLE 4)
Figure 3C.5-4

10079-11D-1389
250C6

Amended: April 2009 TL: E047997

Site File Copy

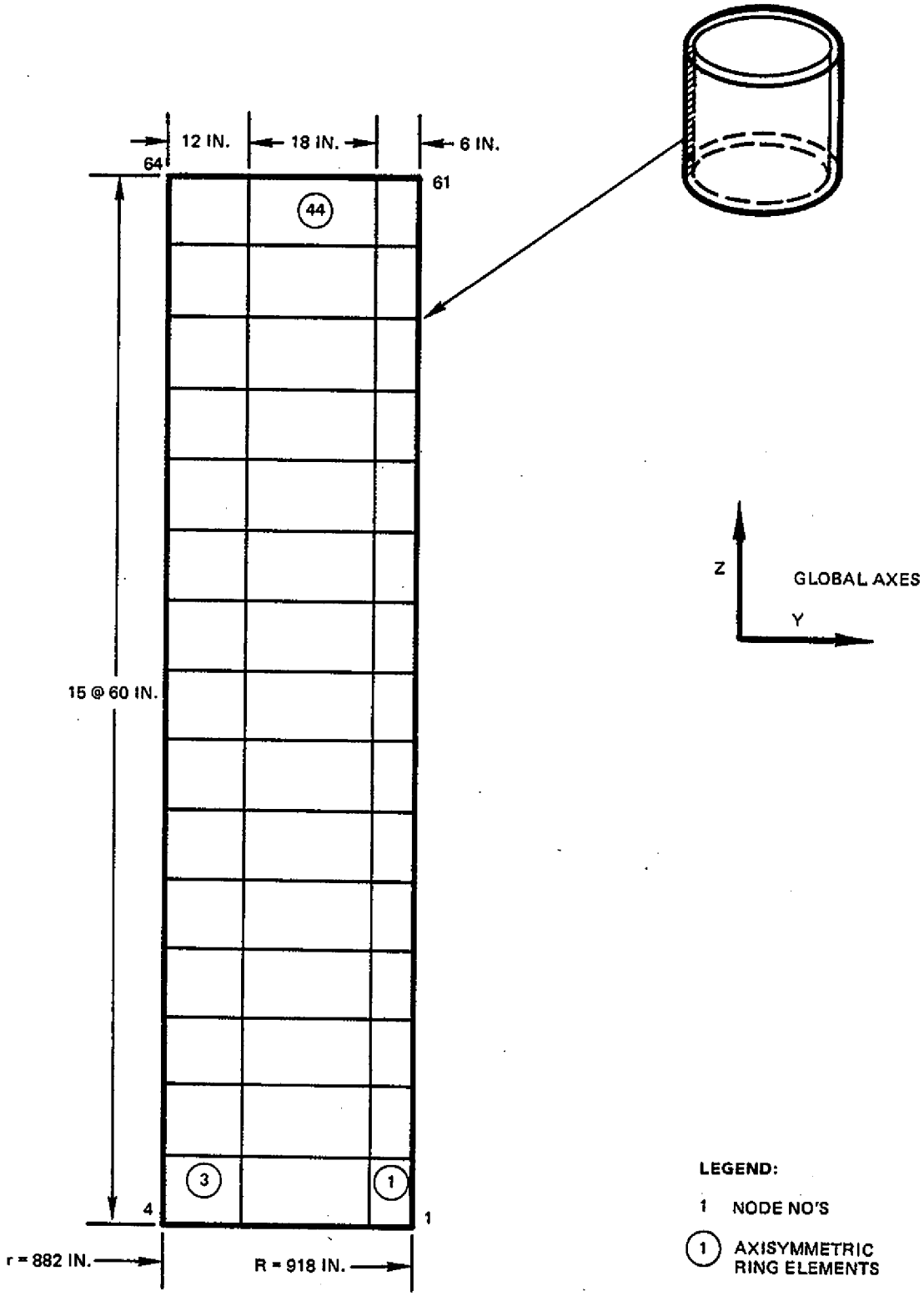

SEGMENT OF CYLINDER WALL

Updated

SAN ONOFRE NUCLEAR GENERATING STATION Units 2 & 3
CYLINDRICAL SECTION COMPOSED OF AXISYMMETRIC RING ELEMENTS (SAP EXAMPLE 5)
Figure 3C.5-5

10079-11D-1390
250C6

Amended: April 2009 TL: E047997

Site File Copy

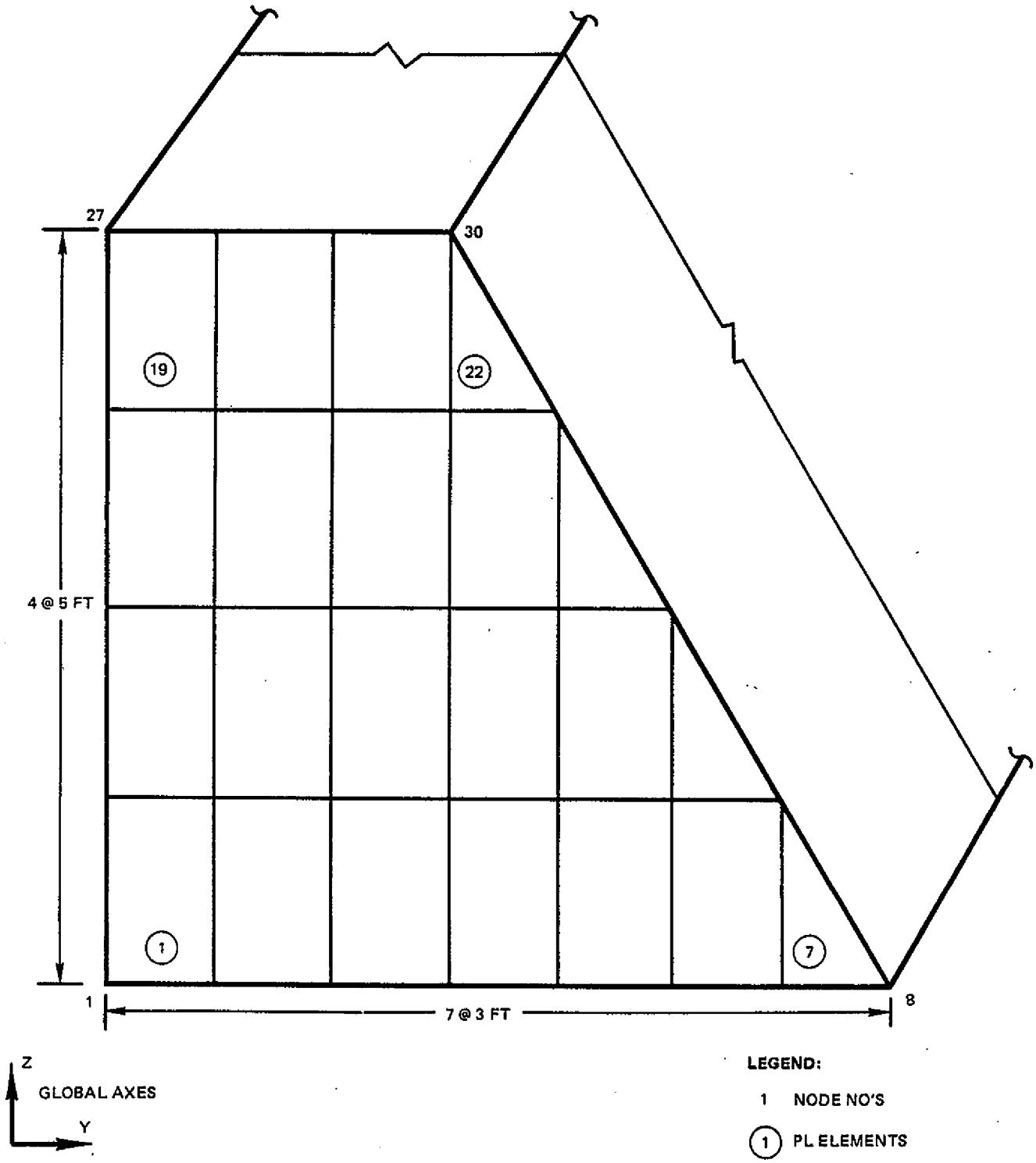

Updated

SAN ONOFRE NUCLEAR GENERATING STATION Units 2 & 3
RETAINING WALL COMPOSED OF PLATE ELEMENTS (SAP EXAMPLE 6)
Figure 3C.5-6

10079-11D-1391
250C6

Amended: April 2009 TL: E047997

Site File Copy

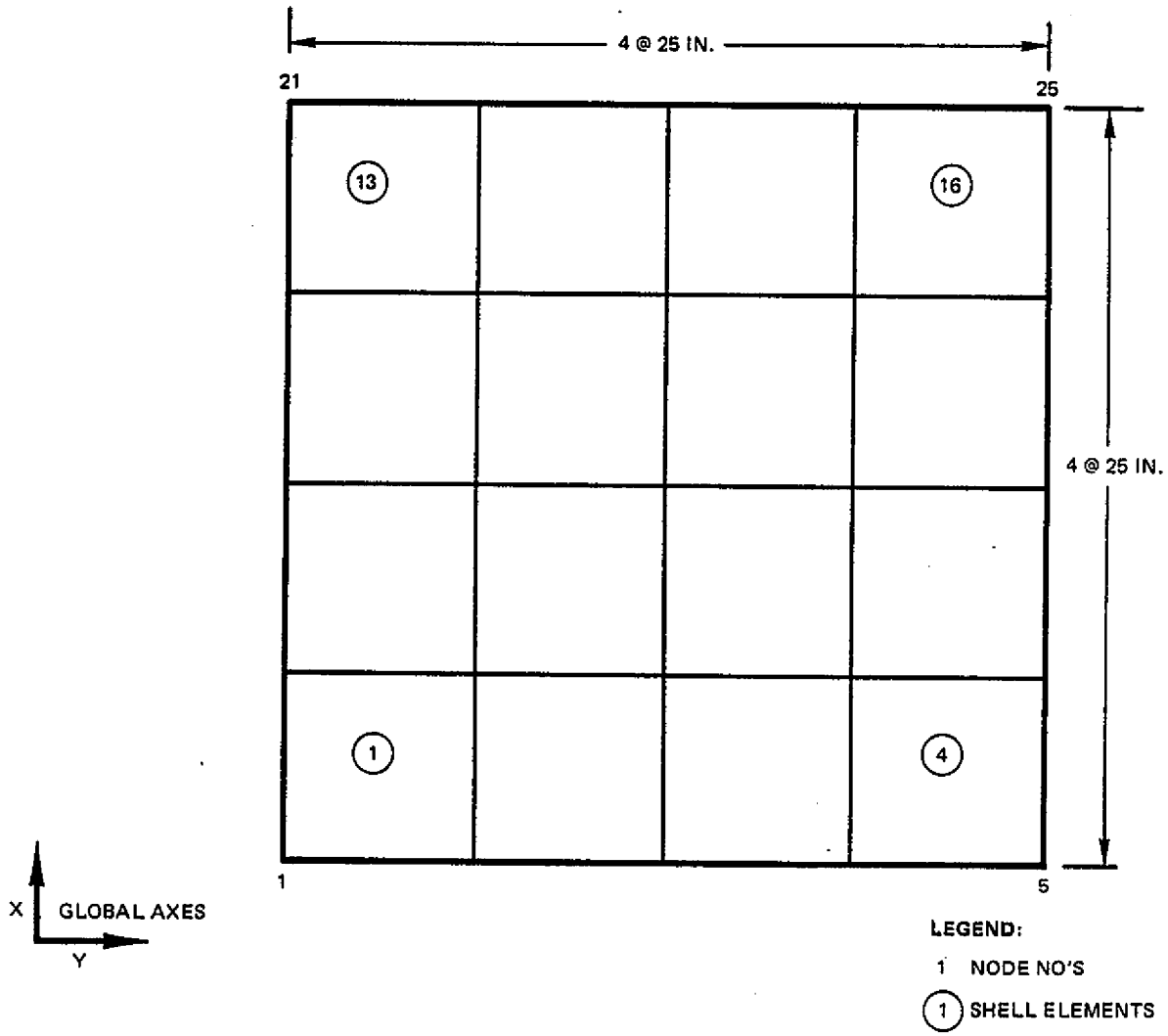

Updated

SAN ONOFRE NUCLEAR GENERATING STATION Units 2 & 3
FLAT PLATE COMPOSED OF SHELL ELEMENTS (SAP EXAMPLE 7)
Figure 3C.5-7

10079-11D-1392
250C6

Amended: April 2009 TL: E047997

Site File Copy

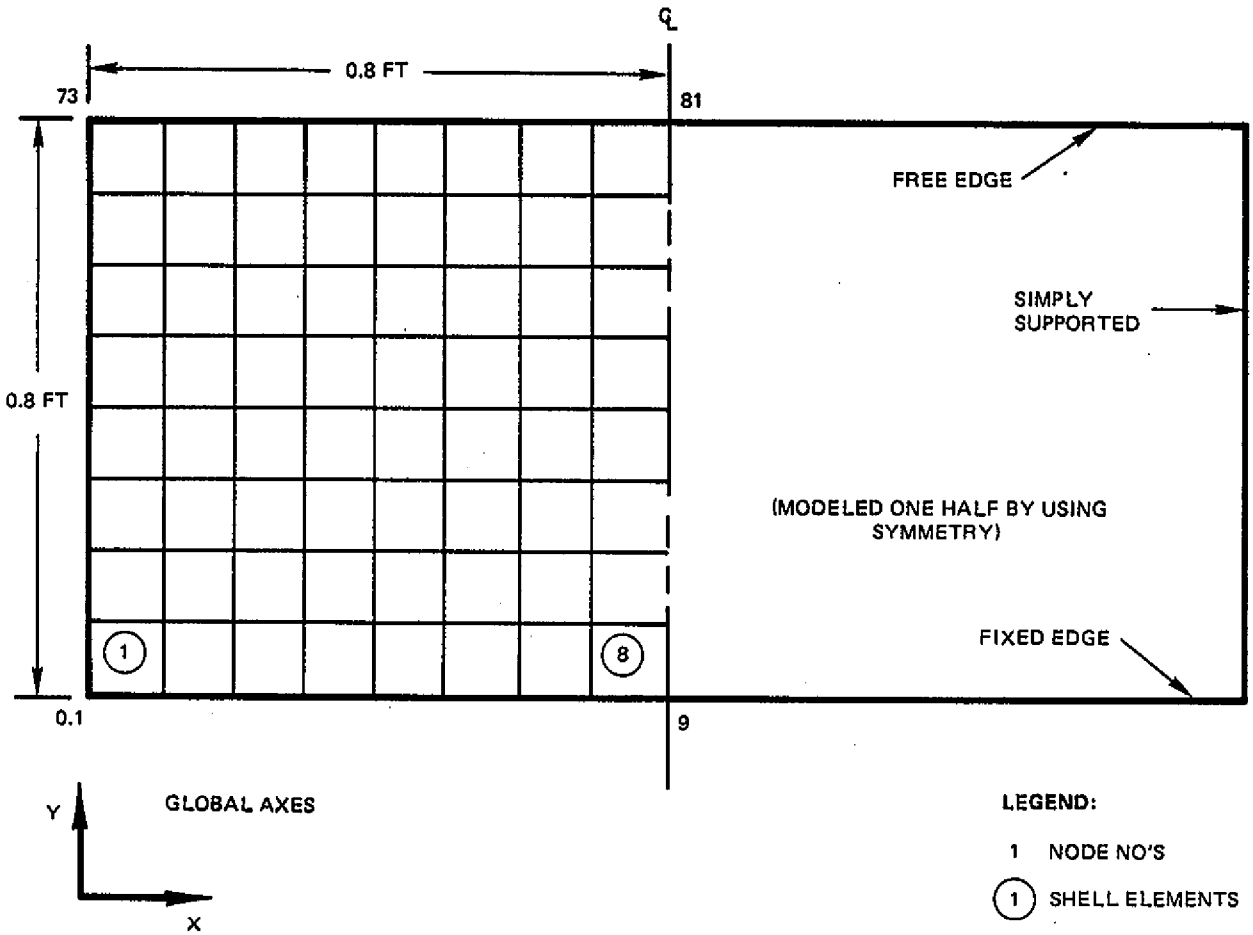

SAN ONOFRE NUCLEAR GENERATING STATION Units 2 & 3
FLAT PLATE COMPOSED OF SHELL ELEMENTS (SAP EXAMPLE 9)
Figure 3C.5-8

10079-11D-1393
250C6

Amended: April 2009 TL: E047997

Site File Copy

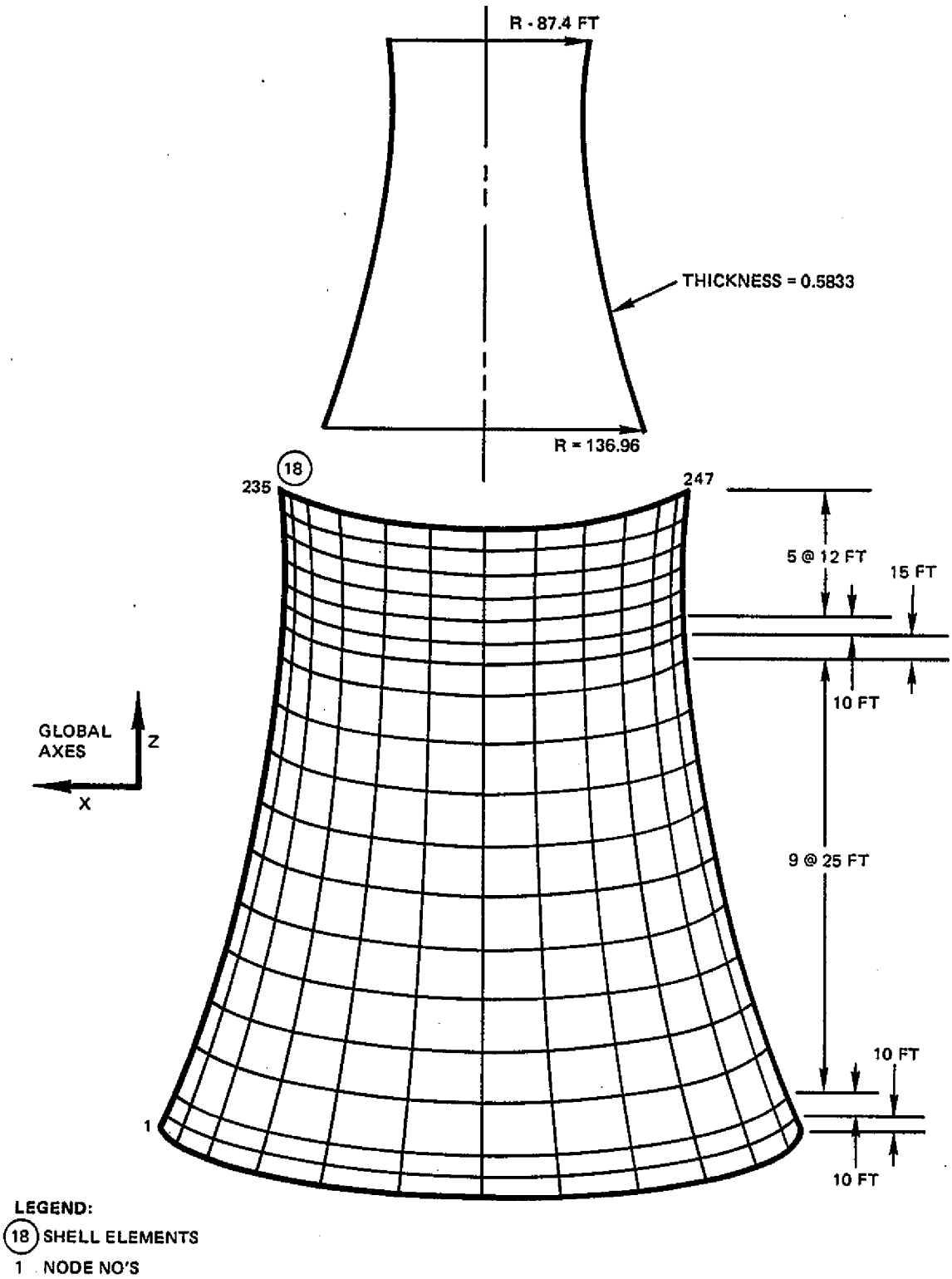

Updated

SAN ONOFRE NUCLEAR GENERATING STATION Units 2 & 3
HYPERBOLIC COOLING TOWER COMPOSED OF SHELL ELEMENTS (SAP EXAMPLE 10)
Figure 3C.5-9

10079-11D-1394
250C6

Amended: April 2009 TL: E047997

Site File Copy

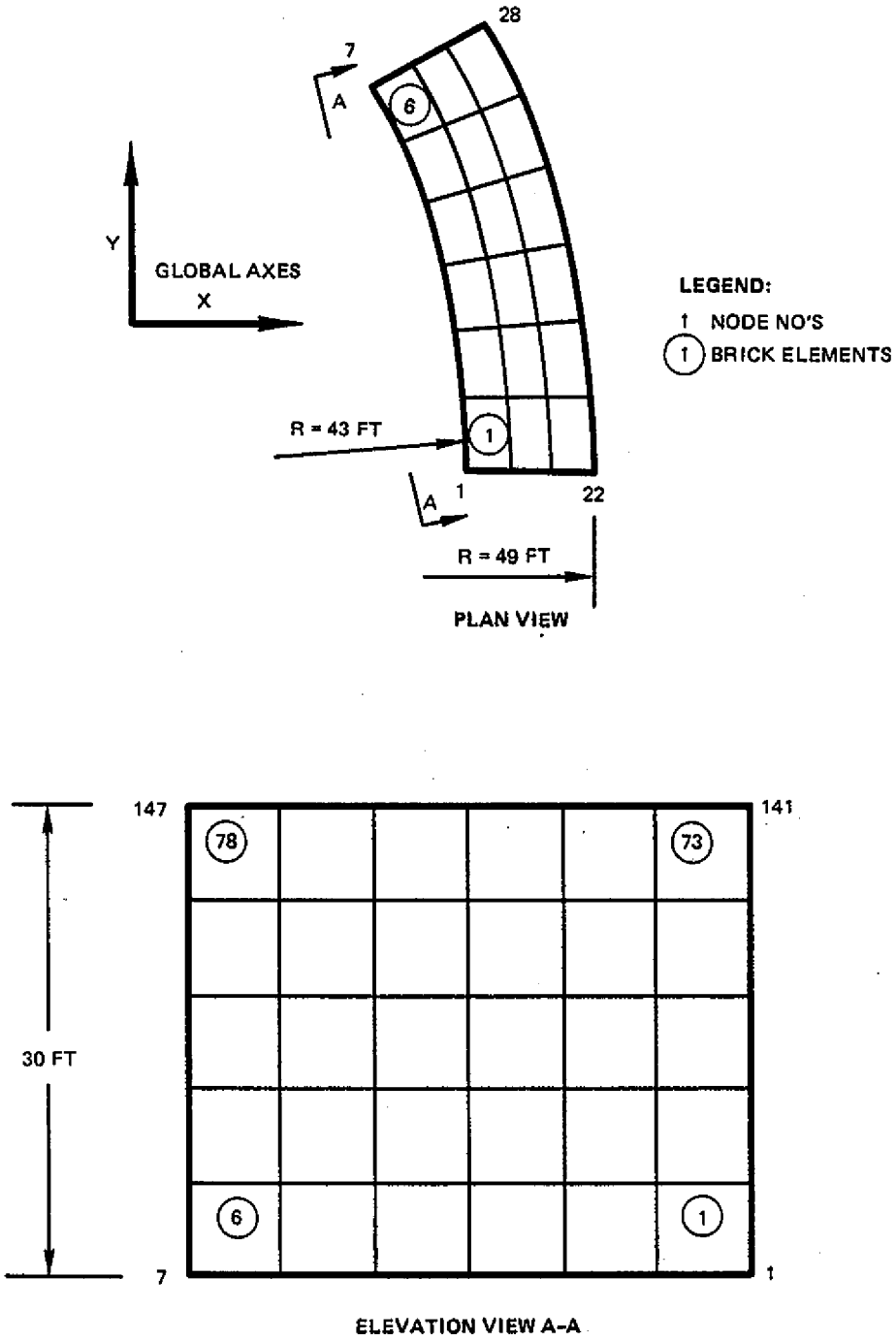

Updated

SAN ONOFRE NUCLEAR GENERATING STATION Units 2 & 3
SEGMENT OF A CYLINDER COMPOSED OF BRICK ELEMENTS (ARCH DAM) (SAP EXAMPLE 11)
Figure 3C.5-10

10079-11D-1395
250C6

Amended: April 2009 TL: E047997

Site File Copy

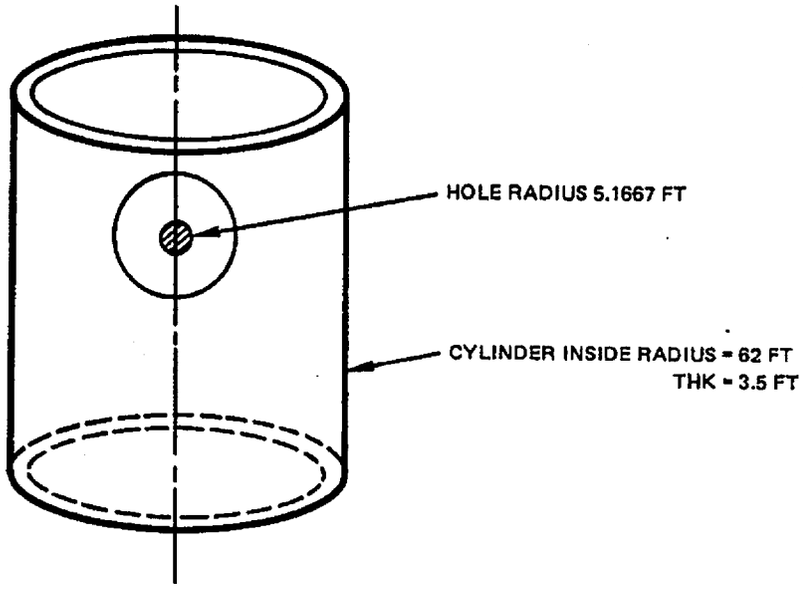

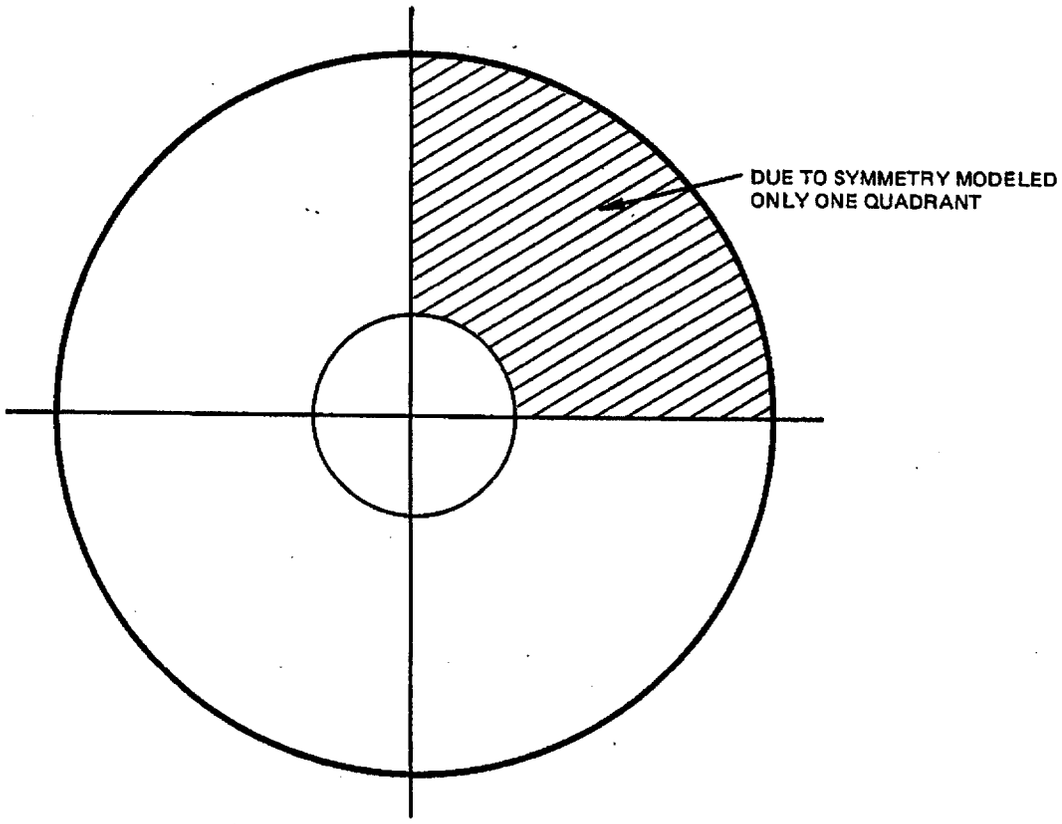

Updated

SAN ONOFRE NUCLEAR GENERATING STATION Units 2 & 3
AREA AROUND A CYLINDRICAL PENETRATION IN A CYLINDER (SAP EXAMPLE 12) (Sheet 1 of 2)
Figure 3C.5-11

Amended: June 2003 TL: E004628

10079-11D-1396
250C6

Site File Copy

Site File Copy

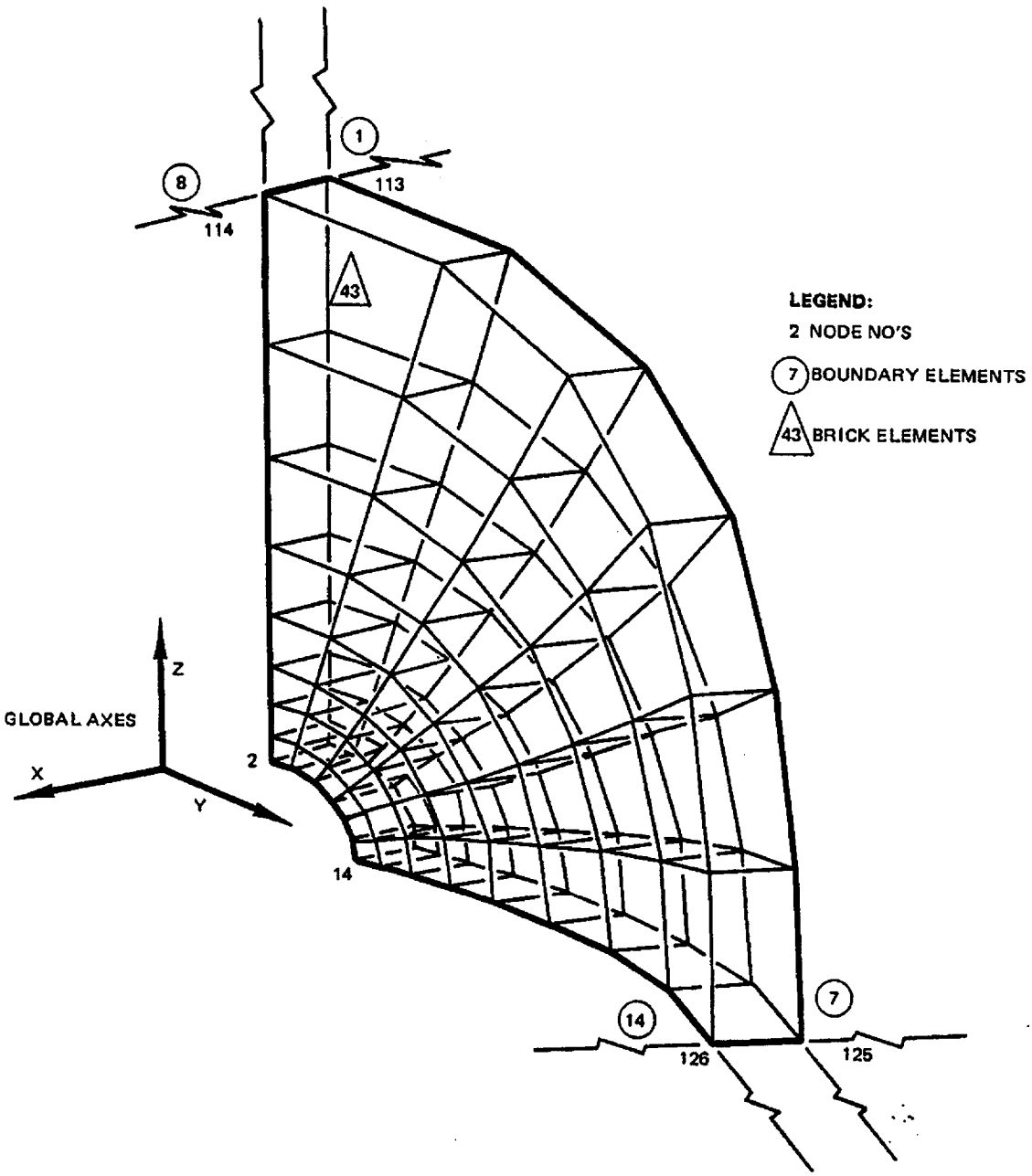

Updated

SAN ONOFRE NUCLEAR GENERATING STATION Units 2 & 3
AREA AROUND A CYLINDRICAL PENETRATION IN A CYLINDER (SAP EXAMPLE 12) (Sheet 2 of 2)
Figure 3C.5-11

Amended: June 2003 TL: E004628

10079-11D-1397
250C6

Amended: April 2009 TL: E047997

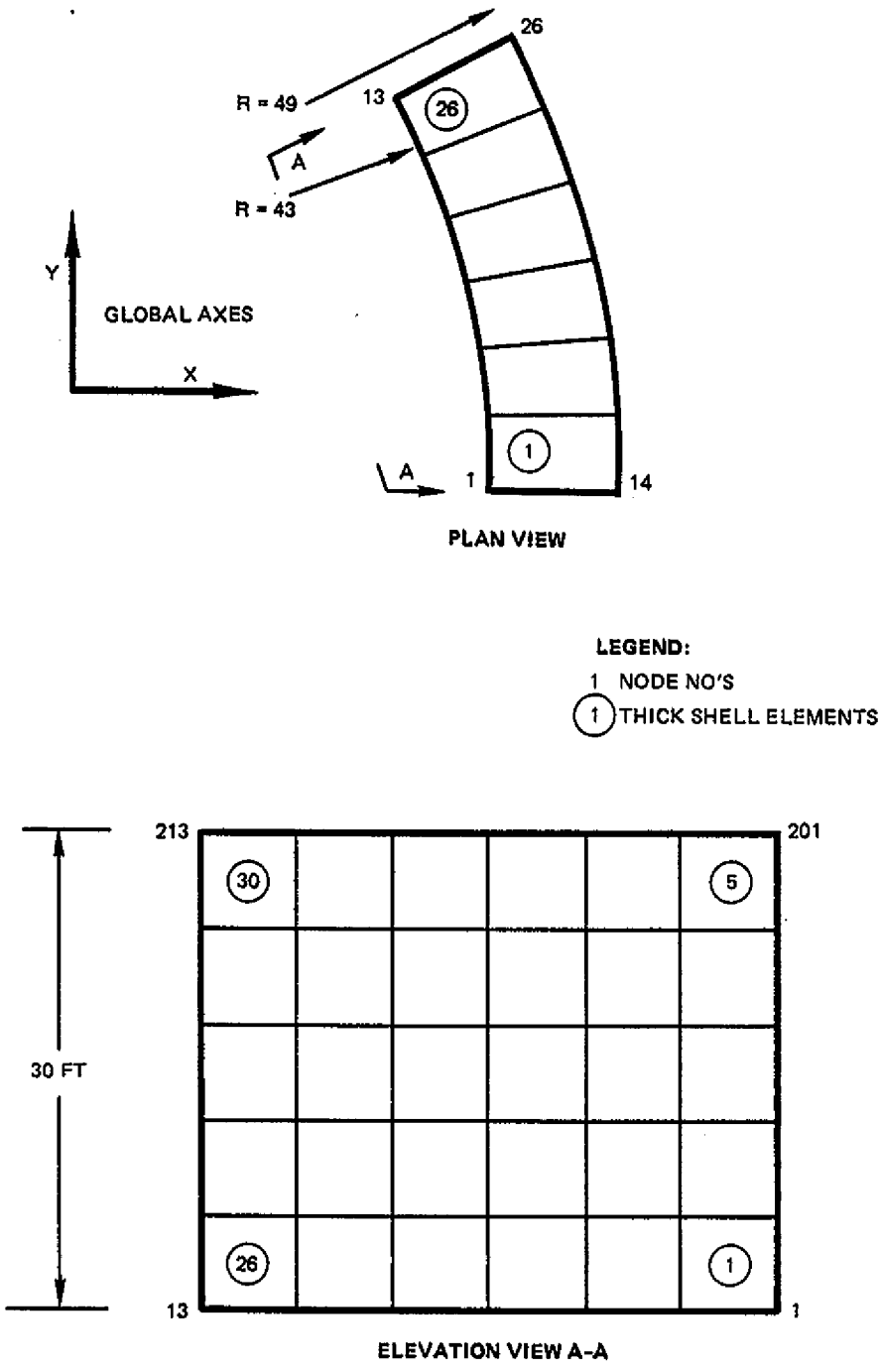

Updated

SAN ONOFRE NUCLEAR GENERATING STATION Units 2 & 3
SEGMENT OF A CYLINDER COMPOSED OF THICK SHELL ELEMENTS (ARCH DAM) (SAP EXAMPLE 13)
Figure 3C.5-12

10079-11D-1398
250C6

Amended: April 2009 TL: E047997

Site File Copy

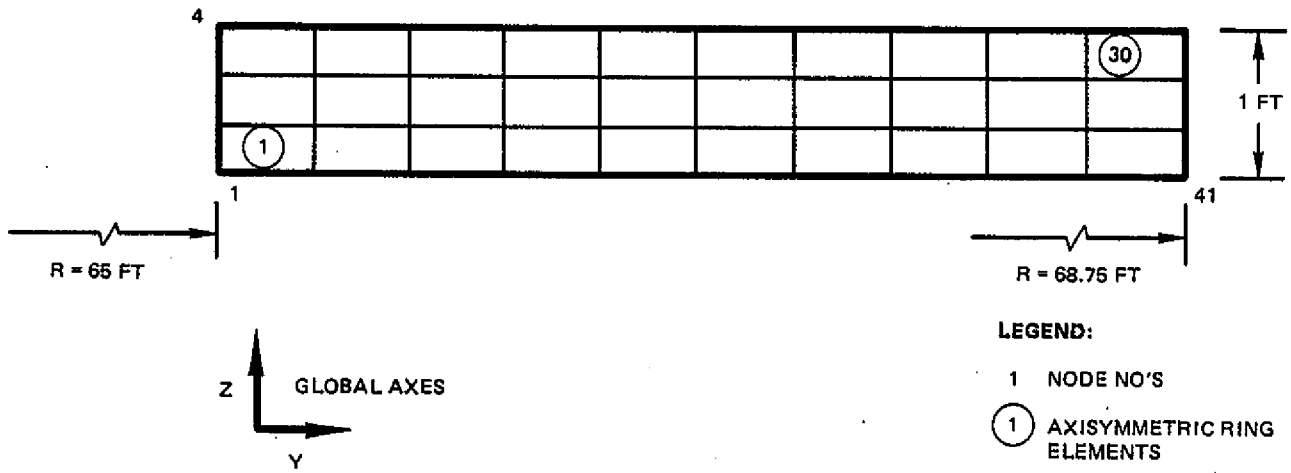

Updated

SAN ONOFRE NUCLEAR GENERATING STATION Units 2 & 3
SEGMENT OF A CYLINDER WALL COMPOSED OF AXISYMMETRIC RING ELEMENTS (SAP EXAMPLE 14)
Figure 3C.5-13

10079-11D-1399
250C6

Amended: April 2009 TL: E047997

Site File Copy

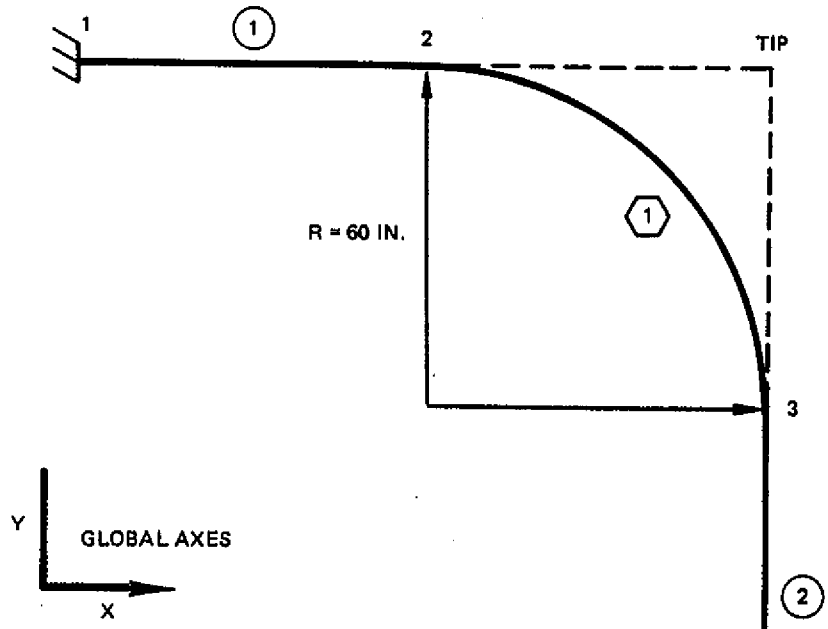

RUN NO. 1

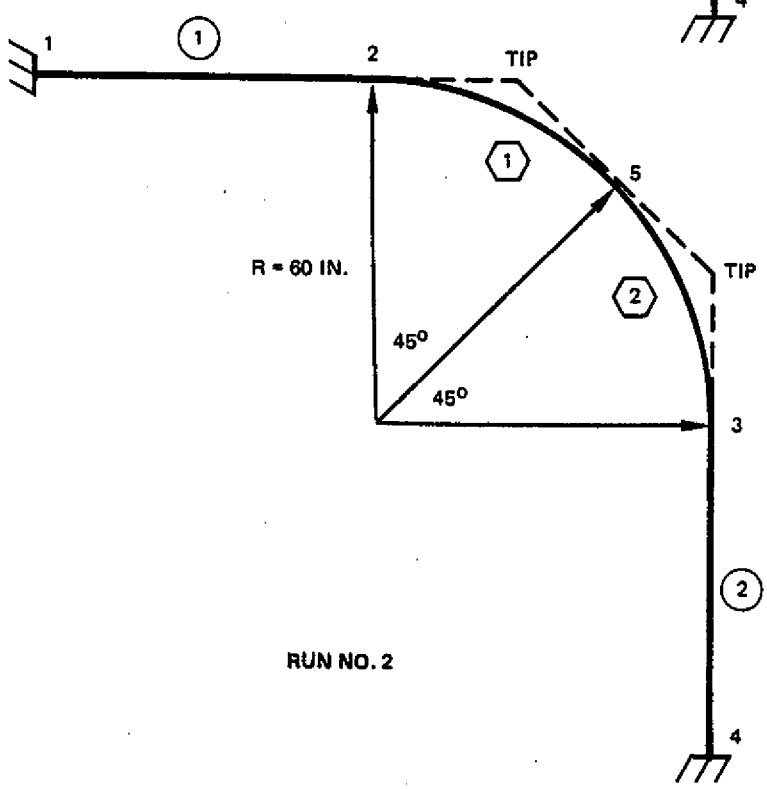

RUN NO. 2

LEGEND:

1 NODE NO'S

(1) BEAM ELEMENTS

⟨1⟩ CU ELEMENTS

Updated

SAN ONOFRE NUCLEAR GENERATING STATION Units 2 & 3
PLANE FRAME COMPOSED OF BEAM AND CURVED BEAM ELEMENTS (SAP EXAMPLE 15)
Figure 3C.5-14

10079-11D-1400
250C6

Amended: April 2009 TL: E047997

Site File Copy

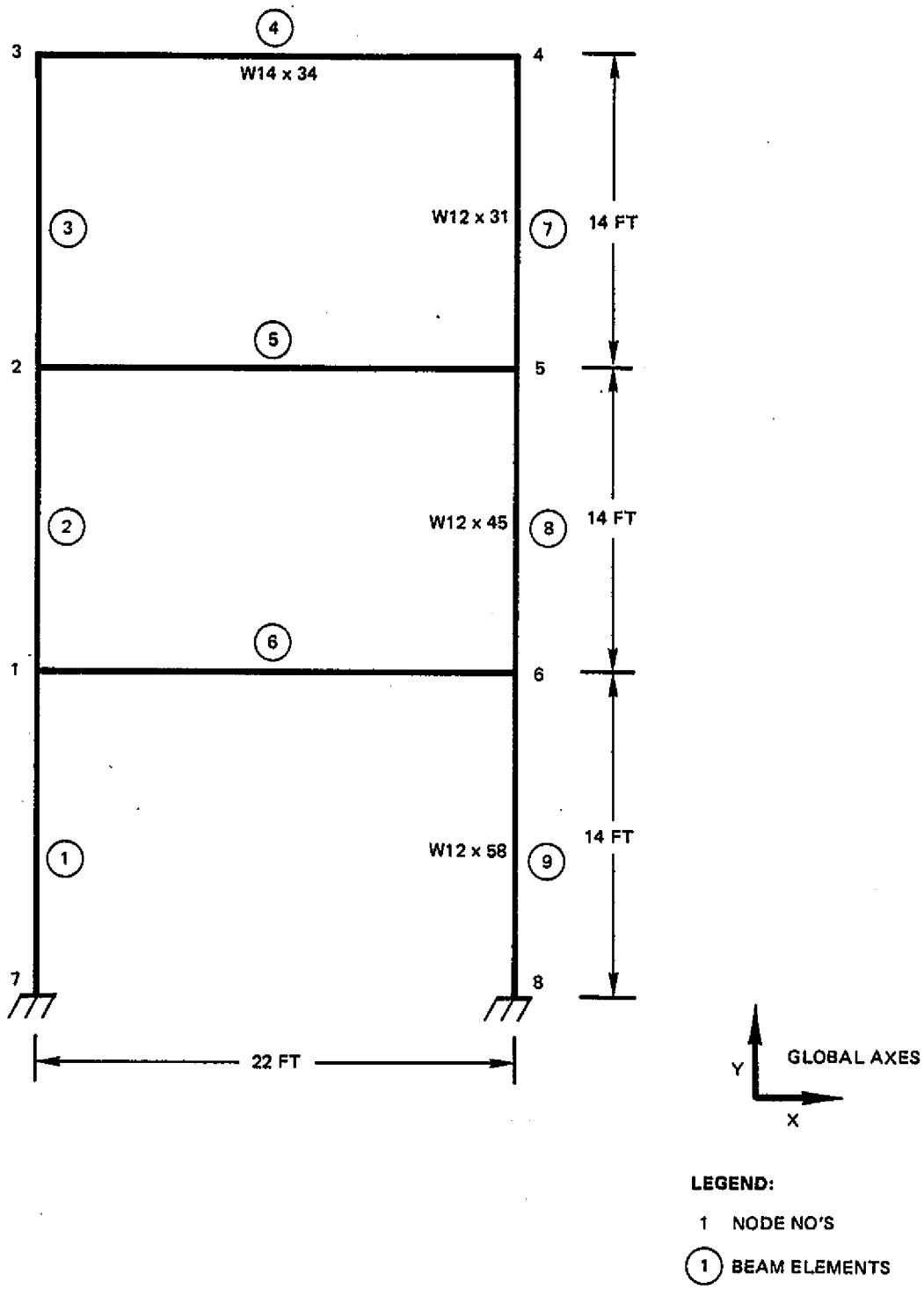

Updated

SAN ONOFRE NUCLEAR GENERATING STATION Units 2 & 3
MULTISTORY PLANE FRAME COMPOSED OF BEAM ELEMENTS (SAP EXAMPLES 16, 19, 24, 25, AND 34)
Figure 3C.5-15

10079-11D-1401
250C6

Amended: April 2009 TL: E047997

Site File Copy

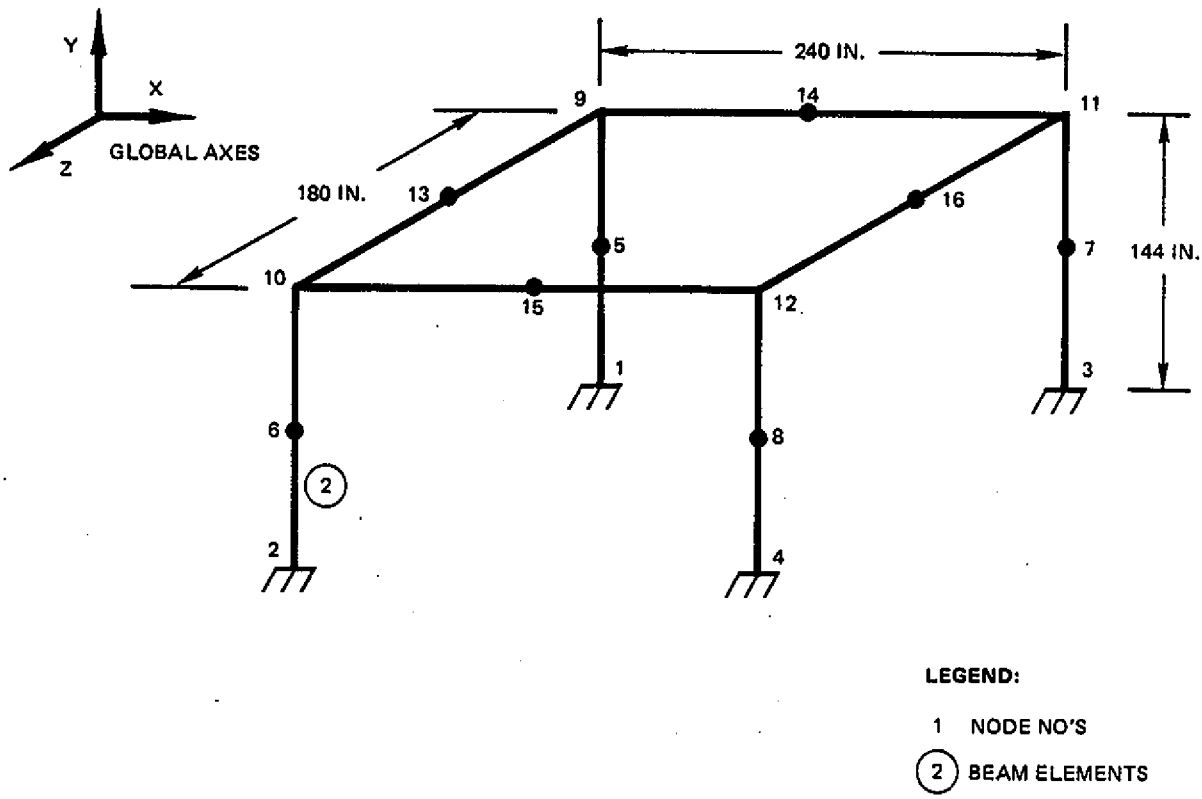

Updated

SAN ONOFRE NUCLEAR GENERATING STATION Units 2 & 3
SINGLE-STORY SPACE FRAME COMPOSED OF BEAM ELEMENTS (SAP EXAMPLES 17, 18, 20, 21, 22, 23, 27, 31, AND 32)
Figure 3C.5-16

10079-11D-1402
250C6

Amended: April 2009 TL: E047997

Site File Copy

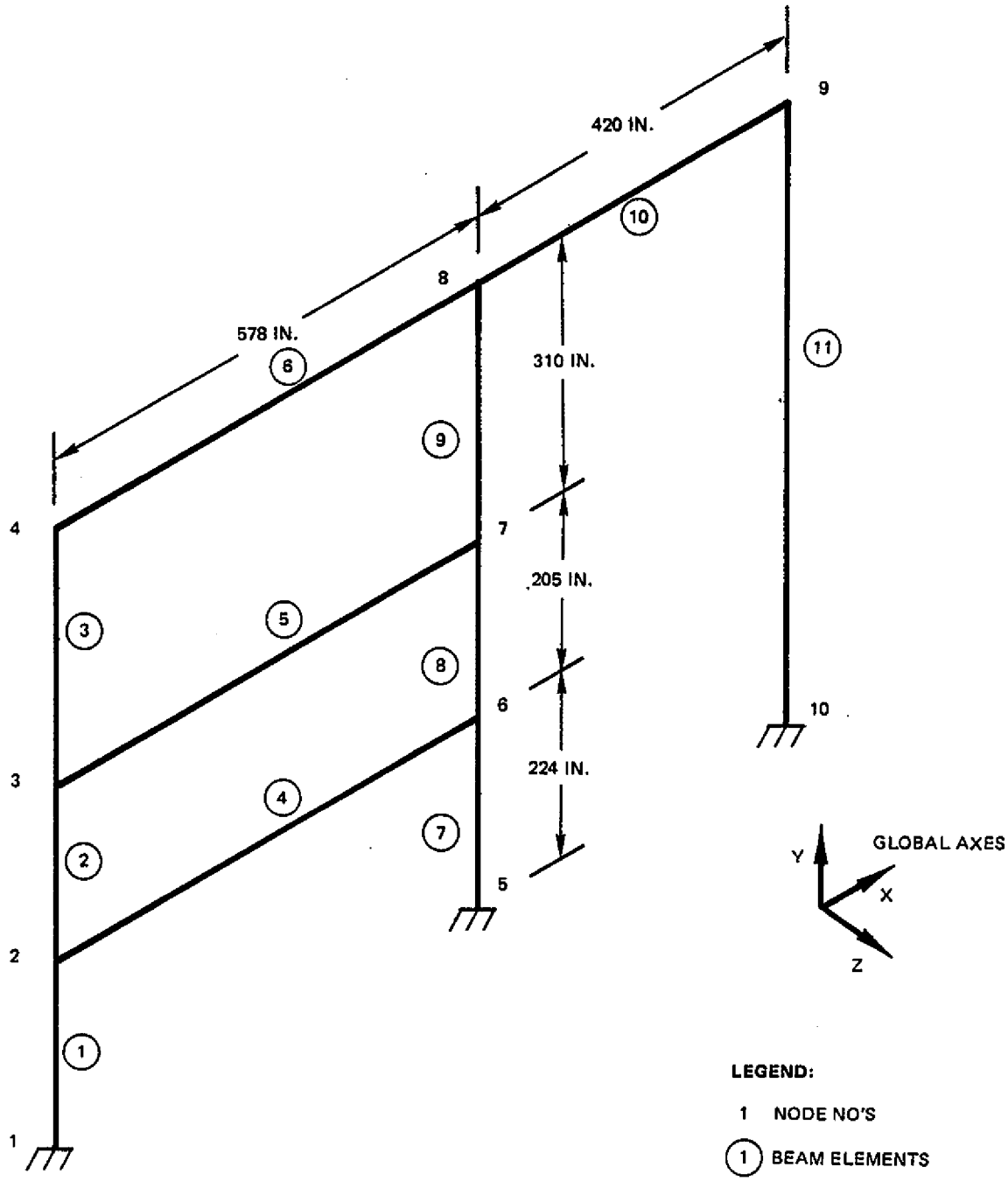

Updated

SAN ONOFRE NUCLEAR GENERATING STATION Units 2 & 3
MULTISTORY SPACE FRAME COMPOSED OF BEAM ELEMENTS (SAP EXAMPLE 26)
Figure 3C.5-17

10079-11D-1403
250C6

Amended: April 2009 TL: E047997

Site File Copy

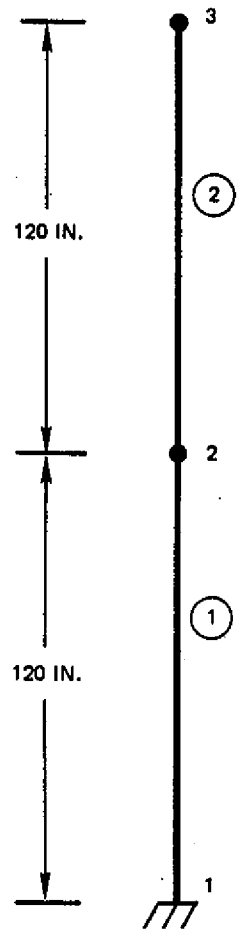

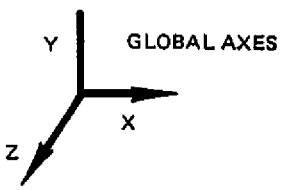

LEGEND:

1 NODE NO'S

(1) BEAM ELEMENTS

Updated

SAN ONOFRE NUCLEAR GENERATING STATION Units 2 & 3
MULTISTORY PLANE FRAME COMPOSED OF BEAM ELEMENTS (SAP EXAMPLE 35)
Figure 3C.5-18

10079-11D-1404
250C6

Amended: April 2009 TL: E047997

Site File Copy

C. STIFFNESS MATRIX

0.60842E+11	.0	.0	.0	-0.91264E+12	0.
.0	0.60842E+11	.0	0.91264E+12	.0	0.
.0	.0	0.76032E+10	0.	0.	.0
.0	0.91264E+12	0.	0.18253E+14	0.	0.
-0.91264E+12	.0	0.	0.	0.18253E+14	0.
0.	0.	.0	0.	0.	0.26940E+13

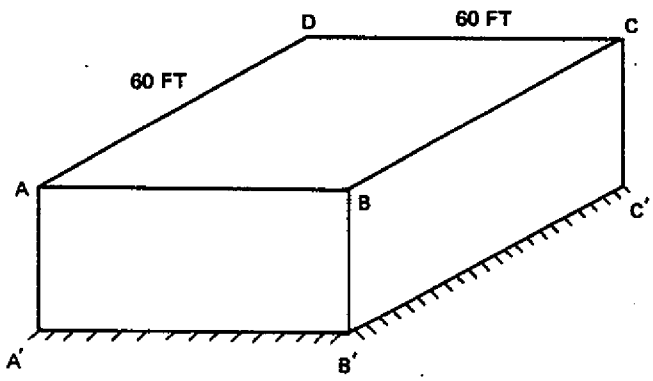

A. THE BOX-TYPE BUILDING

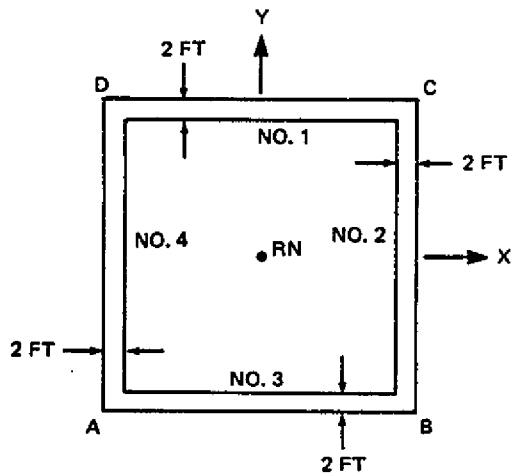

B. GLOBAL AXES

Updated

SAN ONOFRE NUCLEAR GENERATING STATION Units 2 & 3
ARITHMETIC CHECK, THE GLOBAL AXES PASS THROUGH THE REFERENCE NODE (COPK EXAMPLE 1)
Figure 3C.7-1

10079-11D-1410
26OC6

Amended: April 2009 TL: E047997

Site File Copy

$$
\begin{array}{c}
 \\ \Delta X \\ \Delta Y \\ \Delta Z \\ \theta X \\ \theta Y \\ \theta Z
\end{array}
\begin{array}{c}
\begin{array}{cccccc} \Delta X & \Delta Y & \Delta Z & \theta X & \theta Y & \theta Z \end{array} \\
\begin{bmatrix}
\frac{12EI}{L^3} & 0 & 0 & 0 & -\frac{6EI}{L} & 0 \\
0 & \frac{12EI}{L^3} & 0 & \frac{6EI}{L^2} & 0 & 0 \\
0 & 0 & \frac{AE}{L} & 0 & 0 & 0 \\
0 & \frac{6EI}{L^2} & 0 & \frac{4EI}{L} & 0 & 0 \\
-\frac{6EI}{L^2} & 0 & 0 & 0 & \frac{4EI}{L} & 0 \\
0 & 0 & 0 & 0 & 0 & \frac{6I_Z}{L}
\end{bmatrix}
\end{array}
$$

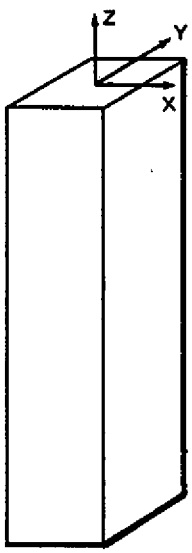

$$AX = AY = 60 \times 4 \times 2 = 480$$

$$I_X = I_Y = \frac{bd^3}{12} - \frac{b'd'^3}{12} = 0.288320 \times 10^6$$

$$\frac{AE}{L} = 0.76032 \times 10^{10}$$

$$\frac{12EI}{L^3} = \frac{12}{30^3} \times 0.4752 \times 10^9 \times 0.288320 \times 10^6 = 0.60892 \times 10^{11}$$

$$\frac{6EI}{L^2} = \frac{6}{30^2} \times 0.4752 \times 10^9 \times 0.288320 \times 10^6 = 0.913398 \times 10^{12}$$

$$\frac{4EI}{L} = \frac{4}{30} \times 0.4752 \times 10^9 \times 0.28832 \times 10^6 = 0.182680 \times 10^{14}$$

Updated

SAN ONOFRE
NUCLEAR GENERATING STATION
Units 2 & 3

ARITHMETIC CHECK, RESULTS OF MANUAL CALCULATIONS FOR THE BOX-TYPE BUILDING SHOWN IN FIGURE 3C.7-1

Figure 3C.7-2

10079-11D-1411
26OC6

Amended: April 2009 TL: E047997

Site File Copy

(ii)
STIFFNESS MATRIX

0.60842E+11	.0	.0	.0	-0.91264E+12	0.
.0	0.60842E+11	.0	0.91264E+12	.0	0.
.0	.0	0.76032E+10	0.	0.	.0
.0	0.91264E+12	0.	0.18253E+14	0.	0.
-0.91264E+12	.0	0.	0.	0.18253E+14	0.
0.	0.	.0	0.	0.	0.26940E+13

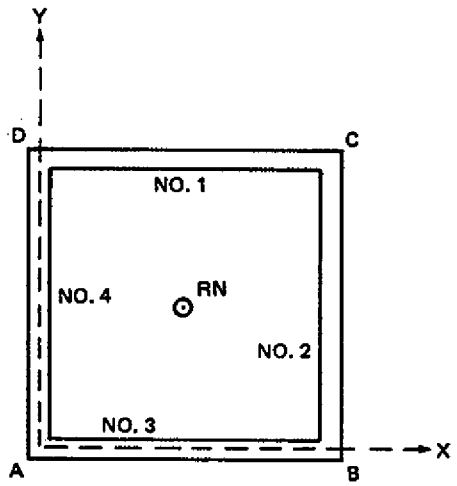

(i) GLOBAL AXES

Updated

SAN ONOFRE NUCLEAR GENERATING STATION Units 2 & 3

ARITHMETIC CHECK, THE GLOBAL AXES PASS THROUGH A CORNER OF THE STRUCTURE (COPK EXAMPLE 2)

Figure 3C.7-3

10079-11D-1412
26OC6

Amended: April 2009 TL: E047997

Site File Copy

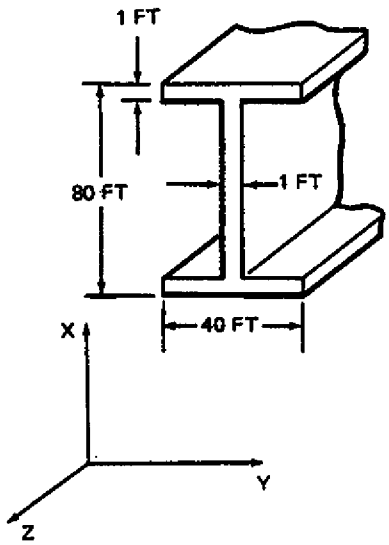

$Av_x = 2 \times 40 \times 0.833 = 66.64$

$Av_y = 78 \times 0.86 = 67.2$

$A_z = 2 \times 40 \times 1 + 78 \times 1 = 158\ FT^2$

$I_x = \frac{1}{12}(80^3 \times 40 - 78^3 \times 39) = 164370\ FT^4$

$I_y = \frac{1}{12}(2 \times 1 \times 40^3 + 78 \times 1^3) = 10673\ FT^4$

$J = 2K_1 + K_2 + 2\alpha D^4$ (REFERENCE 1)

WHERE $K_1 = ab^3\left[\frac{1}{3} - 0.21\frac{b}{a}\left(1 - \frac{b^4}{12a^4}\right)\right]$

$= 40 \times 1^3 \times \left[\frac{1}{3} - 0.21 \times \frac{1}{40}\left(1 - \frac{1^4}{1240^4}\right)\right] = 13.1$

$K_2 = \frac{1}{3}\ od^3 = \frac{1}{3} \times 78 \times 1^3 = 26$

$\alpha = \frac{t}{t_1}\left(0.15 + 0.1 \times \frac{r}{b}\right) = 0.15$

$D = 1.25$

$J = 2 \times 13 + 26 + 0.73 = 52.73$

	Av_x	Av_y	A_z	I_x	I_y	J
MANUAL CALCULATION	66.6	67.2	158	164370	10673	52.7
COPK	66.7	67.3	158	164310	10673	0

Updated

SAN ONOFRE NUCLEAR GENERATING STATION Units 2 & 3

ARITHMETIC CHECK (COPK EXAMPLE 3)

Figure 3C.7-4

10079-11D-1413
26OC6

Amended: April 2009 TL: E047997

Site File Copy

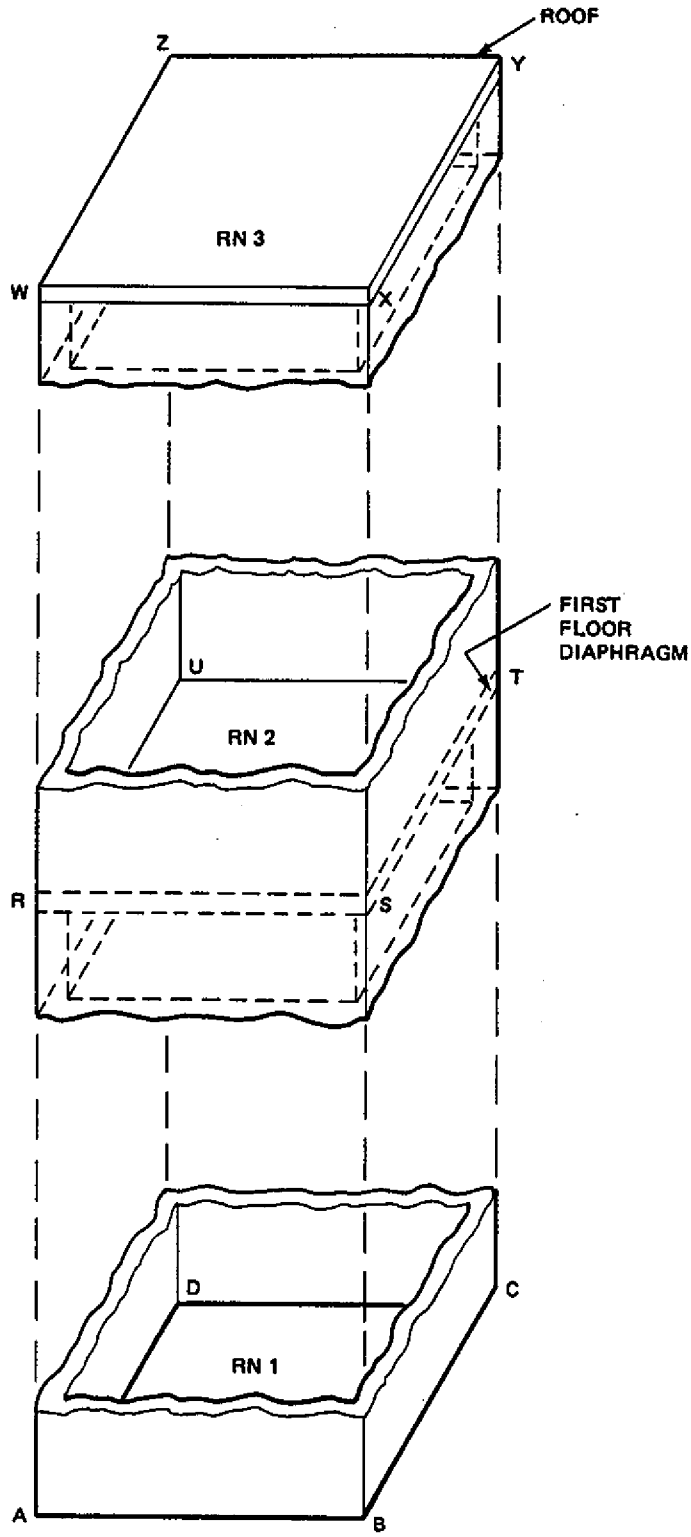

Updated

SAN ONOFRE NUCLEAR GENERATING STATION Units 2 & 3
EXAMPLE BUILDING FOR DEFLECTION CHECK, INTERIOR ASSEMBLIES OMITTED TO SHOW LOCATION OF REFERENCE NODES
Figure 3C.7-5

10079-11D-1414
26OC6

Amended: April 2009 TL: E047997

Site File Copy

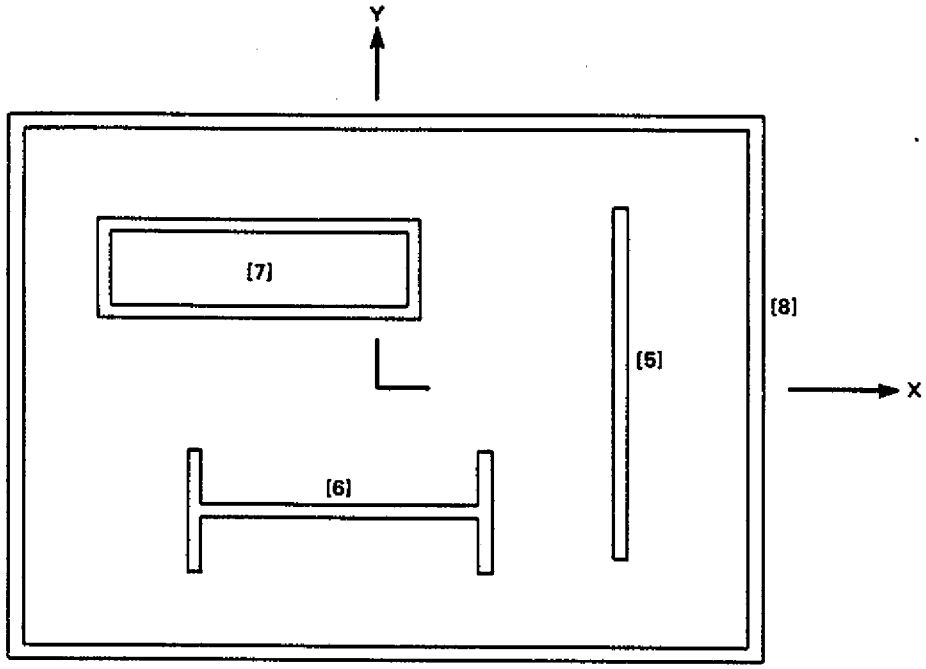

2ND FLOOR

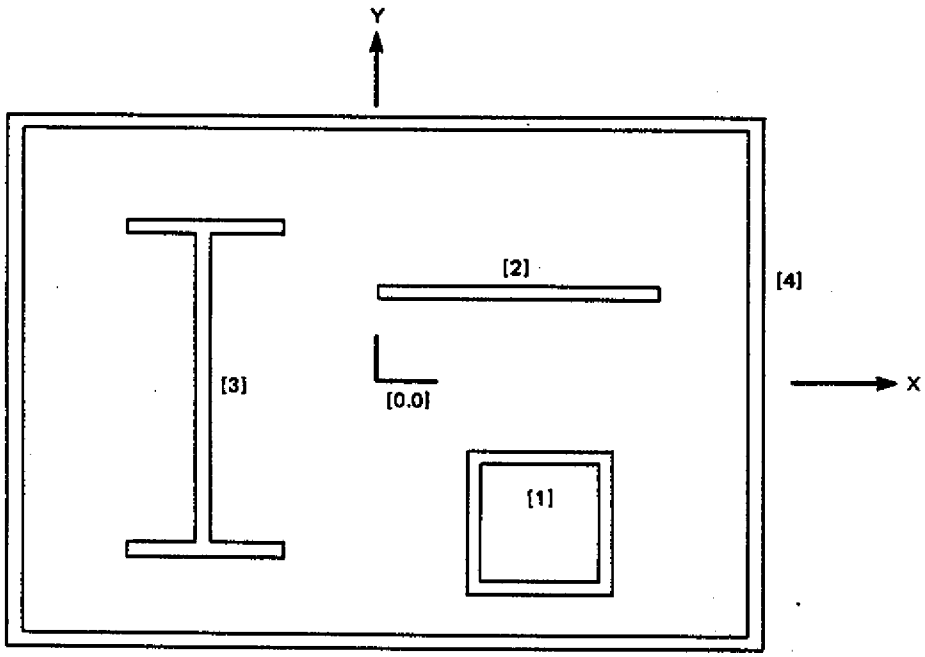

1ST FLOOR

Updated

SAN ONOFRE NUCLEAR GENERATING STATION Units 2 & 3
DEFLECTION CHECK, STRUCTURAL COMPONENTS HAVING GEOMETRICALLY SYMMETRIC CROSS-SECTION
Figure 3C.7-6

10079-11D-1415
26OC6

Amended: April 2009 TL: E047997

Site File Copy

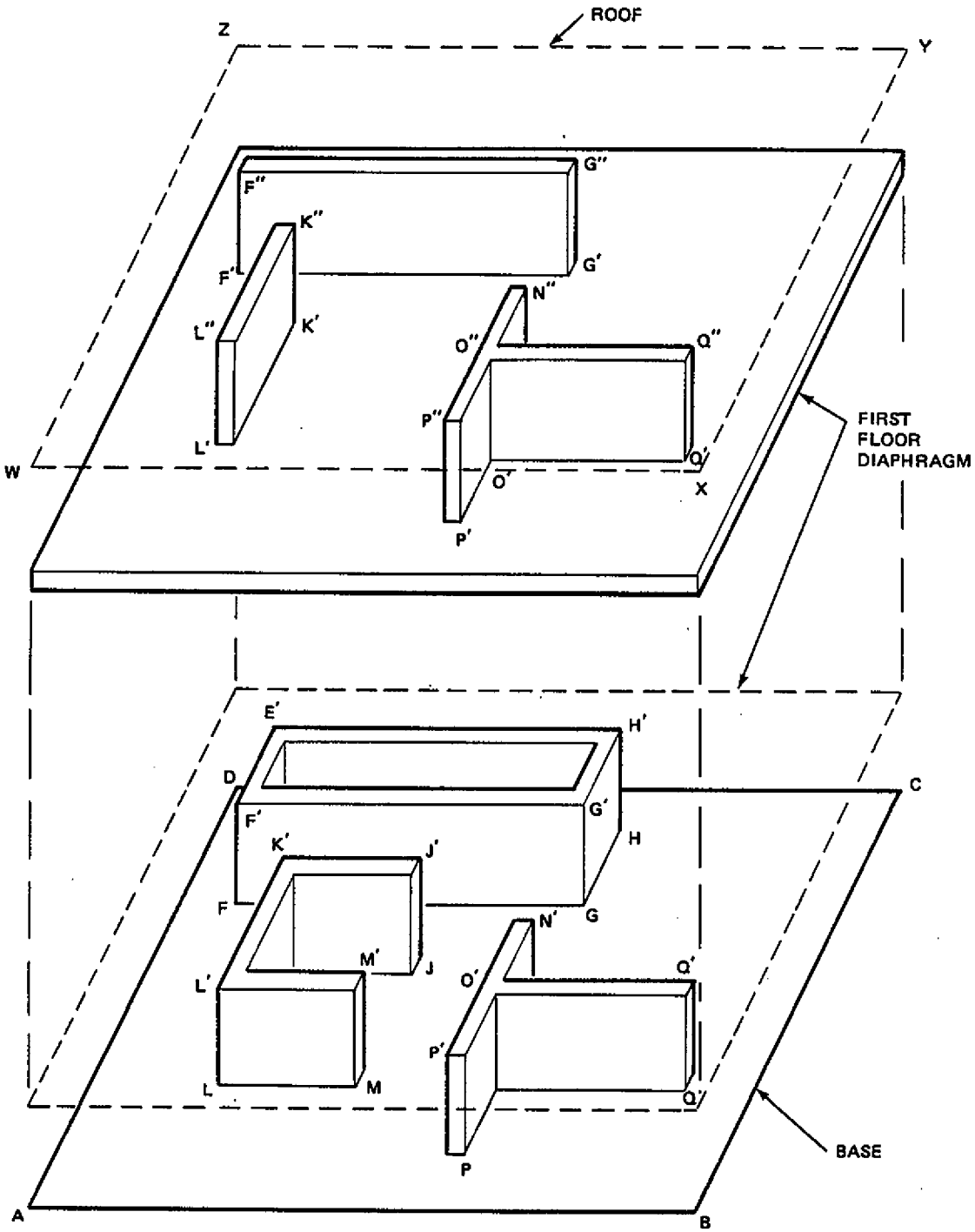

Updated

SAN ONOFRE NUCLEAR GENERATING STATION Units 2 & 3
DEFLECTION CHECK, STRUCTURAL COMPONENTS HAVING GEOMETRICALLY NONSYMMETRIC CROSS-SECTION, EXTERIOR SHEAR WALLS OMITTED TO SHOW INTERIOR ASSEMBLY DETAILS (COPK EXAMPLE 4)
Figure 3C.7-7

10079-11D-1416
26OC6

Amended: April 2009 TL: E047997

Site File Copy

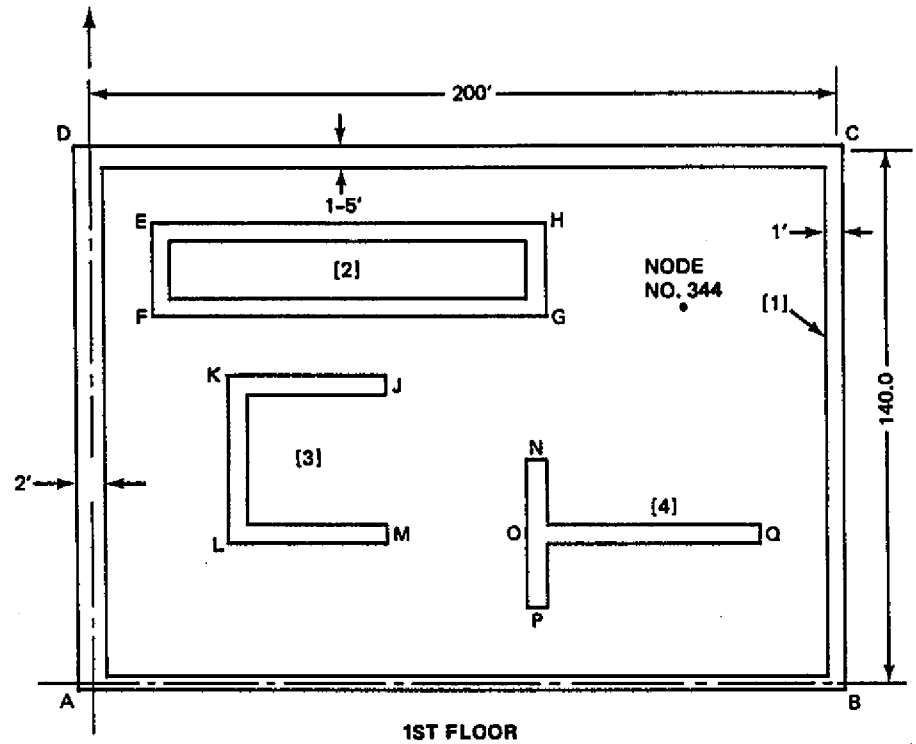

1ST FLOOR

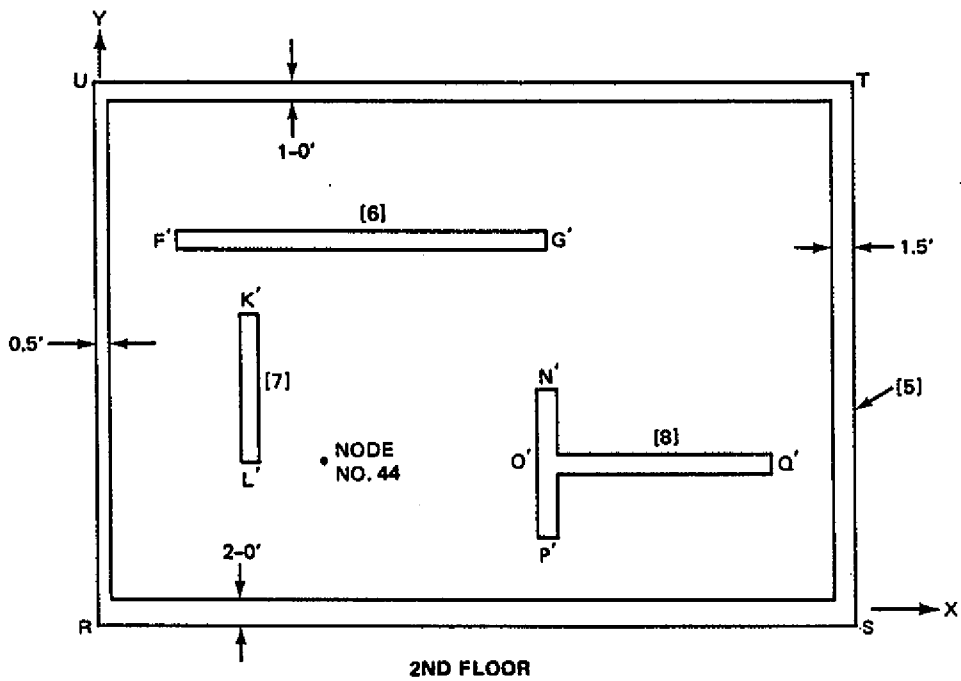

2ND FLOOR

Updated

SAN ONOFRE
NUCLEAR GENERATING STATION
Units 2 & 3

DEFLECTION CHECK, STRUCTURAL COMPONENTS HAVING GEOMETRICALLY NONSYMMETRIC CROSS-SECTION (COPK EXAMPLE 4)

Figure 3C.7-8

10079-11D-1417
26OC6

Amended: April 2009 TL: E047997

Site File Copy

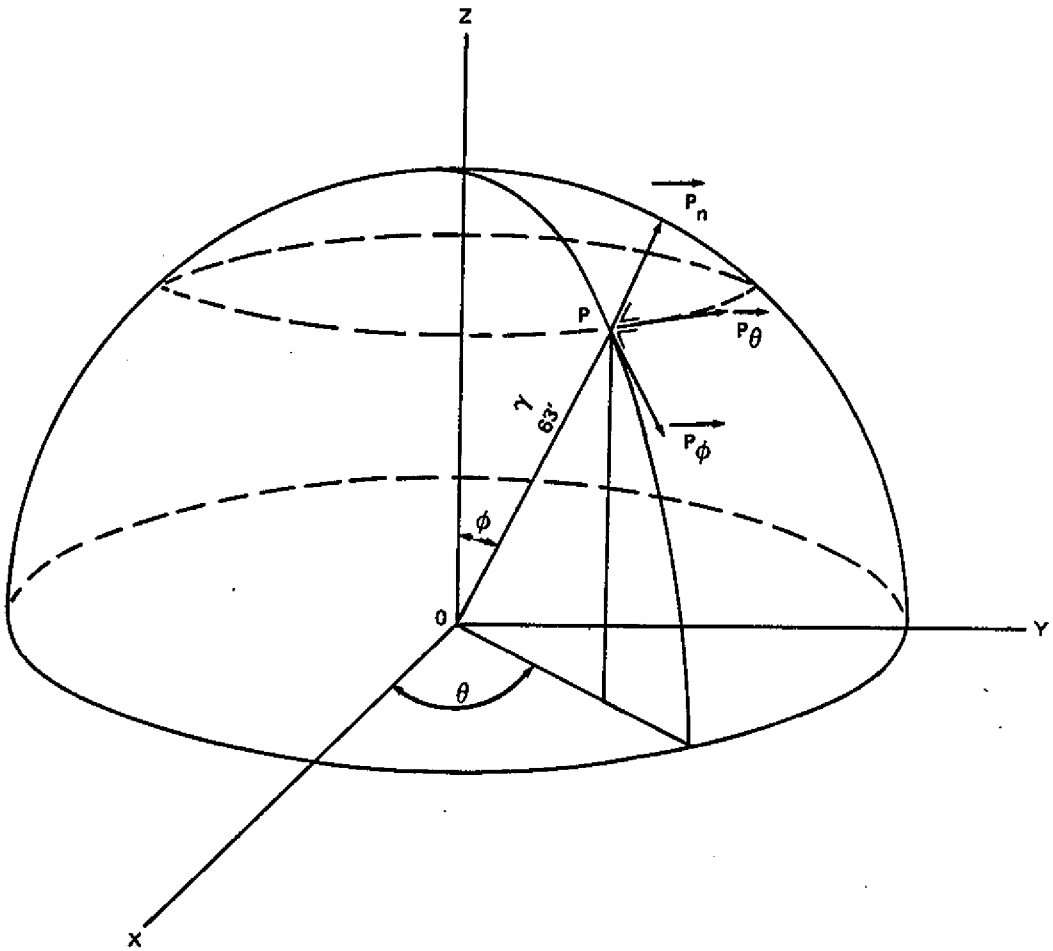

Updated

SAN ONOFRE NUCLEAR GENERATING STATION Units 2 & 3
HEMISPHERICAL DOME
Figure 3C.10-1

10079-11D-1406
26OC6

Amended: April 2009 TL: E047997

Site File Copy

NUMERICAL DATA:

NUMBER OF TENDON GROUPS	2
NUMBER OF TENDONS IN A GROUP	35
ULTIMATE STRENGTH OF TENDON	2120 kips
FRICTION COEFFICIENT	0.160
ANGLE BETWEEN THE FIRST GROUP AND X-AXIS	0°
ANGLE BETWEEN THE SECOND GROUP AND X-AXIS	90°
PRESTRESSING FACTORS – INITIAL	0.759
– FINAL	0.664

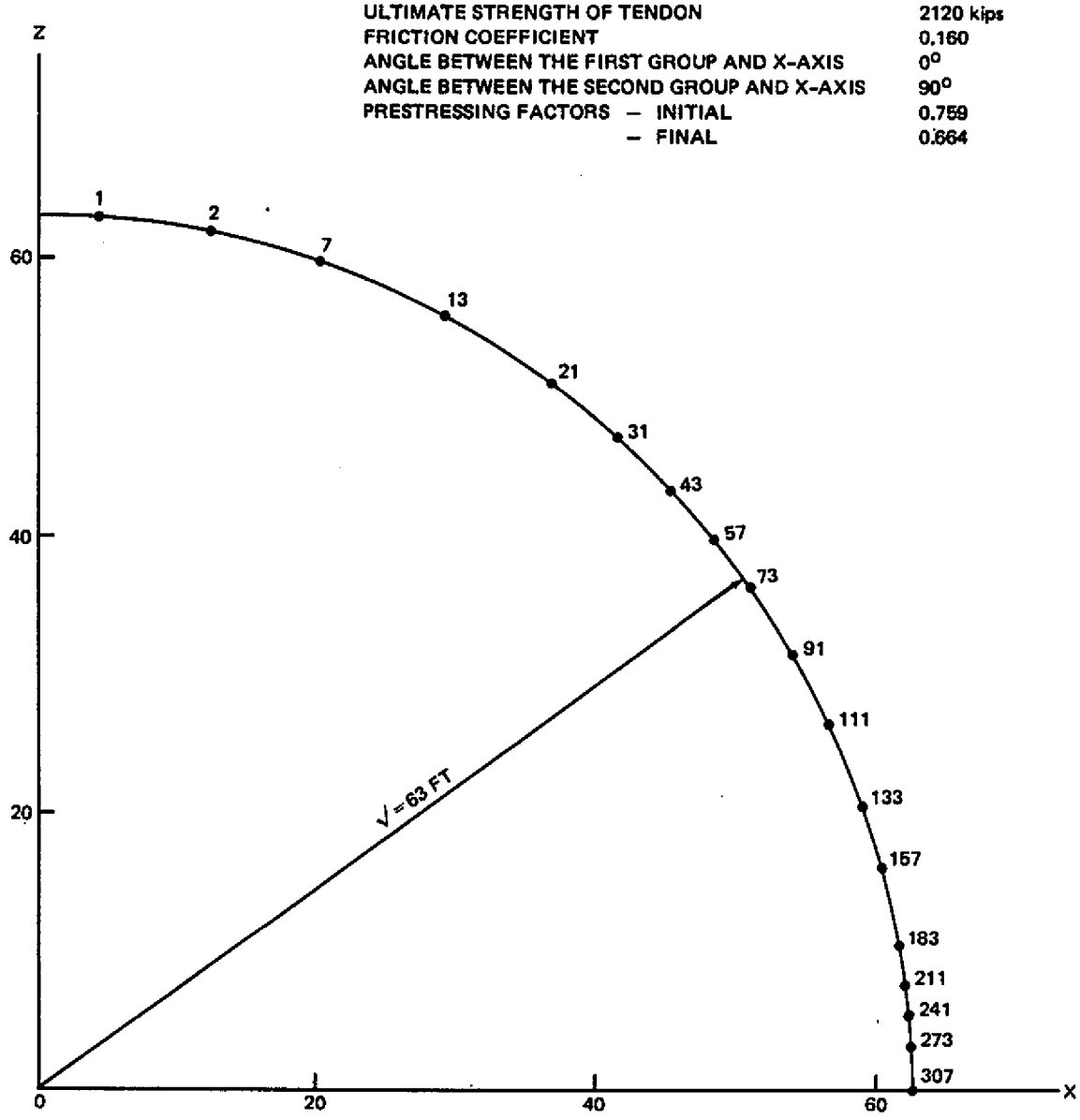

Updated

SAN ONOFRE NUCLEAR GENERATING STATION Units 2 & 3
HEMISPHERICAL DOME - IDENTIFICATION NUMBERS OF THE NODAL POINTS IN THE XZ-PLANE
Figure 3C.10-2

10079-11D-1407
26OC6

Amended: April 2009 TL: E047997

Site File Copy

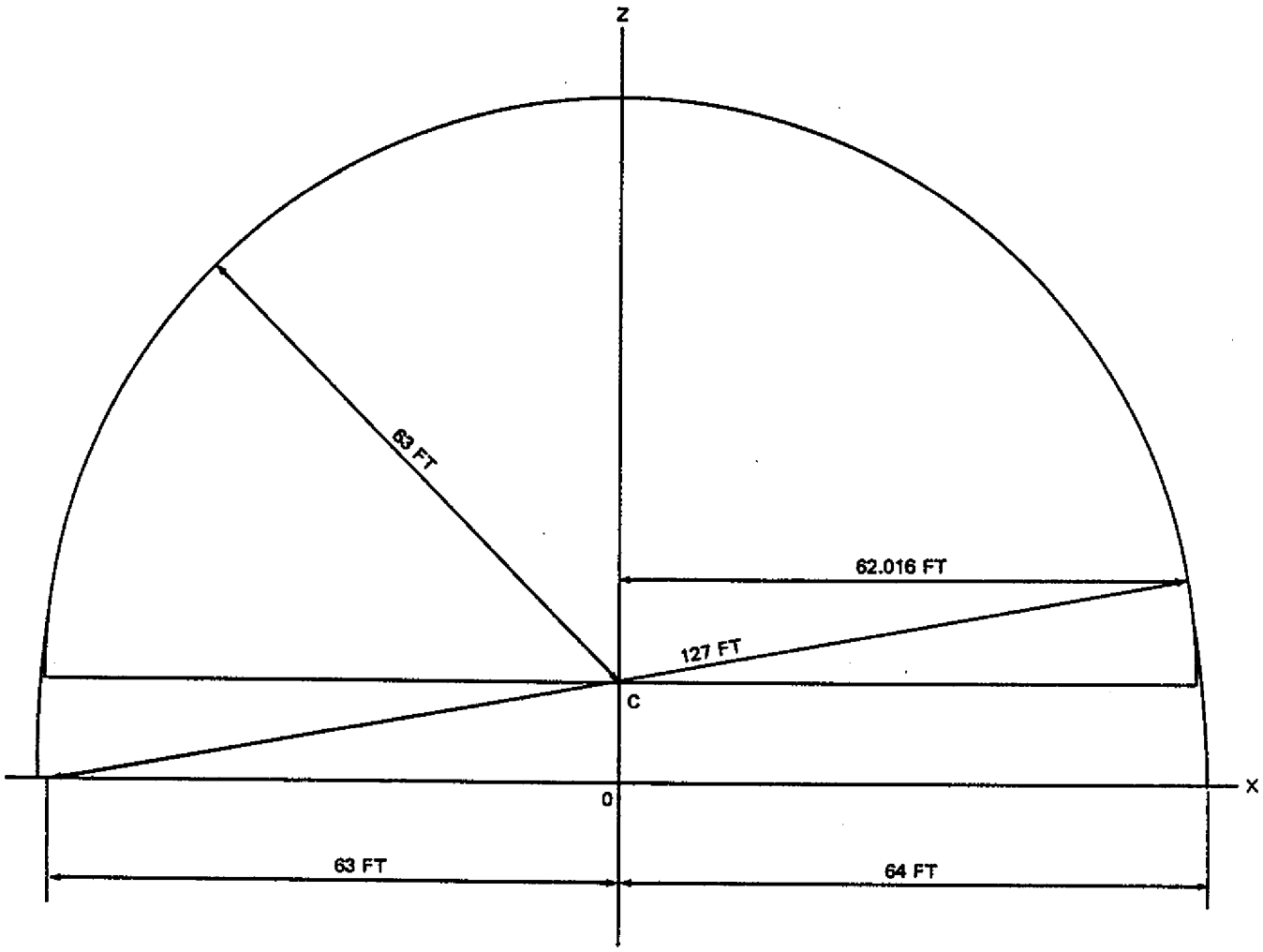

Updated

SAN ONOFRE NUCLEAR GENERATING STATION Units 2 & 3
SPHERE-TORUS DOME
Figure 3C.10-3

10079-11D-1408
26OC6

Amended: April 2009 TL: E047997

Site File Copy

NUMERICAL DATA:

NUMBER OF TENDON GROUPS	2
NUMBER OF TENDONS IN A GROUP	35
ULTIMATE STRENGTH OF TENDON	2120 kips
FRICTION COEFFICIENT	0.160
ANGLE BETWEEN THE FIRST GROUP AND X-AXIS	0°
ANGLE BETWEEN THE SECOND GROUP AND X-AXIS	90°
PRESTRESSING FACTORS – INITIAL	0.759
– FINAL	0.664

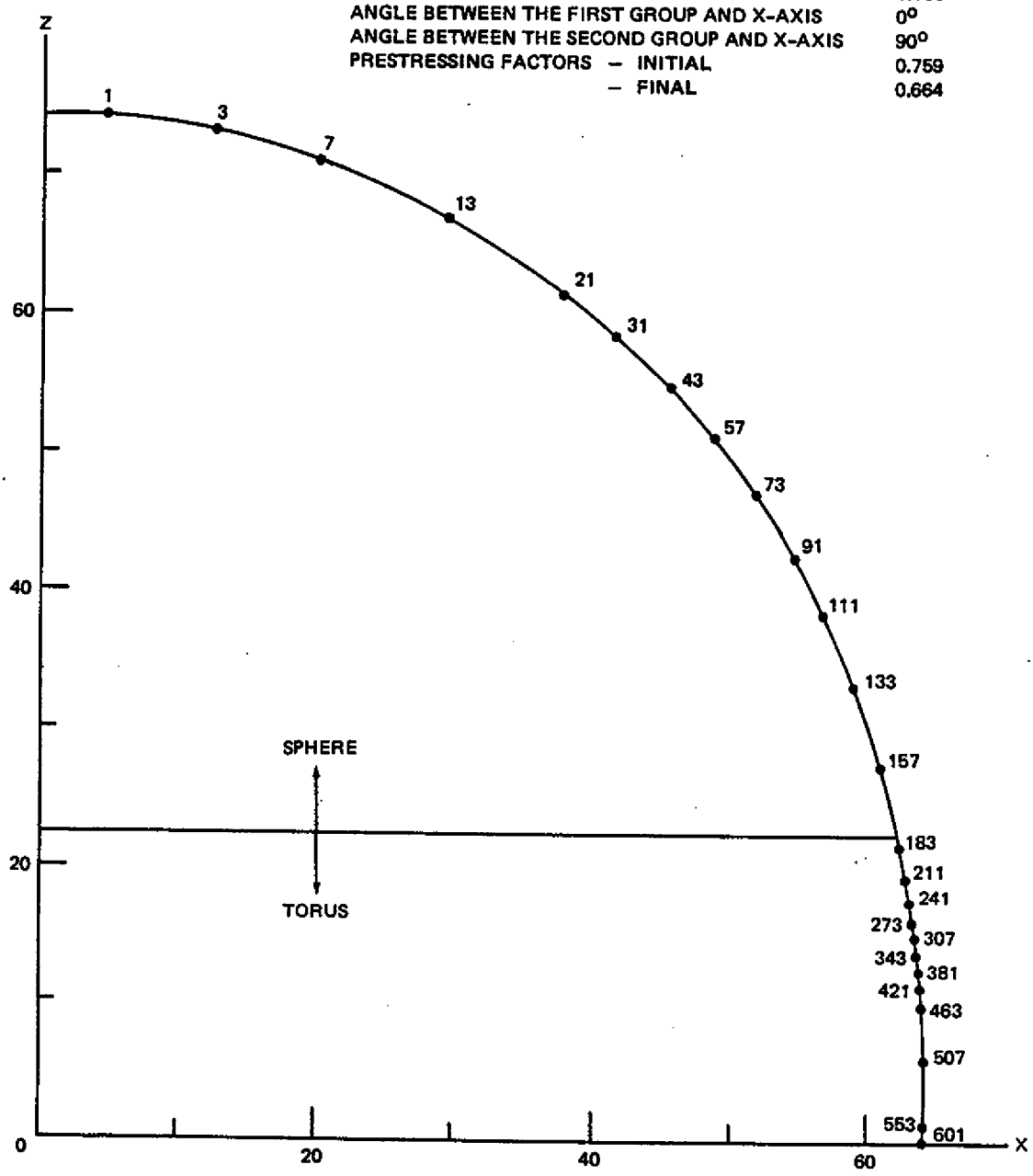

Updated

SAN ONOFRE
NUCLEAR GENERATING STATION
Units 2 & 3

SPHERE-TORUS DOME - IDENTIFICATION NUMBERS OF THE NODAL POINTS IN THE XZ-PLANE

Figure 3C.10-4

10079-11D-1409
26OC6

Amended: April 2009 TL: E047997

Site File Copy

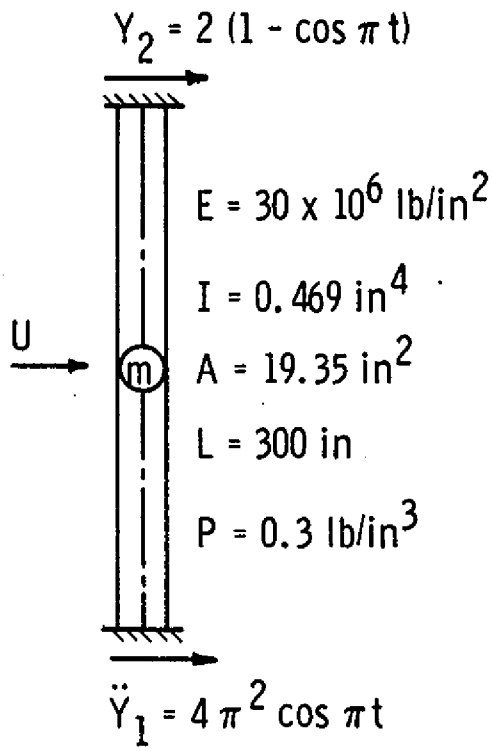

Updated

SAN ONOFRE NUCLEAR GENERATING STATION Units 2 & 3
EXAMPLE PROBLEM FOR TMCALC COMPUTER PROGRAM
Figure 3C.12-1

10079-11D-362
28MY6

Amended: April 2009 TL: E047997

Site File Copy

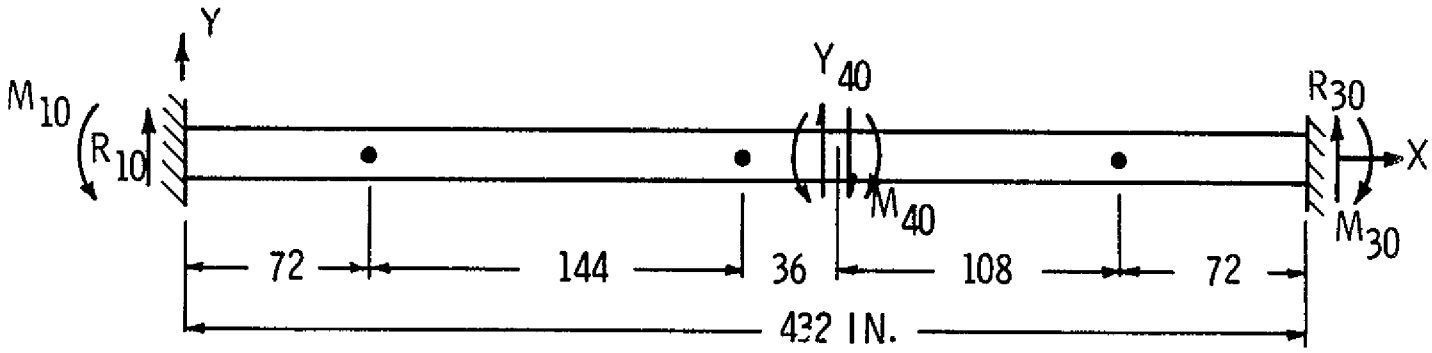

STRUCTURAL PROPERTIES

$AX = 311\ IN.^2$ $AY = 155\ IN.^2$

$IZ = 42,687\ IN.^4$ $E = 27 \times 10^6\ lb/IN.^2$

$\rho = 108\ lb/IN.$

Updated

SAN ONOFRE NUCLEAR GENERATING STATION Units 2 & 3
EXAMPLE PROBLEM FOR FORCE COMPUTER PROGRAM
Figure 3C.13-1

10079-11D-363
28MY6

Amended: April 2009 TL: E047997

Site File Copy